EPA-600/9-83-007
May 1983

PROCEEDINGS:
NATIONAL SYMPOSIUM ON RECENT ADVANCES IN POLLUTANT MONITORING OF AMBIENT AIR AND STATIONARY SOURCES

Proceedings from the National Symposium held at the
Mission Valley Inn
Raleigh, North Carolina
May 4-7, 1982

ENVIRONMENTAL MONITORING SYSTEMS LABORATORY
OFFICE OF RESEARCH AND DEVELOPMENT
U.S. ENVIRONMENTAL PROTECTION AGENCY

NOTICE

This document has been reviewed in accordance with U.S. Environmental Protection Agency policy and approved for publication. Mention of trade names or commercial products does not constitute endorsement or recommendation for use.

ABSTRACT

The second national symposium to explore recent developments that may improve the state-of-the-art for monitoring techniques was presented by the U.S. Environmental Protection Agency, Environmental Monitoring Systems Laboratory (EMSL), May 4 through 7, 1982, at the Mission Valley Inn in Raleigh, North Carolina.

This symposium is part of a continuing effort to explore recent advances in pollutant monitoring of ambient air and stationary sources. Approximately 300 engineers and scientists from industry, universities, and control agencies attended the meeting.

The symposium served as a forum for exchange of ideas and information. The presentations addressed both source emission monitoring and ambient air monitoring. Included were presentations on gaseous organics, particulate pollutants, and personal monitoring. Also presented were findings relative to sampling and analytical methods as well as to a broad spectrum of organic chemicals in outdoor and indoor air.

This publication is intended for those interested in air monitoring and who were unable to attend the symposium. This report includes only those papers submitted voluntarily by speakers. An agenda is included listing all the speakers who participated in the symposium.

CONTENTS

Disclaimer. ii
Abstract. iii
Figures vi
Tables. xvi

Validation of EPA Reference Method 25--Determination of Total Gaseous Nonmethane Organic Emissions as Carbon, Gary B. Howe, Santosh K. Gangwal, R.K.M. Jayanty, Joseph E. Knoll, and M. Rodney Midgett. 1

Evaluation of 2-Propanol as a Liquid Absorbent for Hazardous Pollutants in Stationary Source Gas Streams, Craig M. Young and Larry E. Trejo. 19

Formaldehyde Surface Emission Monitor, T.G. Matthews, A.R. Hawthorne, J.M. Schrimsher, M.D. Corey, and C.R. Daffron. 30

Correlation of Remote and Wet Chemical Techniques for the Determination of Hydrogen Fluoride Emissions from Gypsum Ponds, Howard F. Schiff, Daniel Bause, Mark McCabe, Verne Shortell, William F. Herget, and Mark Antell. 44

Results of the Synthesis and Solid Sorbent Evaluation of Some Porous Copolyamides, Sajal Das, Louis A. Jones, John E. Bunch, and James D. Mulik. 81

Synthesis and Evaluation of a Porous Polyetherimide for the Collection of Volatile Organics, Sajal Das, Louis A. Jones, John E. Bunch, and James D. Mulik 93

Advanced Concentrator/GC Methods for Trace Organic Analysis, S.A. Liebman, T.P. Wampler, and E.J. Levy 103

Air Analysis by a Nondispersive Infrared Method, Philip Hanst 117

Sampling Variability and Storage Stability of Volatile Organic Contaminants, Harold G. Eaton, Frederick W. Williams, and Dennis E. Smith 136

Exposure to Perchloroethylene Associated with the Use of Coin-Type Dry Cleaning Machines, R.H. Jungers and S.J. Howie. 153

Preliminary Results from the Wide Range Aerosol Classifier, R.M. Burton, Dale A. Lundgren, Brian J. Hausknecht, and David C. Rovell-Rixx. 162

Detection of Graphitic Carbon in Collected Particulate Matter, W.A. McClenny 184

Status of Sampling and Analysis of Ambient Nitric Acid, Nitrates and Ammonia, Robert K. Stevens, Robert W. Shaw, Jr., Robert Braman, and C.W. Spicer. 197

A Simple Design for Automation of the Tungsten VI Oxide Technique for Measurement of NH_3 and HNO_3, W.A. McClenny, P.C. Gailey, R.S. Braman, and T.J. Shelley. 202

Ozone Precursor Monitor (OPM) for Investigating Air Pollution, Gordon C. Ortman. 208

A New Reliable Ambient Air Chlorine Monitoring System, Eric F. Mooney 237

The Development of Standard Reference Materials Containing Selected Organic Vapors in Compressed Gas Mixtures, W.P. Schmidt and H.L. Rook 246

Human Exposure to Vapor-Phase Halogenated Hydrocarbons: Fixed-Site VS Personal Exposure, E.D. Pellizzari, T.D. Hartwell, C. Leininger, H. Zelon, S. Williams, J.J. Breen, and L. Wallace. 264

A Personnel or Area Dosimeter for Polynuclear Aromatic Vapors, T. Vo-Dinh. 289

The NBS Portable Ambient Aerosol Sampler, R.A. Fletcher, D.S. Bright, and R.L. McKenzie. 301

Development of a Prototype Active Personal Monitor for SO_2, NO_2, and Airborne Particles, Tahir R. Khan, Jean C. Meranger, and Belinda Lo. 315

Development of SPE Diffusion Head Instrumentation, J.A. Kosek, J.P. Giordano, and A.B. LaConti. 333

Laboratory Studies of a Passive Electrochemical Instrument for Measuring Carbon Monoxide, Vincent A. Forlenza. 358

Results of Testing Diffusion-Type Nitrogen Dioxide Personal Monitors at Low Concentration, James B. Flanagan and Joseph Ryan 369

FIGURES

Number | Page

Howe, Gangwal, Jayanty, Knoll, and Midgett

1 - Single trap sampling train. 3

2 - Modified dual trap sampling train 4

3 - Condensate recovery and conditioning system 6

4 - Byron Model 401 NMOA schematic. 7

5 - Experimental setup for CO_2 interference effect study. 8

6 - Relative responses of the NMOA for several organic compounds. 9

7 - Dry gas volume sampled before plugging versus water vapor content 16

Young and Trejo

1 - Bench-scale test system 21

2 - Eight-inch pilot plant incinerator. 22

3 - Analysis of 1.6 μg CCl_4/ml in 2-propanol. 25

4 - Analysis of 1.3 μg 1,2 - Dichlorobenzene by HPLC. 25

5 - Flow chart of sample analysis 27

Matthews, Hawthorne, Schrimsher, Corey, and Daffron

1 - Conceptual design of the Formaldehyde Surface Emission Monitor 31

2 - Diffusion model for the CH_2O concentration at the surface of the test medium as a function of sorbent-test medium separation and the CH_2O emission rate of the test medium. . . 33

3 - Formaldehyde sampling characteristics of passive samplers containing water (o) and molecular sieve (Δ) sorbents 35

Number			Page
4	-	Comparison of test results for the Hardwood Plywood Manufacturers Association-National Particleboard Association (HPMA-NPA) dessicator and surface monitoring methods	36
5	-	Formaldehyde emission rate of edge-coated wood paneling samples as a function of ambient CH_2O concentration	37
6	-	Urea-formaldehyde foam insulation (UFFI) panel construction	38
7	-	Comparison of CH_2O emission rates from urea-formaldehyde foam insulation (UFFI) panels using dynamic flow and surface monitoring methods	40
Schiff, Bause, McCabe, Shortell, Herget, and Antell			
1	-	Sampling points at CF Industries gypsum ponds	47
2	-	Sampling points at Agrico Chemical Company's gypsum ponds	48
3	-	HF generation system	49
4	-	HF sampling trains utilized in the program (a) prefilter and alkali-treated filter (b) sodium bicarbonate-coated glass tube, and (c) vacuum system for sampling trains	52
5	-	Line of sight of CF Industries	60
6	-	Line of sight at Agrico	61
7	-	The ROSE optical system	63
8	-	Concentration calibration curve for the R(5) line of HF	66
9	-	Clean air and gypsum pond spectra (average of Agrico ROSE Runs 32-38)	67
10	-	Adjusted clean air and gypsum pond absorbance spectra	69
11	-	Transmittance of HF line after background subtraction	70
12	-	Determination of HF line center absorbance by elimination of H_2O interference	71
13	-	Concentration of HF in air assayed by ROSE and manual methods at various time periods	75
14	-	Composite comparison of HF concentrations measured by two techniques	76

Number | Page

Das, Jones, Bunch, and Mulik

1 - Polymers A and B - Copolyamides I, II, and III. 84

Das, Jones, Bunch, and Mulik

1 - Proton NMR of cis-β-phenoxystyrene. 99

Liebman, Wampler, and Levy

1 - CDS 320 sample concentrator 104

2 - Advances in concentrator technology using thermal desorption. 105

3 - Remote sampling of solvents in air. 107

4 - Experimental conditions for remote sampling of solvents in air 108

5 - Test air mixture analysis - Tenax cartridge 110

6 - Test air analysis - Tenax cartridge for diesel fuel 111

7 - Test air mixture analysis - sorbent comparisons 112

8 - Test mixture analysis Tenax/Ambersorb XE-340 cartridge. . . . 114

9 - Test mixture analysis 115

10 - Total organic carbon analysis 116

Hanst

1 - Nondispersive analyzer in negative filter configuration . . . 118

2 - Spectra and detector signals in nondispersive analyzer. 120

3 - Emission spectra of ammonia in nondispersive analyzer 125

4 - Emission spectra of sulfur dioxide in nondispersive analyzer. 127

5 - Detection of SO_2 by nondispersive analyzer. 128

6 - Spectra in nondispersive analyzer tuned for sulfur dioxide. . 129

7 - Spectra in nondispersive analyzer tuned for nonmethane hydrocarbons. 131

8 - Detection of butane by nondispersive analyzer 132

Number | Page

9 - Spectra of hydrogen chloride gas. 133

Eaton, Williams, and Smith

1 - Sampling flask with critical orifice valve. 139

2 - Sampling manifold with one bottle attached. 140

3 - Gas-handling and analytical systems 141

4 - Subsystem-I component analysis. 143

5 - Subsystem-II component analysis 144

6 - Response averages from high-concentration mixture sampling bottles 146

7 - Response averages from low-concentration mixture sampling bottles 147

Burton, Lundgren, Hausknecht, and Rovell-Rixx

1 - Schematic diagram of the mobile sampling system 165

2 - WRAC cumulative mass distributions. 170

3 - WRAC mass distribution histograms for Birmingham, Research Triangle Park, and Philadelphia 171

4 - WRAC mass distribution histograms for Phoenix and Riverside . 172

5 - Normalized mass distributions for Birmingham and Riverside. . 173

6 - Normalized mass distributions for Research Triangle Park, Philadelphia, and Phoenix 174

7 - Mass distribution curves for Phoenix and Riverside. 175

8 - Comparison of sampled vs computed (WRAC) Hi-Vol mass Birmingham, RTP, Philadelphia, Phoenix, and Rubidoux. 179

9 - Comparison of sampled vs computed (WRAC) SSI-IP mass Birmingham, RTP, Philadelphia, Phoenix, and Rubidoux. 180

10 - Comparison of sampled vs computed (WRAC) DICOT-IP mass Birmingham, RTP, Philadelphia, Phoenix, and Rubidoux. 181

Number | Page

McClenny

1 - Schematic of detector cell used in optical measurements of particulate samples (a) front view of disassembled parts, (b) back view. 186

2a - Calibration curve relating optical absorptance and optical absorbance (BL) to sample weight loading of soot in μg per cm^2 of filter area. 187

2b - Calibration curve relating photoacoustic signal to sample weight loading of soot in μg per cm^2 of filter area 187

3 - Ratio, R, of soot estimates by optical absorption and photoacoustics versus total mass loading per filter 190

4 - Schematic representation of model used in calculating light transmitted through and reflected from particle layers in a sample. 191

5 - Model predictions of absorbance ($\ln(I_0/I)$), versus soot loading with mass, M, of scattering particles as a parameter. 193

6 - Model predictions of absorbance, BL, versus experimentally measured values for 18 samples collected in Houston, Texas. . 194

Stevens, Shaw, Braman, and Spicer

1 - Schematic of diffusion denuder nitrate-nitric acid sampler. . 200

McClenny, Gailey, Braman, and Shelley

1 - Schematic of system designed for monitoring HNO_3 and NH_3. . . 203

2 - Schematic of electrical system designed for automated sampling and analysis using time delay relays (TDR) 204

3 - Three-day monitoring sequence using the automated system. . . 206

Ortman

1 - Schematic diagram of ozone precursor monitor (OPM). 211

2 - Irradiation chamber with reaction vessel. 214

3 - Function of integration vessel. 216

4 - GE F40BL lamp spectral output 217

5 - Fluorescent lamp energy maintenance 218

Number | Page

6 - Fluorescent lamp mortality. 219

7 - Ozone yield vs. irradiation time. 222

8 - Ozone precursors and ozone in a small city. 226

9 - Ozone precursors and ozone in a large city. 228

10 - Analytical agreement of OPM's on ambient air. 229

Mooney

1 - Cross-section of probe. 239

2 - Basic chlorine monitoring system using local control or central processing unit 241

3 - LCD alarm graphics on LCU 242

4 - Probe response to 5 ppm chlorine. 244

Schmidt and Rook

1 - Effect of 100 cc/min sample flow rate on equilibration time of cylinder control valve for VCM. 253

2 - Effect of 100 cc/min sample flow rate on equilibration time of cylinder control valve for $CHCl_3$. 254

3 - Effect of sample flow rate and flow volume on equilibration time of cylinder control valve for benzene 255

4 - Effect of 100 cc/min sample flow rate on equilibration time of cylinder control valve for C_2Cl_4. 256

5 - Effect of sample flow rate and flow volume on equilibration time of cylinder control valve for chlorobenzene 257

6 - GC-FID chromatograms of low concentration mixtures prepared by diluting primary standards 260

Pellizzari, Hartwell, Leininger, Zelon, Williams, Breen, and Wallace

1 - Stratified populations in Baton Rouge and Geismar, LA 267

2 - Vest equipped with Tenax GC sampling cartridge, prefilter for particulate and personal pump (in pocket) for collecting vapor-phase halocarbons in personal air 268

3 - Sampling system depicting filter, Tenax GC cartridge and pump for collecting fixed-site air samples. 269

Number | Page

4 - Replicate samples for Tetrachloroethylene - Greensboro, NC study. 273

5 - Replicate samples for 1,1,1-Trichloroethane - Greensboro, NC study. 273

6 - Replicate samples for Chloroform - Greensboro, NC study . . . 274

7 - Replicate samples for Carbon tetrachloride - Greensboro, NC study. 274

8 - Replicate samples for 1,2-Dichloroethane - Baton Rouge/Geismar, LA study 275

9 - Replicate samples for 1,2-Dichloroethane - Greensboro, NC study. 275

10 - Frequency distribution for 1,1,1-Trichloroethane. 278

11 - Frequency distribution for Tetrachloroethylene. 279

12 - Frequency distribution for Trichloroethylene. 280

13 - Comparison of percent detected for fixed-site vs. personal air samples - Greensboro, NC. 281

14 - Comparison of percent detected for fixed-site vs. personal air samples - Baton Rouge/Geismar, LA 282

15 - Spearman Correlation for personal vs. fixed-site air levels of carbon tetrachloride - Baton Rouge/Geismar, LA study . . . 286

16 - Spearman Correlation for personal vs. fixed-site air levels of 1,2-dichloroethane - Baton Rouge/Geismar, LA study 286

Vo-Dinh

1 - Photograph of the PNA dosimeter worn by a worker at a synfuel facility. 291

2 - RTP signal of phenanthrene vapor collected by the dosimeter after two-hour exposure 294

3 - Typical response of the dosimeter to various exposure periods of pyrene vapor 295

4 - Room temperature phosphorescence spectra of quinoline and isoquinoline. 297

Number | Page

5 - Differentiation of isomeric quinolines by synchronous excitation. 298

6 - RTP response of various dosimeters exposed at different locations inside a synfuel plant. 299

Fletcher, Bright, and McKenzie

1 - Schematic of the sampler. 302

2 - Filter collection efficiency as a function of aerodynamic diameter. 305

3 - Schematic of the inlet. 307

4 - Inlet cut curves for 15 μm, 10 μm, and 7 μm cut-points. . . . 308

5 - NBS wind tunnel test facility 308

6 - Horizontal particle concentration profile in the wind tunnel. 309

7 - Inlet sampling efficiency as a function of wind velocity in the wind tunnel. 310

8 - Summary of the NO_2 collection rate for the Dupont Pro-Tek badge 311

Khan, Meranger, and Lo

1 - Schematic of NO/NO_2 flow system for testing solid sorbent . . 317

2 - Schematic of flow system for generating SO_2 + NO_2 + humidified conditions for the testing of sorbent tubes/sampling pumps 318

3 - Sampling arrangement at the Teflon manifold 319

4 - A typical chromatogram of blank (a), 1 ppm standard (b), and duplicate injection of sample (c) 322

5 - Photograph of assembled prototype 326

Kosek, Giordano, and LaConti

1 - Pumped sensor cell assembly 335

2 - Schematic of SPE Diffusion Head Gas Sensor. 338

3 - Remote diffusion head transducer monitor. 339

Number | Page

4 - Transducer and Control Modules Carbon Monoxide Monitor System 340

5 - Effect of a porous metal disk on diffusion sensor cell response. 342

6 - Effect of porous metal on diffusion cell response 343

7 - Response vs. concentration, diffusion sensor cell 344

8 - Application of the SPE Diffusion Cell for the detection of high concentrations of CO. 345

9 - External view, CO diffusion dosimeter 346

10 - Exterior view, CO diffusion dosimeter with interference filter removed. 347

11 - Flow dependence, CO diffusion dosimeter 348

12 - CO diffusion dosimeter linearity data 350

13 - Response of a typical diffusion dosimeter as a function of temperature 351

14 - Exterior view, NO diffusion dosimeter 352

15 - NO diffusion dosimeter flow studies 353

16 - NO diffusion cell response as a function of NO detector response. 354

17 - Temperature dependence of NO diffusion dosimeter response . . 355

Forlenza

1 - ECOLYZER 210 CO sensing system. 360

2 - Instrument reading vs. face velocity at constant gas concentration 362

3 - Ambient readings from the ECOLYZER 210 vs. face velocity at constant CO concentration. 363

4 - ECOLYZER 210 reading at constant CO concentration with and without convection barrier. 364

5 - Percent signal vs. time for ECOLYZER 210-averaged data from five instruments 365

6 - CO vs. LCD readout (ppm). 367

Number		Page

Flanagan and Ryan

1 - Calibration of Palmes tubes analysis system with standard $NaNO_2$ 372

2 - Ratio of Palmes result/CEL versus dose. 374

3 - Palmes results versus dosage. 376

TABLES

Number | Page

Howe, Gangwall, Jayanty, Knoll, and Midgett

1 - Field Test Sampling Conditions. 5

2 - NMO Analyzer Linearity Study Results. 9

3 - Condensate Recovery System Performance Check Results. 10

4 - Textile Plant Field Test Results. 11

5 - Effect of Leak Check Scheme on the Total Measured PPMC for the Plywood Veneer Dryer Field Test Samples 13

6 - Veneer Dryer Plant Corrected Field Test Results 14

7 - Effect of Sampling Train Configuration on CO_2 Interference. . 15

Matthews, Hawthorne, Schrimsher, Corey, and Daffron

1 - Measurements of CH_2O Emission Rates from Major Surfaces in Three Occupied Homes Using the FSEM. 41

2 - Comparison of Measured CH_2O Concentration Levels with Values Predicted from Combined FSEM and ACH Measurements 41

Schiff, Bause, McCabe, Shortell, Herget, and Antell

1 - Results of Laboratory Phase 54

2 - Precision and Accuracy--Laboratory Phase. 55

3 - PPB HF. 56

4 - Preliminary Field Phase: Results and Intersampling Device Precision at Same Site. 57

5 - Preliminary Field Phase Comparison of Results for Analysis by IC and Autoanalyzer. 58

6 - Analysis of Citrate Filters for Fluoride. 58

7 - HF Concentration Data Grouped in Sequence Obtained. 74

Number Page

8 - Statistical Analyses Based on Difference Values for Manual Sampling Data and ROSE Data. 78

Das, Jones, Bunch, and Mulik

1 - Breakthrough Volume of Copolyamide at 25°C (Liter/Gram) . . . 88

2 - Reaction Conditions for the Preparation of Copolyamide-III. . 89

3 - Breakthrough Volumes for Copolyamide III Preparations at 25°C (Liter/Gram). 90

4 - Copolyamide III - Preparation and Properties. 91

5 - Copolyamide III - Breakthrough Volumes (Gm/L) 91

Das, Jones, Bunch, and Mulik

1 - Pertinent Information for the Selected Compounds. 95

2 - U.S. Production/Pollutant Information 95

3 - Porous Polymers Arranged in Order of Increasing Polarity, Determined According to Walraven. 96

4 - Properties of Polyimide Ether 100

5 - Breakthrough Volumes of Polyetherimide at 25°C (Liters/Gram). 100

Liebman, Wampler, and Levy

1 - Test Air Mixture Analysis Tenax Cartridge 40 PPB. 109

Hanst

1 - Detection Limit as Function of System Parameters. 124

Eaton, Williams, and Smith

1 - Contaminants Investigated in the Experiment 138

2 - The Observed Values of the F-Statistics Obtained from the Analysis of Variance. 148

3 - Amounts and Sources of Variance in a Single Observation of Contaminant Concentration (High Levels). 149

4 - Amounts and Sources of Variance in a Single Observation of Contaminant Concentration (Low Levels) 149

Number | Page

5 - Approximate 95 Percent Confidence Intervals for the True Contaminant Concentration in the Test Gas Bottle Based on the Observed Average Concentration in N Flasks with M Analyses for Each Flask (High Concentration Levels) 150

6 - Approximate 95 Percent Confidence Intervals for the True Contaminant Concentration in the Test Gas Bottle Based on the Observed Average Concentration in N Flasks with M Analyses for Each Flask (Low Concentration Levels). 151

Jungers and Howie

1 - Summary of Ambient PERC Concentrations Inside and Outside Laundries (PPB) 158

2 - Comparison of Indoor PERC Between Laundry D and the Apartment Upstairs 159

3 - Summary of Ambient PERC Concentrations Inside a Closed Living Space Where Dry Cleaned Clothing Was Introduced. . . . 160

Burton, Lundgren, Hausknecht, and Rovell-Rixx

1 - Sampler Vs. WRAC Concentration Expressed as Ratio 176

2 - Comparison of Measured Vs WRAC Modeled Mass Loading 182

McClenny

1 - Summary of Mean Values for Parameters Characterizing Particulate Matter Collected on Teflon Substrates 189

Stevens, Shaw, Braman, and Spicer

1 - Levels of Particulate Nitrate and Nitric Acid 200

Ortman

1 - Repeatability of Ozone Yield. 223

2 - Agreement Between OPMs. 223

3 - Line Voltage Effect on Ozone Yield. 224

Mooney

1 - Stability of Calibration. 245

Number | Page

Schmidt and Rook

1 - Toxic Organic Primary Mixtures. 247

2 - Comparison of Gravimetrically Calculated and Analyzed Concentrations for Primary VCM Mixtures 248

3 - Comparison of Gravimetrically Calculated and Analyzed Concentrations for Primary Toluene Mixtures 249

4 - Comparison of Gravimetrically Calculated and Analyzed Concentrations for Primary Chlorobenzene Mixtures 249

5 - Comparison of Gravimetrically Calculated and Analyzed Concentrations for VCM Mixtures: Modified Vs. Original Preparative Procedures. 250

6 - Comparison of Gravimetrically Calculated and Analyzed Concentrations for Primary VCM Mixtures Prepared by the Successive Dilution Technique and the Microtube Technique . . 251

7 - Multi-Component Mixtures With Total Number of Organic Components and Number of Components Showing Significant (±2% Rel) Deviation Between Calculated and Analyzed Concentrations: Modified Vs. Original Preparative Procedures. . 252

8 - Comparison of Gravimetrically Calculated and Analyzed Concentrations for Low-Concentration (<200 PPB) and High-Capacity Cylinder Mixtures. 259

9 - Calibration of Benzene Permeation Tubes at 25.0°C 262

10 - Comparison of Nominal and Analyzed Concentrations for Toxic Organic SRM's 263

Pellizzari, Hartwell, Leininger, Zelon, Williams, Breen, and Wallace

1 - Geographical Areas and Halocarbons Monitored in Personal and Fixed-Site Air. 265

2 - Number of Samples Obtained by Category for Each Geographical Area 270

3 - Quality Control/Quality Assurance 270

4 - Recovery of Halogenated Chemicals From Control Sampling Cartridges - Greensboro, NC Study 271

5 - Recovery of Halogenated Chemicals From Control Sampling Cartridges - Baton Rouge/Geismar, LA Study. 272

Number | Page

6 - Halocarbon Levels ($\mu g/m^3$) in Air for Greensboro, NC Study: Fixed-Site Vs. Personal Samples 276

7 - Halocarbon Levels ($\mu g/m^3$) in Air for Baton Rouge/Geismar, LA Study: Fixed-Site Vs. Personal Samples. 276

8 - Percent Detection in Ambient Air Samples Matched by Participant - Greensboro, NC Study. 283

9 - Percent Detection in Ambient Air Samples Matched by Participant - Baton Rouge/Geismar, LA Study 284

10 - Significant Spearman Correlations Between Period No. 1 and Period No. 2 Measurements 285

11 - Significant Spearman Correlations for Fixed-Site Vs. Personal Air Samples. 285

Vo-Dinh

1 - Limits of Detection (LOD) for Several PNA Compounds by Room Temperature Phosphorescence. 293

Khan, Meranger, and Lo

1 - Collection Efficiency of Tea-Silica Gel Sorbent for NO_2 . . . 323

2 - Sorbent Tube Breakthrough at High Loadings. 323

3 - Effect of Relative Humidity (RH) on Collection Efficiency at 1.0 PPM Level. 324

4 - Life Tests of Candidate Sampling Pumps. 327

5 - Replicate Testing of Sampling Pumps at 1.0 PPM Level and 75 Percent Relative Humidity (RH) 328

6 - Results of Final Testing. 330

Kosek, Giordano, and LaConti

1 - Transducer Module Features. 341

2 - Typical Response Data, CO Diffusion Dosimeter 349

3 - CO Diffusion Dosimeter Linearity Data 350

4 - Dosimeter Coulometer Data 351

5 - NO Diffusion Dosimeters, Coulometer Data. 356

Number | Page

Forlenza

1 - Instrument Error Due to the Effect of Face Velocity 361

2 - Interference Equivalents for CO Diffusion Sensor. 366

Flanagan and Ryan

1 - Results of $NaNO_2$ Calibration. 371

2 - Palmes Tubes NO_2 Exposure Results Stationary Exposure 373

3 - On-Subject Exposures in Chamber 377

4 - Exposure of Palmes Tubes in CEL Chamber 378

VALIDATION OF EPA REFERENCE METHOD 25--DETERMINATION OF TOTAL GASEOUS NONMETHANE ORGANIC EMISSIONS AS CARBON

Gary B. Howe, Santosh K. Gangwal, and R.K.M. Jayanty

Research Triangle Institute
Research Triangle Park, NC

and

Joseph E. Knoll and M. Rodney Midgett

U.S. Environmental Protection Agency
Research Triangle Park, NC

INTRODUCTION

On October 5, 1979, under Section 111 of the Clean Air Act as amended, the U.S. Environmental Protection Agency (EPA) proposed standards limiting the emissions of volatile organic compounds (VOC) from new, modified, and reconstructed automobile and light-duty surface coating operations within assembly plants (1). The standards were based on the Administrator's determination that such emissions contribute significantly to air pollution by producing ozone and other photochemical oxidants that result in a variety of adverse impacts on health and welfare. The standards included a description of a method known as EPA Reference Method 25 for measuring VOC emissions. This method, adapted from a procedure first introduced by Salo et al. (2) has undergone modifications since that date (3) and is the subject of the present study.

The essential feature of this method is that it allows specific measurement of the carbon contained in all types of VOC emissions, including hydrocarbons and oxygenates. However, when the method was used to analyze identical standard organic test mixtures, a wide range of results was obtained by four different laboratories (4). Another shortcoming (labeled as the "CO_2 interference effect") was observed by researchers at Midwest Research Institute (5), who reported that the presence of high concentrations of CO_2 and water vapor in effluent streams resulted in erroneously high values of organics when measured by Method 25.

The Research Triangle Institute (RTI) undertook a systematic evaluation of Method 25 to identify its deficiencies and implement modifications to eliminate these deficiencies. This paper presents the initial results

in an ongoing investigation of Method 25. Presented here are descriptions of the experimental apparatus, the procedures used, the results obtained for preliminary laboratory and field testing, and further examination of the "CO_2 interference effect."

EXPERIMENTAL

The basic principles of EPA Method 25 are as follows. An emission sample is withdrawn from the source stack through a chilled condensate trap and into an evacuated sample tank. Total gaseous nonmethane organics (TGNMO) are determined by combining the results obtained from independent analyses of the condensate trap and sample tank fractions. The organic contents of the condensate trap are oxidized and quantitatively collected in an evacuated vessel, and a portion of the resulting CO_2 is reduced to methane and measured by a flame ionization detector (FID). A portion of the gas collected in the sample tank is introduced into a gas chromatographic (GC) system to achieve separation of the nonmethane organics from CO, CO_2, and CH_4. After this separation, the nonmethane organics are oxidized to CO_2, reduced to CH_4, and measured by an FID. in this way, variations in FID response to different compounds are eliminated and all carbon is measured as methane.

The basic equipment required for Method 25 consists of a VOC sampling system, a condensate recovery and conditioning system, and a nonmethane organic analyzer (NMOA) capable of separating fixed gases, CO_2, methane, and NMO, and of measuring CO_2 and NMO. For preliminary laboratory evaluation, the equipment assembled was similar to that specified in the Federal Register (3). Two field tests of the method were also conducted, and experiments were performed to examine the "CO_2 interference effect." Brief descriptions of the equipment for each phase of the investigation are given below with special reference to features that represent modifications to Method 25 as described in the Federal Register (3). Unless otherwise specified all parts of the equipment were constructed from 1/8-inch or 1/4-inch, 316 stainless steel tubing or fittings.

Field Sampling Trains

The sampling system (train) used during preliminary laboratory evaluation and the first field test (carried out with the effluent from a textile drying plant) is shown in Figure 1. This train involves two minor modifications from the configuration prescribed in the Federal Register (3). First, a bellows seal shutoff valve was used on the sample tank instead of a quick disconnect/connect fitting, and second, the sample tank used was electropolished on its internal surface to minimize sample degradation.

During the second field test (on the exhaust from a plywood veneer drying plant), it was known "a priori" that the exhaust could contain up to 30 percent water vapor. Thus, in order to avoid plugging of the dry ice trap, an ice water trap was added to the sampling train upstream of the dry ice trap, as shown in Figure 2. Three additional modifications were made --a rotameter was added to the system to facilitate maintenance of a

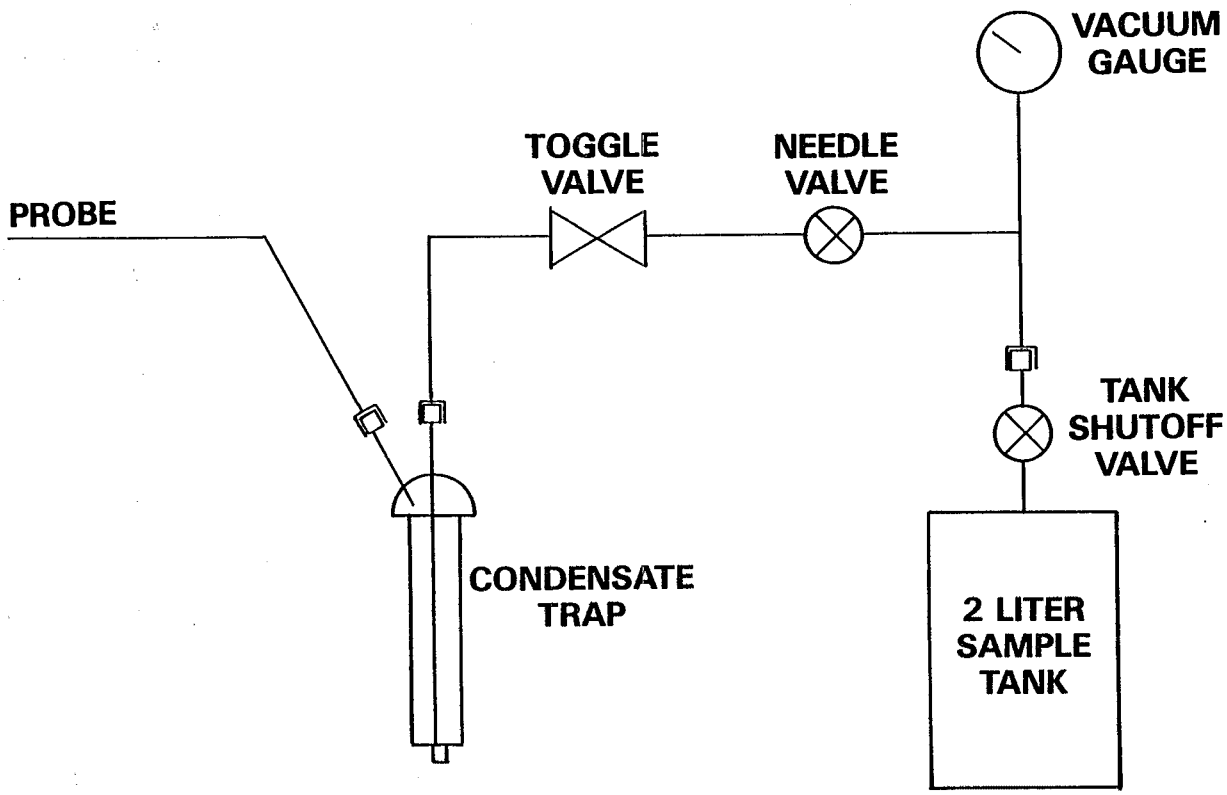

Figure 1. Single trap sampling train.

constant flow rate during sampling; a glass wool filter was added on the probe to prevent particulates from entering the train, and the toggle valve (suspected of leakage during the first field test) was removed from the train. It is to be noted that this toggle valve was near the center of the first sampling train (Figure 1) and was not the same as the one used for sample tank shutoff, which had a screw shut type stem rather than a toggle type stem.

Field Sampling Procedure

The principal objective of the field tests was to determine the precision of Method 25 under actual field conditions. Thus two identical sampling trains (Train A and Train B) were used for each field test, and samples were collected for the same point in the stack with each train. Four sets of duplicate samples were collected during each field test under conditions of sampling shown in Table 1. Pretest and post test procedures, as specified in the Federal Register (3), were carried out for all samples except that the initial and final sample tank pressures were measured for convenience with a Heise compound gauge with 2-mm graduations instead of a mercury manometer, and overall leak check procedures were modified for Runs

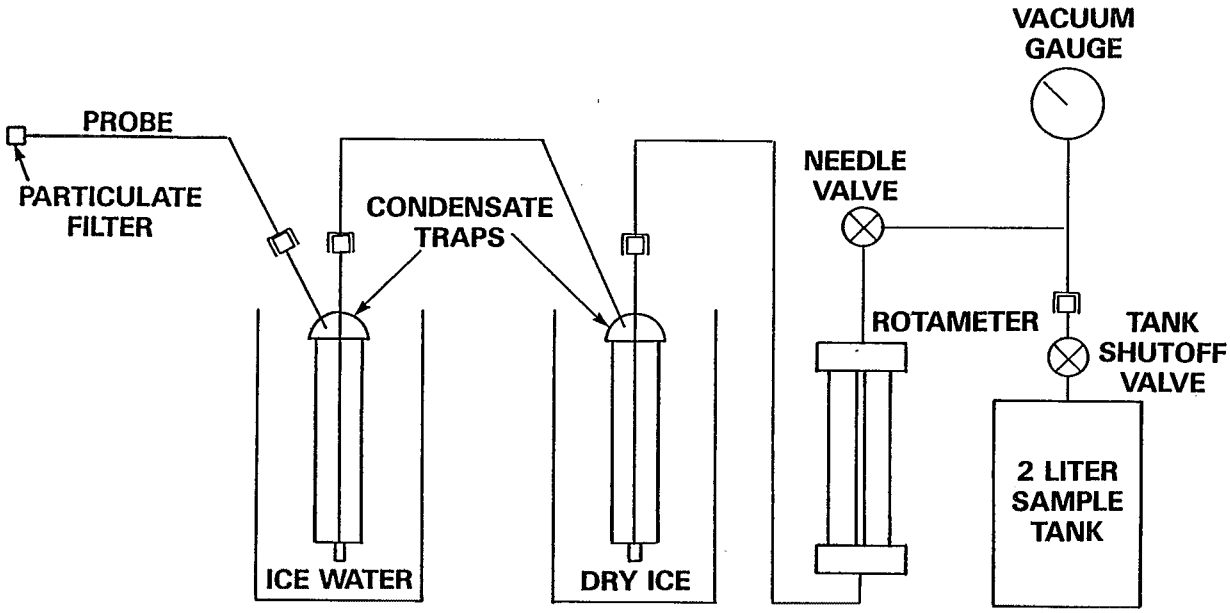

Figure 2. Modified dual trap sampling train.

3 and 4 in the second field test. This is discussed further in the Results and Discussion section. A detailed description of the sampling procedure is available elsewhere (6).

Condensate Recovery and Conditioning System

A schematic of the system for recovering the condensate trap contents by heat desorption and catalytic oxidation is shown in Figure 3. The system is essentially similar to the one specified in the Federal Register (3) except for two modifications. Again, a Heise compound gauge (with 2-mm graduations) was used to measure pressures instead of a mercury manometer and, instead of two four-port valves for diverting gas flow to the oxidation catalyst or to vent, one six-port Valco zero volume valve was used. A detailed description of the system is available elsewhere (6).

Nonmethane Organic Analyzer

Model 401, manufactured by Byron Instruments, Inc., Raleigh, NC, was used as the NMOA for this study. Although descriptions of previous models of this instrument have been published (7,8), it has recently been modified and its present configuration is shown in Figure 4. The instrument is capable of measuring total organic carbon, CH_4, nonmethane organics (NMO), and CO_2 semicontinuously every 12 minutes. Only the measurement of CO_2 and

TABLE 1. FIELD TEST SAMPLING CONDITIONS

	Sample number	Trap(s) type	Sample train A Flow rate (mL/min)	Sample train A Sampling time (min)	Sample train B Flow rate (mL/min)	Sample train B Sampling time (min)
Field test 1	1	D*	35	30	51	30
Textile	2	D	38	20	48	20
Dryer	3	D	54	20	54	20
Plant	4	AIBD†	46	20	50	20
Single trap sampling						
Field test 2	1	ID‡	25	20	25	20
Veneer	2	ID	25	20	25	20
Dryer	3	ID	25	30	25	30
Plant	4	ID	20	30	40	30
Dual trap sampling						

*D = Dry ice.
†AIBD = Ice water for sample train A, dry ice for sample train B.
‡ID = Dual trap system; ice water and dry ice traps in series.

NMO are required for Method 25.

Field Sample Analysis Procedure

All field samples were analyzed according to the procedure described in the Federal Register (3), except for the changes made below. Instead of a separate intermediate collection tank for the condensed organics from the dry ice and ice water traps, the matched sample tank itself was used as the intermediate collection tank after undergoing NMO analysis and evacuation. This repesented a significant improvement of the method since the necessity of measuring tank volumes was eliminated (a time-consuming and error-prone task), because the intermediate collection tank volume and the sample tank volume cancelled out in the calculations (6).

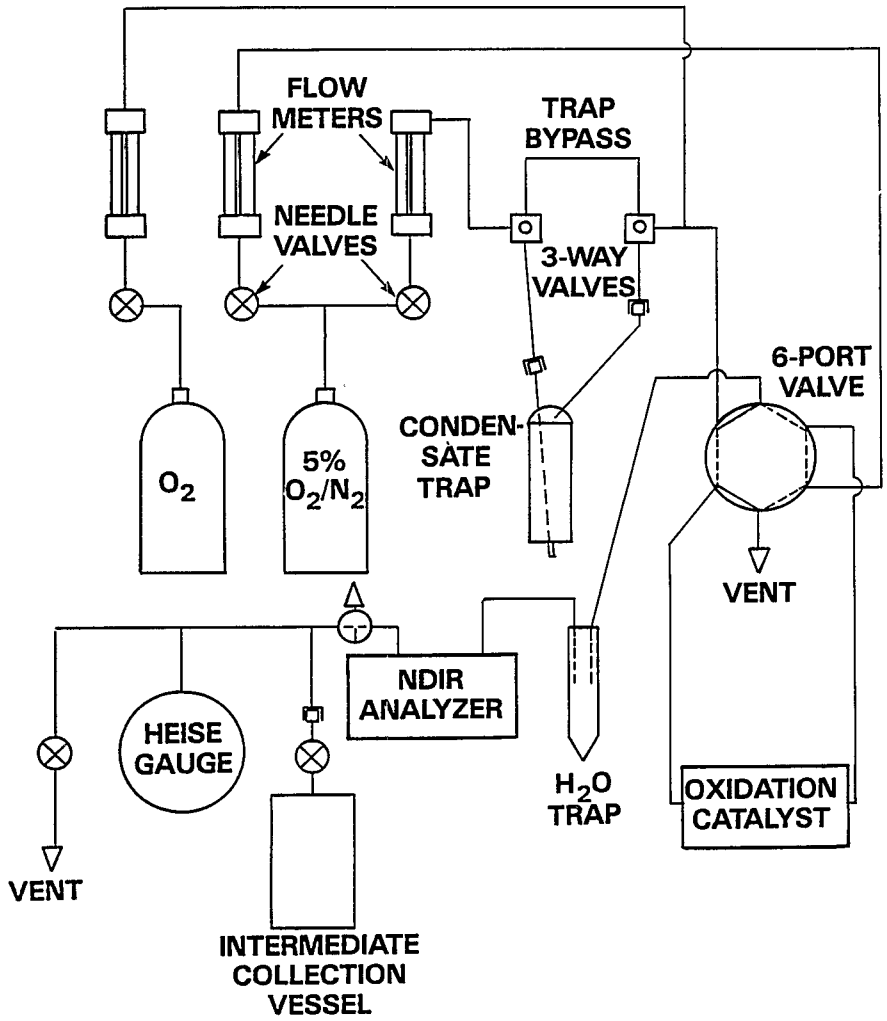

Figure 3. Condensate recovery and conditioning system.

The gas used to bake out the trap consisted of 30 cm^3/min, 5 percent O_2 in N added to 35 cm^3/min pure oxygen for samples from the first field test. Due to low flow and high oxygen content, slight carbonization of the sample was suspected. Thus for samples from the second field test, dilution and total flow were increased with the bake-out gas now consisting of 85 cm^3/min, 5 percent O_2 in N_2 and 15 cm^3/min pure oxygen. A detailed description of the analytical procedure is available elsewhere (6).

CO_2 Interference Effect Study--Apparatus and Procedure

As stated in the introduction, erroneously high values of NMO resulted when Method 25 was used for samples containing a large percent of water vapor and CO_2. Two possible reasons for this are dissolution of CO_2 in the water condensate of the ice water trap or entrapment of CO_2 in the ice condensate of the dry ice trap. The dissolved or trapped CO_2 is unlikely

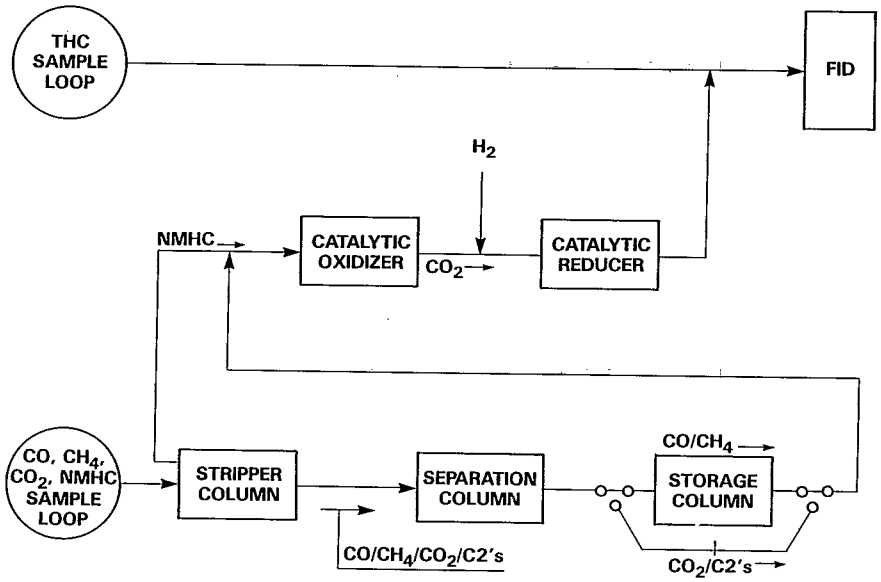

Figure 4. Byron Model 401 NMOA schematic.

to be fully released during the condensate recovery CO_2 purge (since the trap is maintained in ice water or dry ice during this purge to prevent organics from escaping) and would end up being reported as NMO following bake out and measurement.

Further examination of this effect was attempted in this study using the experimental set up shown in Figure 5. An 11.6 percent CO_2 in N_2 standard bottle was used as the CO_2 source, since this concentration approximately represents the CO_2 content of some power plant stacks. Water was pumped by a syringe pump into a heated manifold (120° C), where it was mixed with the CO_2 containing gas. Samples were collected from the manifold at 50 cm^3/min through both the single and the dual trap sampling trains (the evacuated sample tank was replaced with a vacuum pump for both trains) for a series of water vapor concentrations ranging from 0 to 25 percent. Further details of these experiments are presented in the Results and Discussion section.

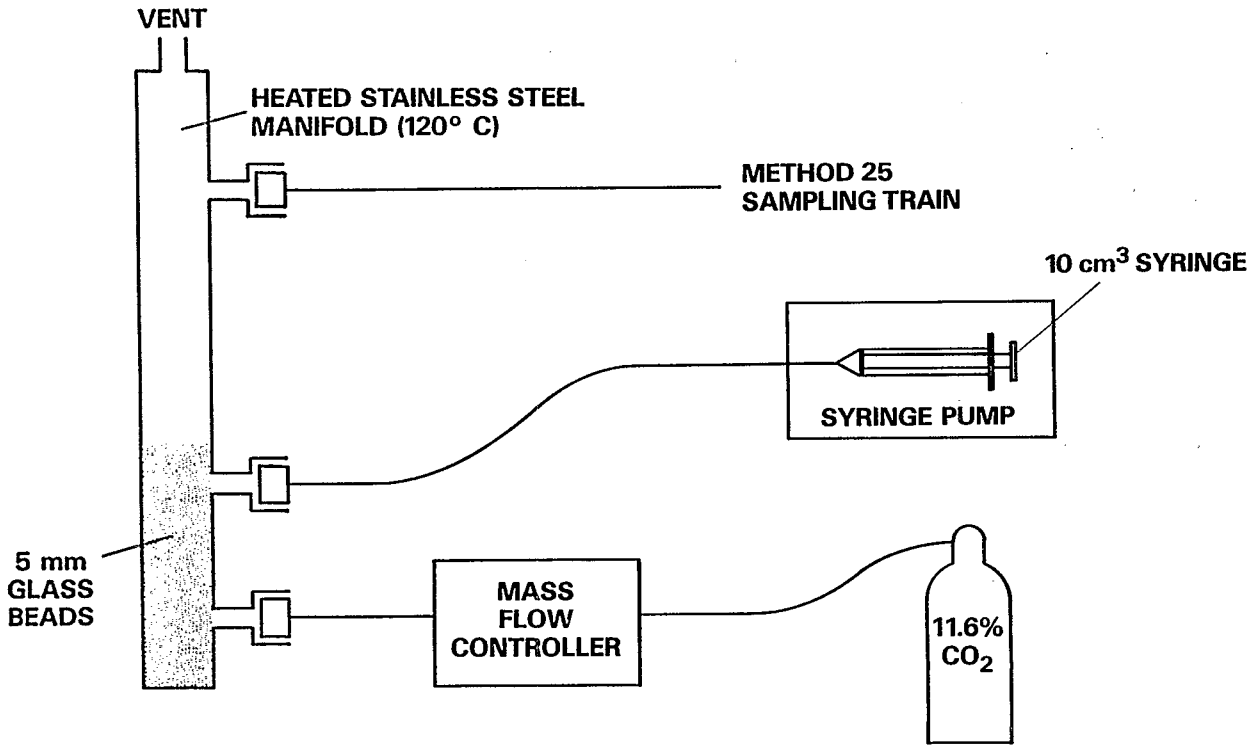

Figure 5. Experimental setup for CO_2 interference effect study.

RESULTS AND DISCUSSION

A preliminary evaluation of the equipment used was completed according to specifications of the Federal Register (3). A detailed description of the preliminary evaluation is available (6). In the interest of brevity, only the highlights are reported here, followed by the results from the field tests and the CO_2 interference effect study.

Preliminary Evaluation

The linearity and compound dependence of the NMOA response were measured for a variety of gases and organic vapors. The instrument showed excellent linearity for several compounds subjected to the linearity study over wide concentration ranges, as shown in Table 2. The compound dependence results are shown in Figure 6. The response variability to different organics is expected to result in inaccuracies for measurement of the volatile portion of the sample, which is not captured by the condensate trap and ends up in the sample tank. The variability of response, however, should have no effect on the precision of results from samples collected via the dual sampling train if all other parts of the sampling and analysis

system are performing properly.

TABLE 2. NMO ANALYZER LINEARITY STUDY RESULTS

Compound	Concentration range	Correlation coefficient*
Propane	59.7 - 9,150	0.999
Benzene	49.2 - 2,090	0.999
Ethylene	9.5 - 40,912	0.999
Propylene	14.8 - 2,050	0.999
Methyl acetate	52.5 - 1,350	0.999
Ethane	590.0 - 1,430	0.962
CO_2	57.3 - 10,000	0.999

*Based on linear least squares fit.

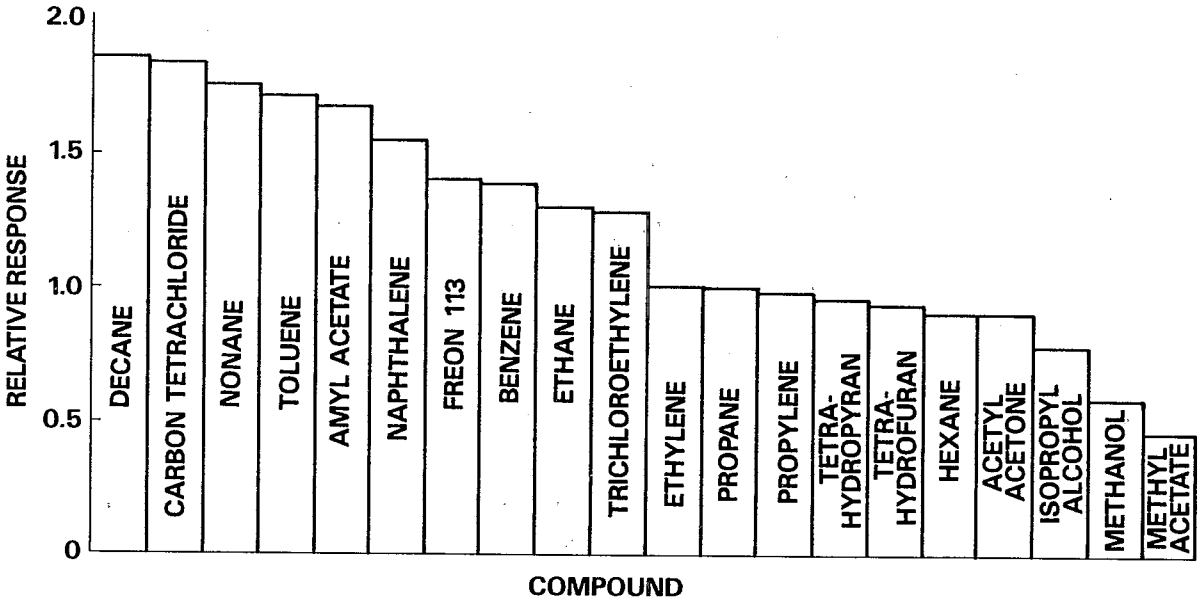

Figure 6. Relative responses of the NMOA for several organic compounds.

The observed response variability could be due to the differences in the oxidation efficiency of the oxidation catalyst of the NMOA for different organics. This was investigated further using a propane (59.7 ppmC) and a toluene (128 ppmC) standard. An oxidation catalyst identical in design to the one used internally in the NMOA was used externally to oxidize the standard propane and toluene gases. Each gas was flowed through the catalyst at 150 cm^3/min into a sampling manifold from which samples were drawn into NMOA for analysis. Both CO and CO_2 resulted from the oxidation, and residual nonmethane organics were also observed to break through the catalyst with either propane or toluene. The most significant difference in the oxidation products was an 18 percent difference in the CO_2 formed per ppmC of organic. Although the higher production of CO_2 from toluene as opposed to propane correlated with its higher response (Figure 6), it was hardly enough to account for the actual response difference that existed between the two gases. Furthermore, since the actual continuous flow conditions of the experiments were not representative of the pulse flow conditions within the NMOA, no definitive conclusions could be drawn from these experiments. Further studies are needed to pinpoint the reasons for the response variability of the NMOA. However, as pointed out earlier, the response differences affect the accuracies but should not affect the precision. For example, evaluation of the field sampling trains in the laboratory showed a 99 percent recovery and a relative standard deviation of 0.08 percent in repetitive sampling of a 603 ppmC propane standard.

The condensate recovery and conditioning system was evaluated by making liquid injections of hexane and toluene at its gas inlet via a heated injection port. These recoveries are shown in Table 3 and were acceptable for the 9 μL injections. For the 100 μL injections, the recoveries were still better than 80 percent. The lower recovery is probably due to a combination of factors, including incomplete recovery and the slight nonlinearity of the NMOA for the high CO_2 concentrations generated (3.2 percent using n-hexane and 4.5 percent using toluene).

TABLE 3. CONDENSATE RECOVERY SYSTEM PERFORMANCE CHECK RESULTS

Compound	Injections (μL)	Percent recovery
n-Hexane	100.0	82.8
n-Hexane	9.0	96.4
Toluene	100.0	81.1
Toluene	9.0	94.0

Field Test Results

The conditions for field sampling were shown earlier in Table 1. The flow rate values shown for the first field test are actually average estimates calculated from the sample tank initial and final pressure, and the tank volume since a rotameter for visual observation and control of the flow rate was not used (Figure 1). For the second field test, however, the flow rates were calibrated on a rotameter (Figure 2). The results from the first field test are shown in Table 4 along with standard deviations for dual train sampling of each run.

TABLE 4. TEXTILE PLANT FIELD TEST RESULTS

Run number	Sample train	Noncondensable organics (ppmC)	Condensable organics (ppmC)	Total (ppmC)	Relative standard deviation* (percent)
1	A	8.7	627	636	45
	B	7.7	320	328	
2	A	<3.0	244	244	15
	B	3.5	193	196	
3	A	4.3	642	646	40
	B	<3.8	360	360	
4	A	160.0	579	738	2
	B	55.6	703	759	

*Relative standard deviation = $\frac{100}{\bar{x}}\sqrt{\Sigma(x-\bar{x})^2/(n-1)}$.
x = Total ppmC.
$\bar{x}$ = Mean for each run.
n = 2.

Another way to look at the precision of the data is on the basis of a pooled relative standard deviation, S_P, shown in Equation (1)

$$S_P = 100\sqrt{\Sigma d^2/2n}\ /\bar{x} \qquad (1)$$

where d is the difference between the paired values, n is the number of runs (=4), and $\bar{x}$ is the overall mean value. The pooled relative standard

deviation for the four runs in Table 4 is 31 percent. Two factors probably contributed most to this imprecision. First, it was discovered during the third run that the toggle valve was leaking. This would normally not be discovered during the leak check procedure, because the probe end is plugged. However, in the process of properly inserting the dual probes in the stack, leakage would be allowed into the train. Another factor that was even more critical was that constant flow rate over the entire duration of the run could not be maintained because of an increase in the sample tank pressures during the run. The effect of this would be higher when the stack concentration is highly variable, as seen in Table 4. Run 4 gave good precision after the toggle valve problem was corrected. It is to be further noted that an ice water trap and a dry ice trap were used during Run 4 for sample Trains A and B, respectively (Table 1). This did not result in a reduced precision for the total ppmC value, although obviously the ice water trap allowed more organics to end up in the sample tank as noncondensables.

The problems observed during the first field test were corrected for the second field test, which was carried out using a plywood veneer dryer plant exhaust. Also, as noted in the Experimental section, due to the high water vapor concentrations of this exhaust, an ice water trap and a dry ice trap in series were used to prevent plugging (Figure 2 and Table 1).

Again, four runs with dual samples were carried out, but this time the Federal Register (3) leak test specifications were not precisely adhered to for Runs 3 and 4. The Federal Register specifies a pretest as well as a post test leak check for the entire sampling train under sample tank vacuum. Thus air contained in the sampling train is allowed to enter the sample tank during the pretest leak check with the probe end plugged. The plug has to be removed following the leak check before sampling can begin. Air thereby enters the train a second time and is again drawn into the sample tank during sampling. Thus two complete dead volumes effectively enter the tank before sampling. During the post test leak check, the train supposedly contains the last stationary portion of the sample. This should not affect the precision as long as the mixing with ambient air of this stationary sample is identical for both trains during the time taken to remove the probes and plug them for the post test leak check.

The leak checks are not representative of the actual conditions existing during sampling since only a small portion of the train from the needle valve exit to the sample tank (Figure 2) is under the influence of the high tank vacuum, the rest of the train being at close to ambient pressures. In order to evaluate the effect of leak checks, the leak check procedures were modified and varied, as shown in Table 5, for Runs 3 and 4. A correction was applied to the total measured ppmC NMO on the basis of the measured dead volume of the sample train ($\sim$86 cm^3). The actual sampled volume was thus reduced by 86 x 2 = 172 cm^3 (which represents the dead volume effect of the pretest leak check) for Runs 1 through 3. The actual sampled volume was reduced by 86 cm^3 only for Run 4, where a pretest leak check was not performed on the entire train. (This would then result in only one dead volume entering the train, as discussed previously.) The corrected total NMOC was then calculated by dividing the measured NMOC with the ratio

of the corrected volume to the uncorrected volume.

TABLE 5. EFFECT OF LEAK CHECK SCHEME ON THE TOTAL MEASURED PPMC FOR THE PLYWOOD VENEER DRYER FIELD TEST SAMPLES

Run number	Leak check scheme	Sample train	Uncorrected values V_s^* (cm^3)	Uncorrected values Total (ppmC)	Corrected values V_s^* (cm^3)	Corrected values Total (ppmC)
1	†	A	672	4,820	500	6,470
		B	672	3,900	500	5,230
2	†	A	672	3,490	500	4,680
		B	672	3,860	500	5,190
3	‡	A	836	4,920	664	6,200
		B	836	4,710	664	5,920
4	§	A	600	5,550	514	6,480
		B	1,200	6,200	1,110	6,670

*V_s = Volume sampled.
† = Pretest and posttest leak checks of entire train.
‡ = Pretest leak check of entire train, posttest leak checkup to needle valve.
§ = Pretest and posttest leak checkup to needle valve.

The dead volume correction would result in the same factor for Trains A and B for Runs 1 through 3, where equal volumes were sampled into the train. Different factors would result when different volumes are sampled as for Run 4. Improvement in precision of the results from the modified leak check procedure is reflected in the standard deviation for Run 4 in Table 6, where data are also presented for the portion of the NMOC partitioned into the sample tank, the dry ice trap, and the ice water trap. Notice that the precision of the data is improved considerably for Run 4 after the leak check correction is applied (without the correction, the relative standard deviation is 7.8 percent, as opposed to 2.0 percent with the correction). Also, the method is seen to be rugged enough that a flow rate variation of a factor of 2 between the two trains in Run 4 caused little effect on the precision of the data. Furthermore, as expected, at a higher flow rate, a larger carryover of the organics into the dry ice trap is observed for Run 4.

The dead volume would have a stronger influence on the accuracy of the results for smaller volumes as collected in this study. The Federal Register (3) specifies a 4 to 6-liter sample tank as opposed to the 2-liter

TABLE 6. VENEER DRYER PLANT CORRECTED FIELD TEST RESULTS

Run number	Sample train	Noncondensable organics (ppmC)	Condensable organics (ppmC) Ice water trap	Condensable organics (ppmC) Dry ice trap	Total (ppmC)	Relative standard deviation*
1	A	352	2,370	3,750	6,470	15.0
	B	612	1,300	3,320	5,230	
2	A	151	842	3,690	4,680	7.3
	B	444	1,020	3,730	5,190	
3	A	887	1,160	4,150	6,200	3.3
	B	677	1,030	4,210	5,920	
4	A	808	1,170	4,500	6,480	2.0
	B	529	894	5,250	6,670	

*Relative standard deviation = $\frac{100}{\bar{x}}\sqrt{\Sigma(x-\bar{x})^2/(n-1)}$.
x = Total ppmC.
$\bar{x}$ = Mean for each run.
n = 2.

sample tank used here for convenience. Assuming a 2 to 3-liter sample is actually collected in practice using Method 25 procedures, the dead volume error would be approximately 6 to 8 percent with a dual trap system (∿172 cm^3 dead volume), and 3 to 4 percent with a single trap system (∿86 cm^3 dead volume).

The pooled standard deviation calculated as before by Equation (1) for the data in Table 6 was found to be 8.3 percent, as opposed to 31 percent calculated for the first field test. This is evidence that the modified procedures (including precise flow control with a rotameter, modified sampling train, the dead volume correction, and the modified leak check procedure) resulted in significant improvement of the precision of the method.

CO_2 Interference Effect

Trap samples were collected using the experimental setup described earlier (Figure 5) with both the single dry ice trap system and the dual ice water and dry ice trap system. These traps were then subjected to the Method 25 procedure to determine the amount of CO_2 that would end up being measured as NMO because of incomplete recovery of the trapped or dissolved CO_2 during the CO_2 purge. These results are shown in Table 7. The CO_2

TABLE 7. EFFECT OF SAMPLING TRAIN CONFIGURATION ON CO_2 INTERFERENCE

Mole percent water vapor	Single dry ice trap sampling		Dual dry ice and ice water trap sampling			
				CO_2 interference*		
	Sampling time (min)	CO_2 interference* (ppmC)	Sampling time (min)	Ice water trap (ppmC)	Dry ice trap (ppmC)	Total (ppmC)
10	60	20.5	60	1.4	0.0	1.4
15	46	17.6	60	30.4	8.0	38.4
20	34	49.3	60	26.9	2.0	28.9
25	23	16.3	60	22.6	∿0.0	22.6

*Corrected for background.
NOTE: Sampling rate = 50 cm^3/min dry basis; sample gas 11.6% CO_2 in N_2 dry basis.

interference ranges from 16 to 50 ppmC for single trap sampling and 1 to 39 ppm for dual trap sampling. These values do not represent a significant interference in sampling sources containing several hundred ppmC or higher concentrations of NMO. However, they would be significant in sampling sources containing NMO concentrations of a few hundred ppmC or lower. The extent of CO_2 interference appears to peak out and then decrease as the water vapor concentration is increased with the dry gas concentration fixed. Although no explanation can be offered for this behavior, it is presently being further investigated. A mathematical simulation of the CO_2 condensation phenomena using transient mass balances and Henry's law is being attempted to predict the amount of CO_2 that will be trapped. The simulation is complicated by the fact that, during the CO_2 purge for Method 25 analysis, portions of the trapped CO_2 could be released and carried out with the inert purge.

The most significant conclusion that can be drawn from Table 7 is the clear superiority of using a dual trap sampling train as opposed to a single dry ice trap sampling train in the sampling of high CO_2 and water vapor-containing samples. It is to be noted that a forced shutdown of sampling resulted each time with the single trap system because of plugging. The dry gas volume that caused plugging is shown as a function of the water vapor content of the sample gas in Figure 7. No plugging was observed for the dual trap system even after sampling for 60 minutes at 50 cm^3/min dry gas with 25 percent water vapor concentration. Also, even though the water admitted into the dual trap system at 20 percent water vapor concentration was almost twice as much as the single trap system, the measured CO_2 interference was less than three fifths.

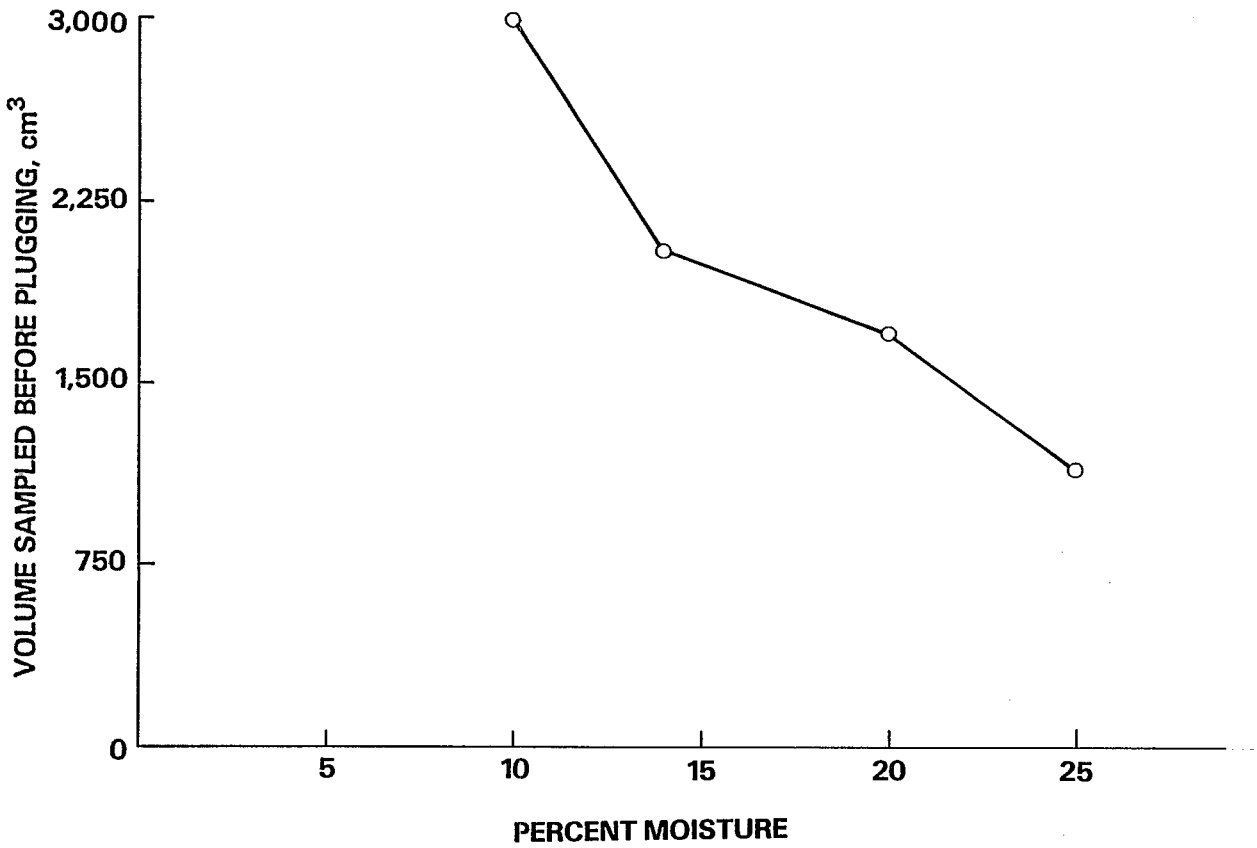

Figure 7. Dry gas volume sampled before plugging versus water vapor content.

Most of the CO_2 interference for dual trap sampling ends up in the ice water trap, which is expected to trap the water as a liquid rather than as a solid. This may be one explanation of the superiority of the dual trap system, because it is probably easier to strip the CO_2 out of liquid water during the purge than it is to purge it out while it is trapped in ice formed within the dry ice trap. Further research into the "CO_2 inteference effect" is continuing.

CONCLUSIONS AND RECOMMENDATIONS

With careful experimentation, good precision can be obtained for source measurement of NMO using Method 25. The accuracy of the results obtained, on the other hand, depends on such additional factors as dead volume of the sampling train and the relative response of the NMOA to different organics. Several modifications were made to the procedures specified in the Federal Register (3), and these modifications in combination were shown to improve the overall precision of the method. The best

relative standard deviation obtained was 2.0 percent for field sampling and 0.08 percent for laboratory sampling.

The "CO_2 interference effect" appears to be minimal when sampling stacks containing several hundred ppmc of NMO, but it is necessary to use a dual trap sampling system to prevent plugging during the sampling of stacks containing high concentrations of water vapor.

Additional studies are required to make theoretical predictions of the CO_2 interference effect, for the design of an NMOA that would produce nearly equal responses to all organics and on the behavior of thermally labile compounds during condensate trap bake out. Further studies are ongoing at RTI on various aspects of Method 25 with a view to improving its accuracy.

ACKNOWLEDGMENTS

This work at the Research Triangle Institute was supported by U.S. EPA Contract No. 68-02-3431.

REFERENCES

1. Federal Register 44:57792-57822 (1979).

2. Salo, A.E., W.L. Oaks, and R.D. MacPhee. 1975. Measuring the organic carbon content of source emission for air pollution control. JAPCA 25:390.

3. Federal Register 45:65956-65973 (1980).

4. Midwest Research Institute. 1981. Evaluation of Method 25 for air oxidation processes--volume I. EPA Contract No. 68-02-2814, Assignment 36. Emission Measurement Branch, U.S. Environmental Protection Agency, Research Triangle Park, NC.

5. Midwest Research Institute. 1981. Investigation of carbon dioxide interference with Method 25. EPA Contract No. 68-02-2814, Assignment 41. Emission Measurement Branch, U.S Environmental Protection Agency, Research Triangle Park, NC.

6. Howe, G.B., S.K. Gangwal, and R.K.M. Jayanty. 1982. Validation and improvement of EPA Method 25--Determination of gaseous nonmethane organic emissions as carbon: manual sampling and analysis procedure--Draft report. EPA Contract No. 68-02-2341.

7. Hilborn, J.C., and N. Quickers. 1975. Evaluation of the Byron Model 233A air quality analyzer. Chemical Instrumentation 6:75.

8. Scott Environmental Technology, Inc. 1978. Evaluation of the Byron Model 401 Hydrocarbon Analyzer. EPA Contract No. 68-02-2813. Emis-

sion Measurement Branch, U.S. Environmental Protection Agency, Research Triangle Park, NC.

EVALUATION OF 2-PROPANOL AS A LIQUID ABSORBENT FOR HAZARDOUS POLLUTANTS IN STATIONARY SOURCE GAS STREAMS

Craig M. Young and Larry E. Trejo

Energy Incorporated
Idaho Falls, ID

INTRODUCTION

General Description

Energy Incorporated is an engineering firm working in the area of fluidized bed combustion systems and, with its manufacturing subsidiary, Energy Products of Idaho, has 40 commercial fluidized bed systems currently in operation. Energy Incorporated (EI) has recently devoted its pilot plant facility to the investigation of the destruction of hazardous wastes. Most studies have been conducted with carbon tetrachloride (CCl_4) and 1,2-dichlorobenzene (DCB) as representatives of chlorinated wastes.

EI needed a method for analyzing off-gas samples from the pilot plant tests that was simple, reliable, and would give rapid turnaround on sample analyses. For these reasons, liquid absorption systems were investigated. From the work done in this study, it was concluded that 2-propanol was an acceptable liquid absorber.

Background

Both liquid and solid absorbers have been used for sampling off-gas streams. Xylene has been used by Continental Can as a liquid absorber for PCBs in combustion gas in boilers fueled with PCB contaminated oil (1). Ferguson and others used a sampling train with a glass probe and three midget impingers to sample for pesticides in the combustion gases from the burning of pesticides. They used benzene, isooctane, 2-propanol, or water as the liquid absorber, depending on the pesticide under study (2). Ethylene glycol was used to sample for DDT and PCBs at General Electric's Pittsfield, Massachusetts, liquid injection incinerator (3). Guilford and Brandon (4) also used ethylene glycol to sample for PCBs in a pilot plant incinerator. They were able to achieve an overall absorption efficiency of 99.64 percent with two impingers. Guilford and Rosenblatt (5) reported a 97.7 percent efficiency with ethylene glycol when sampling for PCBs in combustion gases. Komaniya and Morisaki (6) reported using a three-impinger system to sample for PCBs. Water was contained in the

first impinger, followed by hexane in the other two impingers. Shoemaker (7) has reported the use of a solution of 5 mg/ml aniline in isooctane to sample for bis(cyclohexyl isocyanate) in ambient air.

Probably the most widely accepted method at present for sampling for organics in off-gas streams is the use of solid absorbers in a modified EPA Method 5 sampling train. Several different solid absorbers have been used. Ackerman (8) reported using XAD-2 for absorbing PCBs in a water-cooled sorbent trap. The gas sampled was the combustion gas from a rotary kiln incinerator fed with PCB contaminated capacitors. MacDonald and others (9) reported using a modified Method 5 sampling train with Chromosorb 102 as the solid absorber for sampling the off-gas of a cement kiln burning PCBs. Haile and Baladi (10) evaluated Florisil, XAD-2, and Tenax-GC as solid sorbents for sampling off-gas streams for organics. They determined their optimum configuration to be two impingers containing water, an empty impinger, the solid sorbent, an impinger containing 10 percent sodium hydroxide, and finally, an impinger containing silica gel. The U.S.EPA has recommended in their interim sampling and analysis manual to use Florisil for sampling for PCBs and XAD-2 for other chlorinated organics and general organics (11). Bombaugh and Lee (12) used Tenax GC cartridges when sampling ambient air around synfuel plants. The Source Assessment Sampling System has been developed to sample for organics in gas streams. This system uses cartridges of Florisil, XAD-2, or Tenax GC (13,14).

SYSTEMS STUDIES

Testing Equipment

Energy Incorporated carried out its hazardous waste destruction testing in two stages. The first stage was bench-scale studies in an apparatus shown schematically in Figure 1. For the CCl_4 studies, the water vapor source was a steam generator. In the DCB studies, the water vapor was supplied by bubbling air through heated water. The organic vapor generator, in both cases, was a three-neck flask that was held at a constant temperature and air bubbled through the liquid. The packed bed varied from inert particles to catalytic particles. The number of impingers and their contents were varied according to the goals of the test being run.

The second testing facility, a fluidized bed pilot plant, is shown schematically in Figure 2. Sampling of the gas stream was carried out before and after the spray tower assembly.

Liquid Absorbers Studied

To assure a timely pilot plant development, it would be necessary to analyze the off-gas stream several times per day, since combustion conditions were varied in an effort to optimize destruction conditions. Therefore, a large number of samples would need to be analyzed in a short time to supply the data necessary to set conditions for subsequent pilot plant runs. This restriction eliminated the use of solid absorbers, with their extensive clean-up requirements.

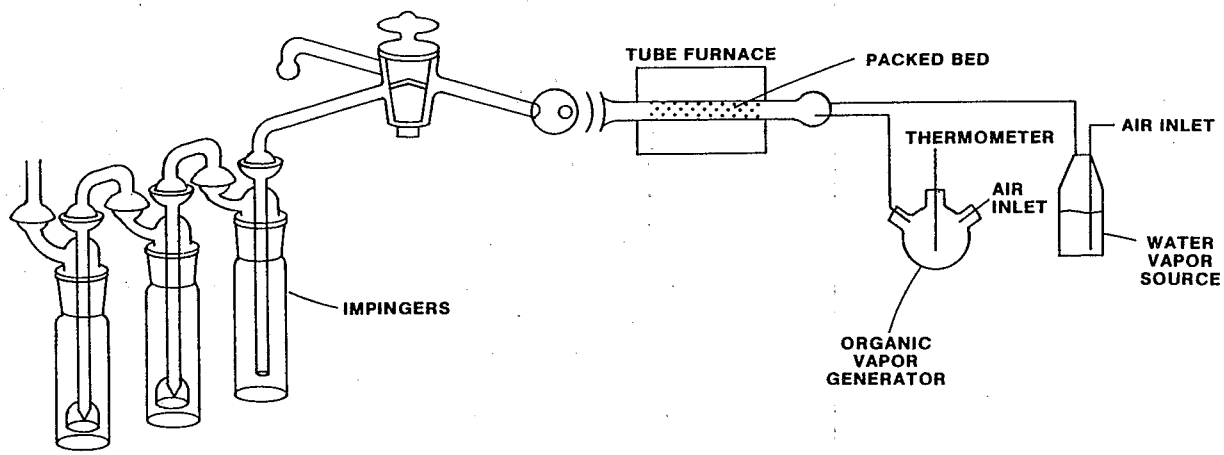

Figure 1. Bench-scale test system.

The use of liquid absorbers was also limited to solvents that are soluble in water. Water vapor would be present in the off-gas from the pilot plant facility and also in the gas stream of the bench-scale assembly. When the destruction of CCl_4 was studied, steam would be injected directly into the system. These large amounts of water would form emulsions or two phases unless a waste-soluble solvent was used. These emulsions or two-phase systems would interfere with the direct analyses of the impinger solution. Direct analysis of the impinger solutions was the major objective of the sampling studies.

After these evaluations, ethylene glycol was chosen for use in the impingers. Figure 1 shows a schematic drawing of the bench-scale apparatus that was used in the first studies with CCl_4 destruction. The first impinger was filled with a sodium hydroxide solution and the next two were filled with ethylene glycol. No CCl_4 was found in the three impingers. The CCl_4 was found in the knock-out flask ahead of the vacuum pump. The first test proved ethylene glycol to be an unsatisfactory absorber for carbon tetrachloride.

At this point, other alcohols were considered. Methanol proved to be too volatile, and it is also toxic. Ethanol, butanol, and higher alcohols were too expensive and were not readily available. 2-propanol was found to be inexpensive and readily available in a pure form. Amyl acetate was also tested, but its low solubility for water and unpleasant odor resulted in its removal from consideration.

Absorption of CCl_4

The test results obtained from the bench-scale studies with carbon tetrachloride showed a chloride closure of 96 percent on the material balance. This was obtained by analysis of the chloride in the first

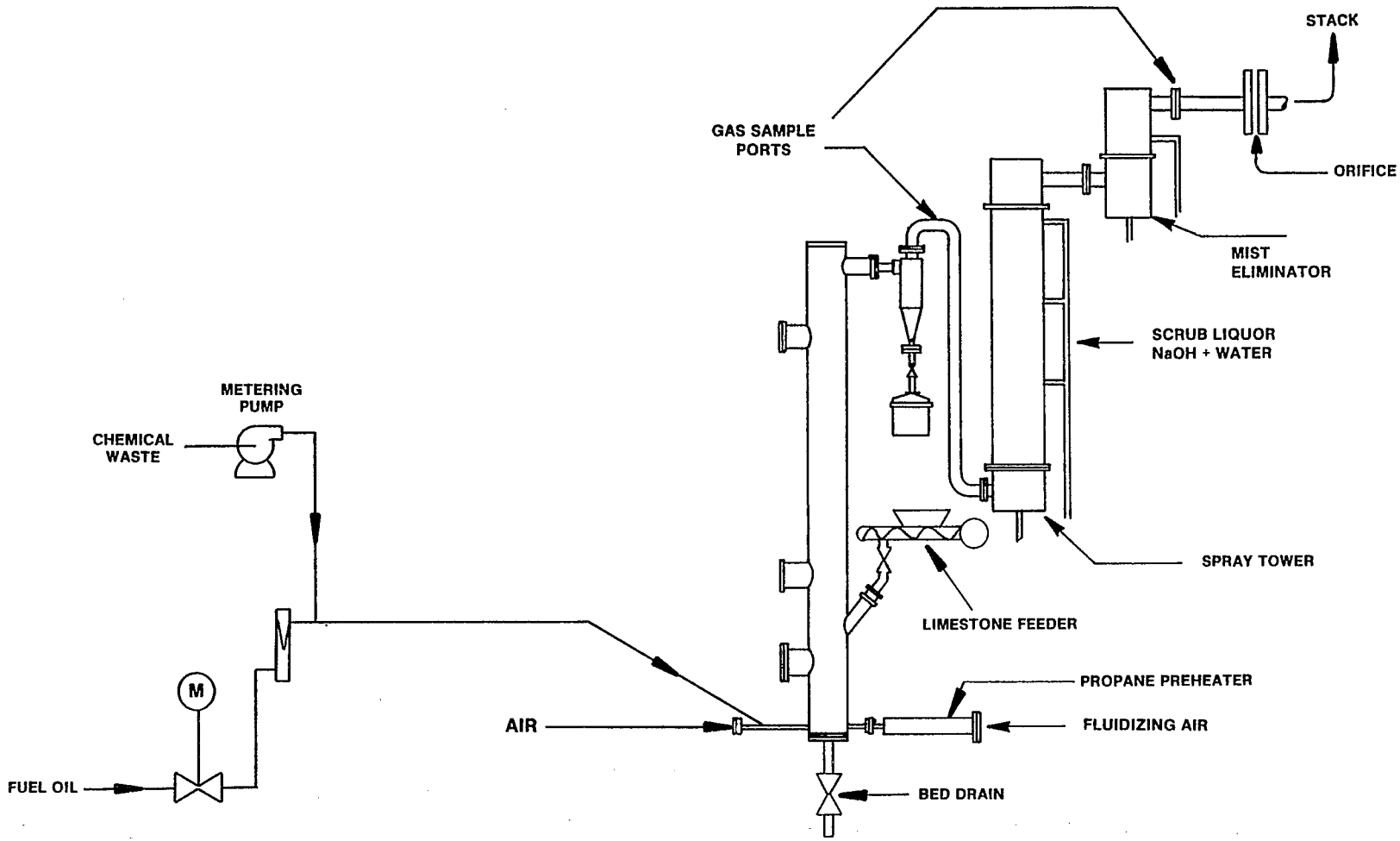

Figure 2. Eight-inch pilot plant incinerator.

impinger and the CCl_4 concentration in the final impingers.

When the tests were conducted in the pilot plant facilities, as shown in Figure 2, three impingers in an ice-water bath were used to sample for CCl_4. The samples were pulled from the off-gas duct through a sample port located ahead of the spray tower. When the impingers were analyzed for CCl_4, 29.3 percent of the CCl_4 recovered was in the first impinger, 46.8 percent was in the second impinger, and 23.9 percent was in the third impinger. The high concentration of CCl_4 in the third impinger led to the conclusion that all of the CCl_4 was not trapped.

The next experimental run used four impingers, with the first impinger cooled in a dry ice/acetone bath. The remaining impingers were cooled in an ice-water bath. The analysis of these impingers showed: 67.2 percent trapped in the first impinger, 23.3 percent trapped in the second impinger, 7.3 percent trapped in the third impinger, and 2.2 percent trapped in the fourth impinger. The CCl_4 concentration decreased by a factor of three in each impinger; it was projected that more than 99 percent of the CCl_4 was being collected in the off-gas. These numbers were the average of three sets of off-gas samples. This test was run at a low temperature to minimize destruction of CCl_4. The off-gas samples accounted for 94 percent of the CCl_4 fed into the system.

Absorption of DCB

When the bench-scale tests were run on DCB, the air was blown through the system and not pulled with a vacuum pump. The second change was that saturated water vapor was used instead of steam. The tube furnace was run at a low temperature as an attempt at recovering all the DCB in the impingers. Four impingers were used, and they were all cooled in an ice-water bath. This resulted in an average of 97 percent of the DCB being recovered. Of the DCB recovered, 98.8 percent was in the first impinger, 1.2 percent in the second impinger, and no DCB was found in the third or fourth impingers.

The pilot plant off-gas samples for DCB were taken by using three impingers cooled in an ice-water bath. The first two impingers contained 2-propanol. The third impinger contained a sodium hydroxide solution to prevent any HCl from going through to the vacuum pump. The recovery of DCB was 92 percent in the first impinger and 8 percent in the second impinger.

Absorption of HCl

The absorption of HCl by 2-propanol was studied along with the destruction of DCB on the bench-scale experiments. The recovery of HCl in the impingers was 97.5 percent in the first impinger, 2.3 percent in the second impinger, and 0.2 percent in the third impinger.

The DCB off-gas samples from the pilot plant were also analyzed for HCl. The recovery of HCl in these samples was 98.3 percent in the first impinger, 1.7 percent in the second impinger, and <0.1 percent in the third impinger.

Absorption of Phenols

Two pilot plant runs were made with mixed phenol feed. The mixture was 50 percent phenol, 25 percent pentachlorophenol, and 25 percent fuel oil. There were very small amounts of phenol and pentachlorophenol collected in the impingers. Therefore, a phenol mixture was run in the bench-scale apparatus to determine the collection efficiency for these phenols. Approximately 0.1 gram of each compound was placed in a combustion boat and placed in the tube ahead of the packed bed. Three impingers containing 2-propanol and one containing sodium hydroxide were used to collect the samples.

The compounds used were phenol, pentachlorophenol (PCP), and 0-,0'-diphenol. It was found that 100 percent of the phenol was trapped in the first impinger, and no phenol was found in the second, third, or fourth impingers. With PCP, 74 percent was collected in the first impinger, 11.5 percent in the second impinger, 13.1 percent in the third impinger, and 1.2 percent in the fourth impinger. With 0-,0'-diphenol, 76.3 percent was trapped in the first impinger, 12.4 percent in the second, 11.4 percent in the third, and none was detected in the fourth impinger.

Absorption of Other Aromatic Compounds

The possibility of the formation of certain additional compounds during destruction testing was considered. Therefore, the collection efficiencies for several compounds in the bench-scale apparatus were examined. Approximately 0.1 gram of material was weighed into a combustion boat. The boat was placed into the tube ahead of the packed bed and the temperature was raised from 200°C to 400°C over a period of 35 minutes. The compounds used were acenaphthylene, biphenyl, and phenanthrene. The collection efficiencies were 97 percent, 90 percent, and 90 percent, respectively. Of the acenaphthylene trapped, 87 percent was collected in the first impinger, 12 percent in the second impinger, and 0.8 percent in the third impinger. Of the biphenyl trapped, 87 percent was in the first impinger, 11 percent in the second impinger, and 1 percent in the third impinger. With phenanthrene, 83 percent was collected in the first impinger, 15 percent in the second impinger, and 2 percent in the third impinger.

Compatibility of 2-Propanol With Analytical Measurement Procedures

The analysis of CCl_4 was performed on a gas chromatograph with an electron capture detector. An electron capture detector was necessary to achieve the sensitivity required to verify that 99.99 percent of the CCl_4 fed to the burner was indeed destroyed, as required by U.S.EPA regulations. Figure 3 shows the analysis of a 1.6 μg/ml CCl_4 standard in 2-propanol. The column used was a 1/8" x 6' Chromosorb 101. The attenuation was X5. There is tailing from the 2-propanol peak, but the CCl_4 peak is not seriously interfered with.

The analysis of DCB was performed by liquid chromatography, with a UV detector set at 210 nm. Figure 4 shows the analysis of a 1.3 μg/ml DCB

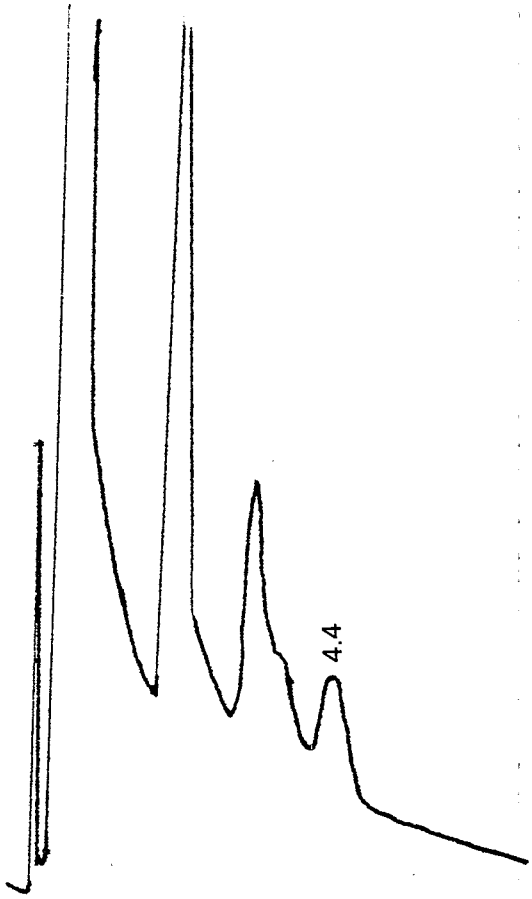

Figure 3. Analysis of 1.6 μg CCl_4/ml in 2-propanol. Chromasorb 101 Column - Ni^{63} Electron Capture Detector.

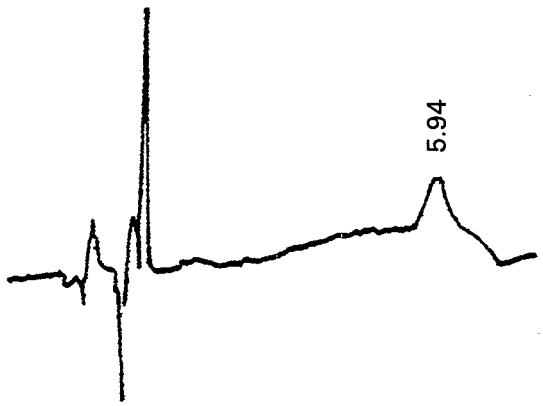

Figure 4. Analysis of 1.3 μgl,2 - Dichlorobenzene by HPLC. Reverse phase C-18 column. UV detector set at 210 nm, 0.05 absorbance units full scale.

standard in 2-propanol. The column used was a reverse phase C18. Absorbance range was 0.05 AUFS. At 210 nm, the absorbance by the 2-propanol is very small and the 2-propanol elutes at about two minutes for an elution volume of 4 ml. The DCB elutes at about six minutes, so there is no interference from the 2-propanol. At 210 nm, there are no signficant impurities in the 2-propanol that interfere with the DCB analysis.

Comparison of 2-Propanol With Solid Absorber System

There are several advantages to the use of 2-propanol as the absorber. The greatest advantage is the sample analysis time saved with this system over the solid absorbers. Figure 5 shows the steps associated with each method. Essentially no sample preparation is needed after the gas samples are taken using 2-propanol. With use of solid absorbers for chlorinated organics, the XAD-2 must be soxlet extracted before sampling to clean it up sufficiently and then again after the sample is taken to desorb the chemical compounds. The impinger contents must be extracted and the organic layer combined with the soxlet extract and evaporated down before analysis by the appropriate method.

Another advantage is the adaptability of the 2-propanol to highly volatile species. Very good trapping efficiencies were demonstrated for CCl_4 and DCB, which are very volatile when compared to PCBs. Haile and Baladi reported decreased trapping efficiencies for the more volatile PCBs (10). When the solid absorber system was tested with DCB in the EI bench scale system, only 82 percent of the DCB was recovered. This compares to the 97 percent that is recovered using 2-propanol. The solid absorber system was also used to sample the gas stream in the pilot plant. A sample was pulled using 2-propanol, then immediately a sample was pulled using the solid absorber system. Immediately after that, a second sample was pulled using 2-propanol. The results using the solid absorber system were a factor of ten lower than the average of the two samples taken using 2-propanol. These findings agree with Haile and Baladi that, as the volatility of the chemical species goes up, the collection efficiency for solid absorbers goes down.

Another advantage of this system over the Source Assessment Sampling System (SASS) is that of cost. The SASS cost is currently in the neighborhood of $14,000 to $25,000, whereas this modified EPA Method 5 system can be set up for a few hundred dollars.

One disadvantage of this system is the volatility of the 2-propanol. When sampling times run past 30 minutes, evaporation of the 2-propanol begins to be a problem. Generally, this can be avoided, but if sample times longer than 30 minutes are required, there will be a loss in volume of the 2-propanol that must be accounted for. Although there is a loss in volume of the 2-propanol, the compounds being sampled in the gas stream will not necessarily migrate from one impinger to the next. An impinger containing 130 μg DCB/ml was placed in the first position in the bench-scale apparatus. The tube furnace was heated to 400°C, and air was pulled through the system for 60 minutes. There was an appreciable loss in volume of the 2-propanol, but only 1 percent of the DCB had migrated from the first impinger to the second.

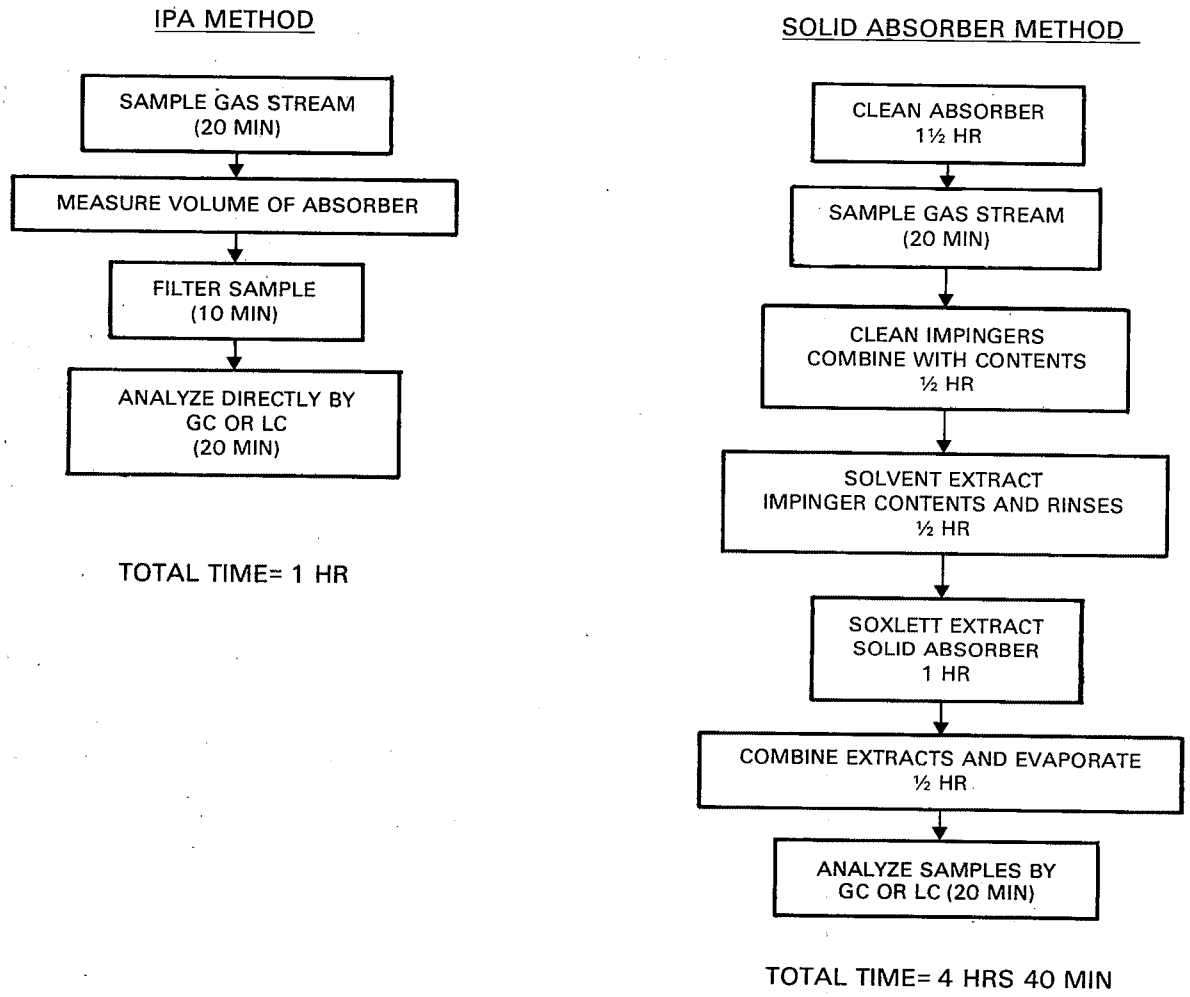

Figure 5. Flow chart of sample analysis.

One advantage of using 2-propanol over other absorbers is that it is probably less hazardous to handle than the other liquid absorbers. There is still a possible fire hazard, but this is encountered whenever an organic solvent is used. The use of solid absorbers is also hazardous because of the extended method steps involving organic solvents.

CONCLUSIONS

From EI studies, we have concluded that 2-propanol is a very good absorber for hazardous pollutants. With proper cooling, it can even sample volatile compounds such as carbon tetrachloride. It offers a technique for direct analysis after sampling a gas stream. With this system, four sets of gas samples can be taken and analyzed in one day by one person.

Absorption efficiencies are generally very good, with most of the compounds being trapped in the first impinger. The number of impingers to be used is dependent on the volatility of the compound being analyzed for. Most organic compounds show good solubility in 2-propanol.

2-propanol has minimal impact on the analysis of CCl_4 and DCB. Some tailing of the 2-propanol does overlap low-level CCl_4 peaks. This tailing is not serious and μg/ml levels of CCl_4 can be easily analyzed.

The use of 2-propanol has many advantages, such as the time saved per analysis. It is easily adapted to sampling of the more volatile compounds. The cost of the sample system is much less than that of systems such as the Source Assessment Sampling System. The major disadvantage of the system is the volatility of the 2-propanol when sampling periods are longer than 30 minutes. Even with this loss in the 2-propanol volume, the chemical compound being trapped does not tend to migrate with the 2-propanol.

REFERENCES

1. Anonymous. 1976. Emission testing at Continental Can Co., Hopewell, VA, July 14-23, 1975. EPA-330/2-76-030, October. U.S. Environmental Protection Agency, Office of Enforcement.

2. Ferguson, T.L., F.J. Bergman, G.R. Cooper, R.T. Li, and F.I. Honla. 1975. Determination of incinerator operating conditions necessary for safe disposal of pesticides. EPA-600/2-75-041, December.

3. Leighton, I.W., and J.B. Feldman. 1974. Demonstration test burn of DDT in General Electric's liquid injection incinerator. U.S. Environmental Protection Agency Region I, December.

4. Guilford, N.G.H., and R.J. Brandon. 1978. Pilot scale evaluation of the destruction of waste PCB by incineration. Ontario Research Foundation, Mississauga, Ontario, Canada, August 28.

5. Guilford, N.G.H., and G. Rosenblatt. 1977. Polychlorinated biphenyl source testing survey, Ontario region. MS Report No. OR-9, September.

6. Komaniya, K., and S. Morisaki. 1978. Incineration of PCB with an oxygen burner. ES&T 12 (10):1205-1208.

7. Shoemaker, R.A. 1981. J. Chromatogr. Sci. 19:321.

8. Ackerman, D.G. 1977. Destroying chemical wastes in commercial scale incinerators. Final report phase II. EPA Contract No. 68-01-2966, November.

9. MacDonald, L.P., D.J. Skinner, F.J. Hopton, and G.H. Thomas. 1977. Burning waste chlorinated hydrocarbons in a cement kiln. Report to Fisheries and Environment Canada. Report No. EPS 4-CoP-77-2, March.

10. Haile, C.F., and E. Baladi. 1977. Methods for determining the PCB Emissions from incineration and capacitor and transformer filling plants. EPA-600/4-77-048, November.

11. Beard, J.H. III, and J. Schaum. 1978. Sampling methods and analytical procedures manual for PCB disposal: interim report. U.S. Environmental Protection Agency, Office of Solid Wastes, February.

12. Bombaugh, K.J., and K.W. Lee. 1981. ES&T 15 (10):1142-1149.

13. Acurex Corporation. 1978. Source assessment sampling system design and development. EPA-600/7-78-018.

14. Arthur D. Little, Inc. 1978. EPA/IERL-RTP interim procedures for level 2 sampling and analysis of organic materials. EPA-600/7-78-016.

FORMALDEHYDE SURFACE EMISSION MONITOR

T.G. Matthews, A.R. Hawthorne, J.M. Schrimsher,
M.D. Corey, and C.R. Daffron

Health and Safety Research Division
Oak Ridge National Laboratory

ABSTRACT

A formaldehyde surface emission monitor is under development for passive, non-destructive measurement of formaldehyde (CH_2O) emission rates from flat surfaces of solid CH_2O sources. The monitor utilizes a solid sorbent, 13X molecular sieve, that provides excellent chemical stability for sorbed CH_2O and permits the monitor to be used in any physical orientation. With a 0.032 m^2-test area, a $\approx$0.01 mg $CH_2O/m^2 \cdot hr$ detection limit can be achieved with a 3-hour sampling period and pararosaniline colorimetric analysis. Preliminary results indicate that the monitor could be used for 1) quality control measurements of commercial CH_2O resin-containing materials such as pressed-wood products, and 2) in-situ measurements of CH_2O emission rates from a variety of CH_2O sources in domestic environments such as pressed-wood, textiles, and urea-formaldehyde foam insulation products.

INTRODUCTION

Formaldehyde (CH_2O) is currently recognized as an important pollutant in a variety of industrial and domestic environments. The 100 ppb CH_2O concentration guideline recommended for indoor air by several European Nations (1) and the American Society for Heating, Refrigeration, and Air-Conditioning Engineers (ASHRAE) (2) reflects a serious concern for prolonged public exposure at low concentrations. As a result, two general needs in monitoring technology have arisen: first, in-situ analysis methods to identify dwellings with high CH_2O levels and the major CH_2O sources within these environments, and second, quality control test methods for a variety of consumer and construction products containing CH_2O-based resins.

Despite a plethora of ambient vapor monitoring techniques for CH_2O, source strength analyses for CH_2O-resin-containing products are currently limited to sample-destructive tests of selected pressed-wood (3) and textile products (4). As a result, the development of a non-destructive

surface emission monitor for CH_2O emission from consumer products could have a major impact on improved quality control and in-situ measurement capability. For quality control applications, a broader testing of construction and consumer products could be performed, resulting in selective grading of materials prior to sale to the consumer. For in-situ monitoring, precise source identification could be accomplished without the destructive removal of numerous samples for subsequent laboratory analysis.

This report addresses the development of the new surface monitoring methodology. The basic design and specific applications to pressed-wood products, urea-formaldehyde foam insulation (UFFI) in simulated wall panels, and CH_2O source identification and potential quantification in three homes is also addressed.

MONITOR DESIGN

The physical design of the formaldehyde surface emission monitor (FSEM) is conceptualized in Figure 1. It is a passive flux monitor for CH_2O emission from a selected area of a solid flat surface. Formaldehyde is collected on a 13X molecular sieve (1.6 mm pellets), suspended in uniform close proximity to the surface of the test media. The CH_2O content is then analyzed via a water-rinse desorption and colorimetric analysis methodology (5). The average CH_2O emission rate of the test media is calculated as a function of the sorbed CH_2O, sampling period, and test area of the monitor (Equation 1).

$$\text{Emission Rate } (\text{mg } CH_2O/m^2 \cdot \text{hr}) = \frac{CH_2O\ (\text{mg}/m\ell) \cdot \text{Sieve Rinse Volume } (m\ell)}{\text{Test Period (hrs)} \cdot \text{Test area } (m^2) \cdot CH_2O \text{ Desorption Efficiency}} \quad (1)$$

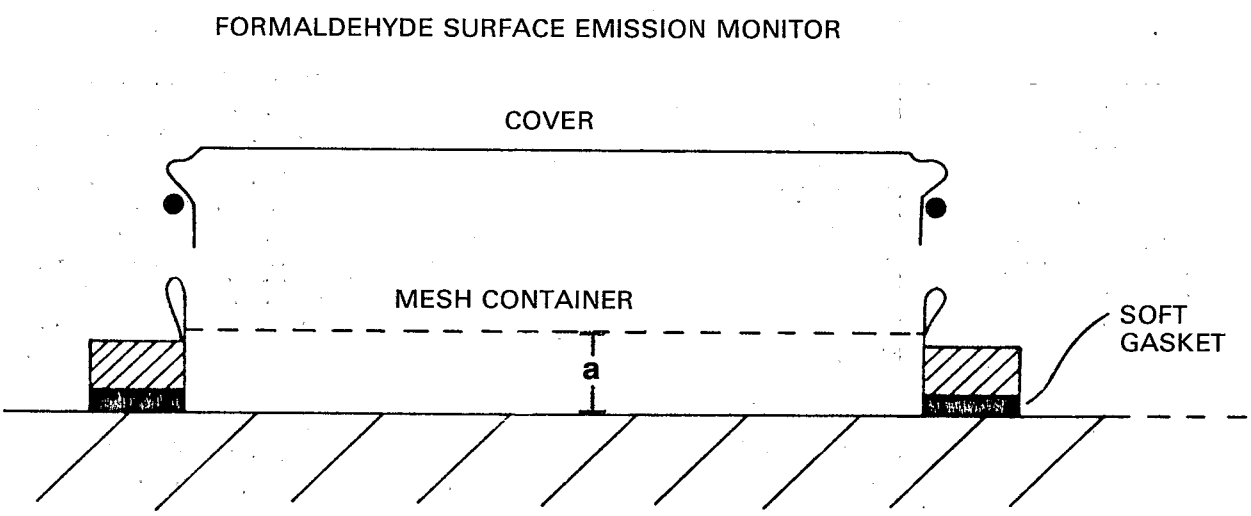

Figure 1. Conceptual design of the Formaldehyde Surface Emission Monitor.

The sieve also sorbs sufficient quantities of water vapor to eliminate potential condensation problems within the monitor.

The sensitivity of the surface emission measurement is proportional to the test area of the monitor and the duration of the sampling period. A large test area is desirable to limit the effects of the inhomogeneity of the test medium. In contrast, a short sampling period is desirable for convenience and to limit any physical changes in the test medium, such as dehydration, that could occur as a function of sampling period.

The separation between the sorbent and emitting surface (distance a, Figure 1) is an additional important design parameter, which has a major impact upon the steady-state CH_2O concentration profile within the passive monitor. In an ideal measurement, the CH_2O concentration within the monitor and in the environment surrounding the monitor should be equal because of the potential for CH_2O concentration dependence of the emission rate of the test media. In practice, the CH_2O concentration within the monitor is dependent upon the source strength of the test media. With an appropriate design, the concentration can be limited to a range consistent with most living environments. A simple mathematical model (Equation 2) for the steady-state CH_2O concentration at the surface of the test media as a function of emission rate and sorbent-test media separation is represented graphically in Figure 2.

$$[CH_2O]\ (\text{ppm}) = \frac{0.8[\text{ppm}/(\text{mg}/\text{m}^3)] \cdot \overset{\text{Emission}}{\text{Rate}}\ \overset{\text{Sorbent-Test Media}}{(\text{mg}/\text{m}^2 \cdot \text{hr}) \cdot \text{Separation (m)}}}{\text{Diffusion Coefficient } (\text{m}^2/\text{hr})} \quad (2)$$

The primary assumptions of this model are simple diffusion behavior and a 100 percent efficient CH_2O sorbent. For emission rates of 0.0 to 1.0 ($mg/m^2 \cdot hr$), typical of most consumer and construction products, a CH_2O concentration range of 0-0.2 ppb is predicted for a separation of ≈2 cm.

The current prototype of the FSEM is constructed from a 20-cm mechanical sieve with a #20 mesh. The load factor within the monitor is ≈20 (m^2 test area/m^3 air volume). The sorbent-test media separation is 2.2 cm. For horizontal operation, the sieve sample (10 g) is sprinkled uniformly over the screen of the mesh container. For vertical operation, the sieve is held in several screen trays attached directly to the screen in the mesh container. With a typical test period of 3 hours, the lower limit of detection is ≈0.01 $mg/m^2 \cdot hr$. This is adequate for all materials normally incorporated in living environments that could have a significant impact upon the ambient CH_2O concentration.

QUALITY CONTROL (QC) APPLICATION FOR PRESSED-WOOD PRODUCTS

Comparison to Current QC Methods

The current analytical method used in the United States for measure-

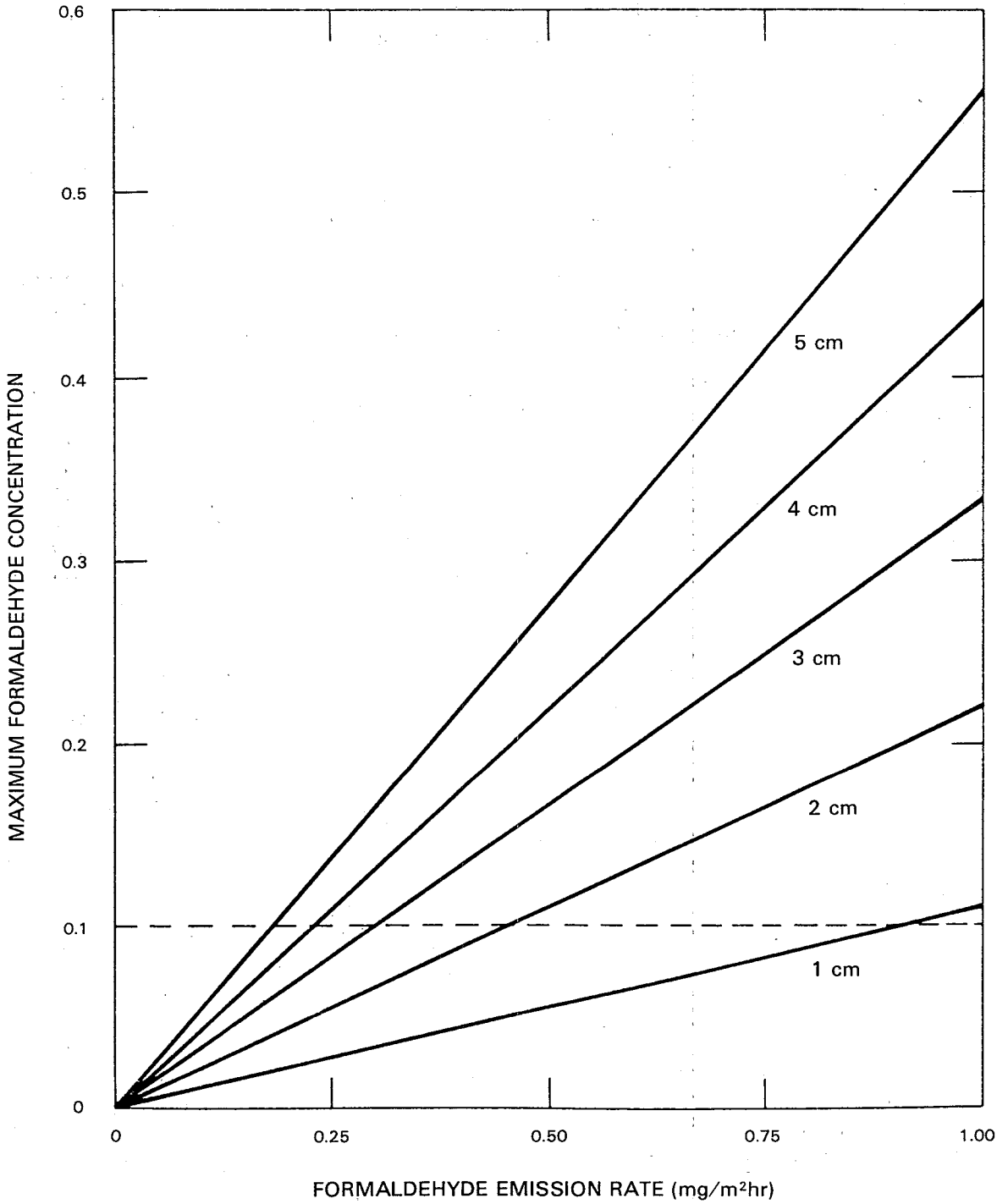

Figure 2. Diffusion model for the CH_2O concentration at the surface of the test medium as a function of sorbent-test medium separation and the CH_2O emission rate of the test medium. The dashed line corresponds to the ASHRAE guideline of 0.1 ppm for indoor air (2).

ments of CH_2O release from pressed-wood products is the 2-hour static dessicator test of the Hardwood Plywood Manufacturers' Association-National Particleboard Association (HPMA-NPA) (3). It is a sample destructive test method that is applied to as few as 1 of every 1,000 to 10,000 sheets of particleboard decking and plywood panels used principally in mobile homes. Prior to testing, the pressed-wood samples (5x13 cm) are conditioned for 1 to 7 days in a 22°C, 50 percent RH environment. The CH_2O sorbent and colorimetric analyses used are water and chromotropic acid, respectively.

The proposed non-destructive method using the FSEM is modeled as closely as possible to the HPMA-NPA method to promote its acceptance as a quality control technique. The primary differences are 1) application to all pressed-wood products, 2) inclusion of new conditioning criteria, 3) use of a solid CH_2O sorbent, 13X molecular sieve, and 4) substitution of the pararosaniline (PA) colorimetric analysis.

Sample conditioning is performed for $\geqslant$2 weeks in an atmosphere at 22°C, 50 percent RH, and 0.10 ppb CH_2O. This allows the emission rate of the test media to stabilize under conditions consistent with typical living environments. In practice, any significant change in environmental conditions (e.g., ±5°C, ±25 percent RH) can cause large fluctuations (e.g., >50 percent) in the CH_2O emission rate, which can require 1 to 3 weeks to stabilize.

The use of the 13X molecular sieve instead of water as a CH_2O sorbent has several advantages. These include 1) the option to use the monitor in any physical orientation, 2) the elimination of water condensation problems, and 3) long-term stability of sorbed CH_2O (5). In addition, the sieve does not appear to suffer from the sampling rate anomalies as a function of sorbed CH_2O concentration as does the water sorbent (Figure 3). In preliminary studies conducted under near-static conditions, the sampling rate of water in a ≈10-cm-diameter open tube sampler demonstrated a non-linear CH_2O uptake as a function of concentration x time. In contrast to the experimental results, which showed an enhanced collection rate, diffusion theory would predict a rollover in the sampling rate at high $CH_2O \cdot H_2O$ concentration levels due to the increased CH_2O vapor pressure above the sorbent. A clear explanation of this sampling rate phenomenon has yet to be made. The sieve exposure was performed using a ≈12-cm-diameter tubular sampler containing a #20 mesh screen to support the sorbent in the center of the unit. Under similar exposure conditions to the experiment with the water sorbent, a linear uptake of CH_2O was observed as a function of concentration x time.

The use of the PA analysis results in a three-fold increase in CH_2O sensitivity over the chromatropic acid (CA) method (5). No difference in the degree of CH_2O selectivity between the PA and CA methods has been observed in the measurement of particleboard, plywood, fiberboard, and paneling samples.

Comparative measurements of four types of pressed-wood products were performed using the 2-hour dessicator and FSEM methods (Figure 4). All measurements were taken 1 to 3 weeks following sample preparation and

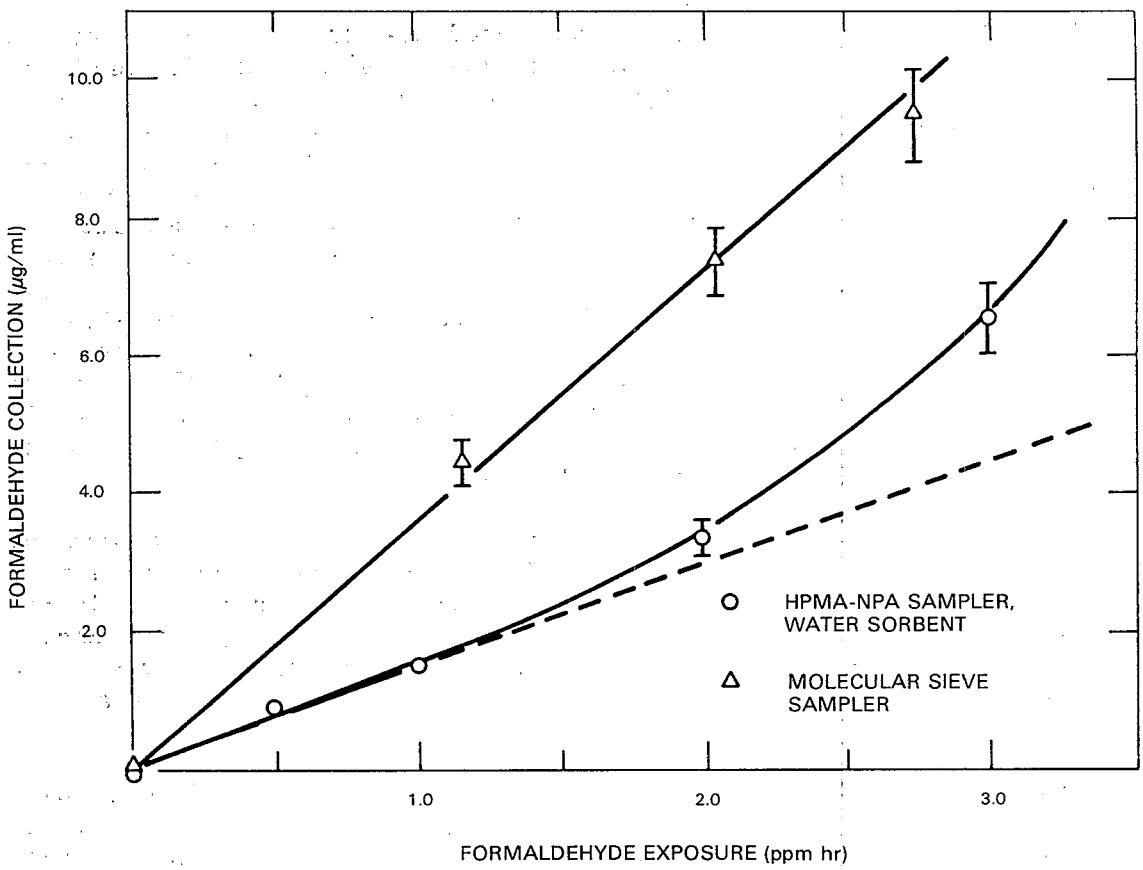

Figure 3. Formaldehyde sampling characteristics of passive samplers containing water (o) and molecular sieve (Δ) sorbents.

conditioning. For low emitters, an excellent correlation is observed between the two test methods. For the strong emitter (paneling sample), a rollover is observed that is consistent with the CH_2O sampling rate anomaly of the water sampler used in the HPMA-NPA test.

Comparison to Dynamic Chamber Tests

Environmental chamber analyses represent the closest laboratory approximation to real-world conditions. Such tests are therefore useful for intercomparison of simple static methods used for quality control applications. The chamber method involved the testing of edge-coated wood product samples at 24°C and 50 percent RH under dynamic flow conditions in a 0.2 m^3 Teflon-lined chamber. The air exchange rate (ACH) and loading factor were varied in the ranges of 0.7-4.4 hr^{-1} and 0.02-1.70 m^2/m^3, respectively. The concentration of the CH_2O vapor exiting the chamber was measured with a modified CEA Instrument (6). The CH_2O emission rate was then determined using Equation 3.

One important result of this analysis was a comparison of the CH_2O emission rates of the test media as a function of CH_2O vapor concentration.

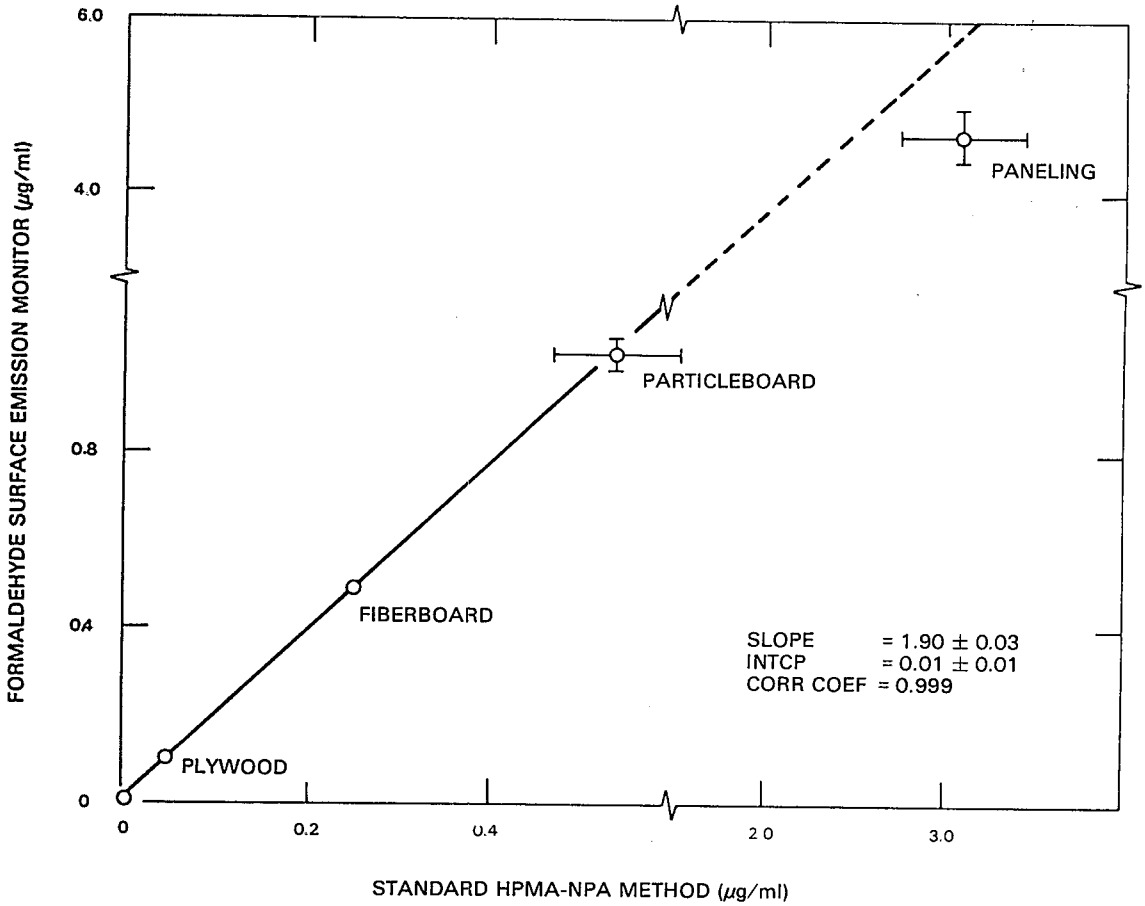

Figure 4. Comparison of test results for the Hardwood Plywood Manufacturers Association-National Particleboard Association (HPMA-NPA) dessicator and surface monitoring methods.

$$\underset{\text{Rate } (mg/m^2 \cdot hr)}{CH_2O \text{ Emission}} = \frac{[CH_2O](ppm) \cdot \text{Flow Rate Through Chamber } (m^3/hr)}{0.8 \ [ppm/(mg/m^3)] \cdot \text{Wood Area } (m^2)} \quad (3)$$

The chamber results for paneling samples (Figure 5) are also representative of the emission behavior observed for particleboard, plywood, and fiberboard samples. The emission rate is strongly dependent upon the CH_2O vapor concentration and increases rapidly below levels of ≈200 ppb. For the paneling sample, the emission rate determined with the FSEM is equivalent to the chamber results observed at 0.1-0.2 ppm. In contrast, the emission rate of the paneling in the HPMA-NPA test is highly suppressed, equivalent to the chamber results observed at ≈1 ppm.

The HPMA-NPA and FSEM test results are consistent with the physical design of the dessicator and surface monitor test apparatus. The larger

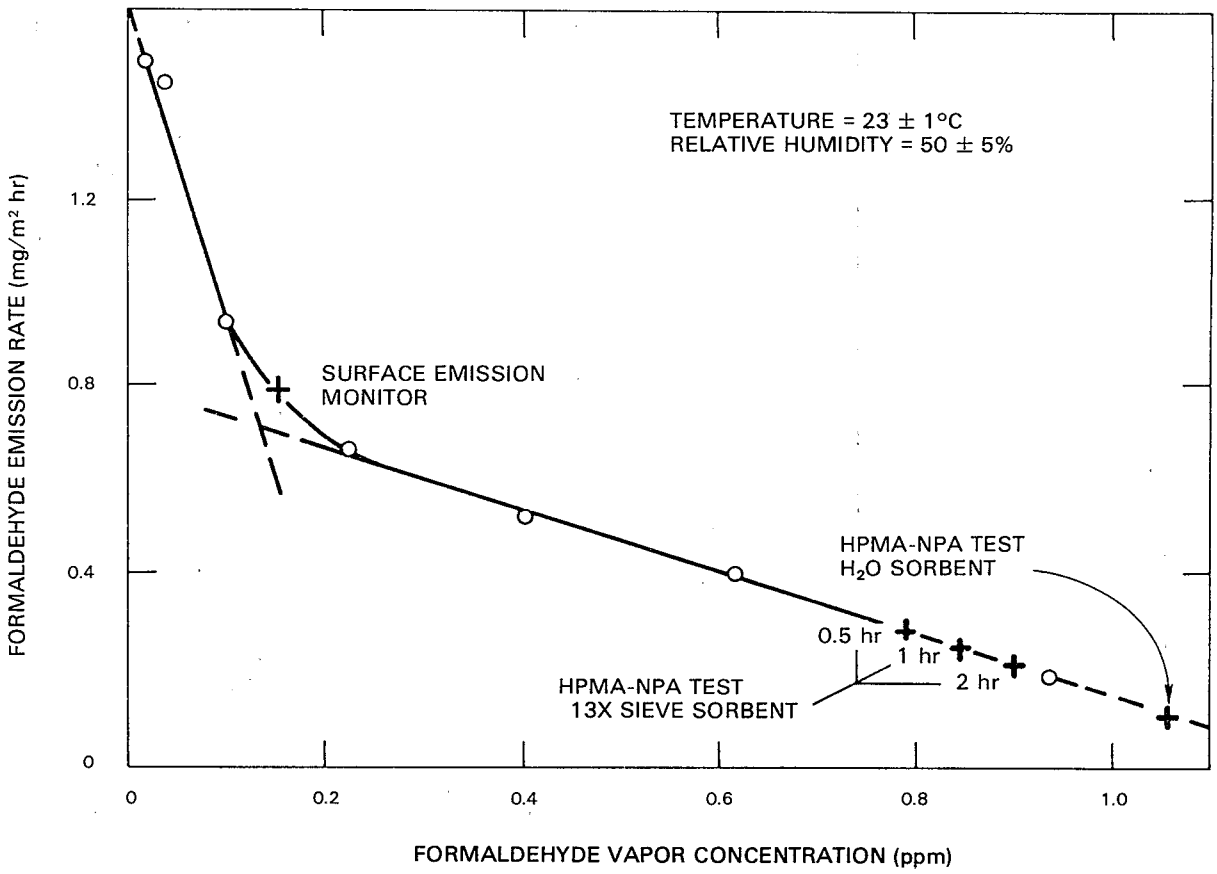

Figure 5. Formaldehyde emission rate of edge-coated wood paneling samples as a function of ambient CH_2O concentration.

test media-CH_2O sorbent separation inherent in the dessicator results in a larger CH_2O concentration at the surface of the test samples. This causes the enhanced suppression of the CH_2O emission rate of pressed-wood products.

IN-SITU SURFACE MONITORING APPLICATIONS

Simulated House Wall Test Panels Containing UFFI

The measurement of CH_2O emission from UFFI through gypsum board represents a separate class of applications for the FSEM where the primary emitting material is only indirectly accessible. To test the efficacy of this type of measurement, a comparison study was performed applying the FSEM and laboratory methods to a selection of simulated house-wall test panels (Figure 6) containing UFFI. The panels were foamed according to manufacturers' specifications at the Franklin Research Institute in March-April, 1980 (7). The reference dynamic-flow determination of the CH_2O emission

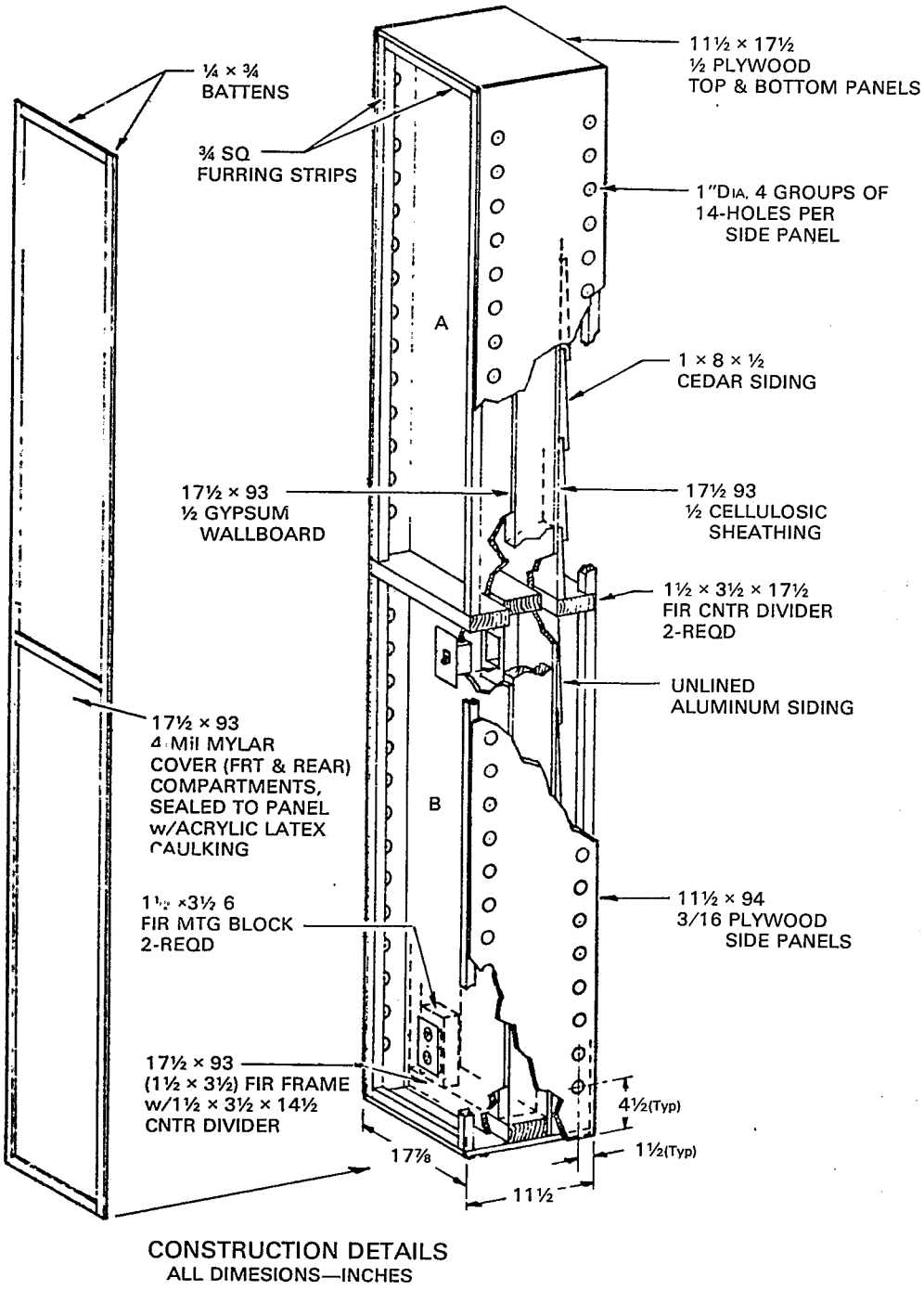

Figure 6. Urea-formaldehyde foam insulation (UFFI) panel construction.

rate was performed by measuring the CH_2O vapor concentration in air passed through an external chamber sealed to the gypsum board side of the panel. This chamber was used to simulate the effects of air exchange rates that are typical of indoor environments. The FSEM measurement was performed by attaching the monitor directly to the surface of the gypsum board.

In a previous study (8) the emission rate through the gypsum board was found to be a strong function of the CH_2O concentration in the chamber exterior to the gypsum board. Below ≈0.2 ppm, the CH_2O emission rate was maximized. At concentrations increasing from ≈0.2 to 2-7 ppm (static conditions), the CH_2O emission rate decreased to near-zero levels where emission from the UFFI was highly suppressed.

For the dynamic flow measurements, the air flow through the chamber was sufficient to maintain a sub-0.2 ppm concentration level. The temperature and relative humidity of the laboratory at the time of the measurements were 16 to 18°C and 30 to 50 percent RH, respectively. This accounts for the low CH_2O emission levels in comparison to previous work that was conducted at 25°C and 50 percent RH (8).

The linear correlation between the FSEM and dynamic flow measurements is excellent (Figure 7). This is strong evidence that both measurement protocols maintained sub-0.2 ppm CH_2O concentration levels at the surface of the gypsum board, thereby maximizing the CH_2O emission rate. The slope of 1.3 is consistent with a slightly larger test area for the FSEM than the specific opening of the monitor. This is probably the result of CH_2O transport through gypsum board adjacent to the opening of the monitor. A 14 percent increase in the radius of the effective test area (i.e., ≈1.3 cm, which is equal to the thickness of the gypsum board) would account for a 30 percent increase in the CH_2O sampling rate.

FSEM Measurements of Surfaces of Walls and Floors in Homes

FSEM measurements were performed on the gypsum board surface of interior-partition and exterior walls, and carpeted and tiled floors of one UFFI and two non-UFFI homes (Table 1). A primary goal was to test the efficacy of the FSEM for localizing and ranking the important CH_2O sources in individual environments. In dwelling 1, no significant CH_2O sources were found. In dwelling 2, the strongest source was the UFFI in the exterior walls. The primary emitter in dwelling 3 was probably the plywood decking; the CH_2O emission could be detected through the carpeting. In all three dwellings the floor tile was an effective blocking agent for CH_2O emission from the wood flooring. In dwellings 2 and 3, the off-gassing from interior gypsum board walls with empty wall cavities indicates the strong sorbtive and desorptive potential of construction materials with significant water content.

A second objective was a comparison of the measured CH_2O concentration levels with concentrations estimated from FSEM and air exchange rate (ACH) measurements. A good correlation between the measured and predicted concentrations would support the quantitative capability of the FSEM for in-situ environmental analyses. For dwellings 1, 2, and 3, the areas of

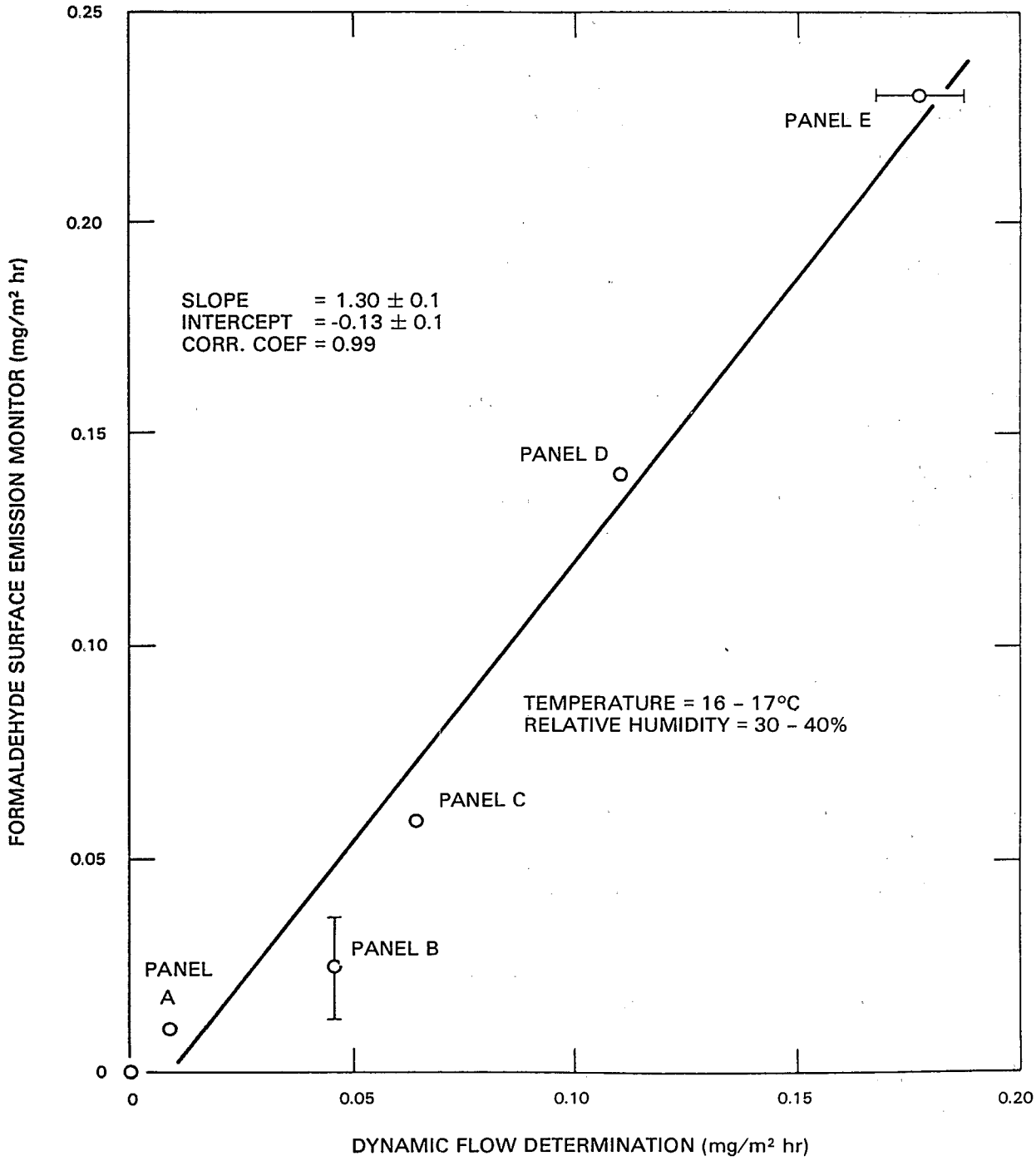

Figure 7. Comparison of CH_2O emission rates from urea-formaldehyde foam insulation (UFFI) panels using dynamic flow and surface monitoring methods.

TABLE 1. MEASUREMENTS OF CH_2O EMISSION RATES FROM MAJOR SURFACES IN THREE OCCUPIED HOMES USING THE FSEM

Dwelling	Formaldehyde emission rate ($mg/m^2 \cdot hr$)			
	Exterior gypsum board wall	Interior gypsum board wall	Carpeted floor	Tiled floor
1 non-UFFI*	0.014 ± 0.005	0.014 ± 0.005	0.011 ± 0.005	0.00 ± 0.005
2 UFFI	0.30 ± 0.03	0.10 ± 0.010	0.095 ± 0.01	0.022 ± 0.005
3 non-UFFI	0.18 ± 0.02	0.22 ± 0.02	0.27 ± 0.03	0.024 ± 0.005

*Urea-formaldehyde foam insulation.

the principal emitting surfaces, including the interior walls (and ceiling), external walls, and carpeted and tiled floors, were estimated for an average room. The emission rate from gypsum board surfaces was reduced by a factor of 1.3 to account for the effective test area of the FSEM determined from the simulated wall panel work. No analogous type of correction factor was applied to the floor data. With the final CH_2O emission rate data for each surface and a measured ACH, a predicted CH_2O concentration was determined via Equation 4.

$$[CH_2O](ppm) = \frac{\{\Sigma \text{Source Area } (m^2) \cdot \text{Emission Rate}(mg/m^2 \cdot hr)\} \cdot 0.8 \ (ppm/(mg/m^3))}{\text{Room Volume } (m^3) \cdot \text{ACH } (hr^{-1})} \quad (4)$$

A comparison of measured and predicted CH_2O concentration levels for dwellings 1, 2, and 3 is given in Table 2. An encouraging correlation is observed for all three dwellings despite the inherent complexity and numerous experimental variables associated with the comparison.

TABLE 2. COMPARISON OF MEASURED CH_2O CONCENTRATION LEVELS WITH VALUES PREDICTED FROM COMBINED FSEM AND ACH MEASUREMENTS

Dwelling	Formaldehyde concentration (ppm)	
	Estimated	Measured
1 non-UFFI*	0.04 ± 0.02	0.036 ± 0.01
2 UFFI	0.16 ± 0.05	0.15 ± 0.05
3 non-UFFI	0.21 ± 0.14	0.18 ± 0.02

*Urea-formaldehyde foam insulation.

SUMMARY

Quality control applications of the FSEM to pressed-wood products have been examined. A comparison of the FSEM and a conventional dessicator method used in the United States showed a strong linear correlation for weak emitting boards. A comparison test with a dynamic chamber method showed that the surface monitor gave results consistent with chamber data at 0-0.2 ppm concentrations.

The feasibility of certain in-situ monitoring applications with the FSEM have been studied. An encouraging quantitative relationship has been observed between the FSEM and a reference method for CH_2O emission from UFFI through gypsum board in simulated wall panels. The results of surface emission monitoring in three homes were also supportive of the quantitative capability of the monitor. A close correlation was observed between measured CH_2O concentrations and CH_2O concentrations estimated from FSEM and ACH measurements.

The potential uses of FSEM for both quality control and in-situ monitoring applications have yet to be fully developed. A non-destructive quality control method for CH_2O is also of interest to the textile and non-UFFI insulation industries. The monitor could also be used to evaluate the long-term decay of CH_2O release from consumer and construction products incorporated in living environments and the efficacy of source removal methods.

ACKNOWLEDGMENTS

Research for this paper was sponsored jointly by the Consumer Product Safety Commission under Interagency Agreement CPSC-IAG-81-1360 and the Office of Health and Environmental Research, US Department of Energy, under contract W-7405-eng-26 with the Union Carbide Corporation.

REFERENCES

1. Borzelleca, J.F. 1980. Formaldehyde-an assessment of its health effects. Report to the U.S. Consumer Product Safety Commission, March.

2. American Society for Heating, Refrigeration, and Air-Conditioning Engineers Standard 62-1981.

3. Tentative test protocol for emission of formaldelhyde from wood products. 1981. Hardwood-Plywood Manufacturers' Association, National Particleboard Association.

4. AATCC Test Method 112-1978. Formaldehyde odor in resin-treated fabric, determination of: sealed jar method.

5. Matthews, T.G., and T.C. Howell. In press. Solid sorbent methodology for formaldehyde monitoring. In Analytical Chemistry.

6. Matthews, T.G. In press. Evaluation of a modified CEA Instruments, Inc., Model 555 Analyzer for the monitoring of formaldehyde vapor in domestic environments. American Industrial Hygiene Association Journal.

7. Osborn, S.W. 1981. Technical report F-C5316-01. The Franklin Research Center, Philadelphia, PA.

8. Hawthorne, A.R. An evaluation of formaldehyde emission potential from urea-formaldehyde foam insulation: Panel measurements and modeling. ORNL/TM-7959.

CORRELATION OF REMOTE AND WET CHEMICAL TECHNIQUES FOR THE DETERMINATION OF HYDROGEN FLUORIDE EMISSIONS FROM GYPSUM PONDS

Howard F. Schiff, Daniel Bause, Mark McCabe, and Verne Shortell

GCA/Technology Division
Bedford, MA

William F. Herget

U.S. Environmental Protection Agency
Environmental Sciences Research Laboratory
Research Triangle Park, NC

Mark Antell

U.S. Environmental Protection Agency
Office of Air Noise and Radiation
Division of Stationary Source Enforcement
Washington, DC

ABSTRACT

Data on concentrations of gaseous hydrogen fluoride in air near an extended area source were collected simultaneously by the Remote Optical Sensing of Emissions (ROSE) system using longpath, high-resolution, Fourier transform infrared (FT-IR) absorption spectroscopy and by standard wet chemical techniques. The program was divided into five phases, including a literature review, pretest survey, sampling and analytical trials in the laboratory, preliminary field phase, and the final, collaborative field phase. Precision and accuracy of standard techniques were evaluated in the laboratory and preliminary field phases.

Field sampling efforts were conducted along gypsum ponds at two phosphate fertilizer facilities. Point sampling efforts utilizing both the double filter cassette and sodium bicarbonate-coated tube methods were conducted simultaneously with the operation of the ROSE system. Four point sampling sites were located at approximately equal intervals along the optical path from the ROSE system light source to the ROSE system van containing the FT-IR system. The fluoride collected by the wet chemical methods was analyzed colorimetrically using a semiautomated method with Lanthanum-Alizarin complexone reagent. The FT-IR data were collected at 0.125 cm^{-1}, spectral resolution, and the HF concentration was determined by

measuring the peak absorption of the R(5) line of HF at 4174 cm^{-1}, after a minor correction for water vapor interference. In 32 independent tests of comparable ambient HF concentrations, the overall average HF concentration was 36.1 ppb (ROSE system) and 36.4 ppb (wet chemical techniques). The standard deviation between the ROSE system data and the manual sampling results was 9.7 ppb.

INTRODUCTION

For several years, the U.S. Environmental Protection Agency (EPA) has used the Remote Optical Sensing of Emissions (ROSE) system to characterize the gaseous pollutants emitted by a variety of point and extended area sources (1). The ROSE system consists of a Fourier transform infrared (FT-IR) interferometer with telescopic optics and has been installed in a van. The system is used either with a remotely located infrared light source to make longpath (up to 1.5 km) atmospheric absorption measurements or in a single-ended mode to measure the infrared emission signal from gases exiting industrial stacks at elevated temperatures.

For the purpose of developing a technical basis for enforcement action to abate human health hazards, it may be necessary to determine concentrations of toxic gaseous pollutants in the vicinity of sources. The ROSE system used in the "active longpath mode" is conceptually capable of evaluating the breathing zone pollutant concentrations. The purpose of this project was to extend the data base of this versatile and promising pollutant sensor by comparison of data generated by the ROSE system with data generated by standard techniques for the measurement of hydrogen fluoride (HF).

A five-phased approach was adopted for conducting the project as indicated below:

- Literature review
- Site survey
- Sampling and analytical trials in the laboratory
- Preliminary field phase
- Collaborative field sampling and analytical phase

Prior to the commencement of the sampling program, it was necessary to determine the wet chemical techniques for sampling and analysis that would facilitate the comparison with the ROSE system data. Ambient sampling for HF is complicated by the low concentrations (ppb level), reactivity of the compound, and the effects of interfering species. The selection of wet chemical methods was based on compatibility with the sampling program; factors studied included sensitivity (minimum sampling time), reproducibility, ease of handling, and freedom from interferences. The literature was reviewed with respect to the above sampling requirements (1-10). The

extensive review of Jacobson and Weinstein (2) for procedures prior to 1976 and NERAC computer search for post-1976 procedures formed the basis of the literature review. The sampling and analytical procedures selected are published as ASTM methods (3) and were modified to fit the requirements of the project. In addition, discussions with Dr. Jay S. Jacobson and Mr. Richard Mandl and Larry Heller of the Boyce Thompson Institute for Plant Research at Cornell University were very helpful in the selection of procedures.

The sampling procedures selected were ASTM D3266-AISI double-tape sampler with citric acid and sodium hydroxide-treated filter papers and D3268-bicarbonate-coated tube samplers. D3266 was modified in that circular filters in 37-mm personal sampling cassettes were used in place of the AISI tape samplers. The analytical procedures selected were ASTM D3269 ion exchange separation followed by conductometric detection--i.e., ion chromatography and D3270-semiautomatic microdistillation spectrophotometric method. The procedures are described in detail subsequently.

SITE SELECTION

The site selection was based on criteria delineated below, and onsite surveys of facilities in the Bartow, Florida, Phosphate complex. The criteria were:

- The site should have geography compatible with the ROSE van and chemical sampling methods. This included an access road for the ROSE van; an unobstructed line of sight of at least 400 meters at the edge of gypsum pond (this provides for a high signal-to-noise ratio for the ROSE system), and no interferences from emissions from the facility or surrounding facilities.

- The facility could permit the use of the wet chemical sampling systems utilizing gasoline-powered electrical generators.

- The facility would have onsite laboratory space and instrumentation for fluoride analyses.

- The concentrations of fluoride in the ponds and the pH of the pond water must be sufficient to release ppb levels of HF into the atmosphere.

Two gypsum ponds, one in the CF Industries, Inc. (CFI), Bartow, Florida, plant, and the other in the Agrico Chemical Company (Agrico), South Pierce, Florida, plant, were found to meet the criteria and were selected for the conduct of the project. The plot plans of each facility are shown in Figures 1 and 2. Sampling line B at both facilities were utilized for the lines of sight in the preliminary and collaborative phases.

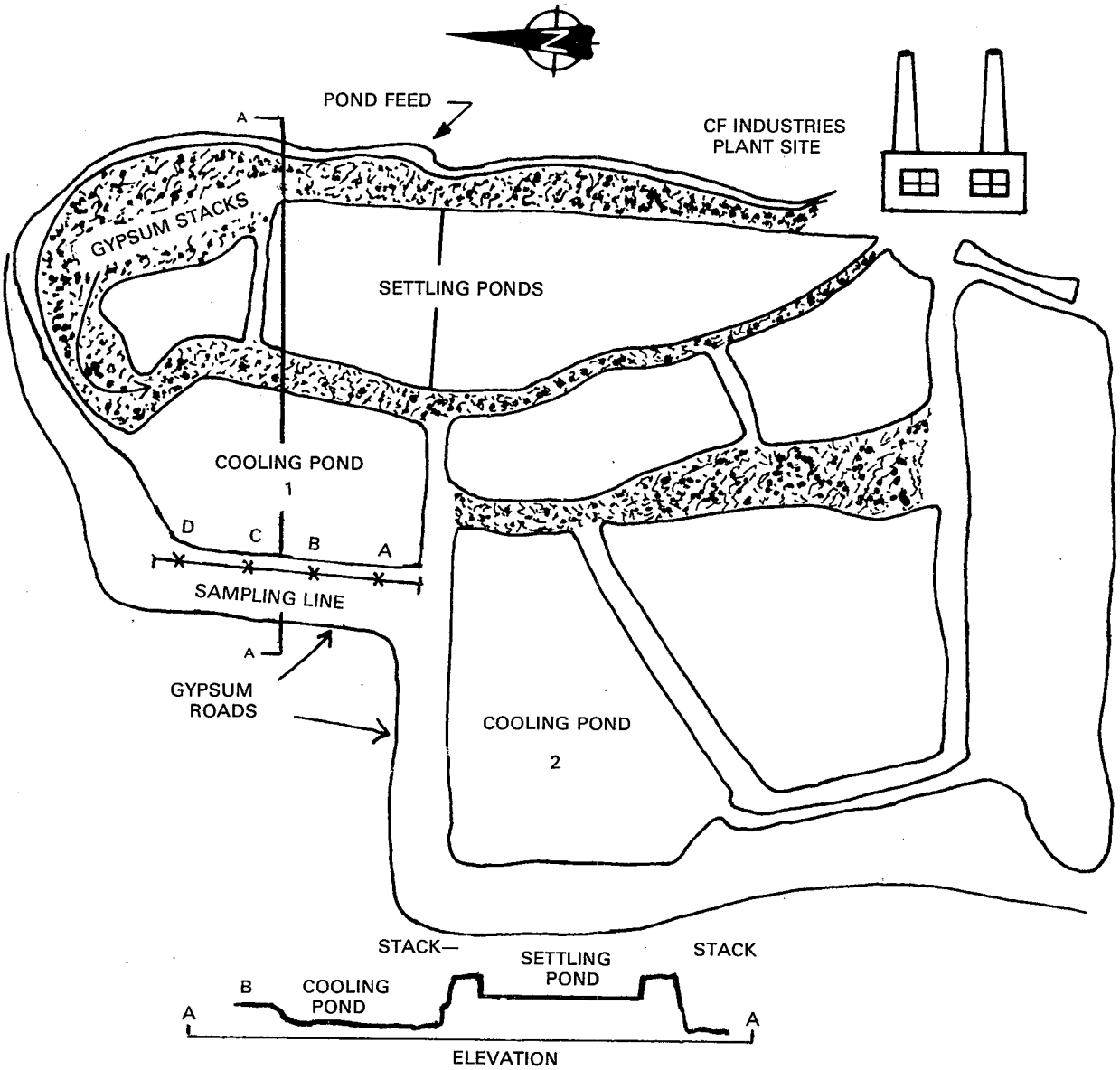

Figure 1. Sampling points at CF Industries gypsum ponds.

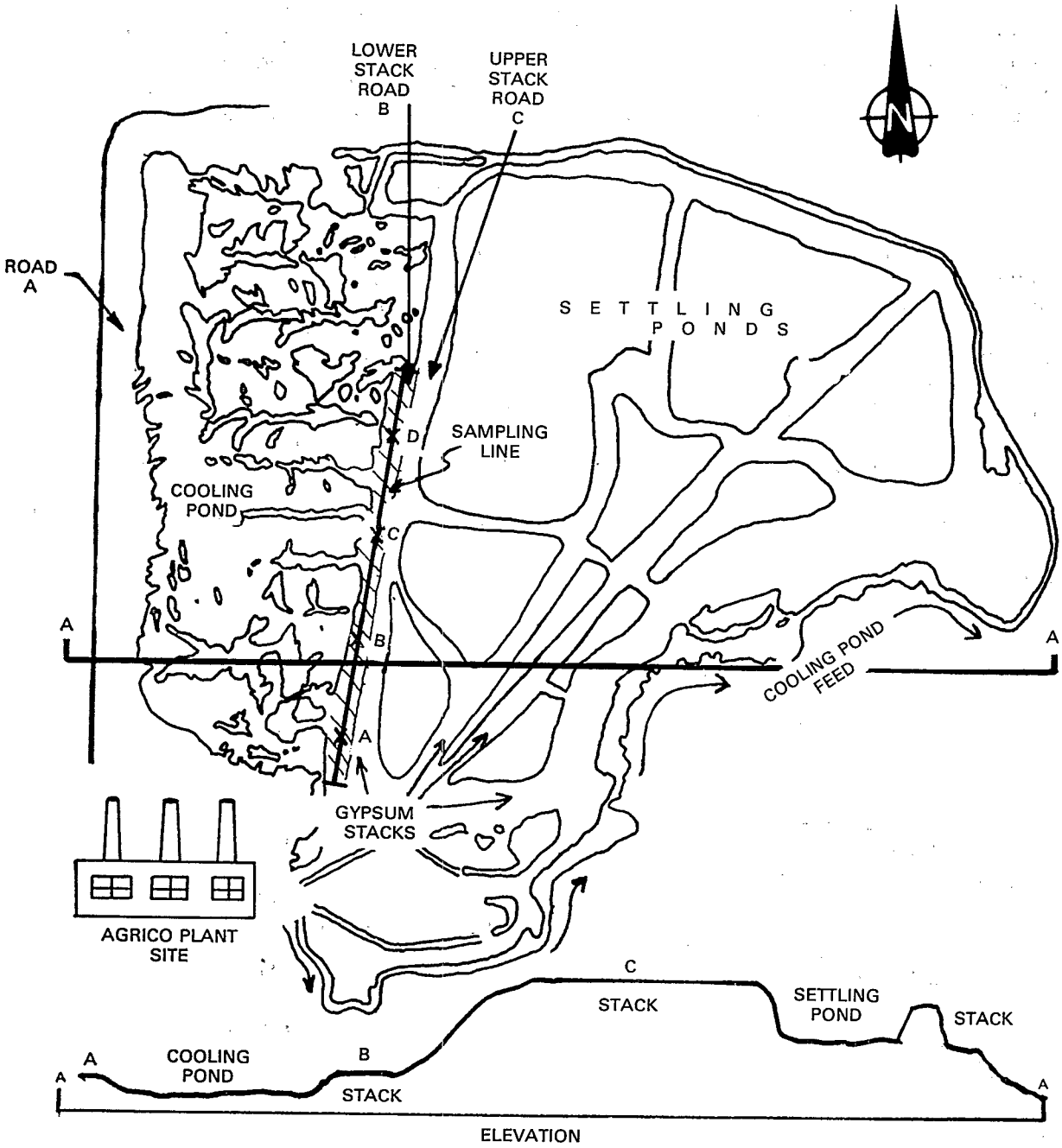

Figure 2. Sampling points at Agrico Chemical Company's gypsum ponds.

LABORATORY PHASE

The laboratory phase was designed to determine the precision, accuracy, and sensitivity of each sampling method under controlled conditions of hydrogen fluoride concentrations. To do so required the generation of precise levels of HF, as described below. Analyses were conducted by ion chromatography with conductometric detection.

HF GENERATION SYSTEM

The design for the HF Generation System and the injection box was supplied by Dr. Jay S. Jacobson of the Boyce Thompson Institute for Plant Research (personal communication of Jacobson and Heller, letter of April 10, 1979). An HF generation system was constructed as illustrated in Figure 3. Air was pumped through an indicating silica gel drying trap, a tube packed with glass wool, and a Whatman 42 filter into heated Teflon tubing at a flow rate of 1.5 dscfm. An aqueous HF solution was pumped at 0.05 ml/min into the heated Teflon tubing (located in the injection box) through which the filtered air flowed. The injection box was kept at 175°F. The fluoride-laden air was then cooled to room temperature in an ice bath and divided. Sampling took place at two points downstream of the flow division. The portion of air that was not sampled was exhausted to a laboratory hood.

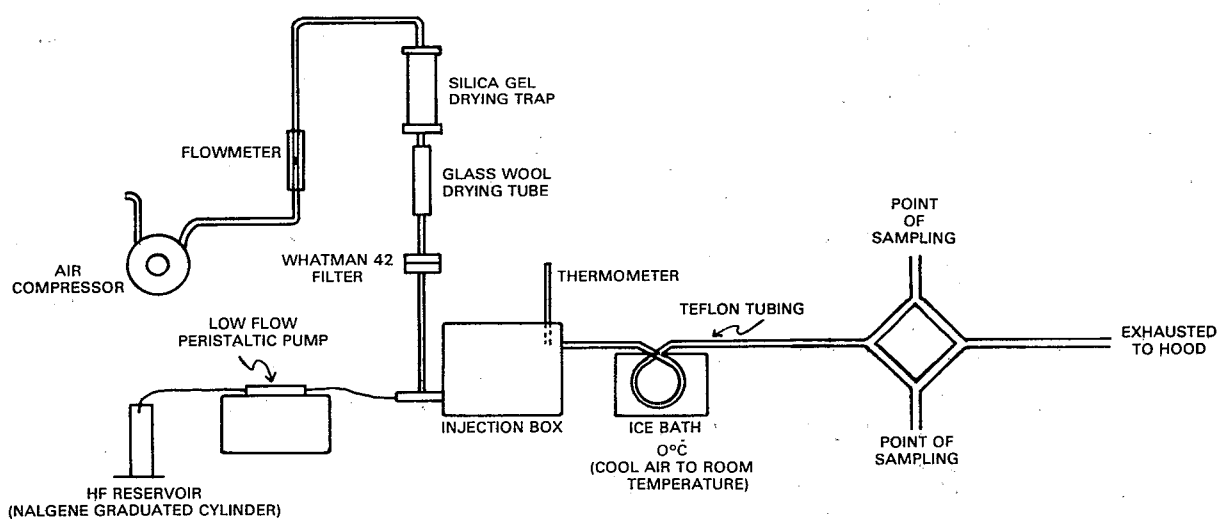

Figure 3. HF generation system.

The amount of fluoride put into the system is dependent on flow rate and the concentration of the HF solution, i.e., the concentration of solu-

tion in the reservoir times the flow rate (μg HF/ml x ml/min = μg HF/min). Adjustment of the air flow rate through the system alters the concentration of fluoride per unit volume of air, but not the amount of fluoride delivered through the system. The latter is controlled by varying the aqueous HF solution concentrations. The concentration of HF in the air stream is determined by the following equations:

$$\mu g\ HF/dsft^3 = \frac{\mu g\ HF\ ml^{-1} \times ml\ min^{-1}}{Vm,\ dsft^3\ min^{-1}}$$

where Vm, $dsft^3$ is at 77°F and 29.92 in Hg

$$\mu g\ HF/dsm^3 = \frac{\mu g\ HF\ dsft^{-3}}{0.02832\ ft^3\ m^{-3}}$$

$$HF\ (ppb) = \frac{\mu g\ HF\ dsm^{-3}}{0.818\ \mu g\ dsm^{-3}\ ppb^{-1}}$$

PRESAMPLING PREPARATION

All glassware and polyethylene sampling bottles utilized in the laboratory phase were cleaned with an Alconox solution and rinsed with tapwater and distilled, deionized water. The glassware was air-dried and capped with parafilm.

The sodium bicarbonate-coated tubes were prepared as outlined in ASTM D3268. The tubes were cleaned with detergent, alcoholic KOH solution, and distilled water. While the inner surface was still wet, a 5 percent (by weight) $NaHCO_3$ solution was poured through the tube to coat the internal surface. Hot, fluoride-free air (prepared by passing air through coiled copper tubing heated by a heating tape) was blown through the tube to dry the sodium bicarbonate on the inner wall.

The Whatman 42 prefilter and Whatman 4 filters were treated with citric acid and sodium hydroxide, respectively, according to ASTM D3266. The filters were immersed in the appropriate solution (either 0.1 m citric acid in 95 percent ethanol or 0.5 N NaOH in 95 percent ethanol and 5 percent glycerin) and dried under an infrared lamp. All filters and tubes were sealed until sampling occurred. At the completion of each sampling run, the filters or tubes were resealed until recovery. The dry gas meters were calibrated according to procedures in APTD 0576.

SAMPLING PROCEDURES

Double Filter Cassette

The double filter cassette sampling train is a modification of ASTM

D3266--i.e., a double filter cassette is used in place of the AISA Automatic Tape Sampler. The constituents of the train (Figure 4) were a 37 mm Millipore filter cassette containing the Whatman 42 filter pretreated with a citric acid solution back to back with the Whatman 4 filter pretreated with a sodium hydroxide solution; a modified Greenburg-Smith impinger containing indicating-silica gel; a dry gas meter and an orifice meter; and a leakless lubricating vane pump.

The sampling rate was 0.5 cfm. Leak checks of all sampling trains were conducted prior to and after each sampling run to determine whether a leak rate greater than 0.02 cfm existed. The cassettes were capped to prevent exposure to the ambient air. After sampling, the inlet and outlet were again plugged. The used filters were placed in clean sample bottles, and 10.0 ml of distilled deionized water and 0.1 ml of 1.0 N NaOH were added. The bottles were sealed tightly until analysis.

Sodium Bicarbonate-Coated Tube

Sampling with the sodium bicarbonate-coated tube was performed as described in ASTM D3268. The train (Figure 4) consisted of a 4-ft glass tube (7-mm ID) evenly coated with sodium bicarbonate, connected directly to a 47-mm polypropylene filter holder containing a citric acid-treated Whatman 42 filter. The tube was followed by the same drying, vacuum, and metering equipment as described for the double filter cassette sampling train.

Both ends of the collecting tube were sealed until sampling took place. After sampling, the ends were capped until recovery. The air to be sampled was drawn through the tube at a rate of 0.5 cfm. Each sampling train was leak-checked before and after the sampling run to determine that no leak greater than 0.02 cfm existed. The collected fluorides were eluted with 8-9 ml of distilled deionized water. One drop of 1.0 N NaOH was added, and the solution was diluted to 10.0 ml. The samples were stored in clean bottles and sealed until analysis.

ANALYTICAL PROCEDURES

The samples from the laboratory phase were analyzed for F^- on a Dionex Model 14 Ion Chromatograph. This automated ion chromatograph incorporates the ion-separating capabilities of the ion exchange column with a conductimetric detection system.

The column system employed for the fluoride analyses consisted of Dionex pre-column (3 x 150 mm) to remove particulates, strongly retained anions, and organic species; a separator column (3 x 250 mm) in the HCO^-_3 form; and a suppressor column (6 x 250 mm) in the H^+ form to remove the background conductivity of the eluent. The eluent, which was a solution of 0.003 M $NaHCO_3$ and 0.0024 M Na_2CO_3, was pumped through the column at a rate of 150 ml/hr. The injection loop had a capacity of 100 µl, and the sample was introduced from a 5-ml disposable syringe fitted with a 0.22-µm Millipore filter to remove particulate matter. A 1N H_2SO_4 solution regenerated

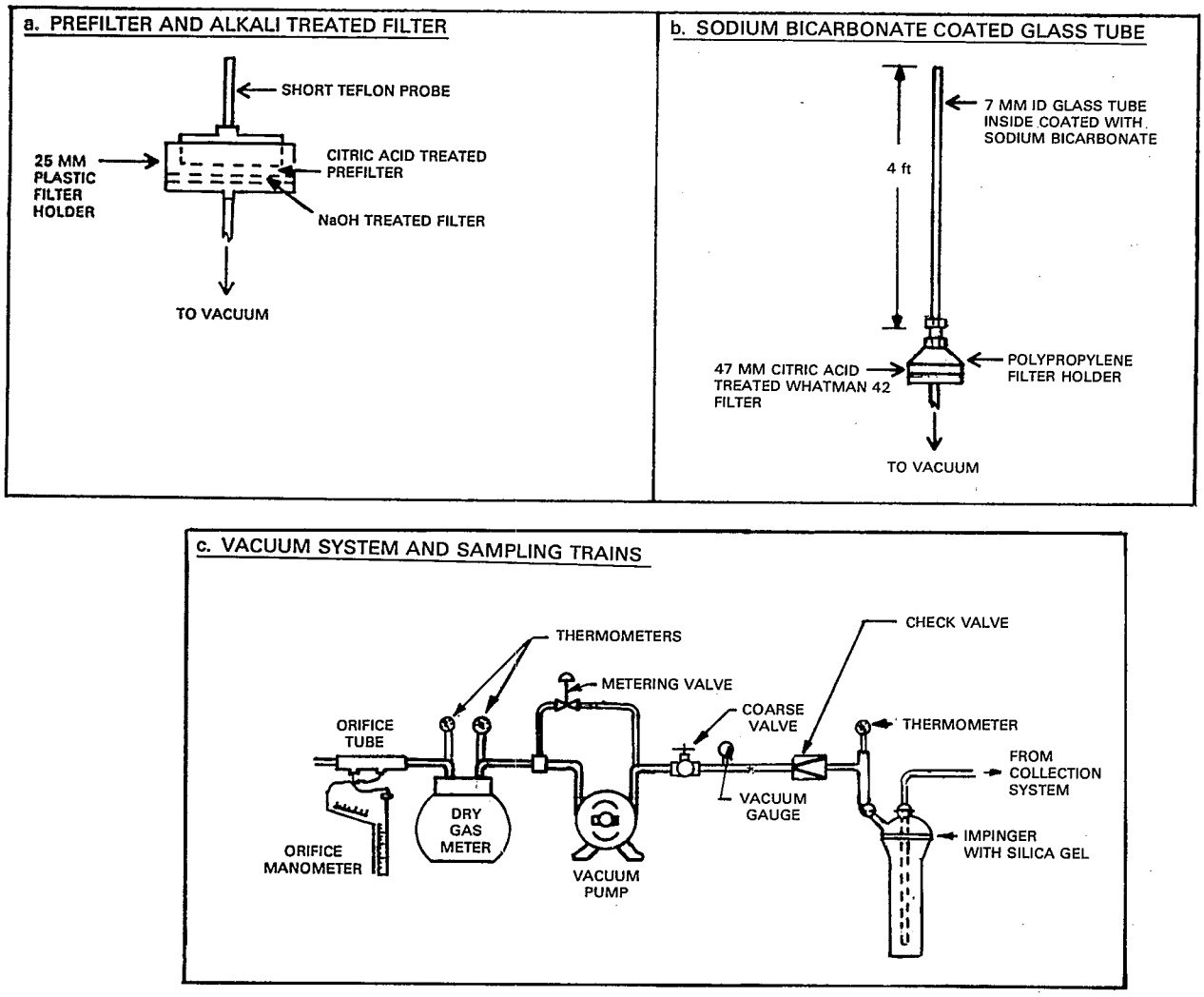

Figure 4. HF sampling trains utilized in the program (a) prefilter and alkali-treated filter (b) sodium bicarbonate-coated glass tube, and (c) vacuum system for sampling trains.

the suppressor column after an 8-hr period.

Blank filters and tubes were prepared and analyzed as previously described for the samples. Values for all samples were blank-corrected.

A series of tests was conducted to determine the intra- and inter-sampling device precision and accuracy at approximately 20, 30, 50, and 60 ppb HF and the sensitivity of the procedures with a sampling duration of 15 minutes. This interval corresponded to the integration period of the ROSE system. Two sets of experiments were performed, one with two of the same sampling device connected to the generation system and the other with one of each sampling device. The results are presented in Table 1. The accuracy--i.e., percent recovery, and inter- and intra-method precision are presented in Table 2. The mean percent recovery of both methods was 100 percent over the range of HF concentrations generated. The mean percent recovery for the filter method was 99.3, and for the tube method was 102.3. The overall precision as measured by the relative standard deviation was less than 8 percent.

PRELIMINARY FIELD SAMPLING PHASE

The preliminary field phase was designed to determine:

1. The compatibility of the selected manual sampling procedures with the sampling location, i.e., the presence or lack of interfering substances, sensitivity levels, etc.

2. The range of ambient HF concentrations at the two ponds.

3. If a sampling period of 15 minutes is compatible with the sensitivity requirements of the analytical techniques.

Sampling Locations

The lines of sight and associated sampling sites for the CFI pond and Agrico pond are shown in Figures 1 and 2. The length of the CFI line was 415 meters and the Agrico line, 630 meters. The lines of sight were divided into four equal segments, and the sampling sites were situated at the center of each segment.

Sampling Protocol

Initially, the double filter cassette was utilized at the four sampling sites at CFI to determine the ambient HF concentration. All four sites were sampled simultaneously. The sampling rate was 0.5 cfm, for a duration of 15 minutes. Three sets of samples were obtained. The filters were treated as described in the laboratory phase and were sent to the GCA laboratory for analysis by IC. The samples were analyzed the next day, and the results were transmitted to the field team. The results are given in Table 3. The values obtained showed that the ambient HF concentration was at a satisfactory level for the sampling and analytical methods. Succes-

TABLE 1. RESULTS OF LABORATORY PHASE

HF generated ppb	HF found ppb							
	Filter 1	Filter 2	Tube 1	Tube 2	Filter	Tube	Tube	Filter
18.2					19	19		
18.2					17	19		
18.2					25	18		
30.8					32	28		
30.8					30	32		
30.8					31	31		
30.8					30	29		
50.1					50	48	48	47
50.1					51	53	55	48
50.1					50	42	49	52
50.1					51	49	49	50
50.1					50	52	50	49
50.1							48	50
50.1							49	
50.1							50	
57.5	54	58						
57.5	58	58						
57.3	54	52						
57.3	54	57						
57.3	55	60						
57.3	58	57						
61.5			59	60				
61.5			67	63				
61.5			82	72				
61.5			62	61				
61.5			63	70				

TABLE 2. PRECISION AND ACCURACY--LABORATORY PHASE

	ppb HF generated	18.2					30.8					50.1					57.4					61.5					$\bar{x}$ F = 47.2 $\bar{x}$T = 48.1, $\bar{x}$ F_T = 49.1					
Group	Parameter	n	$\bar{x}$ ppb R	% recovery	σ_p	RSD_p	n	$\bar{x}$ ppb R	% recovery	σ_p	RSD_p	n	$\bar{x}$ ppb R	% recovery	σ_p	RSD_p	n	$\bar{x}$ ppb HF	% recovery	σ_p	RSD_p	n	$\bar{x}$ ppb	% recovery	σ_p	RSD_p	n	$\bar{x}$ ppb	$\bar{d}$	σ_n	RSD	% recovery
Filter-filter	Within F_1																6	55.5	96.7	1.97	3.6											
	Within F_2																6	57.0	99.3	2.68	4.7											
	Within all filters																12	56.3	98.1	2.38	4.2											
	Between F_1 and F_2																6	56.3		2.88	5.1											
Tube-tube	Within T_1																					5	66.6	108.3	9.07	13.6						
	Within T_2																					5	65.2	106.0	5.44	8.4						
	Within all tubes																					10	65.9	107.2	7.09	10.8						
	Between T_1 and T_2																					5	65.9		6.26	9.5						
Filter-tube	Within filter	3	20.3	111.5	4.2	20.5	4	30.8	100.0	0.96	3.1	5	50.4	100.6	0.54	1.1																
	Within tube	3	18.7	102.6	0.6	3.1	4	30.0	97.4	1.8	6.0	5	48.8	97.4	4.3	8.9																
	Between filter and tube	3	19.5		4.7	24.1	4	30.4		2.5	8.2	5	49.6		4.1	8.3																
Filter	Within all filters											11	49.8	99.4	1.40	2.8																
Tube	Within all tubes											13	49.4	98.6	3.07	6.2																
Filter	Generated-determined																										30	46.9	+0.3	2.73	4.7	99.3
Tubes	Generated-determined																										30	49.2	-1.1	5.05	10.4	102.3
Overall	Generated-determined																										60	48.1	-0.2	3.7	7.6	100.4

σ = n-1 df
R = Recovered
RSD_p = Relative std. dev. = $\frac{\sigma_p \times 100}{\bar{x}}$
σ_p = Precision, as σ either of data or of differences

TABLE 3. PPB HF

Run Site	A	B	C	D
1	50	29	71	95
2	53	35	74	73
3	65	36	76	79

sive samples showed good reproducibility. A concentration gradient along the line of sight was also shown to be present. The wind was blowing from the northeast with a speed of 7-10 mph.

The inter-sampling device experiments were then performed as follows: at both ponds, two sampling trains were set up, one for each device at a sampling site. Because of equipment and power constraints, sites A and B were sampled together and then followed by sites C and D. Five replicates were run. The samples were recovered and returned to GCA for analyses by IC. Some samples were also analyzed by the Agrico Environmental Laboratory using a Technicon Autoanalyzer and the semiautomated spectrophotometric procedure (ASTM D 3270).

The citrate-treated prefilters used in the double filter cassette were also analyzed for fluoride.

Results and Conclusions

Results from the IC method of analysis are presented in Table 4. The data in Table 5 indicate that the filter and tube results are comparable when analyzed by both the IC and spectrophotometric methods. The citrate filter results are presented in Table 6.

Several conclusions can be drawn from the results of the preliminary field phase.

1. A sampling period of 15 minutes was adequate for both the filter and tube collection methods for measuring the HF concentration at each of the gypsum ponds.

2. No interferences were observed when either filter or tube samples were analyzed by either the IC or autoanalyzer methods. A previous ROSE study has found that a possible interferent, SiF_4, was not present in the atmosphere above the gypsum ponds (10).

3. The citrate-treated prefilter was intended to remove particulate matter and was not supposed to remove any HF. The results indicate that essentially no fluoride was collected on the citrate prefilter.

TABLE 4. PRELIMINARY FIELD PHASE: RESULTS AND INTERSAMPLING DEVICE PRECISION AT SAME SITE

Group	Filter ppb HF	Tube ppb HF	d (F-T)	σ_d	Group	Filter ppb HF	Tube ppb HF	d (F-T)	σ_d
	59	41	18						
	50	24	26	14.2		23	21	2	
	28	23	5			29	24	5	
CFI	17	25	-8		Agrico	27	28	-1	4.4
Site A	21	24	-3		Site A	23	30	-7	
	Σ 175	137	38			Σ 102	103	-1	
	$\bar{x}$ 35	27.5	7.6			$\bar{x}$ 25.5	25.8	-0.3	
	43	42	1			54	32	22	
	19	19	0			24	24	0	
	37	36	1	1.6		32	23	9	11.6
CFI	18	15	3		Agrico	39	29	10	
Site B	18	17	1		Site B	36	38	-2	
	Σ 135	129	6			Σ 185	146	39	
	$\bar{x}$ 27.0	25.8	1.4			$\bar{x}$ 37.0	29.2	7.8	
	14	17	-3			35	32	3	
	32	27	5			35	25	10	
	35	30	5	4.8		39	31	8	6.1
CFI	14	21	-7		Agrico	40	42	-2	
Site C	21	18	3		Site C	40	37	3	
	Σ 116	113	3			Σ 189	167	22	
	$\bar{x}$ 23.2	22.6	0.6			$\bar{x}$ 37.8	33.4	4.4	
	57	30	27			19	16	3	
	36	17	19			37	24	13	
	17	36	-19	22.1		43	39	4	7.1
CFI	36	17	19		Agrico	46	38	8	
Site D	42	17	25		Site D	47	45	2	
	Σ 188	117	71			Σ 192	162	30	
	$\bar{x}$ 37.6	23.4	14.2			$\bar{x}$ 38.4	32.4	6.0	

Group		Filter ppb HF	Tube ppb HF	d (F-T)	σ_d
Grand	Σ	1282	1074	208	
n = 39	$\bar{x}$	32.9	27.5	5.3	11.3
CFI	Σ	614	496	118	
n = 20	$\bar{x}$	30.7	24.8	5.9	12.5
Agrico	Σ	668	578	90	
n = 19	$\bar{x}$	35.1	30.4	4.7	6.5

TABLE 5. PRELIMINARY FIELD PHASE COMPARISON OF RESULTS FOR ANALYSIS BY IC AND AUTOANALYZER

Site	Sampling device	ppb/HF IC	AA	d	d^2
CFI A	T	24	21	+3	
CFI A	F	17	38	-21	
CFI D	T	36	34	+2	
Agrico A	F	29	27	+2	
Agrico A	F	38	26	+12	
Agrico B	T	32	35	-3	
Agrico B	T	24	30	-6	
Σ		200	211	-11	647
$\bar{x}$		28.57	30.14	-1.57	
σ_d				10.2	
$\frac{\sigma}{\sqrt{n}} = \sigma_{\bar{d}}$				3.855	
$\frac{\bar{d}}{\sigma_d} = 0.407$					
$t_{.975} = 2.447$					

Note: No significant difference between the two methods of analysis.

TABLE 6. ANALYSIS OF CITRATE FILTERS FOR FLUORIDE

Sample	F^- (μg/mL)	Blank (μg/L)	Net F^- (μg/L)
1	0.37	0.36	0.01
2	0.38	0.36	0.02
3	0.36	0.36	0
4	0.35	0.36	0

4. The precision between the two manual sampling devices is shown in Table 4. In most of the runs, the quantity of ppb collected by each method is comparable; both methods can be used for HF sampling, since the quantities of HF collected are similar for samples collected simultaneously.

FORMAL FIELD PHASE

The objective of the formal field phase of the project was to compare the results of the simultaneous measurement of ambient HF levels as

obtained by manual wet chemical sampling methods with the EPA ROSE system. Both sampling systems were located along the edge of the gypsum ponds at both CF Industries and Agrico Chemical Co. Sampling at CF Industries was conducted on July 24th and 25th, 1979, while samples were obtained at Agrico on July 26, 1979.

Sampling Locations

The sampling line of sight was adjacent to each pond, as shown in Figures 5 and 6. The ROSE van and light source were aligned visually and the distance between them measured with a laser rangefinder. At CF Industries, the line of sight for the ROSE system was 3 feet east of the wet chemical sampling line. At Agrico, the line of sight for the ROSE system was bracketed on each side with the positions of the sampling sites being determined by the configuration of the road. The line of sight established at each pond was divided into four equal segments. One manual sampler was situated at or as close as possible to the center of each segment. The height of the inlet of each of the manual sampling devices was at the midpoint of the light beam, but did not interfere with the beam. The locations designated A, B, C, and D were determined by the restraints of the terrain and positions of the electrical generators.

Sampling and Analytical Procedures

Manual Wet Chemical Methods

Two collection devices were used with the manual sampling trains (Figure 4); i.e., (1) a filter cassette containing a citric acid-treated prefilter followed by a sodium hydroxide-treated filter (designated F), and (2) a sodium bicarbonate-coated pyrex tube (designated T). The vacuum/metering system was a Research Appliance Corporation (RAC) meter control console, which was calibrated according to procedures delineated in EPA publication APTD 0576. The filters and tubes were prepared as previously described. Regardless of the collection device (filter or tube), the sampling train was used at all four sample locations. The air was sampled at a rate of 0.5-0.6 acfm for a period of 16 minutes. Twenty runs were conducted at CF Industries. All odd-numbered runs were executed with the filter cassettes, and the even-numbered runs used tubes for sample collection. The initial 10 runs were conducted on July 24, 1979, and the remainder of the samples at CF Industries were collected the next day. Test samples for 18 runs (No. 21-38) were collected at the Agrico gypsum pond on July 26, 1979. Two sets of samples were collected with the filter cassette, followed by one run with the bicarbonate-coated tube. This sequence was repeated six times. The sampling rate and duration was the same as for the CFI runs.

After completion of the sampling runs, the collection devices were removed and the samples were recovered as follows:

Filter - The sodium hydroxide filter was placed in a 125-ml LPE bottle; 10 ml of distilled deionized water and 0.1 ml of 1N NaOH were added. The bottle was capped and swirled.

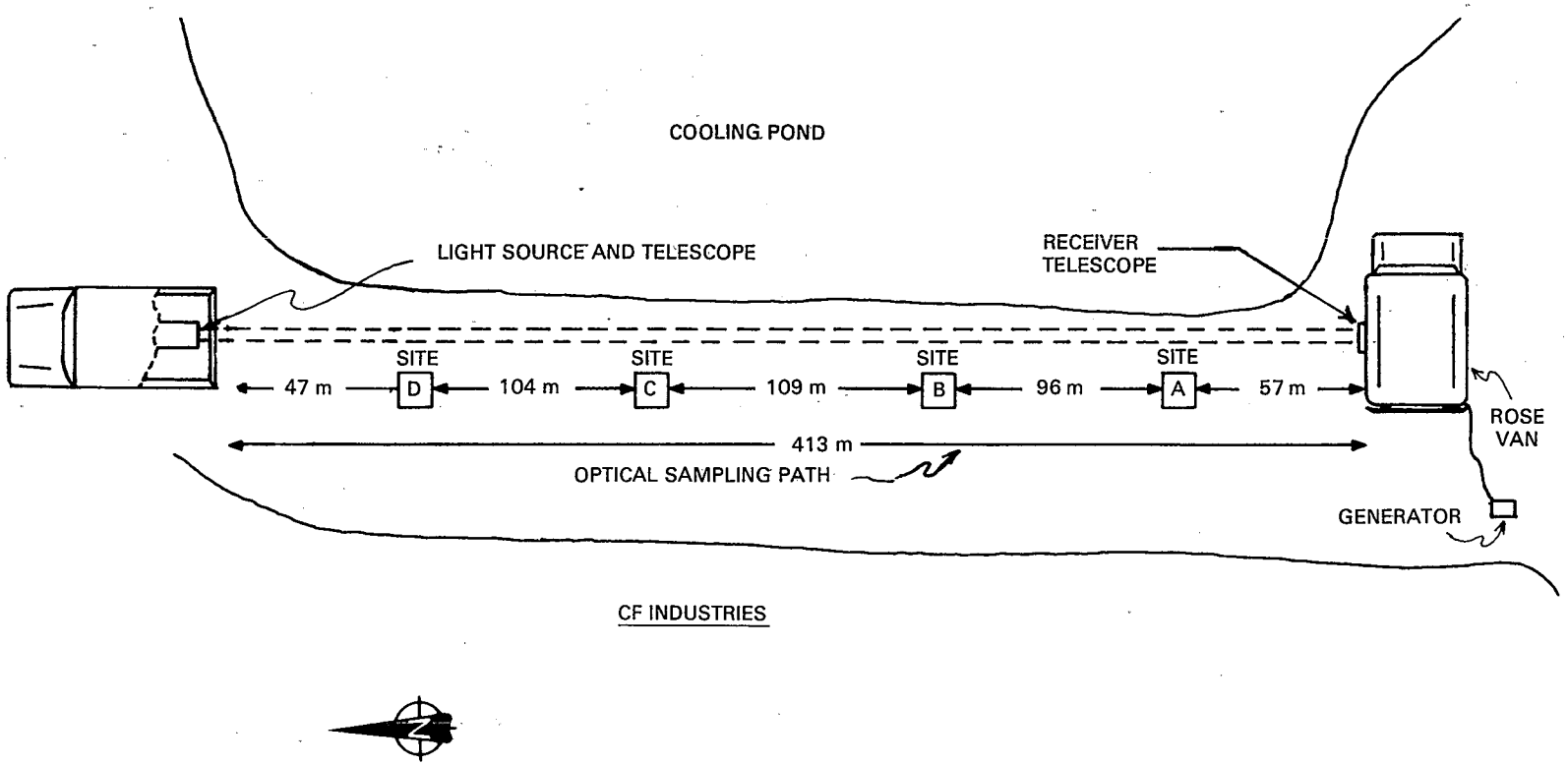

Figure 5. Line of sight of CF Industries.

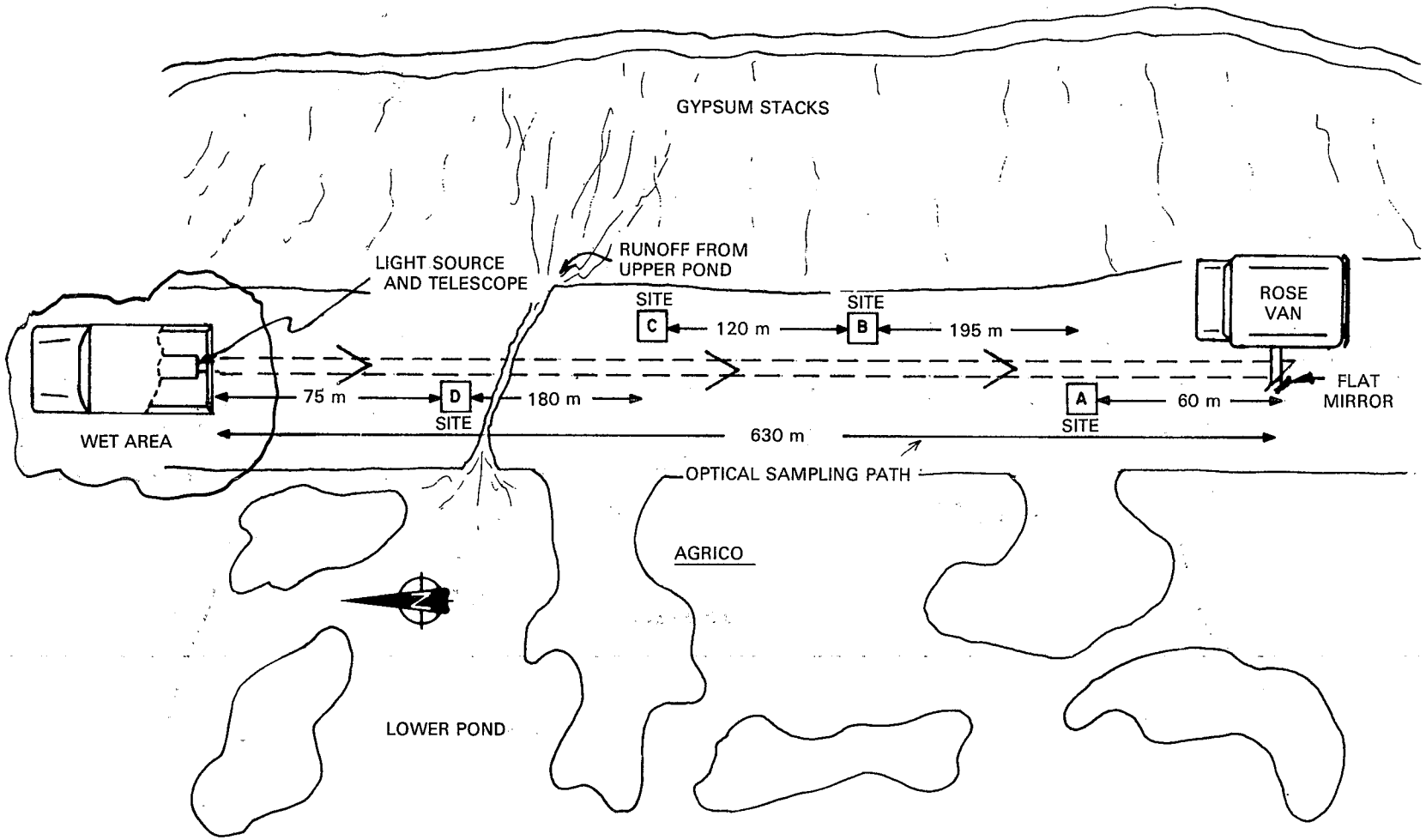

Figure 6. Line of sight at Agrico.

Tube - Two 5-ml portions of distilled deionized water were poured onto the inner surface of the tube; the tube was swirled and the liquid collected in a 125-ml LPE bottle. To preserve the sample, 0.1 ml of 1N NaOH was added. The bottle was capped and swirled.

Blank filters and tubes were also subjected to the above procedure.

All samples were analyzed the day after they were collected at the Agrico Analytical Laboratory using the semiautomated spectrophotometric procedure with a Technicon Auto Analyzer system (ASTM D3270). The remaining aliquots of the CFI samples were brought back to the GCA Laboratory for analysis by IC. Because of difficulties with the ion chromatograph, the samples were analyzed approximately 4 weeks after they were collected. The data for the IC analyses correlated well with the data for spectrophotometric analysis, as was also shown for the preliminary phase data. A t-test indicated no significant difference between the two data sets.

Remote Optical Sensing of Emissions (ROSE) System

The EPA Remote Sensing of Emissions (ROSE) system consists of a commercial Fourier transform infrared (FT-IR) spectrometer system and auxiliary equipment installed in a van. The ROSE system has been used in a variety of source characterization studies and is described in detail in the literature (1,11,12). For the gypsum pond measurements, the system was operated in the longpath absorption mode, as indicated in Figures 5 and 6. The optical system inside the van is shown in Figure 7. The light source is a 1000-Watt quartz-halogen lamp. Energy from the lamp is collimated by a Dahl-Kirkham f/5 telescope with a 60-cm-diameter primary mirror. The collimated infrared beam is transmitted through the atmosphere and passes through a port in the side of the van, where an identical telescope focuses the beam onto the aperture of the interferometer. The interferometer is part of a standard Nicolet Instrument Corporation Model 7199 FT-IR system configured to fit into the van.

Major components of the interferometer system consist of a computer with 40K memory; dual-density disk with a 4.8 million, 20-bit word capacity; teletyper; paper tape reader; oscilloscope interactive display unit; and a high-speed digital plotter. Each traverse of the interferometer mirror produces an interferogram, which is actually the Fourier-transform of the spectrum of the incoming infrared signal. A liquid-nitrogen-cooled InSb/HgCdTe sandwich detector is used to convert the infrared signal to an electrical signal for processing. The InSb detector, which is sensitive over the 1800-6000 cm^{-1} region, was used for the HF measurements. For each 16-minute data set, 100 interferograms were averaged. The data were collected at a spatial resolution of 0.125 cm^{-1}. The computer requires about 12 minutes to calculate the spectrum from the interferograms; each spectrum was permanently stored on disk for later analysis.

Sampling Protocol

The manual collection devices were set into the four sampling trains

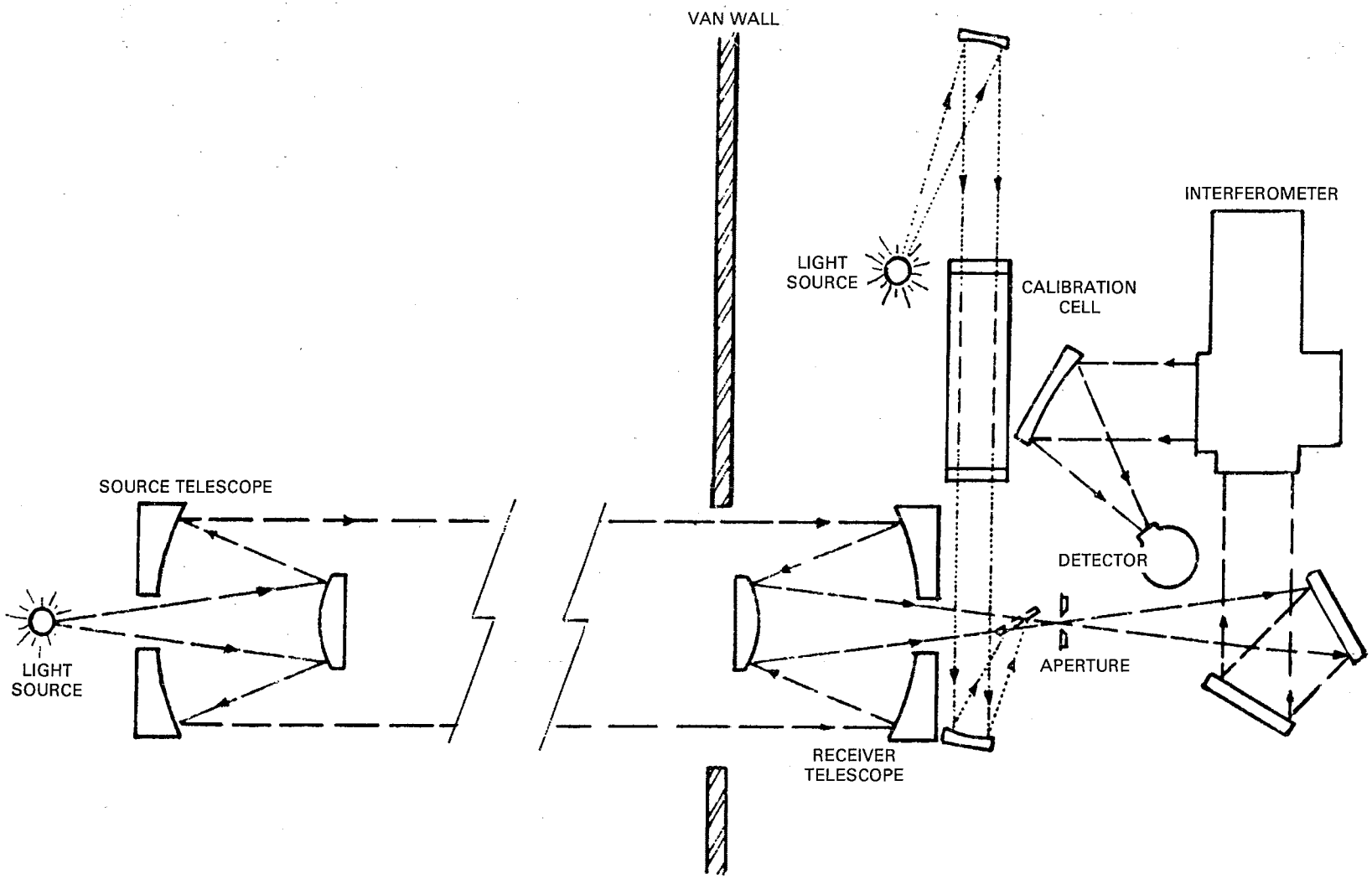

Figure 7. The ROSE optical system.

and initial system readings obtained. The four samplers and the ROSE system were then started simultaneously. The sampling and spectral accumulation proceeded for 16 minutes. All systems were stopped simultaneously. The final readings for the manual samplers were obtained and the spectra obtained by the ROSE were checked. Coordination between the two sampling methods was handled through two-way radio communications and recording of run start times.

Calculations

Manual Methods

1. The volume of dry gas sampled is converted to standard conditions, 777°F and 29.92 "Hg (25°C nd 760 mm Hg).

$$\text{VMstd} = \text{dry std ft}^3 = \frac{537\ (Y)\ (VM)\ \ PB + \frac{PM}{13.6}}{(29.92)\ (TM)}$$

where Y = dry gas meter calibration factor

VM = sample gas volume, ft^3

PB = barometric pressure "Hg

PM = ΔH, pressure at DGM "H_2O

TM = temperature at dry gas meter, °R (°F + 460)

537°R = 77°F + 460

2. Vmstd, dry std., m^3 = Vmstd (dry std. ft^3) x 0.02832 $m^3\ ft^{-3}$

3. The concentration of HF in the ambient air is determined by:

$$\mu g\ HF/m^3 = \frac{\mu g\ F^-/_{ml}\ x\ V_L x \frac{20.006\ (HF)}{18.998\ (F)}}{\text{Vmstd}\ (m^3)}$$

where V_L = volume of sample, ml

4. The concentration in ppb is:

$$\text{ppb HF} = \frac{g\ HF/m^3}{0.818\ \mu g/m^3,\ \text{ppb}}$$

$$\text{where } 0.818 = \frac{20.006\ \mu g/\ \text{mole x } 10^9\ \ L/m^3}{24.45\ \mu L/\ \text{mole x } 10^9\ \text{ppb}^{-1}}$$

5. The four results from each manual sampling run were averaged arithmetically and geometrically.

$$\bar{X} \text{ Arithmetic} = \frac{\sum_{1}^{4} X_i}{n-1}$$

$$\bar{X} \text{ Geometric} = [(X_A)(X_B)(X_C)(X_D)]^{1/4}$$

Calibration of ROSE System Data

Calibration of ROSE system absorption spectra obtained in the field is normally done by measuring the absorption spectra of known amounts of various gases contained in a calibration cell (shown in Figure 7). The transmittance of the gas sample as a function of wavelength (or wavenumber) is related to the cell length and gas concentration by Beer's Law:

$$\tau(\nu) = e^{-K(\nu)CL}$$

where ν = wavenumber (cm^{-1})

C = concentration (ppm)

L = path length (meters)

$K(\nu)$ = spectral absorption coefficient (ppm meters)$^{-1}$.

Once $K(\nu)$ has been determined from the calibration spectra, its value can be used with longpath absorption spectra obtained in the field to calculate the path-average gas concentration (again using Beer's Law). For the field spectra, the path length L from the source telescope to the receiver telescope is measured using a laser range-finder.

Because of its high reactivity, HF requires a special gas handling system for filling calibration cells. Such a system was not available at the EPA laboratory. Therefore, another method, which is based on measuring the area under the absorption curve of the spectral line in question, was used to assist in determining $K(\nu)$. The particular advantage of this method is that the area under the absorption curve is independent of the spectral resolution used, which allows the use of HF data obtained at low resolution (13,14) to be used as calibration data. From the low resolution data, the relationship between the area under an absorption line and the gas optical depth (product C x L) was determined (private communication of D.E. Burch and D.A. Gryvnak, Aeronautic Division of Ford Aerospace and Communications Corporation), and the resulting calibration curve for the R(5) line of HF at 4174 cm^{-1} is shown in Figure 8. The R(5) line was selected for the concentration calculation and because it provides the most suitable compromise between maximum line strength and minimum water vapor interference. The spectral signatures of clean air and the gypsum pond are shown in the 4168 to 4178 cm^{-1} region in Figure 9. It is seen that there

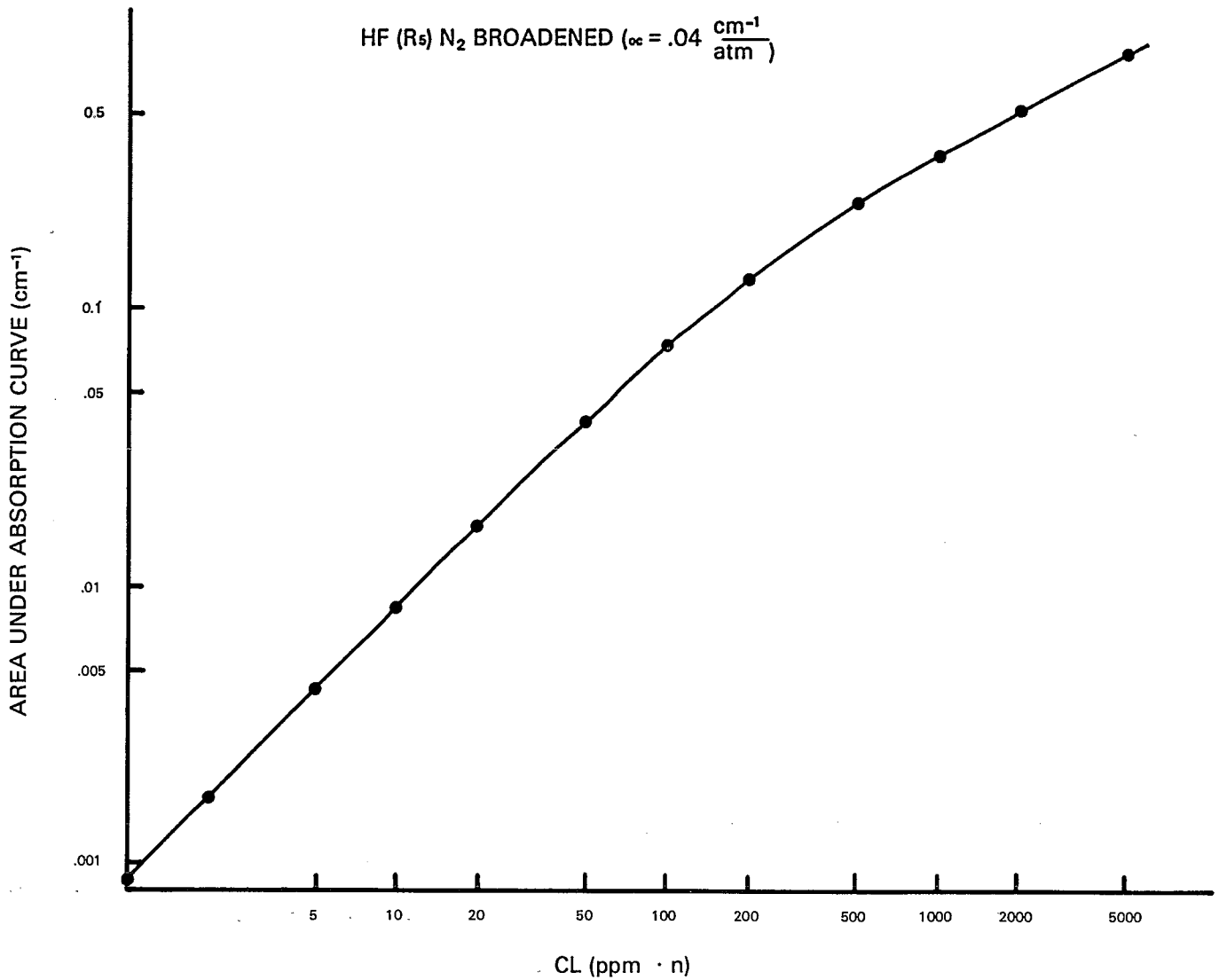

Figure 8. Concentration calibration curve for the R(5) line of HF.

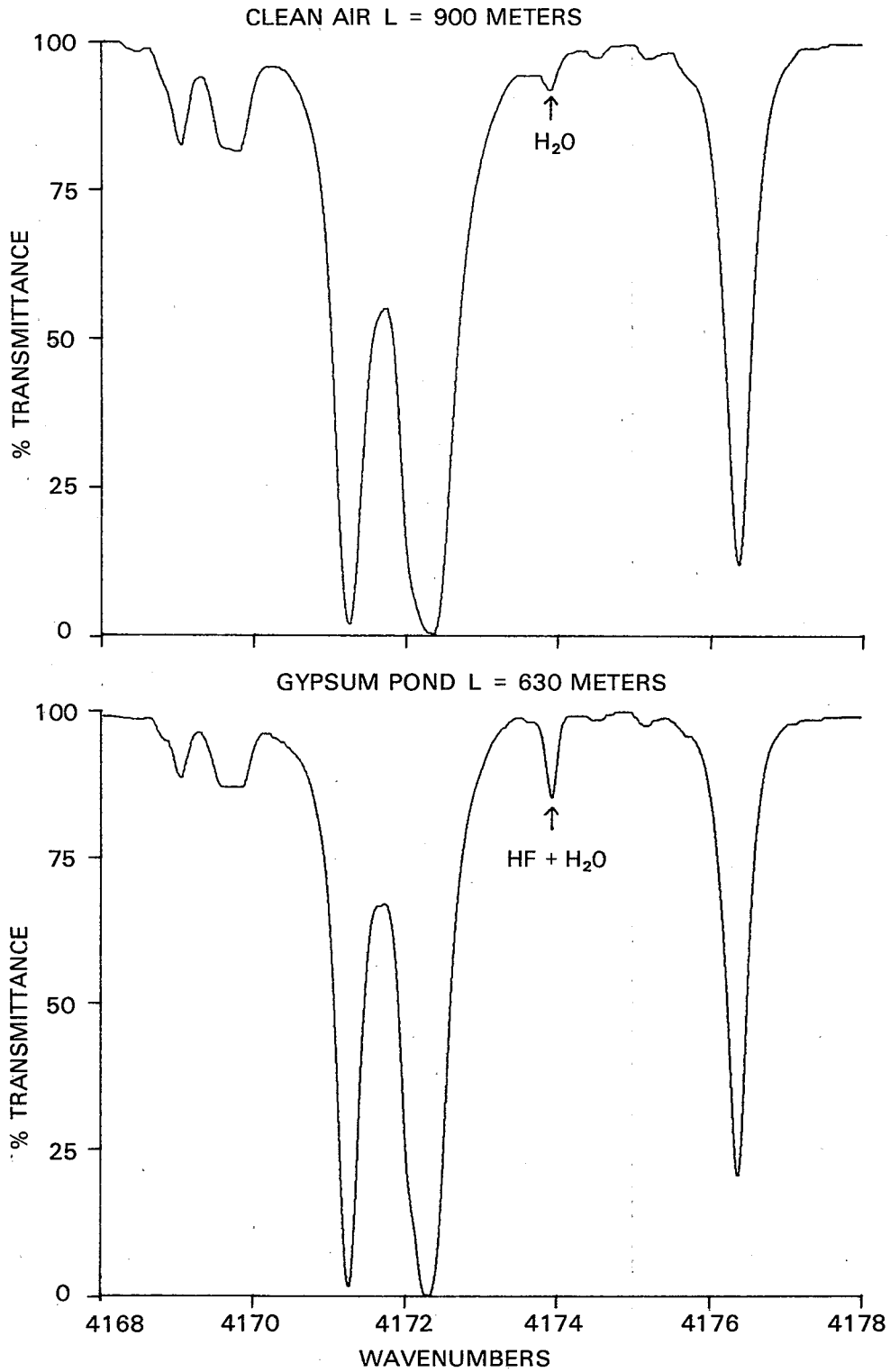

Figure 9. Clean air and gypsum pond spectra (average of Agrico ROSE Runs 32-38.

are weak H_2O lines at approximately 4173.6 and 4173.9 cm^{-1}. The method used to eliminate the H_2O interference and determine the value of $K(\nu)$ is described below.

First, the spectral data from each of the four measurement periods (two mornings at CFL, and a morning and afternoon at Agrico) were averaged to produce four single spectra with excellent signal-to-noise ratios. (Figure 9 shows the average of ROSE system runs No. 32-38.) Next, the clean air and gypsum pond absorption spectra were converted to absorbance [$-\mathrm{Log}\,\tau(\nu)$]. The clean air spectrum was then multiplied by a factor determined so as to make the maximum absorbance of the water vapor line at 4176.4 cm^{-1} equal in both spectra (Figure 10). In this way, the optical depth (C x L) of H_2O was made equal in each spectrum. The background spectrum was then subtracted from the pond spectrum and the result converted back to transmittance (Figure 11). (All of the mathematical operations were carried out with standard system software.) The area under the HF absorption line was then measured manually for each of the four spectra, and an HF concentration was determined from Figure 8. A value of $K(\nu)$ could then be calculated from Beer's Law for each of the spectra, since $\tau(\nu)$, C, and L were now known. The four values obtained were 5.14, 5.04, 5.29, and 5.09 x 10^{-3} (ppm meters)$^{-1}$. The average of these values, 5.14 x 10^{-3}, was taken as the value of $K(\nu)$ for the R(5) line of HF. Each individual pond spectrum could then be calibrated in the following manner.

Each individual pond spectrum was expressed in absorbance over the 4168-4178 cm^{-1} region, and the clean air (background) absorbance spectrum was adjusted as described above to make the H_2O line at 4176.4 cm^{-1} have equal optical depth for each pond and background spectra. The two spectra (each pond and the background) were then superimposed, as shown in Figure 12, in such a manner as to best match the spectral features on each side of the HF line. The absorbance at the HF line center was measured directly from the superimposed plots (difference between pond and background spectra at the HF line center). For the example shown (ROSE Run No. 38 at Agrico):

$$\text{Absorbance at line center} = 0.061$$

$$\tau = 10^{-0.061} = 0.869$$

$$KC\,L = -\mathrm{Ln}\,\tau = 0.140$$

$$KL = 5.14 \times 10^{-3} \times 630 = 3.24$$

$$C = 43 \text{ ppb}$$

The principal error in this measurement is in the baseline determination (i.e., the mismatch of the spectra on each side of the HF line). The maximum error is approximately ±0.005 absorbance units, which is equivalent to approximately ±3.5 ppb.

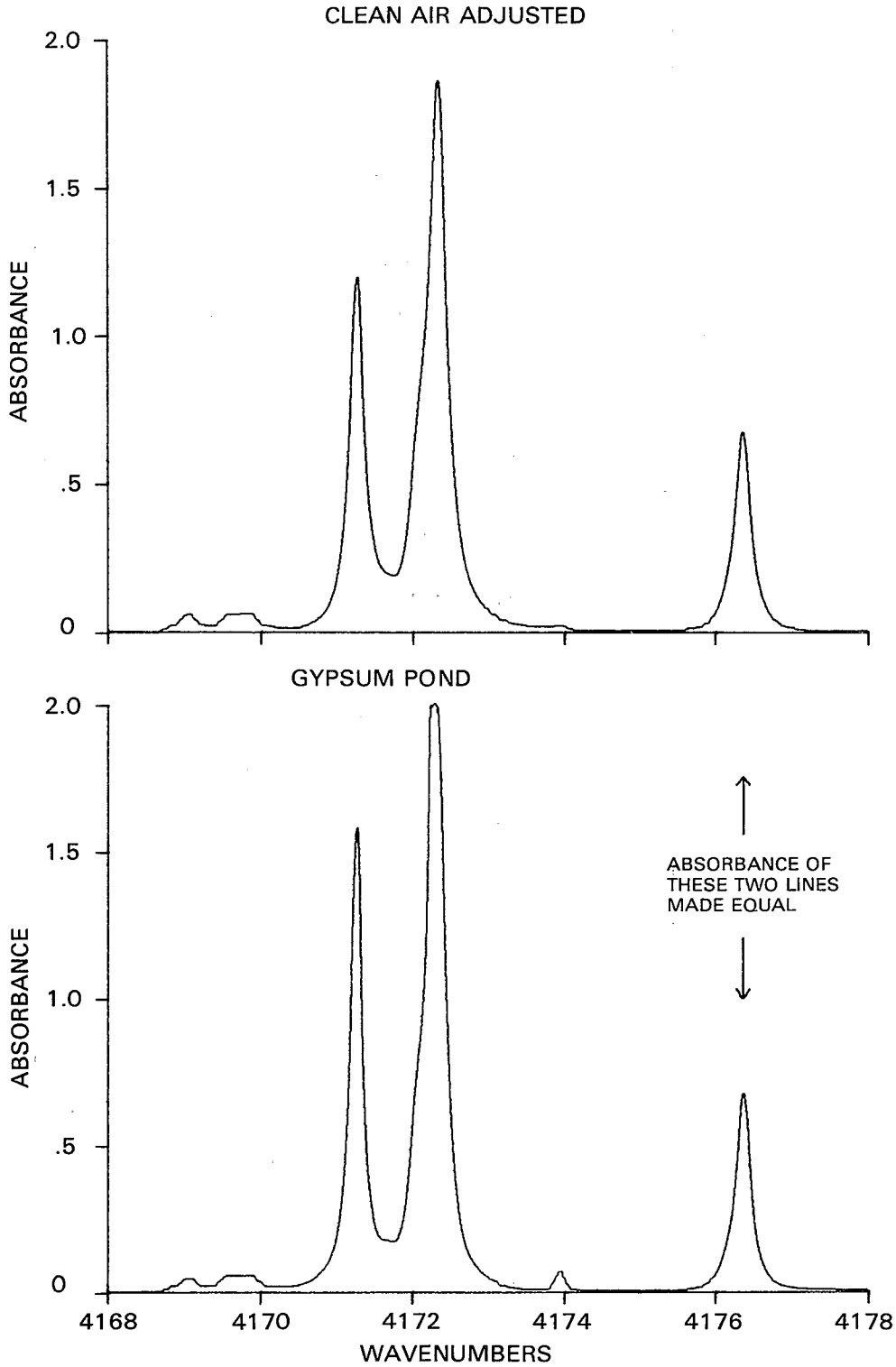

Figure 10. Adjusted clean air and gypsum pond absorbance spectra.

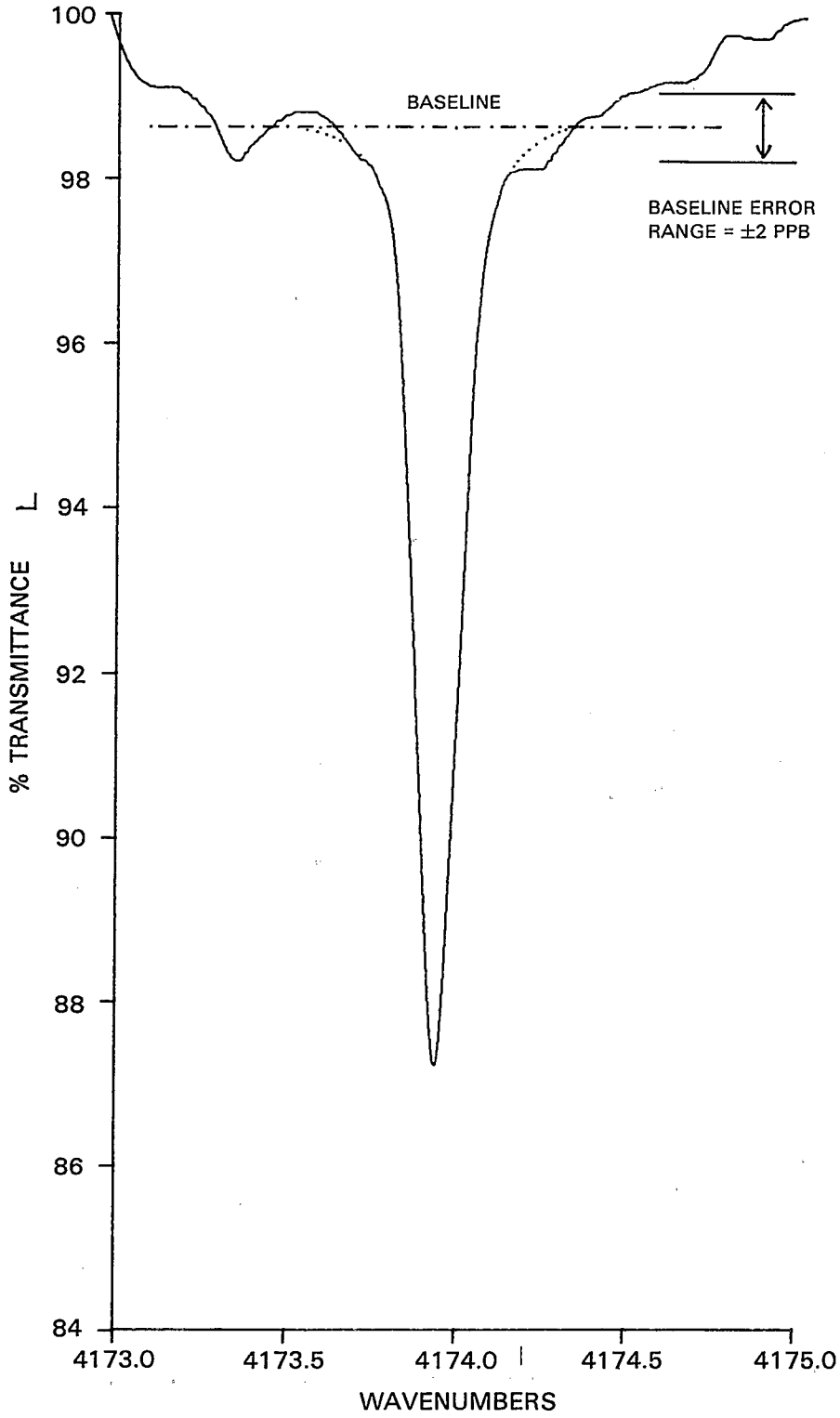

Figure 11. Transmittance of HF line after background subtraction.

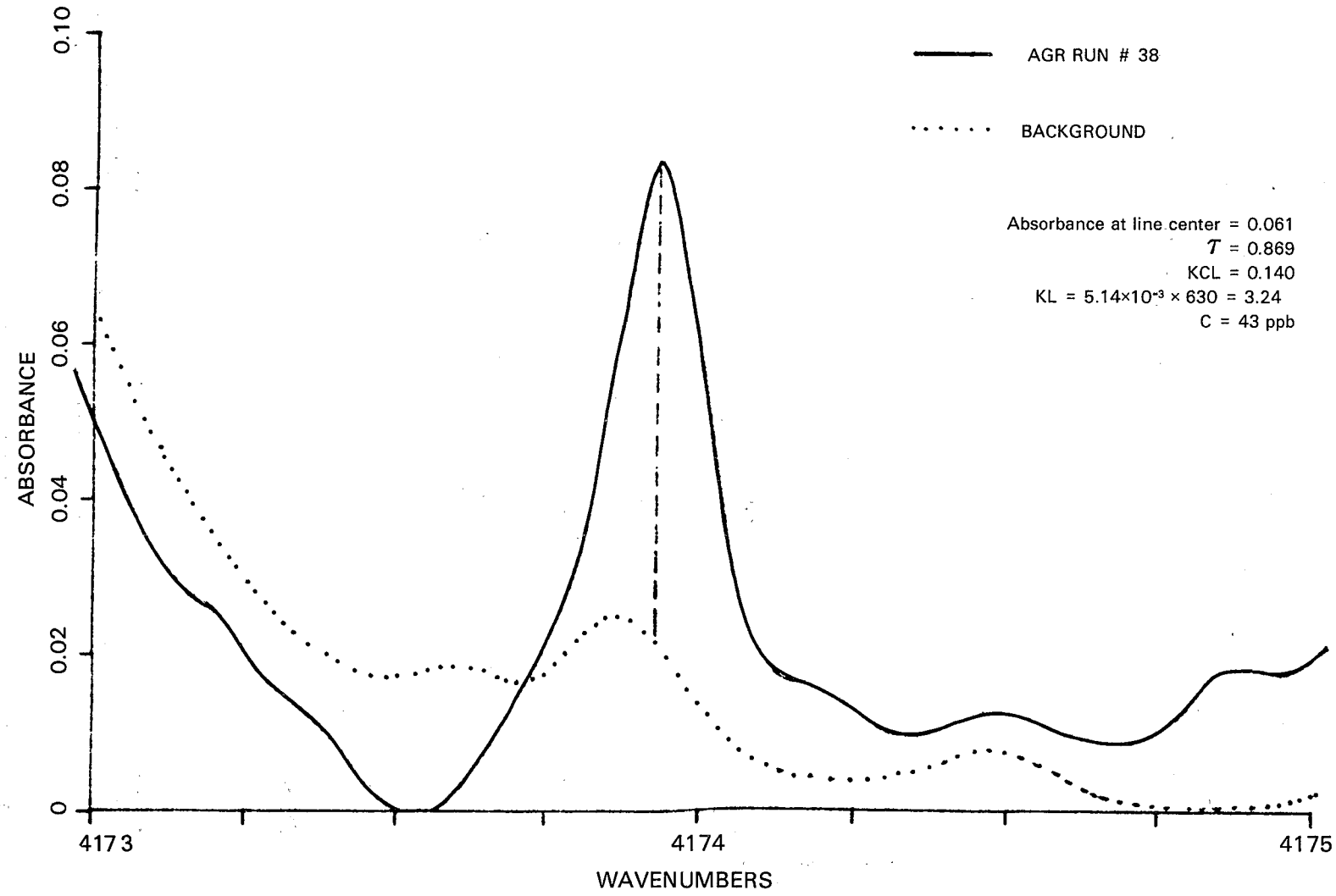

Figure 12. Determination of HF line center absorbance by elimination of H_2O interference.

ROSE System Sources of Error

Potential sources of error in ROSE system measurements have been studied extensively under both laboratory and field conditions. The laboratory studies have addressed system reproducibility and calibration error. The reproducibility of the system was tested by collecting 10 separate sets of interferograms at 0.125 cm^{-1} (50 in each set) on the same gas sample in a cell. Each set was transformed to give a single spectrum. It was found that the peak height of individual absorption lines was reproducible to within ±1 percent of the peak height value. Conventional calibration procedures were evaluated by filling the calibration cell to the same nominal pressure several times and collecting a set of interferograms after each fill. In this case the error was determined by the accuracy with which the pressure gauge in the gas handling system could be read (about ±5 percent). The error in the area method used for the HF calibration is certainly no worse than this value.

Error in field measurements tends to be greater than in laboratory measurements simply because, as the light source is moved further and further from the van, less energy is collected, and the S/N ratio decreases. The most reliable test of the system for field measurements is to compare from run to run the spectra obtained for the gases CO_2 and N_2O. Since these species have essentially constant concentrations, comparison of spectra from different runs gives a measure of the overall instrument reproducibility. Eight runs from Agrico were studied. At the spectral region of maximum S/N, the maximum variation in peak height for eight CO_2 and eight N_2O lines was 5.5 percent of the peak height. Because of the fall-off in detector sensitivity toward shorter wavelength, the S/N ratio is about four times less at the region of HF absorption than at the regions of CO_2 and N_2O absorption. Another CO_2 band, located where the S/N is the same as HF, was similarly studied. For eight spectra, the maximum variation was 14.2 percent of the peak height. A combination of the reproducibility error with the calibration error leads to an estimate that the error in any single HF measurement (average of 100 interferograms) would be ±15 percent.

The two manual sampling methods for the collection of HF have been studied in the laboratory and field and the results of these experiments are presented above. The percent recovery of HF for each method was shown to be about 100 percent, and the precision for each sampling device for the laboratory phase is given in Table 2. For both sampling devices, the relative standard deviation was less than 10 percent for HF concentrations above 18 ppb. The percent recovery and precision, as shown in the above tables, are a reflection of the sources of error in both the sampling devices and the analtyical method. In the laboratory phase, ion chromatography was used to analyze the samples for HF.

The precision obtained in the preliminary field phase is presented in Table 4. Again, ion chromatography was used to determine HF in the samples.

For the formal field phase, the samples were analyzed by the colori-

metric method with an Technicon Autoanalyzer. The precision and accuracy of the semiautomated method have been documented in ASTM-Method D3270. A collaborative study by nine laboratories using the method for the determination of HF in vegetation gave relative standard deviations ranging from 4 to 13.4 percent of different types of vegetation. Replicate analyses of standard NaF solutions by four laboratories had relative standard deviations of 11.4, 3.9, and 3.0 percent for solutions containing 0.28, 1.41, and 2.81 μg/ml, respectively. Replicate analyses of standard NaF solutions by four laboratories showed average recoveries of 101.8, 101.4, and 100.7 percent for solutions containing 0.28, 1.41, and 2.81 μg F/ml, respectively.

RESULTS AND DISCUSSION

The results are presented in Table 7 in the sequence in which the samples were collected. Graphical representations of the data are presented in the following figures.

- Figure 13 plots the HF concentration measured at each site by the manual methods, the arithmetic average of the manual methods, and the ROSE system.

- Figure 14 is a plot of the HF concentration as measured by the ROSE system vs. the HF concentration as determined by the arithmetic average of the manual methods. The theoretical 1:1 correspondence line is indicated.

The ROSE system measures the average concentration of HF molecules in the 30-cm-diameter cylinder extending through the atmosphere from the source to the receiver telescope. The point sampling systems measure the point concentrations of HF. Both the optical and point method measurements were averaged over 16-minute time intervals for each sampling period. If the HF concentration were relatively uniform along the sampling path, fairly small differences would be expected between values obtained at the four sampling sites during a given sampling period, and reasonable agreement between an average of the sampling site values and a ROSE measurement would be expected. If, on the other hand, there were appreciable concentration gradients along the path, then the two methods could give widely differing results without either being "incorrect." The situations that best illustrate this are: (1) a spatially small but high concentration HF pocket could slowly traverse the area of a single point monitor (the result would be a high reading at one site, but no appreciable affect on the ROSE data); and (2) an extended pocket of high HF concentration that slowly passed through the optical path but missed the point monitors (obvious results).

Inspection of data shown in Figure 13, with the above in mind, shows the following:

(1) During the sampling at CFI on July 24 the HF concentration spread between sampling sites is at maximum about ±35 percent of

TABLE 7. HF CONCENTRATION DATA GROUPED IN SEQUENCE OBTAINED

Date	GCA run no.	Sampling start time	Concentration (ppb) Manual sampling Site A	B	C	D	Arith-metic mean	Geo-metric mean	Collec-tion device*	ROSE method
7/24/79 (CFI)	4	1043	27	44	52	27	38	36	T	42
	5	1124	32	32	35	32	33	33	F	39
	6	1200	44	36	--	36	39	39	T	40
	7	1224	35	57	50	50	48	47	F	43
	8	1246	46	24	40	30	35	34	T	30
	9	1307	44	48	43	45	45	45	F	43
	10	1330	42	40	30	40	38	38	T	32
Mean			38.6	40.1	41.7	37.1	39.4	38.0		38.4
7/25/79 (CFI)	12	0830	19	15	22	51	27	24	T	27
	13	0940	34	58	43	48	46	45	F	28
	14	1005	14	98	25	29	42	32	T	32
	15	1027	32	34	51	75	48	45	F	39
	16	1050	22	106	--	24	51	38	T	28
	17	1115	52	37	47	42	45	44	F	29
	18	1145	17	7	44	24	23	19	T	38
	19	1205	43	54	60	53	53	52	F	38
	20	1225	27	31	17	24	25	24	T	43
Mean			28.9	48.8	38.6	41.1	40.0	34.1		33.6
7/26 (Agrico)	21	1040	20	19	--	31	23	23	F	21
	22	1106	21	29	29	40	30	29	T	23
	23	1131	22	27	27	42	29	29	F	32
	24	1150	34	29	32	43	35	34	F	35
	25	1210	34	26	36	45	35	35	T	36
	26	1231	31	29	34	42	34	34	F	41
	27	1252	35	34	35	46	37	37	F	34
	28	1311	37	--	--	45	41	41	T	38
	30	1550	30	36	32	50	37	36	F	39
	31	1608	31	27	46	43	37	36	T	41
	32	1630	23	--	27	38	29	29	F	37
	33	1635	32	33	32	52	37	36	F	46
	34	1722	34	30	33	47	36	36	T	46
	35	1742	26	30	30	39	31	31	F	37
	36	1809	25	22	29	34	28	27	F	41
	37	1827	26	26	30	35	29	29	T	38
Mean			28.8	28.4	32.3	42.0	33.0	32.3		36.6
Grand mean			31.0	39.1	36.1	40.7	36.4	34.0		36.1

*F = Filter cassette.
T = Bicarbonate - treated tube.

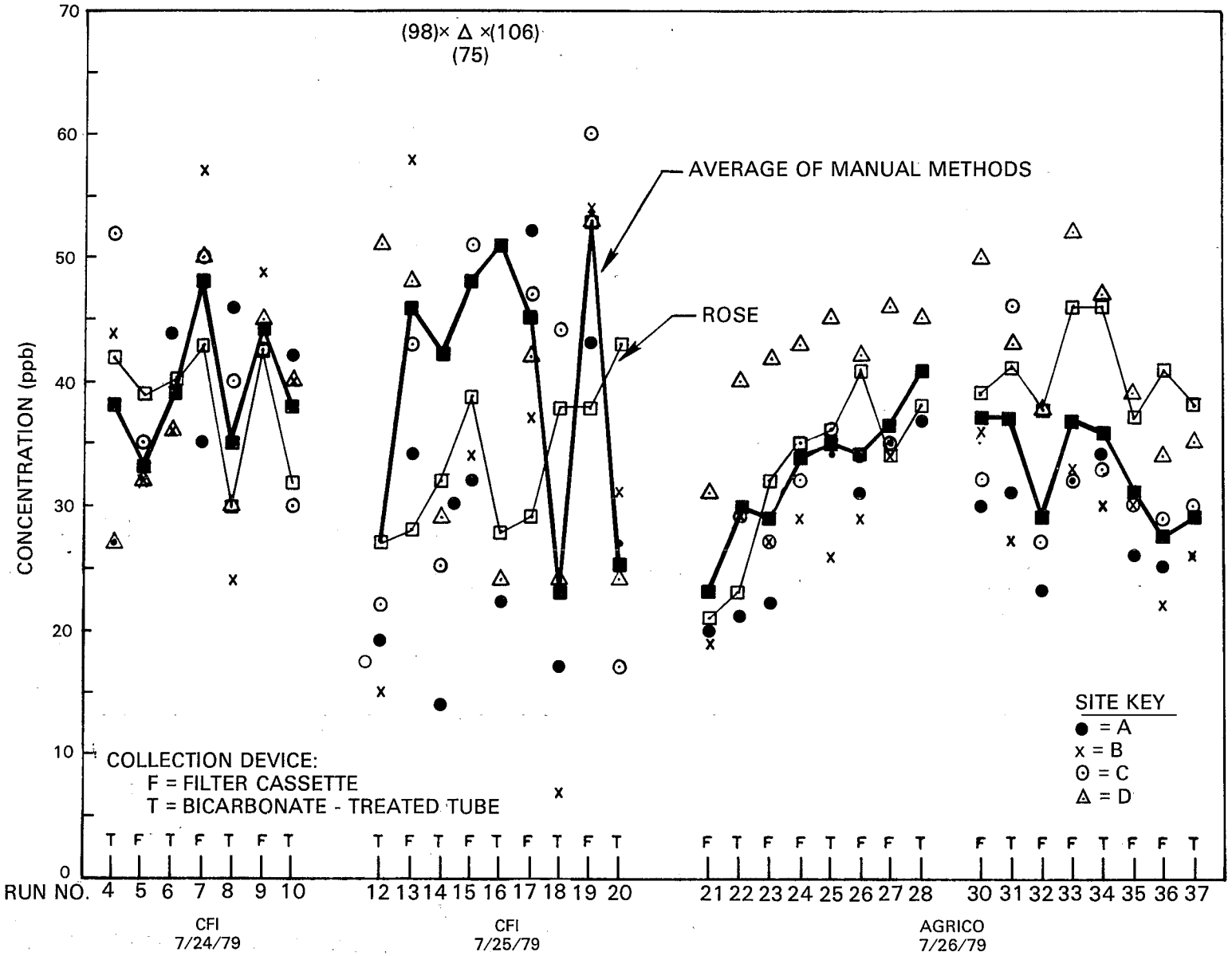

Figure 13. Concentration of HF in air assayed by ROSE and manual methods at various time periods.

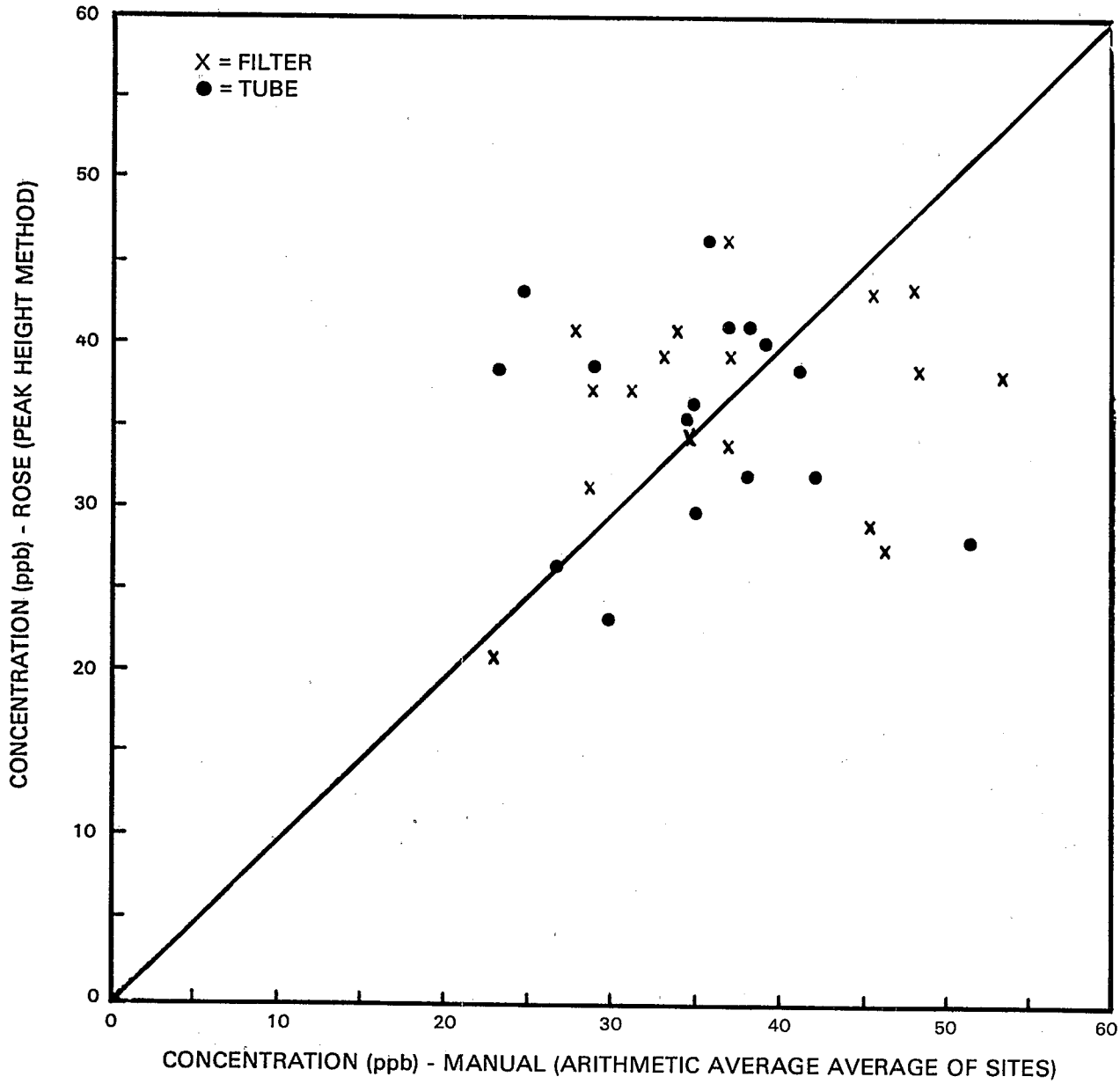

Figure 14. Composite comparison of HF concentrations measured by two techniques.

the average value for a sampling period. The agreement between the ROSE and average point values are all within the estimated ROSE error, and furthermore, each method follows the same up and down trends.

(2) During the sampling at CFI on July 25, the fluctuations between point measurement sites during a given sampling period were much greater than on July 24, and the highs and lows vary between sites for different periods. The point measurements thus indicate widely varying HF concentrations. As might be expected, in this case the agreement between the two methods is not as good as on July 24.

Analysis of the measurements at Agrico shows an appreciable difference from CFI in that a true HF gradient along the sampling path is indicated by the point measurements. Sites A and B are generally the lowest and Site D always the highest (by an appreciable amount) in HF concentration. The readings at Site D can perhaps be explained by the fact that the site was next to a small stream of liquid leaking from an upper gypsum pond. Also, it should be noted that the truck holding the ROSE light source and telescope was in an area moistened by pond runoff. The data fall into two categories:

(1) During the first eight sampling periods (1038 to 1311 hours) the agreement between the methods is excellent.

(2) In the eight late afternoon sampling periods (1548 to 1830 hours) the ROSE data gave HF concentrations always slightly higher than the average of the point sampling data.

The original ROSE data for the last six runs at Agrico were reprocessed a number of times to eliminate the possibility that human error could have caused the difference between the point and ROSE values. Also, the CO_2 and N_2O concentrations measured by the ROSE system were compared for the last six runs. No mistakes in data reduction were found for the HF measurements. The CO_2 and N_2O concentrations were all within ±5 percent of each other (respectively) when measured in spectral regions of maximum S/N. In the spectral region, where the signal-to-noise ratio was about the same for CO_2 as for HF, the apparent CO_2 concentration varied about ±15 percent. The internal checks on the spectral data provided by CO_2 and N_2O show that there is nothing abnormal about the spectra measured by the ROSE system during the last six sampling periods at Agrico. The consistently higher values obtained by the ROSE system during the warm afternoon may have been due to the pond runoff in the vicinity of the light source.

To determine whether any statistical differences existed between the sampling sites at CFI and Agrico, an analysis of variance at the 95 percent level was calculated for the data obtained each sampling day. The results of these analyses indicated no differences among the sites at CFI; however, a significant difference existed among the sampling sites at Agrico.

Statistical analyses based on the differences between the manual sam-

TABLE 8. STATISTICAL ANALYSES BASED ON DIFFERENCE VALUES FOR MANUAL SAMPLING DATA AND ROSE DATA

		Concentrations in ppb					
	n	$\bar{d}$*	Sd†	$\bar{A}$‡	$\bar{R}$§	$(R/\bar{A})$#	Range of $(R/\bar{A})$
All data	32	+8.3	9.7	36.4	36.1	1.04 ± 0.28	0.55 → 1.72
CFI 7/24	7	+1.0	4.8	39.4	38.4	0.98 ± 0.13	0.84 → 1.18
CFI 7/25	9	+6.4	14.5	40.0	33.6	0.94 ± 0.44	0.55 → 1.72
Agrico	16	-3.6	5.6	33.0	36.6	1.11 ± 0.18	0.92 → 1.46
Filters	17	+1.2	8.96	37.5	36.6	1.01 ± 0.24	0.64 → 1.46
Tubes	15	-0.53	10.3	35.07	35.6	1.06 ± 0.32	0.55 → 1.72

*$\bar{d}$ (average of differences) = $\Sigma(\bar{A}-R)/n$

†Sd (standard deviation of differences) = $[\Sigma(d-d)^{-2}/n-1]^{\frac{1}{2}}$

‡$(\bar{A})$ = mean of data for manual methods

§$\bar{R}$ = mean of ROSE values

= _____

$(R/\bar{A}) = \Sigma(R/\bar{A})/n$

pling data and the ROSE values are presented in Table 8 for all of the data and for each day of sampling. The difference between the arithmetic mean of the manual methods ($\bar{A}$) and the ROSE data (R) was computed from the data in Table 7.

The mean HF concentration determined by the manual sampling methods for all of the data was 36.4 ppb, compared to a concentration of 36.1 ppb calculated by the ROSE system. The standard deviation of the difference was 9.7 ppb, with the variation at CFI on July 25, 1979, contributing significantly to raise the overall standard deviation.

Theoretically, random errors should give an overall $\bar{d}$ that is zero or very close to zero. The small $\bar{d}$ indicates a good correlation between the ROSE system and the manual sampling methods. In addition, the overall average of the quotient ($R/\bar{A}$) should be about one if the data from the manual sampling methods and the ROSE system is comparable for any given run. The values for $\overline{(R/\bar{A})}$ approach one for the data.

ACKNOWLEDGMENTS

Research herein was supported by U.S. Environmental Protection Agency Contract 68-01-4143, Task Order 59. This paper is abstracted from U.S. Environmental Protection Agency publication 340/1-80-019.

The cooperation of Mr. Harold Long, Manager of Environmental Control and Mr. Maurice Johnson, Environmental Control, Agrico Chemical Co., South Pierce, Florida; and Mr. William Schimming, Director of Environmental Affairs, CF Industries, Bartow, Florida, is gratefully acknowledged.

Dr. Jay S. Jacobson and Larry Heller of The Boyce Thompson Institute for Plant Research at Cornell University supplied advice and the HF generation apparatus used in the laboratory phase of the program.

The analyses of the formal field phase samples were conducted in the Agrico Environmental Laboratory by Mr. Ed Germain and Mr. Charles Kinsey. Their help is gratefully appreciated.

REFERENCES

1. Herget, W.F., and J.D. Brasher. 1979. Applied Optics 18:3404-3420.

2. Jacobson, J.S., and L.H. Weinstein. 1977. Journal of Occupational Medicine 19:79-87.

3. American Society for Testing and Materials. 1978. Annual book of ASTM standards, D3266-D3270.

4. Intersociety Committee. 1972. Methods of air sampling and analysis. American Public Health Association.

5. Kommers, F.J.W. 1976. Determination of fluorides. Research Institute for Environmental Hygiene, Delft, Netherlands. N79-16435/6WP.

6. Israel, G.W. 1974. Evaluation and comparison of three atmospheric fluoride monitors under field conditions. Atmospheric Environment 8:159-166.

7. Okita, T., K. Kaneda, T. Yanaka, and R. Sugar. 1974. Determination of gaseous and particulate chloride and fluoride in the atmosphere. Atmospheric Environment 8:927-936.

8. Glabisz, U., and Z. Trojanowski. 1976. Metody oznaczania nieorganicznych zwiazkow fluoru w gazach odlotowych z instalacji kwasu i nawozow fosforowych oraz w powietrzu atmosferycznym. Prace Naukowe Akademii Ekonomicznej We Wroclawiv No. 9/113/:253-257.

9. Jacobson, J.S., and L.I. Heller. 1976. Evaluation of probes for source sampling of hydrogen fluoride. APCA Journal 26 (11):1065-1068.

10. Boscak, V., N.E. Boune, and N. Ostojic. Measurement of fluoride emissions from gypsum ponds. Draft final report. TRC - The Research Corporation. Prepared for U.S. Environmental Protection Agency. Contract No. 69-01-4145.

11. Herget, W.F., and J.D. Brasher. 1980. Optical Engineering 19:508-514.

12. Herget, W.F. 1982. Applied Optics 21:635-641.

13. Randall, C.M. 1975. Line-by-line calculations of hot gas spectra including HF and HCl. SAMSO Report TR-75-288. Air Force Systems Command, Los Angeles, CA. December.

14. Meredith, R.E., and F.G. Smith. 1974. Broadening of HF lines by H_2, D_2, and N_2. J. Chem. Phys. 60:3388-3391.

General Reference

Ferraro, J., and J. Basil, eds. 1979. Fourier transform infrared spectroscopy, applications to chemical systems, vol. 2. Academic Press, New York, NY. Chapter 2 - Trace gas analysis, by P. Hanst; and Chapter 3 - Air pollution: ground based sensing of source emissions, by W.R. Herget.

RESULTS OF THE SYNTHESIS AND SOLID SORBENT EVALUATION OF SOME POROUS COPOLYAMIDES

Sajal Das, Louis A. Jones, and John E. Bunch

Department of Chemistry
North Carolina State University
Raleigh, NC

James D. Mulik

U.S. Environmental Protection Agency
Environmental Protection Division
Research Triangle Park, NC

Though Tenax-GC is currently the polymer-of-choice for air sampling, it has demonstrated poor adsorptive capabilities for low molecular weight compounds (1). Of particular concern is its low affinity for aldehydes, nitriles, and amines. Within these classes are acrolein, acrylonitrile, and dimethyl amine; the adsorption of these compounds by Tenax-GC is observed to be insufficient (1). Acrolein and acrylonitrile are known to be mutagenic, while dimethylamine is suspected to be a potential precursor to dimethyl nitrosamine formation in the atmosphere (2). Thus, there is a need for formulation of new, selectively adsorbing materials to permit the determination of these trace low molecular weight toxicants from ambient air. Similarly, Tenax-GC does not efficiently trap propylene oxide, actaldehyde, allyl chloride, vinyl chloride, vinyl bromide, 1-hexene, methyl chloride, and methyl bromide. These toxic organic compounds have been found in trace amounts in ambient air samples (1).

The mechanism of adsorption is a complex phenomenon and has not been completely elucidated. Physical adsorption occurs by impaction of the vapor on the surface of the adsorbent. Polymer porosity, rigidity, surface area, pore volume, pore size distribution, and particle size of the ambient air "aerosol" have been specified as controlling factors that can affect the separation performance of porous polymers (3). It has also been observed that separation is more a function of the surface nature of the porous polymer other than related to its micropore volume or average micropore size (4). Alternatively, chemisorption can be related to interactions involving π-electron density, dipole-dipole interactions, and London dispersion forces, all of which depend on the chemical nature of the sorbent as well as the adsorbate. From thermodynamical consideration, chemisorption is stronger than physical adsorption. The ability of Tenax-

GC to adsorb the higher molecular weight alkenes and aromatics, aromatic halides, alcohols, acids, and amines suggests that the chemisorption process is operative and important, but is not sufficiently controlling to adsorb compounds with diminished π-bond or dipole-dipole interactive properties.

In considering the desirable properties of Tenax-GC, the high thermal stability, ability to be easily handled, lack of demonstrated catalytic activity, and hydrophobicity are of importance (5). As indicated previously, the lack of affinity for lower molecular weight toxicants suggests that a higher π-system/polar group polymer is needed. The argument might be made that the 2,6-diphenyl substitution on the polyphenylene oxide provides this needed π-system. However, the resonance polar property of these phenyl groups is low, as reflected by the low Hammett σ-value of the phenyl group ($\sigma_m = 0.06$, $\sigma_p = -0.01$) compared to that of nitro group ($\sigma_m - 0.71$, $\sigma_p = 0.78$, $\sigma_p^- = 1.27$) or the dimethylamino group ($\sigma_p^+ = -1.7$) (6). A porous polymer with either strongly electron-withdrawing substituents (as a nitro group) or strongly electron-donating (as a dimethylamino group) should exhibit a higher polar affinity for the lower unsaturated and/or polar compounds that constitute a part of the organic toxicants of ambient air.

A desirable porous polymer should contain or possess (a) an aromatic system (for thermal stability), (b) polar groups (for enhanced chemisorption), (c) high molecular weight and tractability, (d) high hydrophobic properties, (e) non-catalytic or chemical activity relative to the toxicants, (f) narrow molecular weight distribution, (g) highly amorphous structure, (h) non-homogeneous surface (7), (i) minimum micro-void to obtain reproducible results, and (j) facile incorporation of functional groups to modify specificity.

Our approach to a systematic study of the effect of polar functional groups on the sorptivity of low molecular weight polar compounds was to prepare a series of copolyamides incorporating N,N'-bispropargyl-4,4'-diaminodiphenylmethane (8), the corresponding benzophenone and 4,4'-diaminodiphenylamine. Thus the effect of $-CH_2-$, $-\overset{O}{\overset{\|}{C}}-$, and -NH- could be determined, and this report describes the preparation and sorptive properties of these new porous polymers.

EXPERIMENTAL

The copolyamides were prepared by a modification of the procedure reported by Wolfe (8) and will be described in detail at a later date. Of importance to subsequent copolyamide preparations (Copolyamides I, II, and III) was the compound N,N'-bispropargyl-4,4'-diaminobenzophenone (VII) and the synthesis utilizing the oxidation procedure of Bell (9), which is summarized in Reaction Scheme I. Polymers A and B were kindly made available by Dr. James Wolfe of Virginia Polytechnic Institute and State University. The structures of the polymers and copolyamides used in this study are shown in Figure 1.

In general, to prepare the bispropargylated copolyamides, a mixture of

Reaction Scheme 1

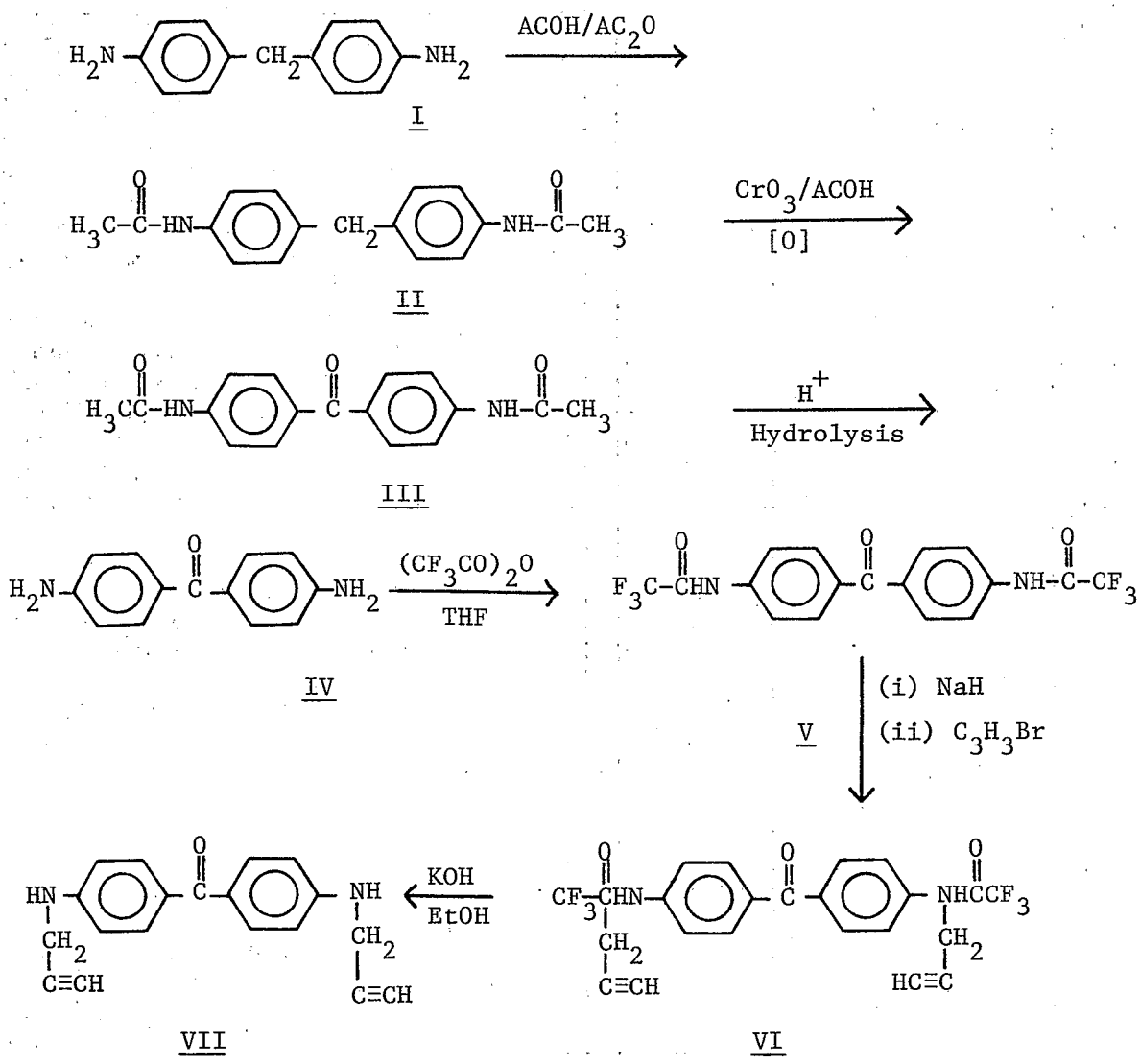

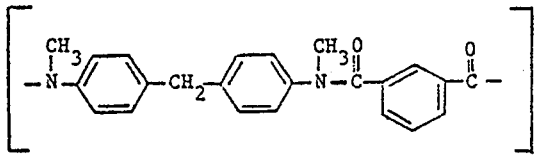

Polymer A

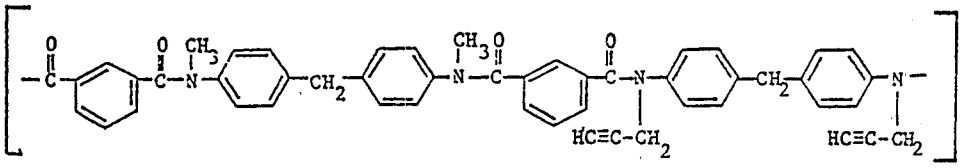

Polymer B

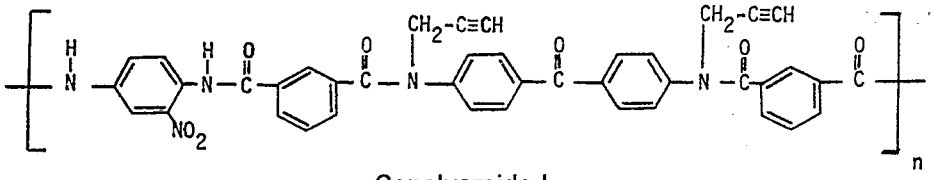

Copolyamide I

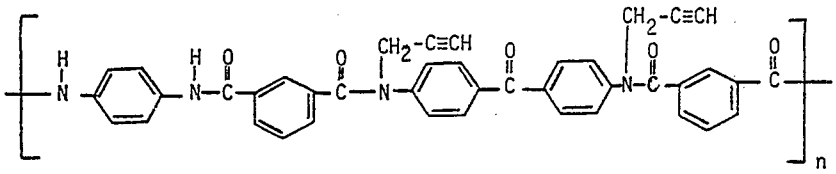

Copolyamide II

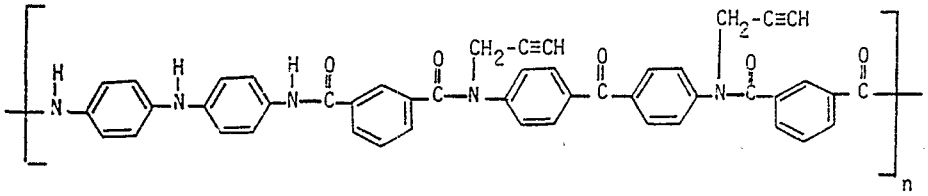

Copolyamide III

Figure 1. Polymers A and B - Copolyamides I, II, and III.

VII and the desired aromatic diamine (ca. 3:1) was dissolved in redistilled N-methylpyrrolidinone (NMP) and to this was added isophthaloyl chloride in NMP at elevated temperatures. When gel formation was observed, the reaction was quenched with methanol, the polymer filtered, washed and/or extracted with methanol, dried under vacuum, and sieved. The 60/80 mesh particle size was collected, packed in 1/8" nickel columns (6 or 3 ft) and the columns conditioned overnight at 150°C under 5 ml/min helium. Breakthrough volumes (BTV's) were determined by the method of Brown and Purnell (10) and consisted of determining the retention volumes from 110°-160° at flow rates of 10 ml/min of helium for each 10° increment, plotting log $\frac{1}{V}$ vs. T (K°) and extrapolating to 25°C.

RESULTS AND DISCUSSION

Although Polymer A does not contain N-propargyl groups, it was considered a necessary "base compound" that could be compared in its sorptive characteristics to Tenax-GC. This compound, a fibrous polymer, could not in itself be packed in a chromatographic (1/8" x 6') nickel column for BTV evaluation due to its non-rigid properties. As a consequence, it was coated on Gas Chrom Q (15 percent load level) and its BTV values evaluted for hexane, benzene, chloroform, methanol, and acetone. Comparison of these values with those of the Tenax-GC showed that, with the exception of methanol, Tenax-GC was at least 100 times more sorptively effective than Polymer A. Polymer B was deposited on Gas Chrom Q (15 percent) and evaluated as before and proved even less sorptive than Polymer A, relative to Tenax-GC. It was apparent from these results that the coating of prepared copolyamides on Gas Chrom Q could not meaningfully be compared with Tenax-GC, which was used in the pure form. Thus future comparison was made between Tenax-GC and the pure polymers prepared.

Wolfe had reported (8) that heating Polymer B led to cross-linking <u>via</u> the propargyl groups, resulting in a more rigid copolyamide. Reasoning that such heating might produce a more suitable GC packing material, researchers in this study converted Polymer B to the crosslinked Polymer C by heating it at 270°C for 6 hours under nitrogen. The resulting slightly tan solid was ground, sieved (30-65 mesh), packed in a GC column, and evaluated as before. The only noteworthy difference in the BTV values was the twenty-fold <u>decrease</u> in the sorptivity of methanol, all other values remaining essentially unchanged and inferior to those of Tenax-GC.

The previous polymers A, B, and indirectly C, were considered to be the base from which changes could be made and related to. In accordance with the aforementioned objective of introducing electron-donating or withdrawing functionalities into the polymer system, the next step would have been the replacement of the methylene group in B and/or C with a carbonyl group to modify the electron density in the polymer system. Although subsequent literature searches revealed that in the curing process of B → C, the -CH- group was simultaneously converted to the $-\overset{O}{\overset{\|}{C}}-$ group (11,12), the predicted need required the independent synthesis of 4,4'-diaminobenzophenone, followed by propargylation (Compound VII) as described in the Experimental.

The first synthesis of a new copolyamide, Cop-I, designed to modify the above results by changing the degree of aromaticity of the polymer system while retaining the thermally stabilizing carbonyl group, was accomplished by the reaction of non-methylated ortho-nitrophenylenediamine with N,N'-bispropargyl-4,4'-diaminobenzophenone (75:25) and reacting the mixture with isophthaloyl chloride to produce Cop-I. This copolyamide was evaluated as before and the BTV values determined as previously described. The significant improvement in the performance of Cop-I relative to Poly A, B, and C prompted the extension of the list of toxic organic compounds to include acrolein and acetonitrile. The BTV values (relative to Tenax) for methanol (104.9), acetone (1.53), acrolein (4.80), and acetonitrile (3.66) suggested that the addition of the polar nitro-group considerably enhanced the ability of the copolyamide to absorb the polar compounds while not particularly affecting the sorptivity for the non-polar compounds.

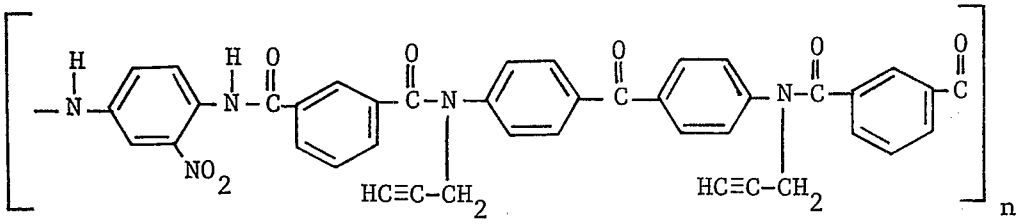

Cop-I

To further test this hypothesis, Copolyamide II, (Cop-II) was prepared, identical to Cop-I except that no ortho-nitro group was present. As anticipated, the BTV values for the polar compounds decreased, while non-polar compound BTV's remained essentially unchanged.

To determine the effect of strongly electron-donating groups on the sorptivity of the test compounds, a new copolyamide, Cop-III, in which the diaminobenzophenone moiety in Cop-II was replaced with 4,4'-diaminodiphenylamine, was prepared using the same proportions. The BTV values for the non-polar molecules were predictably unchanged, while the sorptivity for acrolein and acetonitrile was thirty times larger than that observed with Tenax-GC.

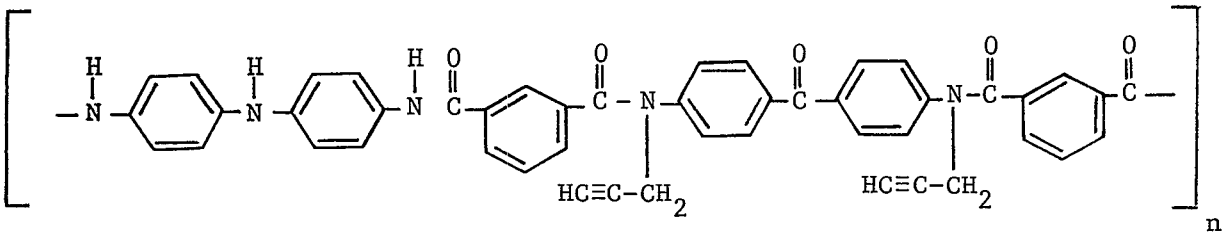

Cop-III

The results are summarized in Table 1.

The dramatic improvement in the BTV values for Cop-III prompted us to repeat the synthesis four more times, varying the reaction temperature, gel time, and purification solvent; Table 2 outlines the conditions employed for each preparation.

The BTV values of each preparation were determined and, as can be seen in Table 3, large variations occur in the BTV's of the different preparations, that of C being the most efficient for acrolein, and second most efficient for acetonitrile. The reason for the inversion of efficiency for these two compounds between A and D versus B and C is not as yet known, but may become more apparent after extensive characterization studies are complete. However, the data only emphasized the need for careful synthetic control, a problem not yet solved even for Tenax.

To determine if the adsorption properties of Copolyamide III could be replicated by preparing the polymer at one temperature, the synthetic procedure was modified such that the propargylated diaminobenzophenone (VII) and the 4,4'-diaminodiphenylamine were (in N-methylpyrrolidinone) heated to 140°C. To this was added isophthaloyl chloride with stirring until gel formation was observed, usually occurring within 7 hours. Reaction Scheme II summarizes the procedure.

Reaction Scheme II

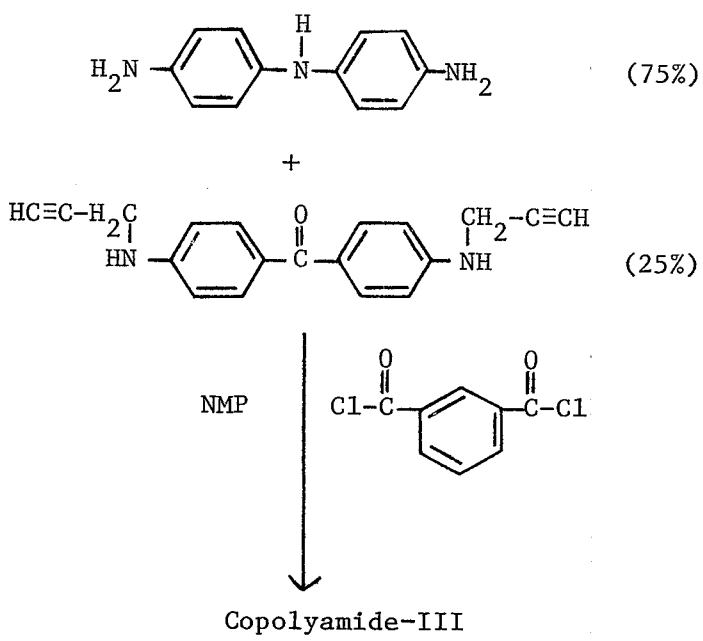

The final product was extracted with methanol, vacuum dried, and sieved. The preparation and properties are summarized in Table 4. After packing in a column, the BTV values were determined and the results are summarized in

TABLE 1. BREAKTHROUGH VOLUME OF COPOLYAMIDE AT 25°C (LITER/GRAM)

Polymer	Methanol	Acetone	Hexane	Chloroform	Benzene	Acrolein	Acetonitrile
Poly A	2.7	0.30	0.021	0.026	0.026	--	--
Poly B	2.3	0.019	0.0092	0.019	0.019	--	--
Poly B*	0.10	0.066	0.00083	0.18	0.0020	--	--
Cop I	4.3	1.3	0.058	0.091	0.060	2.3	4.4
Cop II	2.46	0.901	0.055	0.202	0.1872	1.79	3.39
Cop III	16.20	19.2	0.030	20.3	21.58	48.36	29.68
Tenax GC	0.041	0.85	4.6	4.3	3.9	0.48	1.2

*Poly B - Crosslinked Poly B

TABLE 2. REACTION CONDITIONS FOR THE PREPARATION OF COPOLYAMIDE-III

Preparation	Reaction temperature (time in hours)	Reaction solvent	Gel point	Preparation solvent
A	-5°-0°C (2) 0-25°C (2) 140°C (1.5)	NMP/CH_2Cl_2	Occurred after 1.5 hrs at 140°C	DMAC-MeOH (followed by Soxhlet extrn.)
B	-5°-0°C (2) 0°-25°C (24) 140°C (3.5)	NMP/toluene	Occurred after 3.5 hrs at 140°C	DMAC-MeOH
C	0-10°C (4) 10°-20°C (2) 25°C (18) 130°C (7.75)	NMP	Occurred after 7.75 hrs at 130°C	DMAC-MeOH
D	-5-0°C (2) 0-25°C (2) 140°C (3.5)	NMP/CH_2Cl_2	Occurred after 3.5 hrs at 140°C	DMAC-NMP-MeOH then NMP-CH_2Cl_2-MeOH

TABLE 3. BREAKTHROUGH VOLUMES FOR COPOLYAMIDE III PREPARATIONS AT 25°C (LITER/GRAM)

Sorbate	Preparation A	Preparation B	Preparation C	Preparation D*
Hexane	0.014	0.082	0.030	0.022
Chloroform	0.034	2.81	20.32	3.42
Benzene	0.034	4.09	21.58	6.21
Methanol	4.51	9.82	16.17	10.24
Acetone	5.20	14.83	19.22	36.13
Acrolein	15.02	37.49	48.36	20.00
Acetonitrile	35.04	22.40	29.68	48.16

*Determined as a 2' x 1/8" column, 20 ml/min flow rate.

TABLE 4. COPOLYAMIDE III - PREPARATION AND PROPERTIES

Solvent		Temperature	Reaction time	Yield
NMP	80			
CH_2Cl_2	20	125-130	7 hrs	70%

Inherent Viscosity - dl/c = 0.95
(0.5% in NMP)

T_g (from DSC) - 277°C

Table 5. Although the replicability of the BTV's is acceptable, it is felt that the performance of the polymer can be improved by further study. Of concern is the large BTV for methanol and, by analogy, water. It has been shown that the polymer should have a low affinity for the water vapor present in ambient air samples (13); otherwise, displacement chromatography, in which water vapor displaces the already adsorbed organic molecules, may become an important factor in the adsorption process. Additionally, adsorbed water vapors can cause condensation problems (ice) during the cryogenic concentration phase of the desorption-analytical process (1).

TABLE 5. COPOLYAMIDE III - BREAKTHROUGH VOLUMES (GM/L)

Compounds	Acetonitrile	Acetone	Benzene
Cop III-6	107.2	32.84	1.55
Cop III-7	110.9	31.96	---
Cop III-8	111.8	59.16	1.18

Relative breakthrough volumes of copolyamide III/Tenax GC

Compounds	Acetonitrile	Acetone	Benzene
Cop III-6	228.6	55.07	0.202
Cop III-7	236.5	53.60	---
Cop III-8	238.6	99.21	0.162

The next step then will be to modify Copolyamide III to diminish the affinity for methanol, with minimum adsorptive modification for the compounds of interest.

ACKNOWLEDGMENTS

This research was supported by U.S. Environmental Protection Agency Grant No. CR-807922-01.

REFERENCES

1. Krost, K.J., E.D. Pellizzari, S.G. Walburn, and S.A. Hubbard. 1980. Submitted to Environmental Science & Technology for review. See also E.D. Pellizzari, Publication No. EPA-605/2-74-121, Contract No. 68-02-1228, July 1974.

2. Fishbein, L. 1972. Chromatography of environmental hazards: carcinogens, mutagens, and teratogens. Elsevier, NY.

3. Hollis, O.L. 1966. Anal. Chem. 38:309.

4. Johnson, J.F., and E.M. Barrall. 1967. J. Chromatogr. 31:547.

5. Pellizzari, E.D. 1975. Development of analytical techniques for measuring ambient atmospheric carcinogenic vapors. Publication No. EPA-60012-75-076, November.

6. Johnson, C.D. 1973. Chapter 2 in The Hammett equation. Cambridge at the University Press, London.

7. Sakodynskii, K., L. Panina, and N. Klinskaya. 1974. Chromatographia 7:339.

8. Greenwood, T.D., D.M. Armistead, J.F. Wolfe, A.K. St.Clair, T.L. St.Clair, and J.D. Barrick. 1982. Polymer 23:621.

9. Bell, V.L. 1976. J. Polymer Sci., Polymer Chem. 14:2275.

10. Brown, R.H., and C.J. Purnell. 1979. J. Chromatogr. 178:79.

11. St.Clair, A.K., T.L. St.Clair, and J.D. Barrick. 1980. NASA techical memorandum 81918, January.

12. Androva, N.A., M.I. Bessonov, L.A. Laius, and A.P. Rudakov. 1970. Polyamides, a new class of thermally stable polymers. Techomic Publications, CN.

13. Pellizzari, E.D., J.E. Bunch, B.H. Carpenter, and E. Sawicki. 1975. Environ. Sci. Tech. 9:559.

SYNTHESIS AND EVALUATION OF A POROUS POLYETHERIMIDE FOR THE COLLECTION OF VOLATILE ORGANICS

Sajal Das, Louis A. Jones, and John E. Bunch

Department of Chemistry
North Carolina State University
Raleigh, NC

James D. Mulik

U.S. Environmental Protection Agency
Advanced Analytical Techniques Branch
Environmental Monitoring Division, EMS
Research Triangle Park, NC

INTRODUCTION

In ambient air, there are many carcinogenic and mutagenic volatile polar organic compounds present at extremely low concentration (parts per trillion) (1-3). Most analytical techniques presently available are not sensitive enough to detect these trace quantities. Chromatographic analysis of these contaminants requires first a concentration step followed by thermal desorption (4,5). The commercially available porous polymers are not sufficiently polar to concentrate (high-breakthrough-volume) low-molecular-weight polar substances (6,7). Presently, Tenax GC (2,6,diphenylpolyphenyl ether) is used extensively as a sorbent material for trace-level organic pollutant analysis, but since it is a nonpolar polymer (8), it does not effectively trap lower-molecular-weight polar compounds. The polymeric materials required for concentration and thermal desorption should meet several specifications. The most important features for a polymer adsorbent to have are (a) an aromatic system (for thermal stability), (b) polar groups (for specific interaction), (c) high molecular weight distribution, (d) hydrophobic properties, (e) non-catalytic or chemical activity relative to the toxicants, (f) highly amorphous structure, (g) non-homogeneous surface, (h) large surface area, (i) minimum micro-void to obtain reproducible results, (j) uniform pore volume distribution, (k) high durability to avoid compression and fragmentation under the stress of high flow rates and handling, and (l) facile incorporation of functional groups to modify specificity.

The aim of the present research is to prepare a polyetherimide containing several polar groups (carbonyl, imide, and ether). The starting

material for this polyetherimide is an acetylene-containing imide oligomer, Thermid-600, commercially available from Gulf Oil Chemicals Company, USA. The modification of this oligomer is achieved through the addition of bisphenol compounds at the endcap acetylene groups of Thermid-600.

EXPERIMENTAL

Materials

Thermid-600 was obtained from Gulf Oil Chemicals Company, and was used without further purification. Bisphenol A was obtained from Aldrich Chemical Company, USA, and was recrystallized from toluene. The solvent, N-methyl-pyrollidinone (NMP), was distilled over calcium hydride prior to use and stored over 4 Å molecular sieves.

Polymer Synthesis

The polymer may be synthesized by either melt or solution polymerization technique. A typical solution polymerization can be described as follows: 20 gram (0.087 mole) of bisphenol A was dissolved in 50 ml of NMP in a mini-resin kettle; 20 gram (0.018 mole) Thermid-600 was dissolved in 50 ml of NMP and a few drops of triethylamine was added to the mixture. This mixture was added gradually over a period of 20 minutes to the bisphenol solution at 150°-155°C. The reaction was kept at 160°C for 2 hours. The pot temperature was then raised to 230°C, at which time a highly viscous liquid formed and NMP began to distill off. The pot temperature was dependent on the amount of NMP distilled off. Upon reaching 230°C, the reaction was then run for 2-1/2 hours. Toward the end of the reaction (last half-hour), a slight vacuum was applied to accelerate the removal of NMP. Total distillate collected at the end of the reaction was 75 ml. Gel formation was noticed in the fourth hour of reaction, when the reaction was quenched by pouring into methanol in a blender and the polymer thus obtained was purified by using NMP as a solvent and methanol as nonsolvent. The polymer was further purified by Soxhlet extraction with methanol for 24 hours. The polymer was dried in a vacuum dessicator at 120°C.

The IR spectrum was obtained with a Perkin-Elmer model 521 in KBr pellet. Viscosity measurements were determined using a 0.5 percent (g/ml) solution of the polymer in NMP at 20°C using a Ubbelohde viscometer. Gas chromatographic measurements were performed with a Perkin-Elmer 900 gas chromatograph. Breakthrough volumes were obtained for the polymeric material at several temperatures, whereupon a plot of ln 1/V *versus* T produced extrapolated results to ambient temperatures (7).

RESULTS AND DISCUSSION

The compounds of interest for concentration are tabulated in Table 1, along with their structure, molecular weight, boiling point, and dipole moment. Molecular weight data show that all of the compounds listed are low molecular weight, while boiling point and dipole-moment data are

TABLE 1. PERTINENT INFORMATION FOR THE SELECTED COMPOUNDS

Name	Structure	M.W. (g/mol)	B.P. (°C)	Dipole moment (μD)
Acrolein	$CH_2{=}CHCHO$	56.05	52.5	2.90
Acryonitrile	$CH_2{=}CHCN$	53.06	78	3.51
Acetonitrile	$CH_3C{\equiv}N$	41.0	81.6	3.94
Acetone	$(CH_3)_2C{=}O$	58.08	56.2	2.73
Benzene	C_6H_6	78.11	80.1	0
1,4,Dioxane	$\underbrace{OC_2H_4O}C_2H_4$	88.12	100.1	0
Ethylene oxide	$\underbrace{CH_2H_2O}$	44.05	10.7	1.89
Chloroform	$CHCl_3$	119.38	61.3	1.06
Methanol	CH_3OH	32.04	64.6	1.67

indicative of the volatility and polarity of the compounds, respectively.

Table 2 shows the U.S. production and pollutant information (9).

TABLE 2. U.S. PRODUCTION/POLLUTANT INFORMATION

Compound	U.S. production (10^6 lb/yr)	Pollutant information	
		Carcinogen	Emission* Kg
Acrolein	60	Possible	1.1×10^4
Acryonitrile	1410	Probable	3.7×10^5
Benzene	1400	Probable	5.9×10^7
1,4,Dioxane	14	Probable	1.3×10^6
Ethylene oxide	3960	Possible	3.8×10^4
Chloroform	260	Probable	---

*Emissions, Kg = source emissions, Kg/yr (365 da) x half life, I da.

Tenax GC is a polyphenylene oxide, prepared by oxidative coupling reaction, with cuprous chloride as catalyst and pyridine as solvent, as follows (10):

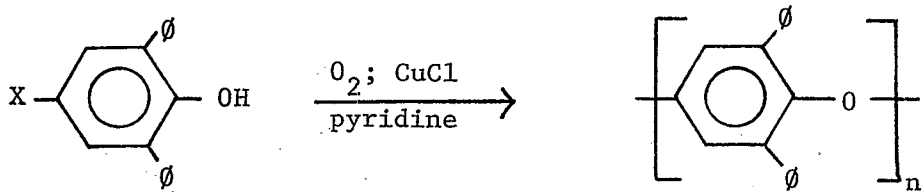

X = H; Cl, Br, I

Tenax GC is a product of AKZO Research Laboratory, Netherlands, and it is distributed through Applied Science, Inc., USA (8). It is a thermostable, hydrophobic polymer (11), has been shown to be an excellent chromatographic packing material (12), and has been extensively used in the field of environmental pollution concentration/analysis (13-15). One of the most important limitations of Tenax GC of present concern is its defined nonpolar character and, presumably because of this, its inability to trap low-molecular-weight volatile organic polar compounds (listed in Table 1). The nonpolar character of Tenax GC is calculated from the retention indices for benzene and ethanol (8) and, according to Walraven, the polarity increases with decreasing ratio of the retention index of benzene and ethanol. From Table 3, it can be concluded that Tenax GC is the least polar polymer on the list.

TABLE 3. POROUS POLYMERS ARRANGED IN ORDER OF INCREASING POLARITY, DETERMINED ACCORDING TO WALRAVEN

Porous polymer	$I_{Benzene}/I_{Ethanol}$
Tenax GC	1.64
Chromosorb 102	1.56
Porapak QS	1.56
Porapak Q	1.56
Chromosorb 101	1.52
Porapak P	1.47
Chromosorb 105	1.47
Porapak S	1.41
Chromosorb 103	1.40
Porapak R	1.36
Porapak N	1.35
Porapak T	1.28
Chromosorb 104	1.21

Recently, a series of copolyamides was synthesized in the laboratory that were shown to be very promising for the present research (16). The structure of the copolyamide for which the best breakthrough volume results were obtained is shown below:

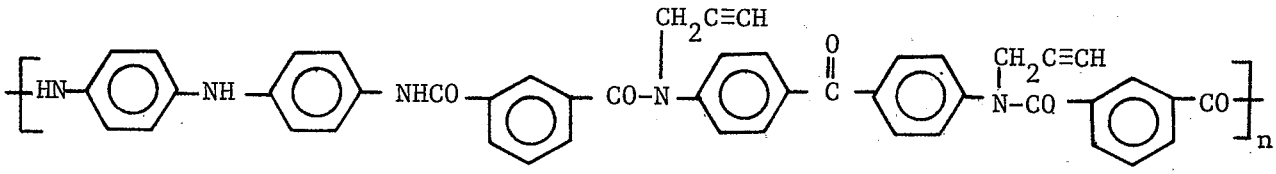

The polar groups in this polymer are the amide group, the carbonyl group, the secondary amine group, and the acetylenic bond. Although the copolyamide shown above gives good results, some of the problems encountered include a high affinity for methanol (and presumably water) and the fact that the N,N'-bispropargyl-4,4'-diaminobenzophenone requires a multistep synthesis (18). However, a commercially available oligomer, Thermid-600 (Gulf Oil Chemicals Company, USA) has similar functional groups, as does the above copolyamide, as well as the polyether linkage of Tenax.

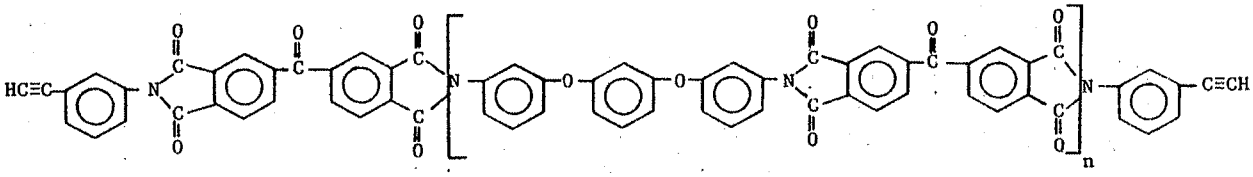

where n = 1-2.

The high softening point (185-200°) and minimal water adsorption (<1 percent after 1000 hours at 125°F, 100 percent R.H.) (19) suggested that a polymer could be prepared having polar character with minimal affinity for water. Thermid-600 by itself could not be evaluated as a packing material since the powder form is too fine for a packing material by itself.

Chemical modification of Thermid-600 was the object at this point.

In 1965, Monsanto Chemical Company, USA, disclosed a patent describing the addition of the hydroxyls in glycols, alcohols, and phenols across the triple bonds of diacetylenic diesters (20). Recently, a polyether ketone was synthesized by the following reaction (21):

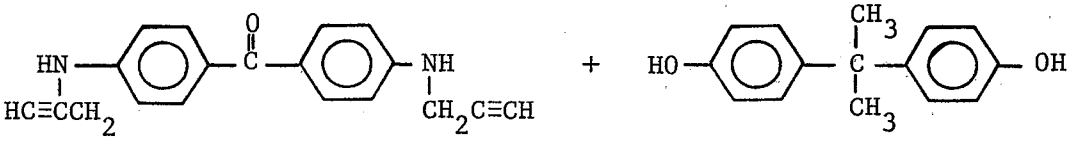

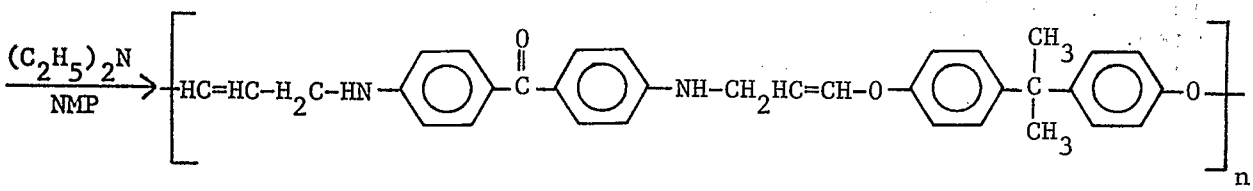

Encouraged by the results of these reactions, researchers reacted the Thermid-600 and bisphenol A similarly, and a polymer was obtained with the following suggested structure:

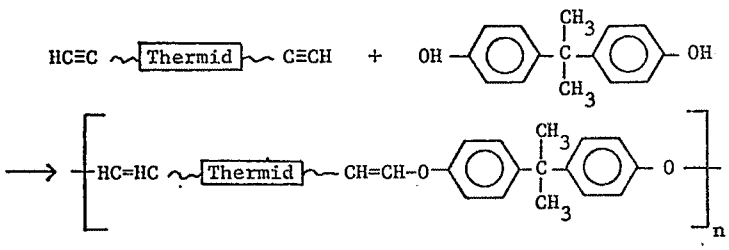

The structure of Thermid is:

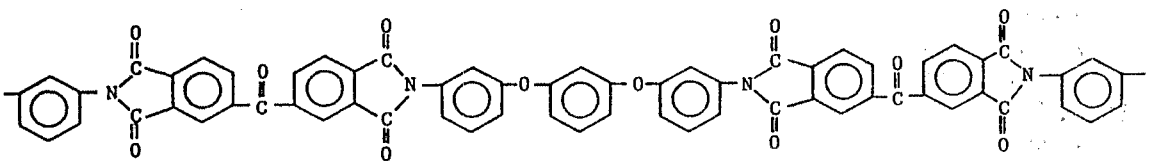

The addition of aliphatic OH across the triple bond is well documented (22), but addition of phenolic OH across the triple bond is not well established. To determine if the latter reaction was feasible, phenylacetylene was reacted with phenol with K_2CO_3 as a base catalyst.

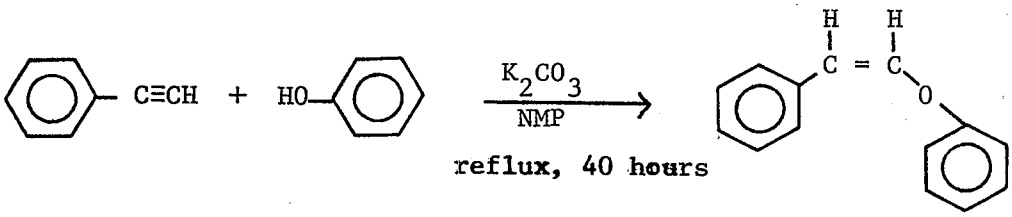

cis β-phenoxystyrene

The product obtained was cis β-phenoxystyrene, characterized by IR, NMR and mass spectra. The IR spectrum showed bands at 1580 cm^{-1}, 1240 cm^{-1}, 1040 cm^{-1}, and 770 cm^{-1}, corresponding to -C=C-, Ø-O, C-O, and cis-HC=CH- groups, respectively. Figure 1 shows the proton NMR. The observed coupling constant for the cis protons is 7Hz, consistent with cis configuration. The mass spectrum indicated a molecular ion of M/Z = 196, and fragmentation was consistent with the structure assigned.

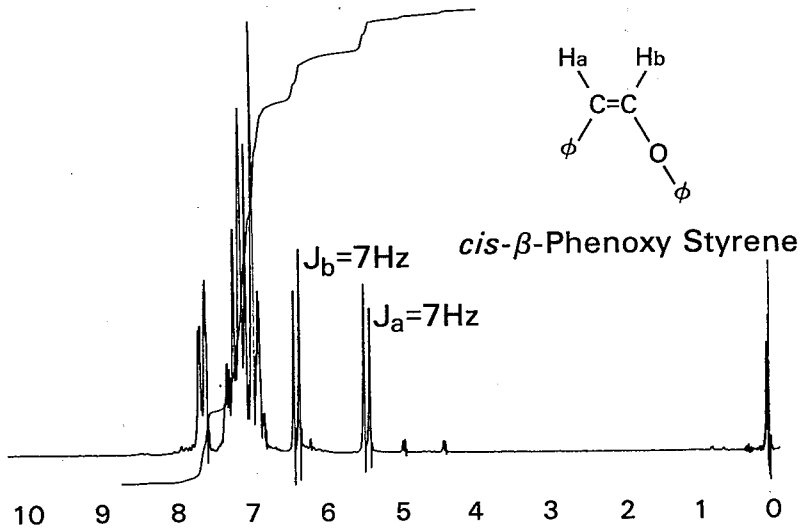

Figure 1. Proton NMR of cis-β-phenoxystyrene.

N-methyl-2-pyrrolidone was selected as the polymerization solvent because of its superior physical and chemical properties compared with other aprotic liquids. The fact that it is highly polar is reflected in its high boiling point of 202°C and high dipole moment value, 4.09 (μD). Therefore, one would predict that it would be a suitable aprotic, dipolar solvent, which is one important criterion for its use under the demanding reaction conditions. Moreover, because of the polar character of the monomer, polymer, and solvent, there is a strong tendency for association, which facilitates the polymerization reactions (23). The N-substituted carboxamide ring has good hydrolytic stability, except in the presence of strong aqueous base or acid at elevated temperatures. Also, it is relatively nontoxic and non-corrosive.

Table 4 shows the general characteristics of the polymer.

TABLE 4. PROPERTIES OF POLYIMIDE ETHER

Color	Pale yellow
Inherent viscosity*	0.91
Yield†,%	65 (SOL)

*0.5% solution in NMP at 21°C.
†Yield is calculated on the basis of Thermid-600.

From inherent viscosity data, it can be inferred that the molecular weight of the polymer is high.

Table 5 shows the breakthrough volumes of the polyetherimide and Tenax GC.

TABLE 5. BREAKTHROUGH VOLUMES OF POLYETHERIMIDE AT 25°C (LITERS/GRAM)

Polymer	Methanol	Acetone	Hexane	Benzene	Acrolein	Acetonitrile
Polyetherimide	1.758	288.91	0.2774	8.61	92.20	124.1
Tenax GC	0.041	0.85	4.6	3.9	0.48	1.20

Breakthrough volumes of all polar compounds like acetonitrile, acetone, and acrolein are much superior compared with Tenax GC. The higher breakthrough volumes for polar compounds suggests that there is a strong interaction between the polar organic compounds and the polymer. Π-Electron-containing compounds, like benzene, are also better retained on the new polymer than on Tenax GC, possibly because the polyetherimide contains many aromatic rings, and the presence of double bonds contributes to the π-electron density of the polymer. The methanol retentivity is greater than Tenax GC, but much smaller than for copolyamides (19). From methanol retentivity, it can be anticipated that water adsorption for the polyetherimide is much less and that it may be considered as a hydrophobic polymer.

CONCLUSION

The present research has developed a polar porous polymer, which is useful for trapping both polar and nonpolar compounds. The water retentivity of this polymer is low. The starting materials for this polymer are available commercially, so extensive monomer synthesis and purification is not necessary. The polymerization technique is also simple, and chances of side reactions are minimal when the reaction is run in equimolar ratio.

ACKNOWLEDGMENTS

This work was financed under U.S. Environmental Protection Agency Cooperative Agreement Grant No. CR-807922-01. The authors thank Mr. Rodney Beaver of this Department for helpful discussions during the course of this study.

REFERENCES

1. Sydor, R., and D.J. Pietrzyk. 1978. Anal. Chem. 50:1842.

2. Bertsch, W., R.C. Chang, and A. Zlatkis. 1974. J. Chromatogr. Sci. 12:175.

3. Pellizzari, E.D., J.E. Bunch, B.A. Carpenter, and E. Sawicki. 1975. Environ. Sci. Tech. 9:552.

4. Pellizzari, E.D., J.E. Bunch, R.E. Berkley, and J. McRae. 1976. Anal. Lett. 9(1):45.

5. Versino, B., M. deGroot, and F. Geiss. 1974. Chromatographia 7(6):303.

6. Krost, K.J., E.D. Pellizzari, S.G. Walburn, and S.A. Hubbard. 1980. Submitted to Environmental Science & Technology for review. See also E.D. Pellizzari, Publication No. EPA-605/2-74-121, Contract No. 68-02-1228, July 1974.

7. Brown, R.A., and C.J. Parnell. 1979. J. Chromatogr. 178:79.

8. Daemen, J.M.H., W. Dankelman, and M.E. Hendriks. 1975. J. Chromatogr. Sci. 13:79.

9. West, D.S., F.N. Hodgson, J.J. Brooks, D.G. DeAngelis, A.G. Desai, and C.R. McMillin. 1981. In Potential atmospheric carcinogens phase 2/3. Analytical technique and field evaluation. Publication No. EPA-600/2-81-106, June.

10. Cooper, G.D., and A. Katchman. 1969. Advan. Chem. Series 91:660.

11. Pellizzari, E.D. 1975. Development of analytical techniques for measuring ambient atmospheric carcinogenic vapors. Publication No. EPA-60012-75-076, November.

12. VanWijk, R. 1969. J. Chromatogr. Sci. 7:389.

13. Bunch, J.E., and E.D. Pellizzari. 1979. J. Chromatogr. Sci. 186:811.

14. Versino, B., M. deGroot, and F. Geiss. 1976. Chromatographia 7(6):302.

15. Bertsch, W., R.C. Chang, and A. Zlatkis. 1974. J. Chromatogr. Sci. 12:175.

16. Jones, L.A. 1982. Porous polymer-adsorption of volatile organic toxicants in ambient air. The synthesis and evaluation of aromatic copolyamides containing N-propargyl groups. EPA Report No. CR-807922-01-1, January.

17. Deanin, R.D. 1972. Polymer structure, properties and applications. Cahners Books, MA.

18. Wolfe, J.D. NASA Grant #NSG-1524. Patent applied for 1980.

19. Gulf Oil Company, Technical Bulletin, Thermid-600 addition curable polyimide resin.

20. Butler, J.M., L.A. Miller, and G.L. Wesp. 1965. U.S. Patent 3201370 (to Monsanto Co.).

21. Das, S., L.A. Jones, J.E. Bunch, and J.D. Mulik. 1982. Polymer Bulletin 6:509.

22. Miller, S.I. 1956. J. Am. Chem. Soc. 78:6091.

23. Sroog, C.E. 1976. Macromolecular Review 11:161.

ADVANCED CONCENTRATOR/GC METHODS FOR TRACE ORGANIC ANALYSIS

S.A. Liebman, T.P. Wampler, and E.J. Levy

Chemical Data Systems, Inc.
Oxford, PA

INTRODUCTION

Gaseous organic pollutant analysis requires reliable and versatile instrumentation. Sampling procedures have been developed with such equipment designed and engineered to provide analysts with the needed information. The CDS 320 Concentrator is a microprocessor-based analytical sampling system (1,2) for air, water, and solids (Figure 1) that permits absolute repeatability throughout the operational sequence to ensure accurate results under appropriate conditions. The role of modern instrumentation is to provide cost-effective analyses with minimal operator training. In trace organic studies, traditional enrichment methods have employed cryogenics, solvent extraction, derivatization, or other time-consuming steps that are difficult to automate. The rationale for emphasizing thermal desorption is outlined in Figure 2 and, as in any analytical situation, the disadvantages must be evaluated relative to the advantages--for example, thermally labile compounds are not successfully handled in this approach. Also, standardization procedures, although basic to any methodology, are particularly critical for trace organic studies at the ppm-ppb levels handled by gas chromatographic (GC) and concentrator technologies.

This paper emphasizes method development, with the concentrator interfaced to a high resolution capillary GC unit using controlled and wide-ranging experimental parameters, including sampling flow rates, thermal desorption/time/temperatures, and varied sorbent trap packings and matrix effects. Additionally, coupling of the concentrator with on-line oxidation/reduction reactors further provided total organic carbon analysis for organics from air-sampling cartridges. The sorbed organics are desorbed in the thermal desorber module of the 320 Concentrator and carried in a helium stream to the microreactors and on-line TCD/FID GC system for analysis of hydrocarbons at the 10 ppb level.

EXPERIMENTAL CONDITIONS

For sampling, organics were sorbed onto a 3" x 1/4" I.D. stainless steel cartridge containing about 100 mg of adsorbent held in place with

A MODULAR SYSTEM DESIGNED AND ENGINEERED FOR:

- **SAMPLING** - AIR, WATER, SOLIDS
  - SPARGE MODULE - PURGE AND TRAP
  - THERMAL DESORBER MODULE
  - BULK SOLIDS ACCESSORY
- **INTERFACING** - GC, MS, FTIR
- **ANALYZING** - TOTAL SYSTEM FOR TOC

Figure 1. CDS 320 sample concentrator.

ADVANTAGES:

USEFUL FOR GAS, LIQUID, AND SOLID MATERIALS
MINIMAL SAMPLE HANDLING
CONTROLLED AND REPRODUCIBLE OPERATIONS
WIDE RANGE OF

1. SORBENT SELECTIVITIES AND CAPACITIES
2. THERMAL DESORPTION TIMES AND TEMPERATURES
3. SEQUENCING OF SPECIFIC SORPTION/DESORPTION STAGES

FULLY AUTOMATED METHODS FOR PPB-LEVEL ANALYSES
AUTOMATED INTERFACING TO GC/GC-MS/GC-FTIR

DISADVANTAGES :

THERMALLY LABILE COMPOUNDS DIFFICULT
REQUIRES APPROPRIATE INTERNAL STANDARDIZATION

Figure 2. Advances in concentrator technology using thermal desorption.

quartz wool. The sorbents, as denoted in the respective figures, were Tenax-GC (obtained from Supelco, Bellefont, PA) CDS modifier, or Ambersorb XE-340 (from Rohm and Haas, Philadelphia, PA). Test mixtures were generated in glass vessels by means of syringe transfer dilutions at ambient or elevated temperatures, as required.

320 Concentrator:

Sample flow: 40 ml/min helium
Trap flow: 30 ml/min
GC carrier: 30 ml/min

Thermal desorber: 260°C, 5 min
Tenax traps: 250°C, 1 min or as indicated
Transfer line: 275°C
Valve oven: 280°C

GC-Varian 3700 FID:

Inj. and Det.: 285°C
Direct Capillary (splitless) injection
30M x 0.32MM,1 micron film; programmed 55°C, hold 3 min, 5°/min to 175°C or as indicated
Att'n: 10^{-11} range
Chart speed: 1 cm/min

Total Organic Carbon Analysis:

Sample: 10 ppb hydrocarbon (C_{10}) sampled at 0.5 l/min for 2 min onto Tenax cartridge

320 Concentrator: Thermal desorber 225°C for 5 min
Tenax trap 225°C/2 min

GC: CDS FID/TCD 14' x 1/8": mixed porous polymer ss column 140°C isothermal

Microreactors: 320 Concentrator effluent from traps led into the CDS 820WP reaction system containing CuO reactor (850°C) followed by Ni catalyst reactor (400°C, hydrogen 5 ml/min). The reaction products, CH_4 and H_2O, were detected by the internal TCD and FID.

RESULTS AND DISCUSSION

Industrial Hygiene Applications

The role of air monitoring in the industrial hygiene field has intensified over the past several years. Mandated monitoring programs require accurate sampling and analysis of trace (ppm-ppb) organics in the work and plant environment. The onsite sampling process using the 320 Concentrator is demonstrated by the results shown in Figure 3 with the conditions given in Figure 4. A test air/mixture was loaded onto a Tenax cartridge by an

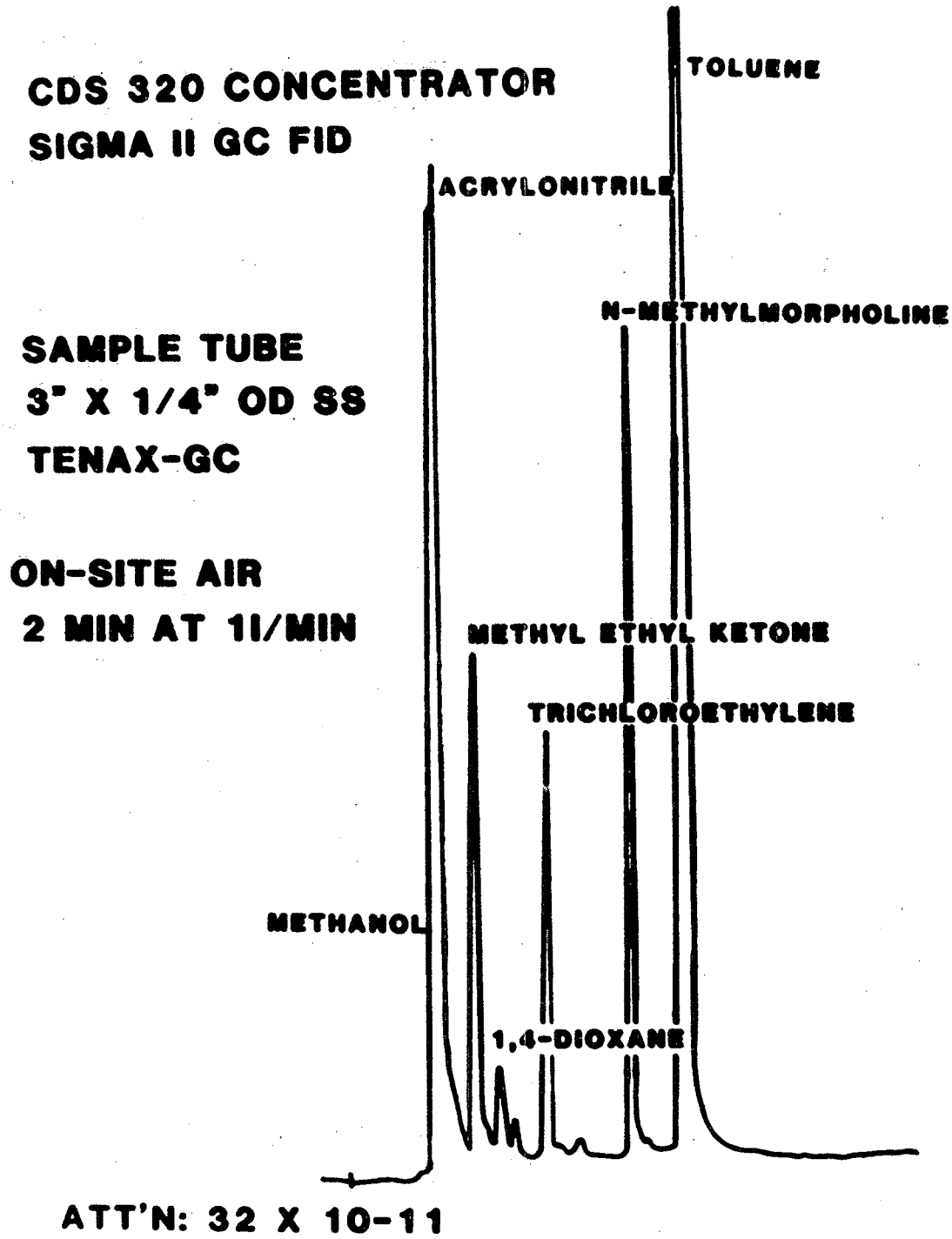

Figure 3. Remote sampling of solvents in air.

CDS 320 CONCENTRATOR

REMOTE SAMPLING:	ON-SITE AIR, 2 MIN, 1 LITER/MIN, 3" x 1/4" OD SS TENAX CARTRIDGE.
320 SAMPLING:	PURGE 1 MIN, 20 ML/MIN HELIUM; NO HEAT. HEAT THERMAL DESORBER, 200°C, 10 MIN., 20ML/MIN TO TRAP. COOL DOWN, 6 MIN.
INJECTION:	BACKFLUSH TRAP 25 ML/MIN HELIUM, 200°C, 4 MIN TO GC.

GC: P-E SIGMA II FID

PRECOL.:	12" x 1/8" OD SS 3% CARBOWAX 1500 ON CHROMOSORB W.
COL.:	8' x 1/8" OD SS 0.2% CARBOWAX 1500 ON CARBOPAK C, 25 ML/MIN HELIUM.
OVEN:	100°C, 4 MIN. THEN 10°/MIN TO 160°C, 10 MIN.
DET:	32×10^{-11}
CHART:	0.5 CM/MIN.

Figure 4. Experimental conditions for remote sampling of solvents in air.

air sampling pump, and the cartridge was then inserted into the 320 thermal desorber module. Packed column chromatography was satisfactory for this purpose, and sampling a test air mixture directly (with GC injection) compared well to the results seen in Figure 3. In this manner, typical industrial solvents are analyzed at low ppm-ppb concentrations.

Priority Pollutants - Quantitative Results

The need to examine sorbents used in the air sampling method is evident, since sorption/desorption efficiencies vary significantly for organic mixtures. Figure 5 shows the results of such test mixture components at the 40 ppb concentrations sampled and analyzed as indicated. The reproducibility of the analyses is shown in Table 1 to have a relative standard deviation of better than 5 percent. Literature results (3) using manual methods for such analyses at the ppb level rarely achieve this reproducibility. Clearly, the closely controlled automated instrumentation of the 320 has provided the much-needed improvement in a cost-effective manner. Furthermore, Figure 6 extends the range of analyses to complex hydrocarbon mixtures with high-molecular-weight components such as those in diesel fuel with the same methodology as that shown in Figure 5. Analysis of trace organics in water with the purge and trap module were reported earlier, with similar results (4).

TABLE 1. TEST AIR MIXTURE ANALYSIS
TENAX CARTRIDGE
40 PPB

Sample	Peak height, mm				Avg. 4 runs	Std. dev.	Std. dev. rel. %
Benzene	94	90	96	95	93.8	2.3	2.4
Toluene	123	112	115	129	119.8	6.7	5.6
Chlorobenzene	120	111	115	123	117.3	9.7	8.2
Heptane	68	72	65	73	69.5	3.2	4.6
O-dichlorobenzene	167	161	172	178	169.5	6.3	3.7
Dodecane	148	142	147	140	144.3	3.3	2.3
						Average	4.7%

Varied Adsorbent

Instead of Tenax adsorbent alone serving as the sorbent bed, comparison cartridges with other solvents were prepared to increase the range for monitoring polar and low-molecular-weight compounds. Figure 7 compares the

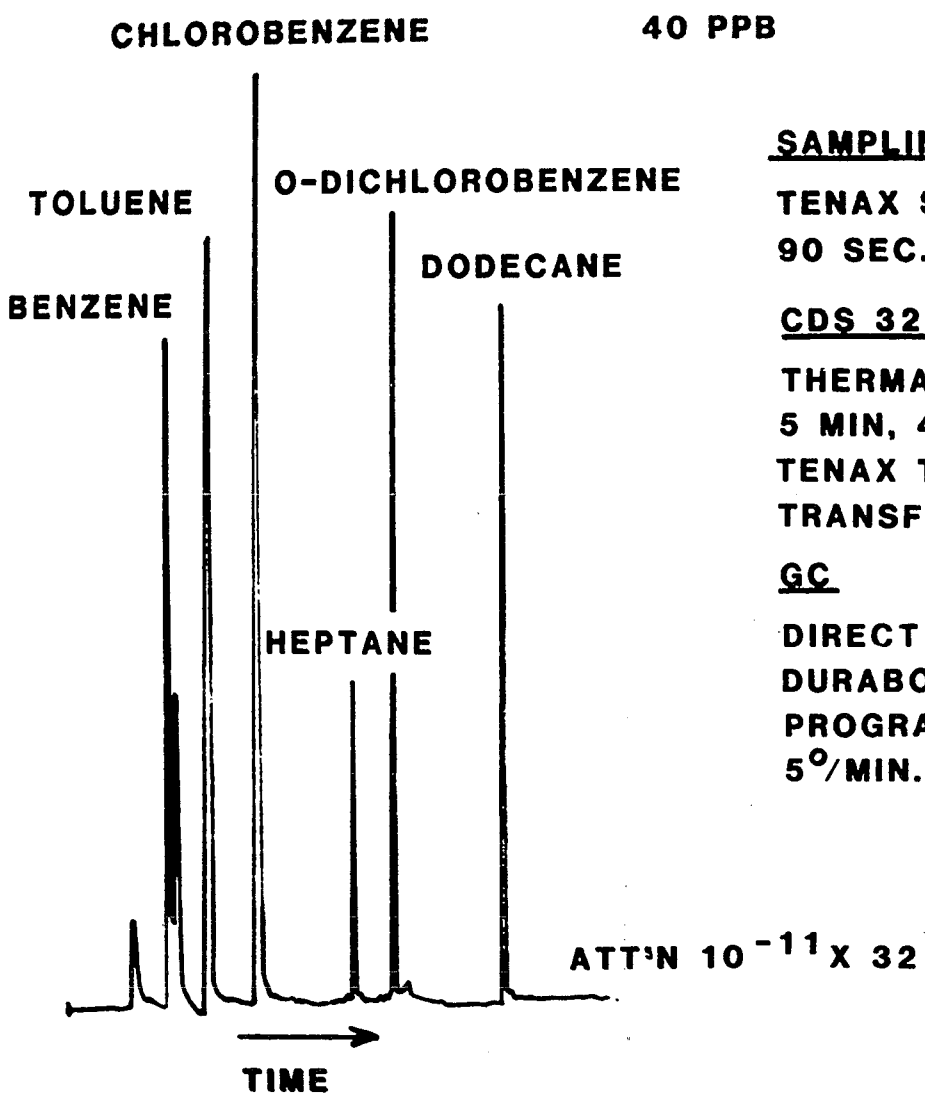

SAMPLING

TENAX SORBENT, 100 mg.
90 SEC. AT 0.5 L/MIN.

CDS 320 CONCENTRATOR

THERMAL DESORBER 260°C,
5 MIN, 40 ml He
TENAX TRAPS, 250°C, 1 MIN.
TRANSFER LINE, 275°C

GC

DIRECT CAPILLARY GC VARIAN 3700 FID
DURABOND DB-5, 30M X 0.32mm, 1 µ FILM
PROGRAMMED 55°C, 3 MIN. HOLD,
5°/MIN. TO 175°C

Figure 5. Test air mixture analysis - Tenax cartridge.

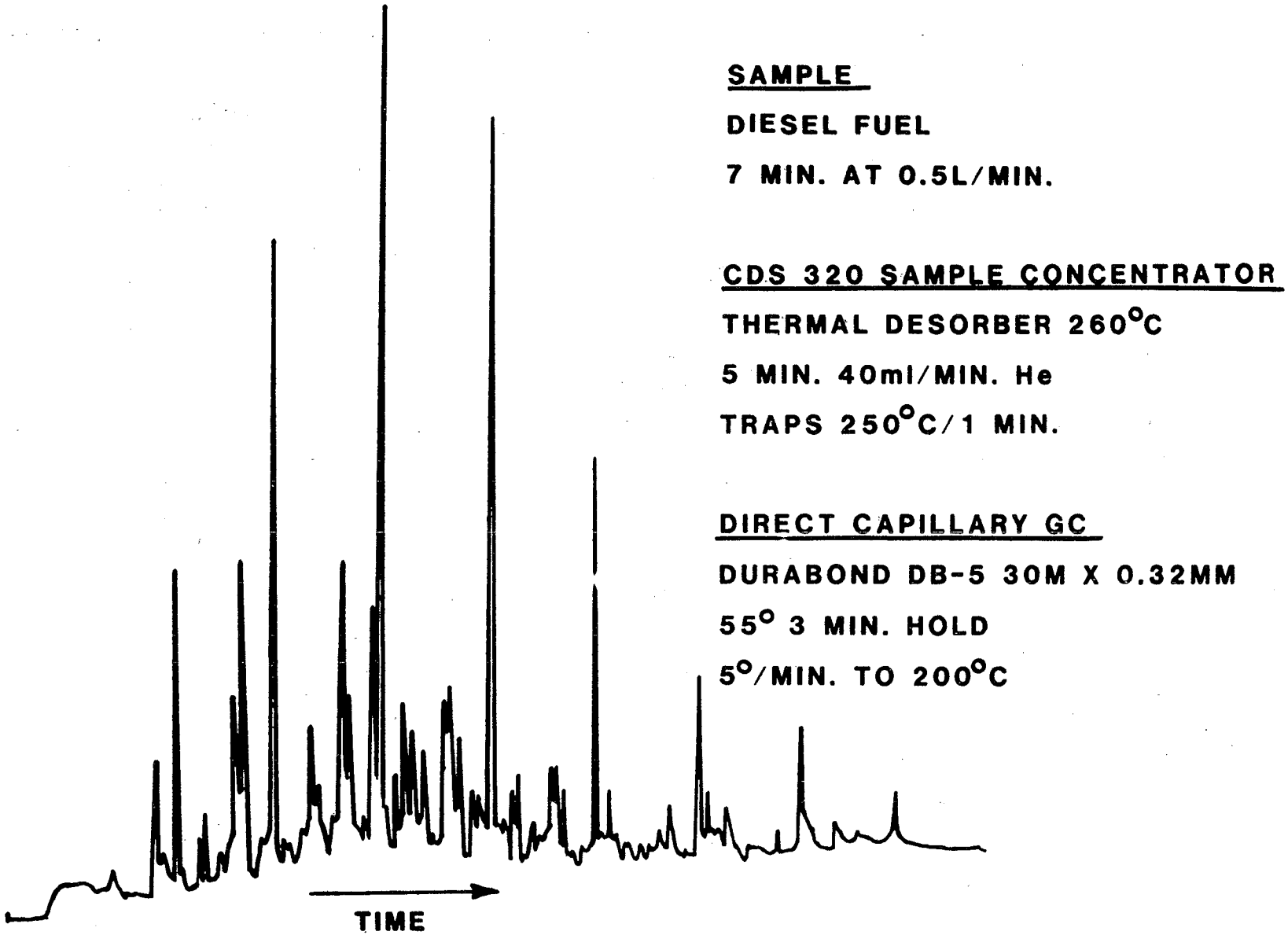

Figure 6. Test air analysis - Tenax cartridge for diesel fuel.

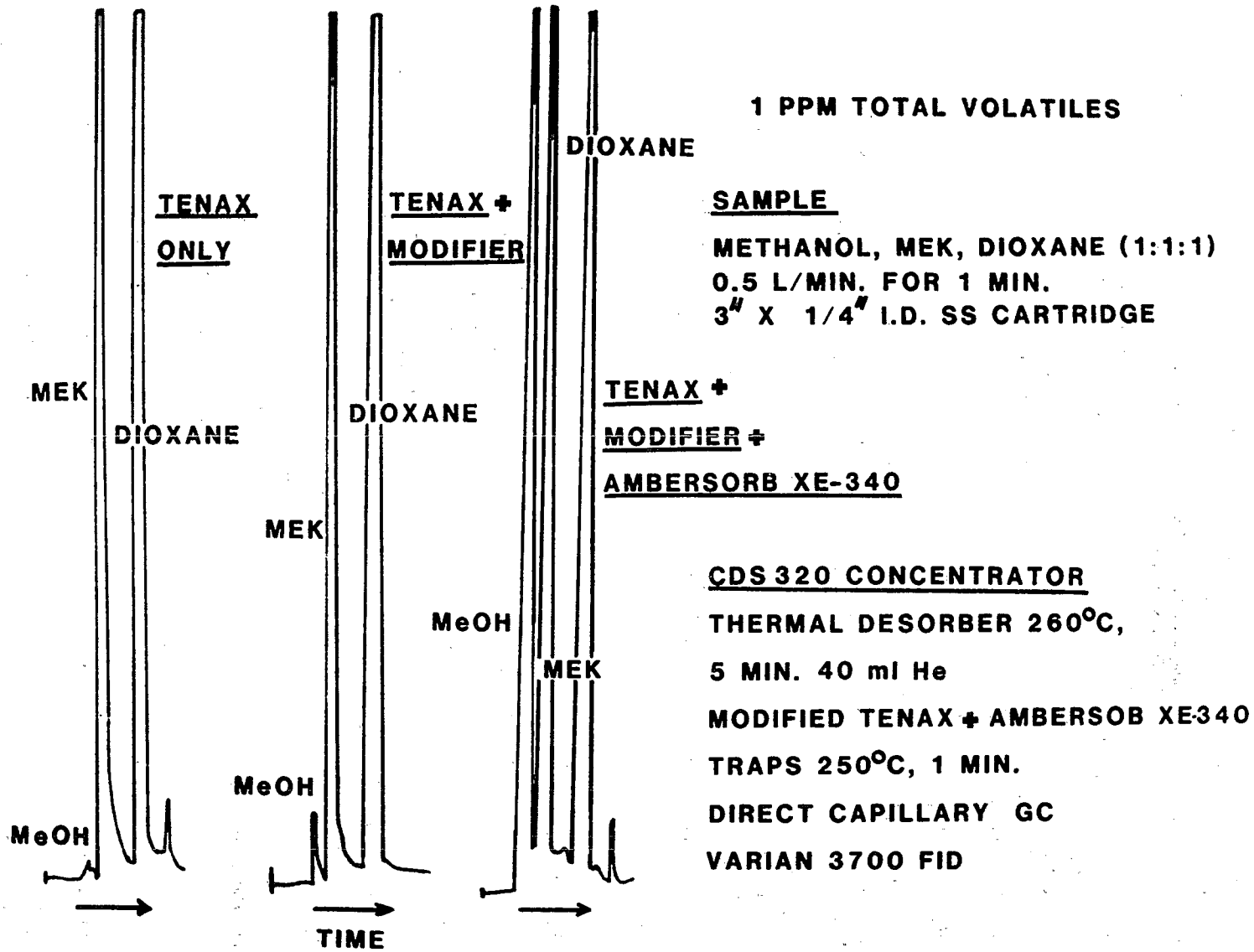

Figure 7. Test air mixture analysis - sorbent comparisons.

results from Tenax cartridges only; Tenax with CDS modifier (1:1); and Tenax + modifier + Ambersorb XE-340 (1:1:1) used for the analysis of a 1 ppm methanol, methyl ethyl ketone, and dioxane (1:1:1) test air mixture. It is shown that the Tenax with these added sorbents makes it possible to trap polar organics for improved detection and analysis. The performance of a Tenax/Ambersorb XE-340 sorbent bed is illustrated in Figure 8, with methyl formate, butyl benzyl phthalate, and naphthalene for a range of polarities and molecular weight components. Likewise, low-molecular-weight, nonpolar alkanes are poorly retained by Tenax sorbent alone, but the excellent retention shown with the Tenax/Ambersorb bed is shown in Figure 9 at the low-ppm level under the nominal sampling and analysis conditions indicated.

Total Organic Carbon Determination

Interfacing the 320 Concentrator in the above studies was achieved with a direct capillary GC configuration for high resolution analysis of the organics. Additionally, the effluents from the trap were directed via a heated transfer line to a CDS microreactor system designed for conversion of the organics to CO_2 and, subsequently, to CH_4 for FID detection. In this manner, high sensitivity detection is shown by the data in Figure 10 for a 10-ppb hydrocarbon sample sampled as indicated. Also, a TCD was in line so that the CH_4 and H_2O reactor conversion products could be chromatographed and detected with the internal GC/TCD system.

SUMMARY AND CONCLUSIONS

The versatility of modern instrumentation to sample and analyze a wide range of organics--low-and-high-molecular-weight, polar and non-polar compounds--has been demonstrated in this study using the CDS 320 Sample Concentrator. Variations in trap contents and instrumental parameters make possible accurate, reproducible analyses with minimal operator training using the microprocessor-based system. Development will continue in order to provide cost-effective methods to meet the challenge of analyzing difficult trace organics.

REFERENCES

1. Gargus, A.G., and C.R. Watterson. 1980. A microprocessor controlled purge & trap GC concentrator. American Laboratory, February.

2. Gargus, A.G., S.A. Liebman, and C.R. Watterson. 1981. Applications of advanced concentrator/GC technology. American Laboratory, May.

3. Application Laboratory. Concentrator bibliography. CDS, Oxford, PA.

4. Gargus, A.G., W. Bowe, W. Dodson, T.P. Wampler, S.A. Liebman, and E.J. Levy. 1982. Applications of concentrator/direct capillary GC system with a purge & trap autosampler. Paper No. 349, Pitts. Conf., Atlantic City, NJ.

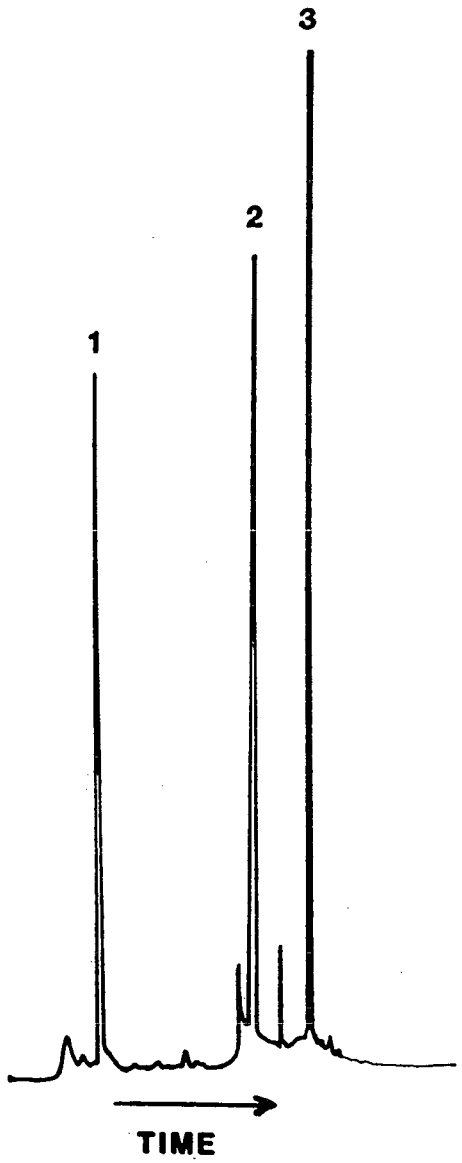

SAMPLE

1 METHYL FORMATE

2 BUTYL BENZYL PHTHALATE

3 NAPHTHALENE

320 SAMPLE CONCENTRATOR

THERMAL DESORBER 260°

5 MIN. 40ml/MIN. He

TRAPS 250°C 1 MIN.

DIRECT CAPILLARY GC

DURABOND DB-5

30 M X 0.32MM 1 μ FILM

55°C 3 MIN. HOLD

10°/MIN. TO 275°

Figure 8. Test mixture analysis Tenax/Ambersorb XE-340 cartridge.

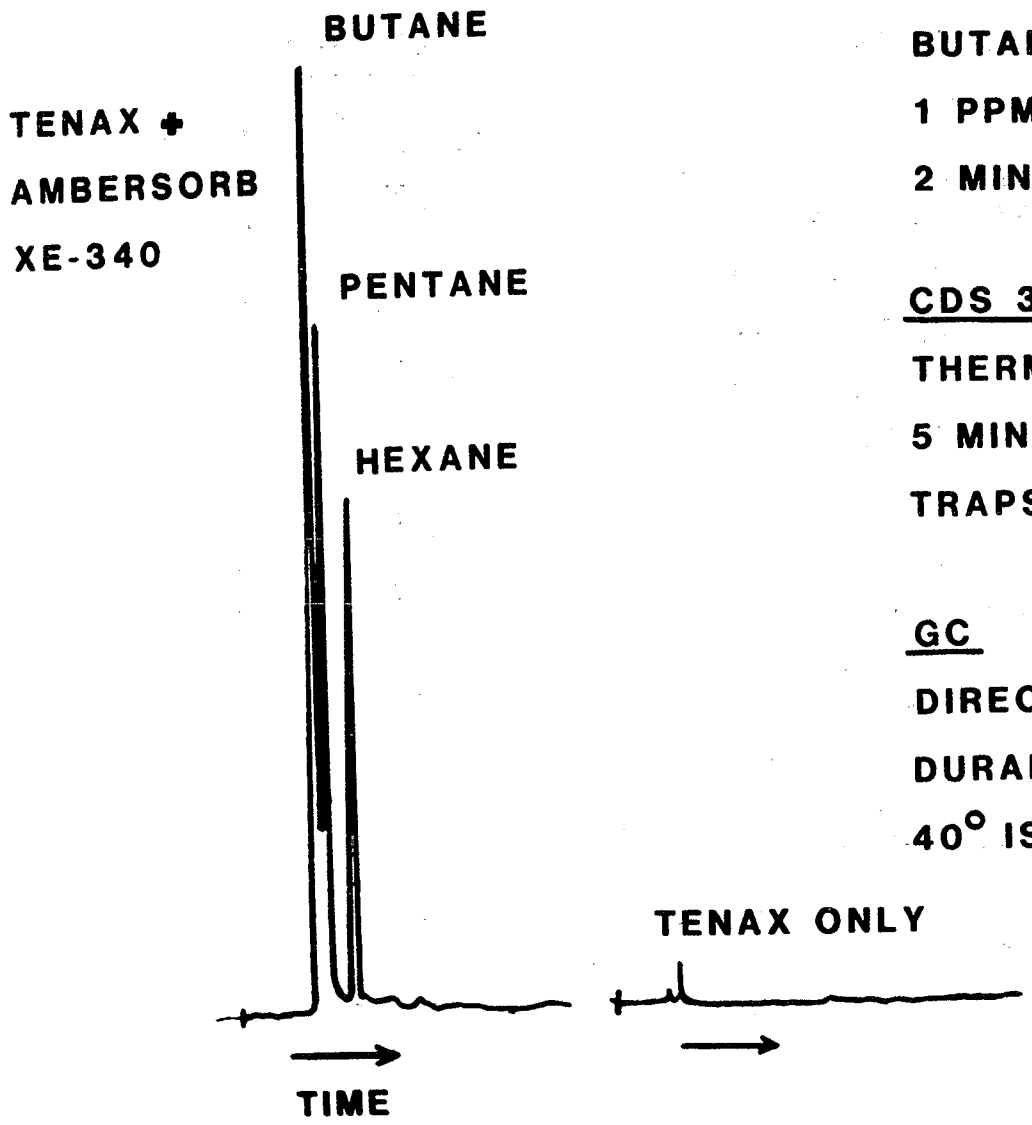

SAMPLE

BUTANE, PENTANE, HEXANE

1 PPM TOTAL VOLATILES

2 MIN. AT 0.5 L/MIN.

CDS 320 CONCENTRATOR

THERMAL DESORBER 260°C

5 MIN. 40ml/MIN. He

TRAPS 250°/1 MIN.

GC

DIRECT CAPILLARY GC

DURABOND DB-5 30M X 0.32MM

40° ISOTHERMAL

Figure 9. Test mixture analysis.

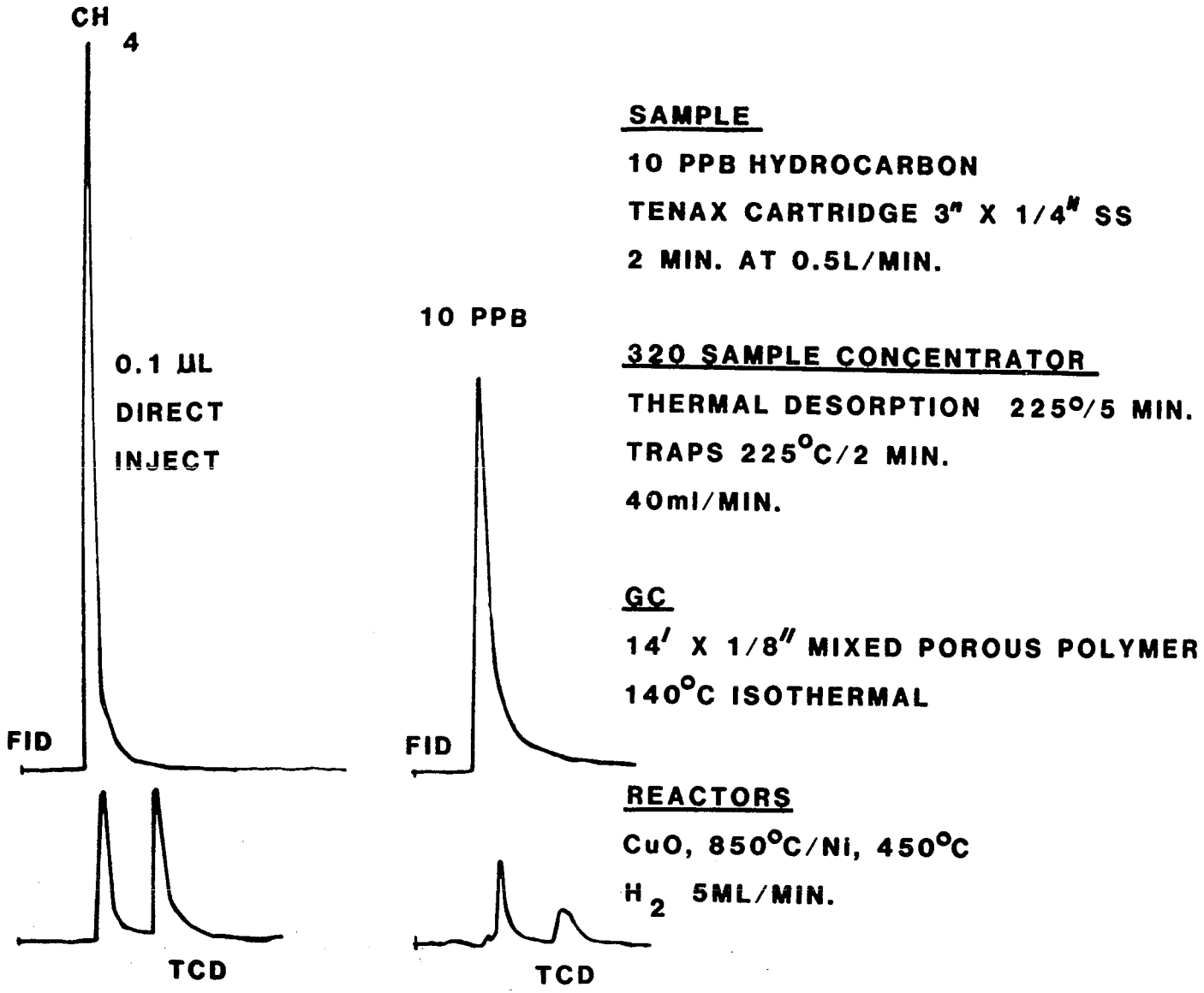

Figure 10. Total organic carbon analysis.

AIR ANALYSIS BY A NONDISPERSIVE INFRARED METHOD

Philip Hanst

INTRODUCTION

A nondispersive analyzer responds to infrared radiation, but does not spatially separate the various radiation frequencies. When compared with instruments that use gratings and slits, a nondispersive instrument shows advantages of high energy throughput, a high degree of spectral multiplexing, and an unlimited degree of spectral resolution. These advantages result from the use of optical components that are inherently responsive to spectral characteristics of compounds being measured, while passing broad bands of frequencies. The performance of the nondispersive optical system depends on correlations between the infrared spectrum of the gas being measured and the spectral response characteristics of the system elements.

For any gas, infrared absorption and emission are spectrally similar. This allows a gas-filled microphonic detector to respond more strongly to radiation from a heated sample of that gas than to radiation from other gases. Using a continuum source, such a detector will also see absorption by the chosen gas more strongly than absorption by other gases. These correlations are the operating basis of widely used nondispersive analyzers called positive-filter systems and described, for example, by Luft (1). The performance of these systems has been mainly limited by interferences from absorbing species other than the one being measured, especially from water vapor.

When the components of a nondispersive analyzer are arranged in what is called the negative filter configuration, a high degree of discrimination between the object gas and other gases is obtained. These negative-filter systems have not yet had as much commercial use as the positive filter systems (based on the microphonic detector), but they have proven their worth in a number of development projects and field tests (2-7). Ambient air pollution measurement requires the high selectivity of the negative filter system.

All nondispersive analyzers have as basic components a radiation source, filters, a sample cell, a radiation detector, and electronics that process and display the detector signal. Nearly all systems have at least one rotating light chopper. The systems currently in use do not differ basically from those studied by Pfund and others in the 1940s (3). Although the principles of operation of the systems have not changed in the last 35 years, capabilities of system components have been greatly expanded. Filters, detectors, and electronics have been especially improved. When these improvements are coupled with gas-filled filter cells for interference removal, it is found that the sensitivity of the nondispersive technique becomes great enough for direct measurement of pollutants in the ambient air.

SYSTEM OPERATIONAL PRINCIPLES

A nondispersive instrument in the negative filter configuration is diagrammed in Figure 1. Radiation sources in instruments described in the literature have included hot wires, globars, Nernst glowers, heated gas, and the sun. The source spectrum may be altered by spectral filters that can be positioned nearly anywhere in the optical train. Typically, source filtering might be done with a narrow band interference filter in combination with a gas-filled filter cell. The emitted radiation is passed through a sample cell, which may be a single-pass type or the many-pass type (White cell). In field studies, the sample has been the open atmosphere. The gas correlation filter cells have usually been just a few centimeters in length, containing the filter gas at a partial pressure of several torr. The optical trimmer is a neutral density filter that can be adjusted to balance the two beams. Wedges or screens can be used for this. Beam-combining optics and a photoelectric detector complete the train of optical components. The beam alternator was the only moving part in the system studied in the present experimental program. Instead of beam alternation, one could choose to modulate each beam at a different frequency and to monitor the intensity ratio of the two frequency components.

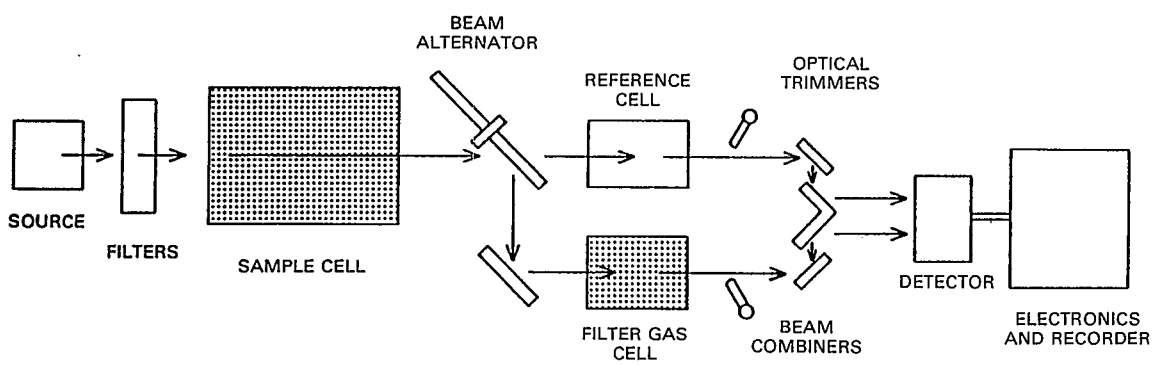

Figure 1. Nondispersive analyzer in negative filter configuration.

System operation can be understood by considering the spectra and

detector signal in the absence and presence of the gas being measured (object gas). Let it be the case that the source and its filters produce a range of frequencies that encompasses two spectral lines of the object gas. Figure 2 (upper half) shows the spectrum in the two channels of the instrument when there is no object gas in the sample cell. The absorption lines appear only in the filter gas channel, and the optical trimmers are adjusted to give equal total intensities with a consequent zero detector signal at the beam alternation frequency. Then, when the object gas does appear in the sample cell (lower part of figure), its absorption lines appear in both channels, the intensities at the detector become unequal, and a signal with the beam alternation frequency appears. The system is called negative filter because the intensity reduction is greater in the reference channel than in the gas filter channel.

Interfering gases will increase the signal when their absorption lines overlap with the lines of the object gas and will decrease the signal when the lines do not overlap. If the interfering gas has many lines in the spectral region being used, the positive and negative interferences might nearly cancel each other.

The following symbols are defined:

V_1, V_2 = Detector output for the filter cell and reference channels

T_1, T_2 = Transmission of the optical trimmers in the filter cell and reference channels (will be between 0 and 1)

$I(\nu)$ = Source intensity as function of infrared radiation frequency, ν

$R(\nu)$ = Response of detector

$T_F(\nu)$ = Transmission of source filter

$T_G(\nu)$ = Transmission of gas-filled filter cell

$T_S(\nu)$ = Transmission of sample under study

For the filter cell channel, V_1 is then given by an integration over all frequencies:

$$V_1 = T_1 \int_0^\infty I(\nu)R(\nu)T_F(\nu)T_G(\nu)T_S(\nu)d\nu$$

If at a given frequency any of the factors has a zero value, then that frequency does not contribute to the signal.

For the reference channel, the detector signal is given by a similar integration without the factor $T_G(\nu)$:

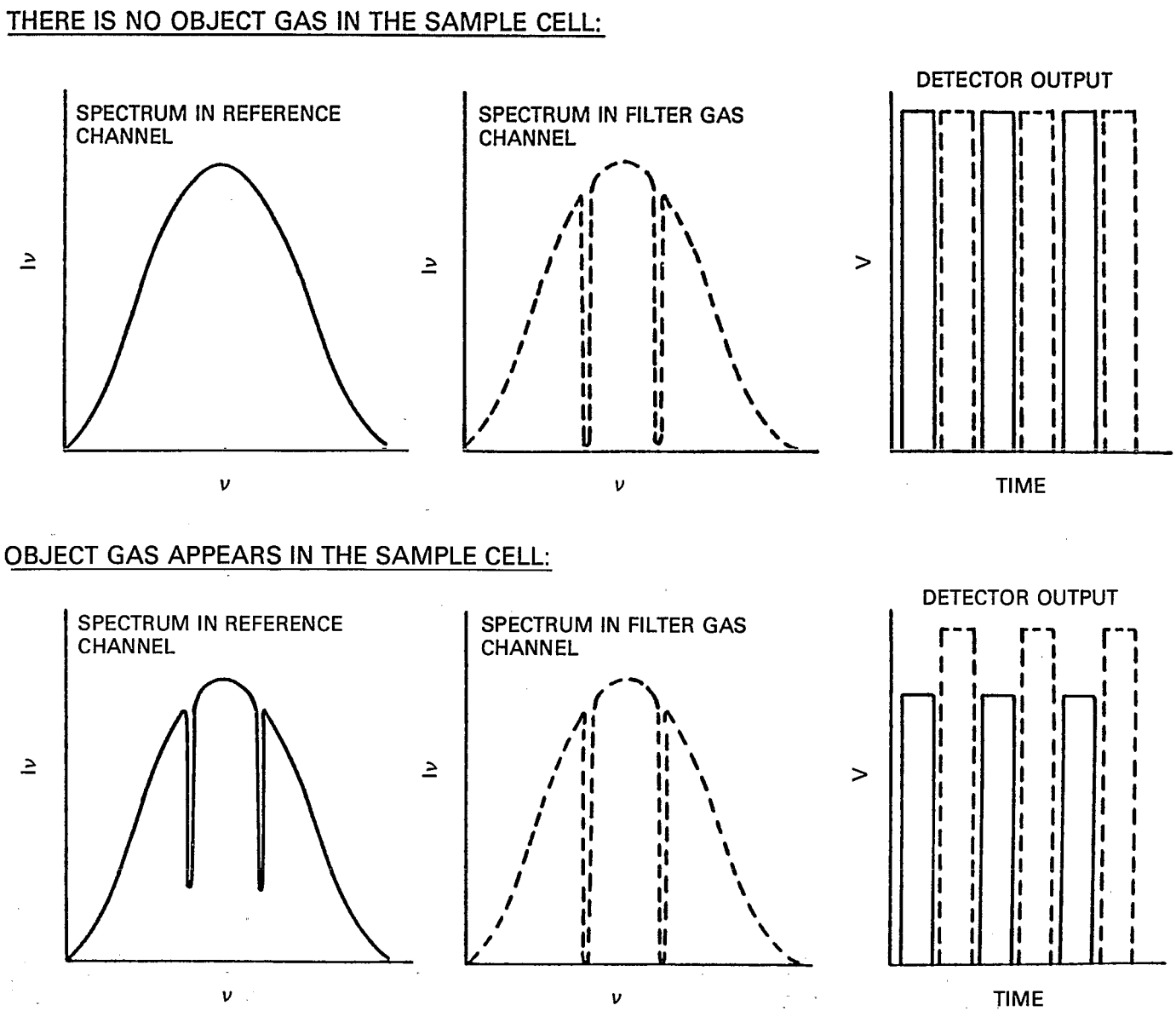

Figure 2. Spectra and detector signals in nondispersive analyzer.

$$V_2 = T_2 \int_0^\infty I(\nu)R(\nu)T_F(\nu)T_S(\nu)d$$

Since the missing factor, $T_G(\nu)$, is always smaller than unity, the signal balance $V_1 = V_2$ will require T_1 to be greater than T_2. In other words, the optical trimming is done mainly in the reference channel.

Detector, filters, and source must be chosen to give a spectral pass band that favors the object gas and discriminates against possible interfering gases. Because the sample transmission, $T_S(\nu)$, will be less than unity, filling the sample cell will cause a decrease in both V_1 and V_2. If $T_S(\nu)$ correlates with $T_G(\nu)$, then the decrease in V_2, (ΔV_2) will be greater than the decrease in V_1, (ΔV_1). If the object gas is the only species in the sample that absorbs in the band pass of the system, the correlation between $T_S(\nu)$ and $T_G(\nu)$ will be so high that ΔV_1 will be near zero and ΔV_2 will be nearly the whole signal. $\Delta V_2/V_1$ is then the apparent integrated absorptivity in the band pass region.

Proper choice of source, detector, and filters will center the band pass around a chosen band of the object gas, thus maximizing the integrated absorption coefficient. If the object gas has a broad absorption band in a spectral region relatively free from interference, then the best system design would include a filter with a band pass slightly wider than the spectral band of the object gas. This would be the case for NO_2 or SO_2, or when using the C-H band to measure hydrocarbons.

If the object gas has a band with only a small number of lines widely spaced, then most of the energy would fall between the spectral lines and the use of a continuum source with a band pass filter will not yield a high absorption coefficient. In this case, a heated sample of object gas could be used as source. The emitted lines would match the absorption lines quite well, with little energy falling between the lines, and therefore the integrated absorption coefficient would be high. This technique can be used for detecting HCl, CO, NH_3, NO, and other thermally stable small molecules.

REMOVAL OF INTERFERENCES

When another gas has no lines within the band pass selected for detection of the object gas, there will of course be no interference. If there are such lines, they can be blanked out of both beams by placing enough of said gas in a filter cell located in the combined beam portion of the optical train. The system will then be "blinded" to the interfering gas. Interference between pollutants is only an occasional problem because the main absorption bands of the major gaseous pollutants do not generally overlap each other and besides, the absorption by each pollutant is very slight. The absorption by water vapor, however, is very great, and the main bands of several important pollutants, such as NO_2, NO, and SO_2, do fall within strong regions of absorption by water. For the detection of these pollutants, the system must be blinded to water vapor.

A small cell cannot be used to blind the system to water vapor because

at ordinary temperatures the vapor pressure of water is no higher than about 0.03 atmosphere. Instead, a long path filter cell is required. Preferably, the product of water vapor concentrtion times pathlength should be greater in the filter cell than in the sample cell. Thus the system requires two long path cells in tandem. On first consideration, it appears that two long path cells would invalidate the system design by being too cumbersome and too sensitive to misalignments. Therefore, a major aspect of this research has been to find a way to build long path cells that are compact, inexpensive, and permanently aligned. This effort has been a success. A cell design has been evolved that has such a degree of stability and permanency of alignment that having two long path cells in tandem is not a limit on system performance.

LONG PATH CELL DESIGN

The multiple-pass optical technique of J.U. White has been used in the cell design (8). Three telescope mirrors, all with the same radius of curvature, are arranged to reflect the beam of radiation back and forth within a tube. The beam is re-focussed on every other pass so that the energy is conserved.

The only major source of energy loss in the mirror system is the absorption by the mirror surfaces. If R is the reflectivity of the mirrors, the fraction of the input energy that will be lost at n reflections will be $(1 - R^n)$. At each encounter, a clean mirror will reflect about 97.5 percent of the incident energy. For such a mirror, the optimum case is to have 40 reflections, which allows about 37 percent of the energy to be transmitted. Adding more reflections than this will decrease the energy faster than the pathlength is increased.

Normally, the mirrors of a White cell are held at the ends of the cell body in spring-loaded kinematic mounts with precision micrometers for adjustment. Such cells are not only costly but are subject to misalignments from vibrations and temperature changes. In the present work, it has been found possible to avoid these limitations by cementing the mirrors permanently within a glass pipe. Alignment is achieved with assistance of a laser beam that is reflected back and forth between mirrors during the cementing process. The mirrors are trimmed to closely fit inside the glass pipes and are fixed in place with epoxy cement. Each cell carries a transfer optics assembly for coupling the radiation in and out. Cells of this type have been found to maintain their alignment over a two-year test period. Since the cell design avoids precision mechanisms, there is no great expense involved in building two such cells into a nondispersive analyzer.

DETECTION SENSITIVITY

Detection sensitivity may be examined in terms of the absorption equation: $\ln I_o/I = k \cdot L \cdot c$. I_o is the incident energy within the pass band, and I is the transmitted energy. k is the absorption coefficient

averaged over the pass band, L is the pathlength through the sample (in centimeters), and c is the concentration of the absorbing species (its partial pressure in atmospheres).

The detection limit is assumed to be reached when the signal reduction due to sample absorption equals the noise level (N) of the total signal (S). Since one is always working in the small absorption range, $\ln I_0/I$ at the detection limit is approximately equal to the noise-to-signal ratio, N/S. There is no apparent reason why the N/S of a properly designed system cannot be 10^{-4} or smaller. In the laboratory breadboard system used for tests described here, the N/S was approximately 10^{-3}. Detector noise was not the limitation. Rather, mechanical stability of the optical system was the limitation. This can be improved by better construction.

In addition to optical system stability, the second major objective of system design is to develop the largest possible absorption coefficient, k, for the object gas. The higher the value of k, the shorter the required pathlength, L. For a strongly absorbing species, when the pass band is properly centered on the absorption band, the value of k can be as high as 50 cm^{-1} atm^{-1}. If the absorption is weak, or if there is difficulty in controlling the pass band, k might be as low as 1 cm^{-1} atm^{-1}.

Because the system always operates in the small absorption range, the output signal is directly proportional to the concentration of the object gas.

The detection limit, c, is listed in Table 1 as a function of noise-to-signal level, absorption coefficient, and pathlength. Tests conducted in the present study have shown that, for many important air contaminants, the bottom line detection limit of 10^{-9} atmospheres is achievable. If the system designer is only seeking parts-per-million sensitivity rather than parts-per-billion, then he can allow the indicated shorter pathlengths and higher values of noise-to-signal ratio.

LABORATORY TESTS

Equipment

An experimental nondispersive analyzer system was set up as diagrammed in Figure 1, using the following components in various combinations:

1. Sources:	Nernst glower, heated gas-filled cells
2. Filters:	Long path cell with humidified air, 10-cm cells with such filter gases as methane, CO_2, etc.
3. Sample cell:	Multiple-pass cells of the type described in text.
4. Beam alternator:	P.A.R., two-channel lock-in chopper with four-aperture blade

TABLE I. DETECTION LIMIT AS FUNCTION OF SYSTEM PARAMETERS

Ratio of noise-to-signal (N/S)	Absorption coefficient k (cm^{-1} atm^{-1})	Path-length L (cm)	Detection limit C (atm)
10^{-3}	1	10^{+3}	10^{-6}
		10^{+4}	10^{-7}
	10	10^{+3}	10^{-7}
		10^{+4}	10^{-8}
10^{-4}	1	10^{+3}	10^{-7}
		10^{+4}	10^{-8}
	10	10^{+3}	10^{-8}
		10^{+4}	10^{-9}

5. Filter gas and reference cells: Cylindrical gas absorption cells 10 cm long and 2.5 cm in diameter

6. Optical trimmer: Optical trimming was done by defocussing one beam or the other at the detector

7. Detectors: Mercury-cadmium-telluride and indium antimonide at liquid nitrogen temperature

8. Electronics: Hughes and Digilab pre-amplifiers with P.A.R. lock-in amplifier

9. Recorders: Tektronix scope and Hewlett-Packard recorder

Ammonia Test Results

Ammonia is a compound that is thermally stable and has many widely scattered lines in its spectrum. It therefore is a candidate for the measurement technique that uses a heated gas sample as the radiation source. A standard type of 10 cm infrared absorption cell wrapped with heating tape was used as the test source. Barium fluoride windows were cemented on with silicone cement. About 50 torr of NH_3 gas was placed in the cell, and the temperature was raised to 300°C. The resulting emission spectrum is shown in Figure 3, bottom half. The emission continuum that underlies the gas lines probably came from the BaF_2 windows, whose emissivity would increase in the lower frequency direction, as seen in the figure. The upper part of the figure shows the spectrum of the radiation after it had passed through the gas filter cell containing a few torr of ammonia gas at room temperature. It can be seen that the strong lines have been removed from the emission spectrum, while the weak lines are only slightly

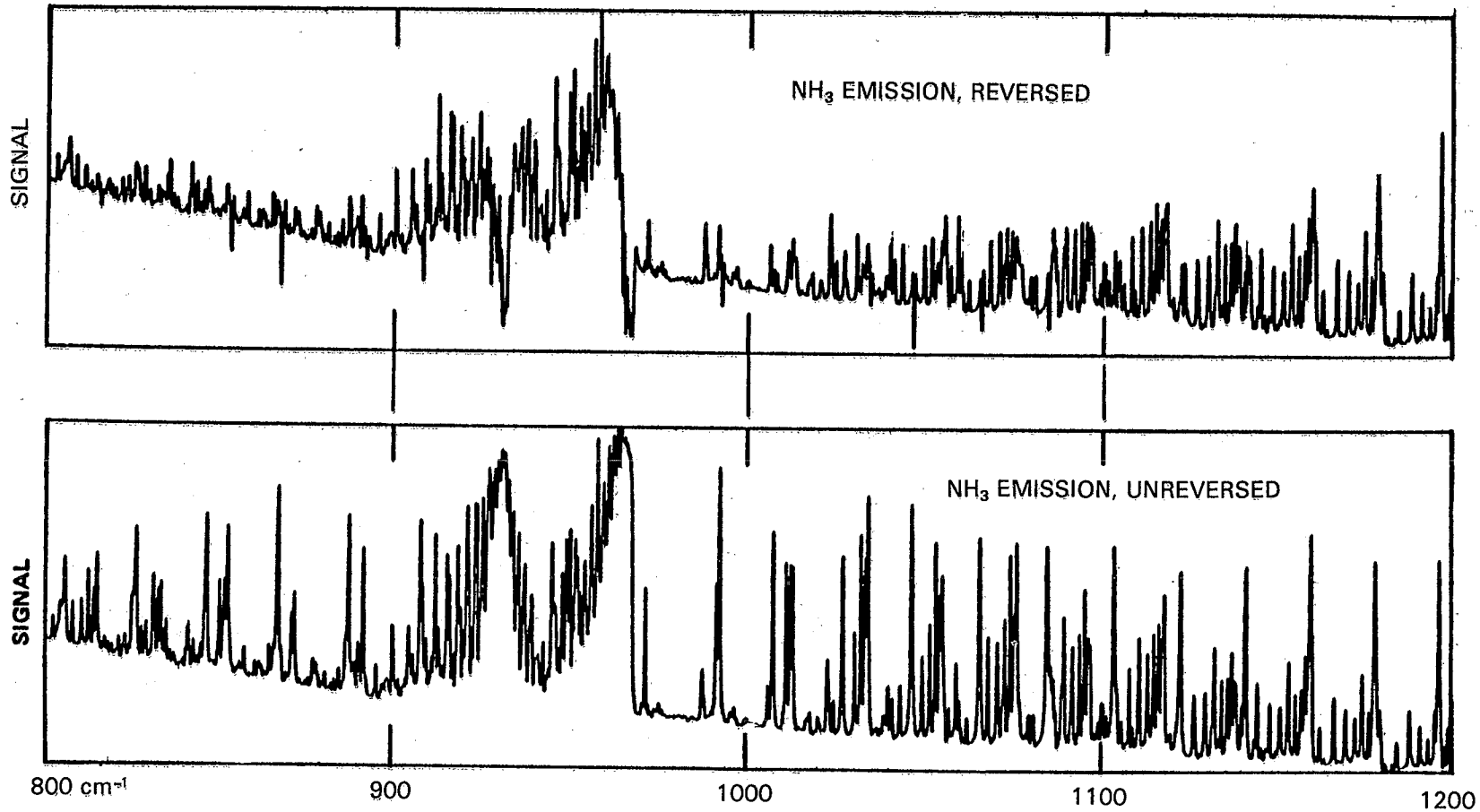

Figure 3. Emission spectra of ammonia in nondispersive analyzer.

attenuated. In the test system, the beam alternation was therefore comparing the reversed spectrum against the unreversed. When ammonia appeared in the sample cell, it caused an imbalance between the two beams with a high absorption coefficient. If the underlying continuum had been eliminated by the use of windows that did not absorb or emit in the pass band, the absorption coefficient would have been still higher.

Since there are only a few water vapor lines in the ammonia emission region, there was no need for a water vapor filter cell. Furthermore, the detailed structure in the ammonia band allowed a highly selective ammonia detection, with practically no interference from other compounds. Ammonia detection was tested using an early version of the test optical system, in which the pathlength was 30 meters and the noise-to-signal ratio of the system was about 10^{-2}. In this test, 5 ppm of ammonia in air gave a signal about 30 times greater than the noise.

Sulfur Dioxide Results

Sulfur dioxide was detected in tests using two radiation sources: (1) heated SO_2 gas, and (2) the Nernst continuum source with band-pass filter. The strong SO_2 band that falls between 1300 and 1400 wave numbers appears to be the best band to use, but this band falls within a region of strong water vapor absorption. To prevent interference by atmospheric humidity changes, it was therefore necessary to blind the SO_2 system to water by including in the optical train a water vapor-filled long path cell. Figure 4 (lower half) shows the emission spectrum of the SO_2-filled source cell heated to about 300°C. The upper part of the figure shows the altered spectrum after the radiation was passed through a sample of SO_2 gas at room temperature.

The system was operated using the SO_2 gas source, but without the long path water vapor filter cell. A sample cell of 30 meters pathlength was used. Ambient air was slowly flushed through this cell and small amounts of SO_2 were introduced periodically. This produced an SO_2 concentration that rose and fell between 0 and 0.1 ppm. The rise and fall in output signal under these conditions is shown in Figure 5 (upper portion).

The second radiation source for SO_2 detection was tested using two long path cells in series, the first being the water-filled filter cell. In this case, the Nernst glower was operated at a temperature of about 1700 K, and its radiation between about 1230 and 1390 cm^{-1} was isolated by use of a band-pass interference filter. Figure 6 shows the spectrum of the radiation at three places in the optical train: (A) after it passed through the long path filter cell containing water vapor, but not the sample cell, (B) after it passed through both the long path filter cell and the long path sample cell with room air, and (C) after it passed through both long path cells and the SO_2-filled filter gas cell. Nearly all the absorption lines in spectra (A) and (B) are due to water vapor. It is to be noted that spectrum (B) shows only slightly greater absorption than spectrum (A), illustrating the blinding of the system to humidity changes. Spectrum (D) is a ratio plot of spectrum (C) divided by spectrum (B), showing the absorption by the SO_2 in the filter gas cell. This is the

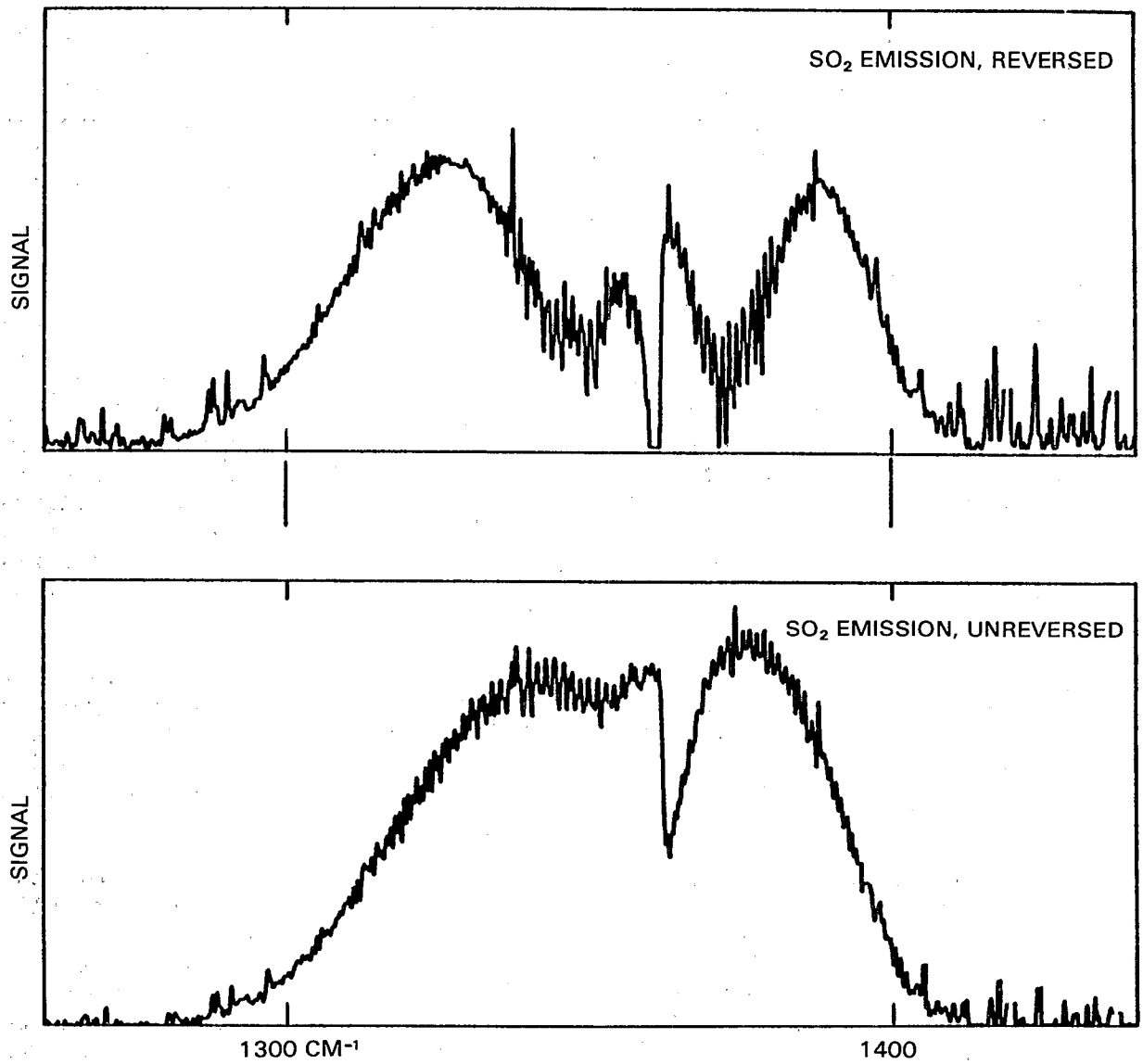

Figure 4. Emission spectra of sulfur dioxide in nondispersive analyzer.

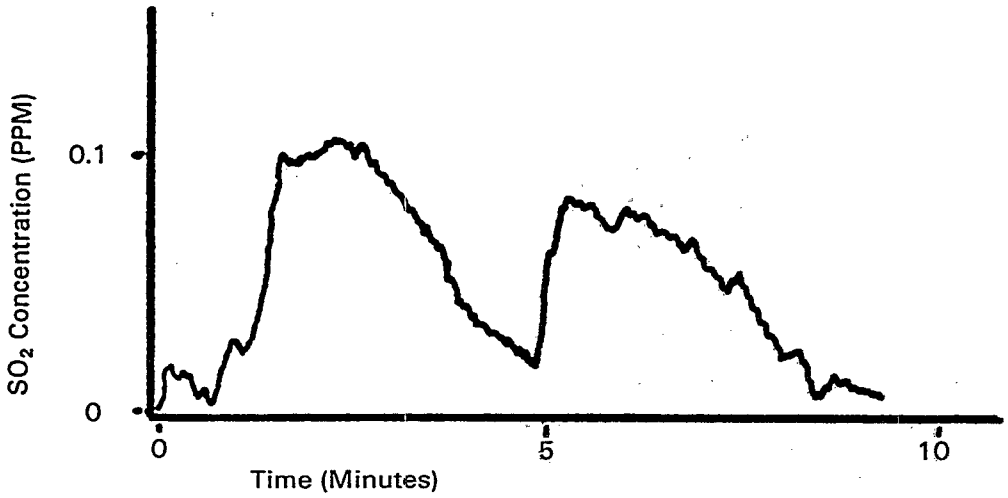

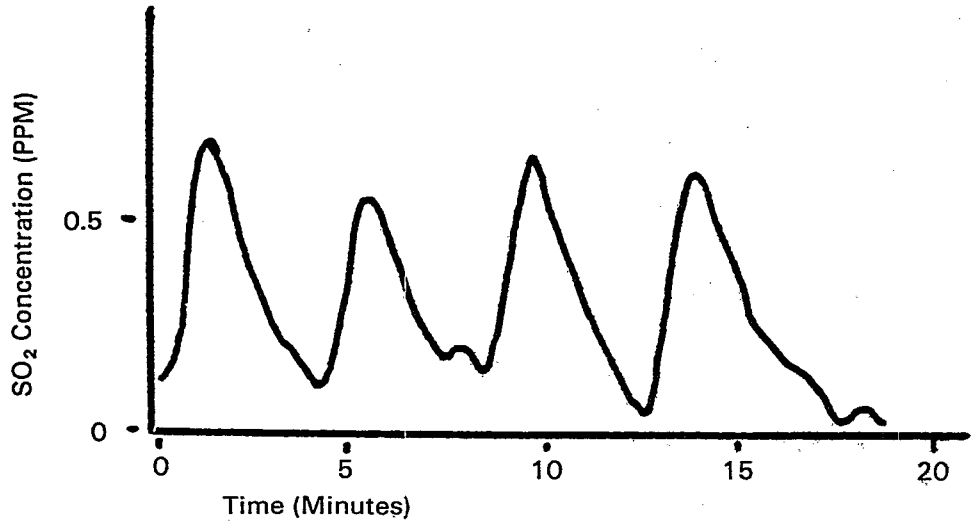

Figure 5. Detection of SO_2 by nondispersive analyzer.
Path = 30 meters.
Upper - Heated SO_2 gas source, no water filter cell; detection time constant = 3 seconds.
Lower - Nernst glower source with band-pass filter; 30-meter sample cell in series with 30-meter water vapor filter cell; detection time constant = 10 seconds.

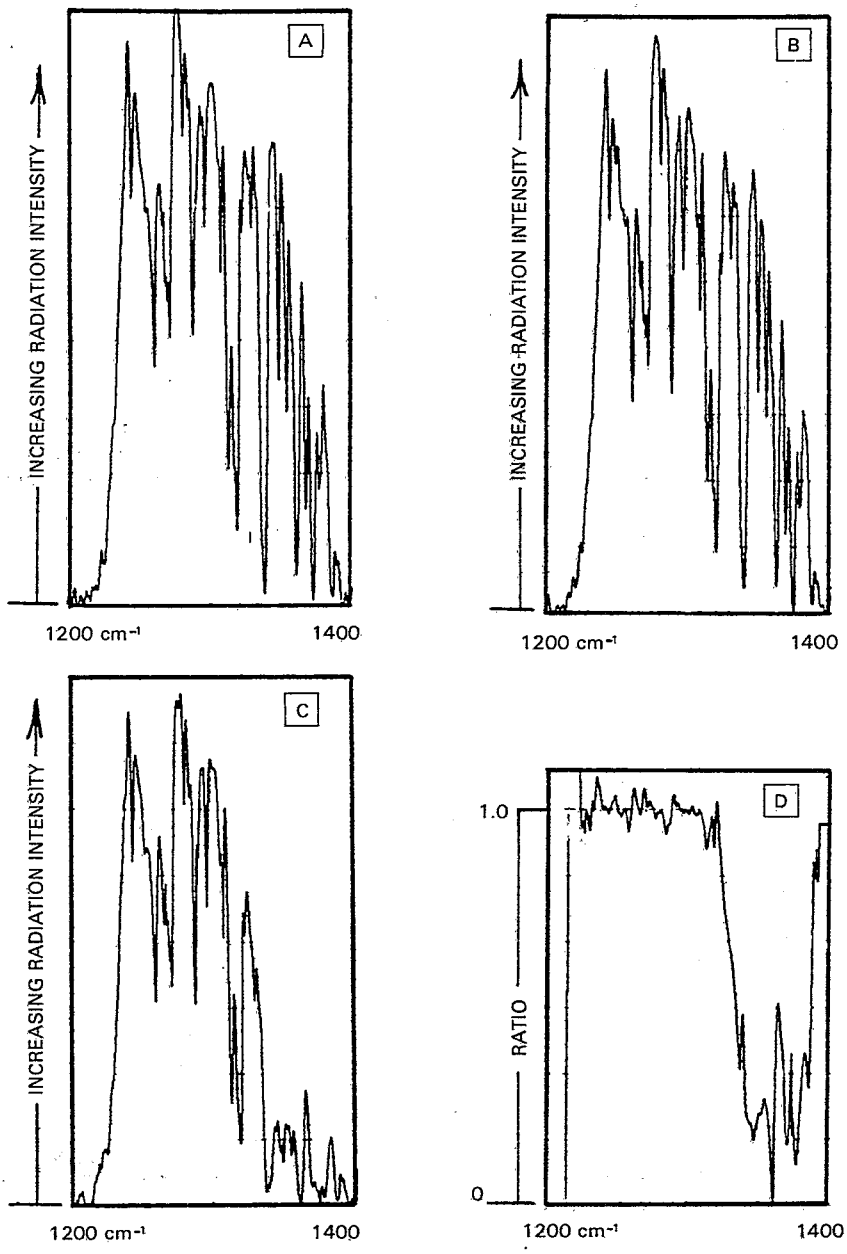

Figure 6. Spectra in nondispersive analyzer tuned for sulfur dioxide.
A - Source radiation through 30-meter filter cell with water vapor; sample cell empty.
B - Source radiation through 30-meter filter cell with water vapor and 30-meter sample cell containing one atmosphere of ambient air.
C - Radiation shown in (B) after passing through sensitizer filter cell with SO_2 gas.
D - Spectrum (C) divided by spectrum (B).

absorption that is compensated by the optical trimming.

This second SO_2 detection system was tested in the same way as the first, by periodically introducing small amounts of SO_2 into the air stream flowing through the sample cell. In this case, the SO_2 amount peaked at about 0.7 ppm, giving the signal changes shown in the lower part of Figure 5.

Hydrocarbon Results

Hydrocarbons were measured using the C-H absorption band near 2900 cm^{-1}. In this case, the Nernst glower source was used with a band-pass filter. For hydrocarbon detection, the analyzer was sensitized by placing butane in the filter cell. The infrared spectra at the several points in the optical train are shown in Figure 7. Part A is the spectrum of the source after the radiation passed through the 30-meter filter cell containing water vapor; B is the spectrum after the radiation passed through both the 30-meter filter cell and the 30-meter sample cell; C is the spectrum after the radiation passed through both sample cells and the butane-filled filter gas cell; and D is the ratio plot of spectrum C divided by spectrum B, showing the butane band that must be compensated by optical trimming.

This dual cell hydrocarbon-tuned system was tested by flowing air through the sample cell while periodically introducing small amounts of butane into the stream. The changes in output signal for a 5-ppm peak concentration of butane are shown in Figure 8. It can be seen in the figure that the signal-to-noise ratio was quite high, even for a detection system response time of 3 seconds, and that it became higher as response time lengthened. Tests showed that system response to an individual molecular species was approximately proportional to the number of carbons in the molecule. Thus, 1 ppm of hexane would give about twice the signal given by 1 ppm of propane.

The hydrocarbon detection sensitivity could have been further improved by narrowing the band-pass. Figure 7 shows a band-pass of approximately 900 cm^{-1}, while the butane band itself was only about 100 cm^{-1} wide. If the band-pass filter had a total width of about 200 cm^{-1}, the absorption coefficient would have been about five times higher.

The hydrocarbon-tuned system will not respond to methane. The system is blinded to methane as well as to water vapor because methane is a constituent of the air in the long path filter cell. Different choices of filters could make the system sensitive to methane and blind to nonmethane hydrocarbons.

Hydrogen Chloride

The measurement of hydrogen chloride gas was found to be difficult because of the weakness of its one infrared absorption band. This band does fall in a clear region of the spectrum so that there is very little interference from other gases, but the band has only a small number of absorption lines spread across a wide spectral region. HCl is a compound

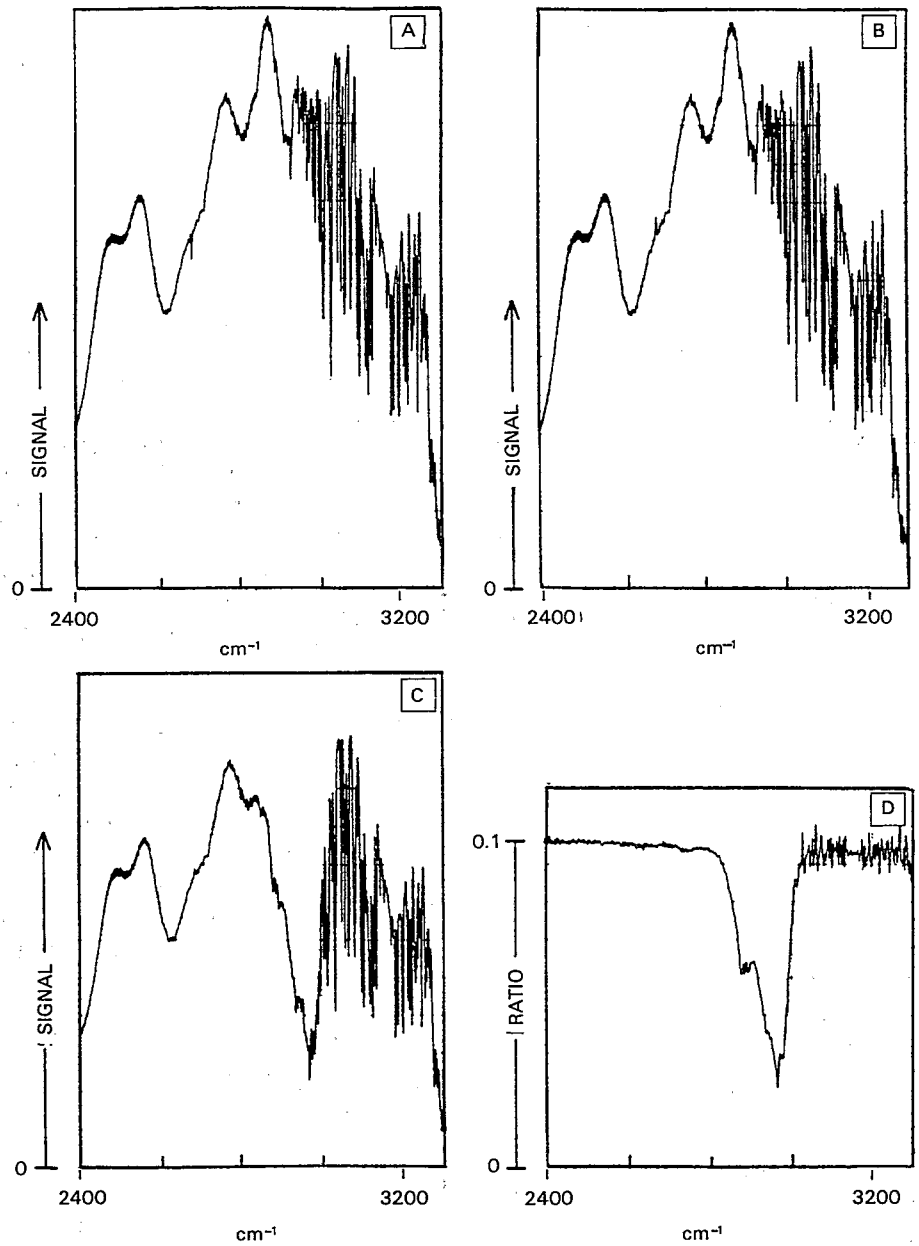

Figure 7. Spectra in nondispersive analyzer tuned for nonmethane hydrocarbons.

A - Source radiation through 30-meter filter cell with water vapor; sample cell empty.

B - Source radiation through 30-meter filter cell filled with water vapor and 30-meter sample cell containing one atmosphere of ambient air.

C - Radiation shown in (B) after passing through sensitizer filter cell with butane gas.

D - Spectrum (C) divided by spectrum (B).

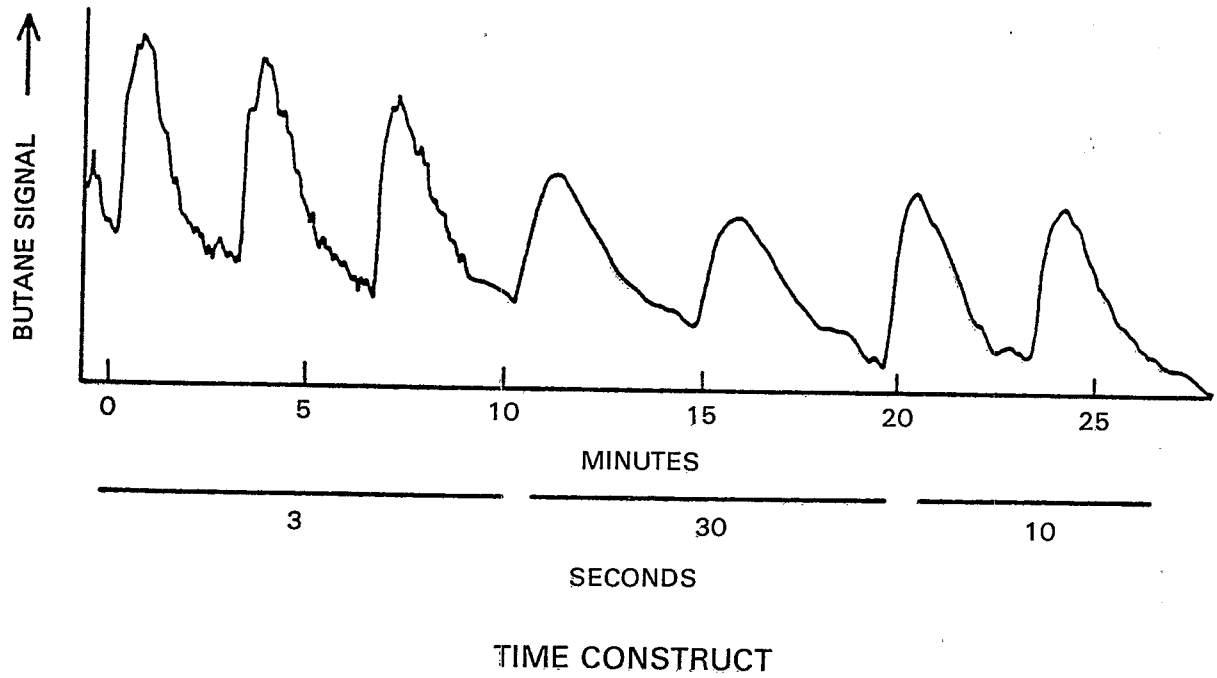

Figure 8. Detection of butane by nondispersive analyzer.
Path length = 30 meters
Band pass = About 700 cm^{-1} (2500 to 3200)
Each peak resulted from adding butane to flow of room air through cell, giving about 5 ppm butane at the peak.

that should best be measured using as its radiation source a cell containing HCl vapor at a high temperature.

Tests with such a source did indeed show substantial increases in sensitivity over tests using a continuum radiation source. Several difficulties were encountered with this source, however, preventing a full test of the potential of the method.

For a gas-filled cell to be successful as a source, its windows must be both nonabsorbing and nonscattering. If the windows absorb, they also emit unwanted continuum radiation that drastically lowers the absorption coefficient exhibited by the object gas. If the windows scatter, they will introduce into the optical path continuum radiation from the cell walls. This radiation will also drastically reduce the absorption coefficient of the object gas.

The fogging of sodium chloride windows on the HCl source cell proved to be a serious problem. Figure 9 shows the emission from an HCl-filled cell (lower spectrum), plus the reversed spectrum (upper) after the emission was passed through a cell containing HCl at room temperature. It can be seen in the figure that there is an underlying radiation continuum. This continuum largely nullifies the advantage of having the HCl emission

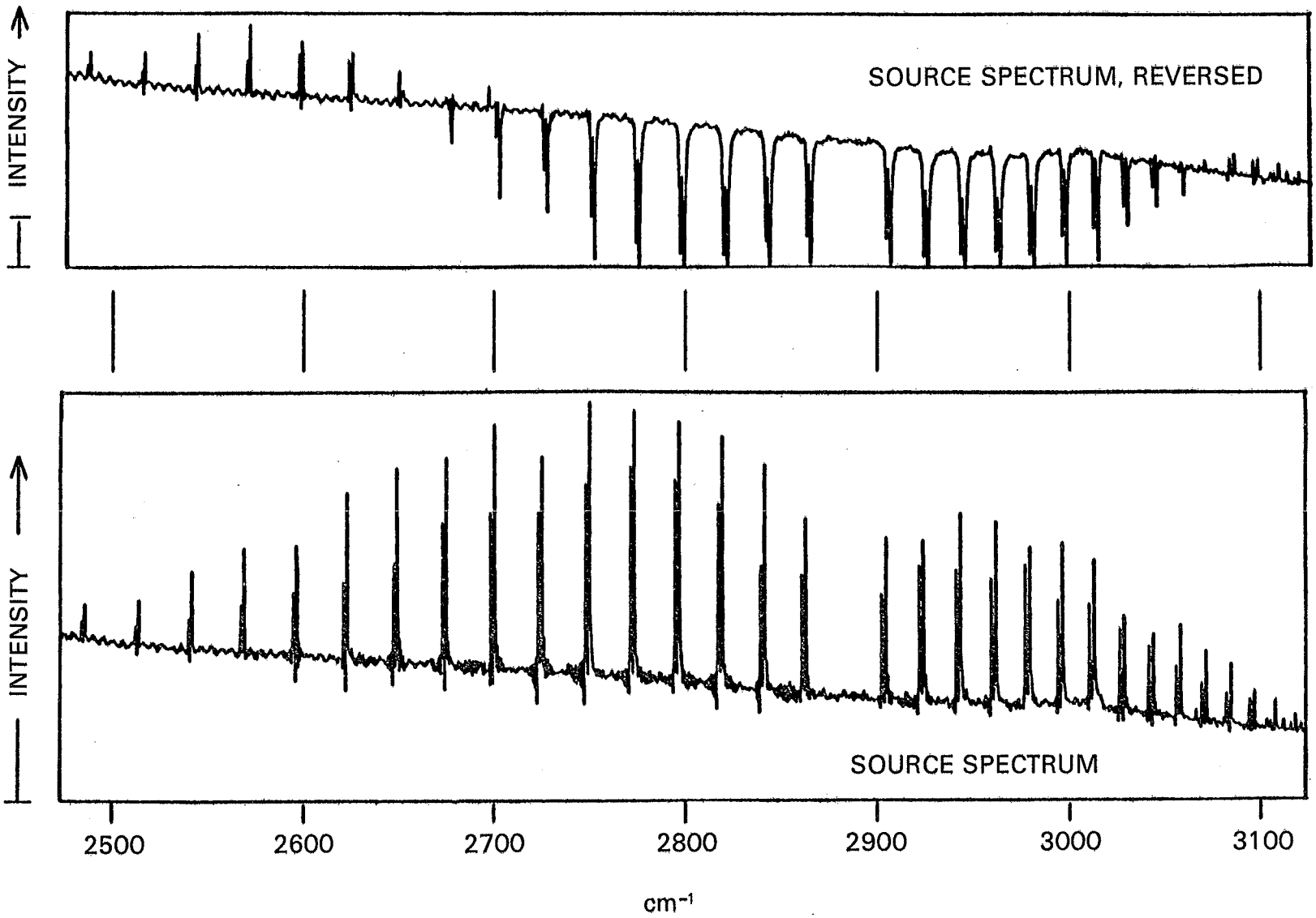

Figure 9. Spectra of hydrogen chloride gas.

lines in the source. An attempt to use CaF_2 windows on the source cell failed because the windows caused the HCl gas to disappear. Perhaps the HCl was attacking the windows and being exchanged for HF. Success in HCl measurements is clearly dependent on source cell improvements.

Other Compounds

Chlorofluoromethanes, vinyl chloride, nitrous oxide, and other compounds were mesured in the nondispersive analyzer with a high degree of sensitivity. These experiments were qualitative in nature, but in each case, the measurement confirmed that the nondispersive method is easily applied to the measurement of molecules that are thermally stable and have strong infrared bands.

CONCLUSIONS

Nearly all gaseous air pollutants can be measured by their infrared absorption, using the nondispersive technique. Filters that select desired regions of the spectrum are the key optical elements that permit the measurement of selected gases within a mixture. It has been demonstrated that appropriate combinations of radiation sources, gas-filled filter cells, band-pass filters and cooled photo-detectors can yield much greater detection sensitivity than has been available to date. It has also been shown that a filter cell containing humidified air will blind a nondispersive infrared system to any humidity change in the air being studied.

These new developments will allow the construction of nondispersive infrared analyzers that will measure pollutants in the ambient air in a passive, nondestructive way. Automatic filter changes will allow a single train of optical components to measure a multiplicity of pollutants. These studies should be followed up by the building of a prototype instrument, based on the physical principles discussed in this article. Success with the prototype could then lead to commercial realization of a new improved class of ambient air analyzers.

REFERENCES

1. Luft, K.F. 1943. Uber eine neue methode der registrierenden gasanalyse mit hilfe der absorption ultraroter strahlen ohne spektrale zerlegung. Z. Tech. Physik, Bd. 24(5):97-104.

2. Bartle, E.R., S. Kaye, and E.A. Meckstroth. 1972. An in-situ monitor for HCl and HF. J. Spacecraft and Rockets 9(11):836-841.

3. Fastie, W.G., and A.H. Pfund. 1947. Selective infrared gas analyzers. J. Opt. Soc. Amer. 37(10):762-768.

4. Fowler, R.C. 1949. A rapid infrared gas analyzer. Rev. Sci. Instrum. 20(3):175-178.

5. Hill, D.W., and T. Powell. 1968. Nondispersive infrared gas analysis in science, medicine and industry. Plenum Press, New York, NY. 212 pp.

6. Sebacher, D.I. 1977. A gas filter correlation monitor for CO, CH_4, and HCl. NASA Technical Paper No. 1113, NASA Scientific and Technical Information Office. 28 pp.

7. Wright, N., and L.W. Herscher. 1946. Recording infrared analyzers for butadiene and styrene plant streams. J. Opt. Soc. Amer. 36:195-202.

SAMPLING VARIABILITY AND STORAGE STABILITY OF VOLATILE ORGANIC CONTAMINANTS

Harold G. Eaton and Frederick W. Williams

Naval Research Laboratory
Washington, D.C.

and

Dennis E. Smith

Desmatics, Inc.
State College, PA

INTRODUCTION

The Naval Research Laboratory (NRL) has been active for many years in the detection, analysis, and control of atmospheric contaminants in enclosed inhabited spaces. These contaminants may be produced by a wide variety of sources, including materials of construction, instruments, human effluents, cigarette smoke, refrigerant gas leakages, paints, degreasing solvents, cooking, diesel fuel, aerosol cans, and others.

NRL initiated a program in 1956 to determine the identity and concentration of contaminants found in the atmosphere of nuclear submarines. Over 200 individual components varying greatly in volatility and concentration were identified, and the bulk of these proved to be hydrocarbons (1,2). Most of this earlier work involved vacuum or steam desorption from exposed charcoal, followed by analysis of the carbon desorbate (3,4). Although this procedure produced invaluable information as to the identity of the contaminants present, it was found that the lower molecular weight (MW), and hence higher volatility type components, were not as effectively adsorbed on the carbon as were the higher MW low volatility types (5). A review of this earlier work has been published (see reference 6 and previous publications listed as references).

At present, some Navy submersibles have on board <u>in-situ</u> type analyzers that are designed to detect a few individual components periodically as well as total hydrocarbon concentrations (7,8). These analyses are complemented with later laboratory analysis of gas samples collected in evacuated stainless steel bottles. These methods are valuable in determining contaminant concentration at a definite point in time, but in

practice do not provide time-integrated contaminant data over an extended period, such as for an 8-hour exposure. For this, a time-integrated sampling method is needed.

Commercially available sampling methods that are applicable for collecting atmospheric contaminants on a time basis include the use of an adsorbent such as charcoal, Tenax GC, and others. They usually consist of a small pump to draw the air through an adsorptive tube to trap atmospheric contaminants. Sampling times, however, are generally limited from one to two hours for each tube exposure. In addition, as discussed previously, low MW components are not quantitatively trapped on charcoal (5). Holzer (9) and Bertsch (10) found that, in general, the lower limit for effectively trapping contaminants on adsorbents was in the C_5 to C_7 range.

NRL has designed, built, and field-tested a time-integrated sampling method capable of collecting contaminants, including low MW components, over various time periods (11-13). This procedure does not employ a pump, but rather, an evacuated stainless steel container equipped with a critical orifice. As discussed in detail below, air to be sampled is allowed to leak into the container across a small orifice until a one-half atmosphere pressure is obtained. Time of sampling is controlled by the size of the orifice.

Because of the fact that in many instances these samples cannot be analyzed for days or months after samples are collected, a statistically designed experiment was set up to study the sampling variability and storage stability of several volatile organic comtaminants within the time-integrating sampling containers. These contaminants were representative of those found in closed inhabited environments (6).

EXPERIMENTAL PROCEDURE

General

In this statistically designed study, a matrix of eleven contaminants in air, listed in Table 1, were evaluated for storage stability in the time-integrated gas sampling bottles. These contaminants will be referred to by the numbers given in Table 1 in this report. Each contaminant in the matrix was evaluated at a high and low concentration. In general, high concentrations were in the range of 60 to 110 ppm by volume per contaminant and the low levels were in the range of 5 to 12 ppm by volume per contaminant. The use of the two levels of concentration permitted the evaluation of concentration levels as a possible effect on storage stability of a component.

The original statistical design for this study was to have a total of 12 bottles each for the high- and low-level concentration matrices. The samples were divided into three groups of four bottles for each concentration. In the procedure described below, each group was attached to a heated manifold and the test gas allowed to enter the four sampling bottles through a critical orifice until a one-half atmosphere pressure

TABLE 1. CONTAMINANTS INVESTIGATED IN THE EXPERIMENT

1	Methane, CH_4
2	Carbon monoxide, CO
3	Dichlorodifluoromethane (R-12), CCl_2F_2
4	1,1,2,2-Tetrafluoro-1,2-dichloroethane (R-114), CF_2ClCF_2Cl
5	Vinylidene chloride, $CH_2 = CCl_2$
6	1,1,2-Trichloro-1,2,2-trifluoroethane (R-113), CCl_2FCClF_2
7	Hexane, $CH_3(CH_2)_4CH_3$
8	Methyl chloroform, CH_3CCl_3
9	Benzene, C_6H_6
10	Trichloroethylene, $CHCl = CCl_2$
11	Toluene, $C_6H_5CH_3$

was obtained. The bottles were analyzed immediately to obtain the zero-day data, and then every 10 days thereafter until 80 days had elapsed.

Time-Integrated Gas Sampling Bottle

The sampling flasks used in this study were 1.64-liter type 304 stainless steel bottles (Alloy Products Corporation, Waukesha, Wisconsin). As seen in Figure 1, atop the bottle at a right angle to the "T" connection is an on-off valve (Whitey, part No. B-14DKM4). This valve was used either to evacuate the sampler when connected to a vacuum system or to connect to a gas chromatograph (GC) for evaluation of the contaminants entrapped after a sampling period. On top of the "T" connection is the gas sampling valve, which houses the critical orifice and protective filter through which the atmospheric sample enters. This valve was actuated by one complete counterclockwise turn. A complete detailed description of this valve and analytical system used to evaluate the contaminants has been published (11-13).

In general, the gas sampling bottle was prepared for atmospheric sampling by first attaching the bottle via the off-on valve to a vacuum system. The bottle was evacuated to less than one Torr pressure. At the time of sampling, the sampling valve was opened by turning counterclockwise. The gas flow into the container through the critical orifice remained constant as long as the criteria for critical flow existed (14). In order for this to occur, the internal pressure of the container remained less than one half of the external atmospheric pressure during the sampling period. Thus, the length of sampling time depended on both the size of the orifice and the volume of the sample container.

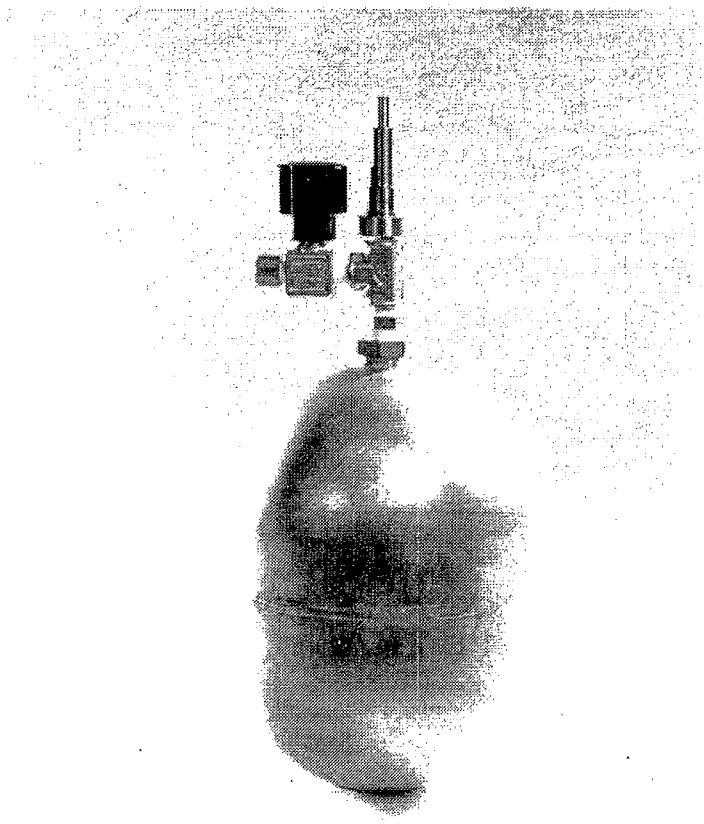

Figure 1. Sampling flask with critical orifice valve.

The equation that governs the gas flow across a critical orifice is as follows (14):

$$\dot{m} = 10^{-5}CAP\left[\frac{\gamma M}{RT}\left(\frac{2}{\gamma+1}\right)^{\frac{\gamma+1}{\gamma-1}}\right]^{1/2} \qquad (1)$$

where $\dot{m}$ = mass flow rate, g sec^{-1}
A = orifice throat area, cm^2
P = external pressure, Ncm^{-2}
γ = specific heat ratio, C_P/C_V
M = molecular weight of the gas, g
T = ambient temperature, °K
R = gas constant, 8.31 joule $mole^{-1}$ $°K^{-1}$
C = discharge coefficient (accounts empirically for boundary layer effect having a range of 0.8 to 0.95 for small orifices).

For this study, a sampling time of one hour was selected, which required

the use of a 38-micron orifice with the 1.64-liter bottle.

Sampler Preparation and Sample Collection

Each group of four bottles was prepared for this study by alternately evacuating and purging the bottles several times with helium. With one atmosphere of helium left in the bottles for 24 hours, they were then analyzed for potential residual contamination as described below. Next, the four bottles were again evacuated and attached at the sampling valve with 6.3 mm (1/4 in.) o.d. Teflon tubing to a heated (80°C) stainless-steel manifold, as shown schematically in Figure 2.

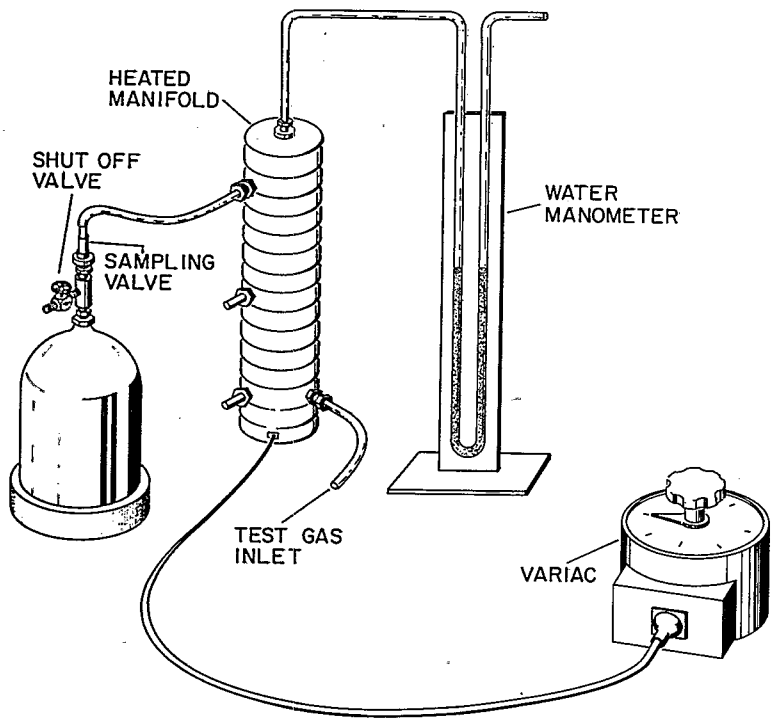

Figure 2. Sampling manifold with one bottle attached.

One end of the manifold was connected via Teflon tubing to a test gas bottle containing the contaminants listed in Table 1 (Union Carbide Corporation, Linde Division, Keasby, New Jersey). After purging the manifold for several minutes with the test gas, the opened end of the manifold was closed. After an in-situ analysis by GC of the manifold gas, the four sampling valves were opened.

One atmosphere pressure of test gas was maintained within the manifold by adjusting the flow of gas from the test gas bottle. At the end of the sampling period, the sampling valves were closed. The bottles were then

analyzed to establish the Day 0 point and every 10 days thereafter to Day 80.

The above procedures were conducted on the remaining groups for both high- and low-concentration levels.

GAS CHROMATOGRAPHIC ANALYSIS

A Beckman (Beckman Instruments, Inc., Fullerton, CA) Model GC-5 equipped with dual hydrogen flame ionization detectors (FID) was used to evaluate the storage stability of the gases collected in the stainless steel bottles. This analyzer was modified considerably to analyze the subambient pressured bottles.

A schematic of the gas handling and analytical system is presented in Figure 3. Subsystem I was designed to analyze all of the organic components with the exception of methane and carbon monoxide, which were analyzed on Subsystem II.

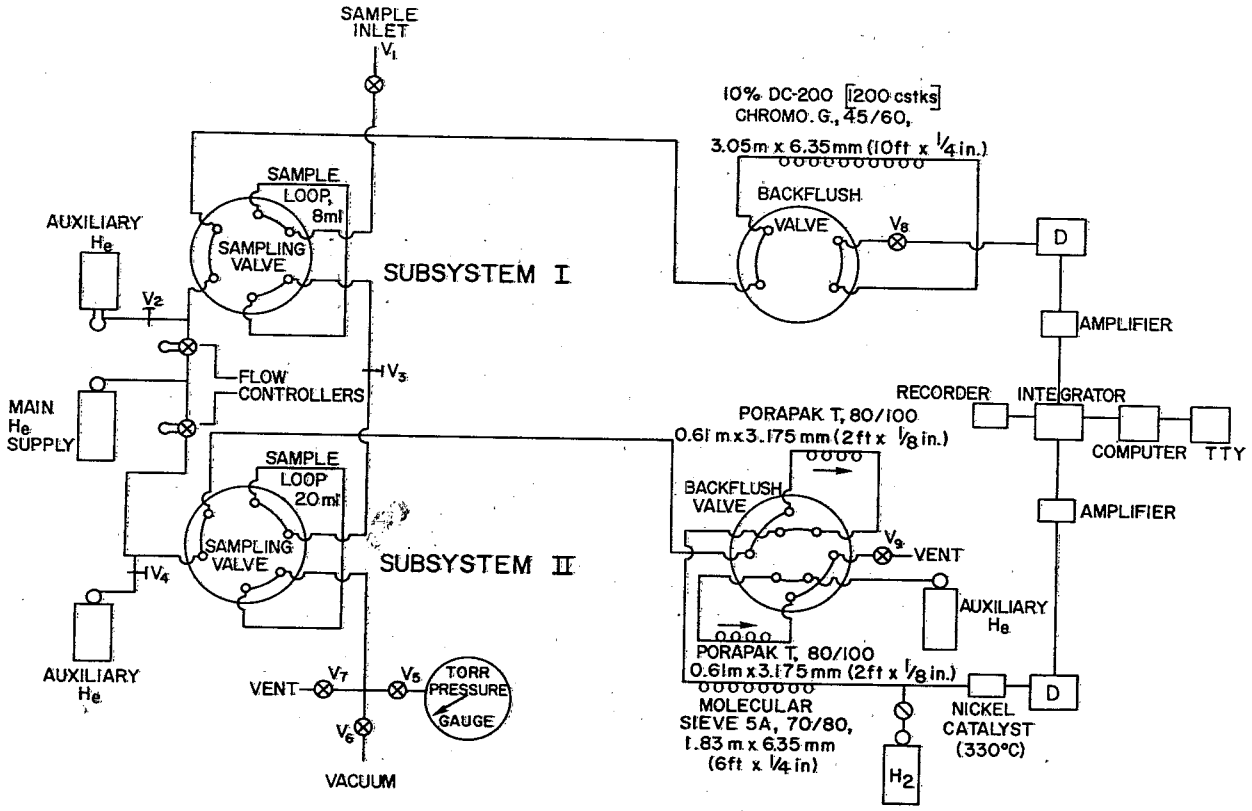

Figure 3. Gas-handling and analytical systems.

The gas sampling and backflush valves were manufactured by Carle Instruments (Carle Instruments, Inc., Fullerton, CA). Other valves used were stainless-steel ball valves (V_1, V_5, V_6, V_7), toggle valves (V_2, V_3, V_4), and fine metering valves (V_8, V_9). All tubing was stainless steel. Tubing connections to and from sampling valves, Subsystems I and II, were 1.6 mm (1/16 in.) o.d. The sample loops were 6.3 mm (1/4 in.) o.d. and of 8 cm^3 and 40 cm^3 volume for Subsystems I and II, respectively. The tubing from valves V_2 and V_4 was 3.2 mm (1/8 in.) o.d. To measure the sample pressure accurately, a Wallace and Tiernan (Belleville, NJ), Model 62A-4A-0100D, 0 to 5000 Torr, pressure gauge was connected by a cross, via valve V_5, to the sample line. A vacuum system was connected at valve V_6 leading also to the cross.

Helium was used as the carrier gas and was purified by the use of tandem columns of molecular sieve and charcoal immersed in a liquid nitrogen container. Flow controllers in the main helium supply to the sampling valves were standard parts of the GC. Secondary or auxiliary helium flows were brought in downstream of the flow controllers through V_2 and V_4 to provide a high-volume flow for rapid compression of the sample during injection (15). In Subsystem I, valve V_8 was used as a restrictor and employed to prevent the FID from blowing out when the backflush valve was actuated. In Subsystem II, the detection of CO with the flame ionization detector was accomplished by converting CO to CH_4 over a nickel catalyst (16). To prevent the contamination of the molecular sieve columns by the other contaminants in the sample, a backflush valve equipped with two precolumns, both Porapak T, 80/100 mesh, 0.6 m by 3.2 mm, was used. Valve V_9 served as a restrictor to minimize pressure fluctuations when this backflush valve was actuated.

The sampling valves for both subsystems were operated at 80°C, the nickel catalyst at 300°C, and the detectors at 150°C. The backflush valve for Subsystem II was operated at room temperature.

The flow rate of the carrier gas through both Subsystems I and II was 60 ml/min. To obtain ideal detector performance from the flame ionization detector, an additional 60 ml/min of helium flow (a total flow of 120 ml/min) was passed through the detector (not shown in Figure 3). Hydrogen flow for the FID was 50 ml/min in each system. As shown, H_2 for Subsystem II was added at the catalyst, whereas for Subsystem I, H_2 was added at the detector. Air flow to the detector was 300 ml/min. These operating conditions were maintained throughout the evaluation of the sampling bottles.

The response from the FID through the amplifier was fed into a Hewlett-Packard, Model 3370B, integrator (Avondale, PA) and a 1-mV strip chart recorder. The digitized signal was processed by a Hewlett-Packard minicomputer, Model 2116C.

SYSTEM PROCEDURE

Preparation of the Sampler for Analysis

The sampler was prepared for evaluation of its contents by connecting the off-on valve to the gas handling system at the inlet port. With the sampler closed, valves V_1, V_3, V_5, and V_6 were opened to evacuate the sampling system to less than 1-Torr pressure. Valve V_6 was then closed. By opening the off-on valve of the sampler, valve V_1 was used to meter in the sample to a pressure of 100 Torr to both Subsystems I and II. Valve V_1 was then closed. Valve V_3 was then closed to separate the sample loops of both subsystems during analysis.

Subsystem-I Analysis

With the sample contained in the sample loop at a pressure of 100 Torr, the sampling valve was rotated to place the loop in the carrier flow. At the same time, valve V_2 was opened to rapidly compress the sample and force it into the smaller-diameter tubing leading to the backflush valve and column. After 20 seconds the sampling valve was returned to its original position and valve V_2 was closed. The flow controller now controlled the flow of the carrier gas. The analysis of components was conducted by program temperature, as indicated in Figure 4.

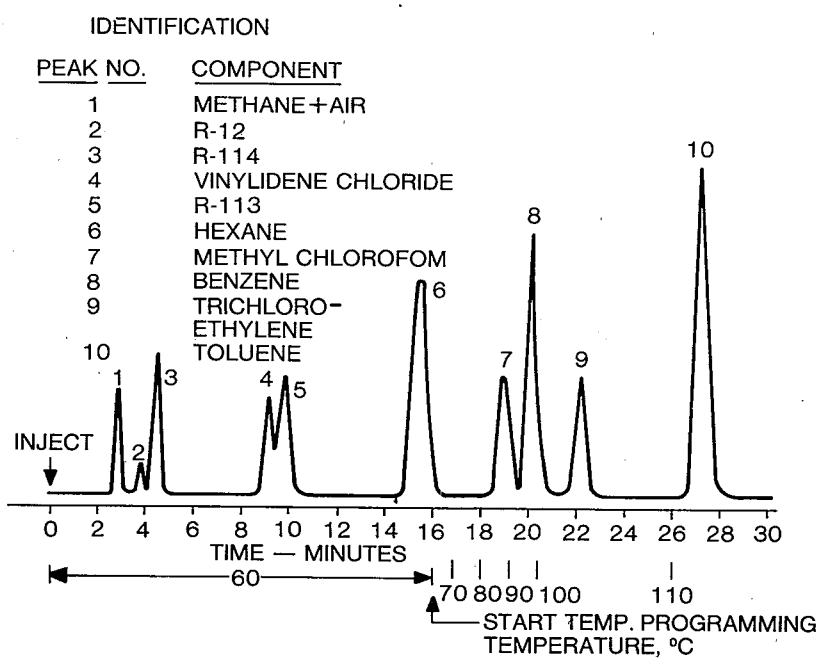

Figure 4. Subsystem-I component analysis.

Subsystem-II Analysis

Subsystem II was designed to detect CH_4 and CO. Although the detection of these components was fairly routine and was accomplished on a molecular sieve column, caution was exercised so that this column did not become contaminated with the other components of the sample. To avoid this contamination, two precolumns, Porapak T, 80/100 mesh, 0.6 m by 3.2 mm, operated at room temperature were used to separate CH_4 and CO from the other gases in the injected sample. After the CH_4 and CO passed through, the other gases still on the precolumn were backflushed.

The sequence of operation (Figure 3) was as follows. With the sample enclosed in the sample loop at a pressure of 100 Torr, the sampling valve was rotated to place the loop in the carrier gas stream. At the same time, valve V_4 was actuated for 35 seconds to rapidly inject the sample as described for Subsystem I. At the end of this time the injection valve was returned to its original start position and valve V_4 was closed. At 55 seconds the valve was returned to its original start position and valve V_4 was closed. By this time, the CH_4 and CO had passed through the top precolumn and were on the molecular sieve column. The backflush valve was actuated, turned clockwise, thereby allowing the auxiliary carrier to flow in the opposite direction on the top column carrying the contaminants out through valve V_9. The main carrier flow continued on the bottom precolumn, now in the opposite direction, to the molecular sieve column. The reversal of flow on the precolumns did not affect the normal forward flow of the molecular sieve column.

To detect the response of CO with an FID, as stated previously, a nickel catalyst was used to convert CO to CH_4. Figure 5 illustrates the results obtained at a column temperature of 60°C.

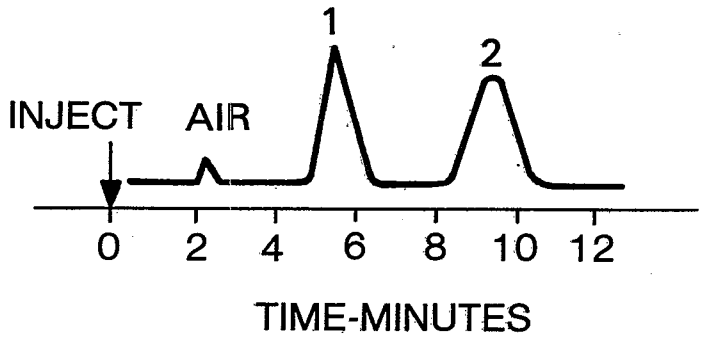

Figure 5. Subsystem-II component analysis.

At the conclusion of this analysis cycle, valves V_7 and V_3 were opened to vent the positive pressure. Valve V_7 was then closed. Valves V_5 and V_6 were opened to prepare both Subsystems I and II for the next analysis.

RESULTS AND DISCUSSION

As discussed previously, the sampling bottles were divided into groups by high- and low-concentration. Each group consisted of four bottles. They were filled to one-half atmosphere pressure, stored at room temperature, and analyzed, but at different times. The number of days between filling and analysis, however, was the same for all groups. Due to equipment defects associated with the sampling bottles during the experiment, such as leaks into the subambient pressured bottles, several bottles had to be rejected. As a result, 9 high- and 7 low-concentration samples were evaluated. This situation resulted in a statistically unbalanced experiment, since the number of samples analyzed were different for different groups of the contaminants.

Two analyses were made of each bottle on Day 0 and every 10 days thereafter, until Day 80. The response average of the contaminants from all of the groups is presented in Figures 6 and 7 for the high- and low-concentration mixtures, respectively. At the low-concentration level, Figure 7, contaminants #1 (CH_4) and #2 (CO) both responded high on Day 70, but returned to a reasonable concentration response on Day 80. In general, at both concentration levels the concentration of the contaminants, and hence detector response, fluctuated very little during the 80-day period.

A more detailed examination of the data base was conducted using the analysis of variance, a versatile statistical technique for studying the overall variation in a set of observations. Analysis of variance permitted an examination of the effects of possible sources of variability. In addition, it was used to test whether any portion of the overall variation was directly attributed to any of these sources. This type of test was based on the observed value of an $\underline{F}$-statistic computed from the data. In general, the larger the observed value, the more evidence that the source being tested had a contributing effect to the overall variation. However, the number of observations on which each specific test was based and the associated degrees of freedom had to be taken into account.

The observed $\underline{F}$ statistic value was compared with tabulated values (17,18). An observed value that was larger than the tabulated value corresponding to a 0.05 significant level, for example, was said to be statistically significant at the 0.05 level. This indicated that if the source being tested had no real contributing effect to the overall variation, there would be less than a 5 percent chance of observing an $\underline{F}$-statistic value that large. Thus, such an observed value would offer strong evidence that the source being tested does, in fact, have a contributing effect.

Table 2 presents a summary of the observed values of the $\underline{F}$-statistics obtained from the various analyses of variance. This table indicated those values that were statistically significant at the 0.05 significance level. Although the results in the table provided no evidence of variability due to time of analysis (i.e., no evidence of time trends or loss of components in the gas mixture due to adsorption) during the 80-day period, they did reveal significant group and flask variability. It was concluded, there-

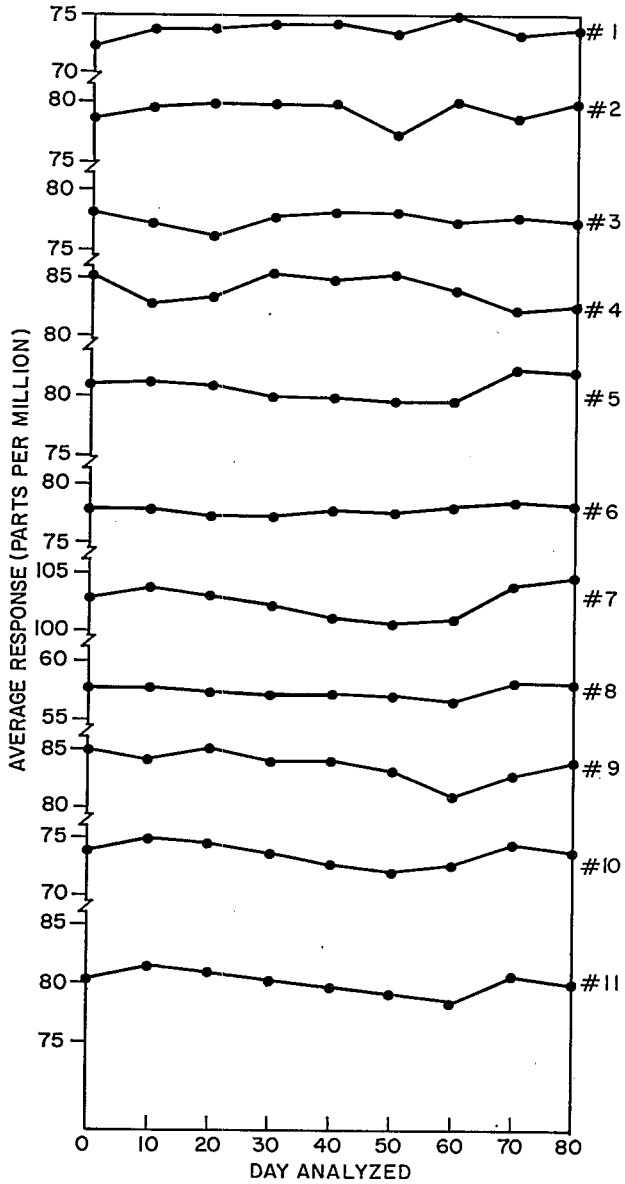

Figure 6. Response averages from high-concentration mixture sampling bottles. For contaminant number identification, see Table 1.

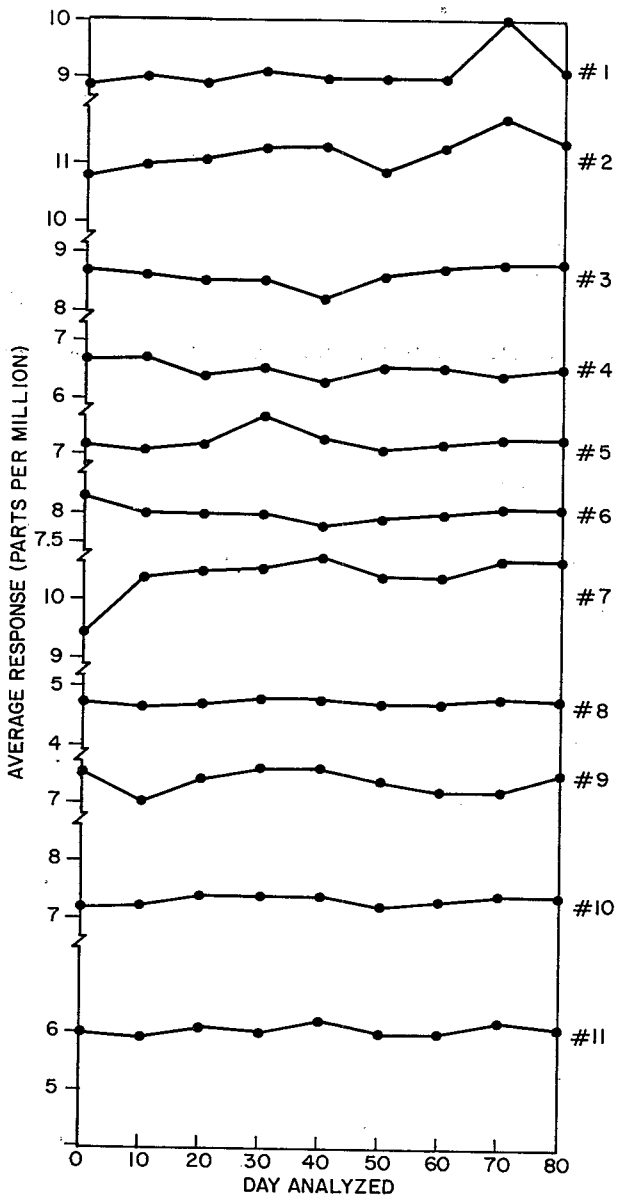

Figure 7. Response averages from low-concentration mixture sampling bottles. For contaminant number identification, see Table 1.

TABLE 2. THE OBSERVED VALUES OF THE F-STATISTICS OBTAINED FROM THE ANALYSIS OF VARIANCE

Source of variation	Contaminant 1	2	3	4	5	6	7	8	9	10	11	Total
High concentrations												
Groups	4.12	1.60	12.25*	0.65	33.83*	19.09*	10.73*	10.30*	5.12	11.46*	6.90*	13.15*
Flasks	1.91	1.91	3.70*	4.44*	32.5*	4.83*	6.16*	7.48*	4.70*	4.92*	5.61*	6.04*
Time	1.44	1.08	0.20	0.50	2.46	0.33	2.12	2.72	0.45	0.85	0.53	1.25
Low concentrations												
Groups	7.79*	6.87*	0.00	0.15	3.29	0.62	5.48	1.87	0.12	1.42	20.72*	8.96*
Flasks	4.61*	3.39*	2.40*	4.50*	11.07*	9.01*	20.74*	3.73*	3.49*	1.92	13.31*	8.51*
Time	1.51	1.73	0.27	0.26	0.43	0.33	0.39	1.71	0.78	0.94	0.68	1.08

*Denotes a statistically significant F-statistic value (using a 5 percent significance level).

fore, that there was noted variability between different observations due to the following three sources of variation:

Source 1: Variation between groups (fillings)

Source 2: Variation between flasks

Source 3: Variation between analyses (measurements)

The variation between groups reflected overall differences in average concentrations in the groups. For example, if for one particular group of high-concentration observations, the average was 83.0 ppm while in a second group the average was 84.2 ppm, this difference would be ascribable to between-group variability. Similarly, variation between flasks reflected overall differences in average concentrations in the flasks within the same group. Likewise, the variation between analyses reflected overall differences between analyses (measurements) performed on the same flask.

If σ^2 denotes the variance of any observed concentration based on a single analysis, then $\sigma^2 = \sigma^2_G + \sigma^2_F + \sigma^2_A$. The three components on the right-hand side denote the portion of variance due to group differences, flask differences and analysis differences, respectively. Each of these three components were estimated statistically from the analysis of variance based on the available experimental data. (See (17,18) for a discussion of estimation process.)

Tables 3 and 4 exhibit the sources and estimated components of variance for each of the eleven contaminants considered. These figures also indicate the percentage of the variance σ^2 attributable to each of the three sources. The estimated components (denoted by $\hat{\sigma}^2_G$, σ^2_F and σ^2_A) can be used to construct approximate confidence intervals based on a single observation or on a number of observations.

In general, shipboard sampling will involve taking samples of an atmosphere in a number of flasks. Because each of these samples is taken independently of each other, variability in sampling includes both filling

TABLE 3. AMOUNTS AND SOURCES OF VARIANCE IN A SINGLE OBSERVATION OF CONTAMINANT CONCENTRATION (HIGH LEVELS)

Contaminant	Estimated variance ($\hat{\sigma}^2$)	Percent of estimated variance attributable to differences between: Groups ($\hat{\sigma}^2_G$)	Flasks ($\hat{\sigma}^2_F$)	Analyses ($\hat{\sigma}^2_A$)
1	2.49	0	48	52
2	3.80	0	49	51
3	7.18	5	72	23
4	12.10	0	83	17
5	4.06	19	50	31
6	3.77	19	57	24
7	6.12	18	46	36
8	1.30	35	27	38
9	4.73	2	67	31
10	3.81	22	36	42
11	4.79	26	29	45

TABLE 4. AMOUNTS AND SOURCES OF VARIANCE IN A SINGLE OBSERVATION OF CONTAMINANT CONCENTRATION (LOW LEVELS)

Contaminant	Estimated variance (σ^2)	Percent of estimated variance attributable to differences between: Groups (σ^2_G)	Flasks (σ^2_F)	Analyses (σ^2_A)
1	0.45	8	52	40
2	0.31	9	62	29
3	0.15	0	80	20
4	0.11	0	81	19
5	0.04	12	64	24
6	0.08	0	68	32
7	0.06	18	71	11
8	0.03	7	21	72
9	0.10	0	67	33
10	0.06	2	16	82
11	0.07	48	38	14

and flask variability. Thus, the sampling variance is equal to $\sigma^2_G + \sigma^2_F$. It should be noted that, by the manner in which the time-integrated experiment was conducted, each of these individual components was able to be estimated. In other words, it can be judged how much of the overall sampling variability is due to differences in filling and how much is due to differences in flasks.

The ultimate aim of sampling is to obtain an accurate estimate of the

contaminant concentrations within the environment of interest. In the experiment, this is the test gas bottle, while in the "real world" this is some specific enclosed environment. To increase the accuracy of an estimate, the number of flasks (the samples taken) may be increased and/or the number of analyses done on each flask may be increased. Of course, there will be trade-offs to be made between greater accuracy and greater cost and time for a larger number of samples or analyses.

Based on the data from this sampling experiment, Tables 5 and 6 present approximate 95 percent confidence intervals (C.I.) for the true contaminant concentration based on the average observed concentration in $\underline{N}$ flasks where $\underline{M}$ analyses are done for each flask. Thus, the entry for $\underline{N} = 1$ and $\underline{M} = 1$ indicates the estimated accuracy of a single observation, while the other entries indicate how increasing the number of flasks or analyses affects the accuracy. The formula for the approximate 95 percent confidence intervals is:

$$95\%\ \text{C.I.} = \pm 2\ [\hat{\sigma}^2_{\underline{G}} + \hat{\sigma}^2_{\underline{F}}/\underline{N}] + [\hat{\sigma}^2_{\underline{A}}/\underline{NM}]^{\frac{1}{2}} \qquad (2)$$

where the values of $\sigma^2_{\underline{G}}$, $\sigma^2_{\underline{F}}$, and $\sigma^2_{\underline{A}}$ are obtained from Tables 3 and 4. As a point of interest, it should be noted that regardless of how many analyses are done for each flask, the confidence interval can never be smaller than

$$\pm 2[(\hat{\sigma}^2_{\underline{G}} + \hat{\sigma}^2_{\underline{F}})/\underline{N}]^{\frac{1}{2}} \qquad (3)$$

TABLE 5. APPROXIMATE 95 PERCENT CONFIDENCE INTERVALS FOR THE TRUE CONTAMINANT CONCENTRATION IN THE TEST GAS BOTTLE BASED ON THE OBSERVED AVERAGE CONCENTRATION IN $\underline{N}$ FLASKS WITH $\underline{M}$ ANALYSES FOR EACH FLASK. (HIGH CONCENTRATION LEVELS)

Contaminant	Avg. conc. (ppm)	Approximate 95 percent confidence intervals (ppm)								
		$\underline{N} = 1$, $\underline{M} = 1$	5, 1	10, 1	1, 5	5, 5	10, 5	1, 10	5, 10	10, 10
1	74.1	±3.2	±1.4	±1.0	±2.4	±1.1	±0.8	±2.3	±1.0	±0.7
2	79.7	±3.9	±1.7	±1.2	±3.0	±1.3	±0.9	±2.9	±1.3	±0.9
3	77.7	±5.4	±2.4	±1.7	±4.8	±2.2	±1.5	±4.8	±2.1	±1.5
4	84.3	±7.0	±3.1	±2.2	±6.5	±2.9	±2.0	±6.4	±2.9	±2.0
5	81.4	±4.0	±1.8	±1.3	±3.5	±1.6	±1.1	±3.4	±1.5	±1.1
6	78.4	±3.9	±1.7	±1.2	±3.5	±1.6	±1.1	±3.4	±1.5	±1.1
7	103.5	±5.0	±2.2	±1.6	±4.2	±1.9	±1.3	±4.1	±1.8	±1.3
8	57.9	±2.3	±1.0	±0.7	±1.9	±0.8	±0.6	±1.8	±0.8	±0.6
9	84.5	±4.3	±1.9	±1.4	±3.8	±1.7	±1.2	±3.7	±1.7	±1.2
10	74.4	±3.9	±1.7	±1.2	±3.2	±1.4	±1.0	±3.1	±1.4	±1.0
11	80.9	±4.4	±2.0	±1.4	±3.5	±1.6	±1.1	±3.4	±1.5	±1.1
Total	876.8	±25.4	±11.4	±8.0	±21.5	±9.6	±6.8	±21.0	±9.4	±6.6

TABLE 6. APPROXIMATE 95 PERCENT CONFIDENCE INTERVALS FOR THE TRUE CONTAMINANT CONCENTRATION IN THE TEST GAS BOTTLE BASED ON THE OBSERVED AVERAGE CONCENTRATION IN N FLASKS WITH M ANALYSES FOR EACH FLASK. (LOW CONCENTRATION LEVELS)

Contaminant	Avg. conc. (ppm)	Approximate 95 percent confidence intervals (ppm)								
		N = 1	5	10	1	5	10	1	5	10
		M = 1	1	1	5	5	5	10	10	10
1	9.1	± 1.3	± 0.6	± 0.4	± 1.1	± 0.5	± 0.3	± 1.1	± 0.5	± 0.3
2	11.2	± 1.1	± 0.5	± 0.3	± 1.0	± 0.4	± 0.3	± 1.0	± 0.4	± 0.3
3	8.6	± 0.8	± 0.4	± 0.2	± 0.7	± 0.3	± 0.2	± 0.7	± 0.3	± 0.2
4	6.5	± 0.7	± 0.3	± 0.2	± 0.6	± 0.3	± 0.2	± 0.6	± 0.3	± 0.2
5	7.2	± 0.4	± 0.2	± 0.1	± 0.4	± 0.2	± 0.1	± 0.4	± 0.2	± 0.1
6	8.0	± 0.6	± 0.2	± 0.2	± 0.5	± 0.2	± 0.2	± 0.5	± 0.2	± 0.1
7	10.5	± 0.5	± 0.2	± 0.2	± 0.5	± 0.2	± 0.1	± 0.5	± 0.2	± 0.1
8	4.7	± 0.3	± 0.1	± 0.1	± 0.2	± 0.1	± 0.1	± 0.2	± 0.1	± 0.1
9	7.4	± 0.6	± 0.3	± 0.2	± 0.5	± 0.2	± 0.2	± 0.5	± 0.2	± 0.2
10	7.3	± 0.5	± 0.2	± 0.2	± 0.3	± 0.1	± 0.1	± 0.2	± 0.1	± 0.1
11	6.1	± 0.5	± 0.2	± 0.2	± 0.5	± 0.2	± 0.2	± 0.5	± 0.2	± 0.2
Total	86.8	± 3.8	± 1.7	± 1.2	± 3.5	± 1.6	± 1.1	± 3.5	± 1.6	± 1.1

The data in Tables 5 and 6 show that increasing N is more effective in narrowing the limits than increasing M.

SUMMARY

We have developed a time-integrated sampling method which is capable of collecting contaminants, including low MW components, over variable time periods. Storage stability of several components at one-half atmospheric pressure within the stainless-steel flasks has been proved over an 80-day period. An analytical technique based on GC has been developed to analyze the subambient pressured flasks.

REFERENCES

1. Piatt, V.R. 1960. Chemical constituents of submarine atmospheres. Chapter 1 in NRL Report 5465.

2. Carhart, H.W., and V.R. Piatt. 1963. Chemical constituents of nuclear submarine atmospheres. Chapter 8 in NRL Report 6053.

3. Nester, F.H.M, and W.D. Smith. 1958. Submarine habitability--Atmosphere sampling and analysis. NRL Report 866.

4. Nester, F.H.M. 1960. Trace contaminants, sampling, and analysis. Chapter 4 in NRL Report 5465.

5. Umstead, M.E., J.C. Christian, and J.E. Johnson. 1960. A study of the organic vapors in the atmosphere of the USS SKATE. NRL Report 1057.

6. Saalfeld, F.E., F.W. Williams, and R.A. Saunders. 1971. Identification of trace contaminants in enclosed atmospheres. American Laboratory 3:8-15.

7. Saalfeld, F.E., and J.R. Wyatt. 1976. NRL's central atmosphere monitor program. NRL Memorandum Report 3432.

8. Eaton, H.G., M.E. Umstead, and W.D. Smith. 1973. A total hydrocarbon analyzer for use in nuclear submarines and other closed environments. J. Chromatogr. Sci. 11:275-78.

9. Holzer, G., H. Schanfield, A. Zlatkis, W. Bertach, P. Juarez, and H. Mayfield. 1977. Collection and analysis of trace organic emissions from natural sources. J. Chromatogr. 142:755-64.

10. Bertsch, W., R. Chang, and A. Zlatkis. 1974. The determination of organic volatiles in air pollution studies; characterization of profiles. J. Chromatogr. Sci. 12:175-82.

11. Eaton, H.G., J.P. Stone, and F.W. Williams. 1976. Personal atmospheric gas sampler with a critical orifice: Part 1 - Development and evaluation, NRL Report 7963; Part 2 - System for handling and analyzing the gas from the sampler, NRL Report 7960.

12. Stone, J.P., H.G. Eaton, and F.W. Williams. 1975. Atmospheric sampling; description of a small flow-control valve unit. Rev. Sci. Instrum. 46:1288-89.

13. Williams, F.W., J.P. Stone, and H.G. Eaton. 1976. Personal atmospheric gas sampler using the critical orifice concept. Anal. Chem. 48:442-45.

14. Anderson, J.W., and R. Friedman. 1949. An accurate gas metering system for laminar flow studies. Rev. Sci. Instrum. 20:61-66.

15. Umstead, M.E. 1974. A sampling technique for subambient pressure systems. J. Chromatogr. Sci. 12:106-08.

16. Porter, K., and D.H. Volman. 1962. Flame ionization detection of carbon monoxide for gas chromatographic analysis. Anal. Chem. 34:748-49.

17. Bennett, C.A., and N.L. Franklin. 1954. Statistical analysis in chemistry and the chemical industry. John Wiley and Sons, Inc., New York, NY.

18. Box, G.E.P., W.G. Hunter, and J.S. Hunter. 1978. Statistics for experimenters. John Wiley and Sons, Inc., New York, NY.

EXPOSURE TO PERCHLOROETHYLENE ASSOCIATED WITH THE USE OF COIN-TYPE DRY CLEANING MACHINES

R.H. Jungers

U.S. Environmental Protection Agency
Research Triangle Park, NC

S.J. Howie

PEDCo Environmental, Inc.
Cincinnati, OH

THE PURPOSE OF THIS STUDY

Nearly all coin-type dry cleaners use perchloroethylene (PERC) as the cleaning solvent (1). Since PERC is a suspected carcinogen (2,3), the potential of human exposure to it by such widespread uses as dry cleaning is an area of great concern. Previous studies have shown that relatively high concentrations may be found in self-service laundries (4) and that exposure to PERC may be expected in residences near its use as well (5).

This study was initiated as the result of a request by the Interagency Regulatory Liaison Group, and was sponsored by the Environmental Monitoring Systems Laboratory of the U.S. Environmental Protection Agency (EPA), in conjunction with the U.S. Consumer Product Safety Commission (CPSC). The purpose was to obtain data demonstrating the potential for public exposure to PERC that may result from coin-type dry cleaning in self-service laundries.

GENERAL DESCRIPTION

The major data base collected during this study consisted of daily indoor and outdoor PERC concentrations measured for seven consecutive days at each of six selected self-service laundries. Additional data were collected to demonstrate PERC levels in a residence above one of the laundries, and in a residence where clothing was brought in from being freshly dry cleaned in a coin machine.

Testing at the laundries and at an overhead apartment was conducted in the Washington, DC vicinity during August and early September, 1980. The clothing study was performed in a private residence near Cincinnati, Ohio

during early October, 1980.

All testing involved the use of standard charcoal sorption tubes, through which measured volumes of air were drawn. The adsorbed PERC was later desorbed at analytical laboratories and analyzed by gas chromatography. Volume of PERC per volume of air was determined for each sample, and all results were reported in terms of parts per billion (ppb). The field work was performed by PEDCo Environmental, Inc., under contract to the EPA. The majority of the analytical work was also performed by PEDCo, with some analyses and support provided by Research Triangle Institute (RTI) and TRW Corporation.

EXPERIMENTAL APPLICATIONS

Technical Approach

Sampling Methods

Previously tested methods of sampling ambient air were used in this study (6,7). These methods involved sampling of air with NIOSH-approved 150-mg charcoal tubes for measured periods of time at constant air flow rates.

Indoor sampling in the laundries was performed with air flow rates set at 75 ml/min for periods of 8 hours. This allowed a sufficient air volume to be collected so that the adsorbed PERC would be measurable by flame ionization detection. This method of sampling was also applied to testing inside the apartment above one of the laundries.

Outdoor testing was performed using air flow rates of 250 ml/min for periods of 24 hours. This allowed a sufficient air volume to be collected so that the adsorbed PERC in these samples would be detectable. Since very low levels were present at outdoor locations relative to inside the laundries, more sensitive detection methods were employed. This method of sampling also applied to testing in the home into which freshly dry cleaned clothing was brought.

In all cases, sampling systems were constructed to allow the tested air to enter directly into the sorption tube. All valving, pumps, and vacuum lines were located downstream from the sample collection point.

Analytical Methods

All analyses of samples were made by desorbing the sample into a suitable solvent (carbon disulfide or carbon disulfide with methanol) and analyzing the solvent by gas chromatography. The indoor laundry and apartment analysis instruments were equipped with flame ionization detection (FID), while the outdoor and clothing study analysis instruments were equipped with electron capture detection (ECD) or mass spectroscopy (MS). In this particular application, ECD and MS are much more sensitive to low levels than the less expensive FID, making their use mandatory in this

case. Determinations of ppb PERC, using the analytical results and the air volume field data, yielded time-weighted average (TWA) results for each appropriate sampling period.

Field Application

Site Descriptions

The six laundries were selected to be representative of various types and sizes of operations. All of them had coin-type dry cleaning machines on the premises as well as regular customer-operated washers and dryers. The physical layouts, ventilation methods, machine operating methods, and number and type of dry cleaning machines varied from laundry to laundry. The apartment above one of the laundries was selected because it had one room directly above several dry cleaning machines and it was generally unoccupied during testing hours. The home that was used for the clothing test was chosen because it was in a semi-rural area, which minimized background PERC levels, and because it had an unoccupied bedroom, which was used in this test. All outdoor test sites in the vicinity of the laundries served as background level indicators. Since these levels were generally much below the tested laundry levels, detailed descriptions of these sites are not necessary to describe the significance of the laundry data. The sites were located from 50 to 1000 meters away from each laundry in order to provide representative background data for each location. Each indoor location was assigned a letter identification for ease in presentation and discussion of results.

Laundry (A)--This spacious, well-ventilated laundry contained 24 customer-operated dry cleaning machines. All of the clothing dropped off by customers for attendant dry cleaning was sent off premises, however, so machine use was generally low. This laundry had good cross-flow ventilation, which was assisted by opposing, open doors.

Laundry (B)--This small laundry had very good ventilation and two attendant-operated machines. Machine usage was high due to the convenience of the attendants' service. One door was kept open during business hours, and large fans provided constant, fresh air inflow.

Laundry (C)--This moderately large laundry had fair ventilation and eight dry cleaning machines. Attendant service was provided for dry cleaning, which led to regular use of the machines. One door was kept open, and some fans were used to assist ventilation.

Laundry (D)-- This older, medium-sized laundry had four customer-operated dry cleaning machines that were regularly used during the study. Ventilation was not consistent throughout the laundry because of the rather complicated floor plan. Although a customer waiting area was next to an open door that allowed plenty of fresh air, the dry cleaning machines were in a somewhat isolated room with little direct ventilation to the outdoors.

Laundry (E)--This medium-large laundry had four attendant-operated dry

cleaning machines that were regularly used during the test. This laundry was the only air-conditioned one that was tested, and hence can be assumed to have the poorest overall ventilation of the laundries tested.

Laundry (F)--This medium-large laundry had eight customer- or attendant-operated dry cleaning machines. Use of the machines was somewhat below normal during the test, since a few scheduled maintenance repairs were being performed. The floor plan was unusual compared to the other laundries, since the shop occupied a narrow property between other shops in a large building. This may have impaired the circulation of fresh air from the open front door to the back of the shop where the dry cleaning was located.

Apartment--This apartment was located directly above the dry cleaning machines in Laundry D. It was not occupied during testing, since the residents, who had no children, worked during normal business hours. Because the apartment was closed when they were working, ventilation was very poor during the test.

Bedroom in private home--The bedroom that was tested for clothing emissions was an unoccupied room in a semi-rural, one-family home. This room was generally closed off during the test and hence had poor ventilation.

Testing Strategy

To obtain data that would present a clear picture of potential human exposure caused by the various environmental factors tested, it was necessary to design a comprehensive sampling scheme. Background PERC levels needed to be established for each test to ensure that the exposure data did not represent existing ambient levels. The tests also had to be designed to provide data generally representative of each tested environment, rather than flukes caused by peculiarities in the vicinity of sampling points.

Background tests--Except for the home clothing emission test, all background data were obtained by operating three to four outdoor monitoring stations in the vicinity of each indoor test. Each outdoor station was at least 50 meters away from known potential PERC sources, and within 1 kilometer of the indoor testing site.

A variety of monitoring locations were chosen to obtain background data. Most background sites were at nearby commercial or retail establishments, and at least one representative residential site per test was chosen. Background data for the home clothing emission test was obtained simply by monitoring the test room prior to the introduction of clothing into the room.

Exposure tests--All indoor tests were designed to show representative levels of PERC that might be inhaled by people occupying the room environment during the monitoring periods. In laundries, this required that sampling points be located in areas of high traffic and use, and that specific points of suspected high and low exposure levels be identified and

tested as well as areas probably representative of the room air as a whole. The specific goals in each laundry were to test one point at least halfway from the dry cleaning machines to the open front door, if applicable, one point in a customer lounge area, one point within 2 meters of dry cleaning machines, one point near customer working areas, and one centrally located point. Since only three points in each laundry were tested, these goals had to be met by combining purposes at single sampling points; occasionally, specific types of samples could not be obtained. In the apartment, testing points were obtained to show levels of high potential exposure (directly above the machines) and "background" levels in the rest of the apartment. The home clothing emission test was similarly arranged, with one sampling point near the closet where the clothing was stored (high exposure level) and the other two at points of high probable exposure durations: the desk and the bed.

Test Schedule

Testing was scheduled to collect consecutive daily data at each sampling site. Exposure tests at laundries were scheduled to run for 8 hours each day during normal business hours, while the home clothing emission test ran continuously, collecting 24-hour samples.

Background outdoor tests collected 24-hour averaged daily results, and were scheduled to coincide with the nearby indoor tests. All tests were run until seven consecutive daily sets of samples were obtained.

RESULTS

Perchloroethylene Levels in Laundries

The indoor ambient PERC levels varied considerably from laundry to laundry and from day to day inside each laundry. The average levels ranged from 90 to 14,000 ppb, which compares to a background range of 0.1 to 7 ppb.

Table 1 presents a summary of the high, low, and 7-day mean PERC concentrations for each laundry and for each network of background monitoring sites. This table shows a fairly wide spread of values between the six different laundries, with 7-day mean values ranging from a low of 130 ppb to a high of 8600 ppb. Each laundry also showed a great deal of variation on a day-to-day basis, with a high to low ratio of about 10:1 for five of the six.

Although most of the information gathered does not explain the daily variations in each laundry, some of the differences between laundries can be understood by reviewing the physical layout and operations of each. In making these comparisons, it is helpful to separate the laundries into low, medium, and high PERC concentration categories, based on the relative average levels found in each.

TABLE 1. SUMMARY OF AMBIENT PERC CONCENTRATIONS INSIDE AND OUTSIDE LAUNDRIES (PPB)

	Indoor PERC concentration			Outdoor PERC concentration			N
	Lowest daily average	Highest daily average	7-day mean	Lowest daily average	Highest daily average	7-day mean	7-day I/O*
Laundry A	91	200	130	0.86	6.7	3.3	59/62
Laundry B	75	700	320	0.34	3.9	1.4	28/29
Laundry C	250	2,700	1,300	1.2	4.5	3.6	33/30
Laundry D	464	3,800	1,500	1.3	4.4	2.5	33/33
Laundry E	1,900	14,000	8,600	0.13	5.0	1.5	62/49
Laundry F	330	3,100	1,300	0.27	4.0	2.0	30/35

*I/O signifies "N" for 7-day means as Indoor/Outdoor, where N is the total number of measurements used in arriving at mean values.

Low PERC Levels

Laundries A and B demonstrated average PERC levels from 100 to 300 ppb, which is much lower than the other four laundries. Laundry A, the lowest of all, probably had the best ventilation of the six due to cross air flow, and the lowest on-premises use of dry cleaning machines due to its practice of sending dropped-off clothing out for dry cleaning elsewhere. Laundry B, with somewhat higher PERC levels than A, also had excellent ventilation. Its higher PERC levels are explainable by the regular use that its dry cleaning machines experienced--this laundry provided convenient operation of machines by a full-time attendant.

Medium PERC Levels

Laundries C, D, and F all averaged between 1300 and 1500 ppb, which is much higher than Laundries A and B, but still much lower than Laundry E. The relatively high levels found in these laundries is probably due to a combination of factors generally related to machine usage and ventilation.

All three generally kept their front doors open during business hours, but in Laundries D and F, the benefits of this may have been reduced since their physical layouts were not conducive to good air circulation. Laundry C, which most likely had better air circulation, probably had higher machine usage than D and F. Laundry C had attendant-provided dry cleaning, unlike Laundry D which was solely customer operated. Finally, Laundry C did not experience any scheduled repairs as did Laundry F.

High PERC Levels

Laundry E showed consistently higher PERC levels than any of the others that were tested. Daily average levels ranged from 1900 to 14,000 ppb, with a 7-day mean of 8600 ppb. Because the operations were similar to those in Laundries B and C, with attendant-provided services, operations alone cannot explain the high levels that were found. The major physical distinction was that Laundry E was air conditioned while none of the others was. This may have led to a concentration of PERC caused by recirculation of indoor air without dilution makeup from the outdoors. In short, the ventilation was very poor.

Perchloroethylene Levels in the Apartment

In the apartment tested above Laundry D, PERC levels were practically identical to those downstairs. Table 2 shows a reasonable consistency between the daily averages found in this apartment and the laundry.

TABLE 2. COMPARISON OF INDOOR PERC BETWEEN LAUNDRY D AND THE APARTMENT UPSTAIRS

	Daily average, ppb						
Location	Day 1	Day 2	Day 3	Day 4	Day 5	Day 6	Day 7
Dry cleaning room of laundry	1550	920	5550	2500	645	1300	1450
Apartment	1100	680	5800	720	2300*	620	1200

*No explanation for this occurrence was recorded in the field notes. This high level may be evidence of reentrainment of exhaust fumes from the dry cleaning machines vented to the outdoors.

The field notes taken during the test indicated an interesting occurrence on Day 3 that probably explains the high PERC levels that were monitored on this day. A PERC spill had occurred near the machines, and had not been cleaned up immediately.

Perchloroethylene Levels in the Private Home

A definite rise in the indoor ambient PERC levels was noted when freshly dry cleaned clothing was brought into the bedoom and allowed to hang in the closet undisturbed. Table 3 shows a steady background concentration of 0.2 ppb that had been observed prior to the arrival of the clothing, after which an immediate rise to 100 ppb was measured. The levels dropped quickly the next day to about 20 ppb, and then gradually declined. After 1 week of exposure, the PERC levels in the room were still 6 ppb, which is distinctly higher than the background amounts.

TABLE 3. SUMMARY OF AMBIENT PERC CONCENTRATIONS INSIDE A CLOSED LIVING SPACE WHERE DRY CLEANED CLOTHING WAS INTRODUCED

Test day	Comments	Mean PERC concentration, ppb
1	No dry cleaned clothing*	0.21
2	No dry cleaned clothing*	0.18
3	First day of exposure†	102
4	Second day of exposure	22
5	Third day of exposure	17
6	Fourth day of exposure	25
7	Fifth day of exposure	16
8	Sixth day of exposure	14
9	Seventh day of exposure	6.2

*Values obtained were used to establish baseline PERC concentration.
†Dry cleaned clothing was introduced at the beginning of this 24-hour period.

CONCLUSIONS

This study showed that the use of coin-type dry cleaning machines can lead to a definite potential human exposure to PERC, and that there are indirect as well as direct routes in which this exposure may occur. The data also demonstrated that, at least in terms of direct exposure potential in laundries, ambient PERC levels can differ enormously, depending on various physical and environmental factors. The specific findings of the study are discussed in detail below.

PERC Levels in Laundries

Significant levels of PERC may be encountered in laundries that use coin-type dry cleaning machines. Ventilation appears to be a key factor regulating the indoor concentrations, as well as relative machine use. Air conditioning, which reduces ventilation, can apparently lead to a concentration of PERC well in excess of that found where direct air flow from the outdoors is present. This is especially important in evaluating the exposure potential for winter operations, when ventilation to the outdoors is reduced.

PERC Levels in Properties Adjoining Laundries

PERC shows an apparent high ability to permeate into adjoining properties, at least insofar as apartments above laundries are concerned. More extensive studies of this nature are required to fully characterize this potential. Since only one apartment was tested during this study, the possibility exists that the data obtained represent an isolated circumstance, not a generally prevalent problem. In addition, it should be emphasized that this was in an older building. The newer laundries were

all one-story affairs in nonresidential areas and it may well be that in the future, laundries with overhead dwellings will become phased out.

PERC Emissions from Clothing

PERC is apparently very persistent in clothing once it has been dry cleaned. The levels measured during this study showed a day-to-day trend that demonstrates a definite, long-term emission pattern. These results do have limitations, however, since they represent data obtained during a single test series. More extensive tests of this nature are needed to establish generalities concerning clothing emissions.

REFERENCES

1. Fisher, W.E. 1977. International Fabricare Institute, Research Division, Silver Springs, MD. Paper presented at the EPA Hydrocarbon Workshop, Chicago, IL. July 20.

2. National Cancer Institute. 1977. Bioassay of tetrachloroethylene for possible carcinogenicity. Publication No. 77-813. U.S. Department of Health, Education, and Welfare, Public Health Service, National Institute of Health.

3. Blair, A. 1979. Causes of death among laundry and dry cleaning workers. American Journal of Public Health 69(5):508-511.

4. Sykes, A.L., and J.E. Bumgarner. 1979. Analytical results of the perchloroethylene study of a coin-operated dry cleaner. U.S. Environmental Protection Agency Contract No. 68-02-2688, Task 13.

5. Verberk, M.M., and T.M.L. Scheffers. 1980. Tetrachloroethylene in exhaled air of residents near dry cleaning shops. Environmental Research 21:432-437.

6. U.S. Environmental Protection Agency. 1979. Measurement of perchloroethylene in ambient air. August.

7. U.S. Department of Health, Education, and Welfare. 1977. NIOSH manual of analytical methods. Second edition, Volume 3, 5335.

PRELIMINARY RESULTS FROM THE WIDE RANGE AEROSOL CLASSIFIER

R.M. Burton, Dale A. Lundgren, Brian J. Hausknecht, and David C. Rovell-Rixx

ABSTRACT

The Wide Range Aerosol Classifier (WRAC) was built under a U.S. Environmental Protection Agency cooperative agreement with Dr. Dale A. Lundgren of the University of Florida (Gainesville). This sampling system provides a mechanism for size-separating and collecting with high efficiency the full spectrum of ambient particulate sizes to include fugitive dusts in the range from 15 to 200μm aerodynamic diameter.

The WRAC was designed with a very large inlet and a high sampling flowrate to permit collection of very large particles with nearly 100 percent efficiency. The system consists of a series of single-stage impactors operating at high flow rates in parallel, thus eliminating the problems of wall loss and transport that are associated with cascade impaction. This sampling concept was demonstrated to be viable, as described in Air Pollution Control Association Journal 24:(12), December, 1975. The sampling results are presented as mass concentration distributions over a complete particulate size range from 0.04 to 200μm.

WRAC field sampling has been conducted at a variety of sites to obtain valid particulate size distribution data. Sites in Birmingham, Alabama (industrial); Research Triangle Park, North Carolina (background); Philadelphia, Pennsylvania (metropolitan); Phoenix, Arizona (high fugitive dust); and Los Angeles, California (automotive generated smog and fugitive dust) have provided a wide range of atmospheric particulate mass size distributions for monitoring.

Preliminary analysis of the data shows the WRAC to be capable of determining the total atmospheric particulate matter mass size distribution together with predicting and validating the fractions collected by the Inhalable Particulate Network samplers.

INTRODUCTION

The present air quality standard for particulate matter is based upon the total amount of suspended particulate matter collected by the reference method, a high volume air sampler. This sampler has been assumed to collect particles less than ∿100μm diameter (Stokes equivalent). Tests conducted by Wedding and co-workers indicate, however, that the sampling efficiency of the high volume air sampler may be as low as 7 percent for 50μm particles and 18 percent for 30μm particles in moderate winds. The high volume air sampler is also sensitive to orientation, showing a 20 percent drop in collection efficiency for particles 15μm in diameter and larger with a 45 degree shift in wind direction. Because the mass of a particle increases as the cube of its diameter, the mass concentrations measured by the high volume air sampler can also vary widely.

The U.S. Environmental Protection Agency (EPA) in 1979 defined inhalable particles (IP) as those less than 15μm and is currently considering an upper size limit of 10μm (1). The EPA has also considered establishing a fine particle standard consisting of particles less than ∿2 to 3μm diameter. Consideration of an IP standard has generated considerable interest in defining the total atmospheric particulate size distribution. Only then will it be possible to determine what fraction of the total atmospheric aerosol is being collected and what fraction would be desirable to collect by existing or proposed sampling devices for inhalable or other particulate measurements.

Lundgren and Paulus previously described a stationary sampling system that effectively sampled large atmospheric particles (up to ∿100μm); they determined the large particle size distribution and total atmospheric mass concentration, then compared their results with collections by dust fall plates and with a standard high volume air sampler (2). That study provided the background for the present project to design, construct, and field-test a mobile large particle sampler that determines the mass distribution of large (10 to 200μm) atmospheric particles. With this sampler, it is possible to characterize the total particulate mass size distribution of ambient aerosol and to compare the results with particulate mass data collected simultaneously by the Total Suspended Particulate (TSP) Hi-Vol, the Size Selective Inlet Hi-Vol (SSI), Small Particle Cascade Impactors, and the Dichotomous Samplers. The sampling system will be especially useful for evaluating areas with high fugitive particulate concentration. Data showing the relationship between total suspended particulate, inhaled particulate, fine particulate, and other measures of particle concentration can be obtained while the total atmospheric particle mass distribution is being measured. Differences in the quantity of particulate mass measured by the various devices can then be rationally explained and properly related to the aerosol size distribution in the atmosphere.

The objective of this project was to design and construct a mobile particle sampler capable of collecting size-separated mass samples providing mass distribution of the total atmospheric particle size range up to 200μm aerodynamic diameter, and to use the instrument to perform field sampling for defining the size distribution of the total particulate matter

mass.

PROCEDURE

The sampler, as shown in Figure 1, is fitted into a trailer and consists of a large, high-flow-rate (1380 CFM) inlet from which five isokinetic samples are withdrawn. Four of the samples are passed through single-stage impactors with different cutpoints, while the fifth is passed through a total particulate matter filter. The four impactors are designed to collect particles greater than 9.6μm, 18μm, 34μm, and 57μm diameter, respectively. Smaller aerosol particles are sized by attaching cascade impactors following the single-stage impactors.

An accompanying analysis lab is set up in a mobile van. Analysis equipment includes a precision balance, optical sizing microscope, and a sample equilibration chamber.

INLET DESIGN

The major task in measuring large atmospheric particles is transporting a true or representative sample of the particles into a measurement device. This difficulty is particularly serious for the collection of particles larger than ∿30μm diameter because of their great inertia and high settling rate.

Particle settling velocity (Vs) is determined by a balance between the force of gravity acting on a particle and the fluid drag force exerted by the medium through which the particle falls. Simply put, settling velocity increases rapidly with increasing particle size. Sampling tube inlets that are pointed upward will capture a greater proportion of large particles than are in the actual distribution due to the settling of large particles into the inlet. The increase in the relative number of large particles sampled is equal to 1 + [Vs/Vo], where Vo equals the sampling tube inlet velocity. The error can be kept reasonably small if the inlet velocity (Vo) is made several times greater than the settling velocity (Vs) of the larger particle desired. Therefore, a Vo of 25 times Vs would give a permissible error of only 4 percent overestimation for a tube pointed upward. The Wide Range Aerosol Classifier meets this criterion for a 55μm-diameter particle, and an 11 percent overestimation for a 100μm-diameter particle is predicted.

Particle inertia is a function of particle mass. From Newton's first law, where force equals mass times acceleration, a larger force is required to accelerate (or decelerate) a larger (heavier) particle as quickly as a smaller (lighter) particle. Because the size of a particle also affects the drag it experiences from the air, the relaxation time (τ) is used as an indication of its ability to accelerate or decelerate. Particle relaxation time (τ) has been defined as: $\tau = Dp^2\rho/18\eta$, where Dp is the diameter of the particle, ρ is its density, η is the viscosity of air, and τ has units of time.

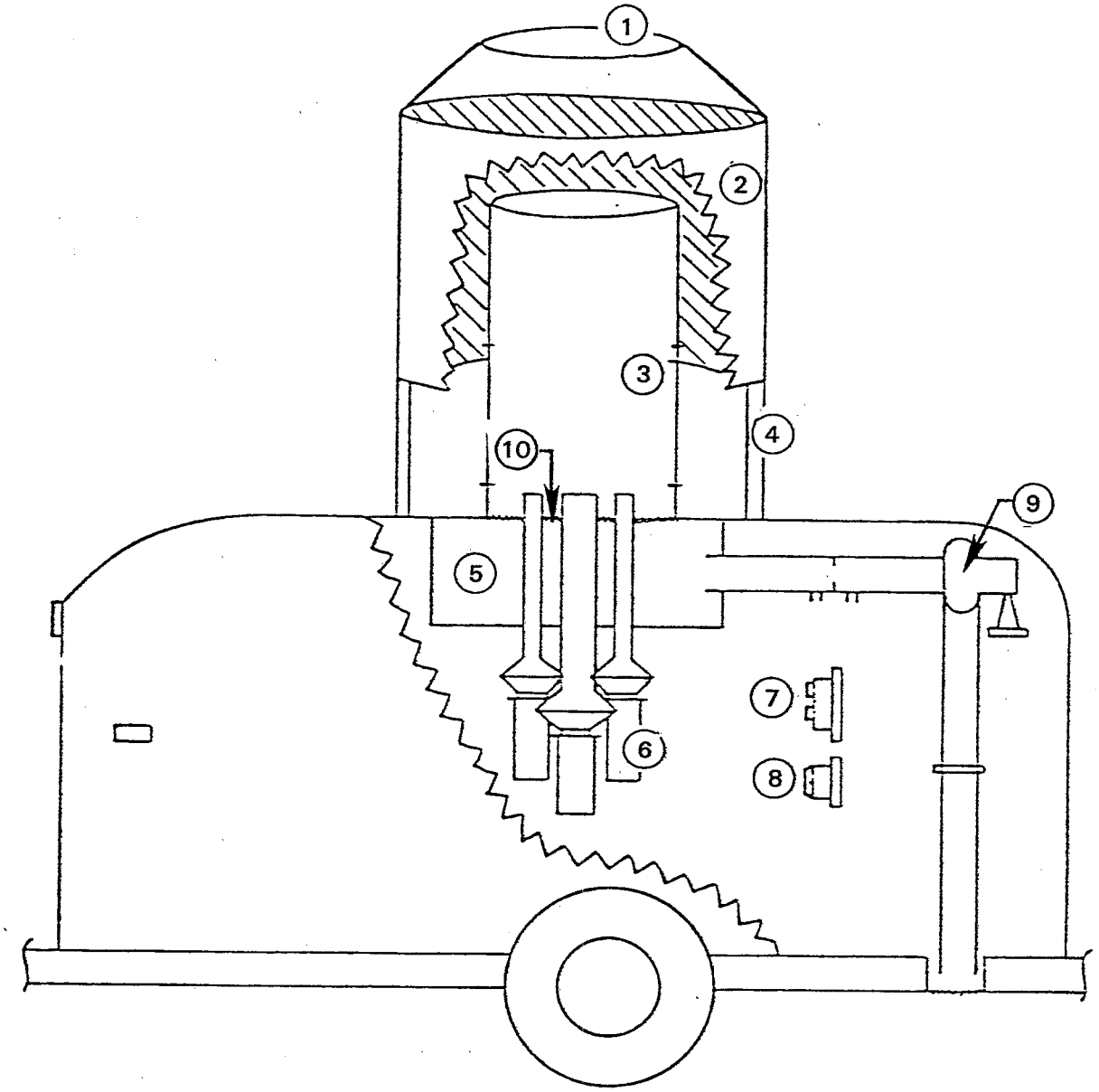

1 Raincap
2 Wind Shroud
3 Main Inlet
4 Shroud Support Pole
5 Air Plenum
6 WRAC Sampler
7 Flow Controller
8 Flow Recorder
9 Auxiliary Blower
10 Coarse Filter

Figure 1. Schematic diagram of the mobile sampling system.

It is also convenient to define particle stopping distance, ℓ, as the distance a particle will travel when decelerated in a fluid medium (air) from an initial velocity (V) to rest. It hs been shown that $\ell = V_{\tau}$.

Davies uses ℓ to evaluate the effect of particle inertia on sampling efficiency for two situations (3). When sampling at a known inlet flow rate, Q, a suction velocity (Vx) will be produced; Vx is a function of the distance from the inlet orifice. To examine the case where Vx is evaluated at a distance ℓ from the center of the orifice, Davies uses the equation $Vx = Q/4\pi\ell^2$, where Q is the flow rate of the sampler inlet and $4\pi\ell^2$ is the surface area of a sphere of radius ℓ.

More appropriate might be an equation determined by Dalle Valle from measured velocity contours of exhaust hoods. For a point at a distance ℓ along the center line from the hood face, $Vx = Q/10\ell^2+A$, where A equals the inlet face area. Davies reasons that if the radius of the inlet (R) is several times larger than ℓ, the effects of inertia will be negligible.

Davies also has examined the situation of sampling in a cross-wind with some velocity (Vs) and reasons that the inlet radius (R) should be much greater than the stopping distance associated with the wind (i.e., $\ell = Vw\,\tau$). He suggests that R should be at least 5ℓ. For the mobile WRAC sampler, the condition that $R = 5\ell$ requires that ℓ be less than 6 cm. At a distance of 6 cm from the inlet orifice, the maximum velocity using the latter equation would be 2 m/s (∿4.5 mph). The stopping distance for a 100μm-diameter particle at this velocity is 6.15 cm. This nearly meets Davies' criteria and suggests that the mobile sampler inlet is dimensionally adequate to efficiently sample 100μm-diameter particles in winds up to ∿2 m/s (4.5 mph).

Several researchers have noted that Davies' theoretical criteria seem overly restrictive for efficient sampling and are not met by several commercially available sampling instruments. A theoretical study of sampling efficiencies by Agarwal and Liu took into account both particle inertia and settling (4). They determined the flow field around a vertical, thin-walled inlet from the Navier-Stokes equations and then calculated particle trajectories. They determined a critical particle trajectory that is a distance, Rc, from the inlet axis, such that the particles inside this radius enter the inlet. Sampling efficiency was calculated by comparing the concentration of particles entering the inlet versus the actual concentration of the air sampled.

Agarwal and Liu noted that the sampling efficiency was a function independent of both the Stokes number ($STK = \rho\, CDp^2 Vo/9\eta D$) and the relative settling velocity ($Vs' = Vs/Vo$). The characteristic length and velocity are in the inlet diameters, D, and the inlet velocity, Vo. Their research indicates that if the product (Stk) (Vs') is less than 0.10, then sampling efficiency will be greater than 90 percent. Agarwal and Liu caution, however, that their criterion for efficiency regards all particles that enter the inlet as sampled, whether or not they impact and possibly stick on the inside wall of the inlet. The value of (Stk) (Vs') for sampling 100μm particles with the mobile sampler is 0.025. Solving for particle

diameter with (Stk) (Vs') equal to 0.10 indicates that the mobile sampler can sample particles as large as 130μm in diameter with an accuracy of 90 percent. These values assume, however, that Stokes Law holds for particles this size.

The shroud of the WRAC was designed to provide a calm air space around the inlet orifice so that the sampler would be less sensitive to cross-winds. To be effective, it was made large enough so that particles would not impact on it but would flow around and over the shroud. To ensure this, it was designed large in comparison to ℓ. Using the same ratio of 1:5, this criterion was met for a particle with a stopping distance less than or equal to one-fifth the diameter of the shroud, or 30 cm. This condition was met for a 100μm-diameter particle in a 9 m/s (20 mph) wind.

A rain shield designed for use when the sampler is operating consists of a 90 cm flat disk supported 30 cm above the top of the shroud and centered above the inlet. It prevents rain from falling directly into the inlet under light wind conditions. A wind-driven rain should fall at an angle and impact on the side of the tube. From there it should run down the side and into the air plenum box and not into the samplers.

SELECTIVE SAMPLER DESIGN

The size-selective sampler inlets were designed to extract an isokinetic sample from the air flowing through the inlet tube. The samplers were constructed of 0.10 mm aluminum. The sampler inlets are of equal area so that an equal volume of air is sampled through each sampler. Each impactor inlet measures 17.8 cm x 6.55 cm. The inlet area was determined by the slot width required for the first impactor; therefore, the Number 1 impactor is a straight nozzle (neither converging or diverging).

To minimize losses and facilitate construction, a rectangular jet design was used. The impactors were designed with the jets 17.8 cm long in order to leave more room for the airflow over the impactor plate to turn down into the filter. This reduces the particle losses on the walls of the impactor.

The fifth sampler, which collects a total particle sample, was designed with a square inlet so that it would fit better between the impactor inlets. The sides of all sampler inlets are straight, to reduce any loss of particles onto the walls. The inlet area of the fifth sampler is the same as for the other samplers.

An additional advantage of using high volume air sampler blowers is that flow controllers are readily available on the market. These flow controllers ensure a constant flow rate through the sampler so that the total air volume for the sampling period is known and that a representative sample is drawn for each hour over the normal 24-hour period. Therefore, if the total sampling time is known and the flow rate is known and constant, the total air volume sampled is known. Aerosol mass concentrations can then be computed. A constant flow rate is additionally critical for

impactors because the aerosol impaction efficiency is a function of the flow rate. Field sampling and evaluation at selected sites has shown that the sampler can provide reliable information on the size distribution of particle mass, including particles up to 200μm aerodynamic diameter. The system is self-sufficient, with the accompanying mobile laboratory, for processing and analyzing the collected samples.

FIELD SAMPLING SITE DESCRIPTION

WRAC field sampling was conducted in five locations throughout the country, each location chosen to represent a distinctively different type of ambient aerosol loading. The five locations are described below.

1. Birmingham, Alabama (industrial)
2. Research Triangle Park, North Carolina (background)
3. Philadelphia, Pennsylvania (metropolitan)
4. Phoenix, Arizona (high fugitive dust)
5. Los Angeles (Riverside), California (automotive-generated smog and fugitive dust)

Each site was selected at an existing EPA Inhaled Particulate Network site in order that Total Suspended Particulate Hi-Vol, Size Selection Inlet Inhalable Particulate Hi-Vol, and Dichotomous Inhalable Particulate measurements could be made simultaneously and concurrently with the WRAC measurements. Sample duration time was 24 hours for sampling at all locations. Since the WRAC gives particle mass by size distribution up to 200μm, cut-point characteristics of the conventional particle samplers used in the study could be evaluated from the WRAC data. Also, a better understanding of the total and inhalable particulate mass particle size distributions around the country would be acquired from the WRAC data.

The analysis van containing an environmentally controlled filter equilibration chamber and a precision balance for filter weighings accompanied the WRAC to each of the five sampling sites for sample processing and weighing.

RESULTS OF FIELD SAMPLING

Data from each sampling site are reported separately for comparison. At each site, several similar runs were selected and averaged to determine a representative average distribution for site-to-site comparison. Selection for averaging was based on similarities in total particulate concentration and distribution. Based on these two parameters, data from Birmingham and Riverside strongly suggest that two distinct distributions were present, depending on the local wind and weather conditions. On this basis, a total of seven data sets were used for comparison purposes: one set each for Research Triangle Park, Philadelphia, and Phoenix; and two sets each for Birmingham and Riverside.

In the following data reporting, each set is referred to by the site

acronym. Where two data sets were used, the descriptive suffix "-High" and "-Low" is used after the acronym. The following is a list of sites, average total concentrations and appropriate acronyms:

Birmingham:	204.6 $\mu g/m^3$	NB-High
Birmingham:	113.0 $\mu g/m^3$	NB-Low
Research Triangle Park:	48.4 $\mu g/m^3$	RTP
Philadelphia:	100.1 $\mu g/m^3$	PA
Phoenix:	111.6 $\mu g/m^3$	PHX
Riverside:	255.1 $\mu g/m^3$	RBX-High
Riverside:	89.5 $\mu g/m^3$	RBX-Low

Calculations were made for each data set to determine the cumulative particle size distribution. The points were plotted on logarithmic normal graph paper as % < Dp versus Dp (impactor cutpoint). The results for the seven data sets are shown in Figure 2. A set of points generating a straight line on a cumulative probability graph describes a log-normal distribution. The shape of a best-fit curve through each set of points indicates that the distributions are not log-normal but bimodal in shape.

Each data set is also illustrated as a histogram in Figures 3 and 4. The partial concentrations are weighted for the particle interval width. Because of the weighting procedure, the area under the histogram represents the total mass of the aerosol; the percentage of the area under a given size interval segment is equal to the percentage of mass in that given size interval.

A comparison of the shapes of the different distributions is made possible by normalizing the concentration for each data set. For each size interval, the partial concentration is divided (weighted) by the total concentrations before being divided by the particle size interval width term. This allows each interval value to be represented as a percentage (decimal value) of the total concentration. Superimposing the histograms of the different data sets allows direct comparison of the shapes, independent of the total concentrations. These histograms are shown in Figures 5 and 6.

The use of small particle (<10μm) impactors in the WRAC further describes the particle size distribution below 10μm. Data from a University of Washington impactor is used to illustrate the average distributions obtained in Phoenix and Riverside. These distributions are illustrated in smooth curve plots in Figure 7. The curves were generated from the normalized histograms for the respective WRAC and Washington impactor data sets. This plot is important because it shows the distinct small particle mode of the RBX-High data below 10μm, which cannot be determined from the plot in Figure 4.

Data for the collected IP Network samplers were averaged together to correspond to the WRAC run groupings. Where several data points (measurements) were not obtained, the average was omitted. To readily compare results site-to-site, the sampler data are reported as ratios to the WRAC total aerosol concentration. These ratios are presented in Table 1. Also

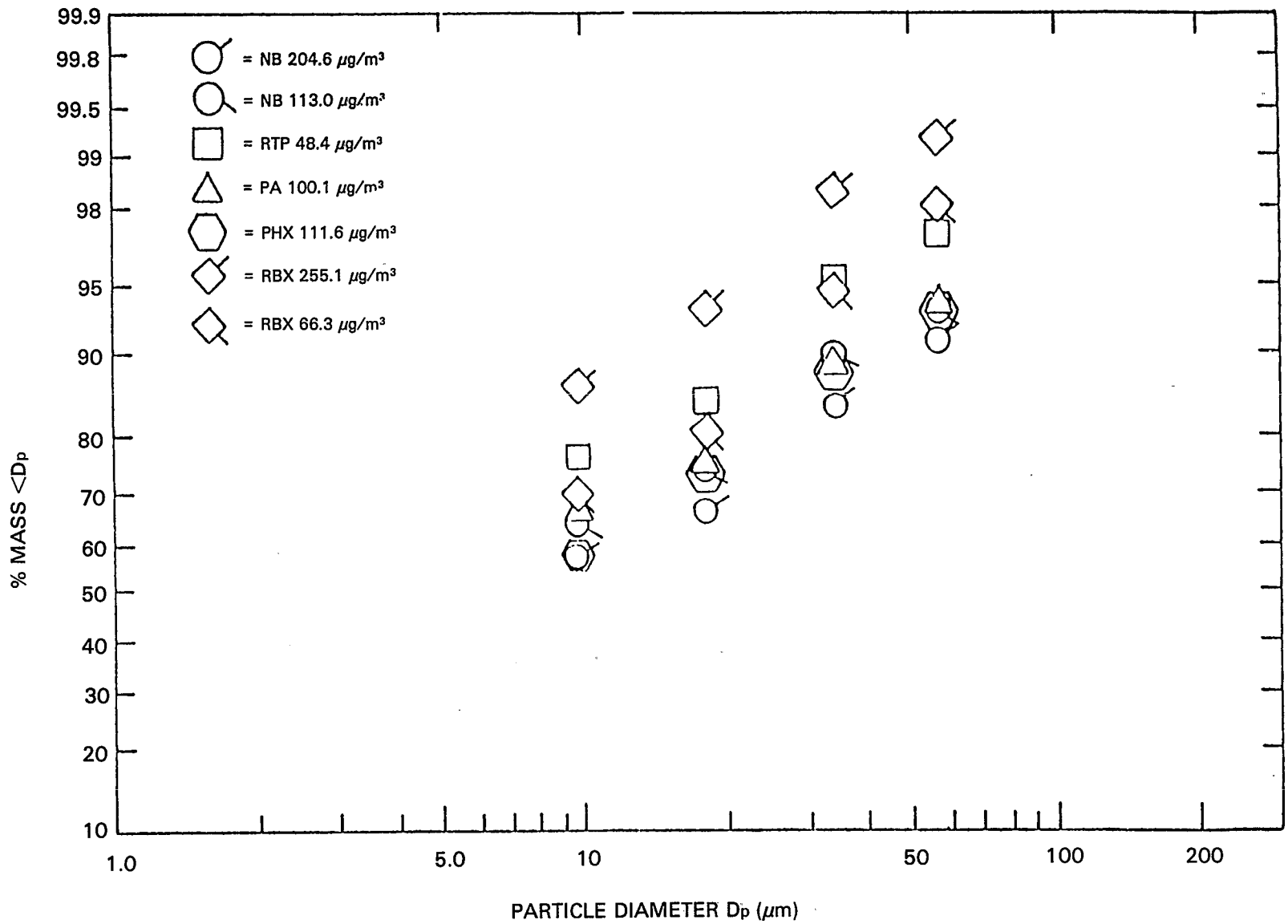

Figure 2. WRAC cumulative mass distributions.

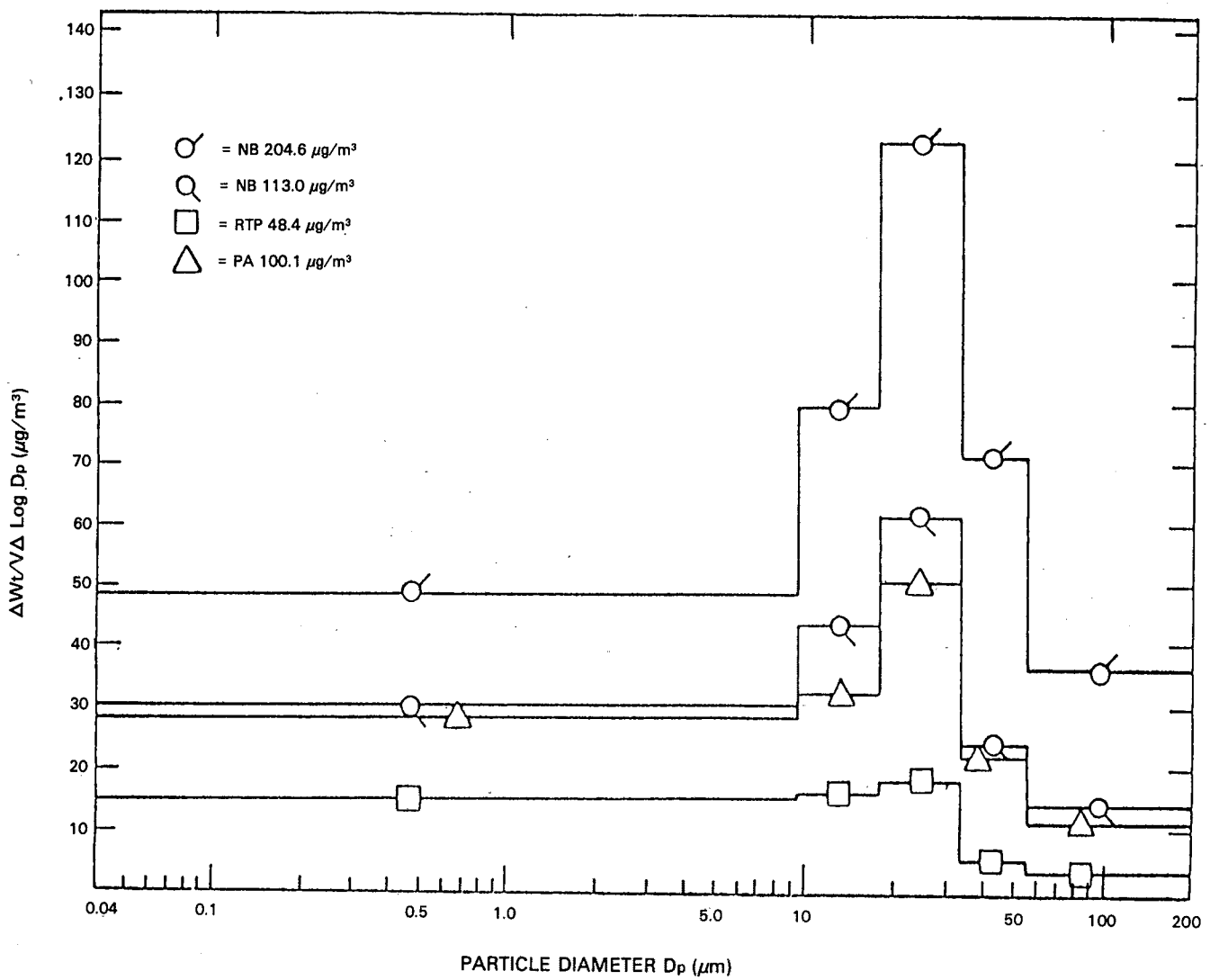

Figure 3. WRAC mass distribution histograms for Birmingham, Research Triangle Park, and Philadelphia.

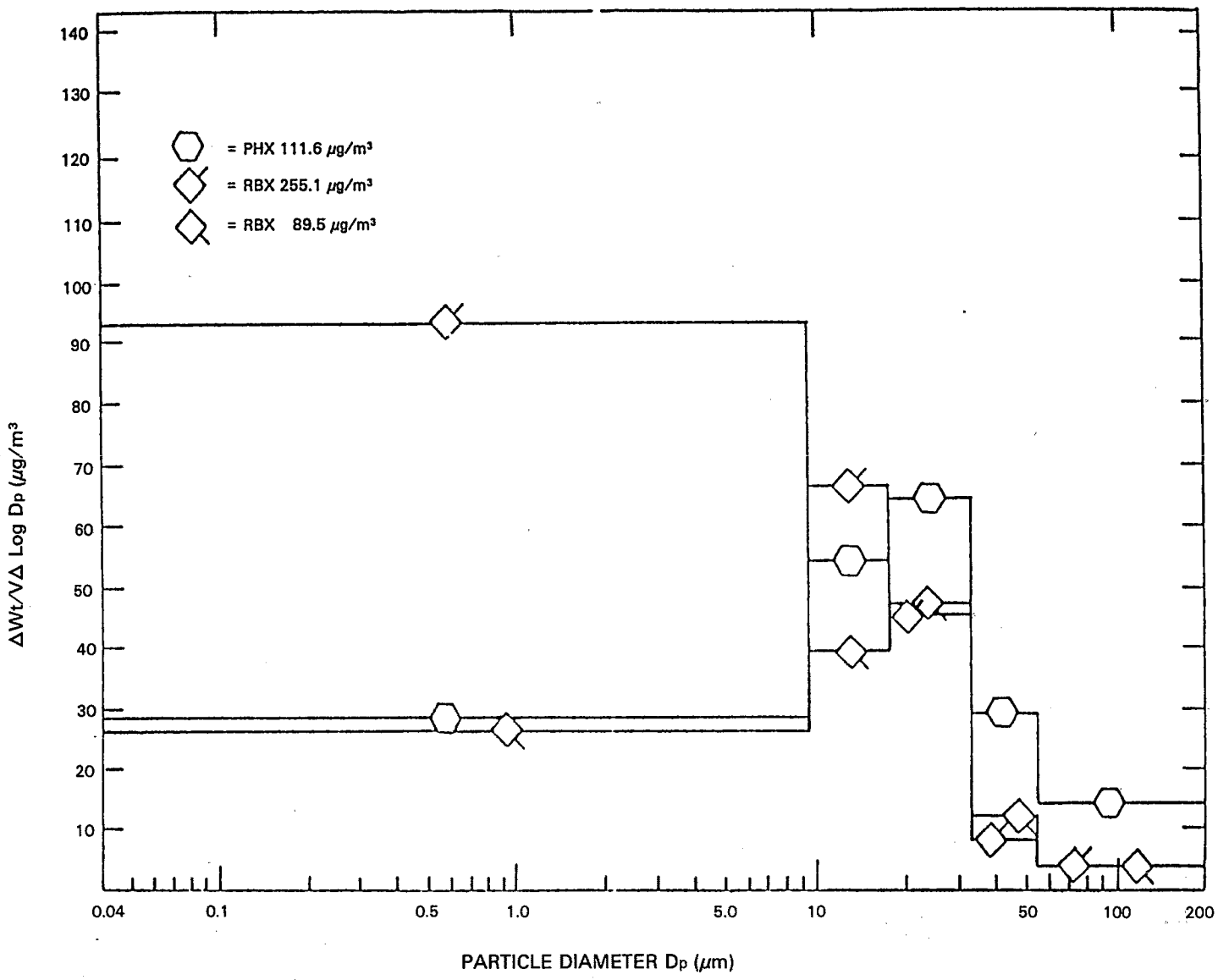

Figure 4. WRAC mass distribution histograms for Phoenix and Riverside.

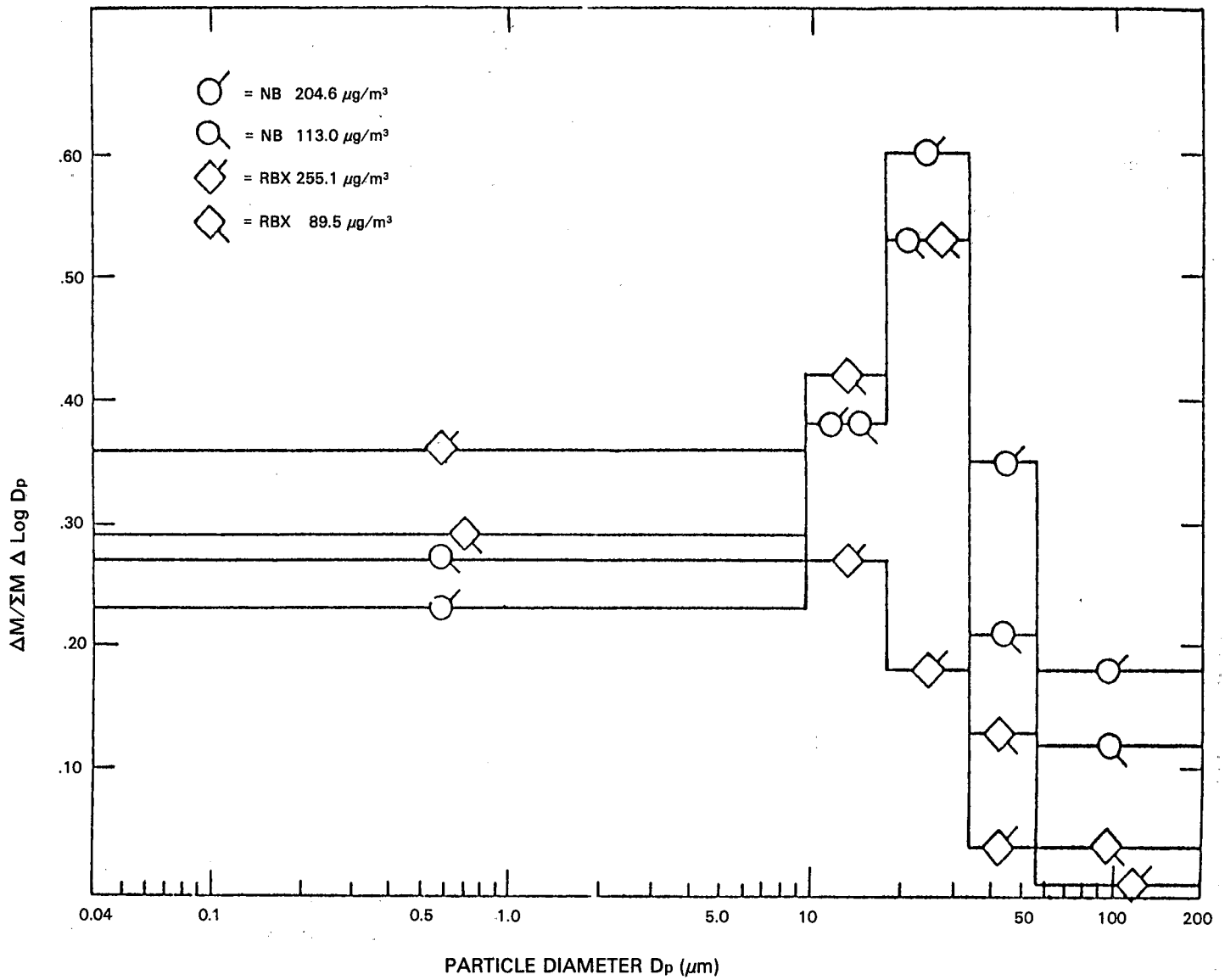

Figure 5. Normalized mass distributions for Birmingham and Riverside.

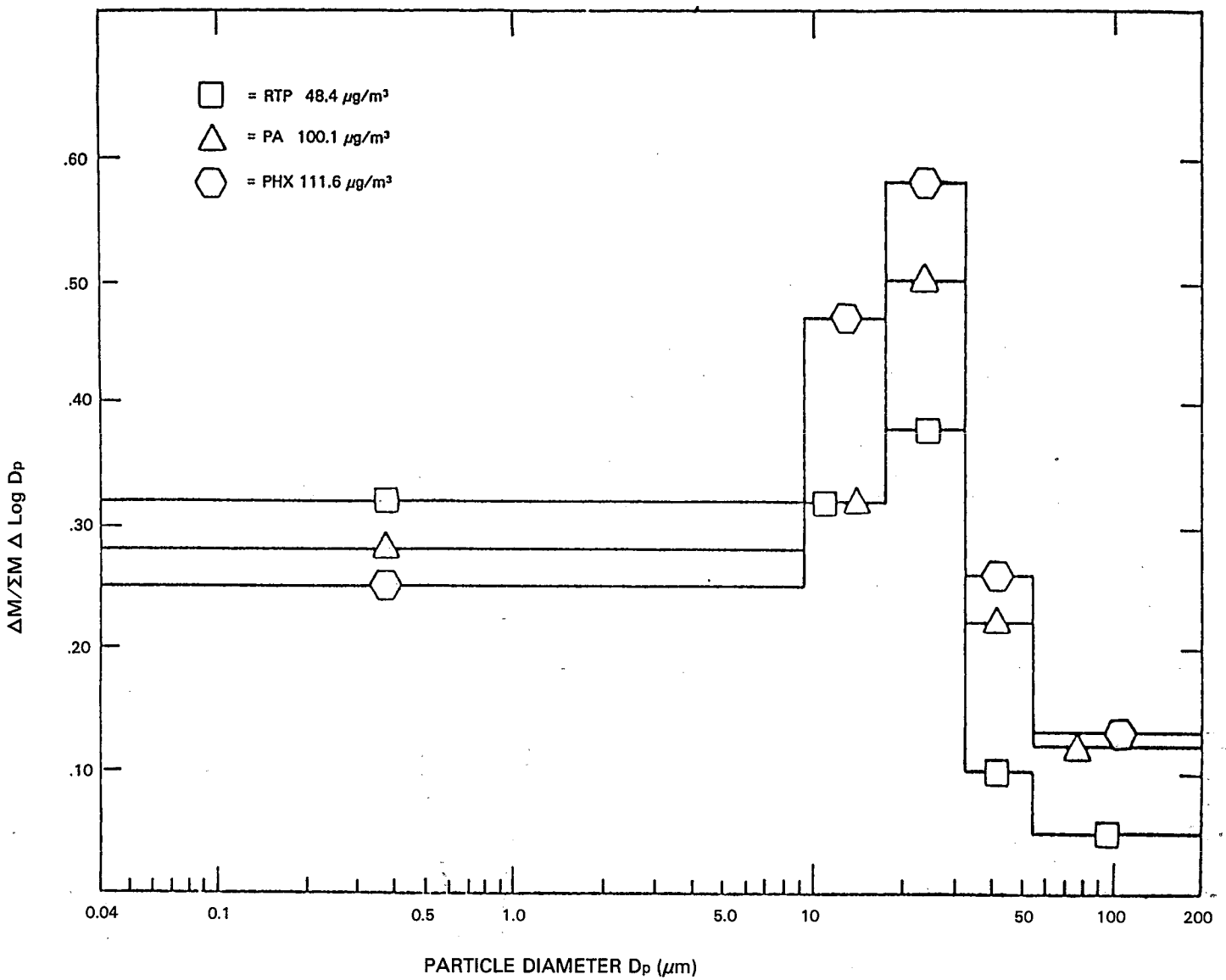

Figure 6. Normalized mass distributions for Research Triangle Park, Philadelphia, and Phoenix.

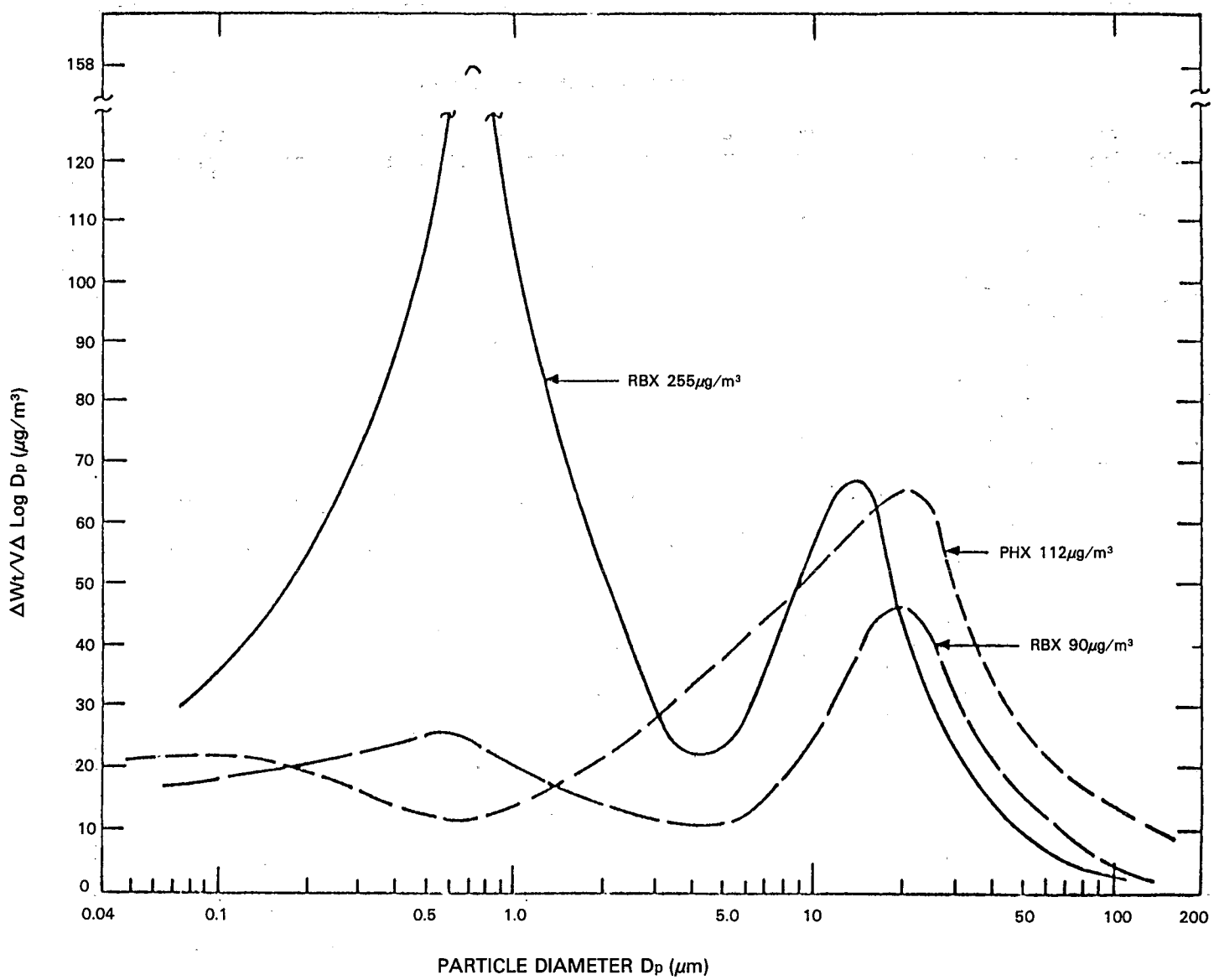

Figure 7. Mass distribution curves for Phoenix and Riverside.

TABLE 1. SAMPLER VS. WRAC CONCENTRATION EXPRESSED AS RATIO

Site	Total* conc "C"	TSP	Sampler concentration/"C" SSI <15μm	Dicot <15μm	Dicot(F) <2.5μm	Dicot(C) <2.5μm
NB-High	204.6	0.84	0.50	0.57	0.13	0.44
NB-Low	113.0	0.95	0.69	0.66	0.26	0.40
RTP	48.4	--	--	0.81	0.46	0.35
PA	100.1	1.08	0.72	0.71	0.35	0.36
PHX	111.6	0.87	0.62	0.55	0.12	0.43
RBX-High	255.1	0.92	0.94	--	--	--
RBX-Low	89.5	0.95	0.74	--	--	--

Site	Total* conc "C"	WRAC concentration > Dp/"C" >57μm	>34μm	>18μm	>9.6μm
NB-High	204.6	0.10	0.17	0.34	0.45
NB-Low	113.0	0.07	0.11	0.26	0.37
RTP	48.4	0.02	0.05	0.15	0.24
PA	100.1	0.06	0.11	0.25	0.33
PHX	111.6	0.07	0.12	0.28	0.41
RBX-High	255.1	0.01	0.02	0.06	0.14
RBX-Low	89.5	0.02	0.05	0.20	0.31

*Total WRAC concentration expressed as $\mu g/m^3$.

presented, for comparison purposes, are ratios of the particle concentration collected on a given WRAC impactor to the total concentration measured.

DISCUSSION OF MASS DISTRIBUTIONS

Particle mass distributions obtained from all of the sampling sites exhibit a biomodal shape. The position and magnitude of the modes varies from one location to another and even varies at different times in the same location. The cumulative probability distributions in Figure 2 are curves that indicate multimodal distributions. The histograms in Figures 3 and 4 clearly show the various positions of the large particle modes, together with their magnitudes. The distribution curves in Figure 7 show that the small particle mode also may vary in position and magnitude.

The great difference in the RBX-High and RBX-Low small particle modes is easily explained by examining the respective sampling conditions. During the days averaged for the RBX-Low distributions, the winds were predominantly from the east, or off of the Santa Anna Desert. The particulate mass was primarily composed of large particles entrained in the wind.

The small particle mass mode was small because most of the mobile sources and other condensation aerosol sources are located to the west, and their contributions were not carried in by the wind.

During the sampling runs used for RBX-High averaging, the wind was primarily from the west, out of the Los Angeles Basin. The wind velocities were, on the average, lower than winds from the east. The air was heavy with small-diameter particulate matter due to the abundance of condensation aerosol (including photochemical aerosol) being blown in from the Los Angeles basin area. This boosted the small particle concentration by about a factor of eight. An interesting observation is that the large particle mode appeared to increase in magnitude with a downward shift in mean particle size. The Los Angeles basin is a moderate source of larger particles, due to the many dispersion sources such as the extensive roadway system. However, with lower wind speeds, the air mass that starts in Los Angeles takes a considerable amount of time to travel to Riverside. This may have allowed most of the larger particles to be removed (or settled out) from the air mass and produce a downward shift in the mean large particle size.

In contrast to this, the observed distributions in Birmingham were characterized by a fairly uniform increase in the whole size spectrum. This condition was usually the result of air stagnation in the immediate area, resulting in an overall increase in concentration of all sizes of particles.

A final comment on the actual distributions refers to the Research Triangle Park site. The overall low concentrations observed were generally expected because of the lack of significant anthropogenic pollution sources in the area. It is interesting to note that the largest size fractions show magnitudes similar to those found in Riverside. This leads to a suggestion that these particles, which included things like insect parts and pollen, are the result of natural generation and exist in relatively clean areas around the country.

By normalizing the mass distributions with respect to concentration, the shapes of the distributions can be compared as in Figures 5 and 6. The figures indicate that, while the general shape of the distributions are similar, the individual interval values can vary greatly. Each distribution measured is the result of a unique set of meteorological and geographical conditions that influence the presence and residence time of each size range of particles. There is no simple pattern that all of the distributions follow. One cannot simply have a generalized distribution with a correction factor to apply for actual concentration. Indeed, the distribution shapes can be quite different when the concentrations in two areas are similar. The result is that ambient particulate distributions must be considered as a function of location, time, etc.

When the concentration obtained by the WRAC is compared to the concentrations obtained by other conventional samplers, as in Table 1, several facts are revealed. The Hi-Vol sampler normally collects between 85 percent and 95 percent of the total suspended aerosol mass present, depending

on the location. The amount of material collected by the > 57μm WRAC sampler can be 1 percent to 10 percent of the total mass. However, these differences are not a function of concentration, but a result of the distribution characteristics. Aerosol distributions that exhibit a low concentration in the large particle mode give much closer correlation between the Hi-Vol and WRAC total aerosol measurement.

COMPARISON OF MEASURED VS WRAC MODELED TSP HI-VOL, SIZE SELECTIVE INLET HI-VOL AND DICHOTOMOUS MEASUREMENTS

Measurements by the conventional TSP Hi-Vol, Size Selective Inlet Hi-Vol, and Dichotomous samplers were made simultaneously with each WRAC measurement. The three conventional sampler types have been recently characterized for particle size separation and collection efficiency definition under EMSL extramural programs. With the particle size cut-off characteristics of the conventional samplers applied to the total particle mass distribution defined by WRAC measurements, it is possible to compute mass loadings that each of the three conventional samplers should be collecting. The results of the modeled predictions are compared to actual measurements by the TSP Hi-Vol, SSI Hi-Vol, and Dichotomous samplers, as shown in Figures 8, 9, and 10, respectively. Correlations are good for all three sampler types. A statistical analysis was performed, with the results shown in Table 2. No significant difference at the 95 percent C.L. was found between TSP Hi-Vol modeled and measured samples for all five cities sampled. SSI Hi-Vol measured vs modeled showed no significant difference at the 95 percent C.L. for all measurements in four of the five cities sampled. Birmingham SSI Hi-Vol measurements were somewhat lower than predictions. Dichotomous sampler measured values were lower than predicted in each of the five cities.

CONCLUSIONS

System testing, along with field sampling and evaluation, have shown that the Wide Range Aerosol Classifier is a viable instrument for collecting size-separated particulate mass samples to include the total ambient aerosol size spectrum. WRAC field data reveal that the amount of particulate matter present in the ambient air greater than 10μm diameter can vary by as much as a factor of 3, with a maximum percentage obtained in this study of 45.

Ambient aerosol distributions tend to display bimodal shapes under a variety of situations such as sampled with the WRAC. In reference to time and location, implementation of a standard will affect some areas of the country more radically than others, due to the large variation in the size distribution of the ambient aerosol.

By use of WRAC particle mass distribution data, precise estimates for the TSP Hi-Volume and Size Selective Inlet Hi-Volume samples of a given <u>total</u> ambient aerosol mass can be made.

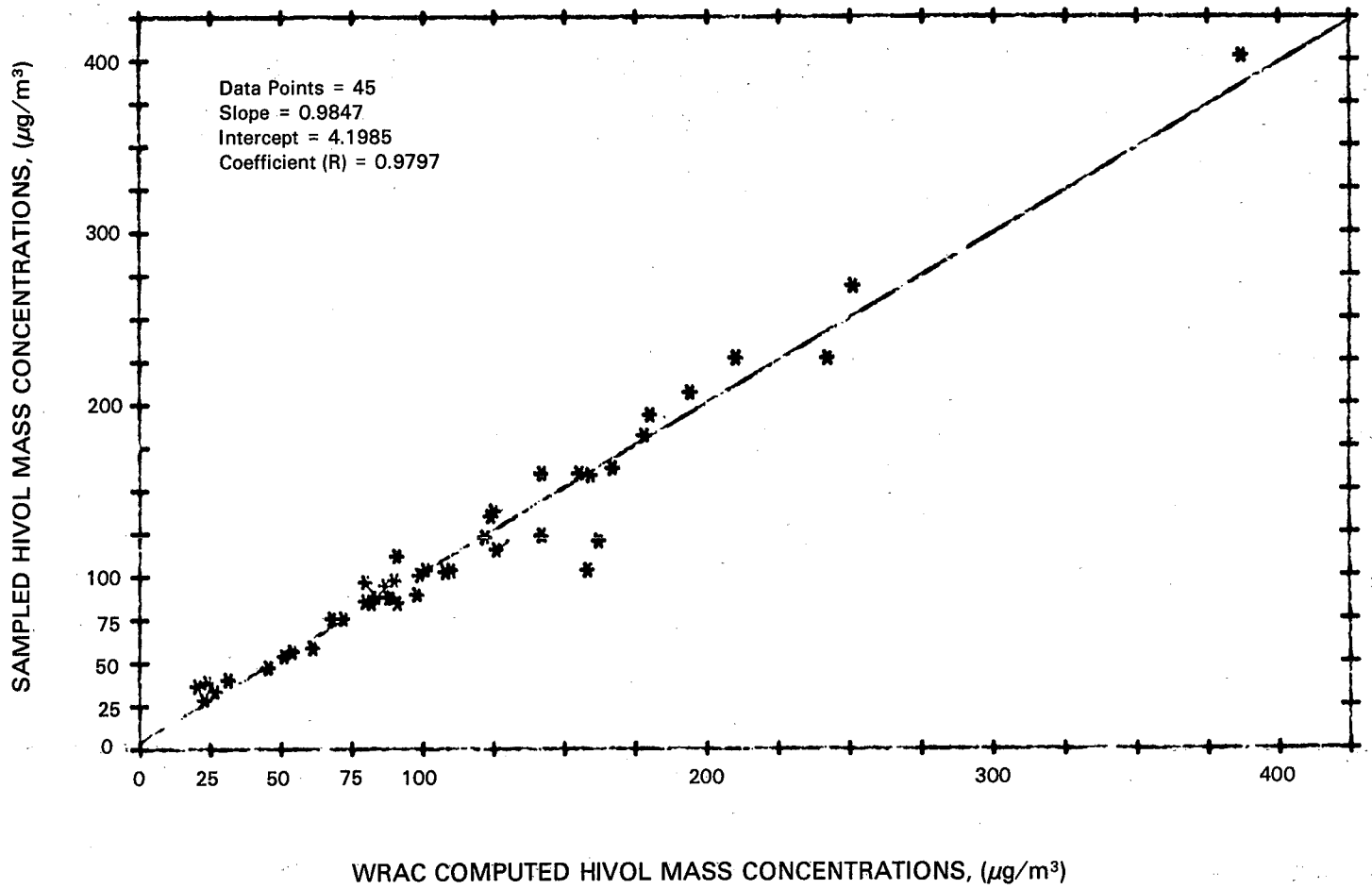

Figure 8. Comparison of sampled vs computed (WRAC) Hi-Vol mass Birmingham, RTP, Philadelphia, Phoenix, and Rubidoux.

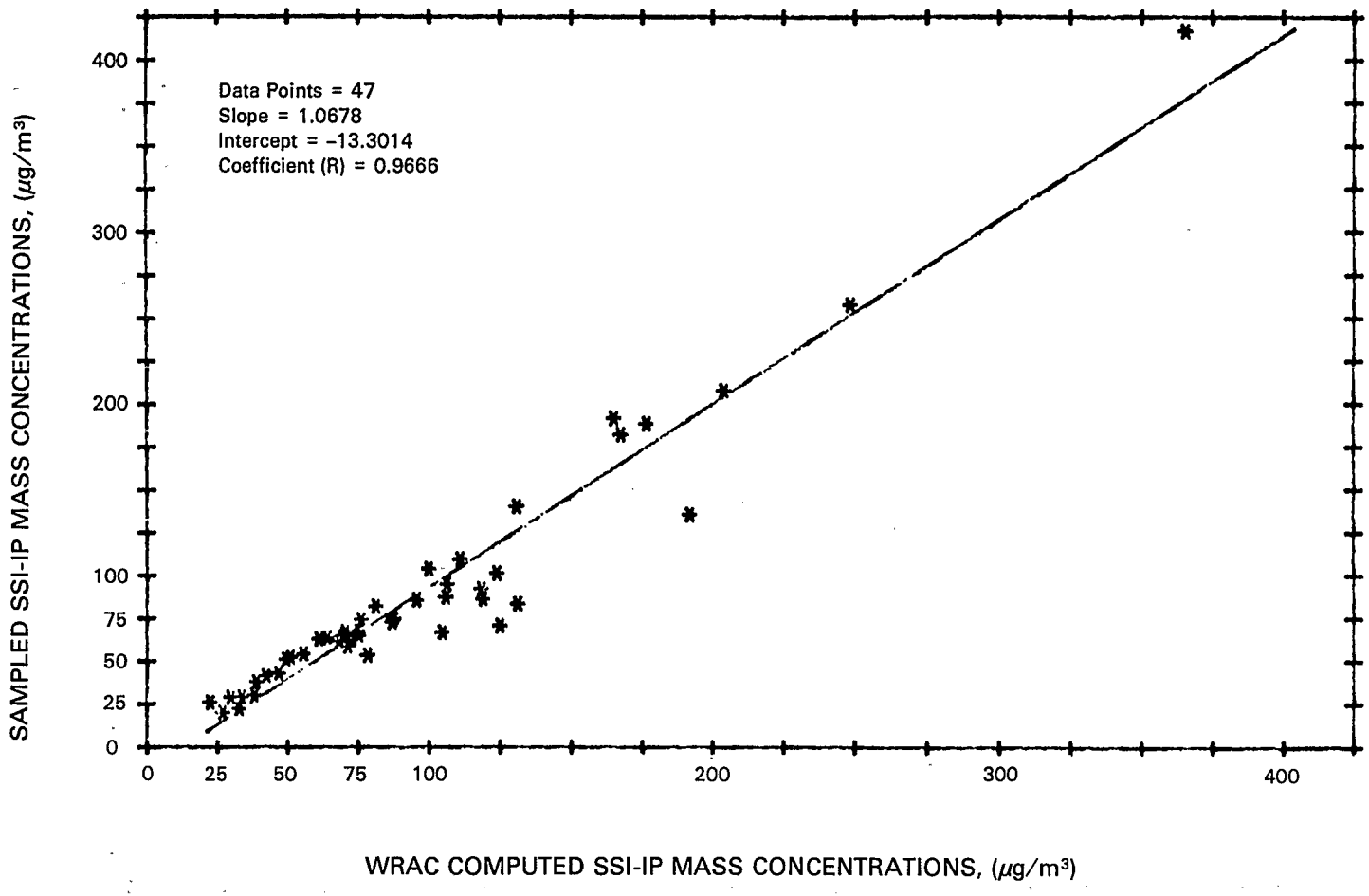

Figure 9. Comparison of sampled vs computed (WRAC) SSI-IP mass Birmingham, RTP, Philadelphia, Phoenix, and Rubidoux.

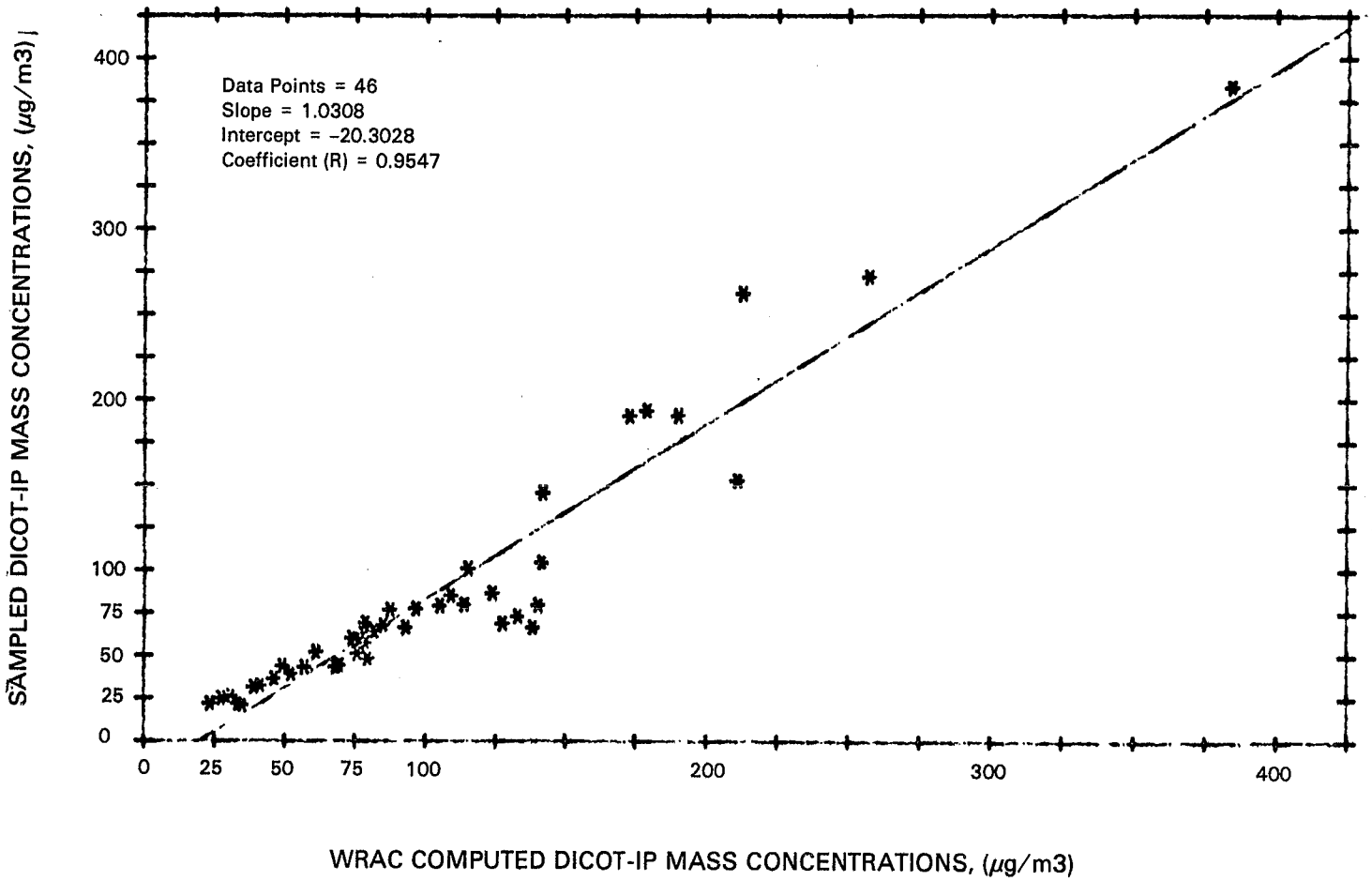

Figure 10. Comparison of sampled vs computed (WRAC) DICOT-IP mass Birmingham, RTP, Philadelphia, Phoenix, and Rubidoux.

TABLE 2. COMPARISON OF MEASURED VS WRAC MODELED MASS LOADING

Sampler type	Mean measured conc. ($\mu g/m^3$)	Mean computed conc. ($\mu g/m^3$)	Mean difference ($\mu g/m^3$)	Mean difference (%)	Corr. coeff.	n	Paired t-test calculated	Paired t-test tabulated	Remarks
Hi-Vol TSP 5 cities	114	116	2.0	1.7	0.9797	45	0.99	2.014	No significant difference at 95% C.L.
SSI Hi-Vol 5 cities	88.8	96.4	7.6	8.2	0.9666	47	2.690	2.012	
SSI Hi-Vol 4 cities	89.9	91.7	2.3	2.5	0.9853	38	1.163	2.024	No significant difference at 95% C.L.
Dichotomous Sampler	86.7	103.8	17.1	18	0.9547	44	5.690	2.022	

REFERENCES

1. Miller, F.J. 1979. Size considerations for establishing a standard for inhalable particles. APCA Journal 29(6).

2. Lundgren, D.A., and H.J. Paulus. 1975. The mass distribution of large atmospheric particles. APCA Journal 25:1227-1231.

3. Davies, C.N. 1968. The entry of aerosols into sampling tubes and heads. Brit. J. Appl. Physics 2(1):921-932.

4. Agarwal, J.K., and B.Y.H. Lui. 1980. A criterion for accurate aerosol sampling in calm air. Am. Ind. Hyg. Assoc. J. 41:191-197.

DETECTION OF GRAPHITIC CARBON IN COLLECTED PARTICULATE MATTER

W.A. McClenny

U.S. Environmental Protection Agency
Research Triangle Park, NC

ABSTRACT

Concentration estimates of ambient light-absorbing carbon in particulate matter collected on Teflon filter substrates have been made, using the optical, nondestructive techniques of differential transmission and photoacoustics. Based on a comparison with similar measurements on laboratory-generated samples, analysis of ambient samples indicates that differential transmission measurements overestimate absorbing carbon by an increasing amount as the total sample mass increases. Photoacoustic measurements appear to be more accurate, but are subject to the influence of thermal properties of the sample and substrate.

INTRODUCTION

This research attempted to measure absorbing carbon in particulate samples collected for X-ray fluorescence analysis. Absorbing carbon is assumed to be synonymous with graphitic carbon in terms of visible light absorption (1). To be compatible with X-ray fluorescence analysis (2), ambient samples were collected over periods of 12 to 24 hours by dichotomous samplers (3) using Teflon filter substrates. The analytical approach used to detect absorbing carbon on these samples has been to make simultaneous photoacoustic and transmission measurements using a visible light source. Measurements were interpreted using calibration curves relating response to loading of flame-generated soot.

EXPERIMENTAL PROCEDURE

We have used an experimental arrangement similar to that described by Lin and fellow researchers (4) to record transmission and photoacoustic signals for ambient samples collected on Teflon filter substrates (Ghia Types 501 and 504). To obtain the transmission value, a fraction of the forward scattered light is measured before and after loading with particulate matter. The relationship of the signal differences to the sample loading of absorbing carbon has been examined. We did not observe the

sampling constraints specified by Lin; other considerations related to compatibility with X-ray fluorescence analysis dictated the sample characteristics. The experimental arrangement also used a photoacoustic cell to provide an analytical signal related to sample absorption.

Figures 1a and 1b show the cell-holding Teflon filters. Light from either a broadband or laser source is directed through a glass window onto the side of the Teflon filter containing the particulate matter. The light is scattered and absorbed within the sample. A portion of the light is forward-scattered through the Teflon filter and opal glass diffuser to a photodiode detector (RCA, 1P39) and recorded as the transmitted signal. In the latest configuration, a 15-mW HeNe laser beam is expanded and directed onto a beam-defining aperture of 1 cm diameter just before passing through the optical cell's front window. The filter is usually placed with the aerosol deposit facing the light source, although it can easily be reversed.

Pressure seals are made with O rings for those Teflon filters bonded into frames, or with the retaining ring in filters not bonded. The opal glass is used to reduce the effect of scattering, and of substrate and sample inhomogeneities, by diffusing the incident beam to form the exiting pattern of a diffuse radiator. An aperture in the aluminum retaining plate for the opal glass limits the exiting beam before it reaches the photodiode.

The light absorbed in the sample causes a slight increase in the pressure of the closed volume in front of the Teflon filter. Because the light beam is mechanically chopped, the pressure variation is periodic. This variation is detected by a Knowles electret microphone (BT 1759) and processed by a lock-in amplifier.

To relate photoacoustic and transmission signals to the graphitic carbon content of the particulate sample, the following sequence is performed. The blank Teflon filter is mounted in the cell and a transmission measurement is recorded. The photoacoustic signal is also measured, but since the light absorbed by the blank filter is quite small (approximately 10 times smaller than the signal for typical ambient loadings), a preloading measurement of the photoacoustic signal is not usually necessary. After the filter is loaded, the sequence of measurements is repeated. A value of absorbance, $-\ln(I/I_o)$, is formed from the two transmission measurements. For the photoacoustic analysis, the same before and after measurements are subtracted to form a net signal value. These system responses are used to find the amount of a reference sample that would have given an equal signal. This correspondence is made using calibration curves that relate system response to reference sample loading. The calibration curve is established by plotting absorbance and photoacoustic response as a function of carbon loading for filters on which known loadings of soot have been placed. Typical calibration curves are shown in Figures 2a and 2b. Figure 2a gives the value of absorbance, $(1-I/I_o)$, as well as $-\ln(I/I_o)$. The measured response of either system is located on the ordinate scale of the corresponding calibration curve, and a value of graphitic carbon loading in micrograms per centimeter squared is located on

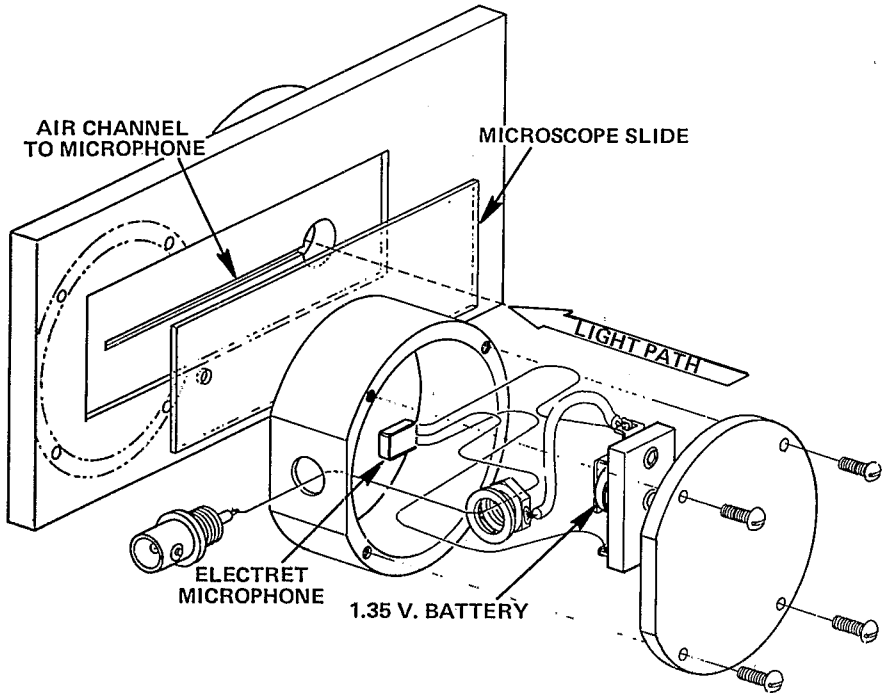

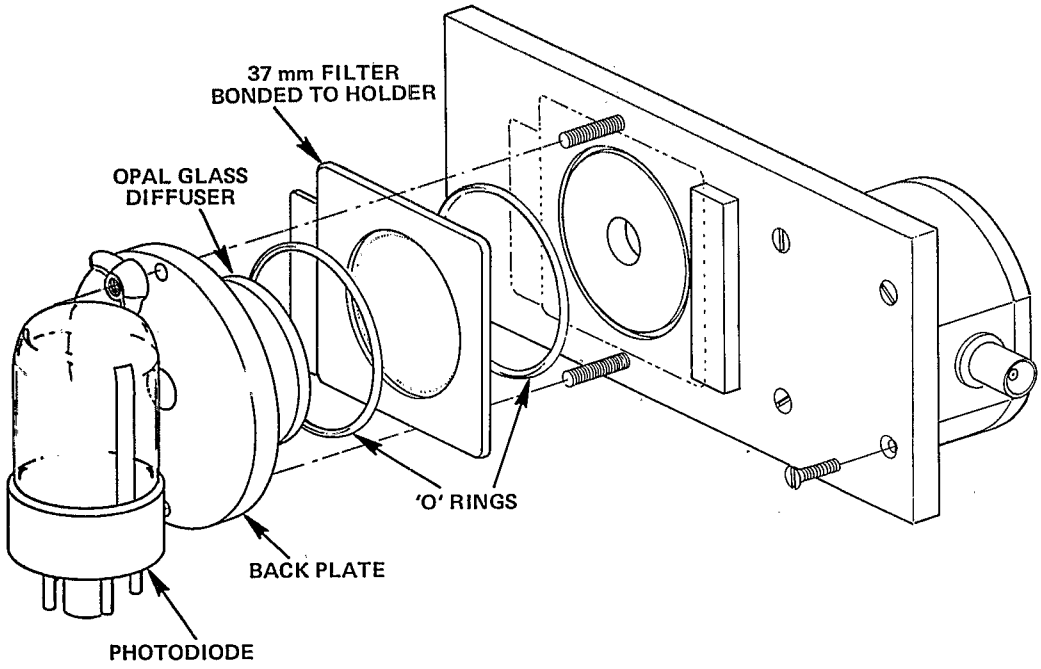

Figure 1. Schematic of detector cell used in optical measurements of particulate samples (a) front view of disassembled parts, (b) back view.

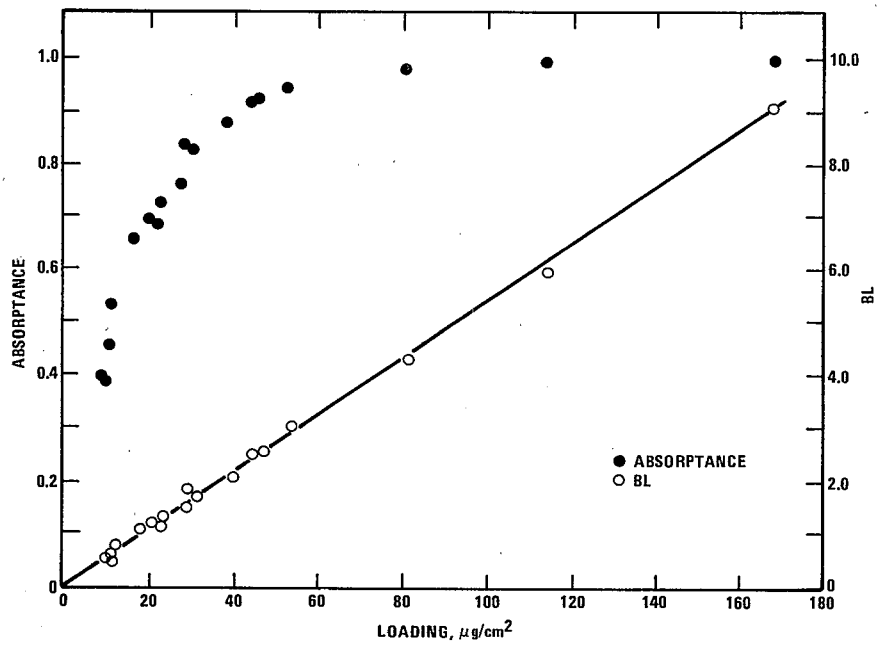

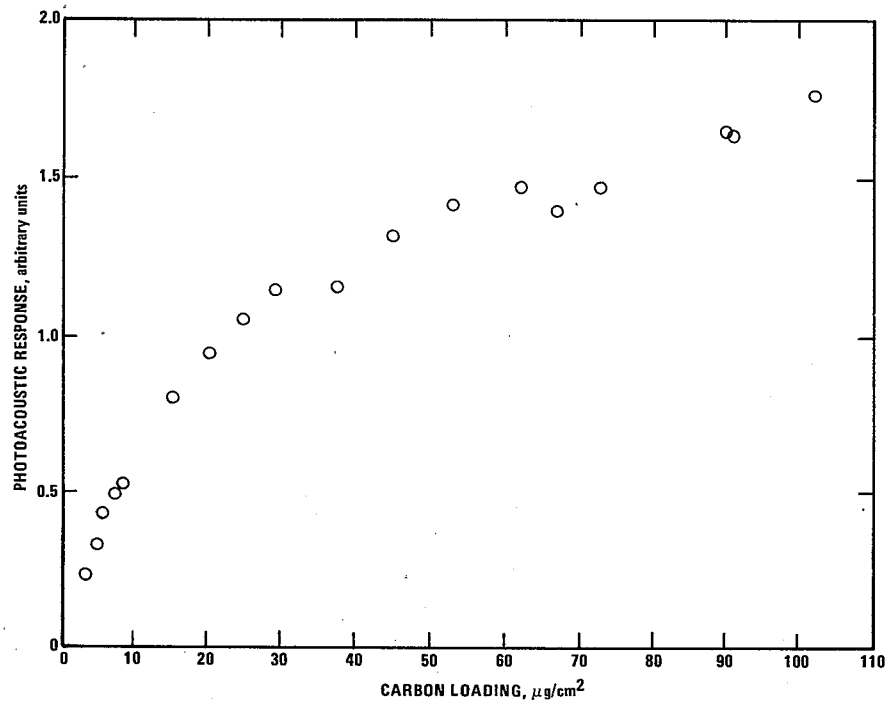

Figure 2a. Calibration curve relating optical absorptance and optical absorbance (BL) to sample weight loading of soot in μg per cm^2 of filter area.

Figure 2b. Calibration curve relating photoacoustic signal to sample weight loading of soot in μg per cm^2 of filter area.

the abscissa scale, using the previously established calibration curve. The usual ambient loadings of absorbing carbon are below 10 $\mu g/cm^2$, so that the calibration curves must be used in a region between actual data points and zero loadings. However, as shown on the calibration curves, the extrapolated curve is well defined. Imprecise weighing of the lightly loaded samples causes this lack of data points in the useful range of loadings.

The soot used in loading a reference set of filters was generated in an oxygen-rich, propane flame, as described by Bennett (5). The soot was mixed with dry air to supply the required flow rate for a manual dichotomous sampler. Soot loadings were weighed on a Mettler balance using a set of certified weights for calibrating the balance. The fraction of graphitic carbon was measured for 13 samples as 0.80 ± 0.06 (one standard deviation) by combustion analysis.

RESULTS

Analysis of Synthetic Samples

Previous research using the experimental apparatus shown in Figures 1a and 1b has been published (6,7), but is limited to analyzing synthetic samples that are intended to simulate ambient samples. Three conclusions are drawn:

1. thermal effects, as well as carbon absorption, determine the photoacoustic response versus soot loading relationship;

2. mixing ammonium sulfate with a given amount of soot significantly increases the apparent absorption values derived from differential transmission measurements; and

3. photoacoustic measurement of absorption values are only slightly changed by mixing ammonium sulfate and soot.

The first conclusion is at least partly due to thermal wave interference (6). The thermal effects are evident in the calibration curves shown in Figures 2a and 2b. In each figure, sample loading for a sample of propane flame-generated soot is plotted as the abscissa, with response as the ordinate. In Figure 2a the response is given in units of absorptance, $(1-(I/I_o))$, and of absorbance, $(\ln I_o/I)$ or βl. The response is given in mv of signal per mW laser output power in Figure 2b. The first of the above conclusions is evident in the shape of the two calibration curves near a loading of 80 $\mu g/cm^2$. At this loading, Figure 2a shows that no additional light is available for absorption, while in Figure 2b the photoacoustic response continues to increase. Conclusions 2 and 3 are shown in graphic form in reference 7.

Analysis of Ambient Samples

During the research on synthetic samples, several sets of ambient samples were analyzed. These samples were the fine fraction of particulate matter collected with dichotomous samplers in special U.S. Environmental Protection Agency (EPA) field studies. A set of routine analytical procedures, consisting of analysis by X-ray fluorescence and mass determinations by beta-gauge (8), was performed on the samples. In some cases, duplicate samples collected on quartz fiber filters were available for analysis of total, volatile, and graphitic carbon (9).

A summary of the data appears in Table 1, as mean values for several measured parameters for each of the five data sets. The sets are ordered so that the value of the parameter BL/PA decreases monotonically. Three tentative conclusions seem consistent with these data:

TABLE 1. SUMMARY OF MEAN VALUES FOR PARAMETERS CHARACTERIZING PARTICULATE MATTER COLLECTED ON TEFLON SUBSTRATES (18-33 filters per set)

Location	EC*	PA†	BL‡	MASS§	BL/PA	CC#
	(micrograms per square centimeter)					
Houston	2.2	2.8	6.1	64	2.1	0.96
Philadelphia	6.1	4.7	8.0	61	1.7	0.77
Shenandoah	---	0.9	1.3	42	1.4	---
Philadelphia	4.6	5.7	6.1	38	1.1	0.86
Houston	---	6.7	6.1	38	0.9	---

*Elemental carbon determined by combustion.
†Absorbing carbon determined by photoacoustic measurements.
‡Absorbing carbon determined by differential measurements.
§Mass of all particulate collected.
#Correlation coefficient for BL and PA measurements.

1. BL/PA and MASS are correlated. Since PA values are not changed by adding ammonium sulfate to a given amount of soot for lab-generated samples, the parameter BL/PA for ambient particles appears to be an enhancement factor in the differential transmission measurement. This enhancement factor is apparently related to MASS.

2. The values of EC, PA, and BL do not appear to be related in any simple way. The combustion value for elemental carbon and the optical value for absorbing carbon probably vary depending on location.

3. The value of the correlation coefficient (C.C.) for paired values of BL and PA is higher for the filter set (Houston, Texas) using the thicker, Type 501, Teflon filters. This

greater value is consistent with other observations in the laboratory. The effect is apparently related to the greater variability in mass for the blank Type 501 filters, which in turn corresponds to a variability in the transfer of energy from the sample to the surrounding air.

A relationship between BL/PA and MASS is also evident for individual filters within a single set. This relationship is shown in Figure 3 for a set of 25 filters taken in Philadelphia, Pennsylvania. The data were fitted using a linear, least squares analysis. An intercept value of 1.0 would correspond to agreement of BL and PA for low loadings of MASS.

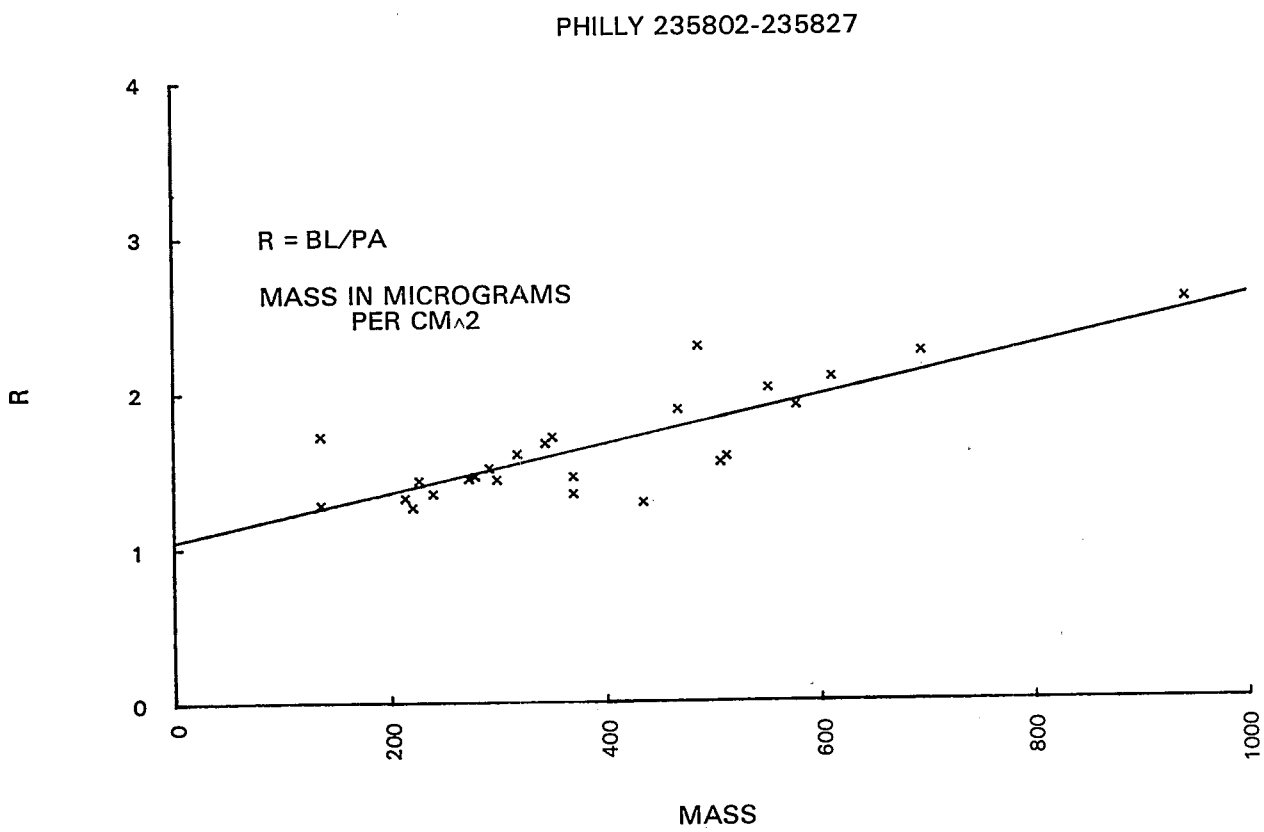

Figure 3. Ratio, R, of soot estimates by optical absorption and photoacoustics versus total mass loading per filter.

Modeling of the Differential Transmission Measurement

A mathematical model has been developed to predict the results of differential transmission measurements. The model simulates the light attenuation with a mixture of absorbing and scattering particles, using a modification of a mathematical treatment listed by Kortum (10). Kortum

assumes that the sample consists of layers that are assigned values of reflectivity, R, and of transmission, T. Using the closed form of a geometric series, the values of R and T are obtained for a combination of two layers. The resultant R and T values are assumed to be for a composite layer, which is combined with an additional single layer to obtain values for R and T for three layers, etc. Thus any number of layers can be considered, as indicated in Figure 4. To adapt this procedure to light transmission through a sample of discrete particles, the following assumptions were made:

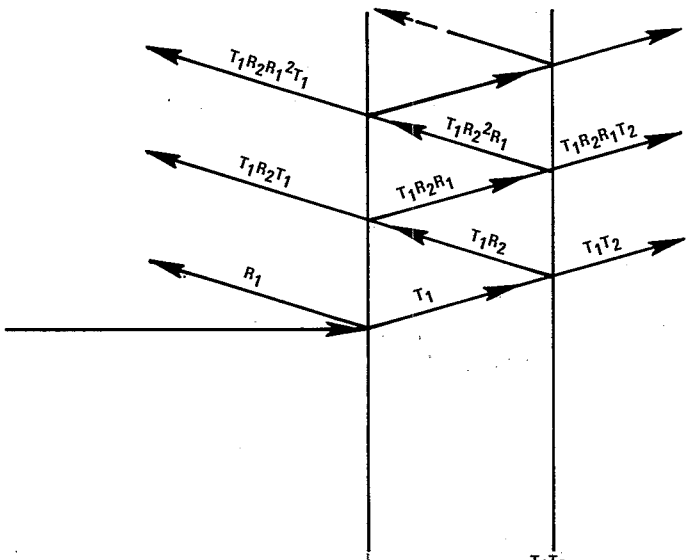

$$T = T_1T_2\,(1+R_1R_2+R_1^2R_2^2+\ldots) = \frac{T_1T_2}{1-R_1R_2}$$

$$R = R_1+T_1^2R_2(1+R_1R_2+R_1^2R_2^2+\ldots) = R_1+\frac{T_1^2R_2}{1-R_1R_2}$$

Figure 4. Schematic representation of model used in calculating light transmitted through and reflected from particle layers in a sample.

1. The particles are divided into two mutually exclusive groups: scattering and absorbing. These correspond to soot and all particles minus soot.

2. All particles are spherical and each group has a single diameter that is specified at the beginning of the treatment.

3. A scattering particle is characterized by a backscatter under uniform illumination that was initially estimated using a Mie theory calculation (11). Contributions of individual particles comprising a layer are summed to obtain a filled layer's reflectivity. This estimate was modified as required to fit

experimental data; the modification appears justified, as the individual particles are so close that assumptions used to derive the Mie formulation are not necessarily valid.

4. Absorbing particles are assigned an absorption coefficient; the light throughput is characterized by the average parallel transmission of light through the intercepting cross-section. The transmission of a single layer is equal to unity minus the reflectivity minus the sum of absorption by individual particles.

5. The last "layer" in the model is the combination of Teflon filter and opal glass, where a reflectivity of 63 percent was measured at 45° and used as the average reflectivity of the last "layer."

The program for calculating sample transmission was begun by specifying the absorption coefficient of soot, B; diameters of particles, D1 for soot and D2 for scattering particles; reflectance of the substrate, R2; mass loadings of soot and scattering particles, L1 and L2, respectively; and a packing fraction, P, which accounted for the amount of available area (84 percent) actually occupied by particles in a layer composed of spherical particles.

The model predictions for absorbance versus the graphitic carbon loading for simulated ambient samples are shown in Figure 5. Individual curves correspond to the indicated loading (M in micrograms per filter) of nonabsorbing particles. The curve for M = 0 is calculated by using the graphitic carbon weight to define the number of particle layers in a sample (i.e., spherical particles of a given diameter closely packed onto a given surface area, with a fractional void area, have a mass which, when divided into the total mass, gives the number of layers in the sample). The remaining curves, M = 100, 300, 500, and 700μg/filter, use the mass of nonabsorbing particles to determine the number of layers and disregard the mass contributed by graphitic carbon. While this simplification is of value in making the mathematical treatment tractable, the resulting curves may not be appropriate for sufficiently high values of graphitic carbon loadings. In fact, the unexpected crossover of the M = 100μg/filter and M = 0μg/filter curves and bending of the remaining curves for the higher graphitic carbon mass to nonabsorbing mass ratios may result. Even with its limitation, the model clearly predicts that: 1)scattering from nonabsorbing particles causes an overestimate of graphitic carbon; and 2) the higher the nonabsorbing particle loading, the greater the overestimate.

Figure 6 shows a comparison of model predictions and experimental measurements of absorbance for a set of field-loaded filters from Houston. Model parameters were: $B = 13 \times 10^6\ m^{-1}$; D1 = 0.02 μ; D2 = 0.084 μ; R = 0.1; R2 = 0.63; P = 0.9. The value of B approximately equals that measured by Rohl and fellow researchers (12). The value of D1 is an estimate based on existing research; the value of D2 was taken from recent work on Denver aerosols (13). The value of P is an estimate; the value of R was adjusted as required to obtain a good fit between experimental results and predicted

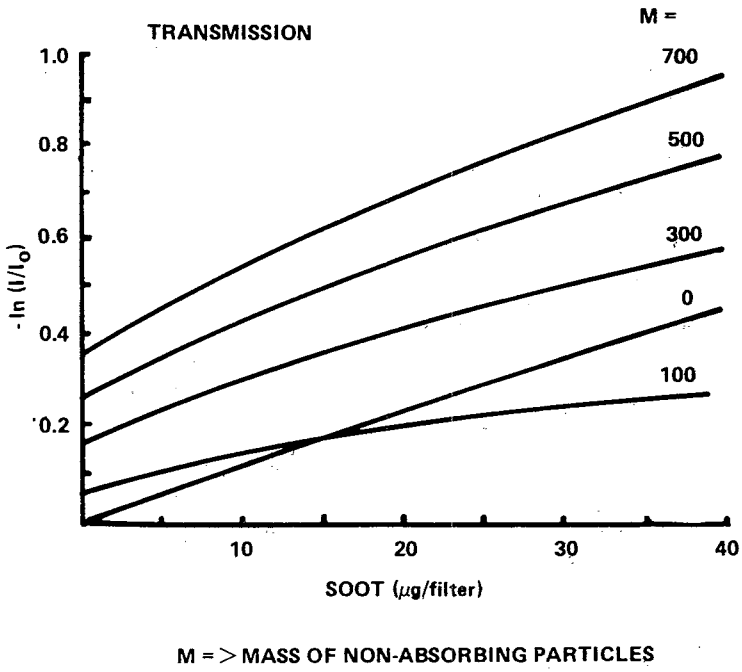

Figure 5. Model predictions of absorbance ($\ln(I_o/I)$), versus soot loading with mass, M, of scattering particles as a parameter.

values. All but one of the points located above the straight line correspond to filters taken during sequential 12-hour sampling periods at the monitoring site (the numbers associated with individual points refer to the order in which the samples were taken). This subset of filters may be physically different from the rest of the set. As noted earlier, the model predictions appear too low for samples having higher values of soot-to-mass ratio. Points corresponding to filters 16 to 19, which are significantly lower than experimental values, have an average soot-to-mass ratio of 0.125, as compared to 0.53 for the remainder of the set.

SUMMARY AND DISCUSSION

The ratio of absorbing carbon estimates BL/PA increases as sample mass increases for mean values of different filter sets and for individual values within a set. Based on similar experiments with laboratory-generated samples, this relationship appears to be due to the enhancement of the BL estimate. Some doubt remains, however, since the laboratory-generated ammonium sulfate particles were considerably larger in mean diameter (0.4 to 0.6 μ) than the ambient particles.

Average estimates of elemental carbon by combustion (for a given filter set) are different from absorbing carbon estimates. The relationship changes from one filter set to another and probably depends on bulk absorp-

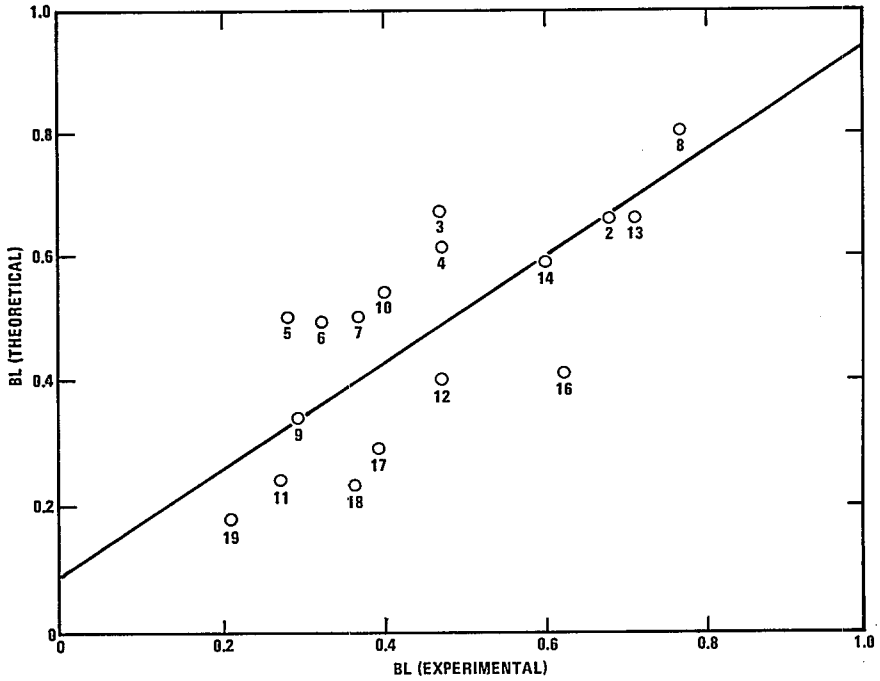

Figure 6. Model predictions of absorbance, BL, versus experimentally measured values for 18 samples collected in Houston, Texas.

tivity of combustion carbon. For individual filters from the two sets of filters loaded in Philadelphia, the relationship between EC and BL is linear, with reasonably low scatter and a correlation coefficient of 0.95 (information from personal communication with W.J. Courtney, Northrop Services, Inc., Research Triangle Park, NC). If BL is being enhanced, then its enhancement is linearly related to EC.

PA estimates of absorbing carbon are less precise for Type 501 Teflon filters. This fact is apparently related to a corresponding variability in the mass (and I_o values) of individual filters within a set. Given the same amount of soot, thick filters give lower signals than thin filters.

The BL values for a set of 18 filters loaded in Houston have been predicted with some success using a multi-layer particle model with adjustable parameters for particle size, layer reflectivity, and absorption coefficients. Prior knowledge of some of these parameters is required before true predictive capability can be realized.

CONCLUSIONS

The following conclusions seem justified based on the experiments so far completed:

1. For input to visibility calculations, use optical measurements of absorbing carbon.

2. Transmission measurements apparently overestimate absorbing carbon for higher filter loadings.

3. For PA estimates of absorbing carbon, use thicker filter substrates, such as Type 501 Teflon or Nuclepore filters.

4. Reference optical measurements to a standard soot sample of known absorption properties to establish comparability among different measurement systems.

ACKNOWLEDGMENTS

The author acknowledges the efforts of Dr. C.A. Bennett, Jr., and Dr. R.R. Patty of the North Carolina State University Physics Department, and Mr. M.A. Mason and Dr. W.J. Courtney of Northrop Services, Inc., for providing the experimental measurements shown throughout this work. Thanks also to Mr. R.K. Stevens and members of his staff for sustained interest in this project.

REFERENCES

1. Rosen, H., A.D.A. Hansen, L. Gundel, and T. Novakov. 1978. Identification of the optically absorbing components in urban aerosols. Appl. Opt. 17:3859.

2. Dzubay, T.G., and D.G. Rickel. 1978. X-ray fluorescence analysis of filter collected aerosol particles. In P.A. Russell and A.E. Hutchings, eds., Electron microscopy and X-ray applications. Ann Arbor Science Publishers, Ann Arbor, MI.

3. Dzubay, T.G., and R.K. Stevens. 1975. Ambient air analysis with dichotomous sampler and X-ray fluorescence spectrometer. Environ. Sci. Technol. 9:663.

4. Lin, C.I., M. Baker, and R.J. Charlson. 1973. Absorption coefficient of atmospheric aerosol: A method for measurement. Appl. Opt. 12:1356.

5. Bennett, C.A., Jr. 1981. Photoacoustic detection of particulate carbon. Master's Thesis, North Carolina State University, Raleigh, NC. 60 pp.

6. Bennett, C.A., Jr., and R.R. Patty. 1981. Evidence for thermal wave interference in thin particulate carbon samples. Submitted to J. Photoacoustics.

7. Bennett, C.A., Jr., and R.R. Patty. 1982. An evaluation of photoacoustic and transmission techniques for monitoring particulate carbon collected on Teflon filters. Appl. Opt. 21:371.

8 Jaklevic, J.M., R.C. Gatti, F.S. Goulding, and B.W. Loo. 1981. A β-gauge method applied to aerosol samples. Environ. Sci. Technol. 15:680.

9. Mason, M.A., and J.W. Tesch. 1980. Carbon analysis on the Dohrmann DC50 Envirotech organic analyzer. Progress report ES-TN-81-02. Northrop Services, Inc., Environmental Sciences, Research Triangle Park, NC. 17 pp.

10. Kortum, G. 1969. Reflectance spectroscopy. Springer-Verlag, New York, NY.

11. Bhardwaja, P.S., J. Hubert, and R.J. Charlson. 1974. Refractive index of atmospheric particulate matter: An in situ method for determination. Appl. Opt. 13:731.

12. Rohl, R., W.A. McClenny, and R.A. Palmer. 1982. Photoacoustic determination of optical properties of aerosol particles collected on filters: Development of a method taking into account substrate reflectivity. Appl. Opt. 21:375.

13. Countess, R.J., S.H. Cadle, P.J. Groblicki, and G.T. Wolff. 1981. Chemical analysis of size segregated samples of Denver's ambient particulate. J. Air Pollut. Contr. Assoc. 31:241.

STATUS OF SAMPLING AND ANALYSIS OF AMBIENT NITRIC ACID, NITRATES AND AMMONIA

Robert K. Stevens and Robert W. Shaw, Jr.

U.S. Environmental Protection Agency
Research Triangle Park, NC

Robert Braman

University of South Florida
Tampa, FL

C.W. Spicer

Batelle
Columbus, OH

INTRODUCTION

As investigators have improved the methods for sampling and analysis of atmospheric nitrate, it has become evident that distribution between the gaseous and particle phases has often been masked by experimental artifacts. Many early particle nitrate data were based on analyses of extracts from glass fiber aerosol filters used in Hi-vol samplers. It is now known that these filters contain active sites that fix gaseous HNO_3 and make it appear as particle nitrate (1).

Other filter materials have also been shown to react with and collect gaseous HNO_3 and create a positive particle nitrate artifact (2). The use of an inert filter material, such as Teflon, removes the "positive artifact" problem, except for the possibility of reaction of gases with the collected aerosol particles. It has been shown, however, that collected aerosol nitrate particles (true particle nitrate) may be lost from filters because of reactions with other materials or evaporation. Loss of particles is known as "negative artifact." Reactive loss may occur if, for example, H_2SO_4 aerosol comes in contact on the filter surface with nitrate aerosol. Evaporative loss may occur if, due to decreases in ambient gas concentrations, the solid and gaseous nitrate phases are no longer in equilibrium. Thus we see that measurements of particle nitrate by means of glass fiber filters are expected to be systematically high. On the other hand, measurements of particle nitrate using inert Teflon filters are expected to be systematically low. The extent of loss due to reaction and

due to reaction and evaporation are difficult to predict. Recent measurements indicate that, because of the distribution between HNO_3 and particle nitrate, the glass fiber filter nitrate overestimates may be considerable.

TECHNIQUES AND THEIR FEATURES

Methods currently under development or used in research studies to measure gas phase nitric acid include the use of continuous (real-time) and semi-continuous monitors, as well as integrative collection of HNO_3 on adsorbing materials. The continuous methods (1) are: a) chemiluminescence and b) Fourier transform long path infrared spectrometry (FTS-LPIR). Methods involving preconcentration (1) are:

(a) collection of HNO_3 on nylon or cotton, followed by extraction, conversion to nitrobenzene ($C_6H_5NO_2$), and analysis by gas chromatography;

(b) reduction to ammonium ion (NH_4^+) of fixed inorganic nitrogen collected on nylon filter, followed by iodophenol ammonia test;

(c) collection of HNO_3 on sodium chloride-impregnated filters, followed by extraction and hydrazine reduction-diazotization analysis of nitrate;

(d) denuder difference experiment--collection of total nitrate from two parallel air streams, removal of nitric acid from one stream using a diffusion denuder, and subsequent determination by difference (3); and

(e) continuous chemiluminescence method--a dual chamber NO_x chemiluminescence monitor is modified so that both sides of the split sample stream pass through molybdenum catalyst convertors to reduce the oxides of nitrogen to NO; one of the sample streams passes through a nylon filter to remove the HNO_3; the difference of the two signals from the instrument is recorded as nitric acid.

(f) Tungsten VI oxide technique--short-term collection of nitric acid on diffusion tubes followed by release and detection using chemiluminescence (4).

This last technique is a considerable advance, permitting measurements down to 0.25 $\mu g/m^3$ of nitric acid for sampling intervals of 20 minutes and also permitting simultaneous measurement of NH_3.

Each technique has unique features. FTS-LPIR is suitable for providing benchwork measurements of HNO_3, because measurement takes place in the atmosphere and identification is made unambiguous by the recognition of characteristic infrared absorption. However, the equipment is not portable, and the method has a minimum detection level of 5 ppb. Chemilumi-

nescence has the inherent sensitivity of a rate sensor, but involves the measurement of small differences in a signal that is frequently large and time-varying due to interferences (for example, total oxides of nitrogen, NO_x; peroxyacetyl nitrate, PAN; and organic nitrates). Collection techniques generally require relatively simple equipment; however, they require documentation of collection and release efficiencies, maximum loading, and possible interferences.

In order to compare a number of techniques for measuring atmospheric nitrate and nitric acid, investigators from Brookhaven National Laboratory, the University of Colorado, the National Center for Atmospheric Research, the University of Michigan, Battelle, the U.S. Environmental Protection Agency, and the University of California at Riverside gathered for a field study in Claremont, California during August 27 to September 3, 1979, with the following objectives: (a) to test and compare measurement systems for HNO vapor and nitrate aerosol; and (b) to determine the extent to which measurement systems are susceptible to artifact nitrate formation or loss and, if possible, to determine the cause of artifacts. The various measurement systems were available at that time, and we believed that their comparison could best be achieved by side-by-side evaluation under field conditions, similar to the EPA Charleston Aerosol Sampler Comparison Study (5). In order to determine the absolute reliability of the instruments, all were run side-by-side with FTS-LPIR, which was the only technique established at that time to be interference-free.

Detailed results of the Claremont study have been published by Spicer and fellow researchers (6). Briefly, consistent results for nitric acid were achieved using chemiluminescence, FTS-LPIR, and the denuder difference experiment. Of four methods using particle filters followed by nitric acid-absorbing filters, two were in agreement with the mean of the other methods and two showed apparent excess nitric acid; hence, these tandem filter techniques may not be used with as much confidence as the other methods. Collection of particulate nitrate on Teflon filters gave generally consistent results, although comparison with the denuder difference experiment suggests that some nitrate loss from Teflon filters did occur. Measurement of nitrate on quartz and glass fiber filters gave greatly varying results, possibly depending on filter history.

During the Claremont study, levels of nitric acid ranged from 2 to $40 \mu g/m^3$ and particulate nitrate from 4 to $26 \mu g/m^3$. The good agreement among measurement methods observed in Claremont may not be reproducible in other areas where nitrate levels are not so high as they are in the Los Angeles Basin. For example, measurements were made during the summer 1980 in Research Triangle Park, NC, using the denuder difference experiment, the Tungsten VI oxide technique, and single filter methods. The denuder difference experiment and the Tungsten VI oxide technique were in good agreement when they were run simultaneously. Simultaneous measurements for particle nitrates using filter collection, compared to nitrates measured by denuder difference method, showed much lower nitrate values, due to evaporative or reactive loss from the filter.

A few reported values from measurements not thought to be subject to

artifact problems are presented in Table 1.

TABLE 1. LEVELS OF PARTICULATE NITRATE AND NITRIC ACID

Location	Date		$\mu g/m^3$ NO_3^-	$\mu g/m^3$ HNO_3	Reference
RTP, NC	July 1980	(day)	1.2	3.4	3
		(night)	0.9	0.7	
Claremont, CA	Aug-Sept 1979	(max)	26	38	6
		(min)	4	1	
Rocky Mountains (10,000 ft)	1979	(max)	--	0.01	7

Recently at EPA, we have modified the denuder difference nitrate-nitric acid sampler, as shown in Figure 1. In this sampler, the aerosol is sampled through an all-Teflon cyclone at 28 liters per minute to remove particles > 2.5μm. From this air stream, two parallel samples at 3 liters per minute are collected simultaneously; one aerosol sample is collected (F_1) on a nylon filter (1 m pore size) and the other sample is collected (F_2) after the aerosol passes through a diffusion denuder coated with MgO. This sampling arrangement minimizes large particle deposition within the sampler and reduces HNO_3 losses within the cyclone due to its inert

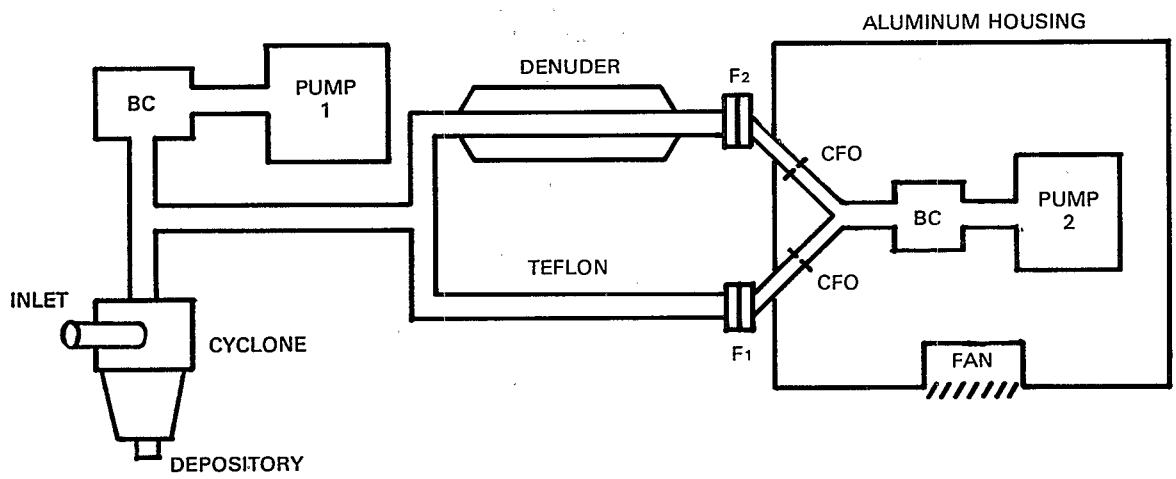

BC - BALLAST CAN
F - NYLON FILTER HOLDER
CFO - CRITICAL FLOW ORIFICE

Figure 1. Schematic of diffusion denuder nitrate-nitric acid sampler.

construction (Telfon) and large sample flow. The nylon filters are extracted with a 1:1 mixture of 0.005 M solutions of $NaHCO_3$ and Na_2CO_3. The extract is analyzed for nitrate by ion chromatography (8).

CONCLUSION

Work is continuing to compare the performance of the denuder difference method with the tungstic acid-chemiluminescent method for nitric acid. Comparisons have been conducted in Denver in 1982, and another comparison is planned in North Carolina. Braman has recently automated his tungstic acid denuder method for NH_3 and NHO_3 to permit measurements of particle nitrate and ammonium. The system typically collects the ambient aerosol for 30 minutes. This is followed by analysis of the aerosol collected for nitrate and ammonium, followed by the analysis of the HNO_3 and NH_3 collected by the denuder as described by Braman (4). The detection limit for nitrates and HNO_3 is $0.2 \mu g/m^3$.

REFERENCES

1. Stevens, R.K., ed. 1979. Current methods to measure atmospheric nitric acid and nitrate artifacts. EPA-600/2-79-05, March.

2. Appel, B.R., S.M. Wall, Y. Tokiwa, and M. Haik. 1979. Interference effects in sampling particulate nitrate in ambient air. Atmos. Environ. 13:319-325.

3. Shaw, R.W., R.K. Stevens, J. Bowermaster, J. Tesch, and E. Tew. 1981. Measurements of atmospheric nitrate and nitric acid; the denuder difference experiment. Atmos. Environ. 16:845-853.

4. Braman, R.S., T.J. Shelley, and W.A. McClenny. 1982. Tungsten VI oxide for preconcentration and determination of gaseous and particulate ammonia and nitric acid in ambient air. Anal. Chem. 54:358-364.

5. Camp, D.C. 1980. An intercomparison of results from samplers used in the determination of aerosol composition. Environ. International 4:83-100.

6. Spicer, C.W., J.E. Howes, Jr., T.A. Bishop, L.H. Arnold, and R.K. Stevens. 1982. Nitric acid measurement methods--an intercomparison. Atmos. Environ. 16:1487-1500.

7. Kelly, T.J., D.H. Steadman, J.A. Ritter, and R.B. Harvey. 1982. Measurement of oxides of nitrogen and nitric acid in clean air. J. Geophys. Res. in press.

8. Stevens, R.K., T.G. Dzubay, D. Rickle, and G. Russwurm. 1978. Sampling and analysis of atmospheric sulfates and related species. Atmos. Environ. 17:55-68.

A SIMPLE DESIGN FOR AUTOMATION OF THE TUNGSTEN VI OXIDE TECHNIQUE FOR MEASUREMENT OF NH_3 AND HNO_3

W.A. McClenny and P.C. Gailey

U.S. Environmental Protection Agency
Research Triangle Park, NC

R.S. Braman and T.J. Shelley

University of South Florida
Tampa, FL

ABSTRACT

The tungstic acid technique for collection and analysis of NH_3 and HNO_3 concentrations in the ambient air has been automated in a simple and cost-effective design. The design allows complete separation of HNO_3 and NH_3 during detection. Unattended operation in field trials has been demonstrated, and a three-day run sequence with hourly updates is shown.

INTRODUCTION

Braman and fellow researchers (1) have recently described a technique for separation and collection of gaseous HNO_3 and NH_3 using a diffusion tube coated with the selective sorbent tungstic acid, H_2WO_4. Application of the tungstic acid technique (TAT) to ambient air monitoring has been reported by McClenny (2). The TAT allows collection of HNO_3 and NH_3 in the presence of particulate matter without the use of in-line filters. The TAT appears preferable to a simple tandem filter arrangement (collection of particulate matter followed by collection of gases on a specially prepared filter), which is subject to particle-to-gas and gas-to-particle conversions, depending on filter type (3). In addition, the TAT is sufficiently sensitive to provide hourly updates of the ambient concentrations. If the TAT is used with a longer-term integrated measurement technique, such as the denuder difference apparatus (3), a successful comparison would provide an extra measure of quality assurance.

The TAT uses a 4 mm i.d. Vycor tube coated along a 35-cm length with tungsten (VI) oxide, which hydrates to tungstic acid. Ambient air is pulled through the tube at 1.0 L/min. The basis for a gas/particle separation is the difference between the diffusion rates of HNO_3 and NH_3 (0.122

cm^2/s and 0.236 cm^2/s, respectively; see reference 4) and the ambient particles containing their corresponding particulate forms (that is, $[NH_4]_2SO_4$ and NH_4NO_3). The longitudinal distribution of HNO_3 and NH_3 along the tube is predicted by Gormley and Kennedy (5), assuming that laminar flow is maintained in the tube, and that every target molecule reaching the tube wall sticks. Sectional analysis of the longitudinal distribution has substantiated the predictions. Under the established conditions of use, greater than 99 percent of the ambient particle mass is expected to pass through the tube, while the combined collection and release efficiency of the two gases is greater than 95 percent (1).

EXPERIMENTAL PROCEDURE

A simple scheme for automating the TAT has been developed as a cost-effective alternative to an automated system used previously (2) and is shown in Figures 1 and 2.

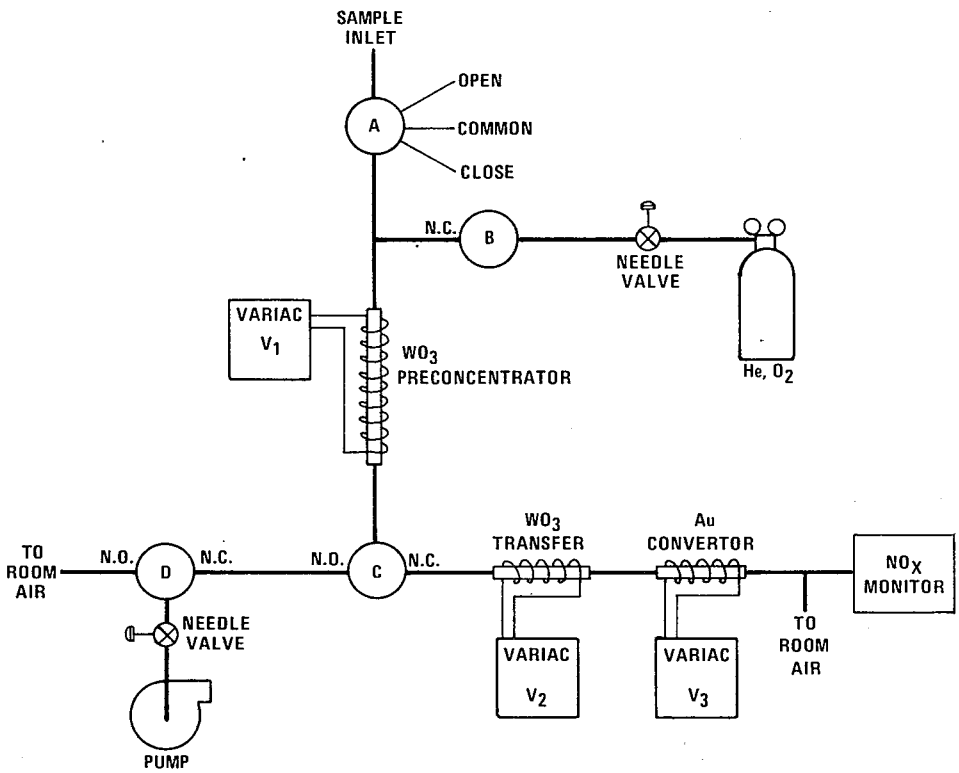

Figure 1. Schematic of system designed for monitoring HNO_3 and NH_3. B, C, and D are Teflon® solenoid valves. A is a Teflon® ball valve.

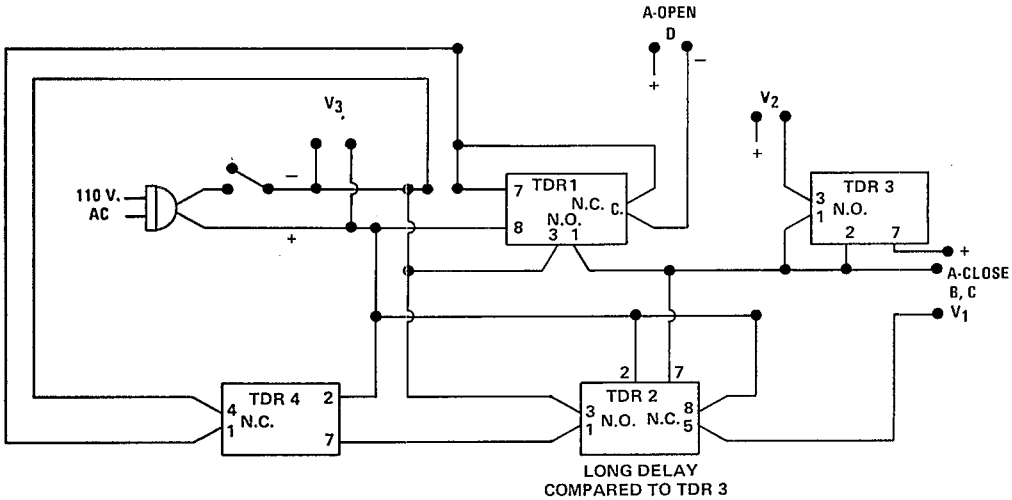

Figure 2. Schematic of electrical system designed for automated sampling and analysis using time delay relays (TDR). NC = normally closed; NO = normally open.

Explanation of Operation

The automated sampler operates in a four-step cycle as described below:

1. Trapping - Ball valve A* opens; solenoid D activated. Pump draws ambient sample through the WO_3 diffusion tube, which scrubs out NH_3 and HNO_3. Timing is controlled by TDR 1 and is typically 12 to 40 minutes.

2. HNO_3 Analysis - Ball valve A closed; solenoid D deactivated; solenoids B and C activated; power supplied to Variac V_1. WO_3 diffusion tube is heated, releasing NH_3 as NH_3 and HNO_3 as NO_2. A helium-oxygen mixture is directed through the diffusion tube. This carrier gas entrains desorbed gases and is diverted through the transfer tube and convertor before entering the NO_x monitor for measurement. The transfer tube scrubs out the NH_3 but allows NO_2 to pass through the NO_2-to-NO converter to the NO_x monitor. The flow rate through the converter is less than that pulled into the NO_x monitor so that room air is sampled. Some variation in baseline signal will occur if any NO is present in the room air. TDR 2 is involved in timing this and the next cycle, and is typically set for 10 to 15 minutes.

*Fluorocarbon Co., 1432 South Allen Street, PO Box 3640, Anaheim, CA 92803, Teflon® ball valve Model EBVI-88.

3. NH_3 Analysis - Conditions remain as in Step 2, except that Variac V_2 is activated. The transfer tube is heated, releasing the NH_3 for measurement. The NH_3 is converted to NO in the Au converter and is sampled by the NO_x monitor. TDR 3 is involved in timing this cycle and is typically set for 3 to 5 minutes.

4. Cooling - Ball valve A remains closed; solenoids B, C, and D deactivated, Variacs V_1 and V_2 deactivated. WO_3 diffusion tube cools before system returns to Step 1. TDR 4 controls the length of this step, which may last from 3 to 10 minutes. This TDR can also provide a time interval between sampling periods, in which case longer time delays may be used.

Switching and timing are performed by Potter and Brumfield time-delay relays with variable time delays. The first relay (TDR 1) completes a circuit, supplying power to the first step's instrument components, while its own time delay begins. When this time delay ends, TDR 1 switches, breaking the circuit of the components that operate in the first step and turning on the second step components and the second relay timer (TDR 2). This process of one relay turning on the next continues until TDR 4 has completed its time delay. Rather than turning on another relay, the switching of TDR 4 interrupts the power to the timer in TDR 1, returning TDR 1 to its normal position and breaking the circuit that powers the timer in TDR 2. TDR 2 deactivates TDR 4 in the same manner. However, TDR 4's deactivation results in power once again flowing to TDR 1, thereby marking the beginning of a new cycle. TDR 3 controls the transfer tube Variac and operates during part of TDR 2's time delay.

Discussion of Components

Reference 1 describes the diffusion tubes and the procedure for making them. During thermal desorption, a coiled heater wire heats the diffusion tube to approximately 350°C. The converter is constructed of thin gold foil, folded and fitted into a 15-cm quartz tube. A coiled heater wire also heats this tube to approximately 600°C. The NO_x analyzer is a Bendix Model 1810B, with an ambient air ozonator feed and a two-stage diaphragm pump for evacuating the reaction chamber to 27 inches of mercury pressure difference. An integrating stripchart recorder, Linear Instrument Co. Model 252A, was used to record and integrate the data. All tubing used for transport of gases was 0.64 cm i.d., thin wall FEP Teflon®.

Field Operations

The system was operated continuously over a 10-day period of ambient measurements to provide 20-minute average concentrations of NH_3 and HNO_3. A 3-day measurement sequence is shown in Figure 3 as a chart recorder trace. Electronic integration of peak areas was also available in a length-of-line format on the chart recorder output, but was excluded to improve clarity. Peak area values above a preset reference level were compared to a calibration curve relating area to calibrated mass loadings

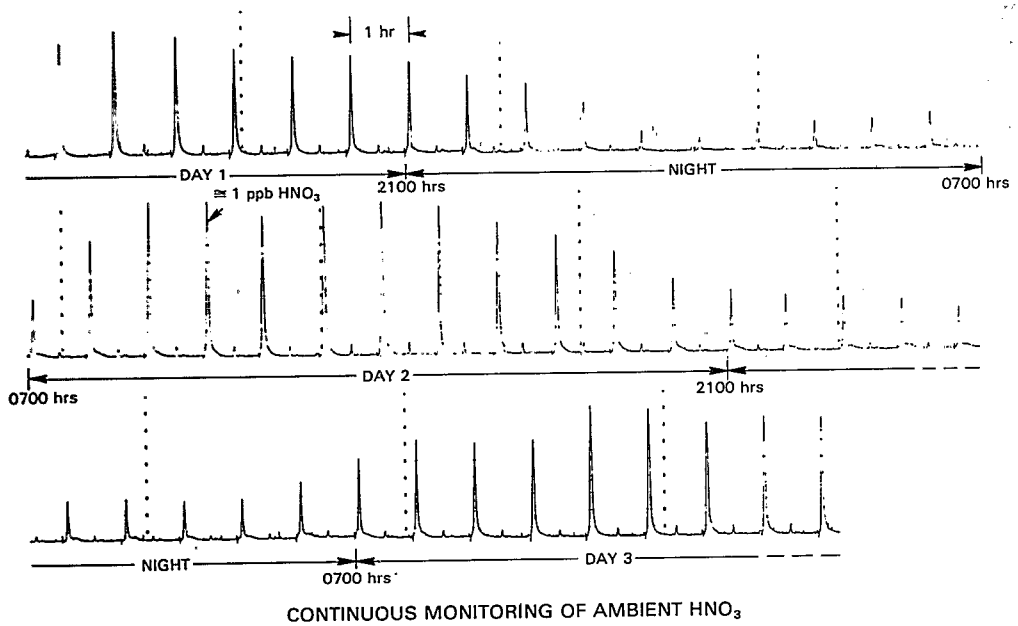

Figure 3. Three-day monitoring sequence using the automated system.

of NH_3 from a permeation tube held at a constant temperature. Because each molecule of HNO_3 or NH_3 is converted to NO before detection, NH_3 calibration was also used to infer HNO_3 concentrations. However, since the system response to NH_3 has been measured as slightly higher than the response for HNO_3 (factor of 1.12; see reference 1), the calibration is considered only approximate. The 1-ppb HNO_3 peak in Figure 3 indicates the approximate value of the individual responses. The range of HNO_3 concentrations is estimated as 0.1 to 1.2 ppb, while the NH_3 concentrations range from 0.05 to 0.3 ppb. Detection capabilities over these ranges imply a monitoring capability in most, if not all, ambient monitoring sites. Test data were consistent with expectations for HNO_3 (that is, diurnal cycling, with midday maximum and low nighttime concentrations).

CONCLUSION

A simple design to automate the tungstic acid technique for monitoring gaseous HNO_3 and NH_3 has been developed and demonstrated. The system can be left unattended to collect and record integrated average values over periods adjusted with time-delay relays. The system has been used to demonstrate that HNO_3 or NH_3 concentrations as low as 0.1 ppb can be detected using 20-minute collection periods.

REFERENCES

1. Braman, R.S., T.J. Shelley, and W.A. McClenny. 1982. Tungstic acid for preconcentration and determination of gaseous and particulate ammonia and nitric acid in ambient air. Anal. Chem. 54:358.

2. McClenny, W.A., P.C. Gailey, R.S. Braman, and T.J. Shelley. 1982. Tungstic acid technique for monitoring nitric acid and ammonia in ambient air. Anal. Chem. 54:365.

Shaw, R.W., Jr., R.K. Stevens, J. Bowermaster, J.W. Tesch, and E. Tew. 1982. Measurements of atmospheric nitrate and nitric acid: The denuder difference experiment. Atmos. Environ. 16:845.

4. Wilke, C.R., and C.Y. Lee. 1955. Estimation of diffusion coefficients for gases and vapors. Ind. Eng. Chem. 47:1253.

5. Gormley, P.G., and M. Kennedy. 1949. Diffusion from a stream flowing through a cylindrical tube. Proc. R. Ir. Acad. 52A:163.

OZONE PRECURSOR MONITOR (OPM) FOR INVESTIGATING AIR POLLUTION

Gordon C. Ortman

Office of Research and Development
U.S. Environmental Protection Agency
Research Triangle Park, NC

ABSTRACT

Ozone is designated by the U.S. Environmental Protection Agency as one of six principal air pollutants. Of the six, ozone alone is classified as a secondary pollutant since it is not emitted by a specific source. Ozone is formed in the lower atmosphere by photochemical reactions involving the precursors of ozone: gaseous organic compounds (mostly hydrocarbons), nitric oxide, and nitrogen dioxide.

This paper describes a new automated method for quantifying the precursors of ozone. An ozone analyzer is coupled to a reaction vessel contained in an irradiation chamber. At timed intervals, discrete samples of outside air are drawn into the reaction vessel and irradiated with ultraviolet light. The amount of ozone produced is a measure of the photochemical reactivity potential of the precursor blend.

The ozone precursor monitor (OPM) is designed for urban air sampling stations where analyzers for the principal air pollutants are routinely operated. The monitor, however, has other uses. Among special applications of the method that are discussed are its use as an early warning device for forecasting elevated ozone concentrations, a screening system for assessing the photoreactivity of solvents, and a procedure for investigating the transport of ozone precursors from urban to rural areas.

INTRODUCTION

Ozone in the earth's atmosphere is a paradox. We want it and we don't want it. We want ozone in the stratosphere, where it forms a protective layer that encircles the earth and screens out harmful ultraviolet radiation that causes skin cancer. While the depletion of this stratospheric ozone layer is of vital concern, the subject of this paper is the harmful ozone in the ambient air we breathe. When the hourly average concentration

of ozone reaches or exceeds the National Ambient Air Quality Standard of 0.12 ppm (120 ppb), our health and welfare are imperiled (1).

Non-methane organic compounds and nitrogen oxides are known to be the precursors of ozone that is produced photochemically in the ambient atmosphere (2,3). In view of the pollution of the atmosphere by organic compounds and their role in the formation of ozone, it is clear that knowledge of their total concentration using non-methane organic carbon analyzers (4) is important. However, knowledge of the total non-methane organic concentration alone makes photochemical air pollution modeling difficult at best and poses a severe burden on the ozone control strategist, since there is an endless possible mix of these organic gases that may number into the hundreds and since these gases vary in their photoreactivity by orders of magnitude. Even with in-depth knowledge of the species of organics present, gained by use of state-of-the-art chromatography, and their photoreactivity level, the assessment of the ozone-forming potential of an air mass is laborious. The assessment is also fraught with uncertainties such as unknown synergistic and opposing reactions. The task is even further complicated by the fact that, in the absence of nitric oxide and nitrogen dioxide, the solar- irradiated organic vapors will not form ozone and because, in the presence of these nitrogen oxides, the amount of ozone formed and the time for its formation will vary depending on the concentration and species of nitrogen oxides present.

As early as 1956, researchers in California made an effort to circumvent the many problems associated with estimating the photochemical smog formation potential of the ambient air in the Los Angeles Basin (5). They developed an empirical approach to the problem embodied in an oxidant-oxidant precusor analyzer. The dominant oxidant of interest was ozone. The basic idea of the analyzer was to expose a flow of sample air in a reaction vessel to intense ultraviolet irradiation to generate photochemical oxidants (primarily ozone) from their precursors. An oxidant analyzer, coupled to the reaction vessel, would alternately measure the oxidant in the sample air entering and exiting the chamber. The difference between the two concentrations would be a measure of the oxidant precursors in the air sample. Conceptually, the analytical approach of the oxidant-oxidant precursor analyzer was very meritorious, and analyzers were installed in 10 sampling stations. However, after several years of trial, the approach was abandoned. The bulkiness of the equipment, and numerous performance and operational problems that included lack of specificity, sluggish response, frequent negative readings caused by sulfur dioxide and heat-induced ozone losses, failure of mechanical components, etc., was cause for shelving of the analyzers.

In recent years substantial gains have been made in the reliability and performance of non-methane organic analyzers (6,7,8). The promulgation in the Federal Register of the reference and equivalency program in 1975 (9) precipitated the widespread improvement of automated analyzers used to measure the principal pollutants, including ozone and nitrogen oxides. Concurrent with the ever-improving data base of the seventies, advanced photochemical models were developed that were intended to aid the control strategist in reducing ozone. However, the usefulness of these models has

been challenged. The problems delineated in the second paragraph of this introduction still exist and the credibility of the data base for the reactivities of organic compounds has been questioned. EPA researchers recently concluded that "Wall-contamination problems raise serious questions as to the utility of Teflon-film smog chambers in determining reactivity of hydrocarbons. . . . With very low-reactivity hydrocarbon (and organic compounds) (sic), the reactivity parameters obtained from these smog chambers are of questionable value. Plastic smog chambers are not reliable for use in multiday irradiations when low levels of pollutants are present" (10).

Two documents are especially invaluable to the researcher seeking in-depth knowledge of the many subjects related to ozone (11,12). Unless otherwise referenced, these documents were the source of archived information contained in this paper.

In October of 1979 the research project reported here was funded. The research proposal outlined the development program for a continuous analyzer that would measure the potential photochemical reactivity of the atmosphere in terms of ozone equivalent units (13). The design of the analyzer would be a modification of the oxidant-oxidant precursor analyzer of the late 1950s that would incorporate state-of-the-art components and advanced technology to eliminate the shortcoming of the instrumental approach of the fifties.

The initial experimental approach focused on optimization of a continuous flow-through system as used with the earlier oxidant-oxidant precursor analyzer. One of the configurations (shared-time) used a single ozone analyzer. Another configuration (dual channel) used two analyzers. However, continuous flow-through methods had several limitations; the most severe was that reproducibility and sensitivity were dependent on sample flow rate--i.e., the ozone yield was a function of residence time in the chamber. A primary goal of the research undertaking was to develop a standard system that would be uniform in construction and operation. It was also highly desirable that any EPA-designated ozone analyzer (14) could be incorporated as a detector for the OPM for the widest appeal. The flow-through system could not satisfy this desired feature, since the EPA-approved analyzers differ in sample flow rates by a factor of four.

It was recognition of these problems that led to the "discrete sampling" approach, a concept similar to the batch-type analysis of an automated chromatograph. The discrete sampling approach renders the performance of the ozone precursor monitor independent of sample flow rate; thus one design can be universally used with any of the dozen EPA-designated ozone analyzers. Moreover, it was found that the ozone yield of the discrete sampling approach for various precursor test mixtures was more than 50 percent greater than the ozone yield using continuous sampling. The discrete sampling approach also was found to have additional operational and performance advantages that greatly enhance the appeal of the OPM for a variety of field and laboratory applications.

The discrete sampling approach breakthrough was made in the last

quarter of the allotted time for the development of the OPM and all of the anticipatory research that the author would have liked to have accomplished with the system was not possible. However, sufficient data were gathered using the discrete sampling approach to adequately demonstrate that the OPM does provide information on the presence and reactivity of ozone precursors in the atmosphere that has been hitherto unavailable and that the OPM could be a useful tool in the research laboratory as well as in the field.

The purpose of this paper is to describe the OPM research and the evaluation of the method.

DESCRIPTION OF INSTRUMENT

The OPM consists of two subsystems (Figure 1).

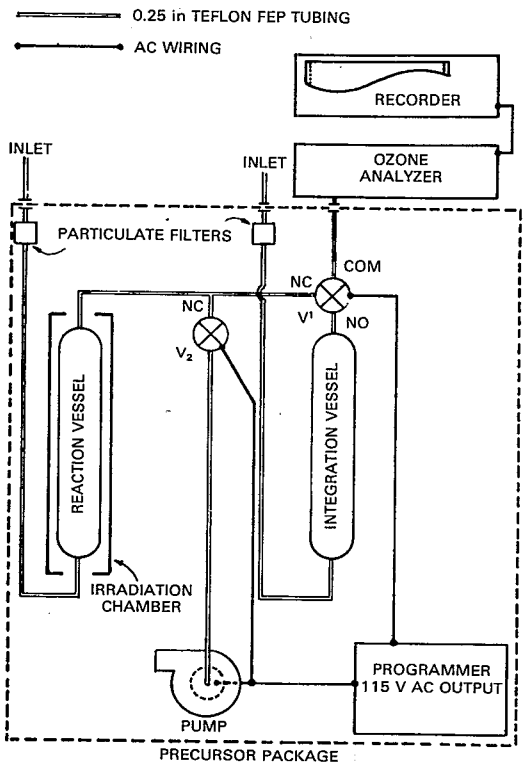

Figure 1. Schematic diagram of ozone precursor monitor (OPM).

The first subsystem, the "precursor package," has two sample inlets with in-line particulate filters. One of the lines connects to a reaction vessel that is contained in the irradiation chamber. The outlet port of the reaction vessel connects to control valves that provide for timed irradiation of the sample in the reaction vessel, subsequent sampling and

analysis of the reaction vessel content for its ozone level, its purging, and the introduction of a new sample into it. The other sample inlet line connects to an integration vessel in line with the sample/analysis valve. An auxiliary pump and an electronic programmer that controls the valves and the auxiliary pump complete the system.

FEP Teflon 1/4" OD tubing and TFE Teflon fittings were used for interconnecting components, except for ground glass ball-and-socket fittings at the inlet and outlet ports of the glass vessels. Ground glass fittings were also used to couple the inlet port of the particulate filters to the glass manifold sampling systems used in air monitoring stations or to glass calibration gas mixture delivery systems. The assembled system was leak-tested by capping the inlet ports and applying a vacuum with a sensitive flow meter in line to the pump.

The second subsystem is composed of a chart recorder and an ozone analyzer with an integral sampling pump. A listing of the EPA-designated ozone analyzers (14) usable for OPMs and a listing of suppliers of all other OPM components is available from the author.

A length of flexible 1/4" OD Teflon tubing connects the two subsystems to make an operable OPM.

INSTRUMENT OPERATION

The electronic programmer is the heart of the OPM. It precisely times the sequence of events that occur during each continuously repetitive 15-minute cycle.

At the beginning of the cycle, or time zero, with solenoid valve #2 closed, solenoid valve #1 (Figure 1) is energized and directs the flow of the sample from the reaction vessel to the ozone analyzer. For the next 2 minutes, the ozone concentration of the irradiated sample is assayed and recorded. Then, at 2 minutes into the cycle, three things occur simultaneously: one--solenoid valve #1 is de-energized and the sample flow to the analyzer is drawn (via the integral sampling pump in the ozone analyzer) from the integration vessel for analysis and recording of the ozone concentration of the non-irradiated ambient air, continuing for 13 minutes until the beginning of the next cycle; two--solenoid valve #2 is energized to its open position; and three--the purge pump is powered. The pump rapidly draws out the remaining residual irradiated air from the reaction vessel and fills it with a fresh parcel of ambient air. The time required for purge is 3 minutes, so at 5 minutes into the cycle, the purge pump is stopped and valve #2 is closed. For the next 10 minutes the newly introduced air parcel, with its ozone precursor loading, is irradiated with ultraviolet energy. The total ozone concentration of this new air parcel, including the ozone generated by irradiation of the ozone precursors, is then again measured and recorded for 2 minutes at the beginning of the next cycle. A single continuous recorder trace shows the elevated 2-minute total ozone concentration that includes the precursor ozone yield alternately with the 13-minute ambient ozone analysis during each 15-minute

cycle.

The details for inputting the program into the OPM's electronic programmer are available from the author.

INSTRUMENT CONSTRUCTION

Two identical OPMs were constructed using mostly off-the-shelf components. The reaction and integration vessels were made to specifications from standard glass tubing and fittings. The irradiation chamber, which required sheet metal work and installation of the electrical sockets and ballasts for the 8 fluorescent lamps, was fabricated in-house. A drawing of the irradiation chamber and reaction vessel is seen in Figure 2. The design of the irradiation chamber was suggested in a report written in 1959 (15).

Ventilation of Irradiation Chamber

The reaction vessel is cooled by an induced flow of room air as it convects upward through the chamber from a circular 4-inch-wide opening above the bottom support frame seen in Figure 2. The air carries the heat from the lamps upward and out the open top. The temperature of the exiting air stream is less than 15°C above ambient.

Portability

The ease of disassembly of the OPM into its component parts with no need for tools is facilitated through the use of glass ball-and-socket clip-on pneumatic connections and plug/receptacle power connections. The irradiation chamber with reaction vessel weighs 70 lbs, and the total weight of the other components, inclusive of the analyzer and recorder (about 70 lbs), is less than 100 lbs.

Precursor Package

Space and power requirements, maintenance and cost - The 5-foot-high irradiation chamber takes up slightly more than a square foot of floor space. Depending on layout, the space requirements for the other components is 2 to 4 square feet. The lamps draw 320 watts. With fixed components, coupled with the Teflon tubing and the glass ball-and-socket fittings, there is built-in flexibility, adjustability, and chemical inertness. Because the inlet filters keep the inside surfaces clean, maintenance-free operation of the OPM's precursor package can be expected for periods of six months, except for the biweekly change of the Teflon filters. The cost of all materials and in-house fabrication (labor), exclusive of the ozone analyzer, was less than $2,000 for each unit.

Integration Vessel

The function of the integration vessel is to "average" the rapid data fluctuations normally observed with EPA-designated ozone analyzers, which

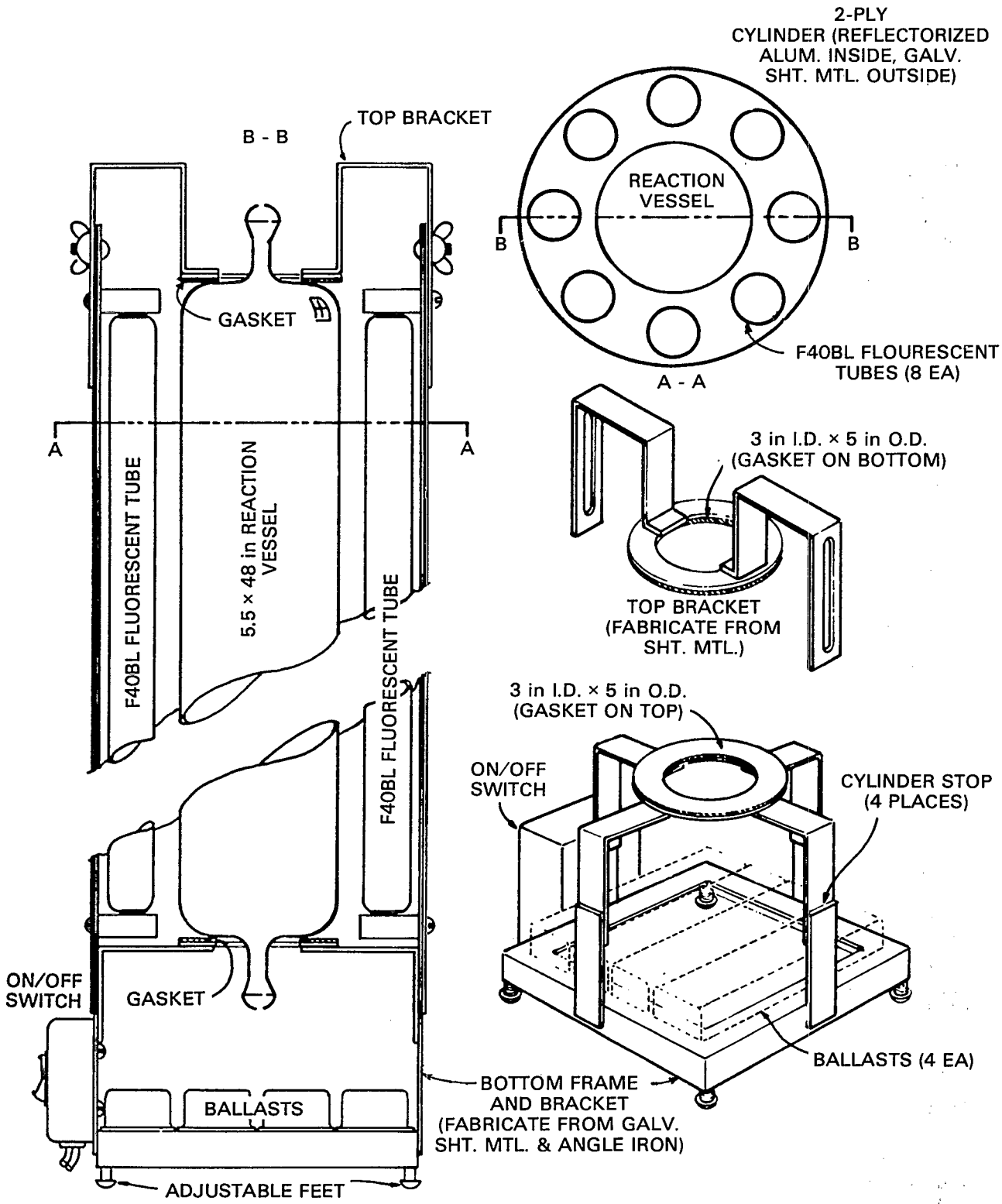

Figure 2. Irradiation chamber with reaction vessel.

have response times typically of 30 seconds or less, while the Federal Register allows for ozone analyzers to have a rise and fall time of 15 minutes and lag time of 20 minutes (16). An integration vessel was deemed essential for the OPM based on the evidence for typical ambient data, seen in Figure 3. The precursor signal is easily masked when there is no integration vessel in the sample line. The author recommends an integration vessel volume to be no more than necessary to give good signal averaging to facilitate data reduction. The 16.8-liter vessel used in this investigation is considered the upper limit of what would be a satisfactory volume using the Dasibi analyzer. If ozone analyzers with lower flow rates are used, the integration volume should be scaled down proportionately.

IRRADIATION LAMPS

Lamp Selection

A wide variety of lamp types from several manufacturers were evaluated for possible use in the OPM. These included fluorescent lamps with peak spectral distributions from 300 nanometers (SunLamp, a Westinghouse product) to 367 nanometers (GE F40BL) as well as mercury vapor and xenon lamps. The reasons for final selection of the GE F40BL include: a reasonably good fit with the sun's spectral output (17) as shown in Figure 4 (18), consistent spectral distribution with lamp aging, relatively long life at reasonably low light output decay rate, and good overall quality with long expected mean time before failure (MTBF).

Lamp Output Decay

All fluorescent lamps show appreciable decay--40 to 50 percent--in light output over their useful life. The life expectancy of the OPM lamps used is greater than 20,000 hours (19). Approximately 50 percent of the total loss of light output occurs in the first 1000 hours, with 5 to 10 percent of the total output lost in the first 100 hours. Based on several sources of information for the type of lamps used (20,21, and personal communication with Elton T. Lappelmeir, Lighting Business Group, General Electric Company, April 15, 1981) and empirical tests, the author recommends that the lamps be burned in for 1000 hours prior to OPM usage. The lamps should then be used for a year (about 9000 hours) and discarded. The expected percent decay during this time is about 12 percent (Figure 5) or about 1 percent per month. By removing the lamps at one year, the probability of any lamp failing is about 3 percent (Figure 6) (21). Lamps used for the OPMs were numbered and a record maintained of their in-service time (hours ON).

Temperature Effect on Lamps

Light output varies with ambient temperature for all lamps, including the fluorescent type. Exact temperature effect information for the GE F40BL could not be located. In general, however, the F40 series has a maximum output at 20°C and the output energy decrease, with temperature increase up to 40°C, is about 10 percent or 0.5 percent per degree centi-

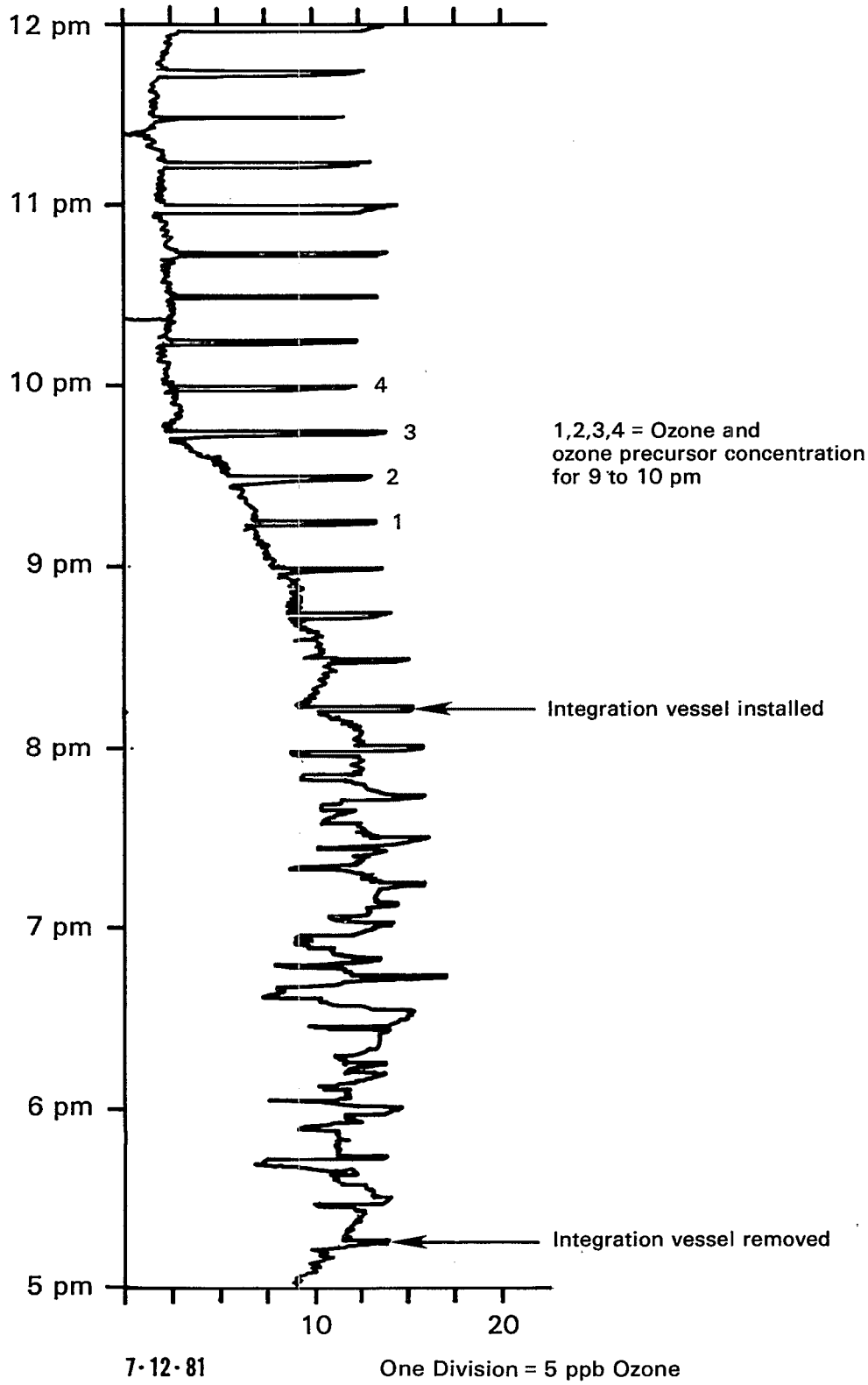

Figure 3. Function of integration vessel.

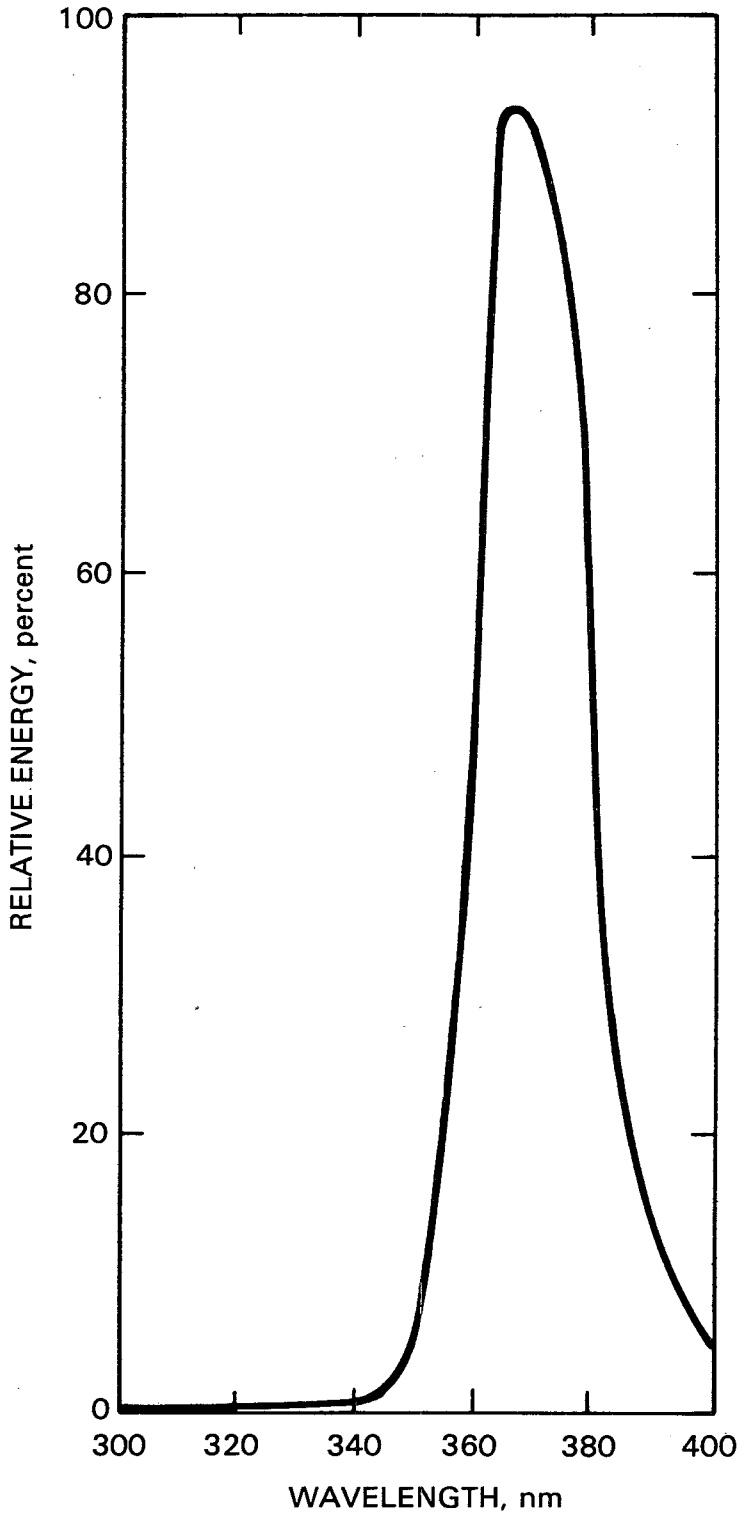

Figure 4. GE F40BL lamp spectral output.

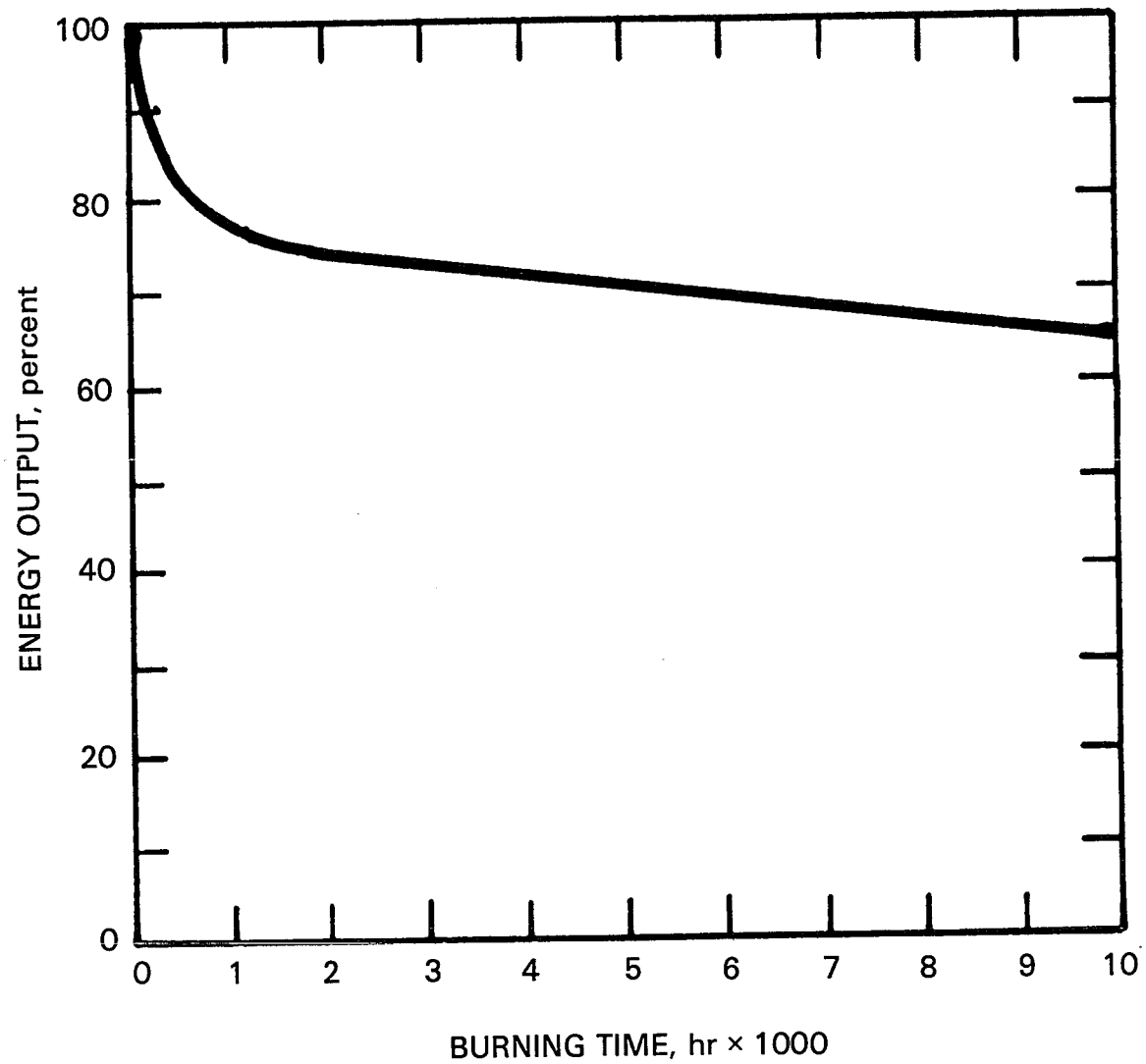

Figure 5. Fluorescent lamp energy maintenance.

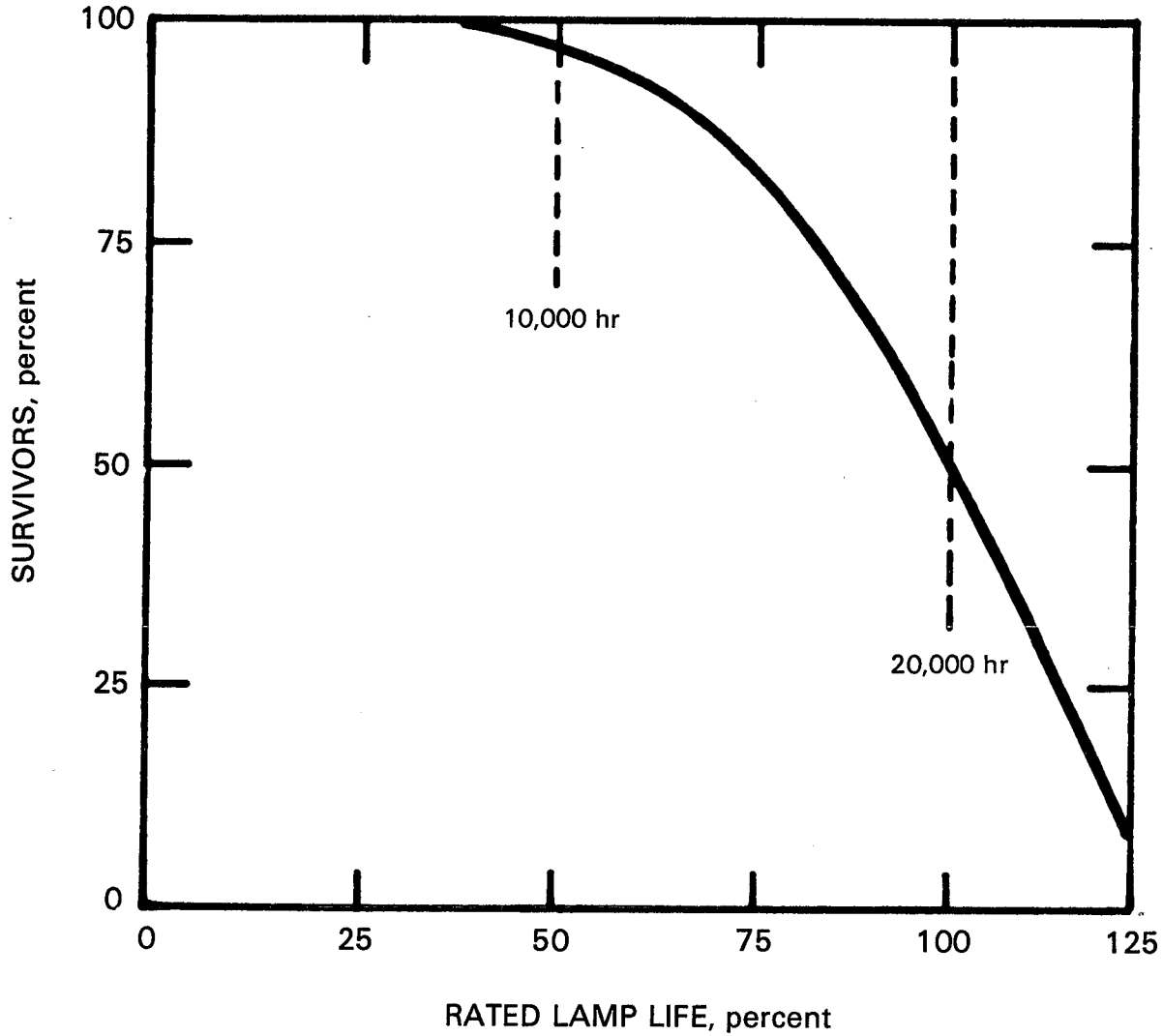

Figure 6. Fluorescent lamp mortality.

grade. The energy output decrease is slightly steeper as the temperature goes down from 20°C. As mentioned earlier, the temperature inside the irradiation chamber is at room temperature at the bottom and 15°C above room temperature at the top. The lamps therefore are operating at an estimated 95 percent of their peak output. As is true with most analyzers, it is desirable to keep room temperature within a set tolerance for optimum performance. For the OPM, ±3°C is suggested.

PREPARATION FOR OPERATION

Precursor Package

To ensure that the surfaces making contact with the air sample were free of contamination, only new materials and components (tubing, particulate filter holders, valves, and fittings) were used. All sample train components were purged with helium, nitrogen, or zero grade air and conditioned with a high concentration (∿50 ppm) ozone in zero air stream. The glass vessels were washed with a chromic acid solution followed by thorough rinsing with distilled water, dried with a heat gun while being purged with zero grade air, and then conditioned by a flowing stream of ozone (∿50 ppm) in zero grade air for about an hour. The ozone in air was stopped and the vessels sealed for 48 hours. The entire system was tested by directing a stream of about 450 ppb of ozone in dry air directly to an ozone analyzer and then through the system. A match of readings confirmed no losses of ozone.

Calibration of Ozone Analyzer

Four Dasibi ozone analyzers were used: two were incorporated as part of the two OPMs; one was a standby and one was used as a transfer standard. All four analyzers were initially calibrated (22) by the Quality Assurance staff of EPA's Environmental Monitoring Systems Laboratory (EMSL). The transfer analyzer was periodically recalibrated by the EMSL for use as a standard in the field (23).

EXPERIMENTAL

Data Reduction and Sample Integration

Reference is made again to Figure 3, which shows typical ambient data at an urban site. The chart speed is 1 inch per hour. The OPM's normal operating range is 0-.5 ppm. This chart scale uses 200 divisions - therefore, one chart division equals 2.5 ppb ozone, or 5 ppb per percent of scale. Zero concentration is at 0.0 percent chart for convenience of illustration. The Federal Register methodology for air pollution analyzers places the recorder zero at +5 percent of scale. Gaseous air pollution concentrations are reported on an hourly average basis. "Eyeballing" the average ozone concentration for the hour 9:00 to 10:00 p.m. gives 25 ppb. Averaging the four precursor readings, 9:15 to 10:00 p.m., gives 67 ppb. The average precursor concentration is therefore 67 minus 25, or 42 ppb

ozone equivalent units.

Test Gases

To carry out a multiplicity of experiments, zero grade air was prepared from outside ambient air by drawing it through a particulate filter, compressing it, and passing it through an ozonizer, chemical and physical scrubbers, and catalytic oxidizers, followed by additional scrubbers and particulate filters. A 30 liter per minute continuous flow of treated air was available at 60 psig. The dry, zero grade air was free of oxides of nitrogen and had a total hydrocarbon content of less than 0.1 ppm carbon. This air was used both in its pure form for zeroing and as dilutent air for making up of test gas mixtures using mass flow controllers to regulate delivery rates.

Lecture bottles of nitrogen dioxide and propylene equipped with specially designed permeation devices provided a source of controlled precursor compounds for the various test mixtures (24).

Ancillary Analyzers

Experimentation in the research laboratory was facilitated by support equipment that included analyzers for oxides of nitrogen and organic carbon as well as instruments for measuring wind direction and velocity, temperature, dew point, and barometric pressure.

Sampling, Calibration, Sampling Precaution

In shifting from a moisturized ambient sample to diluent dry zero air, it was necessary to allow the OPM to stabilize to the condition of dryness of the sample. It has been observed using both photometric and chemiluminescent ozone analyzers that a period of equilibration to a dehumidified sample precedes a true reflection of the ozone concentration in the sample. Similarly, in reversing the condition--i.e., shifting from dry to humidified air--a response delay was encountered. Because of the area of the sample containment surfaces of the OPM, this equilibration period was two or three cycles long. It was essential during this period that both sample sources, the purge/precursor sample and the ambient ozone sample, were at the same humidity level, to allow the OPM's ozone analyzer to properly acclimate.

Lamp Decay Test

After 289 hours of usage of eight new GE F40BL lamps in an OPM chamber, a propylene/nitrogen dioxide in air mixture was introduced and the ozone yield for a normal cycle of operation obtained. The used lamps were replaced with new lamps, the same mixture sampled, and the ozone yield measured. The ozone yield of the used lamps was 16 percent less than for the new lamps. Examination of the earlier referenced Energy Maintenance Curve (Figure 5) shows that the 16 percent loss in yield is consistent with the decrease in energy output for the lamps for the hours-in-use and points out the need for an initial burn-in of 1000 hours to achieve a lower decay

rate.

Characterization of Response

The ascending nature of the precursor response reflects the continuance of irradiation of the sample during the 2-minute readout and increasing ozone yield when the end-point for the sample is not reached (it may be hours before it is). For purposes of data reduction, the author chose the maximum precursor reading.

Ozone Yield

Figure 7 shows ozone yield versus irradiation time. The time of the analysis followed the time of the exposure at an interval of 5 minutes, 10 minutes (the normal operating interval), 15 minutes, and, as indicated in the figure, at increasing intervals up to 420 minutes (7 hours). The test gas contained 120 ppb NO_2 and 0.83 ppm propylene (2.5 ppm carbon) in air. The maximum ozone yield, 925 ppb, was generated at about 300 minutes. It compares well with the yield at 10 minutes of 387 ppb from the standpoint that the latter yield, generated in one-thirtieth the time for the maximum yield, is 47 percent of the maximum yield. Therefore, the 10-minute reading is a meaningful index of the photochemical reaction potential of the precursor mixture.

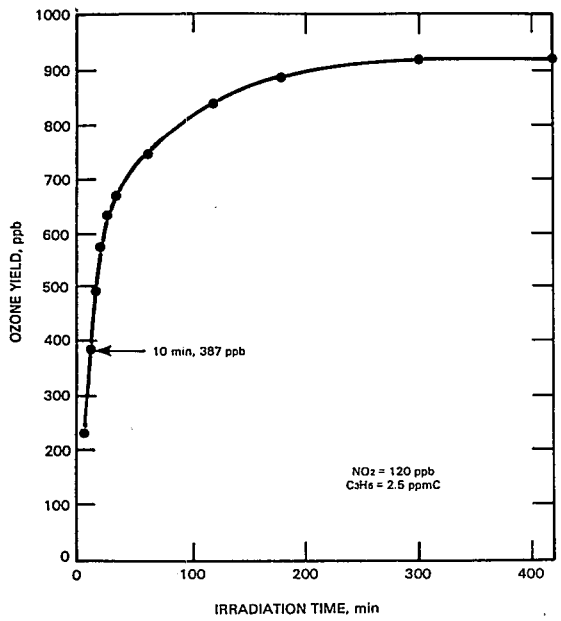

Figure 7. Ozone yield vs. irradiation time.

Repeatability of Ozone Yield

Table 1 shows the results of a 5-hour test to establish the repeatability of the OPM. The test gas contained 0.83 ppm propylene (2.5 ppm carbon) and 120 ppb nitrogen dioxide in pure air. The maximum reading for each of the four precursor readings for each hour is given.

TABLE 1. REPEATABILITY OF OZONE YIELD

	ppb O_3				
	Hour 1	Hour 2	Hour 3	Hour 4	Hour 5
	389	391	390	392	390
	392	393	389	385	386
	394	386	387	386	388
	390	388	387	388	390
Average	391	390	388	388	388

The variation in values in Table 1 reflects the impact of all parameters that can affect the reading, including changes in line voltage, precursor blend, barometric pressure, and ozone analyzer response over the 5-hour test.

Agreement Between OPMs

Table 2 shows the results of repetitive analysis by the two OPMs following calibration of their Dasibi ozone analyzers against the transfer standard. The test precursor mixture contained 0.63 ppm propylene (1.9 ppm carbon) and 111 ppb nitrogen dioxide. The lamps in the irradiation chambers of the two OPMs had been on for 1,867 hours. Readings were taken after the recommended three cycles of operation on the dry precursor test gas.

TABLE 2. AGREEMENT BETWEEN OPMs

Analysis cycle 7/3/81	Ozone yield in ppb OPM A	OPM B
1	348	350
2	350	355
3	354	355
4	352	350
Average	351	352.5

The above data show exceptionally good agreement of results. On five other occasions spanning about 800 hours of on-time for the lamps, similar analyses were made. The average ozone yield readings for the two OPMs agreed within 10 ppb for different precursor mixes that produced ozone yields of 170 ppb to 650 ppb.

Line Voltage Effect on Ozone Yield

A study was made of the effect of line voltage on ozone yield for a test precursor mixture. The results of the study are seen in Table 3.

TABLE 3. LINE VOLTAGE EFFECT ON OZONE YIELD

Irradiation chamber line voltage	Ozone yield in ppb
100	362
110	377
117.4	380
120	390
130	405

Between 100 and 130 volts the ozone yield increased 43 ppb, or 11 percent of the yield of the 117.4 normal line voltage. While the yield is obviously voltage-dependent, an examination of the ozone yield over a "normal" voltage range (110 to 117.4) shows only a 3 ppb or 1 percent change, so the effect is considered minimal except in situations where extreme line voltage fluctuations may occur. Line voltage stabilizers are available for such circumstances.

Loss of Ozone

Photochemical researchers have noted a problem of loss of ozone on surfaces such as Tedlar, Teflon, Mylar, and other plastic films. Tests were conducted on the reaction vessels used in the OPM to determine ozone loss. The 16.8-liter reaction vessels were cleansed and conditioned as noted earlier. A 573-ppb concentration of ozone in diluent air was sampled directly and then through the unused vessels until the exiting concentration was the same as the entering concentration and the vessels capped. An analysis of the content of the chamber was performed 117 hours later; 61 percent of the initial concentration remained. An analysis of the second chamber at 168 hours (1 week) showed 57 percent of the ozone present. After the vessels had been in use for four months, the test was repeated without cleansing the vessels, but conditioning them to a 500-ppb ozone in air test mixture. At 3 hours, 94.5 percent of the initial ozone concentration was present, and at 93.5 hours, 56 percent of the initial concentration remained. Since a full precursor cycle is only 15 minutes, the results indicate the OPM's performance is not impaired by ozone loss. The cleanliness of the vessels during use was maintained by rigorous use of the

particulate filters on the sample inlets. The filters were changed biweekly, after ∿300 hours use. For areas of heavy pollution, weekly replacement of the filters would be necessary.

Efficiency of Purge

The necessity to remove the remnants of the previous discrete sample during a purge cycle is obvious. To test the adequacy of the purge time and flow rate, a stream of 450-ppb ozone was generated in one of two sample streams. The second stream contained zero air. The system was allowed to acclimate for three cycles. Then, in alternately sampling the two streams cycle-to-cycle, the removal of ozone from the reaction vessel was found to be greater than 99 percent. The introduction of the ozone into the reaction vessel was also found to be greater than 99 percent.

Other Experiments

Now that the reader has a familiarity with the experimental procedures followed, capsulation of three critical but straightforward experiments can be presented:

1. No ozone was generated in the chamber in irradiating zero air, even when left in the chamber for several hours.

2. Ozone was generated in sampling nitrogen dioxide in air only. A trace of NO_2 would produce a perceptible ozone yield. This is consistent with the photochemistry of nitrogen dioxide and occurs in nature.

3. No ozone was generated in sampling propylene in air only. This again is consistent with the photochemistry of hydrocarbons.

PERFORMANCE

Ozone Precursors and Ozone in a Small City

Figure 8 shows one day of data (noon to noon) collected at an air sampling site on the fringe of downtown Durham, NC. The recording reflects the typical ozone-ozone precursor profile commonly seen during the months of spring and summer at this location. Attention is drawn to the late evening precursor readings usually observed at the site and to the suppressed ozone readings that sometimes last throughout the night.

The second trace seen on the dual pen recording is the output from a non-methane organic carbon analyzer. The analyzer, calibrated with propane, was operating on the standard 0 to 10 ppm carbon range. Zero was set at 50 percent chart. For 18 of the 24 hours, there is no perceptible organic concentration. There is at all times, however, some evidence of ozone precursors, thus demonstrating the relative ineffectiveness of the non-methane organic carbon analyzer for predicting ozone potential.

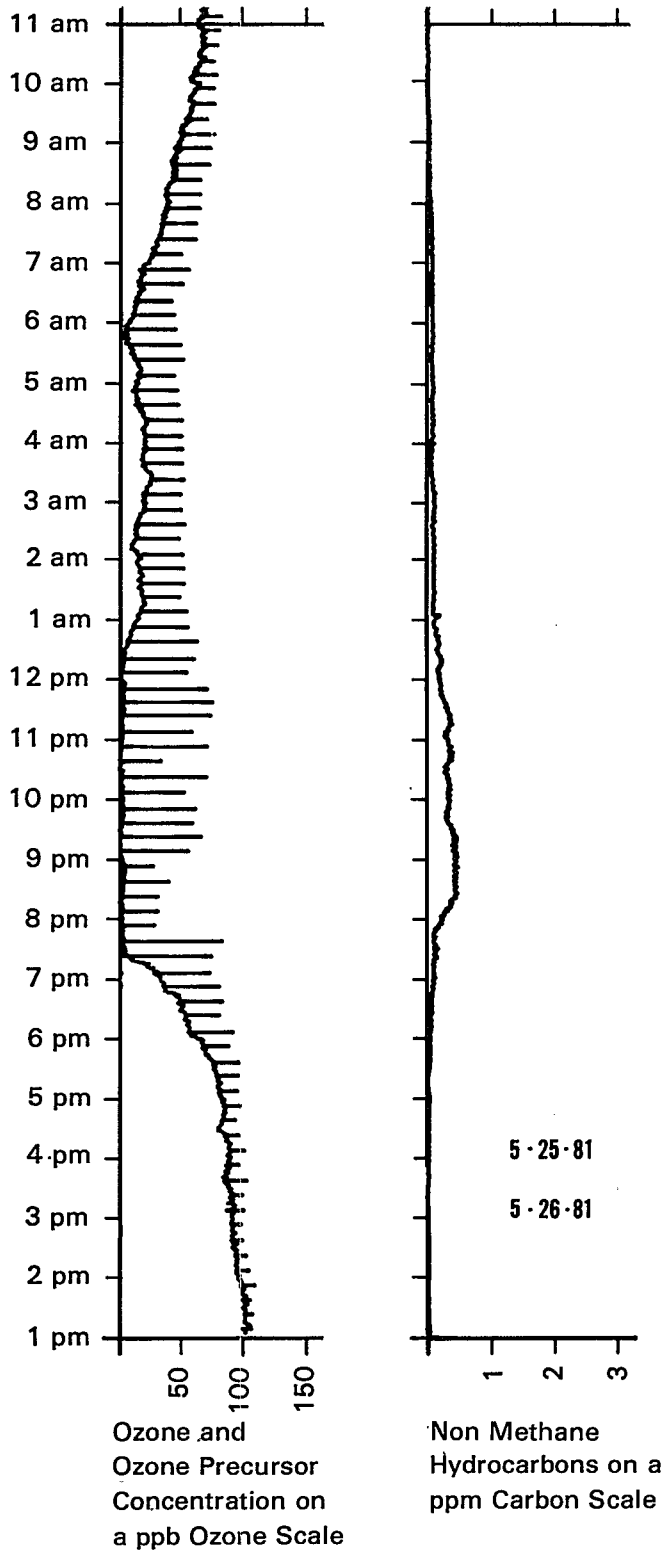

Figure 8. Ozone precursors and ozone in a small city.

Ozone Precursors and Ozone in a Large City

A month-long field study in a major metropolitan area in the southeastern United States was made during the summer of 1981. An OPM was located on the campus of a university near the downtown area. Figure 9 is a reproduction of a single day's run (midnight to midnight) that shows several phenonema. In the early hours of the morning, the ozone concentration was suppressed; nitric oxide was scavenging the ozone. Again, as in the small city, this usually was seen during the late evening/early morning hours.

During the hours between 3:00 and 5:00 p.m. DST, the hourly ozone concentration was 170 ppb, 50 ppb above the standard. Between 9:00 and 10:00 p.m., the ozone precursor hourly average was 99 ppb. At 10:30 p.m., sudden winds that preceded a rainstorm and a drop in temperature carried away the stagnated pollutants, and a noctural ozone concentration of 48 ppb was recorded with passage of the storm front.

The total OPM down-time at the site was 10 hours. Power outage caused 4 hours of lost data, and auditing of the ozone analyzer required 2 hours. Another 2 hours were lost due to operator error. More than 98 percent of both the ozone and the ozone precursor data were usable.

Analytical Agreement of OPMs on Ambient Air

Figure 10 has the tracings of two OPMs operating in tandem off the same ambient sample manifold. The zero for the output of the OPM recording on the left was 0 percent chart. For the OPM on the right, the zero was set at 50 percent chart. Although the OPMs' programs were synchronized with purge and sample operations occurring at the same time, the presentation on the chart shows the tracing on the right about 1/4 inch late due to the offset of the two pens of the recorder.

Sensitivity of OPM

The sensitivity of the OPM can best be appreciated by comparing its response to the response of continuous air pollution monitoring instruments conventionally used for measuring photochemically reactive compounds in the atmosphere. These instruments are nitrogen oxide analyzers operating on a 0-.5 ppm range and non-methane organic carbon analyzers operating on a 0-10 ppm range. On a number of occasions, totaling more than 100 hours during several months of sampling ambient air with these type analyzers, no nitrogen oxides or non-methane organics were detected; however, ozone precursors measured by the OPM during these same times ranged from 0 ppb to 25 ppb. On two occasions, the precursor value (ozone yield) was 0 ppb. These two incidents may have been related to the passage of fronts and ozone-bearing stratospheric air movement into the troposphere (stratospheric intrusion). This hypothesis is supported by the fact that the air did contain 30 to 40 ppb of ozone, as might be expected with such an occurrence.

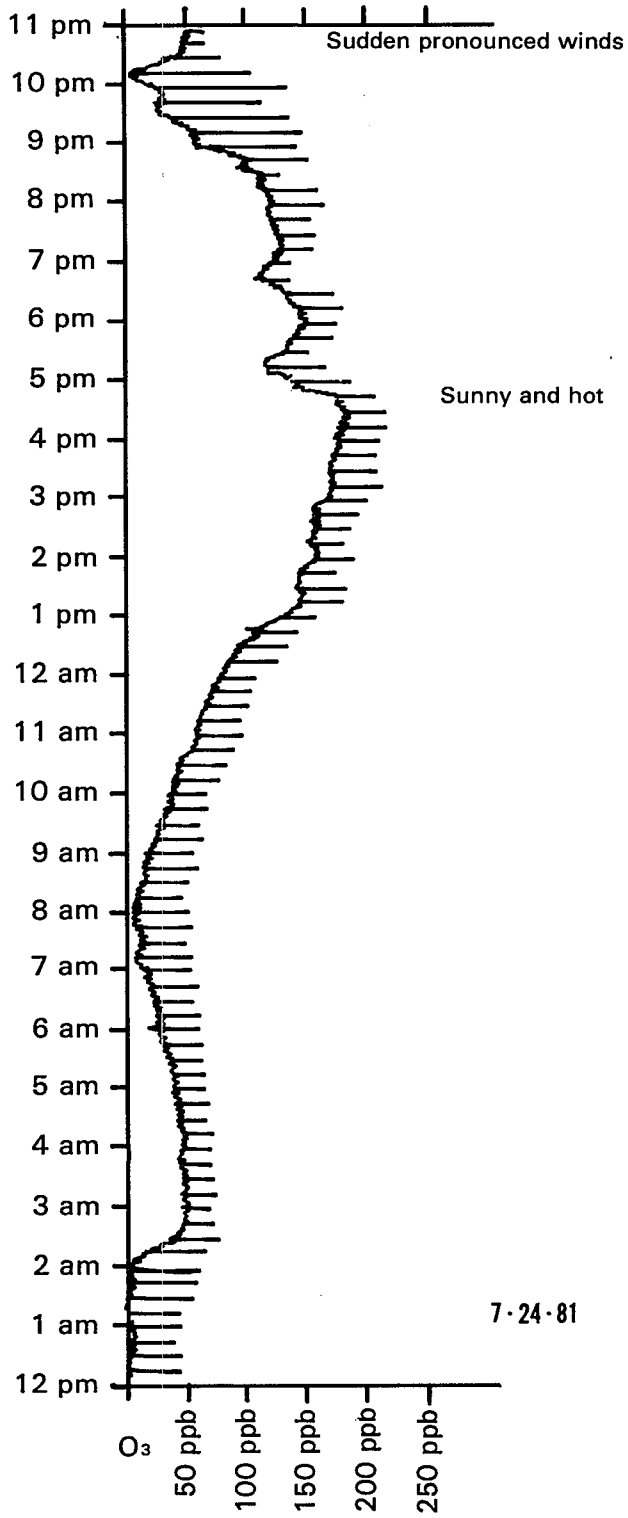

Figure 9. Ozone precursors and ozone in a large city.

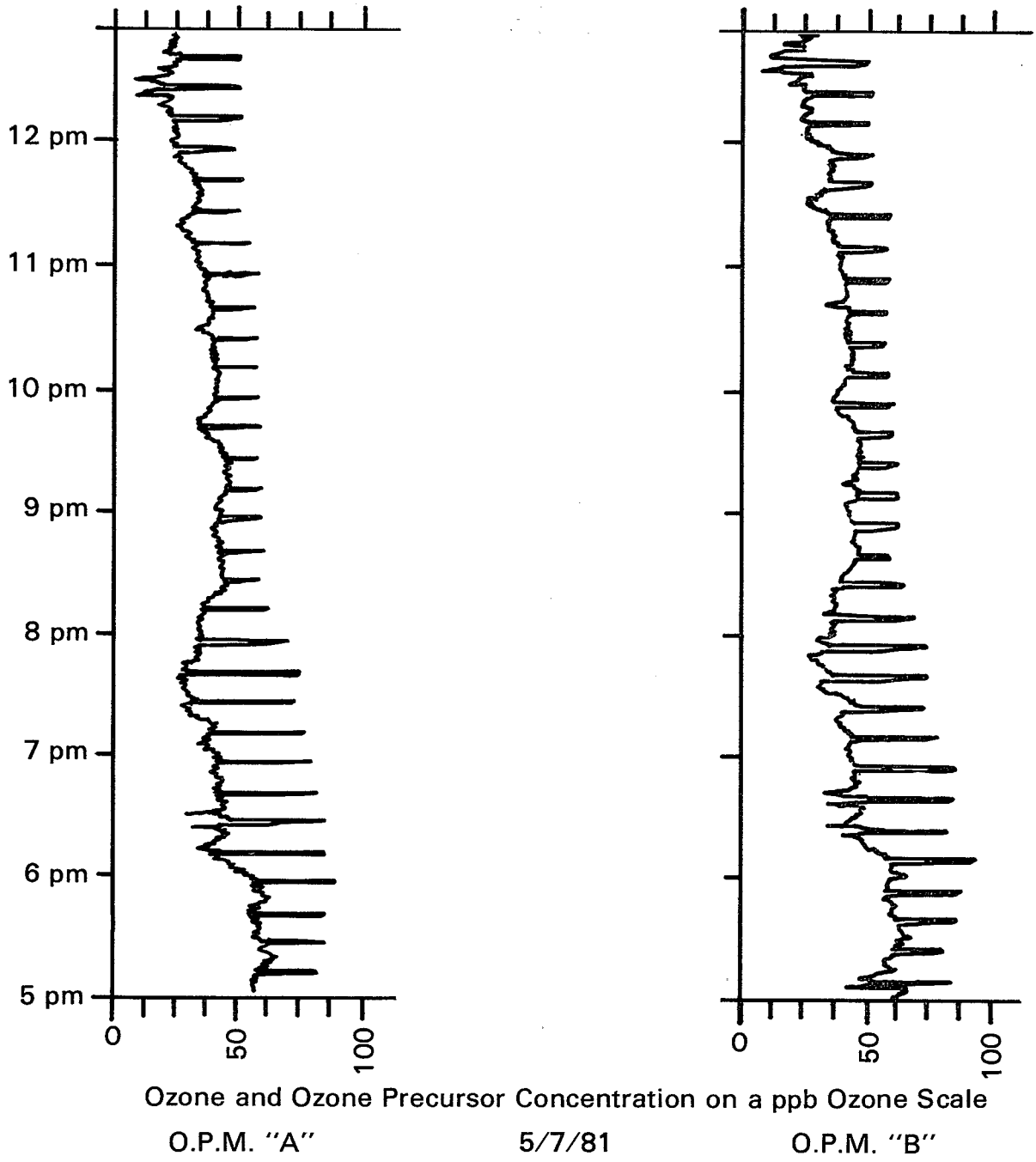

Figure 10. Analytical agreement of OPM's on ambient air.

Performance Specifications

Data in the listing below are based on the use of the Dasibi analyzer (25) and reflects the measurement of ozone in the ambient air on leaving the integration vessel and the measurement of the ozone yield from the OPM's irradiation chamber.

Range: 0.000 to 0.500 or 1.000 ppm
Incremental Sensitivity: 0.001 ppm
Flow Rate: 2 liters per minute nominal
Zero Drift: digital display 0.1 percent/day
Span Drift: digital display 0.1 percent/day
Digital Display: 0.000 to 1.000 ppm
Rise Time: 25 sec.
Fall Time: 25 sec.
Noise: ±0.002 ppm
Interference Sensitivity: 1 percent of full scale or less

In discussing irradiation chamber lamp decay, it was stated that a 1 percent per month loss of energy output is to be expected. Assuming a nominal linear relationship between ozone yield and light energy output for the OPM, the author proposes the normalization of data, collected each month following the installation of conditioned lamps (1000 hour burn-in), to the initial ozone yield. The correction would be 1.00 plus .01 for each month, times the recorded ozone yield concentration. It is believed that this simple procedure will provide an estimated ozone yield tolerance for the 1-year operational life of the lamps of ±2 percent.

DISCUSSION

Maximum Precursor Concentrations

An hourly average precursor reading of 187 ppb ozone was recorded at Durham, NC between 10:00 and 11:00 p.m. during a period of air stagnation. Typically, the highest precursor readings have been observed between 8:00 p.m. and 2:00 a.m. at the Durham Air Monitoring Demonstration Facility (DAMDF).

Sampling Location of OPMs

In general, selection of the monitoring sites for the OPM's dual role of measuring ozone and ozone precursors should be consistent with published guidelines for such an application (26). Briefly, the site should not be in an area subject to the impact of large sources of emissions. However, there could well be special cases where an investigator is interested in localized, concentrated pollution sources. In such cases, additional instrumentation that would include analyzers for oxides of nitrogen and organic compounds would be desirable for a more complete characterization of the air mass. Special siting would be in order for operating OPMs for forecasting ozone episode alerts and for transport studies of ozone precursors in rural areas.

Precaution

All earlier referenced (14) EPA-designated acceptable chemiluminescent analyzers (except the Philips) require an ethylene support gas. Should one of these chemiluminescent analyzers be used, precautions must be taken to ensure that the gas system is free of leaks. The analyzer's exhaust gas, a mixture of ethylene and sample air, should be discharged through a catalytic oxidizer, reducing the ethylene to carbon dioxide and water, to prevent it from being "recycled" into the air being sampled by the OPM. These measures are consistent with published safety precautions for use of ethylene. They are highlighted here because ethylene is a reactive organic that, as part of the sampled air, would be an ozone precursor. The Dasibi and Thermo Electron instruments are photometric analyzers and require no support gases. The Philips, while being a chemiluminescent method, uses an ozone-sensitive Rhodamine B dye and thus needs no gas.

Los Angeles Basin Study

None of the few areas where the OPMs were operated are noted for having an ozone problem. The author had included in his research proposal a three-month study in the South Coast Air Quality Management District (SCAQMD), which includes the Los Angeles Basin. The inhabitants of that area suffer from the most severe ozone pollution problem in the nation nd the location had been considered the ideal setting for siting OPMs. Budgetary constraints, however, precluded the opportunity to research the OPM in the Basin.

APPLICATIONS

Screening of Solvents

Some 200 industrial solvents are unclassified as to their photochemical reactivity. It has been suggested that, using an OPM and an appropriate protocol, these solvents can be rapidly classified for their ozone-forming potential. An initial screening would tell whether a specific solvent (blended with nitrogen dioxide) fell in one of four or five classifications from nonreactive to very reactive. Differential information would then be obtained by adjusting the irradiation time (sensitivity) for each class. The procedure would have incorporated into it a zero air purge/analysis cycle to ensure that no residual solvent remained, in progressing from one to the next solvent. The procedure would provide for uniform treatment of the samples and minimization of artifacts encountered in use of traditional bag sample-in-irradiation-chamber procedures.

Special Air Pollution Surveys

For special surveys, programmed methods are available for simultaneously collecting integrated ambient samples in plastic bags for prescribed time intervals at multiple sites (27). These bags, contained in light shielded black bags, are then returned to a centralized laboratory

for an operator-managed ozone precursor assay using a single OPM. This technique has been successfully used for collecting hydrocarbon samples from multiple sites for subsequent GC analysis (28).

Ozone Episode Forecasting

Several of the EPA Regions in the past several years have given priority ranking to a need for a means to forecast ozone episode alerts. Information from strategically sited OPMs, combined with meteorological information, could be the basis for predicting such episodes. On the basis of the prediction, the public could be alerted and measures could be implemented to reduce ozone precursor emissions. Individuals with respiratory problems or other ailments aggravated by high ozone levels would be advised to stay indoors. For known areas where concentrations exceeding the ozone standard occur frequently, such as the Los Angeles Basin, OPMs could be particularly beneficial.

Rural Ozone Precursor Transport Investigations

Economic loss due to damage to crops and forests by ozone amounts to many millions of dollars annually. It is thought that such losses could be minimized if there were a better understanding of the origin of man-made precursors of ozone transported into sensitive areas. Using data obtained from several OPMs in a network, coupled with readily available meteorological information, the investigator would be able to determine the source of the precursors. Species analysis of the organics in the advancing air could then provide the detailed information that could lead to needed controls if the source were localized. If either the abundance of species making up the precursor mix or the diversity of their origin were to show that little hope for appreciable improvement in the situation could be anticipated, then the planting of crops less susceptible to ozone damage could be the economical solution. However, it might be found that the organic fingerprint would identify a source of emissions that was economically controllable. In the latter case, the air quality manager could take such action appropriate to the situation.

Emission Control Strategy

Recently the EPA Administrator told members of Congress (29) "The more uncertainty there is, the more difficult it is to estimate the proper balance between public safety on the one hand, and the often enormous costs of pollution control on the other. We simply can not afford to err badly in <u>either</u> direction. Better knowledge of the scientific and technical facts almost always reduces the likelihood of such errors."

In a number of metropolitan areas, particularly in Southern California, the ongoing question in ozone abatement strategy debate is, "should multimillion dollar expenditures be made on source control of organic compounds or nitrogen oxides?" (30). With the development of the OPM, a research plan to resolve the above dilemma is feasible. The study, in its simplest form, would involve triplicate collection of integrated samples in ∿100-liter Teflon bags, shielded from sunlight, over a fixed time interval.

The untreated content of bag #1 would be sampled by an OPM for its ozone yield. The contents of bag #2 would be sampled with added nitrogen dioxide; and bag #3 sampled with an added organic. The ozone yields would be compared. The procedure would be performed as often and at such times as necessary to give statistical meaning to the results obtained. Conceptually, the procedure could be embodied in an automated system. The stated problem, as well as the instrumented method advanced for its solution, is intriguing.

CONCLUSION

The principal objective of the research effort that resulted in the OPM was to provide EPA with a means to measure, on a real-time basis, the photochemical reactivity potential of the atmosphere in units of ozone. The measurement method described allows for the fact that there can exist in the atmosphere an unlimited number of combinations of ozone precursors that differ in concentration and photoreactivity. The method treats any conglomerate of ozone precursors in a uniform fashion and provides an ozone value for the mixture sampled.

With deployment of OPMs in geographical areas prone to ozone pollution, it is anticipated that a data base will be generated that air quality managers will find of value. The ultimate goal is enhancement of control strategies and consequent reduction of ozone levels in the many areas of our nation that are not in compliance with the standards established for protection of the health and welfare of the people.

In these times of economic belt tightening, the OPM should be perceived as a money-saving device. With the coupling of the precursor package, as described in the text, to an already operating ozone analyzer, the ability of the air quality manager to assess problems and progress related to ozone precursor emissions will be enhanced with appreciable savings of time and labor power.

The secondary objective of the research effort was to provide EPA with a tool for other applications of varying significance. The use of the OPM for predicting the possibility of hazardous ozone concentrations is one such application. Its use as a method for rapidly screening solvents is another. The method could also be used for reassessing the photoreactivity of a broad spectrum of hydrocarbons where uncertainties exist because of procedural limitations of the past.

ACKNOWLEDGMENTS

The development of the OPM was funded as an innovative research project by the Innovative Research Program of the Office of Research and Development of the U.S. Environmental Protection Agency. Administrative support, facilities, and equipment were provided by the Environmental Sciences Research Laboratory and the Environmental Monitoring Systems Laboratory of the Environmental Protection Agency located at Research

Triangle Park, NC. The author, a member of the Regional Services Staff, is indebted to its Director for the opportunity to participate in the research program and to numerous fellow employees and colleagues in the government and the private sector for their generous assistance.

REFERENCES

1. U.S. Environmental Protection Agency. 1980. Part 50 - National primary and secondary ambient air quality standards. Federal Register 40:523-525 (July 1).

2. Dimitriades, B. 1972. Oxidant control strategies. Part 1. Urban oxidant control strategy derived from existing smog chamber data. Environmental Science & Technology 11(1):80-88.

3. U.S. Environmental Protection Agency. 1977. Uses, limitations and technical basis of procedures for quantifying relationships between photochemical oxidants and precursors. EPA-450/2-77-021a. Office of Air Quality Planning and Standards, Research Triangle Park, NC.

4. U.S. Environmental Protection Agency. 1980. Guidance for collection of ambient non-methane organic compound (NMOC) data for use in 1982 ozone SIP development, and siting criteria for NMOC and NO_x monitors. EPA 450/4-80-011. Office of Air Quality Planning and Standards, Research Triangle Park, NC.

5. Romanovsky, J.C., J.R. Taylor, R.D. MacPhee, and J.E. Dickinson. 1956. Air monitoring of Los Angeles atmosphere with automatic instruments. Proceedings of the 49th Annual Meeting of APCA, Buffalo, NY, May 20-24, 1956. Air Pollution Control Assoc., Pittsburgh, PA.

6. Ortman, G.C., and V.L. Thompson. 1974. Performance of hydrocarbon monitoring instrumentation. Instrumentation for monitoring air quality, ASTM STP 555. American Society for Testing and Materials, Philadelphia, PA.

7. Sexton, F.W., F.F. McElroy, R.M. Mickie, Jr., and V.L. Thompson. 1981. Technical assistance document for the calibration and operation of automated ambient non-methane organic compound analyzers. EPA 600/4-81-015. U.S. Environmental Protection Agency, Research Triangle Park, NC.

8. Sexton, F.W., F.F. McElroy, R.M. Mickie, Jr., and V.L. Thompson. A comparative evaluation of seven automatic ambient non-methane organic compound analyzers. U.S. Environmental Protection Agency, Research Triangle Park, NC. Draft document.

9. U.S. Environmental Protection Agency. 1981. Part 53 - Ambient air monitoring reference and equivalent methods. Federal Register 40:4-37 (July 1).

10. Lonneman, W.A., J.J. Bufalini, R.L. Kuntz, and S.A. Meeks. 1981. Contamination from fluorocarbon films. Environmental Science and Technology 15(1):99-103.

11. National Academy of Science. 1977. Ozone and other photochemical oxidants. Washington, DC.

12. U.S. Environmental Protection Agency. 1978. Air quality criteria for ozone and other photochemical oxidants. EPA-600/8-74-004. Environmental Criteria and Assessment Office, Research Triangle Park, NC.

13. Ortman, G.C. 1979. Prognostic ozone analyzer. Innovative research proposal. Regional Services Staff, Office of Research & Development, U.S. Environmental Protection Agency, Research Triangle Park, NC.

14. U.S. Environmental Protection Agency. 1981. List of designated reference and equivalent methods. Environmental Monitoring Systems Laboratory, Research Triangle Park, NC.

15. Austin, R. circa 1959. Summary of development work on oxidant precursor irradiation chamber. Unpublished work supported by a U.S. Public Health Research Grant.

16. U.S. Environmental Protection Agency. 1980. Part 53 - Ambient air monitoring reference and equivalent methods, Subpart B-Procedures for testing performance characteristics of automated methods. Federal Register 40:13-14 (July 1).

17. Demerjian, K.L., K.L. Schere, and J.T. Peterson. 1980. Theoretical estimates of actinic (spherically integrated) flux and photolytic rate constants of atmospheric species in the lower atmosphere. Page 399 in J. Pitts and R. Metcalf, eds. Advances in Environmental Science and Technology, Vol. 10. John Wiley & Sons, Inc., New York, NY.

18. Leppelmeir, E.T. 1980. Spectral energy graph-F40BL. Lighting Business Group, General Electric Company, Nela Park, Cleveland, OH.

19. General Electric Company. 1980. Fluorescent lamps. Form 9200. General Electric Company, Nela Park, Cleveland, OH.

20. Westinghouse Electric Corp. 1976. Westinghouse "BL" and "BLB" black light fluorescent lamps. Lamp information bulletin. Lamp Division, Bloomfield, NY.

21. General Electric Company. 1970. Fluorescent lamps. Technical Publication 111, Nela Park, Cleveland, OH.

22. Pauer, R., and F. McElroy. 1979. Technical assistance document for the calibration of ambient ozone monitors. EPA-600/4-79-057. U.S. Environmental Protection Agency, Research Triangle Park, NC.

23. McElroy, F.F. 1979. Transfer standards for the calibration of ambient air monitoring analyzers of ozone. EPA-600/4-79-056. Environmental Monitoring System Laboratory, U.S. Environmental Protection Agency, Research Triangle Park, NC.

24. O'Keeffe, A.E., and G.C. Ortman. 1966. Primary standards for trace gas analysis. Analytical Chemistry 38(6):760-763.

25. Ozone monitor. Operating and Instruction Manual. Dasibi Environmental Corp., Glendale, CA.

26. Ludwig, F.L., and E. Shelar. 1978. Site selection for monitoring of photochemical air pollutants. EPA-450/3-78-013. Office of Air Quality Planning and Standards, Research Triangle Park, NC.

27. Seila, R.L., W.A. Lonneman, and S.A. Meeks. 1976. Evaluation of polyvinyl fluoride as a container material for air pollution samples. Journal of Environmental Science Engineering, A 11 (2):121-130.

28. Seila, R.L. 1979. Non-urban hydrocarbon concentrations in ambient air north of Houston, Texas. EPA 600/3-79-010. U.S. Environmental Protection Agency, Research Triangle Park, NC.

29. Gorsuch, A.M. 1981. Statement of U.S. Environmental Protection Agency Administrator. Presented to subcomittee on Natural Resources, Agricultural Research and Environment, Committee on Science and Technolgy, United States House of Representatives, October 22, 1981.

30. Innes, W.B. 1981. Effect of nitrogen oxide emissions on ozone levels in metropolitan regions. Environmental Science & Technology 15(8):904-912.

A NEW RELIABLE AMBIENT AIR CHLORINE MONITORING SYSTEM

Eric F. Mooney

Anacon
A Division of High Voltage Engineering Corporation
Burlington, MA

ABSTRACT

This paper describes a polarographic probe technique for the measurement of low ppm levels of chlorine in ambient air.

Although the range of applications for such a monitoring system are extensive, in many of the installations, the probes are a long distance from the control room. It is therefore imperative that the "state-of-the-probe" be continually monitored. The system has therefore been designed to continually monitor that both the probe and the electronic units are functioning correctly and warning is immediately given should any malfunction occur. Consequently, an indication of zero chlorine concentration is reliable.

Additionally, because the probes are often mounted in remote locations and a large number of probes are frequently installed to monitor the perimeter of a site, or a particular work area where chlorine is handled, the outputs of the probes are multiplexed at a local processing unit (LPU). Data on the chlorine concentration and probe or machine faults are transmitted from the LPU as an RS232 serial data-only link. Thus, the data may be transmitted over normal telephone communication lines and, of course, are ideally suited for connection to a serial I/O port of a smart terminal for further processing.

INTRODUCTION

The requirement for a good ambient air chlorine monitor has long been recognized, as is evident from the amount of work devoted to this problem by the major chlorine manufacturing companies.

A number of methods have been used, including amperometric techniques and solid state sensors. Neither of these techniques is specific for

chlorine and tend to respond to any oxidizing gas such as ozone, sulfur dioxide and oxides of nitrogen, to name only a few of the commonly interfering gases.

There are, of course, a number of colorimetric methods available, but none of these have been used as a continuous monitor to give immediate warning. A method that utilizes the color developed on a tape impregnated with suitable reagents has also been used. This method, again, is not specific, since the same color development is obtained with a range of oxidants and there is some doubt about the stability of the tapes prior to use.

A further complication arises in the measuring of chlorine in paper pulp mills because none of the standard methods are capable of differentiating between chlorine and chlorine dioxide.

The polarographic method offers many advantages because the potential at which the reduction occurs is specific for that compound in the electrolyte medium being used. Thus, two variables, the applied potential and the electrolyte medium, are capable of selecting the specificity of the reduction. Obviously, from a practical point of view, if reduction can occur at zero applied potential, there is considerable advantage in not having to provide this potential.

Jim Young, at Imperial Chemical Industries (ICI) Limited, Mond Division, England, found a suitable electrolyte composition in which chlorine is selectively reduced at zero applied potential, and thus produced a very useful probe (information by personal contact with Jim Young and from ICI internal reports). It should be noted that oxygen, ozone, sulfur dioxide, and oxides of nitrogen are all reduced at negative applied potentials, between -1.5 and -2.5 volts, in the electrolyte solution being used and hence do not interfere with the measurement of chlorine.

It is this probe that Anacon has licensed from ICI for world-wide manufacture and sales.

THE RELIABILITY OF PROBES

There is a general problem with all sensors that are being used for ambient monitoring in that these monitors do not receive the same degree of maintenance as other process instrumentation. This is understandable, since ambient air monitors do not result in any increased productivity of the plant and are simply often regarded as a necessary evil.

Anacon recognized this problem and felt it was most important to have built-in reliability as well as the specific response of the probe to chlorine. If a sensor is indicating zero, owing to a malfunction, it might be said to be better not to have the sensor at all rather than create a sense of false security.

In the new Anacon ambient air chlorine monitoring system, it is

impossible for the probe to be reading zero simply from a malfunction of the probe; any malfunction is immediately indicated.

CONSTRUCTION OF THE PROBE

The probe consists of a bobbin on which is wound a coil of silver wire separated from the outer platinum wire coil by a cellulose insulating layer. A cotton wick is supported between the layers of cellulose insulation, and this wick projects into a reservoir that contains the electrolyte solution. The electrolyte, unlike the amperometric methods, is not consumed, and the total volume of the reservoir is only 1.5 ml.

The two coils are connected via two separate wires to the preamplifier board which, to avoid ingression of moisture, is encapsulated; the probes are frequently mounted outside and exposed to the elements.

The bobbin, the probe sheath, and the housing for the preamplifier board are constructed from polypropylene to minimize any corrosion resulting from exposure to chlorine or hydrogen chloride. The probe is shown diagrammatically in Figure 1.

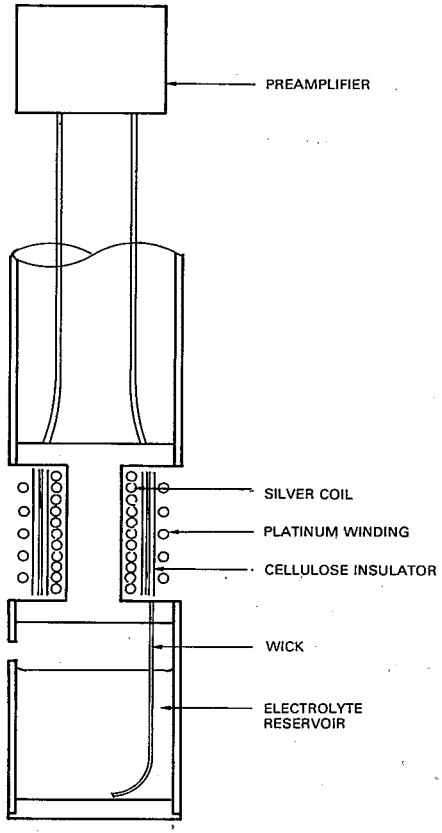

Figure 1. Cross-section of probe.

THE MEASUREMENT OF CHLORINE

On exposure of the probe to chlorine, reduction of the chlorine occurs at the outer platinum coil and chloride ions are formed. The chloride ions are transported across the electrolyte, held in the porous cellulose insulating layers, and then react with the silver coil to form silver chloride; this reaction is the driving force behind the total reaction. It is probably almost certain that chlorine is first absorbed by the wet outer electrolyte layer prior to reduction at the platinum electrode. Under steady-state conditions, if the chlorine is not replenished quickly enough to maintain the equilibrium, the output will decrease.

Under steady-state conditions, the output of the preamplifier is adjusted to give a voltage signal of 4.5 volts for full-scale response of the probe. The normalization of the output of the probe to 4.5 volts for full-scale response is convenient not only for the A to D converter used, but it additionally permits probes of differing ranges to be attached to a single LPU.

THE STATE OF THE PROBE SIGNAL

When the coil is first made and before electrolyte is added, the probe capacitance is very small, on the order of 50 to 60 pF. When the probe is saturated with electrolyte, the capacitance increases to between 40 and 50 mF. The characteristics of the "cell" formed between the platinum and silver windings and the electrolyte, form the basis of the "state-of-the-probe signal."

Should the probe dry out, it will not respond to chlorine, and the capacitance of the probe will decrease. This variation is monitored by the preamplifier and reveals itself as a "high" voltage output in the state-of-the-probe signal train. Normally, a probe operating correctly will display a state-of-the-probe signal between 60 and 600 mV.

THE SYSTEM

In developing the system, considerable thought was given to the requirements for ambient monitoring and methods of dealing with the large amount of data that would be obtained for a comprehensive perimeter monitoring system.

The central intelligence of the system is the Local Processing Unit (LPU), which is capable of accepting up to ten probes. The outputs from all ten probes are multiplexed every three seconds, and when data are taken from each probe, both the voltage from the chlorine concentration and from the state-of-the-probe signals are monitored.

If fewer than ten probes are attached, then the appropriate probe switches in the LPU must be opened; otherwise, an alarm will be given,

indicating that no probe is attached to the system.

Four conductor cables attach the probe to the LPU, and the cable length may be 1000 feet or more; for distances in excess of 1000 feet, the gage of the wire is decreased to avoid any voltage drop along the cable length.

The output from the LPU is an RS232 ASCII data link. Fourteen sets of two-bit codes are given; these will be discussed in detail below. It does mean that, using this data communication system, the LPU may be many miles from the data acquisition or from the Local Control Unit (LCU) with the associated displays. The data may be transmitted along a twisted pair of telephone cables. This is useful for the monitoring of chloride storage tanks that are normally unattended, or left unattended for long periods. Should a leak develop, an alarm may be raised at a remote security or fire department office through standard telecommunication procedures.

Use of the RS232 data link has a further advantage in that the data may be put directly into a serial I/O of a smart terminal or main frame computer, permitting time-weighted averages to be readily calculated.

Visual display of the chlorine levels may be observed using the individual display modules mounted in the LCU. The chlorine concentration is displayed as a bar graph. The same bar graph liquid crystal arrays are also used to indicate probe or instrument errors.

Both the LPU and LCU are powered by 18 to 24V AC or DC, hence installation becomes a relatively simple matter.

The system is illustrated in Figure 2.

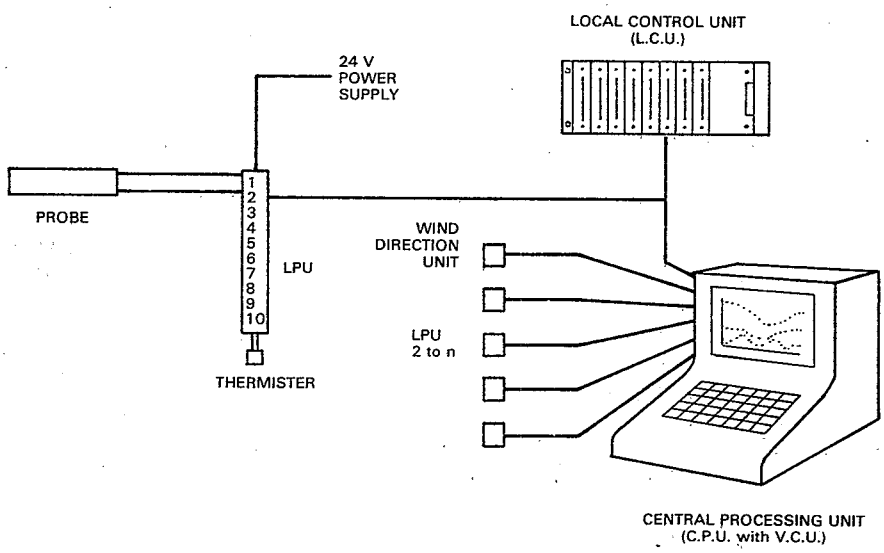

Figure 2. Basic chlorine monitoring system using local control or central processing unit.

THE ERROR SIGNALS

The error signals may conveniently be divided into two classes, the machine errors and the probe errors.

The four machine errors are:

i. Loss of 12-volt power in the LPU
ii. Loss of 12-volt supply to the probe
iii. Loss of 5-volt supply in the LPU
iv. Excess current being drawn by a probe

The ASCII coded error message and the alarm error display shown on the display module are presented in Figure 3.

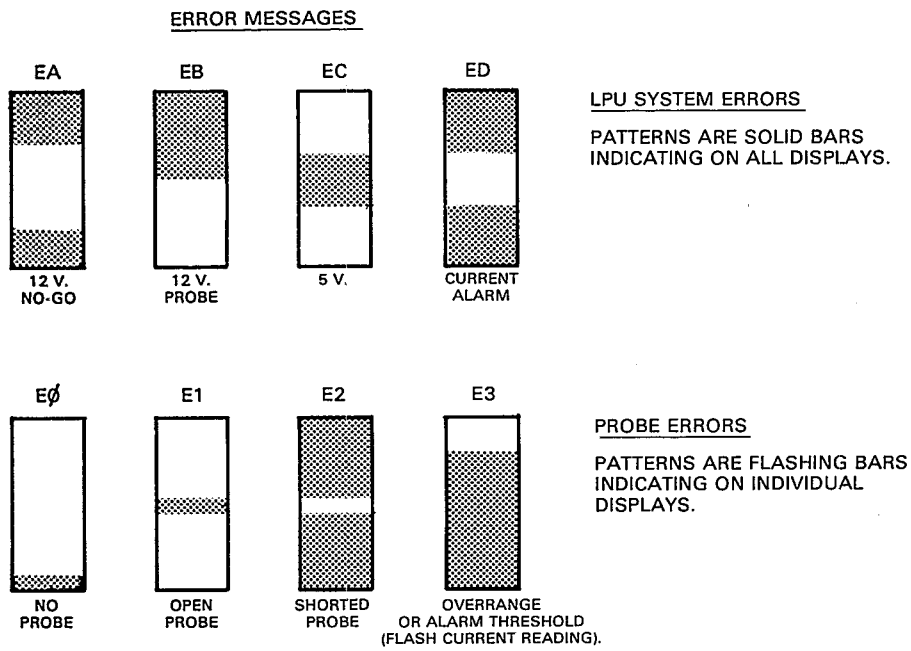

Figure 3. LCD alarm graphics on LCU.

Naturally, should either the 12V or 5V supplies in the LPU be lost, the displays associated with <u>all</u> the probes attached to that LPU will show the same error indication.

The four alarms associated with the probe are:

i. No probe
ii. Open probe
iii. Shorted probe
iv. Overrange - chlorine alarm level exceeded

Again, the ASCII codes and visual display signals are also shown in Figure 3. The overrange (the chlorine alarm level) is obviously not really a probe error, but it is convenient to include here. The probe errors do, however, require some additional explanation.

The no-probe signal appears if one of the display modules is selected to display a probe that is unexpected--for example, the corresponding probe switch in the LPU is open since no probe is attached.

The open-probe signal is obtained if the probe dries out and needs electrolyte replenishing, or also appears if a probe is removed from the connector or if the cable between the probe and LPU port is severed.

The shorted probe signal is obtained if the two coils become shorted or the cellulose insulation becomes degraded.

One further error message is provided and indicates that communication between the LPU and LCU is lost and is shown by the activation of the local sonalert and the red LED "data lost" indicator becomes illuminated. Data loss could arise from complete loss of power at the LPU or when the twisted pair between the LPU and LCU becomes detached or severed.

ASCII CODED DATA

Fourteen sets of two-bit ASCII codes are obtained from the LPU every three seconds, and the line of coded data is terminated by a CRLF (Carriage Return Line Feed).

The first set of data are the machine errors EA to ED; the second and third are not normally used, but were intended to give wind speed and temperature if needed for correction of data. The next ten sets of data are for probes 1 through 10 and show chlorine concentration as ØØ through 99, a percentage of scale. In the computer software, provision must be made to identify the range of the probe. As mentioned earlier, the full-scale output for all probes is normalized to 4.5 volts so that probes of different measurement ranges may be connected to the same LPU. The final set of information is a sum check of the first thirteen sets of data.

Should a probe error be detected, the probe error message EØ to E2 are obtained for the appropriate probe data and of course no chlorine concentration data will be obtained for that probe.

SPEED OF RESPONSE

As with many electrochemical devices, there is an asymptotic approach to the maximum output for a given concentration of chlorine. This characteristic arises because an equilibrium is involved between the chlorine and the rate of reduction. A typical response curve is shown in Figure 4, in which a 5 ppm probe is exposed to 5.0 ppm of chlorine. It will be observed that the normally selected alarm levels of 0.5 or 1.0 ppm are reached

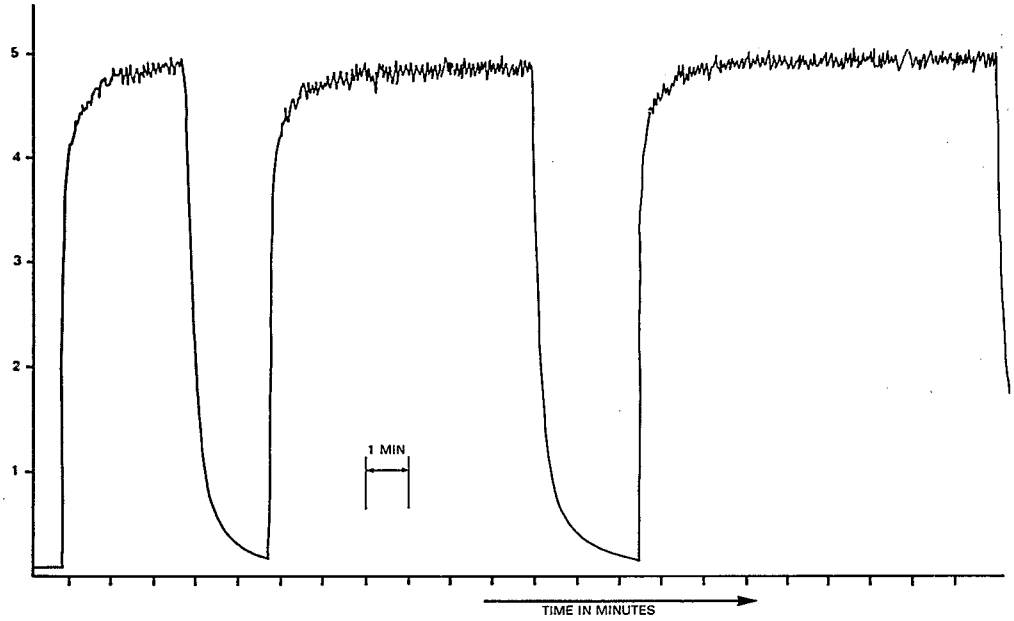

Figure 4. Probe response to 5 ppm chlorine.

within less than 4 to 5 seconds and certainly 80 percent response is reached within 15 seconds.

The equilibrium effect may be readily demonstrated by inserting a probe into a "static" atmosphere containing 5 ppm of chlorine. Initially the output of the probe rises very quickly, but then inverts and decreases as the chlorine is consumed.

There is therefore an airflow effect in the probe, and air velocities in excess of .5 mph are required to maintain the equilibrium conditions. Should a probe be required to be used in an enclosed space, for example, a closed room in which there is little or no air movement, then the probe should be calibrated under static conditions.

CALIBRATION

It was perhaps surprising that, during the initial field trials, the biggest problem for users was to substantiate the calibration of the probe supplied. There was considerable difficulty in obtaining cylinders of gas containing a low ppm of chlorine. We have found one company* that has been particularly successful in providing stable chlorine standards in cylinders that are guaranteed for three months. Our experience has shown that a cylinder was stable for six months.

*Ideal Gas Products Inc., New Jersey

A permeation tube device may also be used, but again, some users have had difficulty in obtaining reliable chlorine permeation tubes.

A fairly simple calibration aid is available in which the probe to be tested is inserted into a calibration chamber and a known concentration of gas passed through the chamber at 3 to 4 liters per minute.

STABILITY OF CALIBRATION

A probe that had been factory-calibrated over the range of 0 to 5 ppm was checked over a period of three months using a permeation device in which 1 and 2 ppm of chlorine could be obtained in the sample gas. These data are shown in Table 1. Although there are differences in the absolute calibration, using the same chlorine source shows remarkably consistent readings over the three months interval.

TABLE 1. STABILITY OF CALIBRATION

Calibration level	0 ppm*	1 ppm	2 ppm
Initial check	0.17 ppm	1.0 ppm	1.83 ppm†
30 days	0.17 ppm	0.78 ppm	1.83 ppm
60 days	0.17 ppm	1.0 ppm	1.72 ppm
90 days	0.17 ppm	1.0 ppm	1.83 ppm
	0.17 ppm	1.0 ppm	1.83 ppm
	0.22 ppm	1.0 ppm	1.83 ppm
	0.22 ppm		
	0.22 ppm		

*The chlorine readings here are believed to arise from the inability to be able to completely isolate the flow through the oven containing the permeation tube. When connected to true zero air, a compressed air supply not connected with the permeation device, values of 0.0 ppm were obtained on every occasion.

†Unadjusted values compared to original factory calibration made using a gas cylinder.

A more detailed study of the stability of calibration has been carried out elsewhere; we are hopeful that these results will be published independently.

CONCLUSION

It will be clear from the above account that, at long last, a reliable chlorine monitor has become available that has a degree of reliability and specificity not previously attained with a chlorine monitor. Further, it is a true monitor, being capable of highly accurate measurements. We can hope that the days are gone when the operator wondered if the monitor was still working when zero chlorine concentration was being indicated.

THE DEVELOPMENT OF STANDARD REFERENCE MATERIALS CONTAINING SELECTED ORGANIC VAPORS IN COMPRESSED GAS MIXTURES

W.P. Schmidt and H.L. Rook

Gas and Particulate Science Division
Center for Analytical Chemistry
National Bureau of Standards
Washington, DC

INTRODUCTION

In the absence of absolute analytical methods for the determination of organic compounds in the atmosphere, accurate and stable primary standards allow comparative analytical procedures to be used with a high degree of reliability. Unfortunately, analytical studies to date on trace organic vapors in compressed gas mixtures have shed little light on the questions of either accuracy or stability (1). Several years ago, the National Bureau of Standards (NBS) undertook research to determine the feasibility of accurately preparing such mixtures and, if possible, to determine their stability with time. Initially, the project was limited to the study of mixtures containing benzene and tetrachloroethylene in high-pressure gas cylinders at concentrations of 0.2-10 parts per million by mole (ppm).

Based on the results of the initial study, the program was expanded to include a total of seven organic compounds in gas mixtures in the concentration range mentioned above. This expanded study included both single-component and, in various combinations, multi-component mixtures. The organic gas mixtures completed thus far include vinyl chloride monomer (VCM), chloroform, benzene, carbon tetrachloride, toluene, tetrachloroethylene, and chlorobenzene. Positive results have been obtained for each of these seven compounds. Gas mixtures containing acrylonitrile have been prepared, but reliable analytical data have not yet been obtained. A list of gas cylinder mixtures showing typical components and concentrations is given in Table 1.

In addition to the detailed study of the gas cylinder mixtures mentioned above, preliminary research into the preparation of lower-concentration primary mixtures (0.05-0.2 ppm) for certain organics has been initiated and the feasibility of the calibration of permeation devices using GC-FID has been ascertained. The results of all of these studies will be discussed in this paper.

TABLE 1. TOXIC ORGANIC PRIMARY MIXTURES

Cylinder no.	Date prepared	Analyzed concentrations, ppm							
		VCM	Acrylo-nitrile*	Chlo-roform	Benzene	Carbon tetrachloride	Toluene	Tetrachloro-ethylene	Chloro-benzene
X-207021	4/18/80				1.390				
X-207093	4/18/80				0.243				
X-207069	4/18/80				0.468				
X-207033	4/18/80				1.878				
X-207080	4/25/80							5.581	
FF 9747	8/05/80			2.239				1.171	0.817
FF 9775	8/05/80			5.060				4.507	
FF 9741	8/05/80			0.226					0.232
FF 9735	8/30/80	0.583		1.848	0.248			0.510	0.363
FF 9766	8/30/80	0.238		0.411					
X-160628	12/4/80		19.484						
X-160649	12/4/80					8.678			
FF 9734	12/4/80	4.862	1.722			3.559	2.737		1.524
FF 9760	12/5/80	2.228	0.625			0.231		0.309	
FF 9772	12/5/80	4.414	0.694		1.325		0.948		1.116
FF 9759	12/5/80	2.541	0.319				0.326		
FF 9755	12/5/80	10.961		6.512					
FF 9738	1/22/81	0.485	0.972			1.121	1.571		3.008
FF 9753	1/22/81	0.197			0.284				
FF 9498	1/27/81		0.221		0.661				
FF 9773	1/27/81	1.000		0.319	0.873				
X-207055	8/07/81		0.276			0.489		0.401	
X-207085	8/07/81		5.222					1.423	
FF 6885	8/07/81	0.802		0.851	0.910			0.930	0.710
FF 9779	8/07/81		1.919				1.381		1.698
FF 9762	8/07/81			1.587		1.436	3.960	15.963	
CAL-6488	9/17/81			0.441				0.988	0.980
FF 12044	9/17/81			1.502		1.491			2.037
CAL-6523	9/22/81			0.776	0.585		2.279	2.001	9.081
CAL-5604	9/26/81					0.433		1.068	
X-160606	9/26/81				0.390				
X-160588	9/26/81				0.871				
X-160619	9/26/81					0.560			
FF 9754	9/28/81			0.235		0.199	0.342	0.476	0.617
FF 9497	9/28/81			0.837	0.281		0.285	1.065	0.584

*Concentrations listed for acrylonitrile are calculated from the gravimetric preparation data.

PREPARATION OF PRIMARY GAS CYLINDER MIXTURES

Primary gas cylinder mixtures for low vapor-pressure organic liquids can not be prepared by the same technique (successive dilutions) used to prepare mixtures for high vapor-pressure compounds. The problems encountered when using this technique for mixtures containing such organics as benzene or tetrachloroethylene include fractionation due to cooling, adsorption of the organic on the walls of the cylinder, and the possible condensation of the organic vapor inside the cylinder. (These problems occur primarily at high concentration levels of the intermediate gas mixtures and cause uncertainty in mixtures prepared by this method.)

To eliminate these problems, a method of preparation was developed that produced the desired low concentration levels by a single dilution. A thin-wall glass capillary tube was sealed at one end and weighed. A small sample (1-20 mg) of the organic liquid was drawn into the tube. The tube was then sealed and reweighed. To aspirate the sample into an evacuated and weighed cylinder, the tube was fitted tightly into a short length of Teflon tubing. The Teflon tubing was then attached to the evacuated cylinder. The cylinder valve was opened slightly and the end of the sample tube nearest the cylinder was cracked. After most of the liquid had vaporized and been drawn into the cylinder, the other end of the tube was carefully broken and atmospheric air was drawn through the remaining portion of the sample tube to sweep any residual vapor into the cylinder. The cylinder was then pressurized with clean air or nitrogen to 12.4×10^6 Pascals and reweighed. Results obtained by this technique for vapors of vinyl chloride, toluene, and chlorobenzene are given in Tables 2, 3, and 4, respectively.

TABLE 2. COMPARISON OF GRAVIMETRICALLY CALCULATED AND ANALYZED CONCENTRATIONS FOR PRIMARY VCM MIXTURES

Cylinder	Date prepared	Calculated concentration	Analyzed concentration	
			January, 1981	September, 1981
FF 9755	12/5/80	10.963 ppm	10.962 ppm	10.961 ppm
FF 9734	12/4/80	4.862	4.868	4.862
FF 9772	12/5/80	4.408	4.421	4.414
FF 9763	8/30/80	3.314	2.284	2.280
FF 9759	12/5/80	2.545	2.546	2.541
FF 9760	12/5/80	2.226	2.236	2.228
FF 9773	1/27/81	1.002	1.002	1.000
FF 6885	8/07/81	0.802	—*	0.802
FF 9735	8/30/80	0.612	0.586	0.583
FF 9738	1/22/81	0.484	0.485	0.485
FF 9766	8/30/80	0.288	0.239	0.238
FF 9753	1/22/81	0.194	0.200	0.197

*Cylinder FF 6885 was prepared after the intercomparison of January, 1981.

TABLE 3. COMPARISON OF GRAVIMETRICALLY CALCULATED AND ANALYZED CONCENTRATIONS FOR PRIMARY TOLUENE MIXTURES

Cylinder	Date prepared	Calculated concentration	Analyzed concentration January, 1981	Analyzed concentration September, 1981
FF 9762	8/07/81	3.952 ppm	--*	3.960 ppm
FF 9734	12/4/80	2.747	2.78 ppm	2.737
CAL-6523	9/22/81	2.276	--*	2.279
FF 9738	1/22/81	1.581	1.58	1.571
FF 9779	8/07/81	1.381	--*	1.381
FF 9772	12/5/80	0.947	0.95	0.948
FF 9754	9/28/81	0.336	--*	0.342
FF 9759	12/5/80	0.325	0.31	0.326
FF 9497	9/28/81	0.287	--*	0.285

*Samples prepared after the intercomparison of January, 1981.

TABLE 4. COMPARISON OF GRAVIMETRICALLY CALCULATED AND ANALYZED CONCENTRATIONS FOR PRIMARY CHLOROBENZENE MIXTURES

Cylinder	Date prepared	Calculated concentration	Analyzed concentration January, 1981	Analyzed concentration September, 1981
CAL-6523	9/22/81	9.081 ppm	--*	9.081 ppm
FF 9738	1/22/81	3.035	3.044 ppm	3.008
FF 9763	8/30/80	2.122	2.125	2.124
FF 12044	9/17/81	2.038	--*	2.037
FF 9779	8/07/81	1.820	--*	1.698
FF 9734	12/4/80	1.544	1.530	1.524
FF 9772	12/5/80	1.119	1.116	1.116
CAL-6488	9/17/81	0.981	--*	0.980
FF 9747	8/05/80	0.818	0.814	0.817
FF 6885	8/07/81	0.744	--*	0.710
FF 9754	9/28/81	0.618	--*	0.617
FF 9497	9/28/81	0.584	--*	0.584
FF 9735	8/30/80	0.500	0.365	0.363
FF 9741	8/05/80	0.235	0.233	0.232

*Samples prepared after the intercomparison of January, 1981.

Two modifications to this micro-gravimetric technique for sample preparation were made to improve the accuracy of this technique when used for either high vapor pressure organics or multi-component mixtures. These modifications were made necessary by a lack of correlation between the gravimetric and analyzed concentrations for both VCM and one or more components in several of the multi-component mixtures. In all suspect samples, the analyzed concentrations were considerably lower than the gravimetric concentrations.

The problems encountered in making VCM mixtures included difficulties in sealing the microtubes containing this organic, polymerization of the VCM in the sealed microtube, and in general, the quantitative addition of the organic to the evacuated gas cylinder. Occasional lower-than-expected concentrations of one or more components in multi-component mixtures were traced to a faulty transfer of the organic compounds to the evacuated gas cylinder.

To solve the inconsistencies in the VCM mixtures, only freshly filled microtubes were used in the preparation of the mixtures, the cylinder valve was opened completely before the end of the microtube was cracked, and a modification was made to the microtube filling technique wherein dry ice was applied to the closed end of the microtube after the liquid VCM had been added to the tube but prior to sealing it. The effect of this modification was twofold. First, the extra cooling allowed a small quantity of air to be drawn through the tip, sweeping the organic further into the tube and eliminating a tendency toward charring and the resultant ashy residue after flame-sealing the tip. Second, the resultant pressure decrease inside the tube allowed a surer seal, since the application of heat during sealing had previously caused an increase in pressure, leading to faulty seals. Samples prepared by this modified procedure showed better agreement between gravimetrically calculated and analyzed concentrations than did samples prepared by the original procedure (Table 5). Mixtures prepared by this modified procedure were compared to mixtures prepared using the successive dilution technique. The results of the intercomparison indicated good agreement (±0.5 percent rel.) between mixtures prepared by both techniques but better precision (±0.2 percent rel.) among mixtures prepared by the modified microtube procedure (Table 6).

TABLE 5. COMPARISON OF GRAVIMETRICALLY CALCULATED AND ANALYZED CONCENTRATIONS FOR VCM MIXTURES: MODIFIED VS. ORIGINAL PREPARATIVE PROCEDURES

Original procedure				Modified procedure			
	Concentration, ppm				Concentration ppm		
Cylinder no.	Calculated	Analyzed	Δ, ppm	Cylinder no.	Calculated	Analyzed	Δ, ppm
FF 9735	0.612	0.583	-0.029	FF 9738	0.484	0.485	0.001
FF 9766	0.288	0.238	-0.050	FF 9753	0.194	0.197	0.003
				FF 9773	1.002	1.000	-0.002

TABLE 6. COMPARISON OF GRAVIMETRICALLY CALCULATED AND ANALYZED CONCENTRATIONS FOR PRIMARY VCM MIXTURES PREPARED BY THE SUCCESSIVE DILUTION TECHNIQUE AND THE MICROTUBE TECHNIQUE

Successive dilution				Micro-tube			
	Concentration				Concentration		
Cylinder no.	Calculated	Analyzed	Δ, %	Cylinder no.	Calculated	Analyzed	Δ, %
000674	9.902 ppm	9.857 ppm	-0.5	FF 9755	10.963 ppm	11.001 ppm	0.3
000335	4.984	4.867	-2.3	FF 9772	4.408	4.412	0.1
000661	0.983	0.984	0.1	FF 9759	2.545	2.547	0.1

The modification to the procedure used in the addition of the microtubes in the multi-component mixtures preparation consisted of changing from a simultaneous addition to a serial addition of the tubes to the cylinder. In the original procedure, all tubes to be added were wrapped together with Teflon* tape and fitted into the end of a 1/4" O.D. Teflon transfer line. The cylinder valve was opened and the ends of the microtubes were broken simultaneously. When four or more microtubes were added in this way, there was insufficient flow through the microtubes to ensure that all of the organic liquid from all of the microtubes was swept into the cylinder. In the modified procedure, a 1/8" O.D. Teflon transfer line was employed and the tubes were added singly. Samples prepared by the modified procedure showed no inconsistencies between gravimetric and analyzed concentrations (Table 7).

ANALYSIS OF PRIMARY GAS MIXTURES

The mixtures were analyzed by GC-FID employing a 10' x 1/8" stainless steel column containing 20 percent SP-2100 and 0.1 percent Carbowax 1500 on 100/120 Supelcoport. The column temperature was 100°C and the carrier flow rate was 60 cc nitrogen/minute. Total time for each separation was 12 minutes.

A modification to the analytical sampling procedure was made during the past year. In the analysis, cylinder control valves were used to sample from the high-pressure gas cylinders. Originally, a sample flow rate of 30 cc/min was established through the sample loop of the automatic sampling valve. It was necessary to maintain this flow rate for several hours prior to the analysis to obtain meaningful responses from the analytical

*Certain commercial equipment, instruments, and materials are identified in this paper in order to adequately specify the experimental procedure. Such identification does not imply recommendation or endorsement by the National Bureau of Standards, nor does it imply that the materials or equipment identified are necessarily the best available for the purpose.

TABLE 7. MULTI-COMPONENT MIXTURES WITH TOTAL NUMBER OF ORGANIC COMPONENTS* AND NUMBER OF COMPONENTS SHOWING SIGNIFICANT (±2% REL) DEVIATION BETWEEN CALCULATED AND ANALYZED CONCENTRATIONS: MODIFIED VS. ORIGINAL PREPARATIVE PROCEDURES

Original procedure			Modified procedure		
Cylinder no.	Total components*	Deviating components	Cylinder no.	Total components*	Deviating components
FF 9735	5	4	CAL-6523	5	0
FF 9734	4	0	FF 9754	5	0
FF 9772	4	0	FF 9497	5	0
FF 9738	4	1			
FF 6885	5	3			
FF 9762	4	0			

*Excluding acrylonitrile.

system. An experiment was undertaken to determine the actual time needed to equilibrate the cylinder control valve to the concentration of the organic being analyzed. The results of this experiment indicated that the equilibration of the valve was dependent on the individual organic compound and the total volume of sample passed through the cylinder control valve, not on the flow rate. The volume of sample necessary for equilibration ranged from about 0.1 L for VCM to ∿10 L for chlorobenzene. Plots of equilibration volumes and times are shown in Figures 1 through 5. The modification to the original procedure consisted of using higher flow rates (∿100 cc/min) and equilibrating the valve for one to two hours prior to the analysis. Once a valve had been equilibrated, the concentration of the organic compound remained constant until the valve was depressurized, e.g., as when it was removed from the gas cylinder.

ANALYTICAL RESULTS OF THE INTERCOMPARISON OF THE PRIMARY MIXTURES

The results of the intercomparisons of the primary gas mixtures for three organic solvents are given in Tables 2 through 4. The agreement between the calculated concentrations based on gravimetric data and the concentrations determined by GC-FID analysis is a demonstration of the precision and accuracy of the preparation of the primary mixtures. As mentioned above, in all cases of significant inconsistencies between the calculated and analyzed concentrations, the calculated concentrations were higher than the analyzed concentrations, indicating losses in the transfer of the organic from the microtube to the cylinder.

PREPARATION AND ANALYSIS OF LOW-CONCENTRATION (∿50 PPB) GRAVIMETRIC GAS MIXTURES

Preliminary studies have been completed on the feasibility of preparation and analysis of low-concentration gravimetric mixtures. Gravimetric

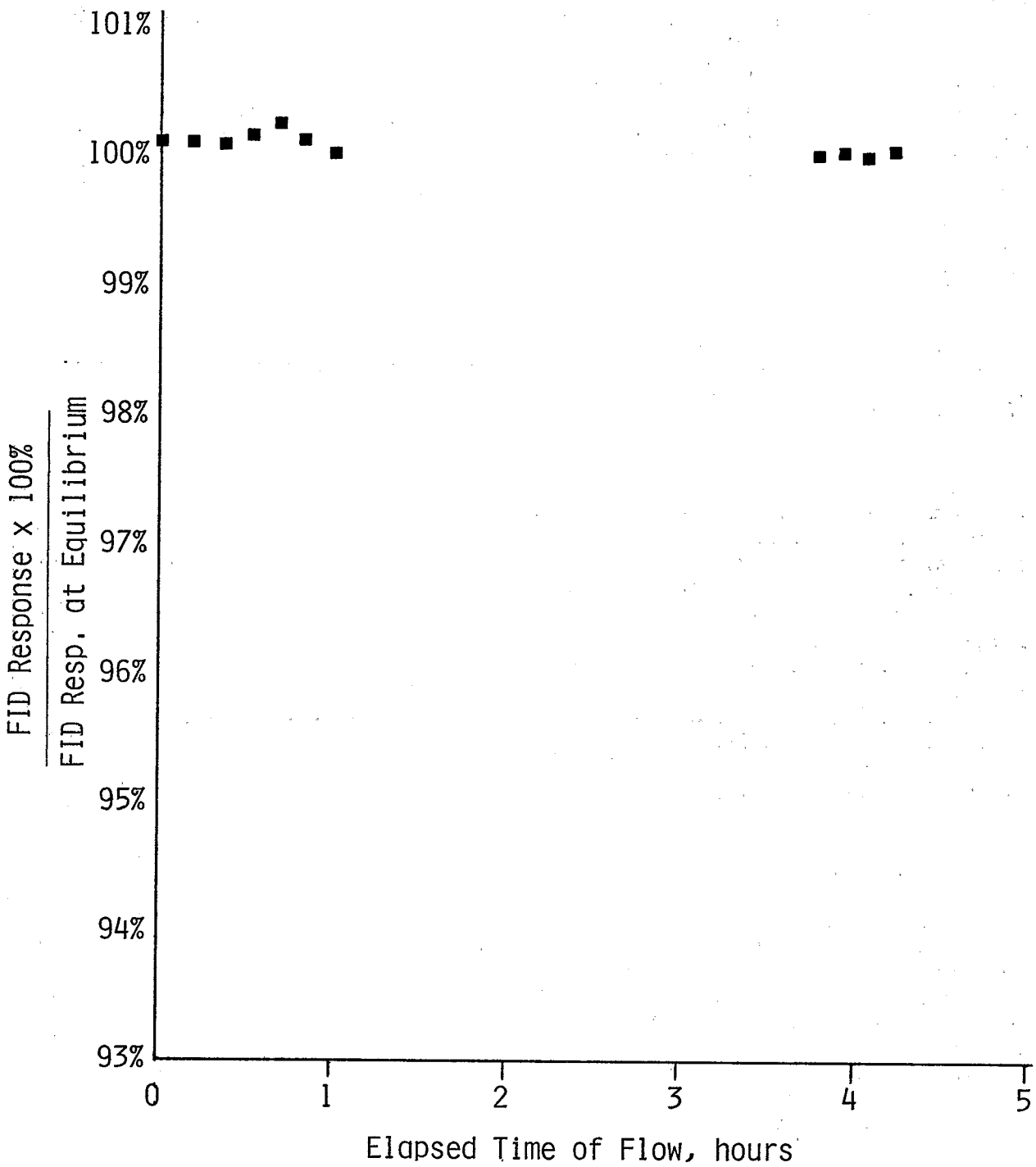

Figure 1. Effect of 100 cc/min sample flow rate on equilibration time of cylinder control valve for VCM.

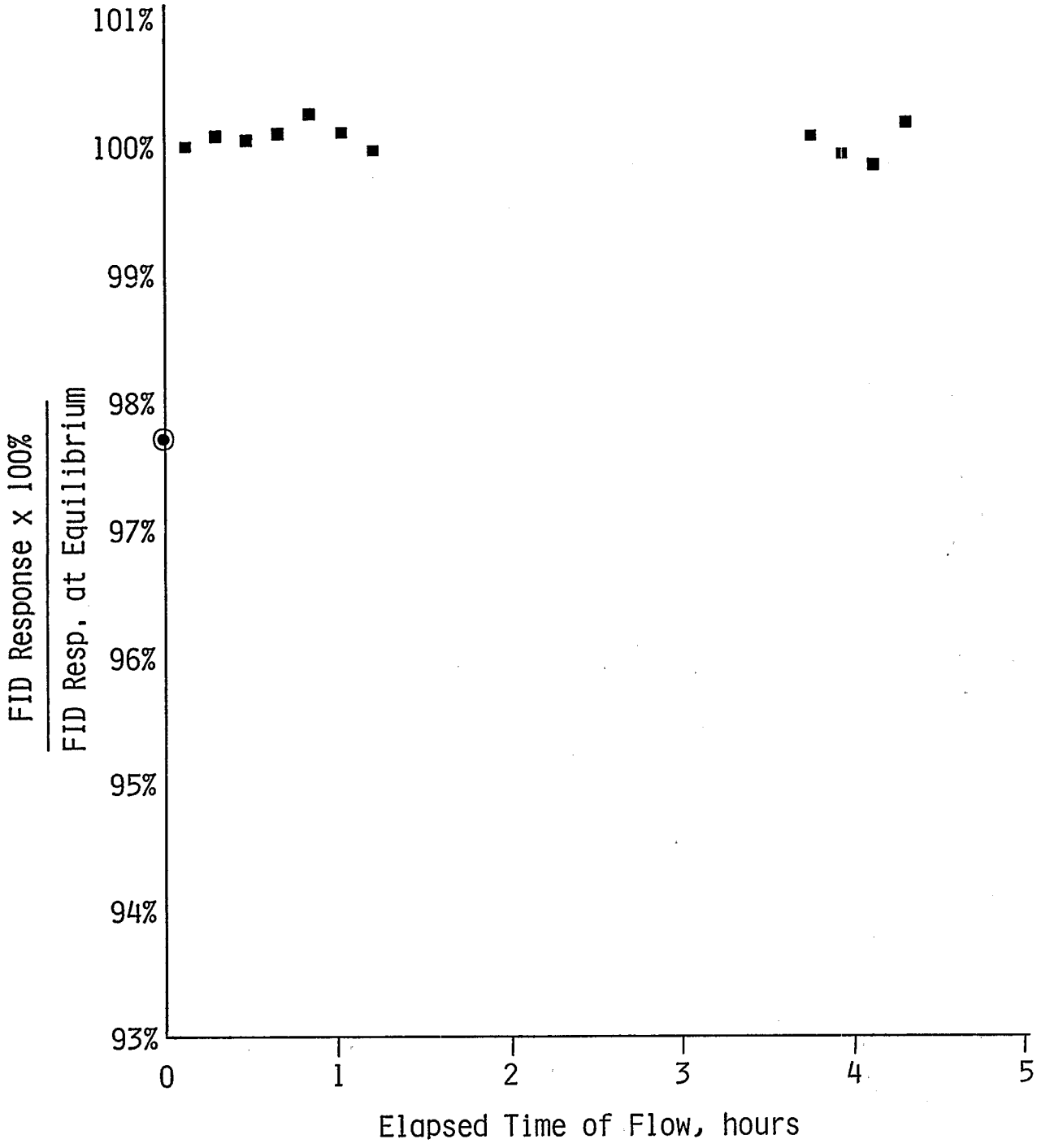

Figure 2. Effect of 100 cc/min sample flow rate on equilibration time of cylinder control valve for $CHCl_3$.

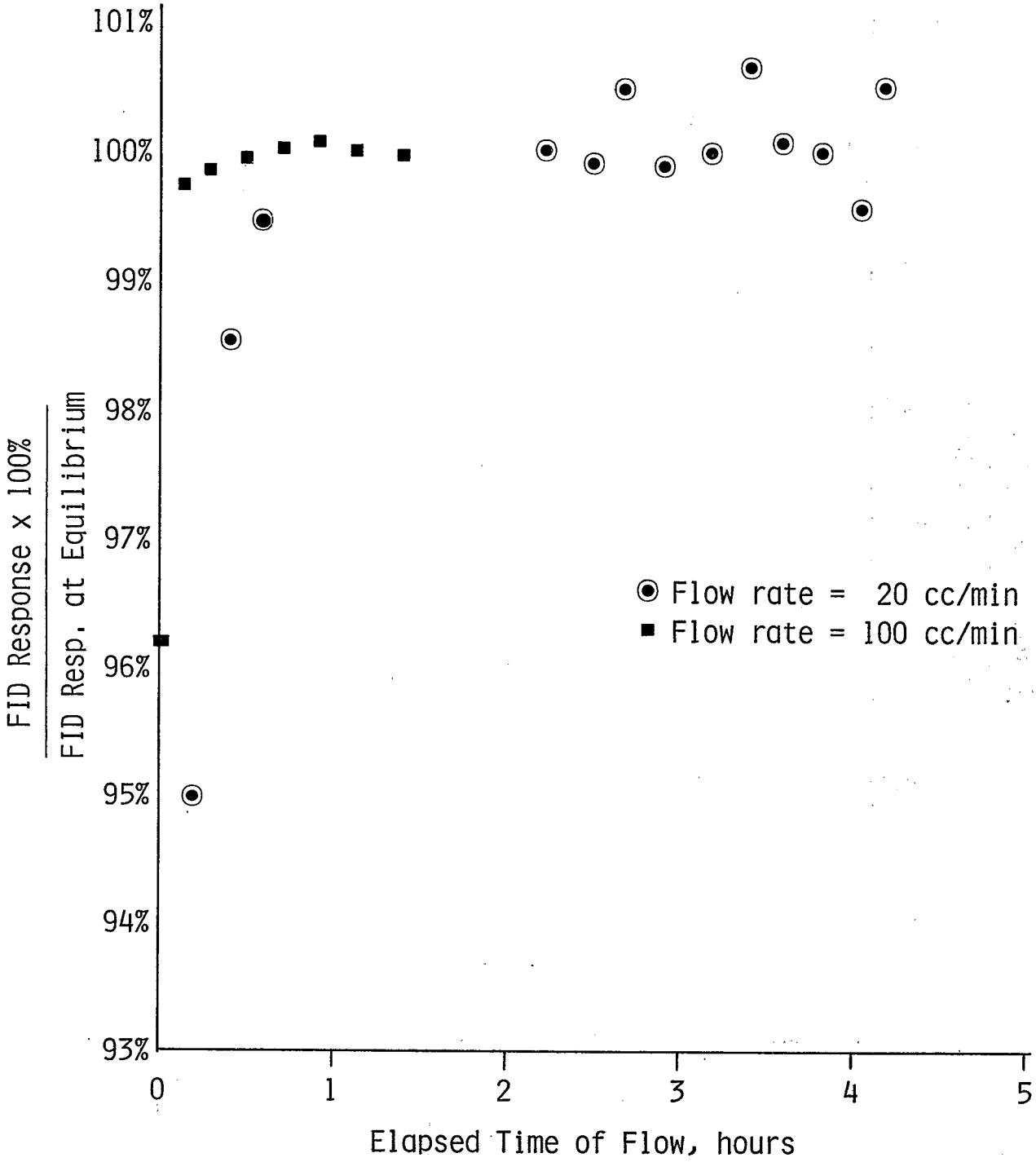

Figure 3. Effect of sample flow rate and flow volume on equilibration time of cylinder control valve for benzene.

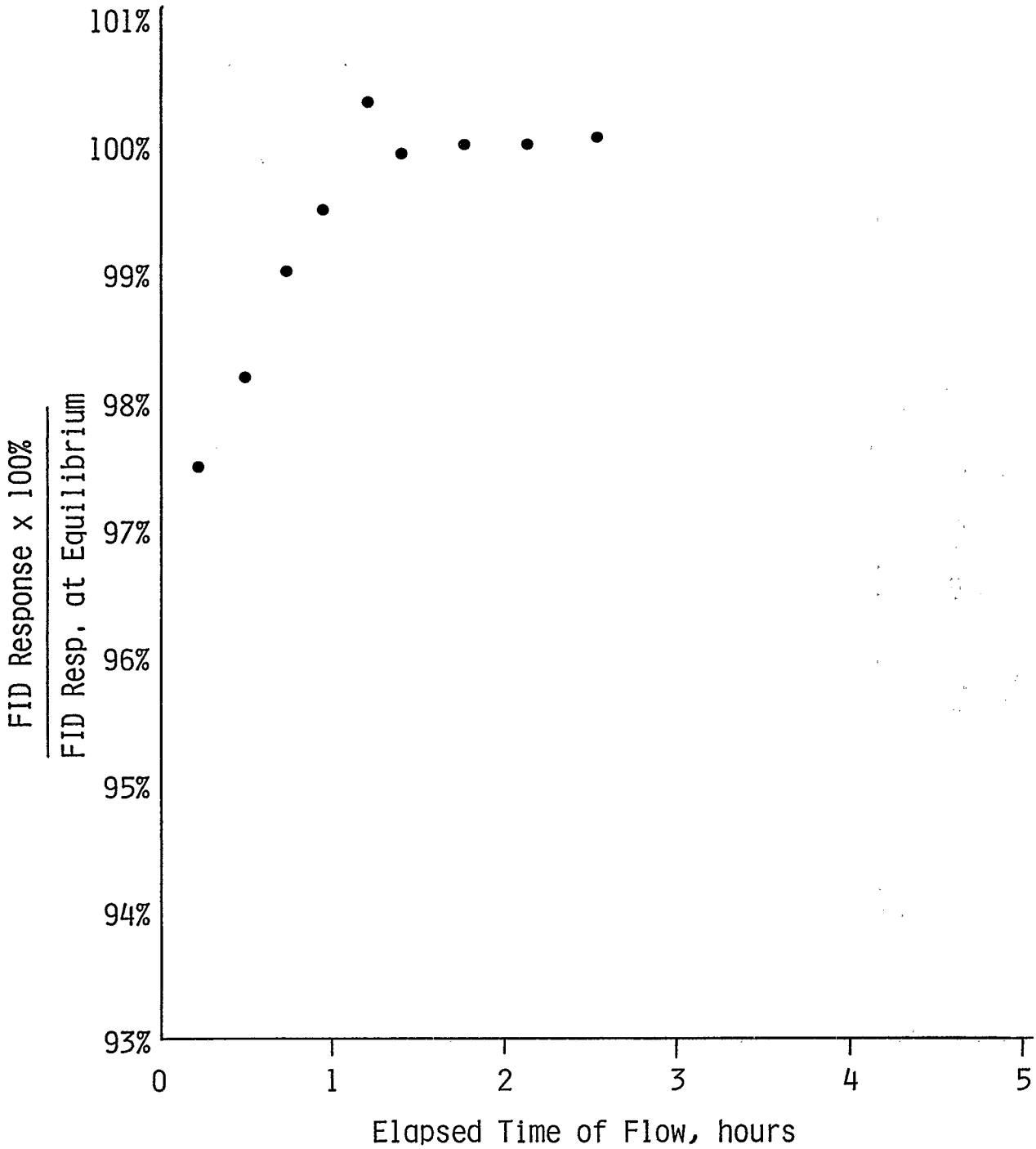

Figure 4. Effect of 100 cc/min sample flow rate on equilibration time of cylinder control valve for C_2Cl_4.

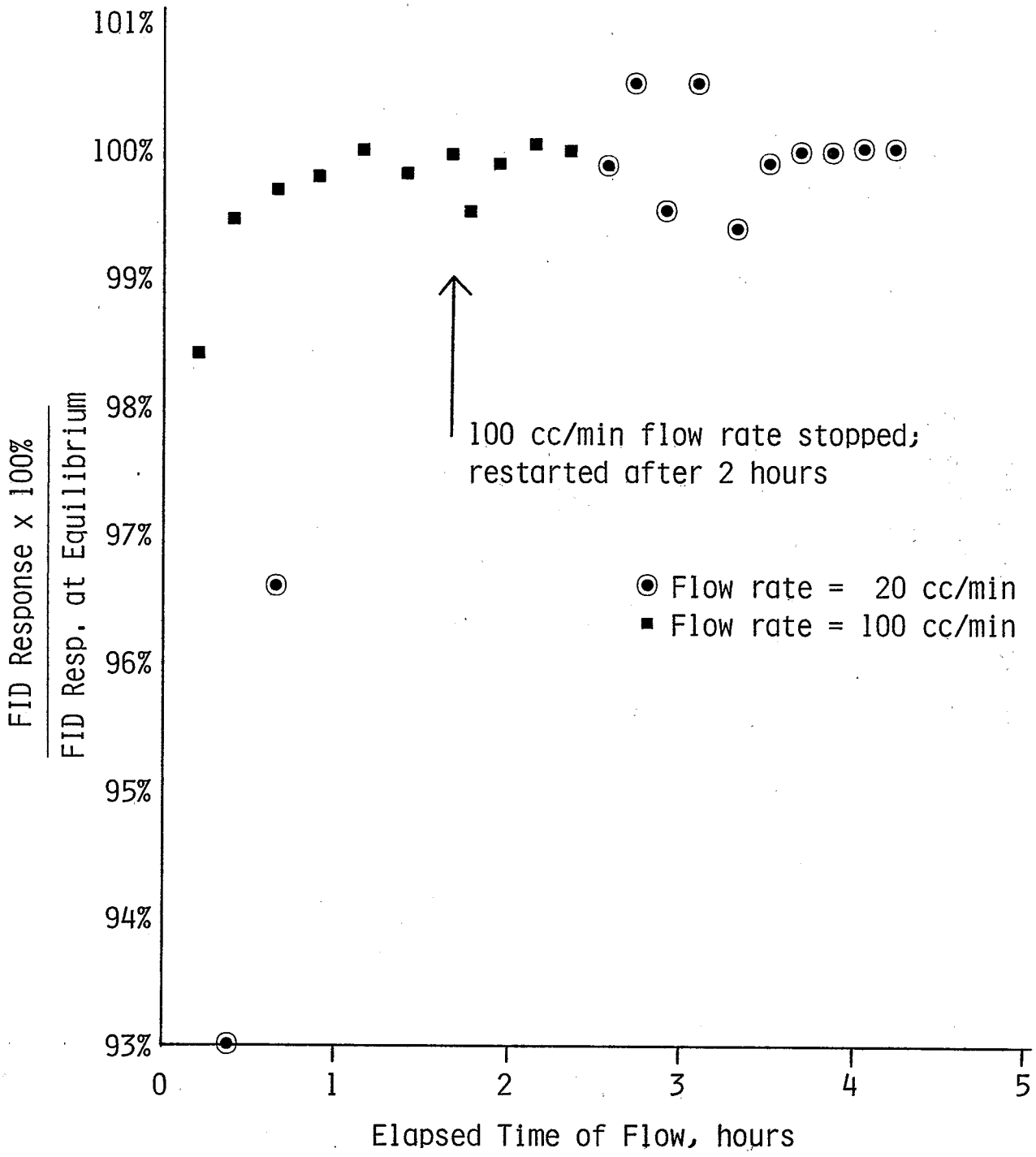

Figure 5. Effect of sample flow rate and flow volume on equilibration time of cylinder control valve for chlorobenzene.

mixtures have been prepared in both 0.85 cubic m (m^3)-size aluminum cylinders and, also, 4.25 m^3-size cylinders. The uncertainty in the accuracy of the standards prepared in the smaller cylinders was determined to be on the order of 5 to 10 percent due to the necessity of weighing microgram quantities of the organic reagent. Larger quantities of the organic were used in mixtures prepared in the larger cylinders, but the weight of these cylinders (∿25 Kg) precluded accurate (±0.5 percent rel.) weight determinations for the diluent gas. Higher concentration mixtures (0.2 to 15 ppm) were also prepared in these larger cylinders to detect any severe problems in the weight determination of the diluent gas. The estimated uncertainties in the accuracy of mixtures prepared in these 4.25 m^3 cylinders was about 3 percent.

These low-concentration mixtures were intercompared (GC-FID) with the higher concentration primary mixtures prepared in the 0.85 m^3 cylinders. A calibration curve was established using the FID response asnd the gravimetrically calculated concentration of the primary mixtures. The gravimetrically calculated and the analyzed concentrations of both the low-concentration mixtures and those mixtures prepared in the 4.25 m^3 cylinders are shown in Table 8. The uncertainties in the analyzed concentrations have not been completely ascertained at this time, but the agreement between the calculated and analytical concentrations demonstrates the feasibility of sample preparation at these levels.

DETERMINATION OF THE MINIMUM DETECTABLE LEVEL USING GAS MIXTURES PREPARED BY THE SUCCESSIVE DILUTION TECHNIQUE

To determine both the feasibility of the successive dilution method of preparation for low concentration mixtures and the sensitivity of the FID to low concentrations of various organic solvents, two primary mixtures that had become depressurized during analysis were diluted with nitrogen to produce low ppb concentration mixtures. The mixture in cylinder FF 9762 was diluted in three steps, each successive mixture being approximately one-tenth the concentration of the preceding mixture. The mixture in cylinder FF 9779 was diluted to one-thousandth of its original concentration in a single step. Final concentrations in both cylinders were approximately equal and ranged from 1 to 5 ppb. Typical GC-FID chromatograms for each of the mixtures are shown in Figure 6 with the retention times and approximate concentrations for each organic compound. The minimum detectable limits (useful primarily for calculations of the concentration of each compound in the diluent gas) are estimated to be:

VCM	2 ppb
chloroform	5 ppb
benzene	1 ppb
tetrachloroethylene	5 ppb
chlorobenzene	1 ppb

TABLE 8. COMPARISON OF GRAVIMETRICALLY CALCULATED AND ANALYZED CONCENTRATIONS FOR LOW-CONCENTRATION (<200 PPB) AND HIGH-CAPACITY CYLINDER MIXTURES

		VCM			Benzene			Tetrachloroethylene		
Cylinder no.	Cylinder capacity	Calculated conc.	Analyzed conc.	Δ, ppb	Calculated conc.	Analyzed conc.	Δ, ppb	Calculated conc.	Analyzed conc.	Δ, ppb
FF 9753	0.85 m^3	194 ppb	197 ppb	3						
FF 9498	0.85 m^3	73	72	-1						
FF 9779	0.85 m^3	11	7	-4						
FF 9755	0.85 m^3				45 ppb	47 ppb	2			
FF 9766	0.85 m^3							103 ppb	103 ppb	0
FF 9595	0.85 m^3							141	142	1
AAL 5915	4.25 m^3	638	633	-5	840	834	-6	1038	1040	2
AAL 5912	4.25 m^3	227	222	-5	258	251	-7			
AAL 6278	4.25 m^3				14765	14813	48	79	73	-6
AAL 6289	4.25 m^3				24	22	-2	9712	9700	-12

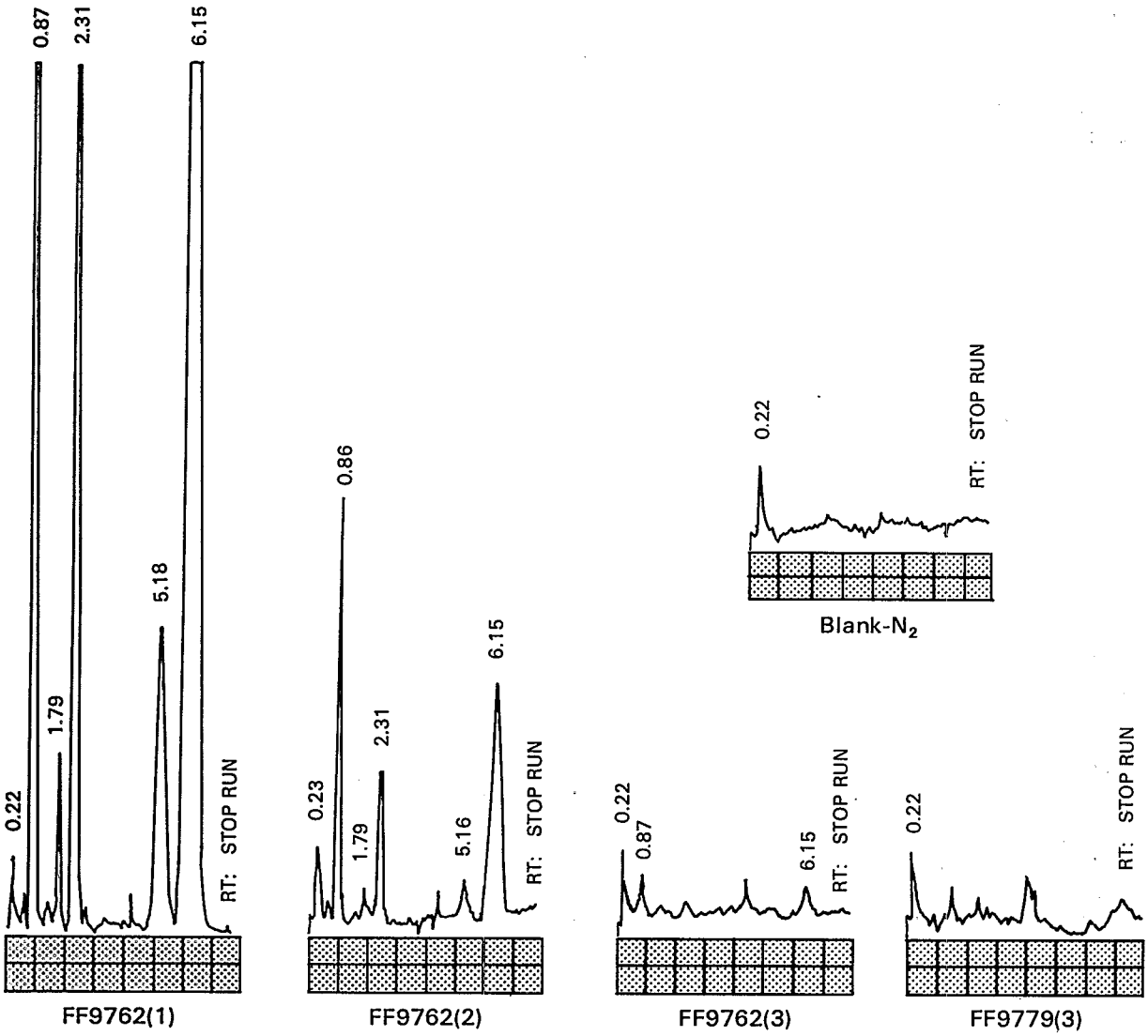

Solvent	Retention Time	FF9762 (1) Concentration	FF9762 (2) Concentration	FF9762 (3) Concentration	FF9779 (3) Concentration
VCM	0.9 min	420 ppb	46 ppb	5 ppb	1 ppb
$CHCl_3$	1.8 min	71 ppb	8 ppb	1 ppb	1 ppb
Benzene	2.3 min	70 ppb	8 ppb	1 ppb	1 ppb
C_2Cl_4	5.2 min	92 ppb	10 ppb	1 ppb	1 ppb
Chloro-benzene	6.2 min	241 ppb	26 ppb	3 ppb	1 ppb

Figure 6. GC-FID chromatograms of low concentration mixtures prepared by diluting primary standards.

The lowest concentrations that can be analyzed using a 5-cc sample loop and a simple (non-preconcentrating) gas injection are estimated to be approximately five times the minimum detectable levels.

The lowest concentration of each organic compound that has been prepared and analyzed and the uncertainty (1σ) in the average of the FID response to replicate 5-cc samples of each is shown below:

Compound	Concentration	Uncertainty
VCM	11 ppb	± 0.6 ppb
chloroform	70 ppb	± 4 ppb
benzene	22 ppb	± 0.4 ppb
tetrachloroethylene	80 ppb	± 2 ppb
chlorobenzene	53 ppb	± 1 ppb

STABILITY OF PRIMARY GAS MIXTURES

The stability of the primary gas mixtures for various periods of time was demonstrated by the lack of change in the relative ratios of the FID response to the gravimetrically calculated concentrations of mixtures prepared at intervals during the course of the study (Tables 2 through 4). For example, mixtures containing chlorobenzene were prepared during 8/80 and were compared with freshly prepared mixtures in 1/81 to determine short- term (5 months) stability. These mixtures were later compared with freshly prepared mixtures in 9/81 to determine long-term stability (12 months). The stability of the mixtures was determined by the lack of a significant change in the analyzed concentrations when compared with the freshly prepared mixtures at the intervals specified. No systematic change in concentration with time was observed for any of the seven organic solvents for which the stability study had been completed.

PERMEATION TUBE CALIBRATION

A set of 100 permeation tubes containing benzene has been calibrated by both gravimetry and comparison with primary mixtures using GC-FID. The results of the calibration of 17 representative tubes from the set are shown in Table 9. The average uncertainty (2σ) in the gravimetric calibrations for these tubes was approximately ±3 percent (relative). The estimated total uncertainty (2σ) in the calibration performed by the comparison with the primary mixtures was ±2 percent (relative). The disagreement between the gravimetric and the comparative calibrations was less than ±1 percent (relative) (Table 9). The precision with which permeation tubes can be intercompared by FID (as shown in Table 9) is better than ±0.5 percent (relative) for all tubes except #1-3. The discrepancy in the calibration data for this tube can not be satisfactorily explained at this time,

TABLE 9. CALIBRATION OF BENZENE PERMEATION TUBES AT 25.0°C. RATES DETERMINED BY GRAVIMETRY AND BY COMPARISON WITH PRIMARY GAS CYLINDER STANDARDS

Permeation tube no.	Permeation rate, 25.0 °C (gravimetric)	FID* response dilution flow = 100 cc/min	Permeation rate, 25.0 °C FID (vs. grav. stds.)	Δ permeation rate (FID - grav.)
3	0.338 μg/min	2504	0.343 μg/min	1.5 % Rel.
5	0.369	2710	0.371	0.5
12	0.355	2600	0.356	0.3
13	0.355	2610	0.357	0.6
20	0.343	2512	0.344	0.2
22	0.372	2711	0.371	-0.2
26	0.358	2618	0.358	0.0
31	0.341	2492	0.341	0.0
53	0.341	2494	0.341	0.0
54	0.356	2595	0.355	-0.2
58	0.371	2713	0.372	0.2
66	0.377	2756	0.377	0.0
70	0.360	2638	0.361	0.3
76	0.339	2494	0.341	0.7
82	0.347	2527	0.346	-0.3
85	0.365	2658	0.364	-0.4
86	0.368	2696	0.369	0.3

*Flame ionization detector.

but this tube had been subjected to higher-than-ambient pressure for a period of several weeks. An effort will be made to quantify the effect of pressure on permeation tube output in the near future.

The demonstrated ability to calibrate permeation tubes by comparison with primary mixtures using GC-FID gives more flexibility to the analysis of environmental effects on the permeation rate. A calibration of permeation rate may be performed in 1/2 hour instead of several weeks. The effects of temperature cycling, flow rate of purge gas, pressure (as mentioned above), and storage parameters can now be determined accurately and quickly.

STANDARD REFERENCE MATERIALS (SRM's) FOR TOXIC ORGANICS

Four sets (50 cylinders each) of gas mixtures containing benzene and tetrachloroethylene at nominal concentrations of 0.25 and 9.5 ppm have been received for the certification process leading to their issuance as SRM's. The concentrations of these mixtures as determined from their comparison with the primary gravimetric gas mixtures are shown in Table 10.

TABLE 10. COMPARISON OF NOMINAL AND ANALYZED CONCENTRATIONS FOR TOXIC ORGANIC SRM's

Cylinder no.	Organic matrix	Nominal concentration	Analyzed concentration
CAL 7216	Tetrachloroethylene	9.5 ppm	9.86 ppm
CAL 6603	Nitrogen		9.82 ppm
CAL 6522			9.83 ppm
CAL 6485	Tetrachloroethylene	0.25 ppm	0.26 ppm
CAL 6499	Nitrogen		0.25 ppm
CAL 6599	Benzene	9.5 ppm	9.79 ppm
	Nitrogen		
CAL 5718	Benzene	0.25 ppm	0.26 ppm
CAL 5715	Nitrogen		0.25 ppm

SUMMARY

Primary gas mixtures have been prepared for seven organic solvents. Increased sophistication in the preparation technique has enabled the preparation of multi-component mixtures with both a large number of components and a greater confidence in the accuracy of the calculated concentrations. Stability studies performed using these mixtures have shown no significant changes in concentration with time over periods of 1 to 2 years.

Permeation tubes have been calibrated by both gravimetry and comparison with primary gas cylinder mixtures using GC-FID. No significant differences were observed between the permeation rates that were obtained by these methods. In the future, permeation tubes can be calibrated by GC-FID comparisons alone, thereby decreasing the time needed for calibration and increasing the flexibility of the calibration procedure.

Accurate low-concentration (0.05 to 0.2 ppm) gas mixtures have been prepared gravimetrically in both 0.85 m^3 and 4.25 m^3 cylinders. The procedure employed in the above preparation appears adequate to prepare samples at low ppb concentration levels.

REFERENCES

1. McGaughey, J.F., A.L. Sykes, D.E. Wagoner, and C.E. Decker. 1979. Research Triangle Institute Report 1808/13-01. Research Triangle Park, NC.

HUMAN EXPOSURE TO VAPOR-PHASE HALOGENATED HYDROCARBONS: FIXED-SITE VS PERSONAL EXPOSURE

E.D. Pellizzari, T.D. Hartwell, C. Leininger, H. Zelon, and S. Williams

Research Triangle Institute
Research Triangle Park, NC

and

J.J. Breen and L. Wallace

U.S. Environmental Protection Agency
Washington, DC

INTRODUCTION

During the past five years, we have been investigating the personal exposure of populations to toxic chemicals, and assessing methods for their analysis in air, water, food, blood, urine, and breath. We have previously reported on preliminary studies of human exposure to benzene and other volatile organics (1-3). Benzene was monitored in lay people in Houston, Texas, and Wood River, Illinois (1), while volatile organics were measured in student populations in Beaumont, Texas, and Chapel Hill, North Carolina (2), and in a nine-person group in Elizabeth and Bayonne, New Jersey (3).

In a larger study, we have investigated the major pathways that contribute to human exposure to volatile halogenated hydrocarbons for populations in two different geographical areas. Although this program addresses the integrated exposure and body burden in populations by measuring volatile halocarbons in the air a person breathes and the water he drinks, and the parent halocarbons and important metabolites in the person's breath, blood, and urine, we wish to report our findings on one route of exposure, air. This paper addresses the use of personal and fixed-station monitoring for assessing exposure of populations to halocarbons. The relative merits of each are discussed.

EXPERIMENTAL

Areas and Halocarbons Selected for Monitoring

Table 1 lists the areas and halocarbons selected for monitoring in

TABLE 1. GEOGRAPHICAL AREAS AND HALOCARBONS MONITORED IN PERSONAL AND FIXED-SITE AIR

Greensboro, NC	Baton Rouge/Geismar, LA
Vinylidene chloride	Vinylidene chloride
Chloroform	Chloroform
Chloroprene	Chloroprene
1,2-Dichloroethylene	1,2-Dichloroethylene
1,2-Dichloroethane	1,2-Dichloroethane
1,1,1-Trichloroethane	1,1,1-Trichloroethane
Carbon tetrachloride	Carbon tetrachloride
1,2-Dichloropropane	1,2-Dichloropropane
Trichloroethylene	Trichloroethylene
Bromodichloromethane	Bromodichloromethane
Dichlorobutane isomer	Dichlorobutane isomer
1,1,2-Trichloroethane	1,1,2-Trichloroethane
Chlorodibromomethane	Chlorodibromomethane
Trichlorobutane isomers	Trichlorobutane isomers
Tetrarchloroethylene	Tetrachloroethylene
Bromodichloroethane	Bromodichloroethane
Chlorobenzene	Chlorobenzene
Bromoform	Bromoform
Chlorobenzotrifluoride isomers	Chlorobenzotrifluoride isomers
1,1,2,2-Tetrachloroethane	1,1,2,2-Tetrachloroethane
Bromobenzene	Bromobenzene
Chlorotoluene isomers	Chlorotoluene isomers
Dichlorobenzene isomers	Dichlorobenzene isomers
Hexachloroethane	
Trichloropentane isomers	
Bis-(Chloroisopropyl)ether	
Chloronitrobenzene	
Methyldichlorophenoxy acetate	
Trichlorohexane isomers	
Dichlorotoluene isomers	
Bromopropylbenzene	
Trichlorobenzene isomers	
1,3-Hexachlorobutadiene	
Trichlorotoluene isomers	
Tetrachlorobenzene isomers	

air. Ambient monitoring data were surveyed (4) and the more prevalent halocarbons were then assessed as to biological activity (4,5). For each halocarbon, potential carcinogenicity and mutagenicity were ascertained from literature reports, and those halocarbons exhibiting activity were included in the monitoring effort (4).

Sample Design

The population in Greensboro, North Carolina was stratified according to three socioeconomic categories, and Baton Rouge/Geismar, Louisiana was stratified relative to suspected point sources of halocarbons of interest. The between-site differences in stratification occurred because Greensboro was considered a reference area with no known major point sources. Figure 1 depicts an example of a stratified area for Baton Rouge and Geismar. This approach considered the U.S. Census data for each area, the average wind rose for the season under study, and potential point sources in the areas.

Counting and listing of households in these areas was then conducted. Households were screened to identify those houses that contained at least one eligible individual. People were considered eligible if they were non-occupationally exposed (to the halocarbons under study), non-smoking adults between the ages of 45 and 64 who had lived in the area for at least one year. In Greensboro, 374 households were screened to yield 101 eligible housing units; 721 households were screened in Baton Rouge/Geismar, producing 190 eligible housing units. Participants were then selected from those persons eligible within the eligible households; final sample sizes were 28 and 66 people, respectively, for Greensboro and for Baton Rouge/Geismar. A probability sample was drawn from the screened households for the stratification variables, and the individuals were solicited to participate in the exposure monitoring effort. Field interviews were performed with each participant, and a demographic questionnaire was administered.

Sampling and Analysis

Acquisition of air samples was conducted during the months of October and November, 1980, in Greensboro, and during January and February, 1981, in Baton Rouge/Geismar. Two sampling periods for ambient air (an overnight and daytime period) were used with each participant. Each period was approximately 11 to 13 hours, with a personal air and a fixed-site air sample collected, concurrently. To collect personal air samples, the volunteer wore a vest equipped with a collection system as shown in Figure 2. The sampling train consisted of a Tenax GC cartridge (6,7) with a prefilter for removing particulate and a small, personal air pump (DuPont Model No. P125 or MSA C-200). The fixed-site sampler was identical to the personal air sampler (Figure 3), except that it was placed outside in the participant's yard for the entire time period. In general, a fixed-site sampler represented a cluster of participants (one to three); however, it always matched a personal sample for at least one participant in each cluster. A nominal sampling rate of 35 mL/min was used; approximately 25 L was sampled per time period.

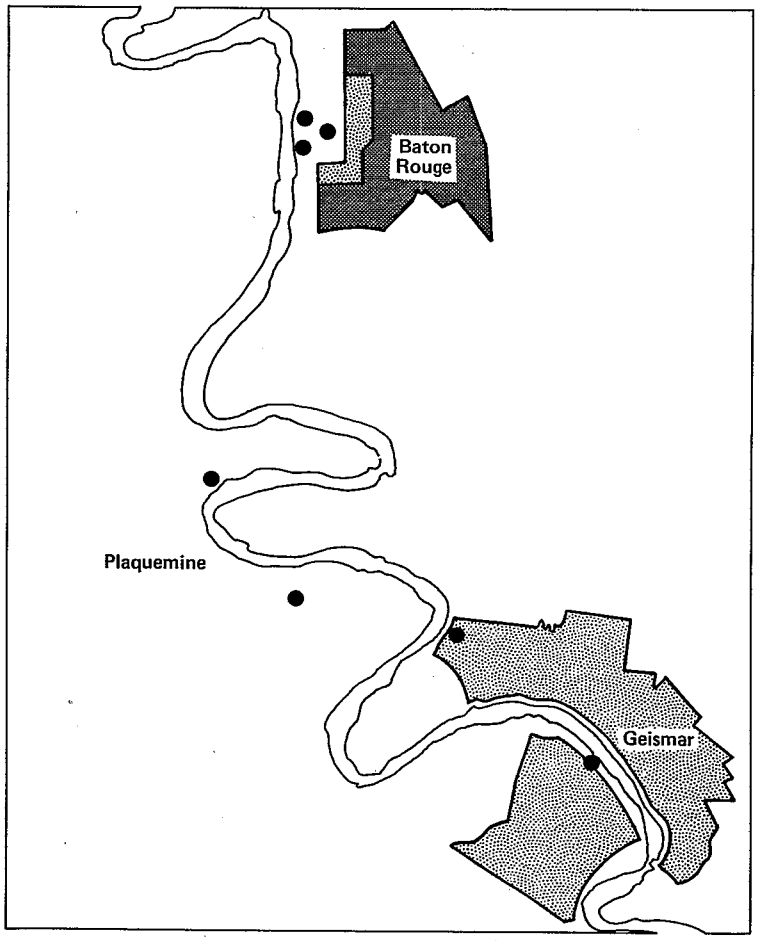

Figure 1. Stratified populations in Baton Rouge and Geismar, LA. Solid circles = suspected sources, light and dark areas represent potentially high- and low-exposure areas (distance between sites not to scale).

Table 2 lists the number of samples obtained by category for each geographical area. In Greensboro, 28 participants were sampled, while 66 people were included in Baton Rouge/Geismar. In addition to primary samples, duplicate samples were also collected.

Analysis of air samples was performed by gas-liquid chromatography/mass spectrometry/computer techniques, as previously reported (6,7).

Quality Control/Assurance

A quality control and assurance program (QC/QA) was maintained for the sampling and analysis procedures. Table 3 gives the major categories of the QC/QA program. For Tenax GC cartridges, laboratory and field blanks

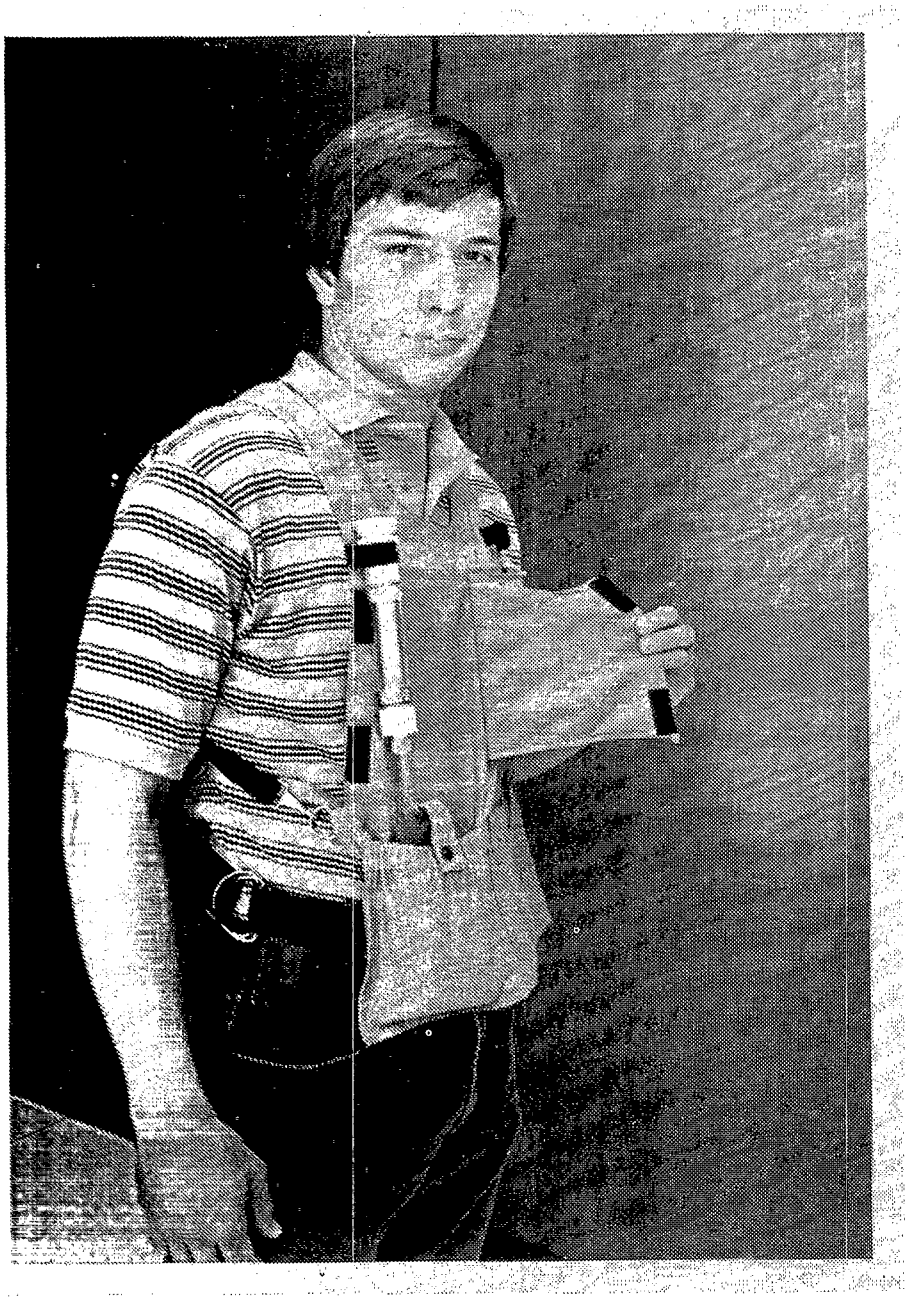

Figure 2. Vest equipped with Tenax GC sampling cartridge, prefilter for particulate and personal pump (in pocket) for collecting vapor-phase halocarbons in personal air.

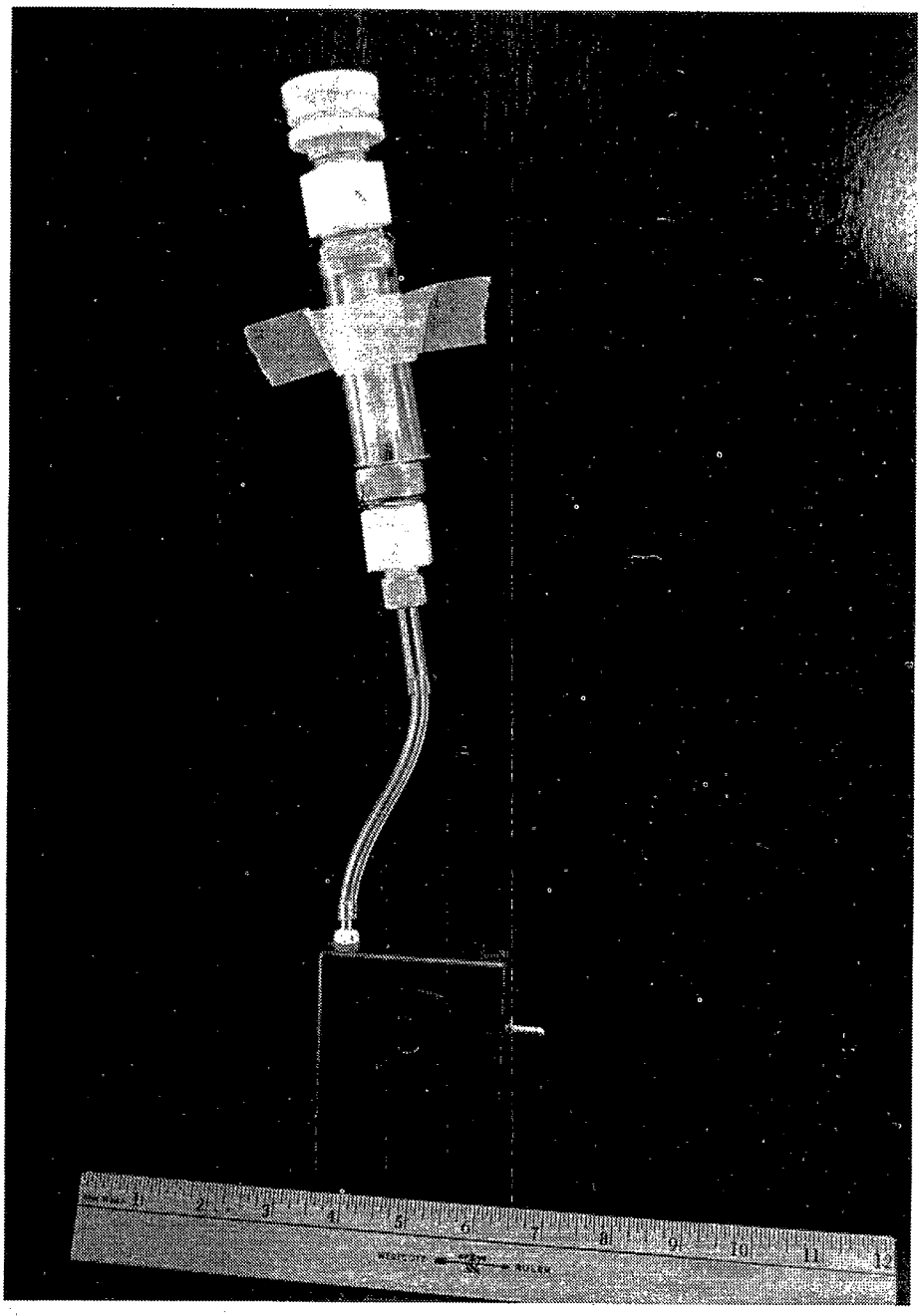

Figure 3. Sampling system depicting filter, Tenax GC cartridge and pump for collecting fixed-site air samples.

TABLE 2. NUMBER OF SAMPLES OBTAINED BY CATEGORY FOR EACH GEOGRAPHICAL AREA*

	Greensboro		Baton Rouge/Geismar	
Sample type	Primary	Duplicate	Primary	Duplicate
Personal Air	53	6	132	19
Fixed-Site Air	37	23	55	11

*Also, an additional 10 percent of the samples in each category were control samples and 10 percent were blanks.

TABLE 3. QUALITY CONTROL/QUALITY ASSURANCE

Tenax GC Cartridges

- laboratory blanks
- field blanks
- laboratory controls (spiked with target halocarbons)
- field controls (spiked with target halocarbons)

Replicate samples

Audit of sampling and analytical systems

- pump flow rates
- battery charge
- GC/MS performance specifications and control charts

were maintained. These were sampling cartridges selected from a batch preparation (∿30-50) of cartridges to demonstrate the potential background, if any, that might develop during the period of sampling and analysis. Field blanks were sampling cartridges transported to the field and returned to the laboratory unused, and analyzed, while laboratory blanks were stored during the entire period. Thus, some indication of the potential contamination that might occur, not only within a batch of cartridges, but also from the influence of transportation was obtained.

Laboratory and field controls were also maintained for each batch production of Tenax GC cartridges. Controls were sampling cartridges spiked with the list of target halocarbons.

Replicate samples (Table 2) of personal and fixed-site air were collected; in general, a minimum of 10 percent were acquired. Also, 10 percent of the total samples collected also had a representative number of blanks and controls.

Each sampling train was internally audited before, during, and after sampling in each geographical area. Flow rates were checked with a bubble meter to assure that the proper rates were attained. Battery charge was verified on personal samplers to ensure that the flow rates were maintained for each sampling period. Recharging was instituted after each sampling period.

A chain-of-custody procedure was maintained for each sample, blank and control, throughout the period of sampling and analysis.

RESULTS AND DISCUSSION

The recoveries of target halocarbons from control sampling cartridges for Greensboro and Baton Rouge/Geismar are given in Tables 4 and 5. The data are mean recoveries and percent relative standard deviations for each halocarbon, representing the entire time period from preparation to their analysis, along with field samples. In some cases, the time span reached a period of five weeks. In general, acceptable recoveries were obtained, and thus, none of the field sample data were corrected for this potential bias in accuracy.

TABLE 4. RECOVERY OF HALOGENATED CHEMICALS FROM CONTROL SAMPLING CARTRIDGES - GREENSBORO, NC STUDY

Halogenated chemical	% Recovery ± S.D. (%RSD)*
Chloroform	79 ± 10 (13)
1,2-Dichloroethane	93 ± 8 (9)
Trichloroethylene	102 ± 7 (7)
Tetrachloroethylene	115 ± 14 (12)
1,1,1-Trichloroethane	111 ± 21 (19)
1,2-Dichloroethylene	81 ± 12 (15)
Carbon tetrachloride	79 ± 15 (19)
1,1,2-Trichloroethane	105 ± 19 (18)
1,1,2,2-Tetrachloroethane	92 ± 2 (2)
Chloroprene	93 ± 5 (5)
Chlorobenzene	102 ± 12 (12)
p-Chlorotoluene	94 ± 11 (12)
Bromodichloromethane	88 ± 14 (16)
Hexachlorobutadiene	111 ± 33 (30)
1,3,5-Trichlorobenzene	125 ± 13 (10)
2,4-Dichlorotoluene	102 ± 34 (33)
1,2-Dichloropropane	112 ± 9 (8)

*N = 9.

Replicate field samples for personal and fixed-site air were analyzed for precision. These data are presented in Figures 4 through 9. Only field duplicate samples that yielded measurable values in both samples are

TABLE 5. RECOVERY OF HALOGENATED CHEMICALS FROM CONTROL SAMPLING CARTRIDGES - BATON ROUGE/GEISMAR, LA STUDY

Halogenated chemicals	% Recovery ± S.D. (%RSD)*
Chloroform	63 ± 15 (23)
1,2-Dichloroethane	102 ± 23 (22)
Trichloroethylene	109 ± 23 (21)
Tetrachloroethylene	98 ± 16 (16)
1,1,1-Trichloroethane	92 ± 23 (25)
Carbon tetrachloride	98 ± 18 (18)
1,1,2-Trichloroethane	100 ± 24 (24)
1,1,2,2-Tetrachloroethane	116 ± 15 (13)
1,2-Dichloropropane	81 ± 25 (31)

*N = 16.

represented; non-measurable or trace values were omitted. Thus, for many chemicals, insufficient data were available for performing linear regression analysis. Figure 4 depicts the replicates for tetrachloroethylene measured in Greensboro samples. The data are plotted on a log-log scale. Linear regression analysis of these data reveals a correlation (r) of 0.990 and 0.997 for fixed-site and personal air samples, respectively. Included are ±25 and ±50 percent limits from the 45° line.

As indicated in each figure (4 through 9) a reasonable correlation was obtained between each measurement. For 1,1,1-trichlorethane (Figure 5), two sets of duplicates were considerably removed from the 45° line; however, acceptable linear correlations were obtained for both personal and fixed-site samples due to the relatively large range of compound values.

The limits of detection (LOD) and quantifiable limits (QL) were, for initial analysis, arbitrarily defined as 4 σ (signal:noise) and 16 σ, respectively. Thus, measurements below the LOD were reported as non-measurables, and those between 4 σ and 16 σ, as trace (T) levels. Only numerical values above 16 σ were reported.

Summary Statistics

Tables 6 and 7 give the halocarbon levels in personal and fixed-site air samples for Greensboro and Baton Rouge/Geismar, respectively. All measurements for the overnight and daytime period are presented; however, only measurements above the LOD were used to calculate the mean, standard deviation, and median. Trace values were entered as the midpoint between the LOD and the QL in these calculations. These summary statistics for fixed-site and personal air samples are preliminary data. They are not necessarily accurate estimates of the study populations, since the weighting factors for the sample selection design have not been included. Similarly, the statistical tests must be based on assumption of simple random sampling and thus are tenuous, given the stratified cluster design. Nevertheless, the general conclusions are sufficiently accurate for an

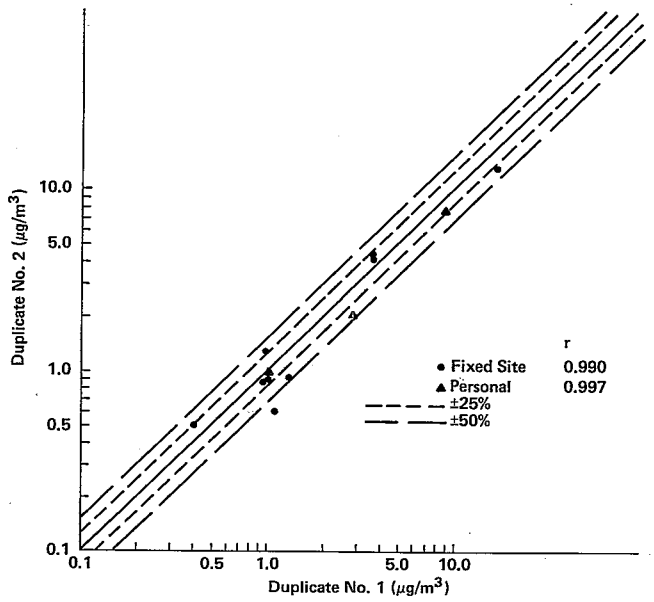

Figure 4. Replicate samples for Tetrachloroethylene - Greensboro, NC study (— is 45° line).

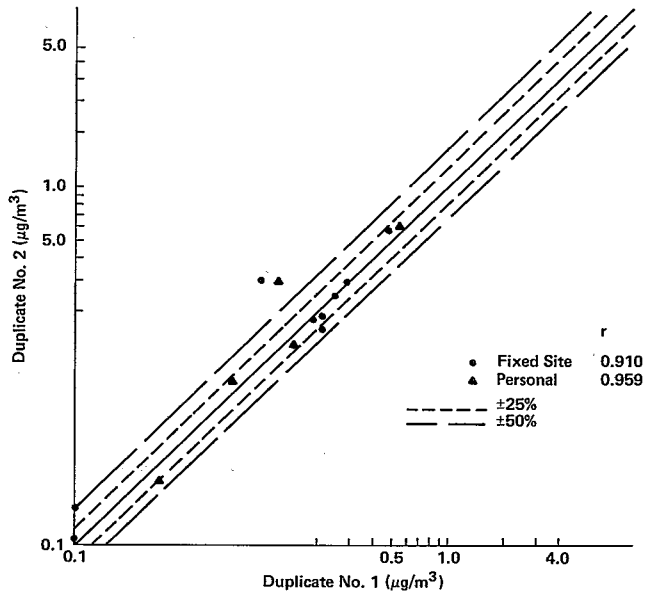

Figure 5. Replicate samples for 1,1,1-Trichloroethane - Greensboro, NC study (— is 45° line).

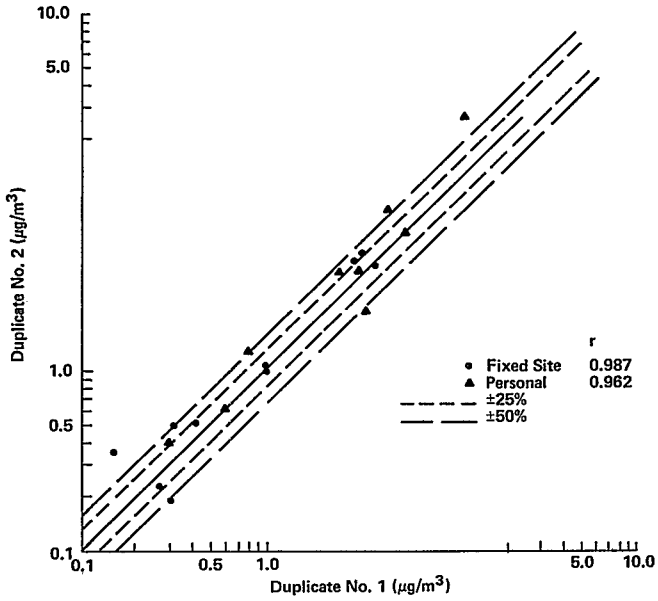

Figure 6. Replicate samples for Chloroform - Greensboro, NC study (—— is 45° line).

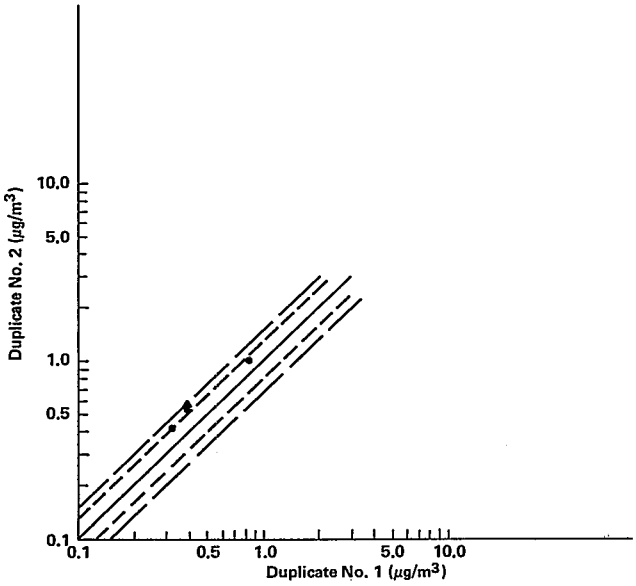

Figure 7. Replicate samples for Carbon tetrachloride - Greensboro, NC study (— is 45° line).

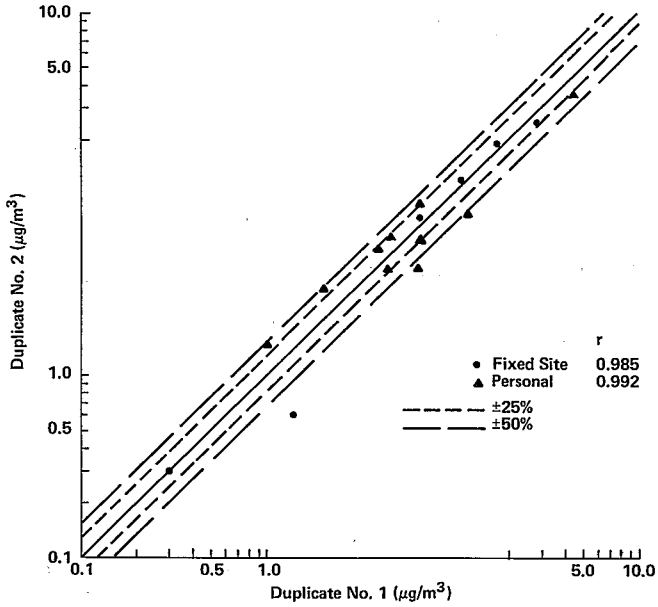

Figure 8. Replicate samples for 1,2-Dichloroethane - Baton Rouge/Geismar, LA study (— is 45° line).

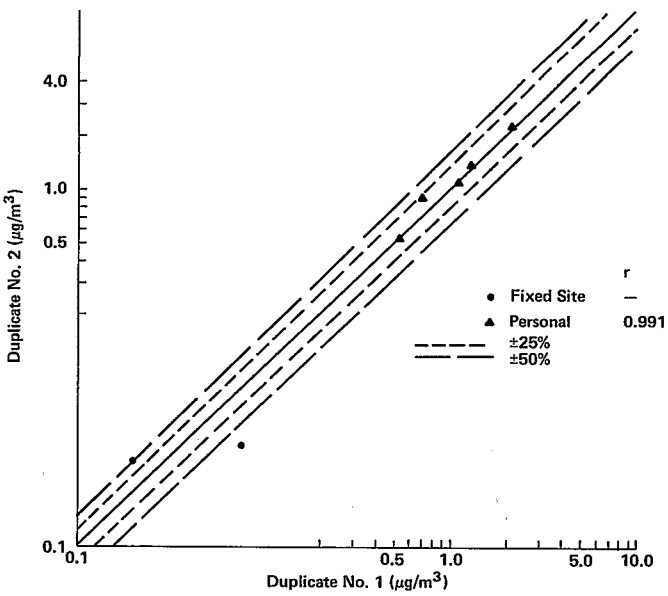

Figure 9. Replicate samples for 1,2-Dichloroethane - Greensboro, NC study (— is 45° line).

TABLE 6. HALOCARBON LEVELS ($\mu g/m^3$) IN AIR FOR GREENSBORO, NC STUDY: FIXED-SITE VS. PERSONAL SAMPLES*

Chemical	Fixed					Personal				
	N(LOD,QL)†	Range	Mean	±S.D.	Median	N(LOD,QL)	Range	Mean	±S.D.	Median
Chloroform	41 (21,1)	0.03-8.9	1.1	±1.9	0.43	53 (5,0)	0.03-26	4.4	±4.8	3.0
1,2-Dichloroethane	41 (24,0)	0.03-13	0.91	±3.1	0.11	53 (35,0)	0.03-140	11	±33	0.22
1,1,1-Trichloroethane	41 (10,0)	0.06-52	5.2	±10	1.9	53 (2,0)	0.06-11000	240	±1500	10
Carbon tetrachloride	41 (21,0)	0.04-1.7	0.63	±0.39	0.50	53 (21,1)	0.03-1300	42	±230	0.61
Trichloroethylene	41 (24,0)	0.03-1.0	0.27	±0.27	0.15	53 (22,3)	0.03-14	1.9	±3.1	0.61
Chlorobenzene	41 (22,0)	0.02-0.60	0.17	±0.18	0.11	53 (34,0)	0.01-7.0	0.63	±1.6	0.12
Dichlorobenzene isomer	41 (22,0)	0.003-1.4	0.44	±0.45	0.23	53 (26,0)	0.02-260	24	±53	4.0
Tetrachloroethylene	41 (9,0)	0.02-21	2.5	±4.4	1.1	53 (1,2)	0.02-54	6.1	±8.8	2.5

*All measurements are used to express the range; only measurements above the LOD are used to calculate the mean, standard deviation, and median.
†LOD = number of measurements below the limit of detection; QL = number of measurements for which a trace was found.

TABLE 7. HALOCARBON LEVELS ($\mu g/m^3$) IN AIR FOR BATON ROUGE/GEISMAR, LA STUDY: FIXED-SITE VS. PERSONAL SAMPLES*

Chemical	Fixed					Personal				
	N(LOD,QL)†	Range	Mean	±S.D.	Median	N(LOD,QL)	Range	Mean	±S.D.	Median
Vinylidene chloride	57 (15,5)	0.10-4.6	0.48	±0.67	0.40	132 (86,31)	0.05-25	2.4	±4.3	1.0
Chloroform	57 (48,1)	0.02-9.3	2.7	±2.9	1.4	132 (108,1)	0.03-47	11	±13	6.3
1,2-Dichloroethane	57 (1,0)	0.10-54	6.0	±11	2.2	132 (9,16)	0.05-69	7.2	±11	3.6
1,1,1-Trichloroethane	56 (24,2)	0.08-73	5.6	±13	1.6	131 (59,6)	0.08-492	43	±84	12
Carbon tetrachloride	57 (30,4)	0.05-24	2.4	±4.6	0.9	132 (39,39)	0.08-35	2.3	±4.4	1
Tetrachloroethylene	55 (42,0)	0.08-33	6.1	±10	1.5	131 (37,26)	0.05-69	4.4	±9.9	1.4
1,2-Dichloropropane	57 (36,5)	0.03-6.3	1.3	±1.8	0.50	132 (73,46)	0.03-5.7	0.52	±0.81	0.31
Dichlorobenzene isomer	57 (51,1)	0.01-3.8	1.5	±1.4	1.2	132 (8,22)	0.05-351	34	±73	4

*All measurements are used to express the range; only measurements above the LOD are used to calculate the mean, standard deviation, and median.
†LOD = number of measurements below limit of detection; QL = number of measurements for which a trace was found.

exploratory analysis of this nature. A weighted analysis will be reported elsewhere. Although the list of target compounds monitored was larger than presented here, these halocarbons were the principal ones that yielded measurable values. For each halocarbon, the LOD was very close, if not identical, between personal and fixed-site samples within a geographical area. However, they differed significantly between areas and thus such comparisons are not made here.

As indicated by the means and medians, personal air samples appeared to yield higher absolute levels than fixed-site samples within a geographical area. These trends were, of course, also reflected in their ranges. Because of these trends, we examined personal versus fixed-site sample values in more detail to elucidate the significance of these data.

Comparison of Personal and Fixed-Site Data

In order to uncover trends in these data, an assorted number of statistical analyses were performed, first examining data for overall trends; then, detailed stratifications of data were tested for significance.

The frequency distribution for all air values (duplicates were averaged) from personal and fixed-site monitors were plotted for a few of the halocarbons. Figures 10 through 12 depict results for 1,1,1-trichloroethane, tetrachlorethylene, and trichloroethylene, respectively. It is seen clearly from these frequency distributions that personal samples yield higher values over the major part of the dynamic range than do fixed-site samples for both the Greensboro and Baton Rouge/Geismar areas.

Figures 13 and 14 show bar diagrams for a comparison of the percent detected between personal and fixed-site air samples in the Greensboro and Baton Rouge/Geismar areas, respectively.

In Figure 13, the comparisons are for (left to right) chloroform, methylchloroform, bromodichloromethane, tetrachloroethylene, chlorotoluene isomers, dichlorotoluene isomers, trichlorobenzene isomers, carbon tetrachloride, trichloroethylene, 1,1,2,2-tetrachloroethane, dichlorobenzene, 1,2-dichloroethane, and chlorobenzene. The percent detected for many of the halocarbons were statistically significant (indicated by asterisks) between personal and fixed-site samples. These data represent 53 personal and 37 fixed-site samples. Except for 1,2-dichloroethane and chlorobenzene, the personal air sample exhibited a higher percent detected.

The same phenomenon was observed with personal and fixed-site samples from Baton Rouge/Geismar (Figure 14). For many halocarbons, the percent detected in personal air samples was higher than fixed-site and statistically significant at the 0.05 level. The reverse trend was observed for three halocarbons, 1,2-dichloroethane, 1,1,2-trichloroethane, and vinylidene chloride. In fact, the fixed-site percent detected for vinylidene chloride was significantly greater (0.05 level) than for the personal air samples. A point source for these three halocarbons was suspected and may be responsible for this association.

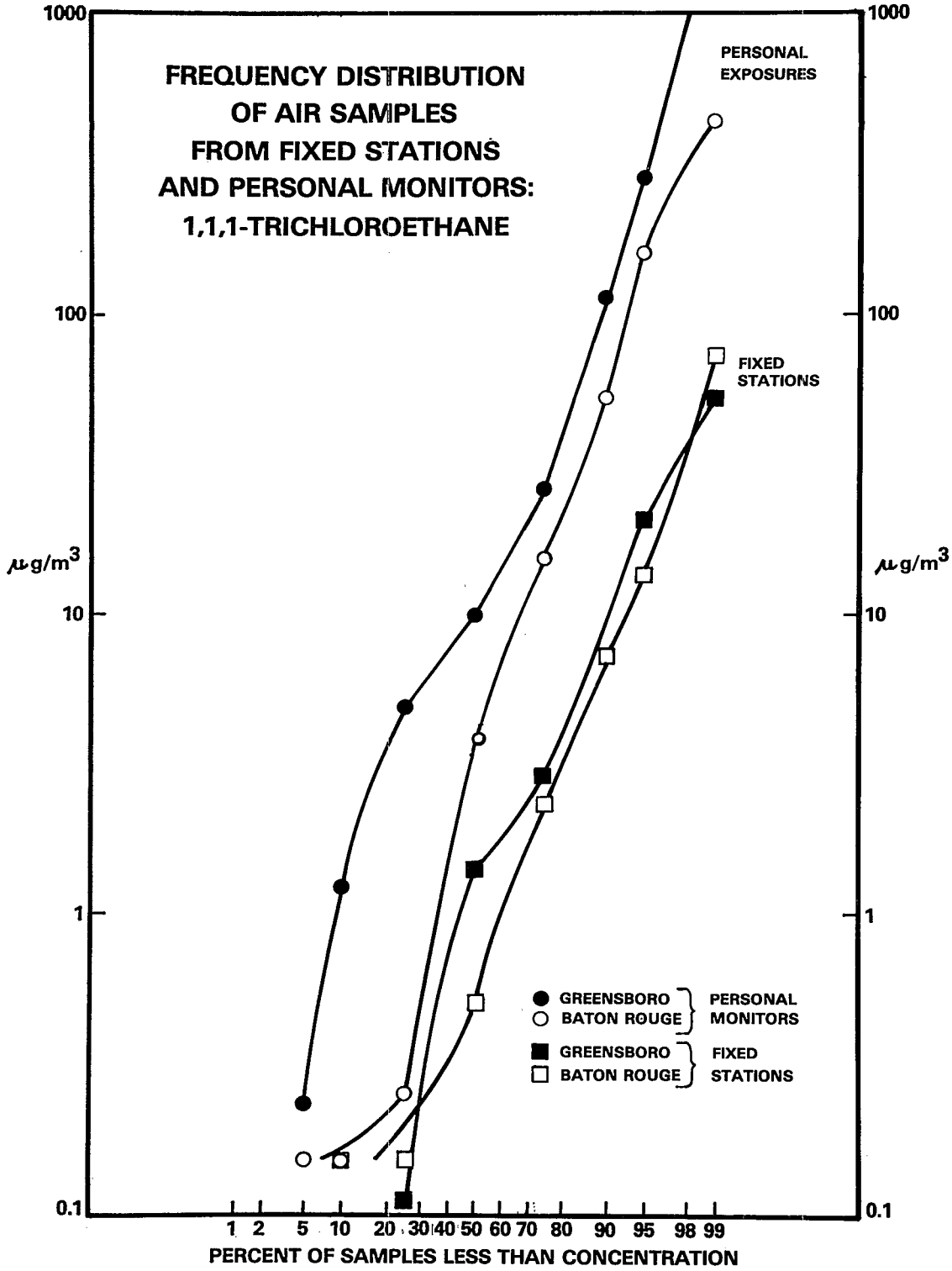

Figure 10. Frequency distribution for 1,1,1-Trichloroethane.

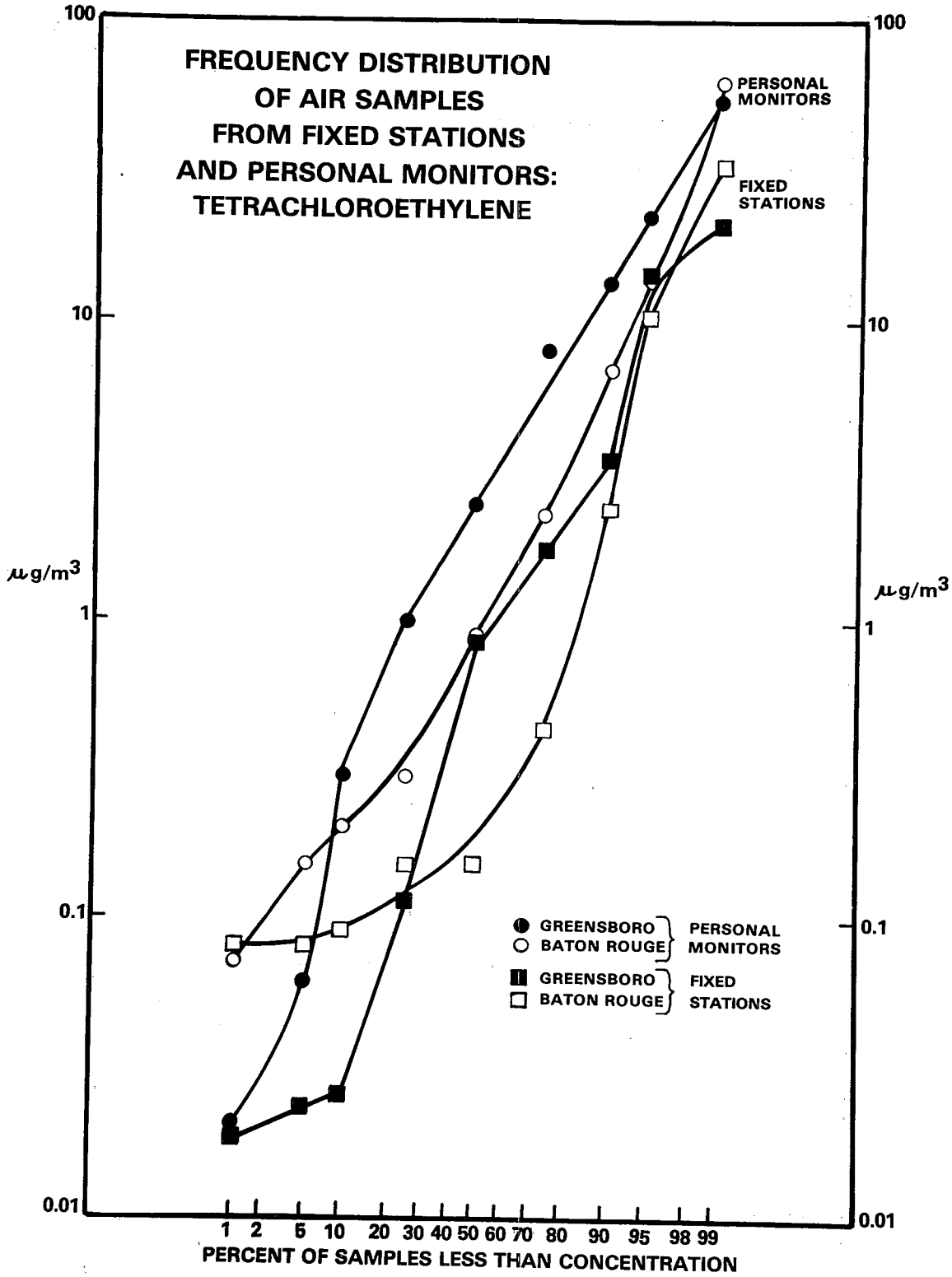

Figure 11. Frequency distribution for Tetrachloroethylene.

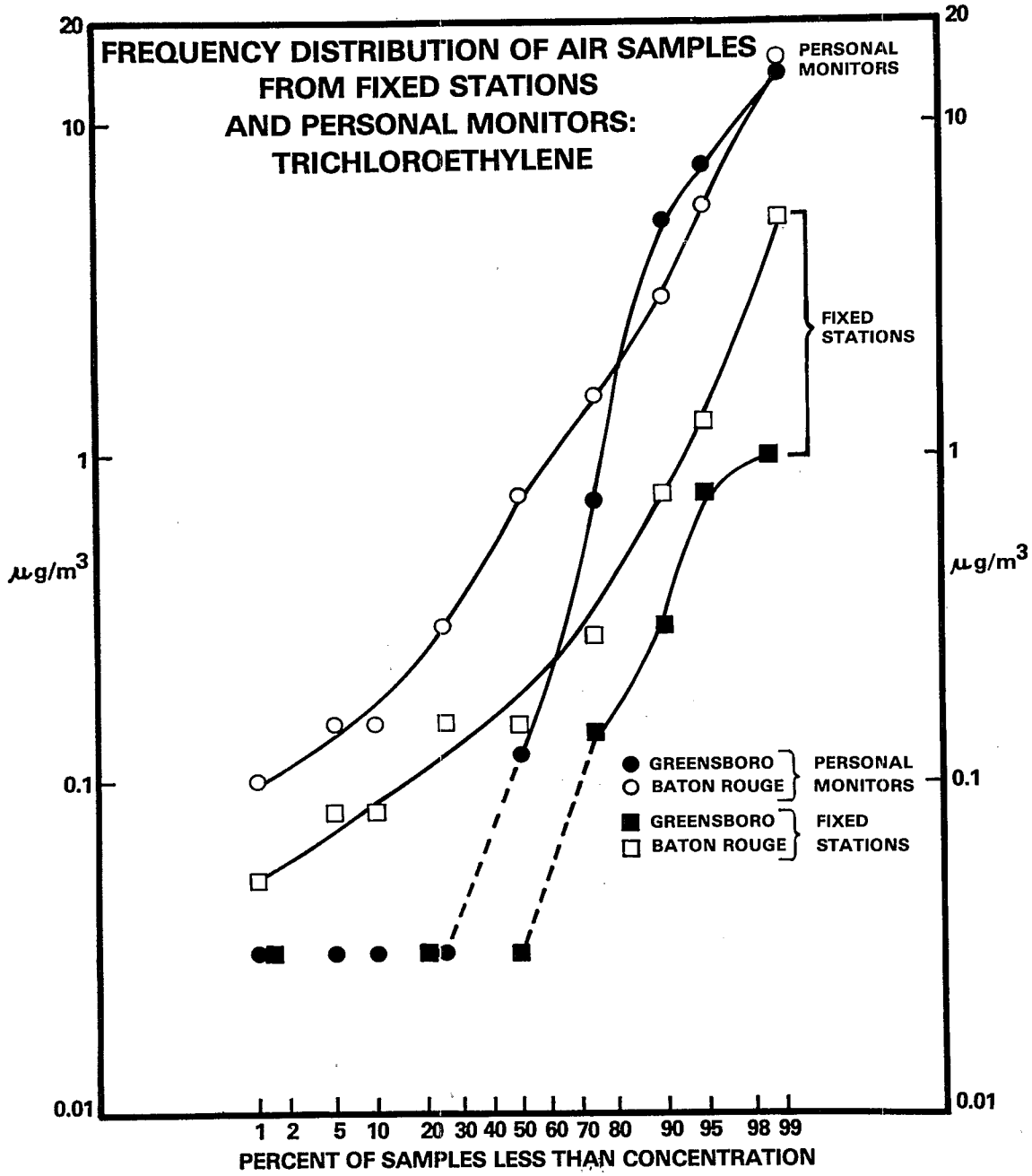

Figure 12. Frequency distribution for Trichloroethylene (dashed lines are extrapolations to the LOD).

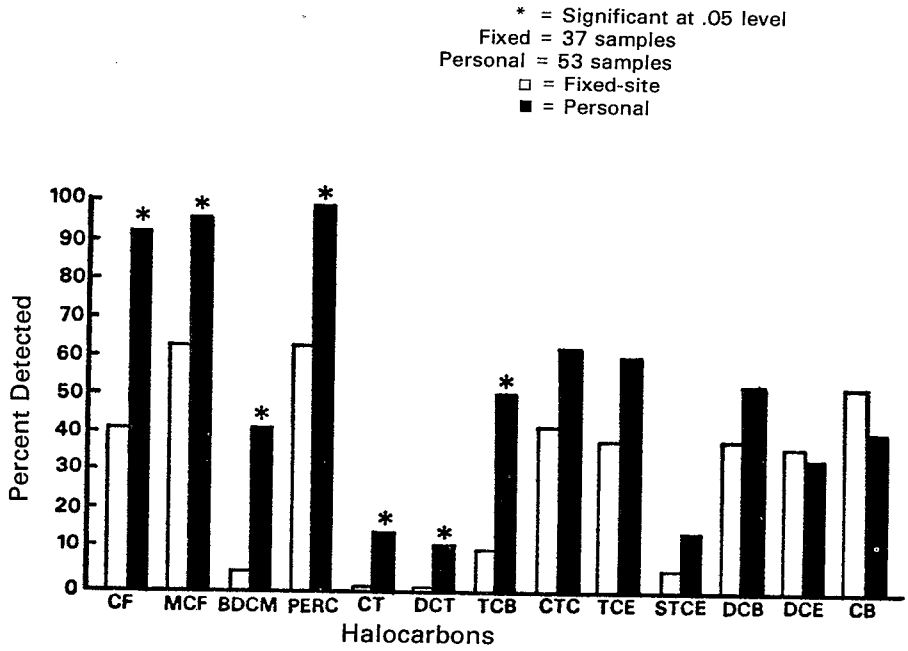

Figure 13. Comparison of percent detected for fixed-site vs. personal air samples - Greensboro, NC.
CF = chloroform, MCF = 1,1,1-trichloroethane, BDCM = bromodichloromethane, PERC = tetrachloroethylene, CT = chlorotoluene, DCT = dichlorotoluene isomers, TCB = trichlorobenzene isomers, CTC = carbon tetrachloride, TCE = trichloroethylene, STCE = 1,1,2,2-tetrachloroethane, DCB = dichlorobenzene isomers, DCE = 1,2-dichloroethane, and CB = chlorobenzene.

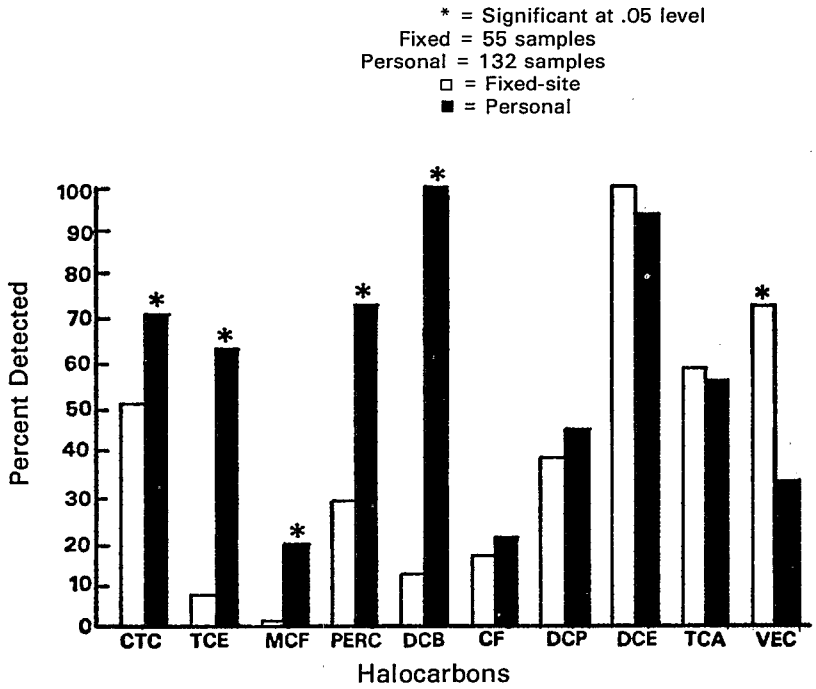

Figure 14. Comparison of percent detected for fixed-site vs. personal air samples - Baton Rouge/Geismar, LA. See Figure 13 for key, in addition, DCP = 1,2-dichloropropane, TCA = 1,1,2-trichloroethane, and VEC = vinylidene chloride.

The question of percent detected between personal and fixed-site samples was examined further. The data were stratified so that only matching pairs of samples were included in the analyses. The data for the participant whose fixed-site sample was in his/her yard were matched with the same participant's personal sample data; the remaining air data from the "cluster" were excluded from statistical analysis. The data were also grouped for analysis according to sampling period. Table 8 lists the percent detected for matching pairs for Greensboro. For the overnight period, a significant difference was observed for chloroform and trichlorobenzene isomers (0.05 and 0.01 level, respectively). Chloroform (0.01), 1,1,1-trichloroethane (0.05), and tetrachloroethylene (0.05) were significantly different between personal and fixed-site for the daytime period. The trends corroborate the previous data (Figure 13), where all data were included in the analyses. Fewer results are given in Table 8 than in Figure 13, since the reduced sample size yielded fewer significant differences.

TABLE 8. PERCENT DETECTION IN AMBIENT AIR SAMPLES MATCHED BY PARTICIPANT - GREENSBORO, NC STUDY

	Period no. 1*		Period no. 2*	
Chemical	Fixed-site	Personal	Fixed-site	Personal
N† =	18	18	16	16
Chloroform	56	94‡	19	94§
1,2-Dichloroethane	33	33	37	25
1,1,1-Trichloroethane	67	94	50	94‡
Carbon tetrachloride	44	61	44	50
Trichloroethylene	44	61	31	37
Bromodichloromethane	6	33	6	19
Tetrachloroethylene	67	94	62	100‡
Dichlorobenzene isomer	39	44	31	50
Trichlorobenzene isomers	0	61§	12	21

*Period no. 1 = 1800-0700 hrs; Period no. 2 = 0700-1700 hrs.
†Field samples included in sample size.
‡Significant differences between the two types of air samples at the 0.05 level.
§Significantly different at the 0.01 level.

Table 9 gives similar information for Baton Rouge/Geismar. An interesting observation is that vinylidene chloride was significantly different (0.01) between fixed-site and personal air, for both sampling periods. The trends were similar to those in the data discussed earlier for all measurements (Figure 14).

Further analyses were performed, specifically to determine whether correlations between the overnight and daytime periods existed for personal and fixed-site air samples. Spearman correlations were used, since the data were highly skewed.

TABLE 9. PERCENT DETECTION IN AMBIENT AIR SAMPLES MATCHED BY PARTICIPANT - BATON ROUGE/GEISMAR, LA STUDY

		Period no. 1*		Period no. 2*	
		Fixed-site	Personal	Fixed-site	Personal
Chemical	N† =	26	26	24	24
Vinylidene chloride		81	23	71§	37
Chloroform		19	15	8	25
1,2-Dichloroethane		100	96	96	96
1,1,1-Trichloroethane		69	54	48	67
Carbon tetrachloride		58	77	48	65
Trichloroethylene		8	69‡	8	71‡
Tetrachloroethylene		35	73‡	18	64‡
Dichlorobenzene isomer		8	88‡	12	100‡

*Period no. 1 = 1800-0700 hrs; Period no. 2 = 0700-1700 hrs.
†Field samples included in sample size.
‡Significantly different at the 0.01 level.
§Significant differences between the two types of air samples at the 0.05 level.

Table 10 lists the significant Spearman correlations that were observed for each of the halocarbons statistically analyzed. Remarkably, a number of halocarbons exhibited significant Spearman correlations for personal and fixed-site samples between the overnight and daytime periods, both in Greensboro and Baton Rouge/Geismar. The highest Spearman correlation observed was for carbon tetrachloride (0.70) in personal air from Greensboro. This suggests that the levels between overnight and daytime periods were related to each other.

The significant Spearman correlations found between fixed-site and personal air samples are given in Table 11. These correlations indicate that, for certain compounds, the values for matched fixed and personal samples track reasonably well with each other, i.e., as one increased, the other also increased or vice-versa. The best evidence of this phenomenon was for carbon tetrachloride (0.71) in the Baton Rouge/Geismar data.

The linearity between personal and fixed-site values for each study participant was more evident when plotted as shown, for example, in Figures 15 and 16 for carbon tetrachloride and 1,2-dichloroethane, respectively. As the measurable values approach the detection limit of the analytical method, the variation appears to increase.

Analyses of personal and fixed-site data suggest that personal monitoring gives higher exposure values for individuals. Secondly, fixed-site samples for a selected number of halocarbons do track the personal air samples, while the absolute values appear to be lower. These data suggest that personal samples may better represent the exposure of individuals to indoor air pollution, where many of the participants spend a higher percentage of their time in a 24-hour period. Again, attention should be drawn

TABLE 10. SIGNIFICANT* SPEARMAN CORRELATIONS BETWEEN PERIOD NO. 1 AND PERIOD NO. 2 MEASUREMENTS

Sample type	Chemical	Greensboro Corr.	Greensboro N†	Baton Rouge/Geismar Corr.	Baton Rouge/Geismar N
Fixed-air	1,2-Dichloroethylene	0.58	20	0.44	27
	Carbon tetrachloride	0.53	20	0.51	27
	1,2-Dichloropropane	0.52	20	0.53	27
	Trichloroethylene	0.53	20	--	--
	Vinylidene chloride	-- ‡	--	0.48	27
Personal air	Chloroform	0.46	24	--	--
	Carbon tetrachloride	0.70	24	0.29	59
	Trichloroethylene	0.42	24	0.47	59
	Tetrachloroethylene	0.41	24	0.37	58
	Dichlorotoluene isomers	0.41	24	--	--
	Vinylidene chloride	--	--	0.31	59
	1,2-Dichloroethylene	--	--	0.35	59
	1,1,1-Trichloroethane	--	--	0.43	58
	1,2-Dichloropropane	--	--	0.41	59
	Dichlorobenzene isomer	--	--	0.35	59

*Significant at 0.05 level.
†Number of measurements.
‡Not significant at 0.05 level.

TABLE 11. SIGNIFICANT SPEARMAN CORRELATIONS FOR FIXED-SITE VS. PERSONAL AIR SAMPLES*

Period no.†	Chemical	Geographical area: Greensboro	Geographical area: Baton Rouge/Geismar
1	Carbon tetrachloride	0.68 (20)‡	0.71 (27)
	Trichloroethylene	0.52 (20)	--
	1,2-Dichloroethane	--§	0.69 (27)
	Dichlorobenzene isomer	0.49 (20)	--
2	1,2-Dichloroethane	0.60 (18)	0.67 (25)
	Trichloroethylene	0.49 (18)	0.41 (25)
	Chloroform	--	0.45 (25)
	Carbon tetrachloride	--	0.47 (25)

*Significant at the 0.05 level.
†Period no. 1 = 1800-0700 hrs; Period no. 2 = 0700-1700 hrs.
‡Number of samples given in parenthesis.
§Not significant at 0.05 level.

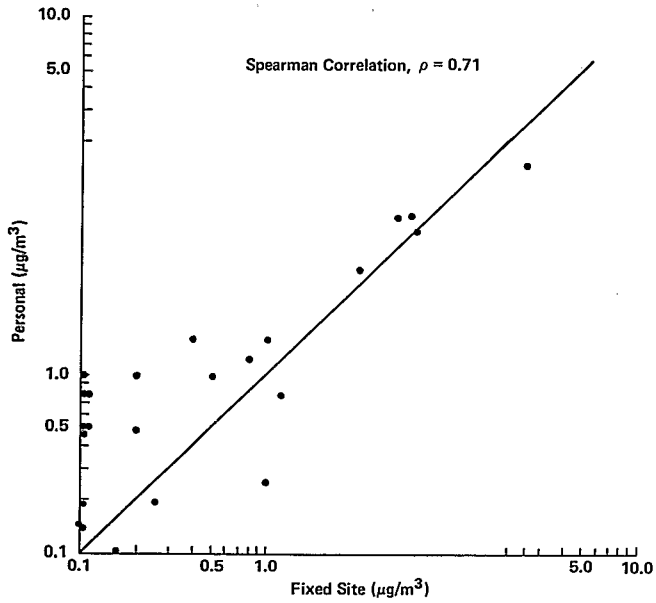

Figure 15. Spearman Correlation for personal vs. fixed-site air levels of carbon tetrachloride (overnight sampling period) - Baton Rouge/Geismar, LA study (45° line depicted).

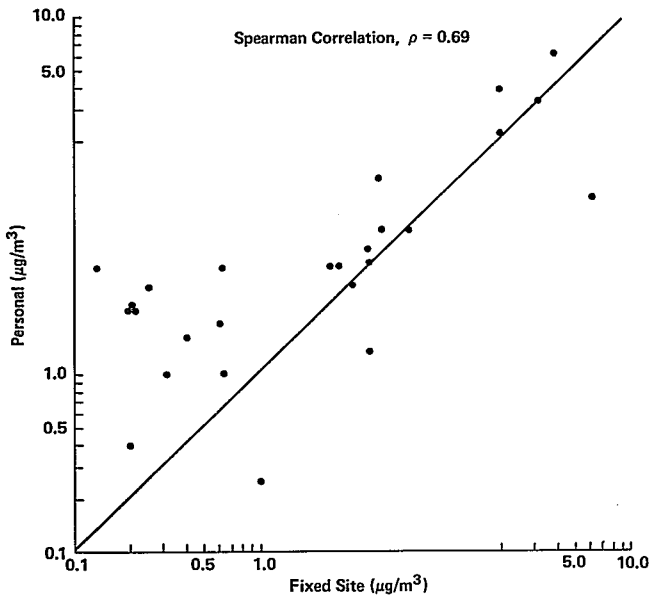

Figure 16. Spearman Correlation for personal vs. fixed-site air levels of 1,2-dichloroethane (overnight sampling period) - Baton Rouge/Geismar, LA study (45° line depicted).

to the situation that the overnight personal sample can, for practical purposes, be considered as an indoor fixed-site sample and thus indoor/outdoor air quality can be directly compared for matched samples.

Some caution, however, should be noted in evaluating these data. For example, the comparison of overnight and daytime period samples for personal samples may be confounded by the inclusion of housewives in the statistical analyses, and thus, significant correlations between overnight and daytime samples are heavily reflecting of exposure near and inside their home. Because the sample participant size is not sufficiently large, further post-stratification of the data could not be performed.

SUMMARY

Personal and fixed-site air monitoring was conducted to assess exposure of lay populations to halocarbons. Twenty-eight people in Greensboro, North Carolina, and 66 people in Baton Rouge/Geismar, Louisiana, participated in a 24-hour sampling program. A QC/QA program was maintained for the sampling and analysis procedures. This included blanks, controls, and replicate field samples.

The significant findings were:

1. mean recovery of halocarbons from Tenax GC cartridges were 79 to 125 percent (except chloroform, 63 percent);

2. for personal and fixed-site air samples, between replicate variability of sampling and analysis was ±25 percent for 1,1,1-methylchloroform to ±50 percent for chloroform;

3. the levels of halocarbons in personal air samples were higher than fixed-site samples;

4. a majority of the halocarbons exhibited a statistically significant higher percent detected in personal than fixed-site air samples within each geographical area;

5. statistically significant correlations (at 0.05 level) were observed for carbon tetrachloride, trichloroethylene, 1,2-dichloroethane, dichlorobenzene isomer, and chloroform between personal and fixed-site air levels,

6. statistically significant correlations (at 0.05 level) were found between overnight and daytime period halocarbon levels (five for fixed-site and 10 for personal).

ACKNOWLEDGEMENTS

The authors wish to thank the many people who have contributed to the success of this study, and especially the participants who graciously gave

their time. This research was supported by EPA Contract Nos. 68-01-4731 and 68-01-3849.

REFERENCES

1. Zweidinger, R.A., S.D. Cooper, B.S.H. Harris, III, T.D. Hartwell, R.E. Folsom, Jr., E.D. Pellizzari, A.W. Sherdon, T.K. Wong, and H.S. Zelon. 1980. Measurement of benzene body-burden for populations potentially exposed to benzene in the environment. EPA-560/13-80-028, December.

2. Wallace, L., R. Zweidinger, M. Erickson, S. Cooper, D. Whitaker, and E.D. Pellizzari. In press. Monitoring individual exposure--measurements of volatile organic compounds in breathing-zone air, drinking water, and exhaled breath. Environ. Intl.

3. Pellizzari, E.D., T. Hartwell, H. Zelon, C. Leininger, M. Erickson, and C. Sparacino. 1982. Total exposure assessment methodology (TEAM): prepilot study - Northern New Jersey. U.S. Environmental Protection Agency Final Report. Contract No. 68-01-3849.

4. Pellizzari, E.D., M.D. Erickson, and R.A. Zweidinger. 1979. Formulation of a preliminary assessment of halogenated organic compounds in man and environmental media. EPA-560/13-79-006, July.

5. Huffman, R.D., C.M. Latanick, T.K. Collins, J.A. Caldwell, and J.D. Wiese. 1979. Metabolism summaries of selected halogenated organic compounds in human and environmental media, a literature survey. EPA-560/6-79-008, April.

6. Pellizzari, E.D., M.D. Erickson, and R.A. Zweidinger. 1979. Analytical protocols for making a preliminary assessment of halogenated organic compounds in man and environmental media. EPA-560/13-79-010, September.

7. Krost, K.J., E.D. Pellizzari, S.G. Walburn, and S.A. Hubbard. 1982. Collection and analysis of hazardous organic emissions. Anal. Chem. 54:810.

A PERSONNEL OR AREA DOSIMETER FOR POLYNUCLEAR AROMATIC VAPORS

T. Vo-Dinh

Health and Safety Research Division
Oak Ridge National Laboratory
Oak Ridge, TN

ABSTRACT

A new passive dosimeter has been developed for monitoring airborne vapors and liquid aerosols of potentially hazardous polynuclear aromatic compounds. The device is a self-contained, badge-size unit that passively collects on filter paper the compounds to be monitored at a diffusion-controlled rate. Collection is followed by in-situ, room temperature phosphorescence analysis of the compounds adsorbed on the dosimeter. The dosimeter can detect pyrene, phenanthrene, and quinoline at sub-part-per-billion for an 8-hour exposure.

INTRODUCTION

Polynuclear aromatic (PNA) compounds are produced primarily as a result of incomplete combustion of organic matter. They are believed to be present in the atmosphere in many industrial and residential environments as both vapor and aerosol. With the advent of increasing public awareness of the potentially long-term health hazards associated with PNA compounds, great emphasis has been placed on the development of new instrumental monitoring techniques to detect those compounds in the atmosphere. However, because of their low equilibrium vapor concentration, vapors from multiring PNA compounds are difficult to detect by simple methods. Conventional procedures to monitor these species involve 1) collection of PNAs by drawing large volumes of air through a sorbent material, 2) thermal or chemical desorption of the PNAs, 3) chromatographic fractionation of the samples, and 4) identification and quantification of the extracted materials. These procedures are usually elaborate, time-consuming, and not suitable for routine applications or field measurements.

This paper reports on the development of a new type of personnel dosimeter that has been recently developed for monitoring select PNAs in vapors and liquid aerosols. This dosimeter collects the PNA compounds via molecular diffusion and sorption. Collection is followed by direct identification and quantification of the analyte compounds via room temperature

phosphorimetry (RTP). There is no requirement for a prior chemical extraction or chemical desorption protocol. The results of the evaluation of the dosimeter for various homocyclic as well as heterocyclic PNAs during laboratory-controlled experiments and field-test measurements are presented here.

A PASSIVE DOSIMETER FOR PNA COMPOUNDS

The PNA dosimeter is a self-contained, badge-size passive monitor. The device is lightweight (∿200g) and can be conveniently worn by a person or placed at a stationary location. Figure 1 shows a photograph of the pen-size dosimeter worn on the pocket of a person at a synfuel facility. The monitor basically consists of a holder, a filter paper substrate, and an interchangeable diffusion chamber. The heart of the dosimeter is the sample collection substrate of filter paper that is treated with a heavy-atom chemical (1-3). The monitoring procedure is based on the measurement of the quantity of the PNAs transferred to the substrate surface via molecular diffusion in air. The unique feature of this dosimeter is the dual use of the heavy-atom chemical both as a sorbent agent and as an RTP inducer. The sorbent material (paper/heavy-atom chemical) maintains the concentration of the PNA compounds at the collection surface at zero or near-zero concentrations while the air outside the dosimeter is at ambient concentration. This sets up a concentration gradient for diffusion of the compounds from the outside of the dosimeter to the inside. Interchangeable diffusion chambers of different sizes can be used to select the rate of molecular diffusion. The concentration gradient provides the driving force to move the PNA molecules onto the paper, eliminating the need for a pump. The transfer of the PNA compounds by diffusion is described by Fick's First Law:

$$J = -D \frac{dc}{dl} \qquad (1)$$

where

J = diffusion flux

D = coefficient of diffusion of the PNA compounds

$\frac{dc}{dl}$ = concentration gradient dc along diffusion path dl.

If the concentration gradient is constant, ($dc/dl = C/L$ = constant), the mass of PNA compounds collected at the sorbent surface is given by:

$$M = D \cdot \frac{A}{L} \cdot C \cdot t \qquad (2)$$

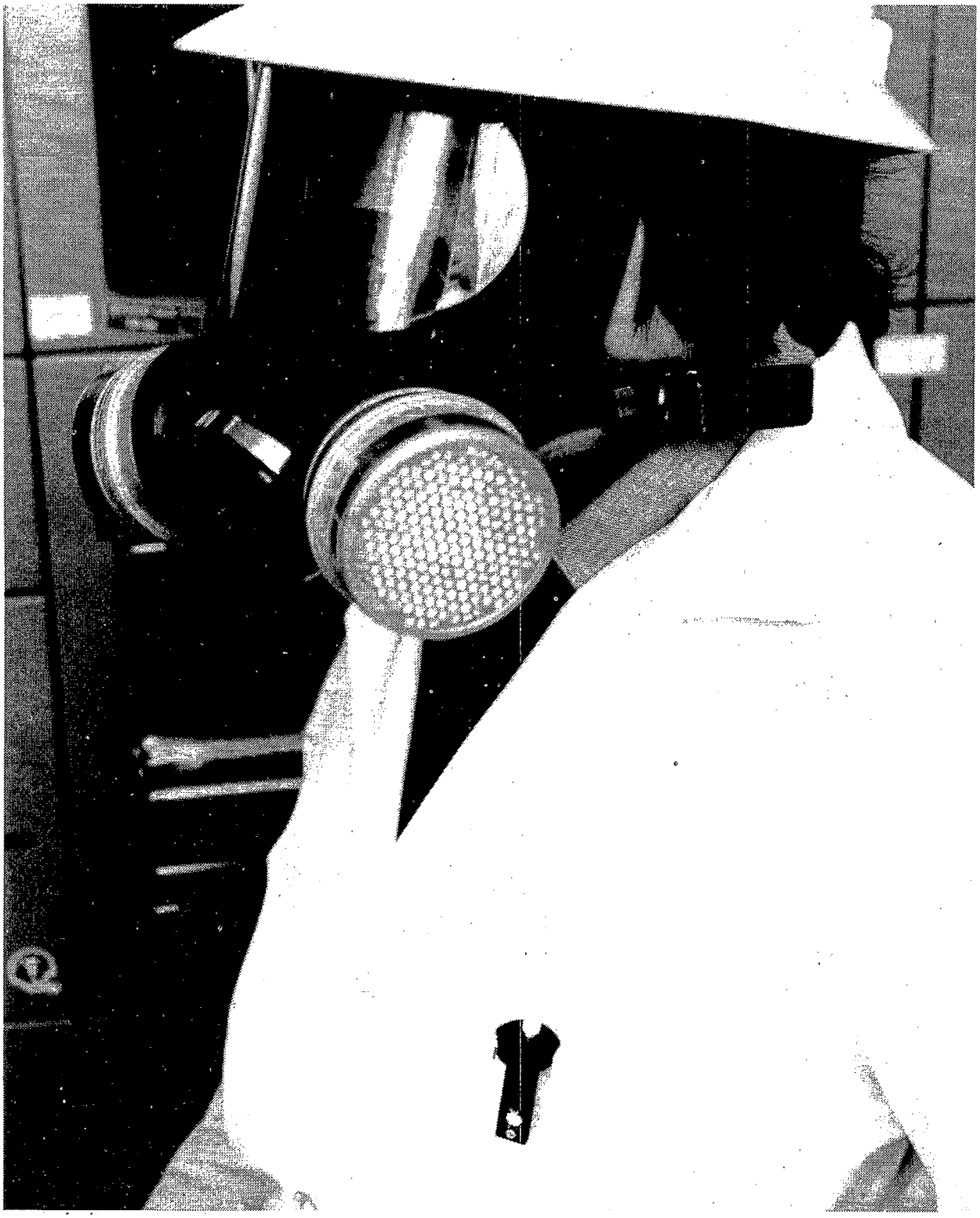

Figure 1. Photograph of the PNA dosimeter worn by a worker at a synfuel facility.

where

A = collection area of the dosimeter

L = diffusion path length of the dosimeter

C = ambient concentration

t = exposure time.

After exposure, the dosimeter is inserted into a luminescence spectrometer for identification and quantification of the PNAs collected on the monitor using the RTP technique (4).

RTP DETECTION

The RTP method is a relatively new approach in phosphorescence based on the emission of organic compounds adsorbed on various solid substrates such as filter paper, silica gel, sodium acetate, etc. At room temperature, phosphorescence is normally a very weak emission that is difficult to detect in liquid solutions or in the gas phase. This is due to the fact that the phosphorescence is almost totally quenched by collisions in solutions or air, or is deactivated by intramolecular vibrations and rotations. The conventional phosphorescence technique, therefore, requires low-temperature equipment and frozen solvents to reduce the probability of these quenching processes so that the phosphorescence signal may be more easily detected. Unlike conventional phosphorimetry, the RTP technique does not use cryogenic technology. This feature is one of the main attributes of this method for routine applications and field measurements.

The paper substrate of the dosimeter is treated with a heavy-atom chemical that is used to increase the adsorption characteristics of the collection surface and to enhance the RTP emissions of the PNA compounds. This latter process, known as external heavy-atom perturbation, provides an invaluable aid to RTP detection (4). The presence of heavy-atom species in the vicinity of a molecule can enhance a photophysical process, known as spin-orbit (S-O) coupling, which is responsible for phosphorescence emission. Qualitatively, the S-O coupling arises from the interaction of two magnetic fields resulting from the nuclear and electron spin motion (5). Since the magnitude of the nuclear magnetic field is directly proportional to the nuclear charge and hence to the atomic number, the S-O coupling increases with increasing atomic number. The method based on the S-O coupling enhancement by the heavy-atom effect has been developed into a practical and simple tool of considerable analytical interest in the areas of air pollution analysis (6). Table 1 shows that the detection limits for several homocyclic and heterocyclic PNA compounds by RTP are in the picogram range.

TABLE 1. LIMITS OF DETECTION (LOD) FOR SEVERAL PNA COMPOUNDS BY ROOM TEMPERATURE PHOSPHORESCENCE

Compound	λex* (nm)	λem† (nm)	LOD (ng)
Homocyclics			
Benzo[a]pyrene	395	688	0.07
Benzo[e]pyrene	335	543	0.001
2,3-Benzofluorene	343	505	0.025
Benzo[ghi]perylene	398	626	0.6
Chrysene	330	518	0.03
1,2,3,4-Dibenzanthracene	295	567	0.08
1,2,5,6-Dibenzanthracene	305	555	0.005
Fluoranthene	365	545	0.05
Fluorene	270	428	0.2
Phenanthrene	295	474	0.007
Pyrene	343	595	0.1
N-Heterocyclics			
Acridine	360	660	0.4
5,6-Benzoquinoline	355	502	0.06
7,8-Benzoquinoline	353	509	0.04
Carbazole	296	415	0.005
Dibenzocarbazole	295	475	0.002
Quinoline	315	505	0.1

*λex = excitation wavelength.
†λem = emission wavelength.

MONITORING PNA VAPORS AND LIQUID AEROSOLS

The detection of a typical PNA compound, phenanthrene, by the dosimeter is illustrated in Figure 2. This figure shows the RTP spectrum obtained after exposing the dosimeter for two hours in a chamber containing phenanthrene vapor at 40°C. The RTP response due to the background emission of the paper substrate of an unexposed dosimeter is also shown in Figure 2 (dashed curve). A typical response of the dosimeter exposed for various time periods to vapors of another PNA compound, pyrene, is given in Figure 3.

The dosimeter is able to detect homocyclic as well as heterocyclic compounds, such as the important family of aza-arenes. Aza-arenes are widely distributed in the atmosphere and studies have shown significant levels in marine sediments, tobacco smoke, urban particulates, automobile exhausts, synfuel plants, and effluents from many industrial sources. The dosimeter can detect various aza-arenes such as quinoline, phenanthridine, and acridine in the vapor phase. From the standpoint of human health

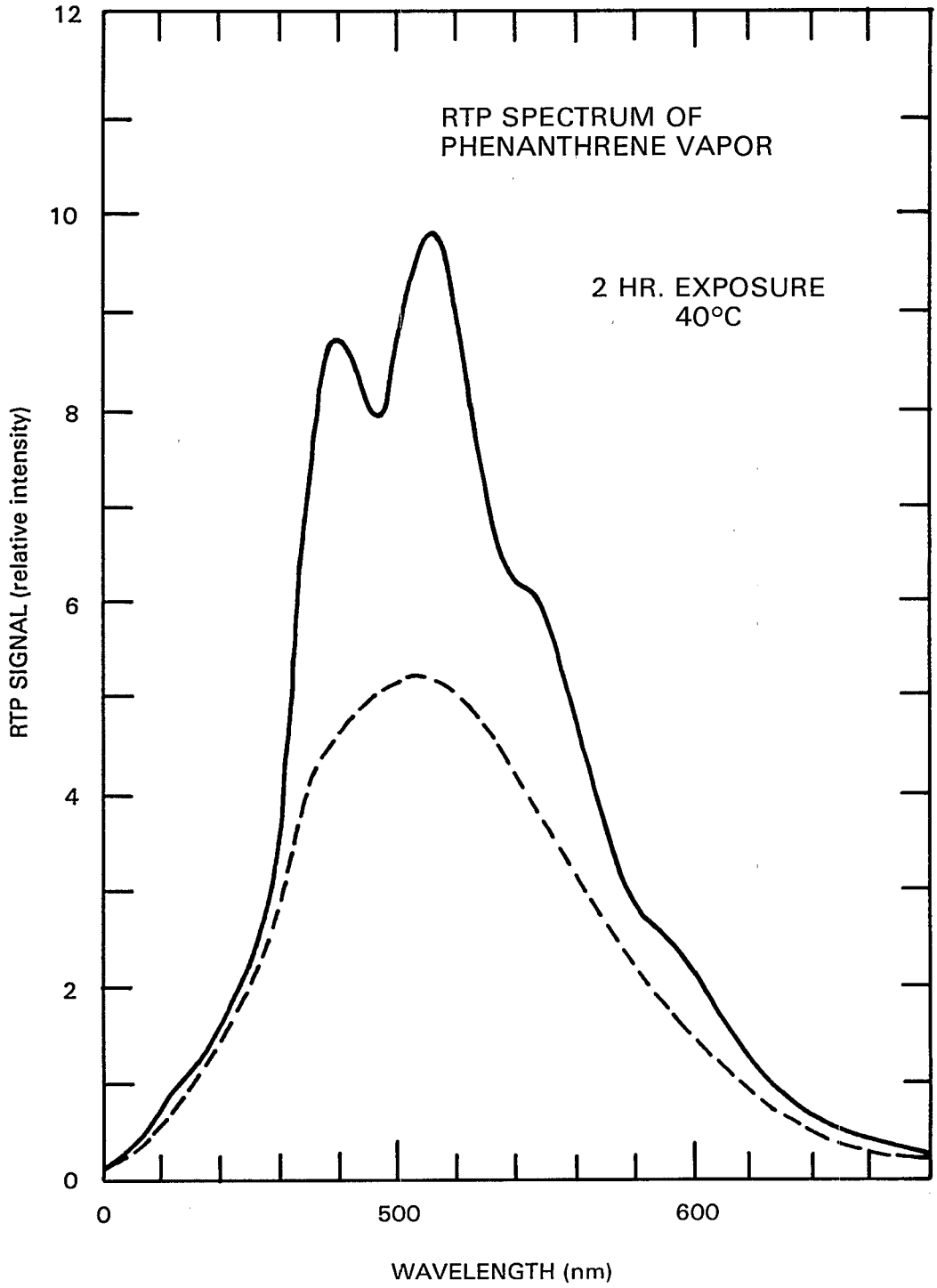

Figure 2. RTP signal of phenanthrene vapor collected by the dosimeter after two-hour exposure.

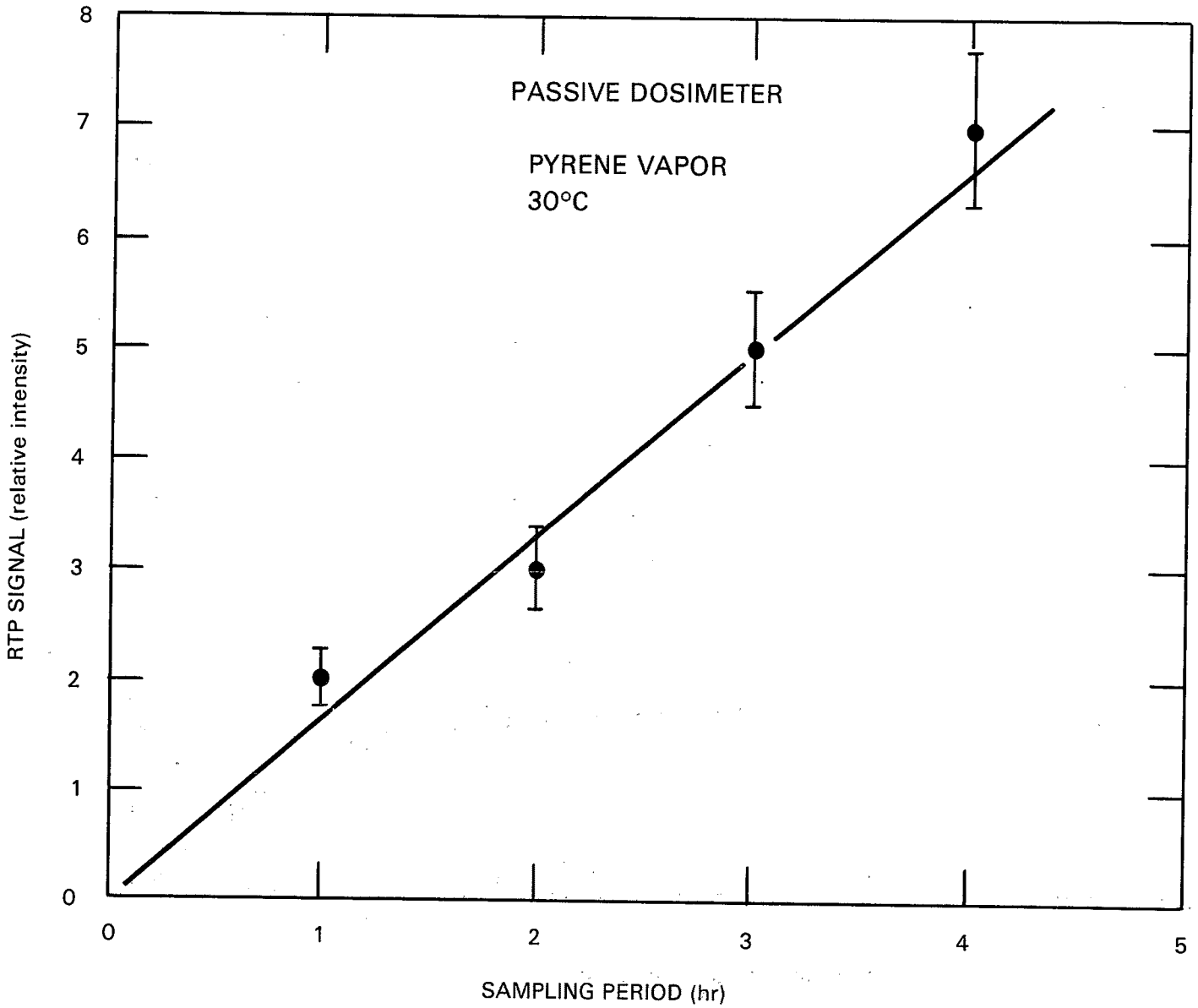

Figure 3. Typical response of the dosimeter to various exposure periods of pyrene vapor.

consideration, quinoline is a very important compound. This compound was found to induce hepatoma in rats and to increase the carcinogenic activity of benzo[a]pyrene (7). Current methods for detection of quinoline are elaborate, involving active pump filtration, desorption, fractionation of collected samples, and analysis by chromatographic techniques. Since quinoline has a relatively high vapor pressure and is easily desorbed by forced-air flow, the values reported for this compound may well be far below the true ambient concentrations.

The dosimeter can effectively monitor quinoline in the vapor phase. The detection limit for quinoline is 0.75 ppb x hr. Figure 4 shows the RTP spectra of quinoline and isoquinoline detected by the dosimeter. The 15-nm spectral shift in the RTP spectra shows that it is possible to differentiate quinoline from its isomer. When these two compounds are both present in a mixture, the specificity to characterize them individually can be further enhanced using the synchronous scanning method by which both emission and excitation wavelengths are simultaneously varied (8). The synchronous scanning method results in much sharper emission bands and allows greater selectivity. The band-narrowing effect of the synchronous excitation method is illustrated in Figure 5 for quinoline and isoquinoline.

The PNA dosimeter has been used to monitor a single component as well as various compounds under actual field-monitoring situations. Figure 6 illustrates the capability of the dosimeter for multi-component detection during field test measurements. The figure shows the RTP signals of four sets of dosimeters exposed at four different areas at a synfuel production plant. Three dosimeters were used per set, and the variation of dosimeter responses within one set was typically 15 percent. The RTP response of the dosimeters placed in a clean room showed a broad emission. This emission was similar to that of a background RTP signal of an unexposed dosimeter and indicated that the location had no detectable levels of PNA compounds. In contrast, the dosimeters placed at the location near a fractionator (FTR) revealed the predominant presence of phenanthrene. Other compounds detected at this location included fluorene and pyrene. Fluorene and phenanthrene were also detected by the dosimeter exposed near a vacuum tower (VAC TWR). Finally, the dosimeters exposed at a location near the bottom of a fractionator (FTR-BOT) detected fluorene and quinoline. The detailed results of these field measurements will be reported elsewhere (currently in preparation by the author and G.H. Miller).

CONCLUSION

The development of personal monitors is an essential step in the quantification of human exposure for health protection, epidemiological, and regulatory purposes. Whereas active samplers can provide real-time detection of hazardous pollutants, these devices often are not the most practical and economical choice for monitoring individual exposure to airborne pollutants. Passive dosimeters offer the advantages of lower capital expense, simplicity, and compactness. The dosimeter described in this work is a valuable tool for monitoring personal exposures to PNA pollutants that

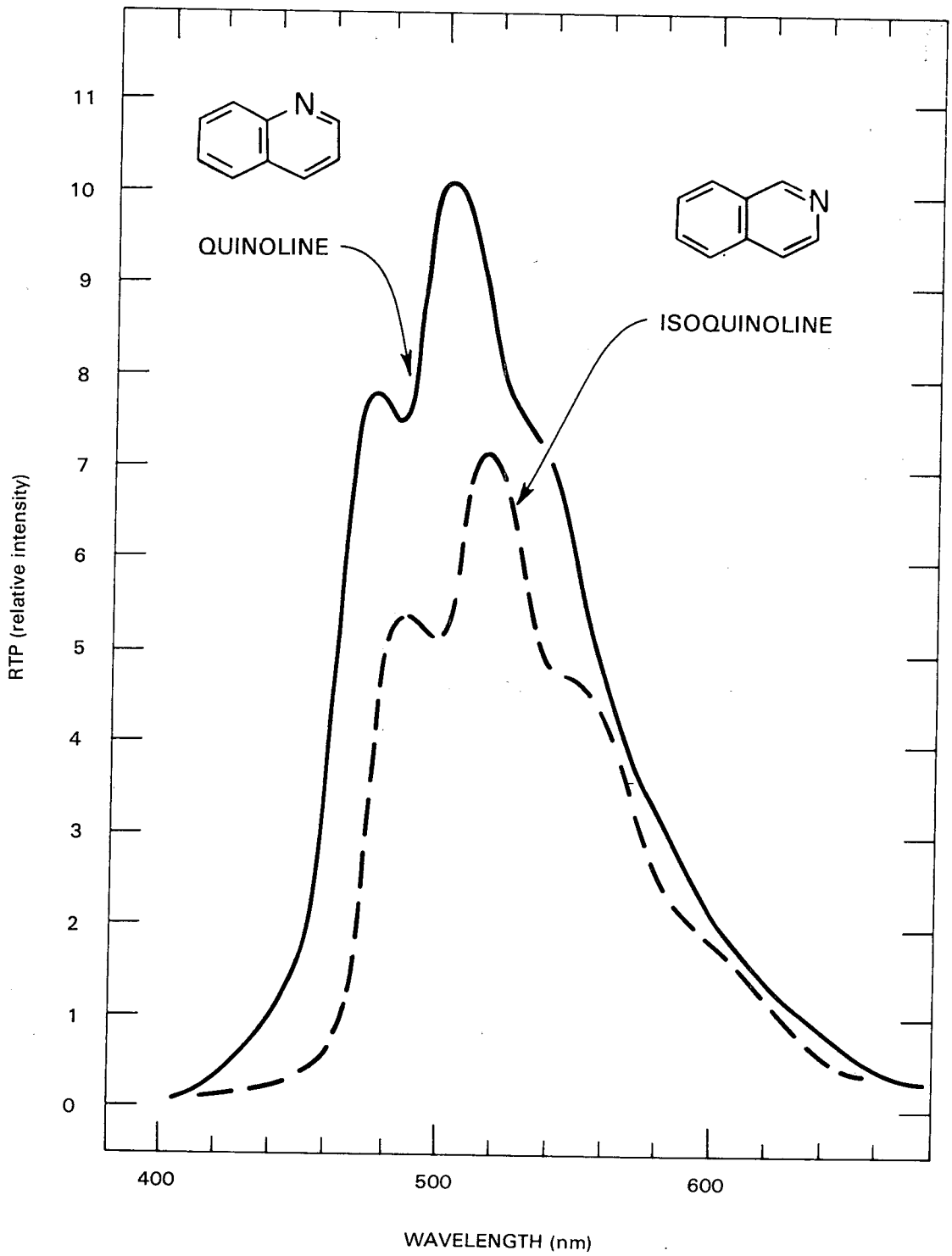

Figure 4. Room temperature phosphorescence spectra of quinoline and isoquinoline.

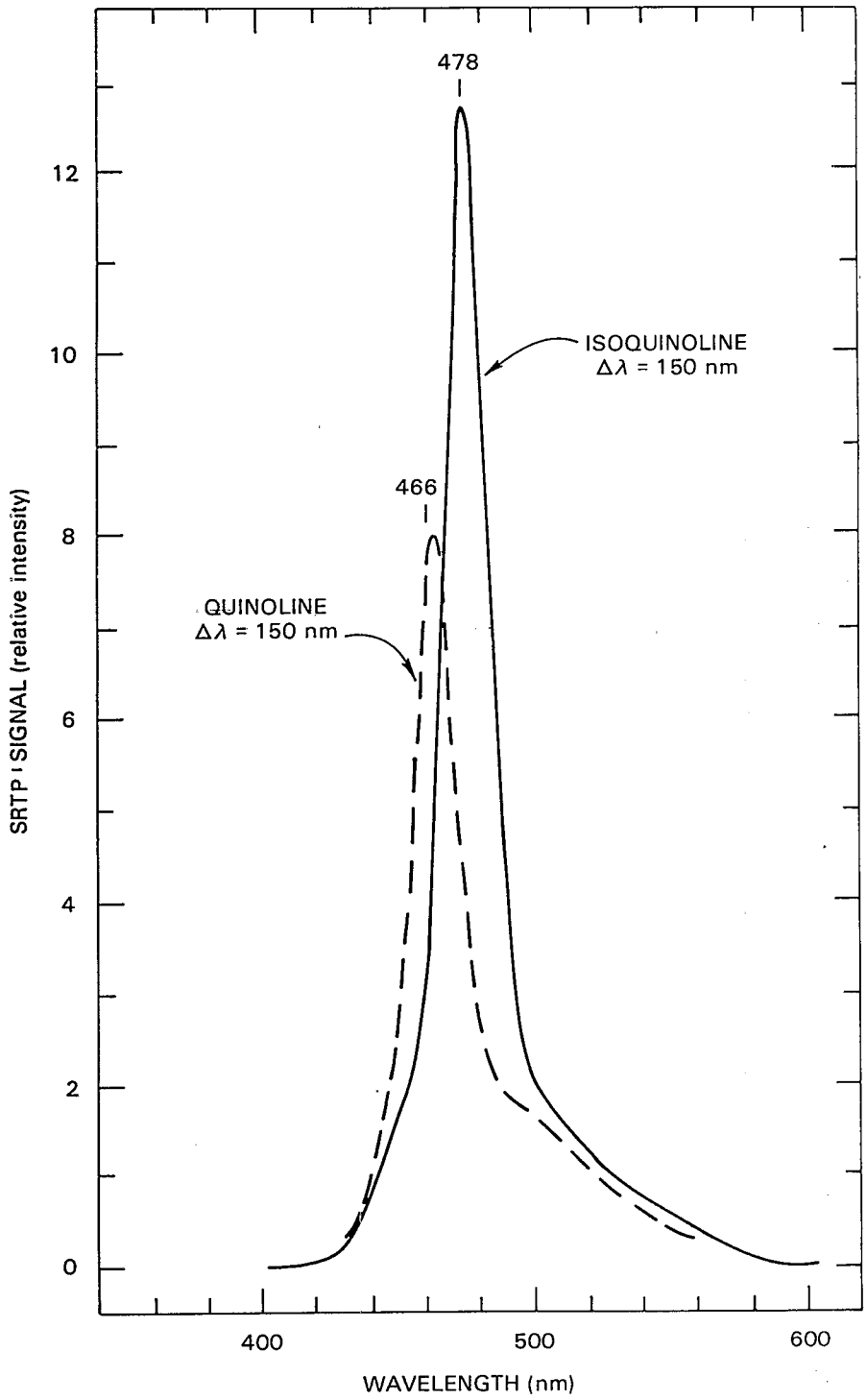

Figure 5. Differentiation of isomeric quinolines by synchronous excitation.

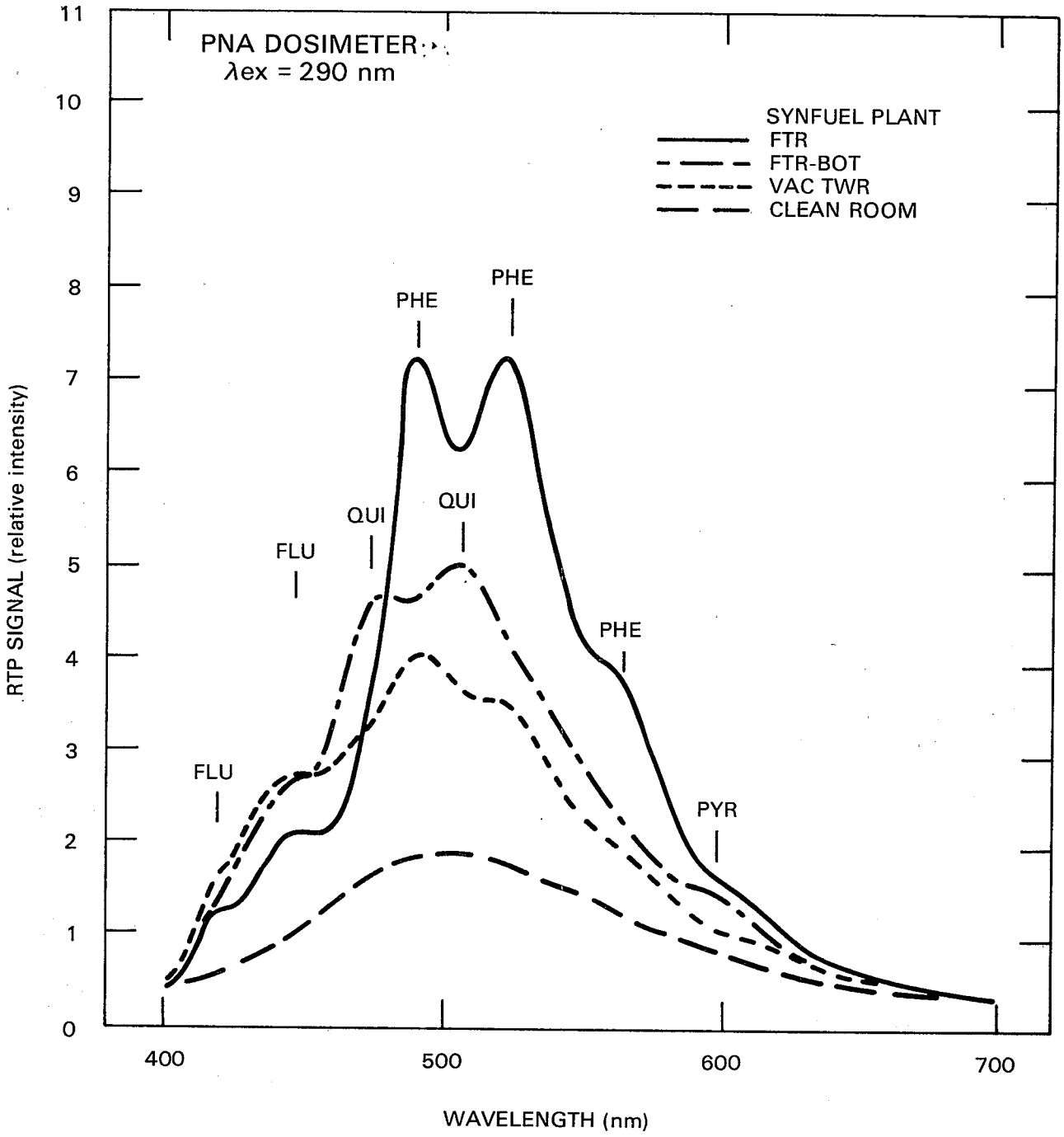

Figure 6. RTP response of various dosimeters exposed at different locations inside a synfuel plant.

can provide critical information to assess the health implications of exposure to these compounds.

ACKNOWLEDGMENTS

Research presented here was sponsored by the Office of Health and Environmental Research, U.S. Department of Energy, under contract W-7405-eng-26 with the Union Carbide Corporation.

REFERENCES

1. Vo-Dinh, T. 1981. InTech 5:45; also, 1982, U.S. patent pending.

2. Vo-Dinh, T., and G.H. Miller. 1982. Proceedings of the 1982 Pittsburgh Conference, Atlantic City, NJ.

3. Vo-Dinh, T. 1981. Proceedings of the 1981 Instrument Society of America, St. Louis, MO.

4. Vo-Dinh, T., and J.R. Hooyman. 1979. Anal. Chem. 51:1915.

5. McGlynn, R., T. Azumi, and Kinoshita. 1969. The triplet state. Academic Press, New York, NY.

6. Vo-Dinh, T., R.B. Gammage, and P.R. Martinez. 1981. Anal. Chem. 53:253.

7. Dong, M., I. Schmeltz, E. Lavoie, and D. Hoffmann. 1978. Page 97 in Carcinogenesis. P.W. Jones and R.I. Freudenthal, eds., Raven Press.

8. Vo-Dinh, T. 1981. Page 167 in Modern Fluorescence Spectroscopy. E.L. Wehry, ed., Plenum Press.

THE NBS PORTABLE AMBIENT AEROSOL SAMPLER

R.A. Fletcher, D.S. Bright, and R.L. McKenzie

ABSTRACT

A portable, lightweight, battery-powered particle sampler for collecting ambient level concentrations of inhalable particles has been developed at NBS. The unit has a flow rate of 6 liters per minute and is capable of operating for longer than 24 hours on a single battery charge. It separates and collects the ambient inhalable and respirable particulate size fractions by series filtration. The first filtration stage, an 8μm pore size Nuclepore* filter collects the "coarse" fraction of the inhalable particles ($\geq$ 3.5μm aerodynamic particle diameter). The smaller particles (< 3.5μm or respirable fraction), which pass through the first filter, are collected by a high-efficiency Zeflour filter. Both filtration stages are weighable to ±10μg certainty and are amenable to subsequent chemical or physical analysis of particulate material. The sampler inlet removes particles larger than 15μm aerodynamic diameter (or other preselected sizes) by impaction. The sampling efficiency of the inlet has been tested in a wind tunnel using a series of monodisperse test aerosols. Wind tunnel tests showed that the sampling efficiency of the inlet has some wind velocity dependence. Design and use of the wind tunnel testing is discussed.

The sampling protocol, which is well suited for indoor particulate monitoring, is also useful for NO_2 pollutant monitoring. A common indoor gas pollutant is NO_2, which results from gas-fired flame sources. Test results for a passive NO_2 sampler that could be fitted to the portable particle sampler is presented.

INTRODUCTION

The increasing concern for measuring personal exposure to particulate and gaseous pollutants (1) and the recognition that such exposures cannot

*Certain commercial equipment, instruments, or materials are identified in this report to specify adequately the experimental procedure. Such identification does not imply recommendation or endorsement by the National Bureau of Standards, nor does it imply that the materials or equipment identified are necessarily the best available for the purpose.

always be extrapolated from outdoor monitoring measurements (2,3) has resulted in the need to develop personal exposure samplers for indoor use. The NBS portable ambient aerosol sampler (Figure 1) was developed with this application in mind. It is a small, quiet, unobtrusive sampler capable of collecting analytically significant samples in sampling periods as short as 8 hours (depending on average ambient concentration levels). The samples collected are quantified gravimetrically and can subsequently be analyzed by other chemical or physical analytical techniques (for example, x-ray fluorescence, microscopy, ion chromatography).

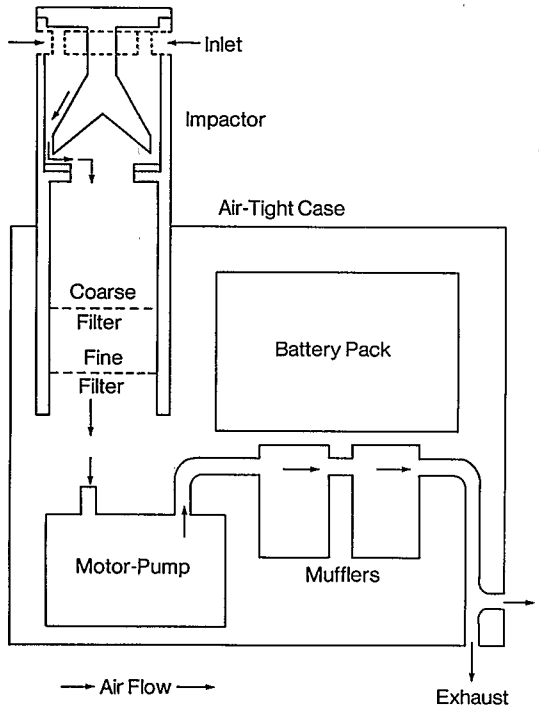

Figure 1. Schematic of the sampler.

The following are some of the characteristics of the sampler:

a. 6 liter per minute (L/min) flow rate stable to within 10 percent (up to 350-400μg mass loading) for in excess of 24-hour operational time period;

b. Particle size separation by means of tandem filtration, with sample collection in the range of 15-3.5μm (or 10-3.5) aerodynamic diameter and $\leq$3.5μm aerodynamic diameter;

c. An inlet that samples only particles $\leq$15μm (or optionally, $\leq$10μm);

d. Collection of an analyzable sample during an 8-hour integrated sampling period under normal ambient particulate concentrations (4-6).

The sampler components have been extensively tested to characterize the sampler performance, including the pump-battery system, the tandem filter unit, and the inlet using a wind tunnel to determine sampling efficiency. These tests are discussed in detail. Additional information is available in references 4, 5, and 6, and a components list is available from the authors.

Because pollutant gases such as NO_2, are frequently present (1) in the indoor environment, we evaluated the feasibility of incorporating NO_2 sampling capabilities into the portable aerosol sampler for use in indoor pollution monitoring situations. A small passive NO_2 sampler with high sensitivity can be used with the aerosol sampling unit that is capable of collecting measureable quantities of NO_2 during an 8-hour exposure to ambient level concentrations.

The following discussion describes the performance characteristics of these various components of the NBS portable ambient aerosol sampler.

DESCRIPTION AND EVALUATION OF THE NBS PORTABLE AMBIENT AEROSOL SAMPLER

Tandem Filter

The NBS portable sampler achieves a particle size separation (50 percent cut) at approximately 3 to 3.5μm aerodynamic diameter using a tandem filter unit (7,8) to collect the respirable particle fraction ($\leq$ 3.5μm) (9) of the inhalable particles ($\leq$ 15μm). The filter unit is composed of an 8μm pore-sized 37-mm Nuclepore filter in series with a highly efficient (10) 3μm pore-sized 37-mm Zeflour filter. The Nuclepore filter is precoated with a small amount of Apiezon L grease to reduce particle bounce (8). Particles in the 15-3.5μm aerodynamic diameter size range are collected by the Nuclepore, while the $\leq$ 35μm aerodynamic diameter particles penetrate that filter and are subsequently collected by the Zeflour filter. The particles are uniformly distributed on both filter surfaces, making the samples amenable to analysis by x-ray fluorescence. The tandem filter arrangement has the practical advantage of being convenient, low cost, and good for gravimetric analysis due to low water retention. This filter unit has high flow conductance at 6L/min (drawing only 15 cm H_2O), which is an important factor in determining battery power and pumping energy requirements. Two disadvantages are that the 50 percent cut-point at 3.5μm is not sharp, and that filter clogging for heavy particle loadings may change the sampler flow rate and collection efficiency. These two disadvantages will be discussed later.

Cut-point tests on the Nuclepore filter were made using monodisperse solid (ammonium fluorescein and ammonium sulfate) and liquid (dioctylphthalate-DOP) particles generated by a vibrating orifice particle generator (VOPG) (11). An optical particle counter was used as the particle

detector downstream of a 37-mm filter holder (12,13). The number of particles of known aerodynamic diameter penetrating the filter was compared to the number of test particles of the same aerodynamic diameter measured with the filter removed from the holder. (Particle aerodynamic diameter was determined by particle sedimentation measurements in air.) The collection efficiency of the filter is defined as

$$E = 1 - \frac{\text{number of particles through holder with filter in place}}{\text{number of particles through holder without filter}}$$

The results of the filter collection efficiency tests are shown in Figure 2 for clean and preloaded (with >150μg of particulate matter) Nuclepore filters. Liquid (sticky) particles are more efficiently collected by the Nuclepore filter than the solid (resiliant) particles because the solid particles "bounce" off the filter surface and thus have a better chance of flow reintrainment that penetrates the filter (12,13). Liquid particles are collected at 50 percent efficiency for 2.3μm-diameter particles, whereas only 35 percent of the solid particles of that diameter are collected. The collection efficiency curve for preloaded filters is shifted toward smaller particle size for liquids, probably because the effective pore size of the filter is reduced by the material deposited on the filter surface. The shift is not so pronounced for solid particles, perhaps because the deposited particles enhance the bounce effect by covering the grease layer.

The cut-point differences reported above will be somewhat moderated when sampling ambient particles, as they will often be characterized by properties intermediate to those of liquid and solid test aerosols. This will minimize, to some extent, the importance of the variability in the 50 percent cut-point. A second factor that will minimize the importance of this variability is that there is a minimum in most naturally occurring bimodal ambient particle concentration distributions at about 3μm (14). The effects of filter clogging are not significant for mass loadings of less than 400μg (on the Zeflour filter), and only in cases of sampling high-concentration environments would the filter unit need replacing in time intervals less than 8 hours.

Pump and Power Supply

The flow rate of the sampler is an important parameter in setting the sampling time required to collect a sufficient sample for gravimetric analysis. There is a ±10μg uncertainty in weighing a clean filter; therefore, the sample must weigh at least 100μg if it is to be determined to an uncertainty of 10 percent or less. Thus, for normal ambient aerosol concentrations (coarse + fine modes) of 50 to 100μg/m^3 (15,16), $\geq$4 m^3 must be sampled. The portable sampler has a flow rate of 6 L/min or .36 m^3/hr. The minimum sampling time, in hours, to collect sufficient sample on the filter (100μg) for $\leq$10 percent uncertainty in the gravimetric analysis is $2.8 \times 10^2/c$, where $\bar{c}$ is the concentration of the particulate in μg/m^3 of the fraction (inhalable or respirable) of concern.

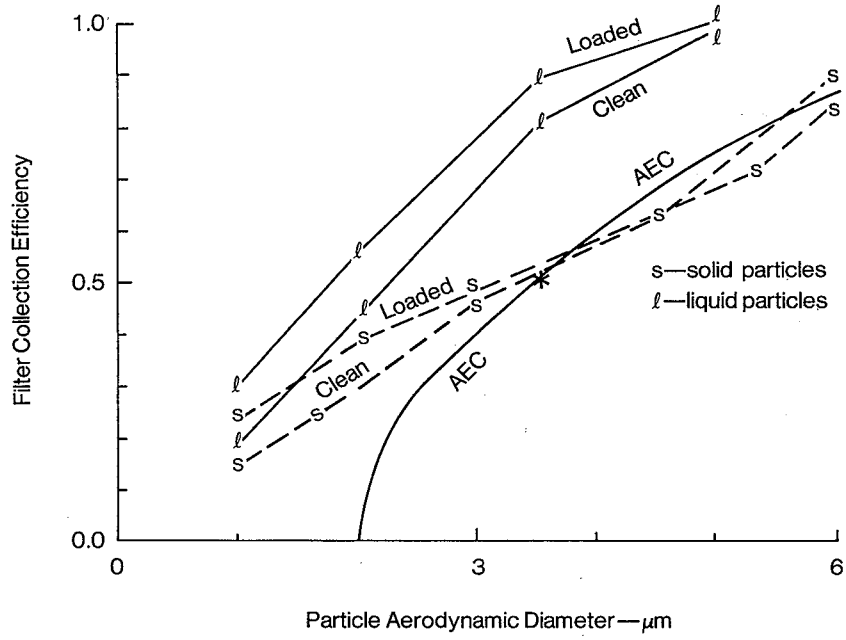

Figure 2. Filter collection efficiency as a function of aerodynamic diameter. The symbols (l) and (s) denote liquid and solid particles. The Atomic Energy Commission's respirable curve is also shown.

Changes in the flow rate of the sampler can introduce two errors: an uncertainty in the total volume of air sampled, and shifts in the inlet and coarse filter cut-points. The flow rate decreases if the voltage driving the pump decreases or the pressure drop of the system increases. The batteries selected will maintain constant voltage under the load presented by the pump for over 24 hours. The pressure drop of the system is primarily that of the filters and filter loading. As the filters load, the flow becomes restricted. A loading of 400μg on the filter unit reduces the flow rate by 12 percent. Our studies show, however, that a flow rate reduction of 33 percent, i.e., from 6 L/min to 4 L/min changes the cut-point on the Nuclepore filter by only 7 percent. Calculations indicate that a similar reduction in flow rate leads to only a 7 percent change in the inlet cut-point (4). Thus, filter loadings normally encountered will not cause a large enough decrease in flow rate to have any significant effect on the sampler performance. The uncertainty in the calculation of the particle mass concentration, $\mu g/m^3$, is a result of uncertainties in weighing the mass and obtaining the total volume of air sampled. The uncertainty in total sample volume resulting from flow rate changes will in most instances be less than the weighing uncertainties. However, for extreme cases, flow rate monitoring may be necessary. It may also be possible to count the piston strokes of the pump to obtain a more precise measure of the total volume sampled.

Inlet

The sampler inlet should perform two major functions--first, it defines the upper aerodynamic diameter limit of the particles to be sampled, and second, it minimizes wind velocity and orientation biasing of the sampler (17,18). The inlet used in this sampler was made by scaling down an inlet designed by Walter John and Steve Wall (19). The sampled air enters the entrance slits of the inlet (see Figure 3) and passes between the inverted "funnel" and the annular impaction surface directly beneath. Particles larger than the cut-point are removed from the air stream by impaction on the oil-soaked frit used as the impaction surface. The dimensions of the "funnel" determine the cut-point of the inlet. We have designed inserts that have 15, 10, or 7μm cut-points. The oil-soaked sintered annular ring provides a long-lived sticky surface that minimizes particle bounce (19). The inlet is connected directly to the 37-mm tandem filter cassette by an o-ring seal.

The cut-point of the impactor was determined by measuring percent penetration as a function of particle diameter, using the vibrating orifice generator to produce monodisperse oleic acid droplets and using the optical particle counter as the detector. The results of the cut test are shown in Figure 4 for the 15μm, 10μm, and 7μm inserts. The two boxes define the region of unacceptable performance for a 15μm inlet designed to sample inhalable particulates according to the criteria by Smith, et al., (20). These measurements were made under quasi-static wind velocity conditions to define the cut-point characteristics of the inlet impactor. To determine the sampling efficiency of the inlet, it is necessary to conduct wind tunnel tests.

Inlet Testing

The sampling efficiency of inlets is difficult to predict on the basis of theoretical models (17). The existing theoretical treatments (21-24) deal mostly with calm (zero wind velocity) conditions. Wind tunnel testing, therefore, has been necessary to characterize inlet performance (17,18,25-29). The wind tunnel (Figure 5) used at NBS is made of corrosion resistant stainless steel, has a 0.46 m x 0.46 m cross-section, and has a working length of 2.4 m. Air is drawn through the tunnel by a variable speed fan-type blower located on the exit end. Over the entire velocity range (0.3-2.4 m/s), the turbulent levels do not exceed 4 percent of the wind velocity values. The turbulence value is defined as the RMS of the fluctuating longitudal wind velocity component. A turbulent mixing grid and an airfoil are used to stabilize the aerosol plume (Figure 5). Narrow (Figure 6), but stable (with respect to particle concentration) aerosol plumes are employed to provide a more concentrated particle stream, which reduces sampling time (4).

The inlet sampling efficiency is defined as the ratio of the particle concentration measured by sampling through the inlet to the particle concentration measured by sampling with an isokinetic probe (an ideal sampler). The monodisperse test aerosol was oleic acid-fluorescien dye particles generated by the VOPG. The aerosol was sampled through the inlet or

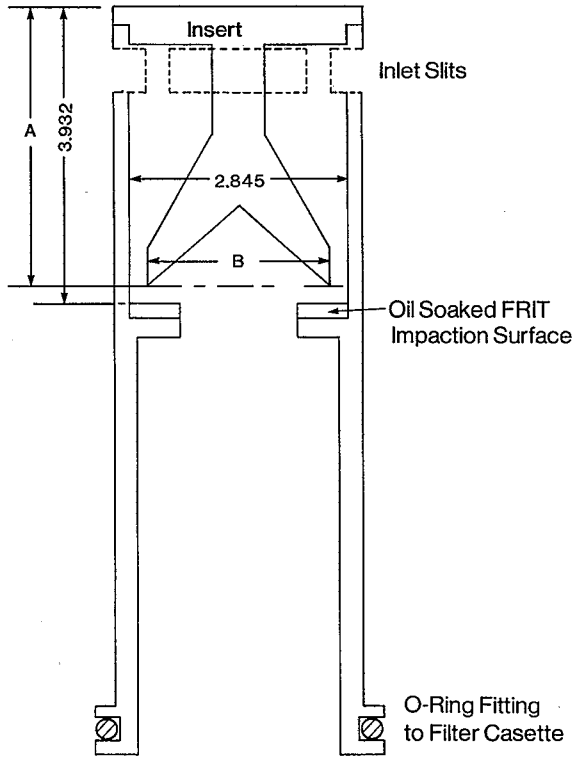

Figure 3. Schematic of the inlet. The values of A and B determine the cut-point.

Critical dimensions for funnel inserts

Cut-point (μm)	A (cm)	B (cm)
15	3.696	2.372
10	3.863	2.568
7	3.871	2.675

an isokinetic probe, and the particles collected on 0.3μm pore (37-mm diameter) Nuclepore filters. A particle-laden filter was then washed with 3 mL of 0.1 N ammonia solution and the fluorescien concentration determined spectrophotometrically. The sampling efficiency was calculated from the measured fluorescien concentration, the known sampling flow rate, and the sampling duration.

The results of the inlet sampling efficiency tests, shown in Figure 7, show that the inlet is somewhat wind velocity- and orientation-sensitive. The cap or hood present on the full size model (19) has not been used on the scaled-down inlet, and considerable influence by wind on the inlet without the hood is expected (information from personal communication with J.B. Wedding, Colorado State University, 1981). The relative standard deviation of the inlet data is about 10 percent. In some instances the

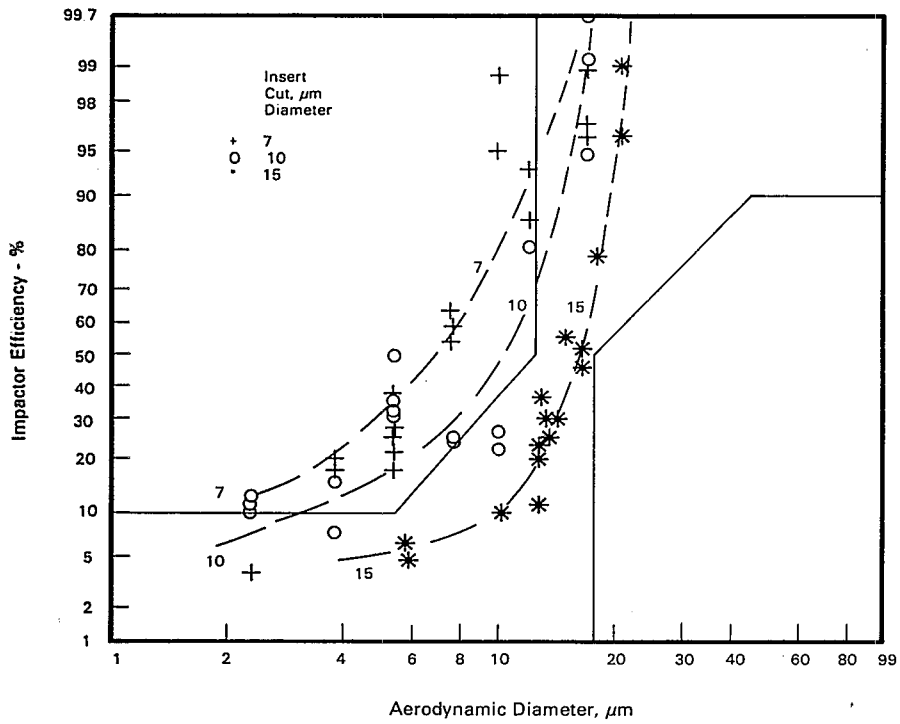

Figure 4. Inlet cut curves for 15μm, 10μm, and 7μm cut-points. Collection efficiency is plotted versus aerodynamic particle diameter.

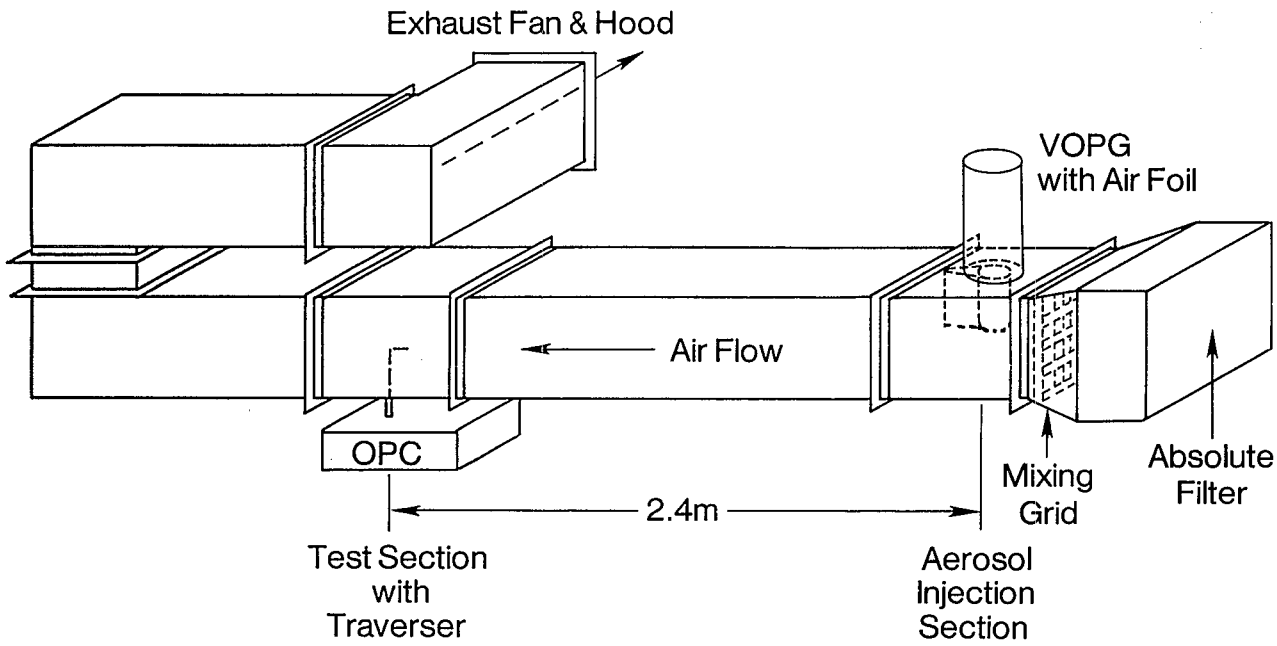

Figure 5. NBS wind tunnel test facility.

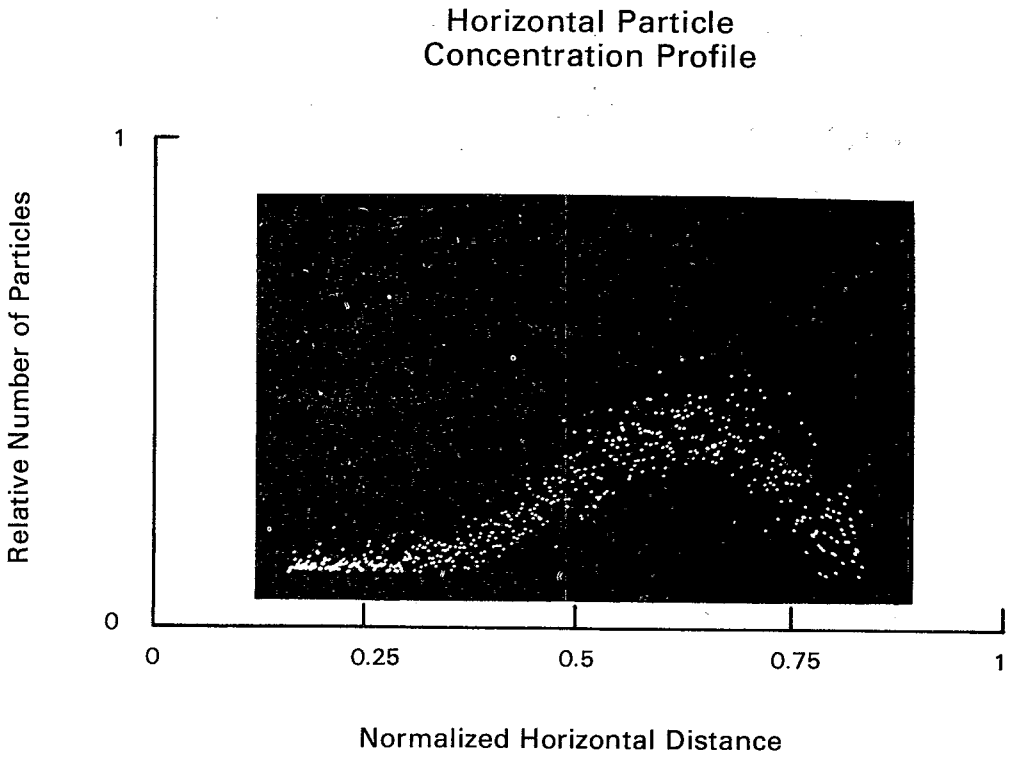

Figure 6. Horizontal particle concentration profile in the wind tunnel.

inlet has a sampling efficiency greater than 100 percent. Such oversampling is predicted for large particles at low wind velocities (21-23) and has been observed for full-scale inlets (18). At high wind velocities, the inlet does not sample large particles efficiently. At low wind velocities the inlet sampling efficiency is essentially independent of wind velocity, making the portable sampler better suited for indoor sampling applications where the wind velocity averages 0.15 m/s and rarely exceeds 0.5 m/s than for outdoor environments where the wind velocity can reach much higher ranges.

INCORPORATION OF NO_2 SAMPLING CAPABILITY

The NBS portable ambient aerosol sampler monitors the particle concentration of the sampled environment. In many instances, there is equal concern for health and/or safety reasons over the concentration of other airborne pollutants, such as SO_2, organics, radon, and NO_2, which are common indoor pollutants (1). The sampling capability of portable aerosol samplers can, in principle, be easily expanded to include gas sampling without increasing the bulk of the sampler or its energy requirements by means of passive gas sampling techniques. Passive gas sampling employs the kinetic energy of the gas to transport (diffusional transport) the species of interest to a trapping agent. The Palmes tube (30) sampler for NO_2 is an example. For indoor ambient monitoring, the gas monitor must be small

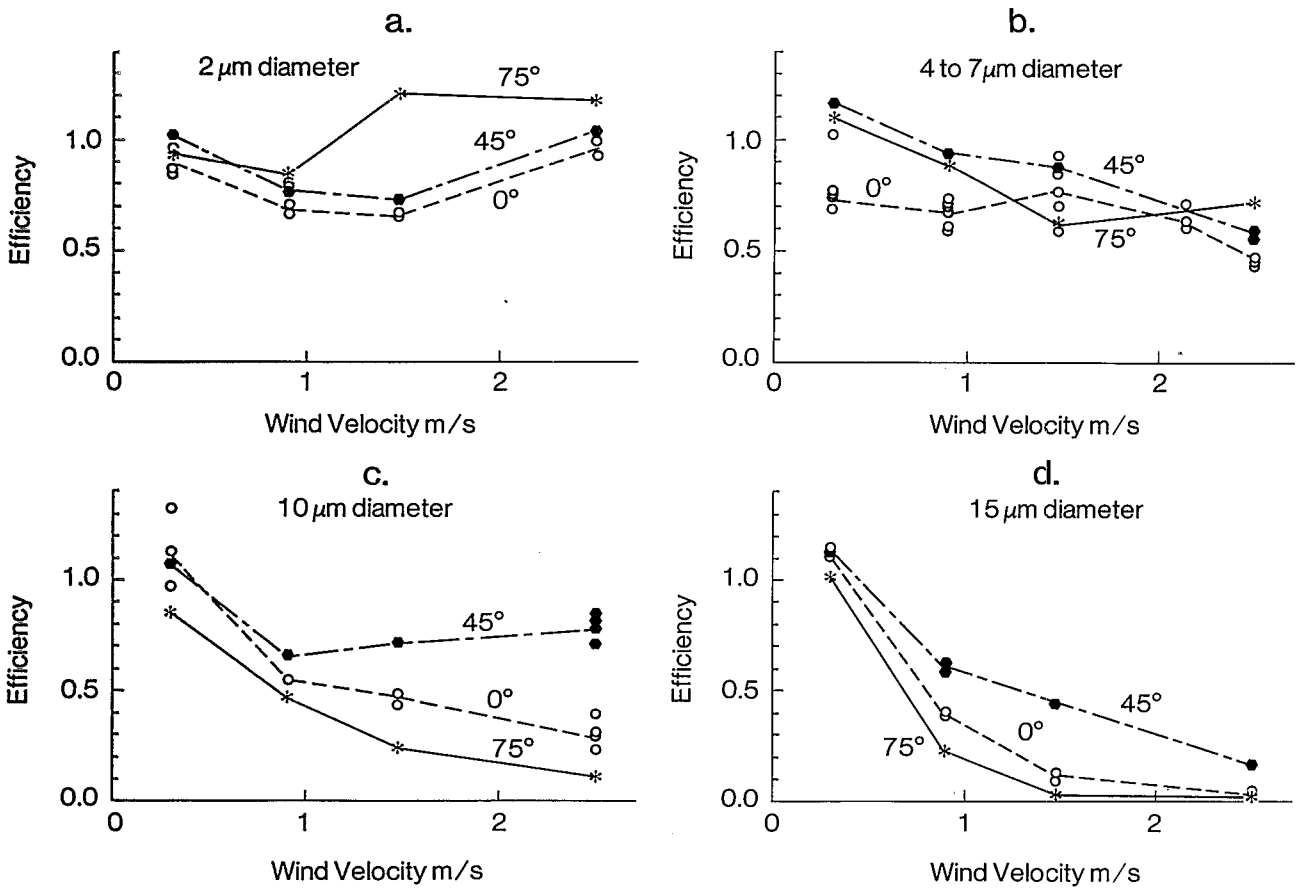

Figure 7. Inlet sampling efficiency as a function of wind velocity in the wind tunnel. Inlet orientation is shown where (o) is upright 0° angle, (●) is for 45° angle tilt forward into wind, and * is a 75° angle tilt forward.

and have a high collection rate. The Palmes tube sampler is small but requires about 24 hours at normal ambient NO_2 levels to collect a detectable sample of NO_2. Because the portable sampler can potentially collect sufficient particle concentrations in as short as 8-hour sampling periods, it is useful to have an NO_2 sampler that can collect a measurable sample in the same time period. The development of a small passive NO_2 monitor that has a high collection rate has become possible by modifying the patented Dupont Pro-Tek organic vapor badge (31,32). The collection medium is a 1 cm x 6 cm Gelman A filter strip soaked in a 1/10 (by volume) solution of triethanolamine (TEA) in acetone (information from personal communication with B. Cadoff, NBS, 1981). TEA has been used as an NO_2 trapping agent for many applications (33-37).

The sampling rate by the Pro-Tek badge is defined by diffusion from the outer surface through 280, 1-mm-diameter holes to the collection surface (TEA-soaked filter paper). The glass fiber filter provides a high surface area collection medium for the NO_2. The sampling rate (Figure 8) of the device was determined from the quantity of NO_2 collected by the sampler for a known NO_2 exposure. The NO_2 collected, which was generated using permeation tubes, was measured by treating the filter strip with Saltzman reagent and analyzed spectrophotometrically. The sampling rate is 5.3 µg NO_2 collected per ppmxh exposure, which is approximately 50 times the sampling rate of the Palmes tube sampler.

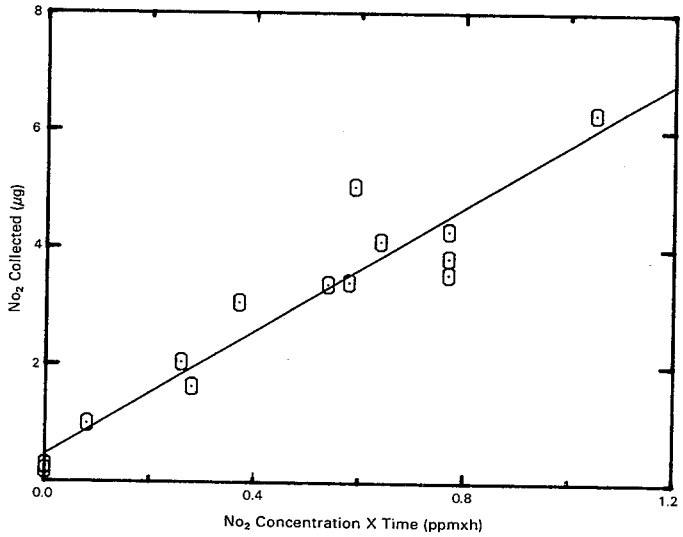

Figure 8. Summary of the NO_2 collection rate for the Dupont Pro-Tek badge. The collected NO_2 mass in µg is plotted as a function of NO_2 concentration in parts per million multiplied by the time in hours.

SUMMARY

The NBS portable sampler fills the need for an ambient atmospheric pollutant personal exposure monitor. It is capable of monitoring ambient concentrations of inhalable particulates and NO_2 in order to assess individual exposures to these pollutants, which may not always be accurately determined by conventional stationary outdoor monitoring systems. The sampler separates and collects the coarse (3.5μm to 15μm-diameter) and the respirable ($\leq$3.5μm-diameter) fractions of the inhalable particulates by series filtration. The collected fractions are gravimetrically quantified and can be subsequently chemically analyzed if desired. The high sampling rate of 6 L/min makes it possible to collect analytically significant (analyzable with 10 percent precision) samples at ambient environmental concentration levels in as short as an 8-hour sampling period. The sampler includes a specially designed inlet that transmits only the less-than 15μm (or alternatively 10μm) aerodynamic diameter particulates. The larger particles are removed by impaction in the inlet. The sampling performance and characteristics of the various components of the sampler have been extensively laboratory- and/or wind tunnel-tested, and the entire unit is now being field-tested. A small passive NO_2 sampler capable of incorporation into the portable particulate sampler extends the monitoring capability of the sampler to simultaneously measure NO_2 exposure. The NO_2 sampler has a high sampling rate (50 times that of the Palmes tube sampler commonly used in occupational monitoring situations).

REFERENCES

1. Committee on Indoor Pollutants, Board of Toxicology and Environmental Health Hazards. 1981. Indoor pollution. Assembly of Life Sciences, National Research Council. National Academy Press, Washington, DC.

2. Dockery, D.W., and J.D. Spengler. 1981. J. Air Pollut. Control Assoc. 31:153.

3. Repace, J.L., and A.H. Lowrey. 1980. Science 208:464.

4. Bright, D.S., and R.A. Fletcher. In press. Amer. Ind. Hyg. Assoc. J.

5. Fletcher, R.A., and D.S. Bright. 1981. International Conference on Powder and Bulk Solids, Cahners Exposition Group, Chicago, IL.

6. McKenzie, R.L., D.S. Bright, R.A. Fletcher, and J. Hodgeson. In press. Environ. International.

7. Parker, R.D., G.H. Buzzard, T.G. Dzubay, and J.P. Bell. 1977. Atmos. Environ. 11:617.

8. Cahill, T.A. 1977. J. Air Pollut. Contr. Assoc. 27:675.

9. Miller, F., and D.E. Gardner. 1979. J. Air Pollut. Contr. Assoc. 29:610.

10. Liu, B.Y.H., D.Y.H. Pui, K.L. Rubow, and G.A. Kuhlmey. 1978. EPA progress report (May). EPA Grant R 804600.

11. Berglund, R.M., and B.Y.H. Liu. 1973. Environ. Sci. Tech. 7:147-153.

12. John, W., S. Hering, G. Reischl, and J.J. Wesolowski. 1980. Final report, Interagency Agreement ARB A7-139-30, Air and Industrial Hygiene Laboratory Section. Lab Services, Berkeley, CA. CA/DOH/AIHL/SO-21.

13. John, W., G. Reischl, S. Goren, and D. Plotkin. 1978. Atmos. Environ. 12:1555.

14. Whitby, K.T., R.B. Husar, and B.Y.H. Liu. 1972. J. Colloid Interface Sci. 29:177.

15. Macias, E.S., and R.B. Husar. 1976. Environ. Sci. & Tech. 10:904.

16. Lewis, C.W., and E.S. Macias. 1980. Atmos. Environ. 14:185.

17. Liu, B.Y.H., and D.Y.H. Pui. 1980. Page 383 in Proceedings of EPA conference on advances in particle sampling and measurement, October 1979, Daytona Beach, FL. EPA-600-9-80-004, January.

18. Wedding, J.B. 1981. Environ. Sci. & Tech. 16:154.

19. John, W., S.M. Wall, and J.J. Wesolowski. 1981. Air and Industrial Hygiene Laboratory, California Department of Health Services. Report CA/DOH/AIHL/SP-27.

20. Smith, W.B., K.U. Cushing, M.C. Thomas, R.P. Wilson, and D.B. Harris. 1980. Page 316 in Proceedings of EPA conference on advances in particle sampling and measurement, October 1979, Daytona Beach, FL. EPA-600-9-80-004, January.

21. Davies, D.N. 1968. Brit. J. Appl. Phys. (J. Phys. D.) 1:921.

22. Fuchs, N.A. 1975. Atmos. Environ. 9:697.

23. Fuchs, N.A. 1964. The mechanics of aerosols. Pergammon Press, New York, NY.

24. Agarwal, J.K., and B.Y.H. Liu. 1980. Amer. Ind. Hyg. Assoc. J. 41:191.

25. May, K.R., N.P. Pomeroy, and S. Hibbs. 1976. J. Aerosol Sci. 7:53.

26. Ogden, T.I., and J.L. Birkett. 1978. Ann. Occup. Hyg. 21:41.

27. Pattenden, N.J., and R.D. Wiffen. 1977. Atmos. Environ. 11:677.

28. Caplan, K.J., L.J. Doemeny, and S.D. Sorenson. 1977. Amer. Ind. Hyg. Assoc. J. 38:83.

29. Wedding, J.B., A.R. McFarland, and J.E. Cermak. 1977. Environ. Sci. & Tech. 11:387.

30. Palms, E.D., A.F. Gunnison, J. Dimattio, and C. Tomczyk. 1976. Amer. Ind. Hyg. Assoc. J. 37:870.

31. Pro-Tek Organic Vapor Air Monitoring Badges. Laboratory validation protocol for diffusion-type air monitoring badges with solid sorbents. Copyright 1981 by E.I. duPont de Nemours and Co., Inc., Wilmington, DE.

32. Lautenberger, W.J., E.V. Kring, and J.A. Morello. 1980. Amer. Ind. Hyg. Assoc. J. 41:737.

33. Levaggi, D.A., W. Siu, E.L. Kothny, and M. Feldstein. 1972. Environ. Sci. & Tech. 6:250.

34. Levaggi, D.A., W. Siu, and M. Feldstein. 1973. J. Air. Pollut. Contr. Assoc. 25:30.

35. Willey, M.A., C.S. McCammon, Jr., and L.J. Doemeny. 1977. Amer. Ind. Hyg. Assoc. J. 38:358.

36. Fletcher, R.A., D.S. Bright, B.C. Cadoff, and J.A. Hodgeson. 1980. EPA/NBS annual report.

37. Blacker, J.H. 1973. Amer. Ind. Hyg. Assoc. J. 34:390.

DEVELOPMENT OF A PROTOTYPE ACTIVE PERSONAL MONITOR FOR SO_2, NO_2, AND AIRBORNE PARTICLES

Tahir R. Khan, Jean C. Meranger, and Belinda Lo

Environmental Health Directorate
Health Protection Branch
Health and Welfare Canada
Ottawa, Ontario

INTRODUCTION

Traditionally, air pollution monitoring has been carried out at fixed-station networks. During the past several years, however, it has become apparent that a significant portion of the air pollution burden that a person is exposed to in the course of daily activities occurs in the indoor rather than the outdoor environment (1,2,3). Typically, people in North America spend about 90 percent of their time indoors (4,5). Indoor pollutants may originate from specific sources such as home cooking and smoking, and may have levels different from ambient air monitored by a fixed-station network.

Indoor/outdoor air pollution comparisons are being made with increasing frequency in an attempt to determine relationships between fixed-station community monitoring results (ambient air) and actual community exposures. Ambient air quality results would then be used to predict the frequency distribution curve for the exposure of a community.

A potentially more serious problem arises, however, when the criteria upon which air quality objectives are based are derived from dose-response data that incorporate ambient pollutant measurements rather than integrated indoor/outdoor exposures and doses. Thus, health effects criteria have been based on exposure data that may have underestimated (or overestimated) the response due to a presumed level of exposure.

The variability of individual human response to air pollutants and of human exposure to them complicates the situation. Even if ambient air quality, with respect to the pollutants of interest and their indoor/outdoor air quality relationships, are known reasonably accurately, the very different daily patterns of individual human activity may confound an attempt to relate exposure estimates to the likelihood of human health effects. In this sense, personal dosimetry of air pollutants may be essential to determine whether current indoor/outdoor (daily activity) doses of criteria pollutants are causing detectable health effects. More precisely,

personal dosimetry may be necessary to determine the sub-population that may be experiencing air pollution-related morbidity.

Earlier we reported that no dosimeter for monitoring personal exposure was currently available or is likely to be produced commercially in the near future (6). Certain promising devices were found, however. These either measured only one of the pollutants, Harvard/EPRI (7), or did not have the required sensitivity or operational life required, GAGE (8). We initiated a project with the aim of assembling a prototype personal dosimeter from the most promising commercially available air pump, a solid sorbent media of the desired collection properties for NO_2 and SO_2 and an H&H cyclone with a Teflon filter for collecting size-selected particles.

Five candidate pumps were chosen primarily on the basis of results from our earlier study on personal dosimeters for SO_2, NO_x, O_3 and particulates (6). The Geomet respiration controlled sampler was not chosen because of its inherent flow variability. The Gage Research Institute pump was excluded from further testing, since it failed to deliver the target sampling rate of 2 liters per minute (L/min). Two sorbents, triethanolamine (TEA)-impregnated silica gel and molecular sieve, were tested for collecting NO_2 and SO_2. The results of these investigations, and the prototype finally assembled are described in this paper.

EXPERIMENTAL

NO/NO_2 Sampling System

The sampling train used in evaluating the collection efficiency of triethanolamine (TEA)-impregnated silica gel (Merck, 35-70 mesh) and molecular sieve (Linde Company, 13X, 1/16" size) for NO_2 is shown in Figure 1. Matheson (Whitby, Ontario)-certified NO_2 (49.7 ppm) gas was diluted with zero air (Matheson-certified) to generate the desired concentrations. The diluted gas was standardized routinely against NBS cylinder gases every week. The calibration curve was constructed by plotting NO_x analyzer (Monitor Labs Model 8840) response against several dilutions of the NBS Standard. The flow rate of each gas, including zero air, was measured precisely with Matheson-calibrated mass flowmeters before these gases were allowed to mix in the precision calibrator (Thermo Electron, Model 102). The calibrator was used only for mixing the test gas and zero air at atmospheric pressure. Stainless steel regulator, fittings, and Teflon tubings were used to assemble the NO_2 and NO_2/SO_2 sampling system.

NO_2/SO_2 Sampling System

This system, shown in Figure 2, was used to evaluate the collection efficiencies of TEA-coated 13X molecular sieve, 45/60 mesh (Chromatographic Specialties), and operational parameters of the prototype personal monitor for the collection of mixed SO_2 and NO_2 gases. It incorporates water-filled gas bubblers maintained at 55°C to humidify the test gases. Scrubbed laboratory air supplied by the Gast Manufacturing's (Benton Harbor, Michigan) double diaphragm pump was used as the diluent. The first

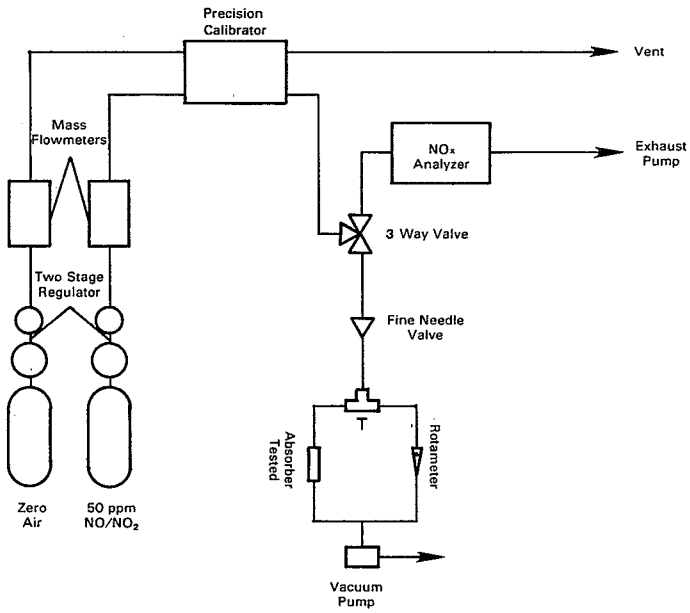

Figure 1. Schematic of NO/NO_2 flow system for testing solid sorbent.

three scrubbers removed moisture, the fourth removed SO_2 and NO_2, and the fifth scrubbed the remaining SO_2. The final scrubber was to remove organics and to act as a final back-up scrubber. The silica gel and back-up charcoal scrubber were replaced daily. Scrubbed air was checked for contamination daily by the use of a sampling pump/TEA-sorbent tube set-up at the outlet of the last scrubber. Standard NBS traceable gases--50.6 ppm SO_2 and 41.4 ppm NO_2 in air--used in this assembly were supplied by Scott Environmental Technology of Pennsylvania. After humidification, the gas stream enters an all-Teflon 32 cm x 7.5 cm I.D. mixing chamber and then goes to a Teflon sampling manifold (Figure 3). The manifold consisted of a cylinder 32 cm x 7.5 cm I.D. x 9.5 cm O.D. with friction-fit caps and three equally spaced holes on the sides to allow the cyclones to be placed within the manifold.

The flow to the manifold was 10 L/min, with a maximum of 6 liters being drawn off for test purposes. The remaining 4 liters were allowed to vent. Of that, 200 cm^3/min was pulled through a liquid impinger containing 25 mL of 1 percent hydrogen peroxide oxidant. The impinger was subsequently analyzed for SO_4^{2-}, and provides a reference point for the amount of SO_2 expected to be collected by the sorbent tubes.

The cyclone (H&H Custom Work, West Hill, Ontario) used was identical to those currently employed by the U.S. Environmental Protection Agency (information from personal communication with R.K. Stevens of the EPA), and was designed to operate between 1.9 and 2.1 L/min. The particle cut-off diameter is 5μ when operated at 1.7 L/min (NBS). Filters used in the cyclone were 25 mm diameter, 1.0μ pore size, FALP Teflon (Millipore Corporation) mounted on a stainless steel support screen. The filter material

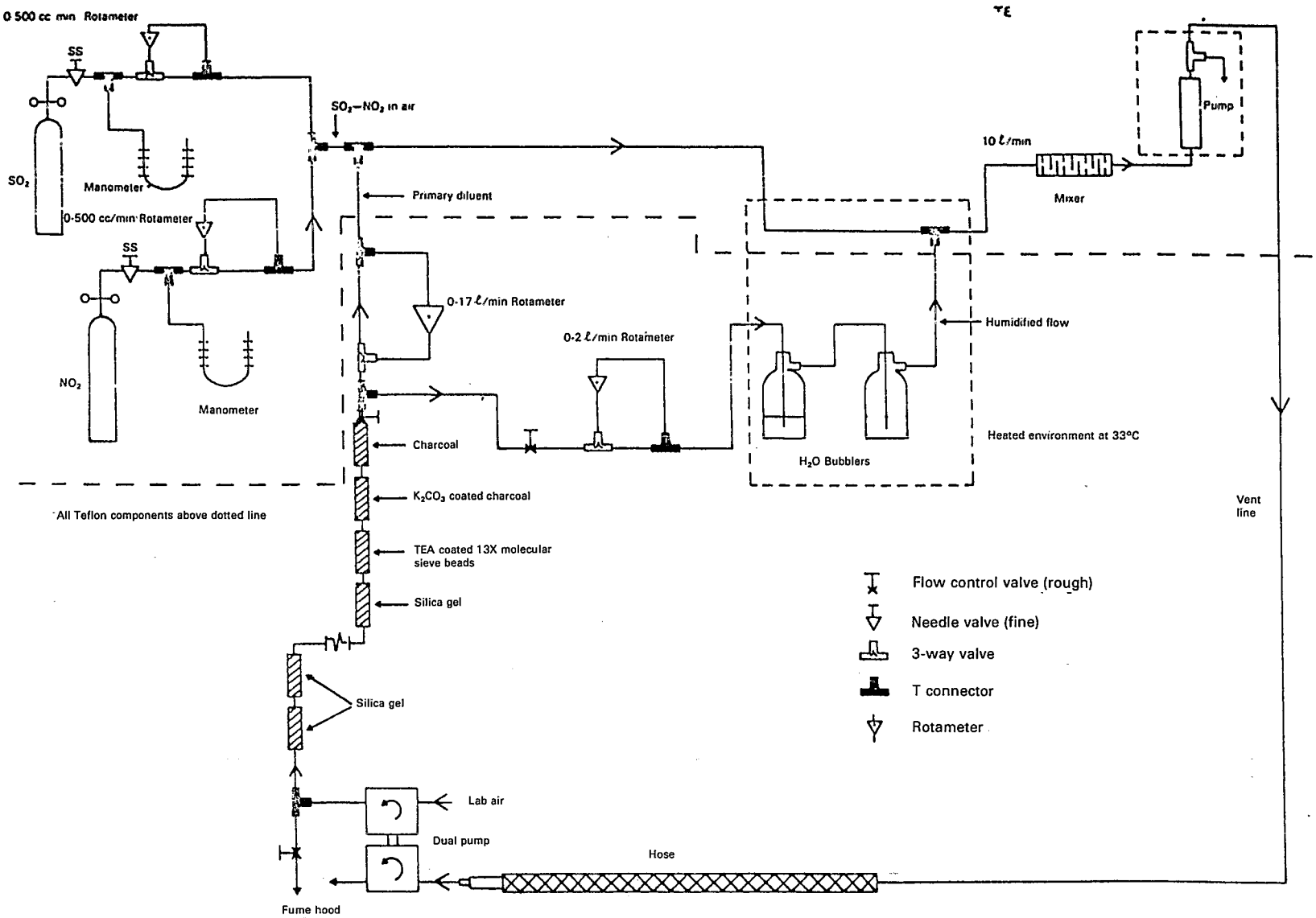

Figure 2. Schematic of flow system for generating SO_2 + NO_2 + humidified conditions for the testing of sorbent tubes/sampling pumps.

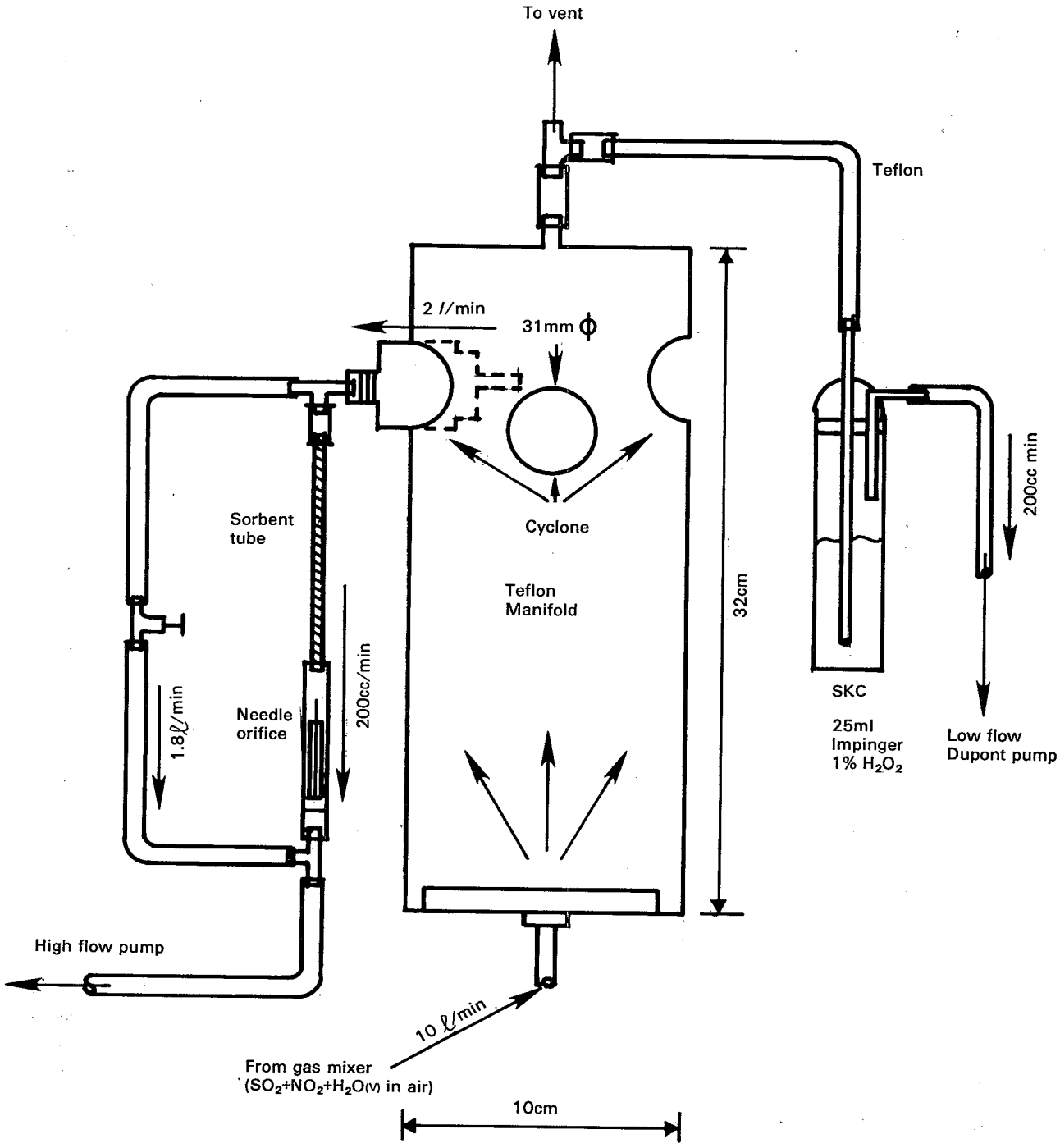

Figure 3. Sampling arrangement at the Teflon manifold.

chosen was reported to be ideal for NO_2/SO_2 sampling (9) and exhibits high (99.9%) particle collection efficiencies (10). The high-flow pump sampled 2 L/min through the cyclone and a restrictor by-pass, achieved by placing an 18-gauge syringe needle immediately behind the sorbent tube, was used to set the flow through the sorbent tubes to the desired level (Figure 3).

Preparation of Sorbent Tubes

Both substrates, silica gel and molecular sieve, were thoroughly washed until free of Cl^-, NO_3^-, and PO_4^{3-}. These were then coated with TEA by using the procedure described by Vinjamoori (11) with some minor modifications. The Chromatographic Specialties' molecular sieve used with the NO_2/SO_2 sampling system was dried, after coating, in an oven at 95°C with the nitrogen purged every half-hour.

A Dionex System 10 ion chromatograph (IC) was used for analysis using the following operating conditions: a 100-mm pre-column, 250-mm plastic separator, 250-mm suppressor, .003-M $NaHCO_3$/.0024 Na_2CO_3 standard eluent, flow rate 30 percent, loop 300 or 500 μL and sensitivity 3 or 10 μMHO.

Procedure

The procedure followed for the extraction of NO_2 from the silica gel used in the NO_2 sampling system was the same as described by Vinjamoori (11), except that the use of H_2O_2 was eliminated. For extracting NO_2 and SO_2 from the molecular sieve, the exposed sorbent was placed in a 1-oz (28-mL) "Nalgene" bottle containing 10 mL standard eluent, swirled for a few minutes, and allowed to stand for 5 minutes. Exactly 8 mL of the extract was placed in another 1-oz (28-mL) bottle containing 2 mL of 0.1 percent H_2O_2 and was analyzed after a brief mixing period. The concentrations of NO_2 and SO_2 were calculated by subtracting the blank and by referring to the standard peak height-to-concentration ratio determined prior to each sample injection.

RESULTS AND DISCUSSION

Nitrogen Dioxide Measurements

During the analysis it was observed that the molecular sieve (Linde Company) extracts contain suspended material (most likely alumina), and cannot be removed completely either by filtration or by centrifugation. This resulted in clogging of the pre-column of the ion chromatograph. Silica gel, on the other hand, produced clear extracts. It was also noted that the ratio of NO_2^- to NO_3^- peak heights varied over a wide range in the molecular sieve experiments as compared to the silica gel. An estimate of peak height ratios in ten experiments showed a variance of 3.6 with a mean of 4.5 for molecular sieve and a variance of 0.98 with a mean of 8.3 for silica gel. On the basis of these observations, silica gel was used for further testing.

For calculating the NO_2 concentrations from spectrophotometric and

other measurements, a stoichiometric factor is used to account for the theoretical formation of half a mole of NO_2^- for each mole of NO_2 (gas). The variations in the peak height ratios indicate that the factor can vary even for a given sorbent and depends upon the type of the sorbent used. Different values varying between 0.72 to 1.0 have been reported in the past (12). We estimated the stoichiometric factor from the mean value of silica gel results and found it to be 0.64, identical to the Vinjamoori estimate (11). However, a factor estimated from molecular sieve results would differ significantly from this value. Two inferences can be drawn from this discussion:

1. The methods in which NO_2 recovery is unaffected by the variations in stoichiometric factor should be preferred for the analysis of NO_2.

2. For the methods determining NO_2^- only (e.g., colorimetric), a careful measurement of the stoichiometric factor for the given sorbent should be made in order to achieve an accurate quantification of NO_2 (gas).

Ion chromatography enables simultaneous quantification of NO_2^- and NO_3^- and eliminates the use of a stoichiometic factor. We measured both NO_2^- and NO_3^- concentrations independently from the chromatograms and added them together to compute the recovery of NO_2 (gas). A typical chromatogram is shown in Figure 4. Nitrogen dioxide was collected on one sampling tube freshly filled with 0.4 gm TEA-impregnated silica gel and analyzed. The results are shown in Table 1. The set-up for the first set of exposures was such that the main stream was divided into two streams through a tee for simultaneous collection of NO_2 gas in duplicate sorbent tubes. For Set 2, only a single tube was used. The values in Set 2 represent an average of at least two independent measurements with a maximum variation of ±4 percent. Similar variation is found in the duplicate exposure of Set 1 (Table 1). Recoveries in both cases average 98 percent. Since the recoveries were good, no further experiments were performed with back-up tubes to study the collection efficiency. Percent recovery is viewed as the collection efficiency of the sorbent tested. The effect of humidity on the quantitative collection and analysis of NO_2 and the breakthrough studies of the sorbent are now being conducted. The work presented above is intended to show that silica gel coupled with IC is very effective for collection and analysis of NO_2 and involves a simpler procedure because filtration of the extract is eliminated from the process.

Prototype Nitrogen Dioxide and Sulfur Dioxide Personal Monitor Components Tests

Solid Sorbent

Two sorbent tubes, (1.6-g sieve in the front and 0.8 g in the back-up tube) were sampled at 250 and 325 cm^3/min using higher flow Dupont pumps to sample 2 L/min through the cyclone and, by means of the restricter arrangement, the desired flow through the sorbent tubes. The sample results with the test conditions given in Table 2 show that SO_2 collection efficiency

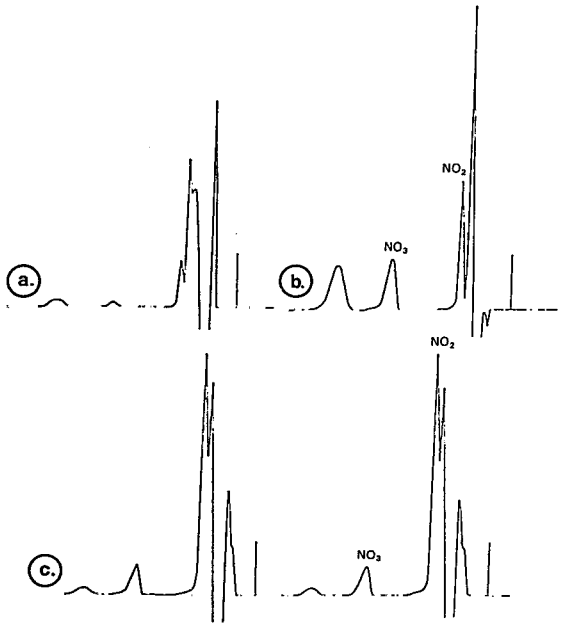

a. Blank
b. 1 ppm standard
c. Duplicate Injection of Sample

Figure 4. A typical chromatogram of blank (a), 1 ppm standard (b), and duplicate injection of sample (c).

exceeded 100 percent, while that of NO_2 was approximately 40 percent. The level of NO_2 in the scrubbed air, as detected by a sorbent tube placed at the end of the scrubbing train, was negligible. High concentration levels (25 percent), however, were detected for SO_2. The high SO_2 collection efficiencies probably arise from sampling blanks not accounted for in the corrections.

To study the effects of relative humidity (RH) on the collection efficiency, tests were conducted near 25, 50, 70, and 100 percent RH at 1 ppm NO_2 and SO_2 concentration levels. Triplicate sorbent tubes (Teflon) were exposed at about 200 cm^3/min flow rate. The results are shown in Table 3. Generally, the SO_2 collection efficiencies did not appear to vary significantly with humidity, although for NO_2 there was a distinct increase above 50 percent RH. At 75 RH, for example, these average 91 percent and 56 percent for NO_2 and SO_2, respectively. Impingers show, on the average, 85 percent efficiencies (ignoring the outlying 65 percent).

As an indication of whether the Teflon filter absorbed any NO_2 or SO_2 with change in humidity, the filters were removed and analyzed for NO_2^- and SO_2^-. For the most part, the filters did not absorb more than 0.2 percent of the exposed concentrations, as would be expected (9,10).

TABLE 1. COLLECTION EFFICIENCY OF TEA-SILICA GEL SORBENT FOR NO_2

Flow through sorbent tube cm^3/min	Exposure hours	NO_2 ppm Expected	NO_2 ppm Found	Percent recovery
	Set 1 (.3-.5-ppm exposure levels)			
90.0 *	6	.50	.51	102
91.5 *	6	.50	.48	96
86.5	6	.30	.27	90
85.0	6	.30	.26	87
93.2	4	.49	.52	106
88.0	4	.49	.54	110
89.0	4	.31	.28	90
91.0	4	.31	.29	94
			Av.	97%
	Set 2 (1-ppm exposure level)			
39.5	5	.94	.90	96
21.0	5	.96	.90	94
59.5	2.5	.96	.92	96
31.5	2.5	.94	.94	100
28.5	2.5	.96	1.01	105
31.6	1.5	1.00	.92	92
50.5	1	.94	.94	100
			Av.	98%

*Bracketed values are from the simultaneous exposures of the main stream branched off into two equivalent sub-streams.

TABLE 2. SORBENT TUBE BREAKTHROUGH* AT HIGH LOADINGS

Flow through sorbent tube	Sampled volume	Total µg expected NO_2	Total µg expected SO_2	µg Found† Front NO_2	µg Found† Front SO_2	µg Found† Back NO_2	µg Found† Back SO_2	Front tube collection efficiency,% NO_2	Front tube collection efficiency,% SO_2
250 cm^3/min^{-1}	90.0 L	340	463	138	469	0.4	6.2	41	101
325 cm^3/min^{-1}	117 L	442	600	174	719	0.6	12.6	39	120

*Conditions: 1.99 ppm NO_2; 1.97 ppm SO_2; 51% relative humidity; 24°C room temperature; glass sorbent tubes; flow of 2 L/min^{-1} through cyclone with filters, high-flow Duponts used; 1.6 g TEA-coated 13x molecular sieve, front, 0.8 g, back; 6-hour test.
†Sorbent blank corrected.

TABLE 3. EFFECT OF RELATIVE HUMIDITY (RH) ON COLLECTION EFFICIENCY AT 1.0 PPM LEVEL*

RH %	ppm		Sorbent tube flow, cm^3/min^{-1}	Sampled volume, L	µg, Expected		µg, Found†		Collection efficiency	
	SO_2	NO_2			NO_2	SO_2	NO_2	SO_2	NO_2	SO_2
23.3	1.03	1.03	283	101.9	199	273	92.7	119	47	44
			215	77.4	152	207	78.9	97	52	47
			200	72.0	141	193	76.4	81	54	42
			Imp.‡ 200	72.0	NP§	193	NP	155	--	80
48.5	1.22	1.00	283	88.3	169	280	73.9	99.5	44	36
			215	77.4	146	245	69.5	69.5	48	28
			200	72.0	136	228	73.9	68.8	54	30
			Imp. 200	79.2	NP	251	NP	163	--	55
75.8	1.05	1.05	283	101.9	202	277	215	182	106	66
			215	77.4	154	211	127	104	82	49
			200	72.0	143	196	120	103	84	53
			Imp. 210	75.6	NP	205	NP	189	--	92
102	1.02	1.02	283	≈85	≈164	≈224	218	126	≈133	56
			215	77.4	150	204	116	72.0	77	35
			200	72.0	139	190	134	68.0	96	36
			Imp. 215	77.4	NP	204	NP	169	--	83

*Conditions: As above, and: room temperature 22.5-23°C; Teflon sorbent tubes; 2 L/min^{-1} through cyclone with filters inserted, high-flow Duponts used; 1.6 g TEA-coated 13x molecular sieve sorbent tubes; 6-hour tests.

†Sorbent blank corrected.

‡Imp. - impinger at manifold exit.

§NP - Not pertinent.

Sampling Pumps

The five sampling pumps chosen were based primarily on an earlier study (6). Life tests were performed on these pumps in order to determine the total time that the units would be able to sample the 2 L/min required for the prototype based on the use of the particulate cyclone and filter. The pumps were tested under conditions simulating the back pressure (≈50 cm H_2O) of sampling according to the full sampling train depicted in Figure 5. The pressure was simulated by constricting the sampling line to the pump. All pumps tested were fully charged prior to use, and pumps were tested twice each. Results are shown in Table 4. Data for the Harvard/EPRI system are not reported because the batteries in the unit tested were five years old.

The results indicated that, based on the ability of the pump to maintain constant flow for a 12-hour period, the Dupont P4000 was clearly the best overall performer when compared to the Dupont P2500 and the Gilian HFS-113. All pumps were generally good for 6 hours, but at 8 hours, only the Dupont P4000 and the Gilian HFS-113 were performing satisfactorily.

The Gage Research Institute pump (with liquid impinger removed) could not deliver 2 L/min; therefore, it was excluded from further testing. It should be noted that the Gage pump used was the first-generation pump. There is at present a second-generation unit, but unfortunately it could not be made available at the time of testing. The second-generation pump unit is equipped with two sampling pumps and also, provision for a 1.7 L/min cyclone has been incorporated.

Replicate testing of the Gilian, Harvard/EPRI, Dupont P4000, and Dupont P2500 was then performed at a relative humidity of 75 percent and SO_2 and NO_2 concentrations ≈ 1.0 ppm. The sampling rate through the cyclone (with filters) was set at 2 L/min, while the flow through the sorbent tube was set at 200 cm^3/min.

Prior to each test, all pump flows were set and were identical (±5 percent) to each other. Sorbent tubes (Teflon) containing 1.6 g sieve were used for all tests. The results given in Table 5 indicate that, for the test performed, the Dupont 4000 again performed best. On inspection of the actual sorbent flows, the following remarks may be made:

1. The Gilian and P2500 pumps always showed lower than nominal flows.

2. The Harvard pump always showed more than nominal flow.

3. The P4000 was closest to the set flow.

4. The mean collection efficiency for NO_2 is twice as much as for SO_2, an observation that was made in the earlier set of exposures (Table 3). Impinger efficiencies again average close to 100 percent.

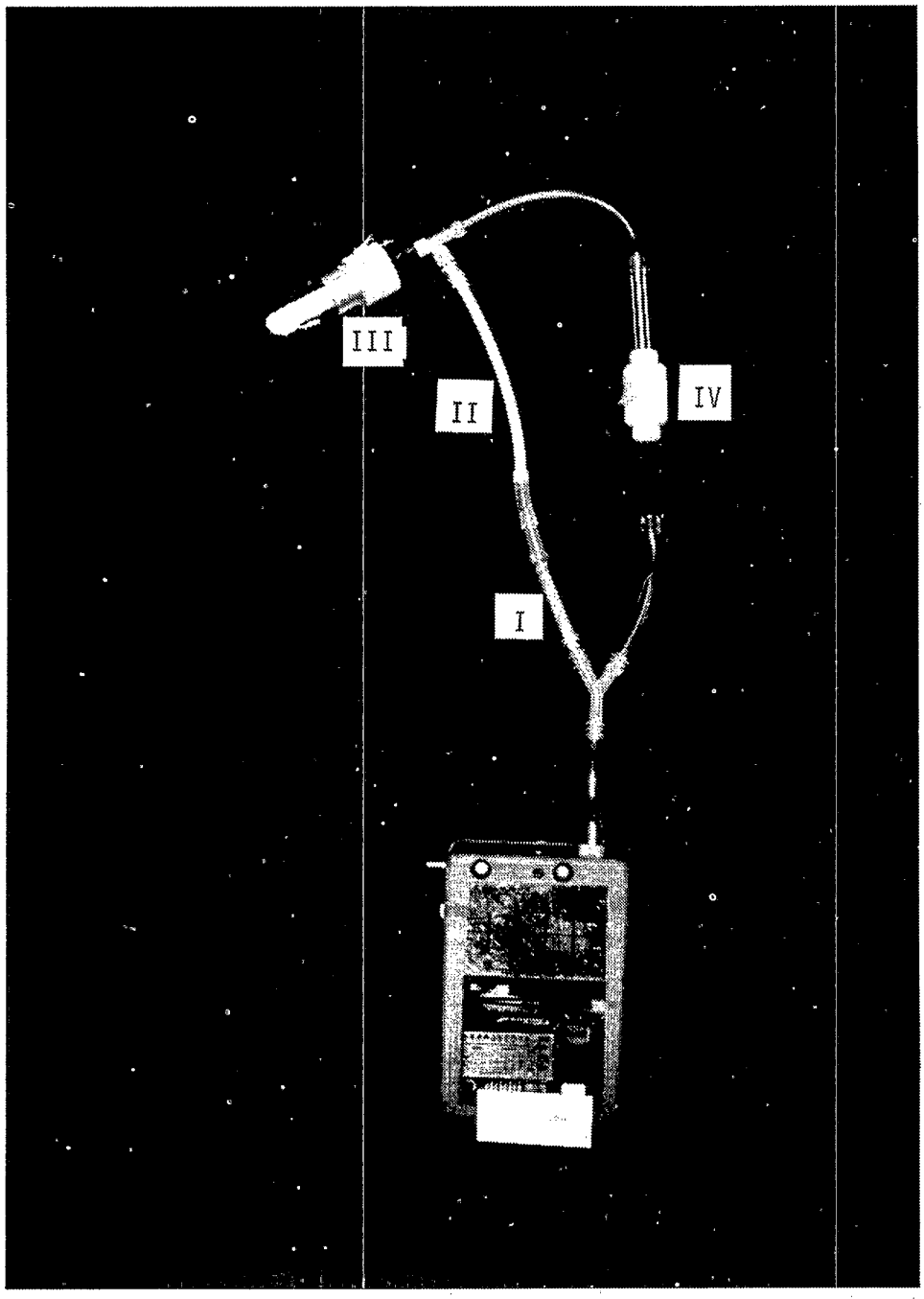

Figure 5. Photograph of assembled prototype.

TABLE 4. LIFE TESTS OF CANDIDATE SAMPLING PUMPS*

Dupont P2500			Dupont P4000			Gilian HFS-113		
Time	Sorbent flow cm^3/min	Total flow L/min	Time	Sorbent flow cm^3/min	Total flow L/min	Time	Sorbent flow cm^3/min	Total flow L/min
Start	200	2.00	Start	200	2.00	Start	200	2.00
6 hr	170	1.95	6 hr	200	2.00	6 hr	162	1.92
7 hr	157	1.95	7.5 hr	190	2.00	8 hr	157	1.88
8 hr	102	1.44	9 hr	190	2.00	10 hr	175	1.88
8.5 hr	Total was <1.0		10 hr	180	1.90	11 hr	141	1.84
			12 hr	167	1.85	15 hr	141	1.88
			13 hr	Total was <1.0		20 hr	165	1.85
						21 hr	Stopped	
Start	200	1.98	Start	200	2.10	Start	200	2.00
6 hr	185	1.94	6 hr	207	1.95	6 hr	141	1.80
8 hr	175	1.94	8.5 hr	200	1.95	8 hr	141	1.75
9 hr	175	1.92	10 hr	193	1.96	10 hr	135	1.69
10 hr	142	1.65	11 hr	203	1.94	12 hr	141	1.92
11 hr	Stopped					13 hr	135	1.91
						14 hr	Stopped	

*Of four individuals listening to the noise level of the sampling pumps, all found the Gilian extremely loud and the Dupont pumps in the middle range.

TABLE 5. REPLICATE TESTING OF SAMPLING PUMPS AT 1.0 PPM LEVEL AND 75 PERCENT RELATIVE HUMIDITY (RH)

Test conditions*	Pump	Sorbent flow† cm^3/min set (actual)	Sampled volume, L set (actual)	µg Expected NO_2	µg Expected SO_2	µg Found‡ NO_2	µg Found‡ SO_2	Collection efficiency NO_2	Collection efficiency SO_2
#1 75.8% RH	P2500	200 (194)	72 (69.4)	144	197	72.7	64.1	51	33
1.05 ppm SO_2	Gilian	200 (185)	72 (66.6)	144	197	60.2	47.1	42	24
1.05 ppm NO_2	Harvard	200 (218)	72 (78.1)	144	197	188	90.8	131	46
	impinger	212	74.2	NP§	202	NP	157	NP	78
#2 76.0% RH	P4000	200 (193)	72 (69.7)	141	193	124	90.0	88	41
1.03 ppm SO_2	Harvard	200 (206)	72 (74.2)	141	193	104	111	72	51
1.03 ppm NO_2	P2500	200 (193)	72 (69.7)	141	193	111	89.1	79	41
	impinger	210	75.6	NP	203	NP	229	NP	113
#3 75.8% RH	Harvard	200 (210)	72 (75.6)	144	197	129	99.1	90	50
1.05 ppm SO_2	P4000	200 (194)	65 (63)	130	178	77.4	37.5	60	21
1.05 ppm NO_2	Gilian	200 (167)	72 (66.1)	144	197	88.4	52.9	61	27
	impinger		75.6	NP	205	NP	222	NP	108
#4 74.7% RH	Gilian	200 (182)	67.6(61.3)	131	179	83.4	37.5	64	21
1.02 ppm SO_2	P2500	200 (184)	67.6(62.0)	131	179	103	57.5	79	32
1.02 ppm NO_2	P4000	200 (200)	67.6(67.6)	131	179	139	90.0	106	50
	impinger	210	71.0	NP	189	NP	207	NP	110
							Av.	72	Av. 36 (excluding impinger)

*Conditions: All 6-hour tests, except #4, which was 338 minutes; 1.6 g TEA-coated 13x molecular sieves in Teflon sorbent tubes used.

†Actual flow is average flow during the course of the test.

‡µg, found = actual found less blank (unexposed) sorbent tube NO_2 and SO_2 levels.

§NP - Not pertinent.

The Dupont P4000 pump has several features that make it useful and attractive for deployment in a prototype sampler, most notably the automatic timer shut-off and the visual indication of cumulative sampling time. The final testing incorporated several changes based on the results of the sampling phases completed. An impinger filled with 25 mL of 1 percent H_2O_2 was placed immediately after the charcoal scrubber to make an accurate assessment of the amount of SO_2 escaping the scrubber system. The mean 100 percent collection efficiency of the impinger at the manifold for SO_2 compared to the much lower efficiencies of the solid sorbent led us to suspect the quality of the latter. A fresh batch of 13X molecular sieve was washed, dried, and coated with an increase in the concentration of TEA and ethylene glycol (50 g TEA + 8 g glycol + 25 mL acetone + water diluted to 75 mL) according to the procedure given earlier. The sieve was removed from the oven at the first sign of free-flow. In order to accurately set flows through the sorbent tube while passing 2 L/min through the cyclone, the restricter-bypass arrangement was not employed. The Dupont P4000 pump was used for high flows (1.8 to 1.9 L/min) through the cyclone, and a low-flow pump was employed to pump the desired flow through the sorbent tube. The total flow through the cyclone would therefore be 2 L/min.

Sampling blanks were determined with the scrubbed air only at flow rates of 100, 150, and 200 cm^3/min at 75 percent relative humidity. The results of these tests are shown in Table 6. The recoveries for NO_2 at the concentration levels investigated are nearly 100 percent, with relative standard deviation of 6.5 percent. For SO_2, recoveries average 96 percent, with a relatively large standard deviation of 32 percent. The corresponding impinger recoveries including those obtained in the earlier tests (Tables 3 and 5) exceed 85 percent and do not show such variations. The variance is believed to be due to inefficient collection of the sorbent under the test conditions. SO_2 losses in the 60 to 90 percent humidity range have been reported by Vinjamoori (11).

The Prototype

The prototype personal monitor (Figure 5) was assembled with the following components (numerals in parenthesis refer to Figure 5):

(a) a Dupont P4000 sampling pump

(b) an 18-gauge syringe needle restrictor/bypass to allow low flows through the sorbent tube (I)

(c) a 6-mm OD Teflon tube containing 1.6 gm TEA-coated 13X molecular sieve (II)

(d) an H&H particulate cyclone with 25-mm-diameter FALP (Millipore Corporation) 1μ Teflon filter (III)

(e) a side-arm restrictor (Teflon needle valve) (IV)

The operational parameters of the device can be summarized as follows:

TABLE 6. RESULTS OF FINAL TESTING

Test conditions*	Average sorbent flow, cm^3/min^{-1}	Sampled volume, L	µg Expected NO_2	µg Expected SO_2	µg Found† NO_2	µg Found† SO_2	Collection efficiency NO_2	Collection efficiency SO_2
#1 75.3% RH	91.5	32.9	63.9	87.5	64.6	54	101	62
1.02 ppm SO_2	148	53.1	103	141	101	108	98	77
1.02 ppm NO_2	197	70.7	137	188	153	125	111	66
	Imp. - 205	73.8	NP‡	196	NP	193	NP	98
#2 75.1% RH	102	37.1	14.1	15.3	13.6	13.3	97	87
0.159 ppm SO_2	150	54.8	20.9	22.7	19.0	22.0	91	97
0.201 ppm NO_2	195	71.2	27.2	29.5	28.4	27.9	104	95
	Imp. - 205	74.8	NP	31.0	NP	33.9	NP	109
#3 74.0% RH	103	37.8	14.2	15.4	18.4	33.3	130§	216§
0.161 ppm SO_2	149	53.6	20.6	22.4	22.1	34.0	107	152
0.201 ppm NO_2	196	70.6	27.1	29.5	25.9	38.0	96	129
	Imp. - 215	77.4	NP	32.3	NP	35.1	NP	109
							RSD 6.5%	32%

*Conditions: As above, and: room temperature 23.5 to 24°C; Teflon sorbent tubes containing 1.6 g freshly coated sieve; flow of 2 L/min^{-1} passing through cyclones, with filter inserted; flow through solvent tubes controlled by low-flow Dupont pumps; one impinger containing H_2O_2 operated at outlet of scrubbed lab air; all 6-hour tests.

†Corrected for sampling and sorbent blanks.

‡NP - Not pertinent.

§Outlier.

1. The pump operates unattended at a sampling rate of 2 L/min over a 12-hour period.

2. The FALP Teflon filter in the cyclone poses no flow restriction problems and appears to absorb a maximum of only 0.5μg SO_2 and negligible NO_2.

3. The bypass/restrictor arrangements set the desired flow through the sorbent tubes while simultaneously passing 2 L/min through the cyclone. Flow stability of ± 5-10 percent are readily achieved at a constant pump flow.

4. The TEA-coated 13X molecular sieve effectively collects 0.2 and 1.0 ppm concentration NO_2 exposures at 75 percent relative humidity, at flow rates between 100 and 200 cm^3/min for 6 hours. For SO_2, collection efficiency is about the same, although there appears to be a lesser dependence on relative humidity.

5. The capacity of 1.6 g of the sorbent in a Teflon tube appears to be 80μg SO_2 and 200μg NO_2. Sampling air at the rate of 100 cm^3/min through the sorbent tube at a concentration of 1 ppm SO_2 and NO_2 is well within the capacity of the sorbent tubes.

The photograph of the assembled prototype is shown in Figure 5. The ion chromatographic analysis is well suited for the quantification of the target in the extracts. Below about 1 to 2μg SO_2 or NO_2 collected, the analysis is performed close to the detection limit. Higher injection volumes would increase the sensitivity. Arrangements are underway to carry out the validation tests of the prototype in an exposure chamber. The results will be reported later.

ACKNOWLEDGMENTS

Part of this work was conducted by Concord Scientific Corporation under Contract Reference No. 808.

REFERENCES

1. Godin, G., G. Wright, and R.J. Shepard. 1972. Urban exposure to carbon monoxide. Arch. Environ. Health 25:305.

2. Wright, G.R., J. Jewczyk, J. Onrot, P. Tomlinson, and R.J. Shepard. 1975. Carbon monoxide in the urban atmosphere. Arch. Environ. Health 30:123.

3. Ott, W.R., and D.T. Mage. 1975. A method of stimulating the true human exposure of critical population groups to air pollutants. Page 2097 in Recent advances in the assessment of the health effects of environmental pollution. Commission of the European Communities, EUR 5300, Luxembourg.

4. Chapin, F.S. 1974. Human activity patterns in the city. Wiley-Intersciences, New York, NY.

5. Szalai, A. 1972. The use of time: Daily activities of urban and suburban populations in twelve countries. Mounton, The Hague.

6. Meranger, J.C., T.R. Khan, and R.B. Caton. 1981. State-of-the-art of commercially available personal monitors for NO_x, SO_2 and particulate matter in ambient air. Proceedings of the 15th Conference on Trace Substances in Environmental Health, University of Missouri, Columbia, MO.

7. Dockery, D.W., and J.D. Spengler. 1981. Personal exposure to respirable particulates and sulfates. JAPA 31:153.

8. Mintz, S., R.H. Hosein, B. Batten, and F. Silverman. n.d. A personal sampler for three respiratory irritants. The Gage Research Institute, Toronto, Ontario, Canada.

9. Appel, B.R., Y. Tokiwa, S.M. Wall, E.M. Hoffer, M. Haik, and J.J. Wesolowski. 1978. Effect of environmental variable and sampling media on the collection of atmospheric sulfate and nitrate. California Air Resources Board, Contract ARB5-1032, January.

10. Appel, B.R., S.M. Wall, Y. Tokiwa, and M. Haik. 1979. Interference effects in sampling particulate in ambient air. Atmospheric Environment 13:319-325.

11. Vinjamoori, D.V., and C. Ling. 1981. Personal monitoring method for NO_2 and SO_2 with solid sorbent sampling and ion chromatographic determination. Anal. Chem. 53:1689-1691.

12. Blacker, J.H. 1973. Triethanolamine for collecting nitrogen dioxide in the TLV range. Am. Ind. Hyg. Assoc. J.:394.

DEVELOPMENT OF SPE DIFFUSION HEAD INSTRUMENTATION

J.A. Kosek, J.P. Giordano, and A.B. LaConti

General Electric Company
Direct Energy Conversion Programs
Wilmington, MA

INTRODUCTION

General Electric has developed a line of electrochemical sensors for monitoring such gases as CO, NO, and NO_2 in mine and industrial atmospheres, using a unique solid polymer electrolyte electrochemical cell technology (1-3). The sensor development has been carried out largely under contract to the U.S. Bureau of Mines, supplemented by an in-house IR&D program. Several models of carbon monoxide instruments are now in commercial production. These instruments include a direct-reading CO detector and a CO dosimeter, both of which use an air-sampling pump to bring a gas sample to the electochemical sensor cell. A feature common to all these instruments is the use of a solid polymer electrolyte membrane as the sole electrolyte in the electrochemical sensor cell. Catalytic electrodes are integrally bonded to the membrane to form a unique unitary structure. Use of the SPE sensor cell eliminates problems such as corrosion and containment associated with caustic or acidic electrolytes and leads to highly invariant sensor cell response and long-life operation with minimal maintenance and calibration.

Recently, the family of instrumentation has been expanded to include diffusion head sensor cells. In these instruments, the air sampling pump has been removed, and the electrochemical sensor cell has been modified such that an air sample reaches the sensor cell by means of natural gaseous diffusion.

A diffusion-based instrument offers several advantages over conventional, pumped instrumentation. First, the pump is usually the least reliable component in the instrument. Therefore, elimination of the pump increases the reliability of the instrument. Secondly, in a battery-powered instrument or in one that has a backup battery system for power, the pump usually requires the most power of any component in the instrument. Elimination of the pump decreases the current draw of the instrument and increases usable battery life. Also, elimination of the pump and its associated tubing and rotameters results in a size and weight reduction that is important for hand-held portable instrumentation.

The SPE gas detectors are intended for use by military, government, and industrial personnel involved in air quality measurements. The commercial SPE CO dosimeter and direct-reading detection instruments are being widely used by steel mills, fire departments, and various city, state, and federal regulatory agencies.

EXPERIMENTAL

The membrane and electrode assembly used in the CO sensor cell has three electrodes of identical composition: sensing, counter, and reference. These electrodes are fabricated from a platinoid black catalyst composition blended with a Teflon (T.M.--E.I. DuPont) binder. A transition metal screen is embedded into the electrodes to obtain improved mechanical integrity and current collection. The counter electrode is the same size (2.4 cm^2) and configuration as the sensing electrode. The reference electrode has an area of approximately 0.32 cm^2. The electrodes are bonded to the membrane by a proprietary method developed by General Electric. The spatial configuration of the resultant membrane and electrode assembly has been developed to achieve good vapor phase transport and to provide a high output signal.

A schematic of the hydrated solid polymer electrolyte sensor cell used in a pumped instrument is depicted in Figure 1. The membrane and electrode assembly is housed in Lexan (T.M.--General Electric Company) polycarbonate hardware. Lexan was selected because of its good physical properties (transparency, shock resistance), and chemical inertness/minimal elution. The catalytic sensing and reference electrodes are positioned on one side of the cation exchange membrane; a catalytic counter electrode is positioned on the other side of the membrane opposite the sensing electrode. The counter electrode compartment is flooded with water. Electrolytic contact between the sensing electrode and the platinoid metal/air reference is achieved through a hydrated solid polymer electrolyte membrane bridge. The performance characteristics and other properties of the cell are highly dependent on the morphological structure of the membrane and the method of hydrating the membrane to achieve a fixed water content.

All work has been accomplished using perfluorosulfonate ion exchange membranes manufactured by E.I. DuPont and sold under the trade name Nafion. Nafion is a copolymer of polytetrafluorethylene (PTFE) and polysulfonylfluoride vinyl ether containing pendant sulfonic acid groups. The sulfonic acid groups are chemically bound to the perfluorocarbon backbone.

An example of the composition is shown below. EW, or equivalent weight, is defined as the weight of XR resin that neutralizes one equivalent of base.

1. RESERVOIR HOUSING
2. CAP
3. SUPPORT PLATE
4. M & E ASSEMBLY
5. BASE PLATE
6. GASKET
7. CONTACT PIN
8. THERMISTOR
9. NYLON SCREW
10. TEFLON TAPE
11. GASKET
12. GASKET
13. COUNTER ELECTRODE
14. SENSOR ELECTRODE
15. REFERENCE ELECTRODE
16. THERMISTOR

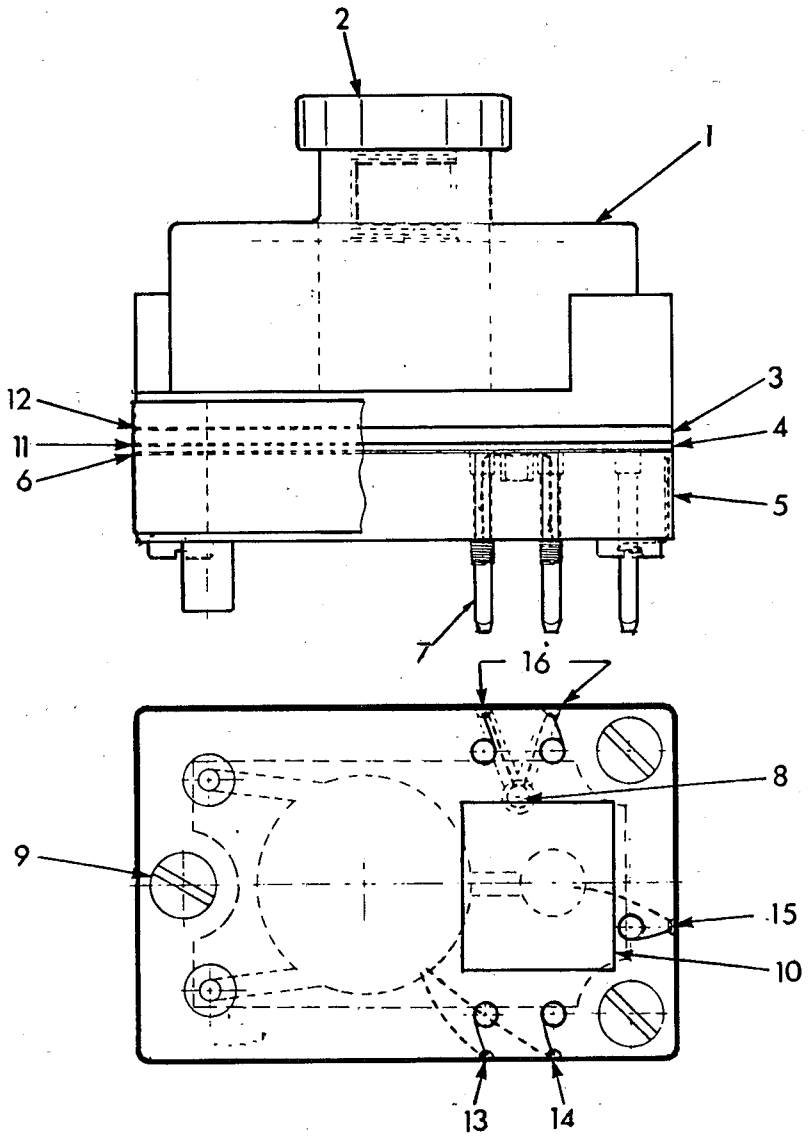

Figure 1. Pumped sensor cell assembly.

1240 EW

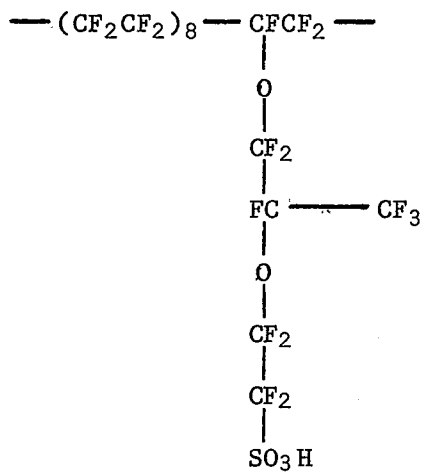

Membranes are also characterized by their ion exchange capacity (IEC) - milli-equivalents (meq) of sulfonic acid/dry weight of membrane. The relationship between IEC and EW can be expressed as:

$$IEC = \frac{1000}{EW} \tag{1}$$

Generally, IEC is determined by acid/base titration methods and gravimetric weight analysis.

Three electrode potentiostatic systems utilizing the hydrated solid polymer electrolyte as the electrolyte for the electrochemical sensor cell were used in all cases. Among the unique design characteristics of the SPE sensor are:

- The electrolyte is embedded in the solid polymer material, providing longer life, greater stability, and improved reliability.

- Electrodes are firmly attached to and embedded in the electrolyte sheet, also contributing to enhanced life and reliability.

- The sensor contains no corrosive liquids--the only liquid in the sensor is distilled water.

A detailed description of pumped SPE CO sensor cell response characteristics may be found in reference 3.

THEORETICAL

Prior to experimentation, a rudimentary theory of sensor response was

derived in order to assess the predicted order of magnitude of sensor response to carbon monoxide diffusion conditions (that is, μA/ppm CO). Pure diffusion in unsteady-state conditions is given by the following expression.

$$D \frac{\partial^2 C}{\partial X^2} = \frac{\partial C}{\partial t} \tag{2}$$

D = diffusion coefficient
(0.175 cm^2/sec for CO)

C = CO concentration (moles/cm^3)

X = distance up the tube

t = time, sec (from time of admission of sample to base of tube)

The general solution to the equation is:

$$C = (a/t^{1/2}) \exp(-X^2/4Dt) \tag{3}$$

where a is a parameter to be determined. Next, at X = 0 (base of tube) the CO concentration is the ambient value, C_*. With this substitution we arrived at

$$C = C_* \exp(-X^2/4Dt) \tag{4}$$

The flux of CO molecules at the electrode surface is as follows:

$$J = DA \frac{\partial C}{\partial X}, \text{ (at } X = L) \tag{5}$$

$A = \pi d^2/4$ is the cross-sectional area of the tube. With the reasonable assumption that all CO molecules that hit the electrode surface react, the electrochemical current generated is:

$$i = zFJ = -zFDA \left(\frac{\partial C}{\partial X}\right)_{x = L} \tag{6}$$

$(\partial C/\partial X)$ is obtained by differentiation of Equation 4. Finally, we arrived at an expression for current, i:

$$i = \frac{zFALC_*}{2t} \exp(-L^2/4Dt) \tag{7}$$

The steady-state current occurs when di/dt = 0 i.e., at

$$t = L^2/4D \tag{8}$$

Substitution of Equation 8 into 7 yielded

$$i = \frac{2zFAC_{*}D}{L} \quad \exp(-1) \tag{9}$$

First, an estimate can be made of expected response time from Equation 8. Tube length is L = 10 cm and D = 0.175 cm^2/sec. Using these values, t = 143 seconds was computed. Secondly, the steady-state current was estimated for 1 ppm CO by means of Equation 9. Note that tube area A = 2.85 cm^2, zF = 2 x 96,500 coul/mole, and 1 ppm CO is equivalent to 4.08 x 10^{-11} moles/cm^3. Using these numbers, a sensor response of 0.29 μA/ppm CO was calculated. The simplified diffusion model provided predictions of operating characteristics that were sufficiently promising to proceed with an experimental study.

RESULTS AND DISCUSSION

Wall-Mounted Transducer Module

A simplified schematic diagram of a typical diffusion sensor cell is shown in Figure 2. With this device, ambient air enters the open end of the diffusion tube, diffuses the length of the tube to the sensing electrode through an integral interference filter (not pictured), and reacts at the sensing electrode. As will be described later, the geometry of the diffusion tube greatly influences the observed diffusion sensor cell response.

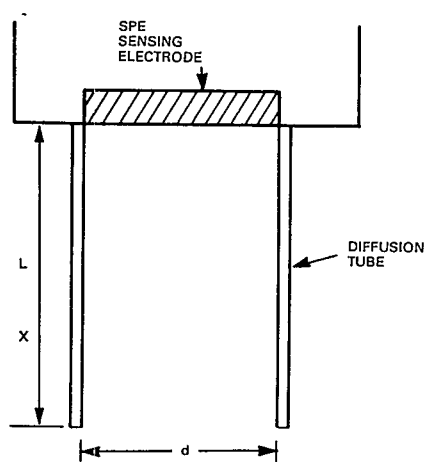

Figure 2. Schematic of SPE Diffusion Head Gas Sensor.

A photograph of a prototype instrument incorporating a diffusion sensor cell is shown in Figure 3. The diffusion head transducer module, designed for long-term unattended use, is a wall-mounted instrument for

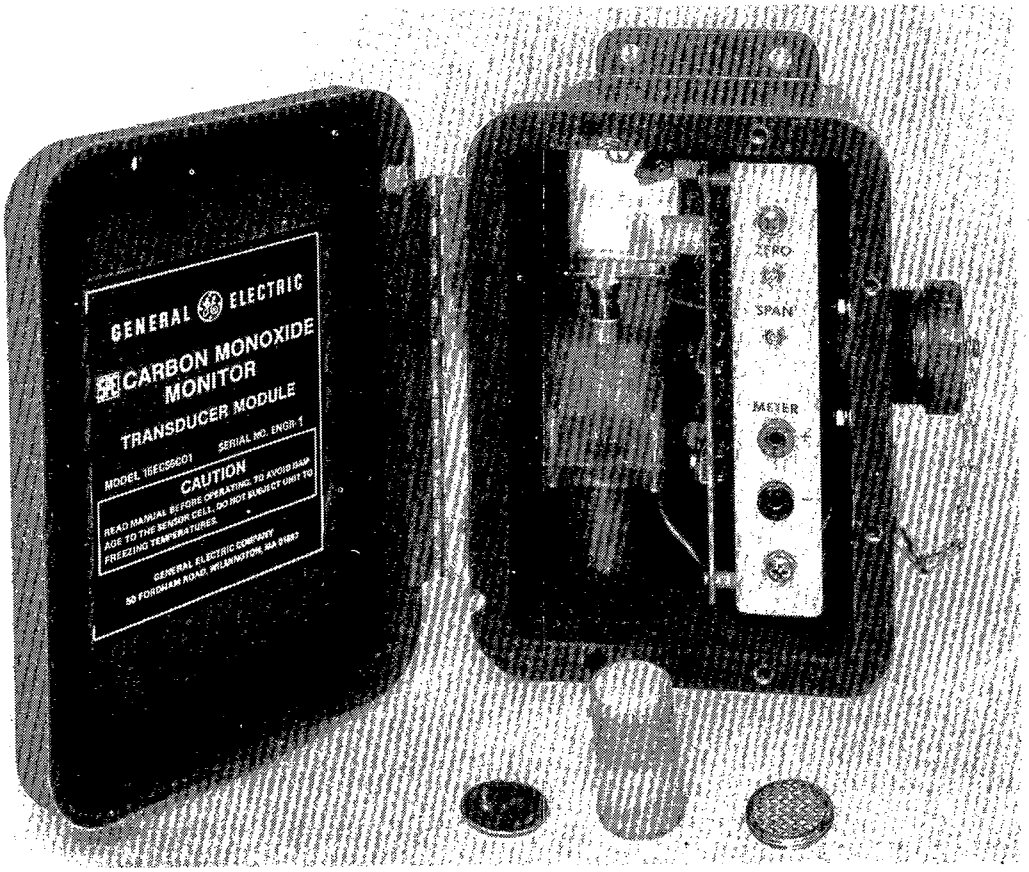

Figure 3. Remote diffusion head transducer monitor.

monitoring ambient levels of CO. The output of the transducer module, when used in conjunction with a dedicated control module shown in Figure 4, can be displayed directly in parts per million (ppm). The control module also supplies power to the transducer module. The transducer module can also operate in conjunction with specified external power and data acquisition systems. The present system is designed to operate over a +7.2 to 21 VDC range of input voltage and to produce an output voltage of 0 to 5 VDC. When used with the control module, CO concentration readings are obtained over the range from 0 to 100 ppm CO. If an external power and data acquisition system is used, the instrument range is 0 to 50 ppm CO. In operation, total current draw of the transducer module is less than 5 ma. Calibration of the unit is readily accomplished directly at the transducer module.

Also visible in Figure 3 is the removal tube that houses the integral interference filter. In use, the interference filter is located directly beneath the sensing electrode. Using a dry gas stream, this filter had a lifetime of 23,300 ppm-hr before breakthrough was observed. Use of the removable tube facilitates changing the interference filter without removal of the sensor cell from the transducer module assembly. Not visible in Figure 3 is the porous metal disk incorporated as part of the diffusion tube assembly to improve the flow/response characteristics of the

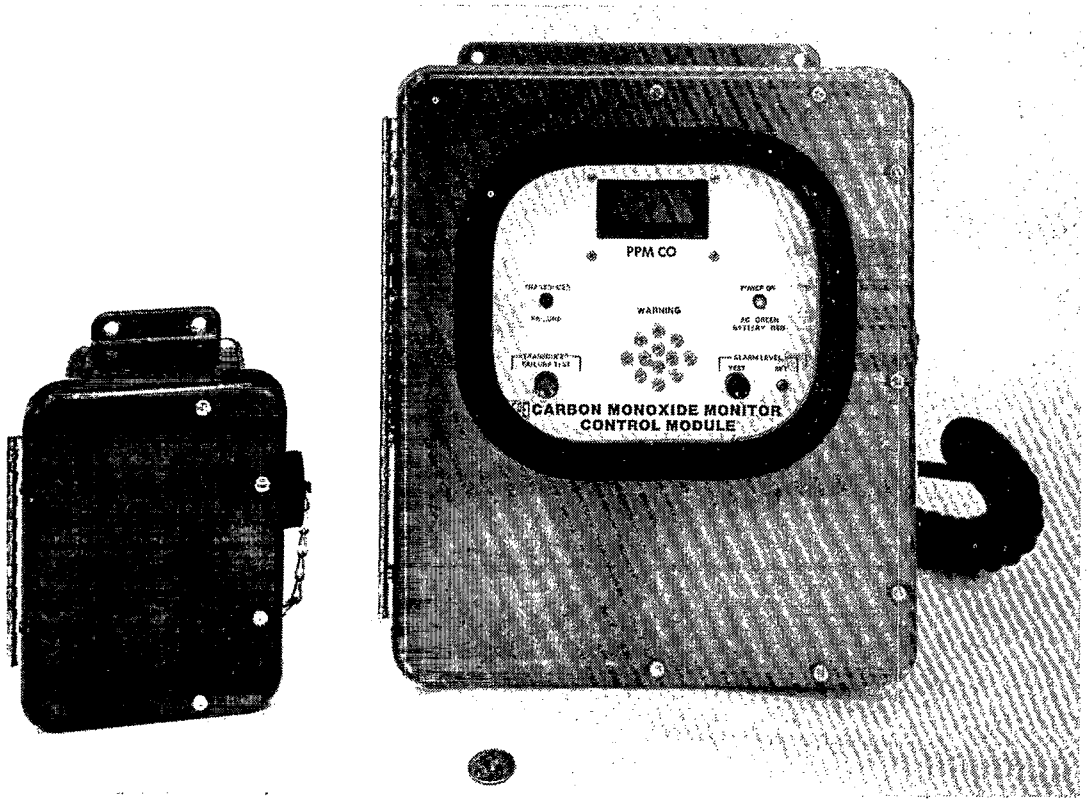

Figure 4. Transducer and Control Modules Carbon Monoxide Monitor System.

transducer module. The only routine maintenance for the transducer module is periodic (biannual) filling of the water reservoir with distilled water and checking the interference gas filter. The unit contains no moving parts. Features of the transducer module are summarized in Table 1.

Through proper choice of the geometry of the diffusion tube, especially by varying the length to diameter ratio (L/D ratio) of the diffusion tube, a diffusion sensor cell response that was independent of the external air flow rate could be obtained. One problem associated with the use of such a diffusion sensor cell was an increase in the flow dependence of the diffusion sensor cell response when the diffusion tube length was decreased. A porous metal disk, incorporated as an integral part of the diffusion tube assembly, minimized this flow dependency.

Figure 5 shows the effect of external air flow rate on diffusion sensor cell response for a diffusion sensor cell having an L/D ratio of 0.91. In this particular example, the diffusion tube was completely open, with no interference filter present. As is clearly visible, the diffusion sensor cell response was highly dependent on external air flow rate.

Also shown in Figure 5 are results obtained with the same diffusion sensor cell, but this time with a porous metal disk across the entrance to

TABLE 1. TRANSDUCER MODULE FEATURES

VISUAL DISPLAY - CASE OPEN

- Water level, Purafil color

VISUAL DISPLAY - CASE CLOSED

- None

FRONT PANEL (INTERNAL) CONTROLS AND ADJUSTMENTS

- Zero adjustment
- Span adjustment

POWER INPUT VOLTAGE

- 7.2-21 VDC

OUTPUT VOLTAGE

- 0-5 VDC (0.5-4.5 VDC linear)

REMOTE OUTPUT

- 0-100 mVDC, linear (for calibration - within case, banana jack fittings)

ENCLOSURE

- Fiberglass case, NEMA 4 or equivalent, 7 1/4" (H) x 5 1/2" (W) x 4 3/4" (D)

SAFETY

- Intrinsic safety for methane-air mixtures (Class 1-D) to pass MSHA approval and certification

CO SENSOR CELL

- Diffusion tube, operate at mine air velocities of 50-400 fpm
- Noise: less than 1 ppm CO
- Zero drift (30 days): ±1 ppm CO
- Precision (30 days): ±5% of reading
- Relative humidity: 0-99+% RH
- Operating temperature: 1-40°C
- Accuracy: ±1 ppm to 10 ppm CO, ±10% of reading over range of 10-100 ppm CO
- Response time: 2 minutes to 90%
- Interferents: highly selective to CO in presence of CH_4, NO, NO_2, CO_2, H_2, NH_3, H_2O vapor with Purafil filter. Filter removal where early fire warning required.

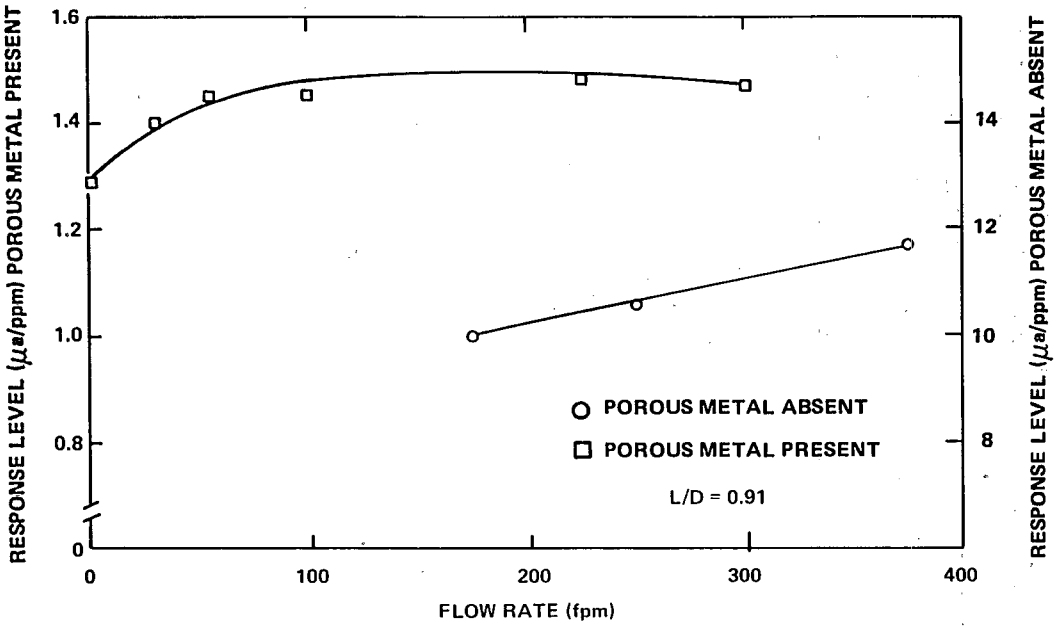

Figure 5. Effect of a porous metal disk on diffusion sensor cell response L/D = 0.91.

the diffusion tube.

Without the porous metal disk, a 12 percent rise in response was noted as the external air flow rate was increased from 175 to 375 feet per minute (fpm). However, with the porous metal disk present, only a 2 percent variation in signal was noted over the range 60 to 300 fpm.

It should also be noted in Figure 5 that the response of the diffusion sensor cell without the porous metal disk present was an order of magnitude higher than the response observed when the porous metal disk was present. The very high response level in the absence of the porous metal disk was due to air flow into the diffusion tube. The response of an electrochemical sensor cell is dependent on the sample flow rate striking the sensing electrode surface. The presence of a porous metal disk across the diffusion tube entrance significantly decreased the amount of direct flow into the diffusion tube and up to the sensing electrode, greatly improving the diffusion contribution and minimizing the flow contribution of the diffusion sensor cell response.

A diffusion sensor cell response level of 1.53 μa/ppm was predicted for the diffusion sensor cell utilized in this phase of testing. The average diffusion sensor cell response level of 1.45 μa/ppm over the range from 60 to 300 fpm was in excellent agreement with the predicted response.

Figure 6 shows the effect of external air flow rate on a diffusion sensor cell having an L/D ratio of 2.39. This diffusion sensor cell was identical to that located inside the transducer module, but had an interference filter located inside the diffusion tube. A porous metal disk was threaded into the bottom of the diffusion tube. Results are shown both with and without the presence of the porous metal. Over the range 40 to 250 fpm, a 17 percent rise in signal was noted for the diffusion sensor cell system without the porous metal, while almost no change was noted for the same diffusion sensor cell over a wider flow rate range after the addition of porous metal. Equation 9 predicts that a diffusion sensor cell having an L/D ratio of 2.39 will have a response level of 0.45 μa/ppm CO. Diffusion sensor cells placed in prototype wall-mounted transducer modules had L/D ratios of 2.39, with observed response levels on the order of 0.45 μa/ppm.

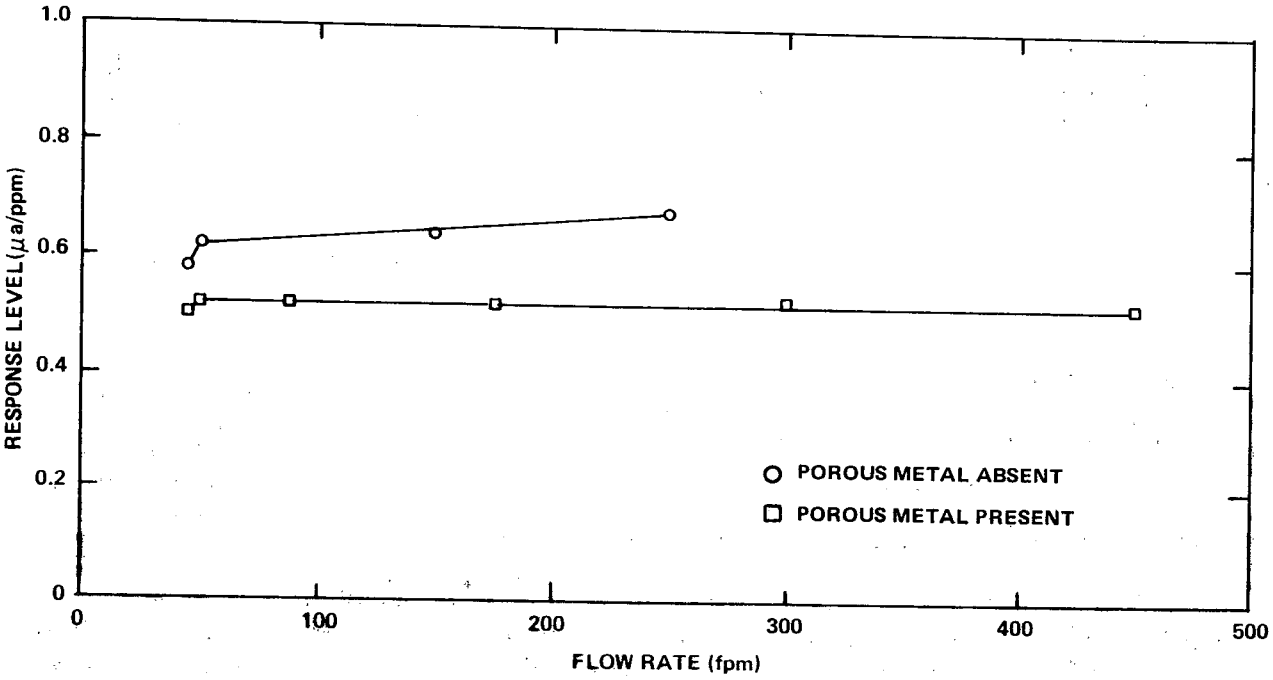

Figure 6. Effect of porous metal on diffusion cell response L/D = 2.39.

Equation 9 also predicts that, for a given sensing electrode area, the response of a diffusion sensor cell is inversely proportional to the length of the diffusion tube. This is demonstrated in Figure 5 and 6, where increasing the length of the diffusion tube (decreasing the L/D ratio) resulted in a decrease in diffusion sensor cell response level. Figures 5 and 6 also demonstrate that, without a porous metal disk, the smaller the L/D ratio, the greater the chance for direct-air flow into the diffusion tube, resulting in a more flow-dependent response.

The response of the tranducer module was tested as a function of CO

concentration. These results are shown in Figure 7. A linear relationship was observed between the diffusion sensor cell response and CO concentration. This line has a slope of 0.58 μa/ppm, in good agreement with the predicted response level of 0.45 μa/ppm, and an intercept of -0.19 μa(-0.33 ppm). The correlation coefficient of the data points is 0.997, demonstrating excellent linearity. The prototype transducer module shown in Figure 3 was designed for operation over the range from 0 to 50 ppm CO; the data displayed in Figure 7 demonstrate that the transducer module has the required linearity over this range of CO concentrations.

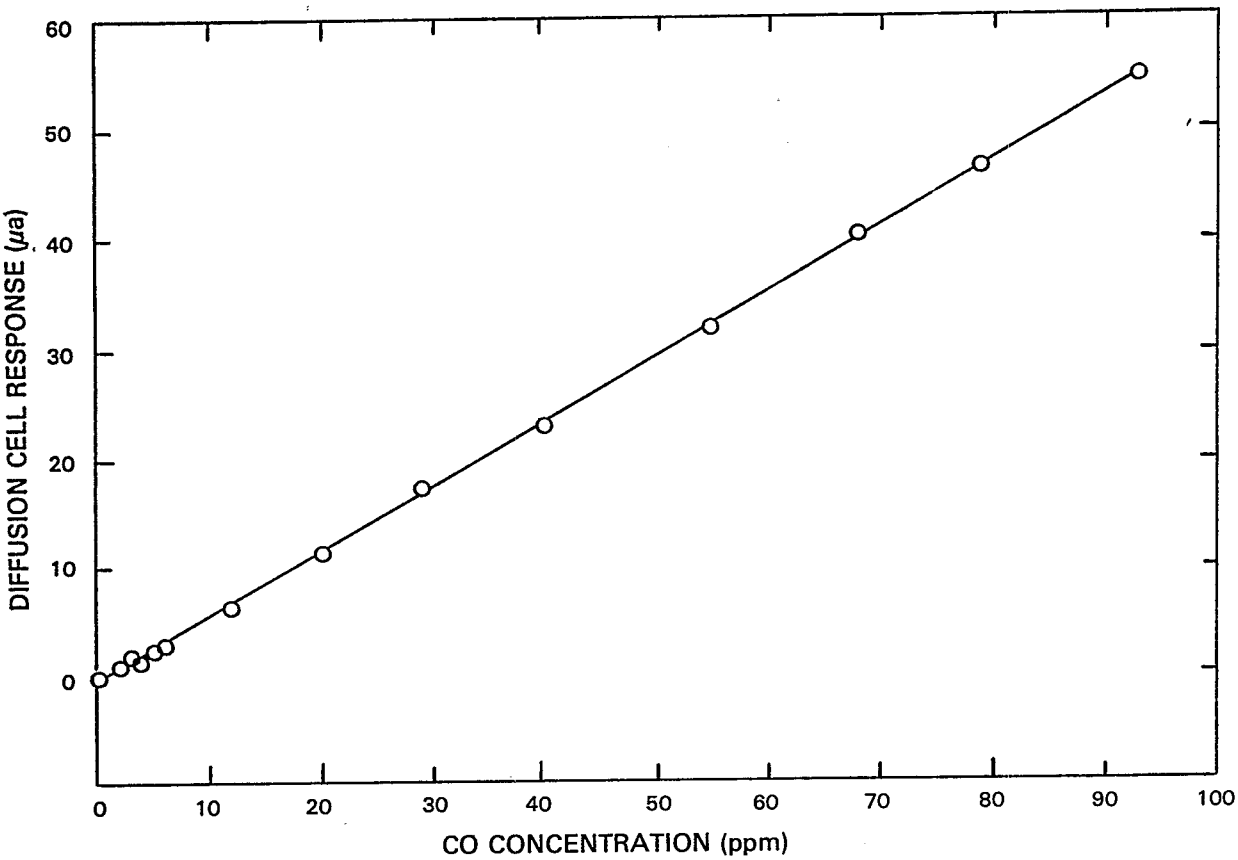

Figure 7. Response vs. concentration, diffusion sensor cell.

The transducer module was also tested to determine response at extremely high CO concentrations as might be observed during an underground mine fire. These results are shown in Figure 8. Pumped sample CO sensors may show severe signal non-linearity at extremely high (i.e., 1-5 percent) CO levels as a consequence of diminishing availability of surface reaction sites or interference by desorption of CO_2 reaction product (4,5).

Increased linearity is observed with a diffusion instrument in comparison with a pumped instrument, especially at high concentrations of CO.

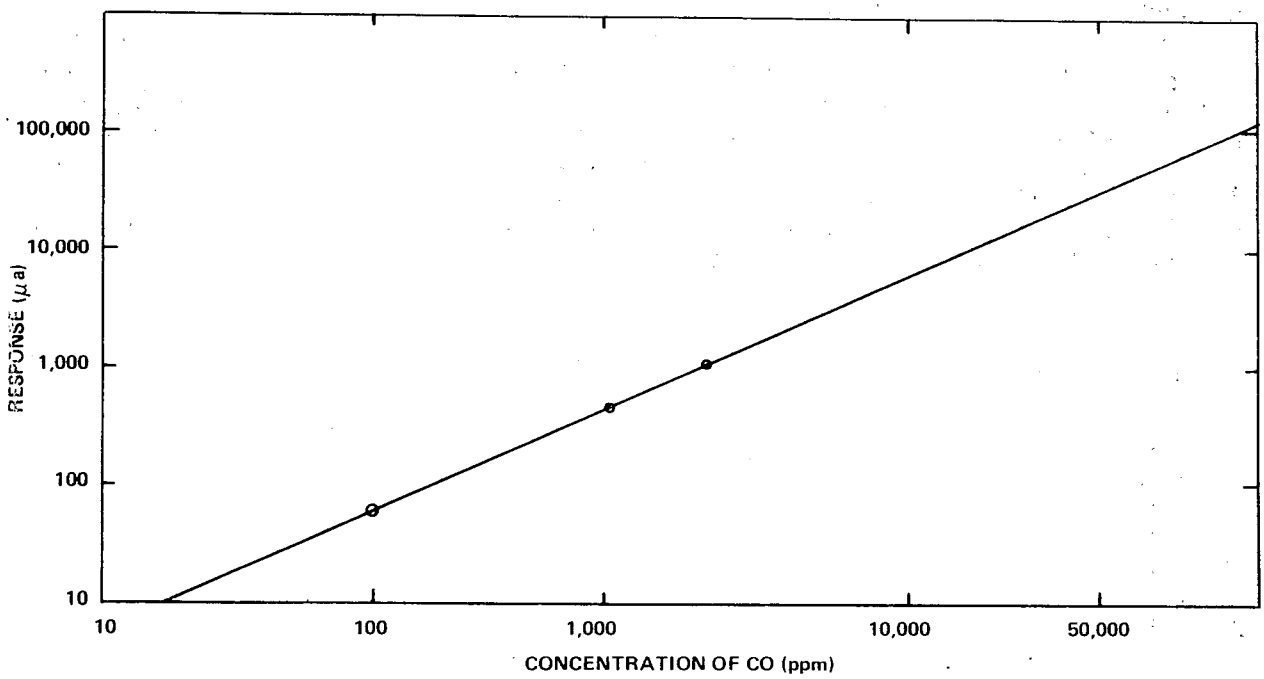

Figure 8. Application of the SPE Diffusion Cell for the detection of high concentrations of CO.

This is due to the concentration gradient established over the length of the diffusion tube. The sensing electrode experiences a CO concentration lower than that actually present at the entrance to the diffusion tube. The concentration gradient across the diffusion tube is given by Fick's first law of diffusion:

$$J = -D\ (\partial C/\partial X) \qquad (10)$$

where J is the flux of the diffusing species per unit area, D the diffusion coefficient of the species of interest, and C the concentration of the diffusing species at any point X along the diffusion path.

The response of a diffusion sensor cell having an L/D ratio of 2.39 was tested at three concentrations of CO/air and 5 percent CO/N_2. A linear response was obtained up to 1000 ppm (0.1 percent CO/air). After 10 minutes of sampling 5 percent CO/N_2, the diffusion sensor cell was responding at 70 percent of its expected value as shown in Figure 8. These data clearly show that the diffusion CO sensor can function at extremely high concentrations.

The transducer modules were also tested to determine response over the range 0-40°C. A background change of 1 to 2 ppm CO was measured over this temperature range, with only a minimal change in span response observed. It was further verified that the transducer module assembly, when

thoroughly dried, may be subjected to storage temperatures as low as -55°C with no harm to the module.

Long-term calibration stability testing has revealed the rate of loss of sensitivity to be 1 percent per month, indicating that monthly calibration checks are sufficient.

Personal Dosimeters

SPE Diffusion Cell CO Dosimeter

A prototype personal dosimeter utilizing a CO diffusion sensor cell was also designed, constructed, and tested. Unlike the wall-mounted transducer module, the diffusion dosimeter may be worn either clipped onto a belt or in a shirt pocket. A photograph of the prototype diffusion dosimeter is shown in Figure 9. The diffusion tube in this instrument has an L/D ratio of 0.91. A replaceable interference filter is an integral part of the diffusion tube assembly; a photograph of the diffusion dosimeter with the filter removed is shown in Figure 10.

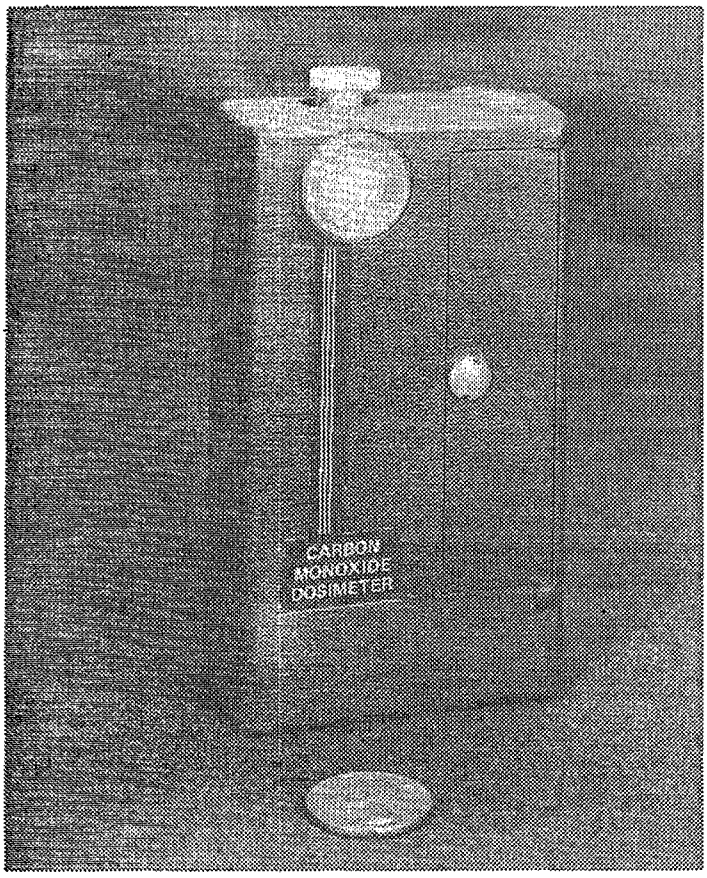

Figure 9. External view, CO diffusion dosimeter.

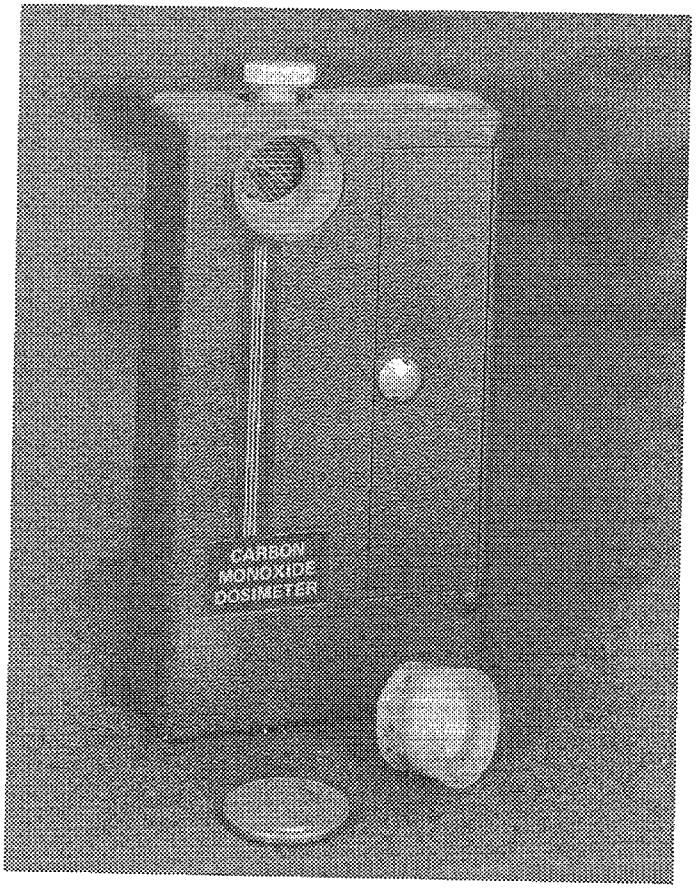

Figure 10. Exterior view, CO diffusion dosimeter with interference filter removed.

The response of the CO diffusion dosimeter as a function of external air flow rate is shown in Figure 11. Data for the dosimeter were obtained with the removable interference filter in place. The abscissa in Figure 11 is the ratio of the diffusion dosimeter response to that of a standard, pumped dosimeter manufactured by General Electric (Model 15ECS1C02). Only a 6 percent increase in signal was observed over the entire range of 40 to 600 feet per minute.

CO diffusion dosimeters were also tested to determine their response as a function of external air flow angle of incidence and air flow rate. Responses of the diffusion dosimeters were measured for flow directly into the diffusion tube, flow at ±45° and ±90° from normal to the diffusion tube entrance.

Typical results for this testing are shown in Table 2. The response of the diffusion dosimeter is expressed as the previously defined response ratio. At a given flow rate, the response ratio changes about 6 percent as the direction of air flow changes. This indicates that the response of the diffusion dosimeter is only slightly dependent on external air flow rate.

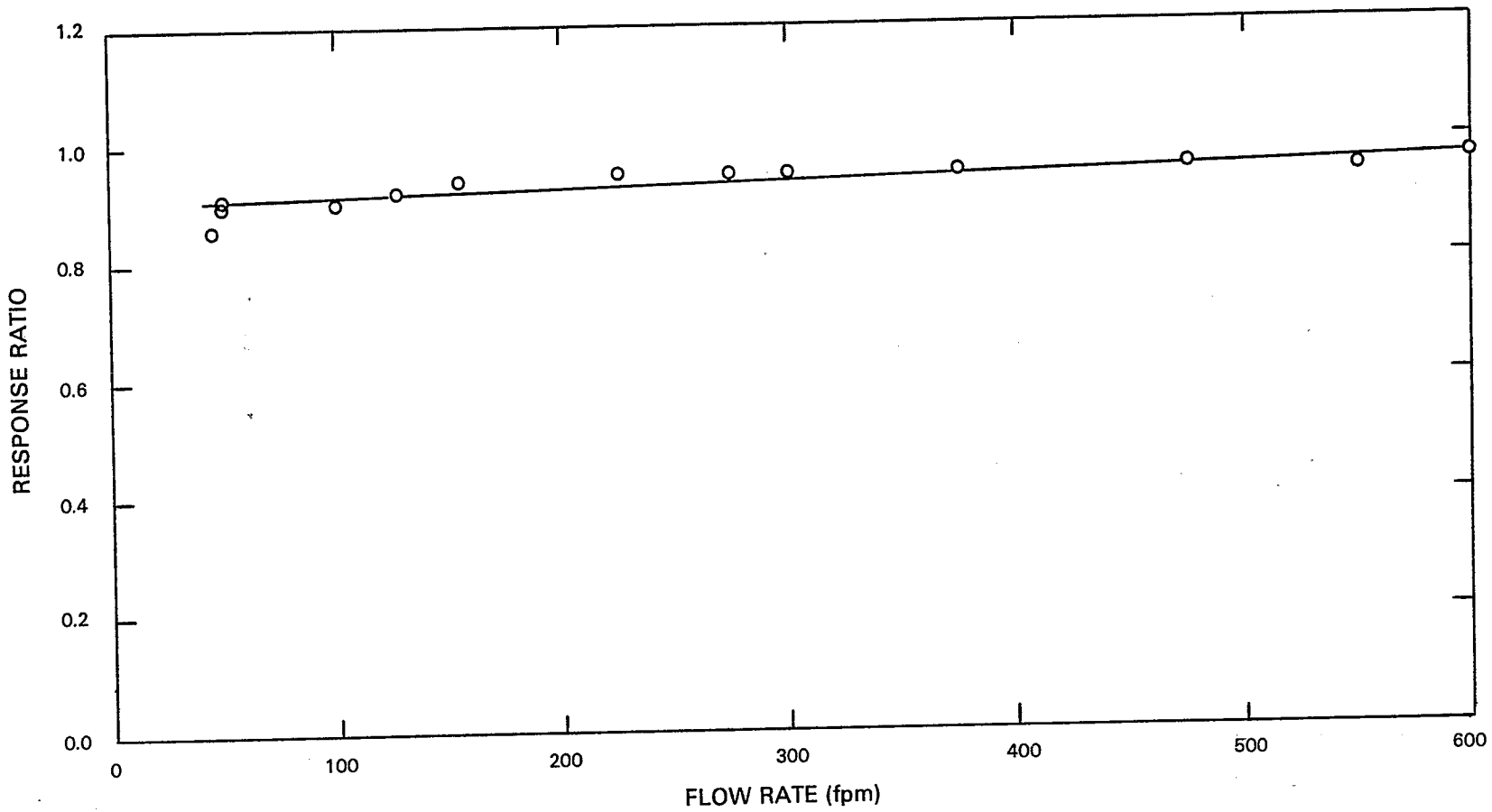

Figure 11. Flow dependence, CO diffusion dosimeter.

TABLE 2. TYPICAL RESPONSE DATA, CO DIFFUSION DOSIMETER

Flow rate	Angle of incidence	Response ratio
200 fpm	0°	1.10
	+45°	1.11
	-45°	1.13
	+90°	1.11
	-90°	1.13
	0°	1.11
400 fpm	0°	1.13
	+45°	1.14
	-45°	1.14
	+90°	1.18
	-90°	1.20
	0°	1.14
600 fpm	0°	1.15
	+45°	1.21
	-45°	1.22
	+90°	1.23
	-90°	1.24
	0°	1.18

Further studies are being performed to minimize this dependence.

Linearity studies were performed over the range from 0 to 80 ppm CO and 100 to 1010 ppm CO. In the former case, a diffusion dosimeter and a standard pumped dosimeter were both placed inside a glove box. Span gas was introduced to the glove box, and the air inside agitated for a two-minute period. This was done to ensure that a uniform CO/air mixture was present inside the glove box. At the end of the two-minute period, the responses of both dosimeters had stabilized, indicating a uniform mixture was present. The dosimeter responses were then recorded. The results, plotted in Figure 12, indicate a linear response/concentration correlation between the CO diffusion dosimeter and the standard pumped dosimeter.

In the second test, span gas was introduced to the diffusion dosimeter by means of the calibration device for a two-minute period. The diffusion dosimeter responses were allowed to relax to background values between exposures to the various test gas concentrations.

The calibration device used in the linearity testing contains a small (0.95-cm-diameter) cavity, which plugs directly into the diffusion tube entrance. Span gas is introduced to the backside of the calibration device at a flow rate of 100-120 cm/min.

Results of the linearity testing presented in Table 3 demonstrate a

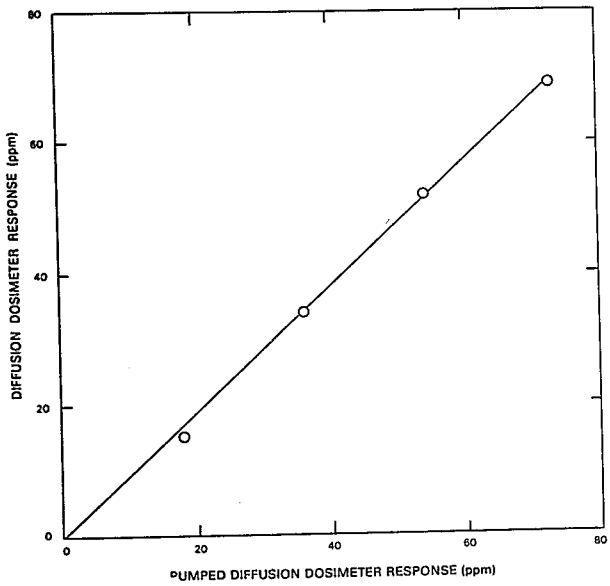

Figure 12. CO diffusion dosimeter linearity data.

TABLE 3. CO DIFFUSION DOSIMETER LINEARITY DATA

Diffusion dosimeter	Response to test gas*			
	100 ppm	491 ppm	750 ppm	1010 ppm
R0462	100	101	101	100
P0588	100	99	101	98
P0624	100	101	99	101
P0622	100	104	103	99
R0056	100	98	98	97

*All values expressed as a percentage of the test gas concentration.

linear response for each dosimeter over the range 100 to 1010 ppm CO. The values in Table 3 are the diffusion dosimeter responses expressed as a percentage of the test gas concentration.

The CO diffusion dosimeter responses were also tested as a function of temperature over the range from 1 to 40°C. Typical results are shown in Figure 13. Thermistor circuitry was included to compensate very closely the span response over the temperature range of interest. Figure 13 shows both the uncompensated diffusion sensor cell response (in μa) and the compensated diffusion dosimeter output (in ppm).

The dosimeter function of the diffusion dosimeter was tested against that of a standard dosimeter. Typical data are shown in Table 4. To obtain these data, the diffusion dosimeter was placed in an air stream

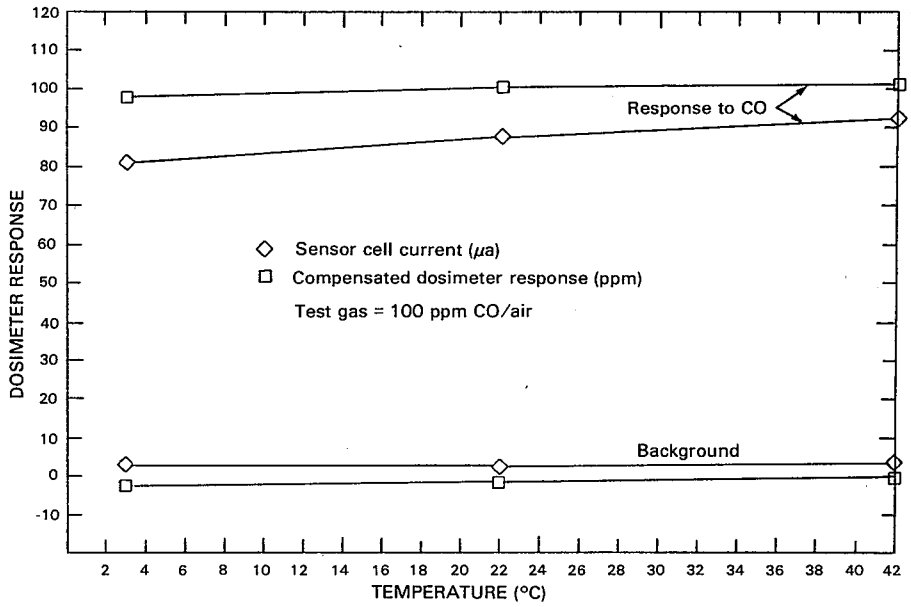

Figure 13. Response of a typical diffusion dosimeter as a function of temperature.

TABLE 4. DOSIMETER COULOMETER DATA

Time (min)	Diffusion response (ppm)	Pumped response (ppm)
0	60	61
5	58	58
10	60	59
15	60	59
20	59	58
25	60	59
30	61	60
Average	59	59
Calculated Coulometer output	29.5 ppm-hr.	29.5 ppm-hr.
Measured output	30 ppm-hr.	30 ppm-hr.

flowing at 400 fpm. CO concentrations were measured with both a diffusion dosimeter and a standard dosimeter. After the response of both dosimeters had stabilized, their coulometers were discharged. CO levels were then integrated for one-half hour, and the coulometer values read after this period. During this test period, instantaneous CO concentrations were recorded at five-minute intervals.

The data shown in Table 4 include the instantaneous dosimeter response, the average value, the calculated dosimeter value, and the dosimeter value as read out on the support console. Very good agreement was obtained between the two dosimeter values in all cases tested. This showed that the diffusion dosimeter will function as efficiently as a standard (pumped) dosimeter.

Long-term stability testing of the diffusion dosimeter response indicated that the calibration stability dropped less than 10 percent over a three-month period. This indicates that monthly calibration checks are sufficient for accurate instrument usage.

SPE Diffusion Cell NO Dosimeter

The diffusion cell technology described previously for the CO diffusion dosimeter was applied to the development of an NO diffusion dosimeter. The diffusion sensor cell utiized for detection of NO was identical to that for CO, except the sensing electrode catalyst was changed to a graphite/Teflon mixture. To avoid interferences from such gases as NO_2, H_2S, and SO_2, an interference filter consisting of triethanolamine (TEA) on a molecular sieve was placed in front of the sensing electrode; CO does not react on the graphite sensing electrode.

The NO diffusion dosimeters were packaged in cases similar to those for the CO diffusion dosimeter; a photograph of an NO diffusion dosimeter is shown in Figure 14. As with the CO diffusion dosimeter, the interference filter may be removed easily to facilitate changing the filter material.

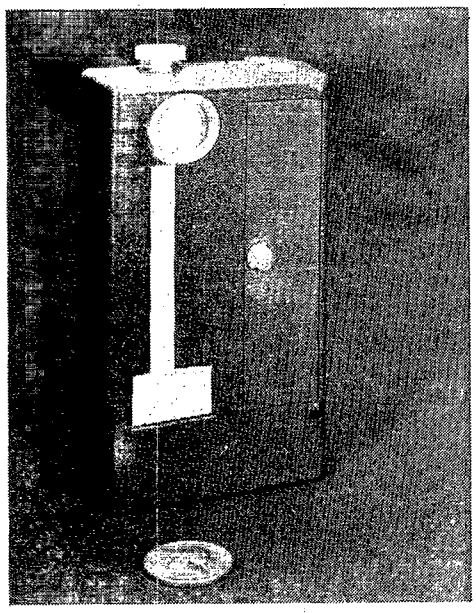

Figure 14. Exterior view, NO diffusion dosimeter.

Figure 15 shows the results of flow testing for three diffusion dosimeters. Each data point is the average of six values, corresponding to various orientations of the diffusion dosimeters in the moving air stream. Diffusion dosimeter responses were compared with NO levels as measured by a prototype pumped direct-reading NO detector. The response ratio plotted in Figure 15 is defined as the ratio of diffusion dosimeter response to direct-reading detector response, and is plotted as a function of external air flow rate. NO concentrations were held at ∿50 ppm. The three dosimeters exhibited less than a 10 percent variation in response over the wide range of air flows indicated.

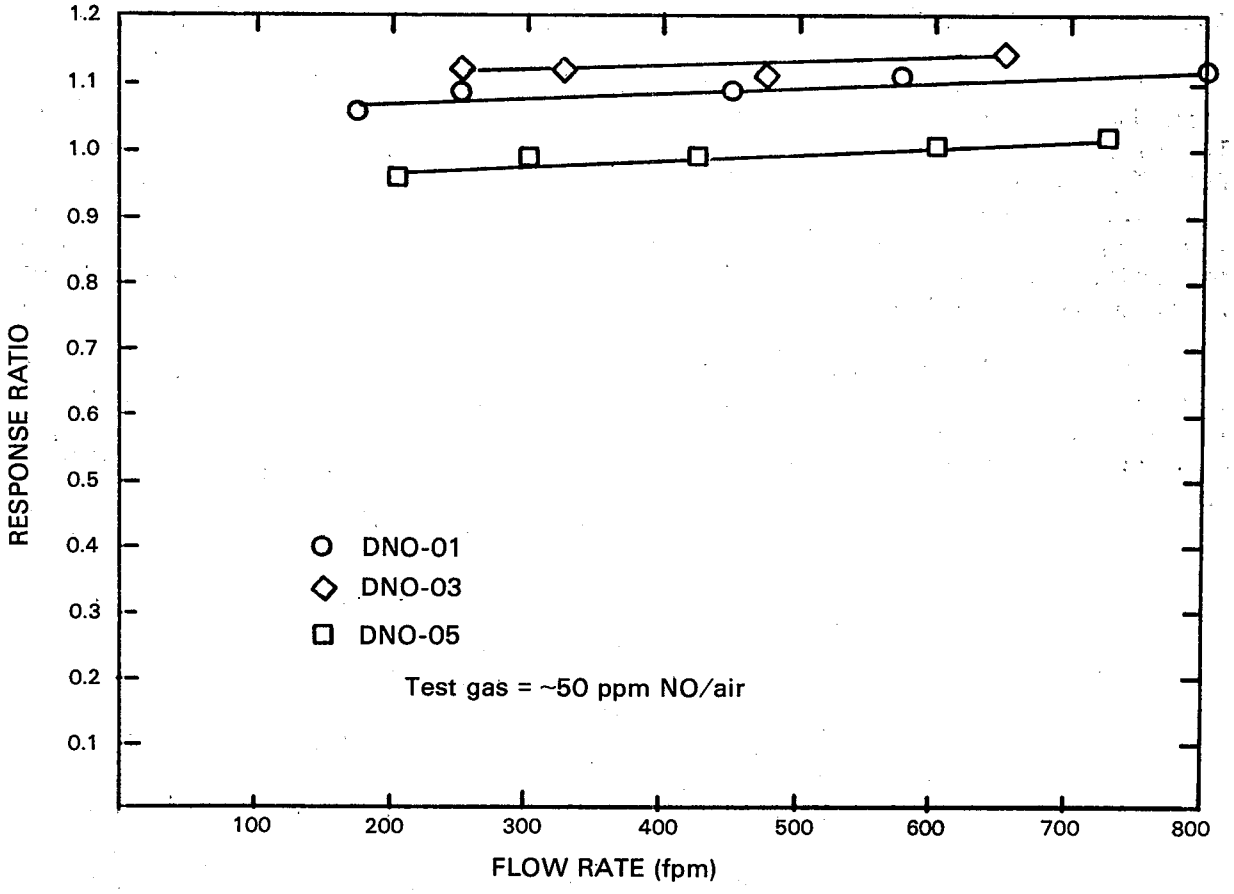

Figure 15. NO diffusion dosimeter flow studies.

A plot of diffusion dosimeter response versus the direct-reading detector response is shown in Figure 16. Data points were obtained for NO concentrations from 0 to 100 ppm. A least-squares analysis of the data plotted in Figure 16 yielded a slope of 0.99 μa/ppm and an intercept of 0.1 μa. This shows the response of the diffusion dosimeter is as linear over the range 0 to 100 ppm NO as is the response of the direct-reading NO detector.

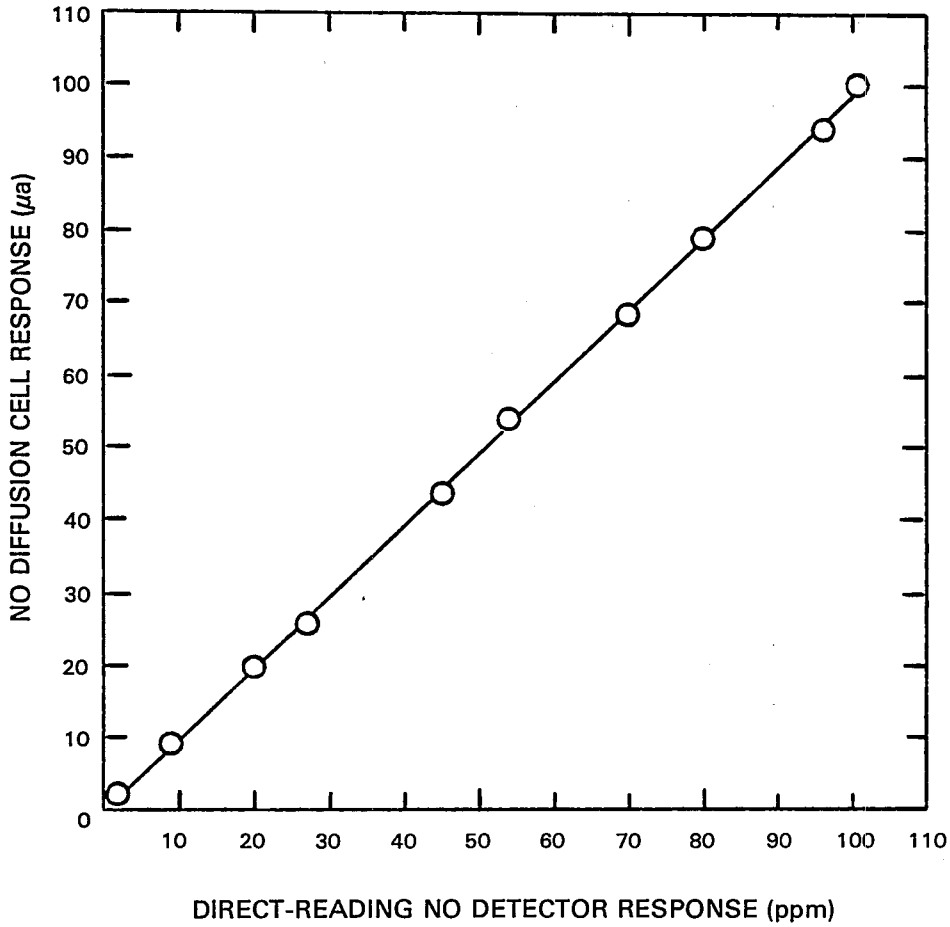

Figure 16. NO diffusion cell response as a function of NO detector response.

The variation in diffusion dosimeter output as a function of temperature is plotted in Figure 17. Both the diffusion sensor cell output (in μa) and the diffusion dosimeter response (in ppm) are shown for background and span response to 28 ppm NO. Thermistor temperature compensation circuitry was used to compensate the span response.

The compensated diffusion dosimeter response varies by ∿10 percent over the temperature range from 0 to 40°C. For this experiment, the diffusion dosimeters were placed inside an environmental chamber, and 28 ppm NO was introduced through the calibration device.

Table 5 lists results of coulometer tests for three diffusion dosimeters. The coulometer calibration was tested by introducing 28 ppm NO to the diffusion dosimeters for 30 minutes at a flow of 120 cc/min. Column 2 of Table 5 lists the calculated coulometer response, in ppm-hr, while Column 3 gives the actual observed values. As can be seen, excellent agreement was obtained in all cases.

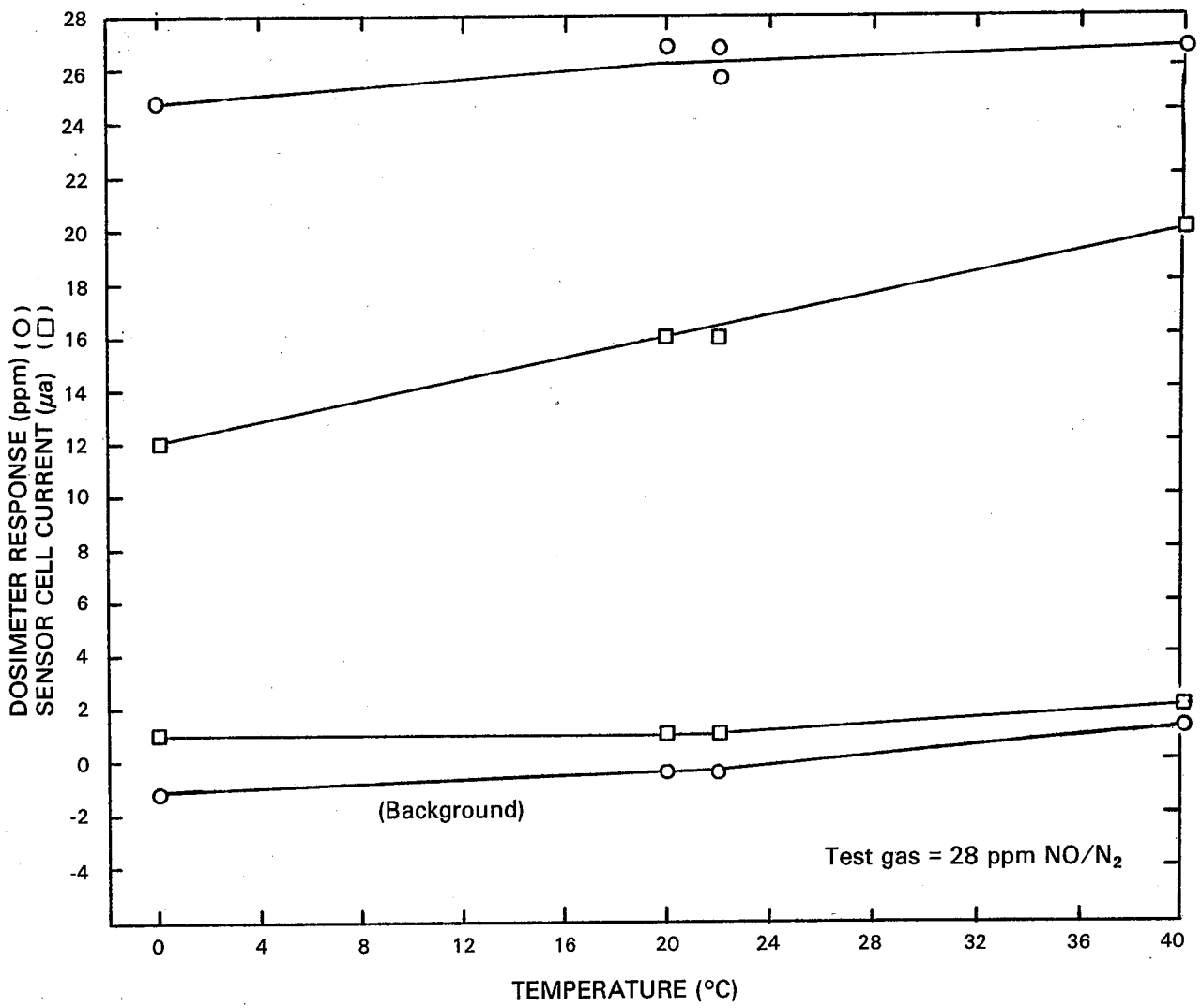

Figure 17. Temperature dependence of NO diffusion dosimeter response.

TABLE 5. NO DIFFUSION DOSIMETERS, COULOMETER DATA

Dosimeter no.	Calculated reading	Actual reading	Background	Time
DNO-01	14.5 ppm-hr	14 ppm-hr	0 ppm-hr	4 1/4 hr
DNO-03	14.5 ppm-hr	14 ppm-hr	0 ppm-hr	4 1/4 hr
DNO-05	14.0 ppm-hr	14 ppm-hr	0 ppm-hr	7 1/3 hr

The fourth column lists the results of background coulometer studies. For this experiment, the coulometers were discharged and the diffusion dosimeters placed inside a glove box. The units were removed after the time periods indicated, and the coulometers were read out. No observable drift was detected in the coulometer output over the time frame of these experiments.

SUMMARY

Gas detection instruments highly specific for CO and NO utilizing diffusion sensor cells have been developed. All diffusion sensor cells utilize a solid polymer electrolyte with integrally bonded fuel-cell electrodes. Linear responses were obtained over wide ranges of test gas concentrations. Responses independent of external air flow rate, over a wide range of air flow rate, were also observed. The instruments are fully temperature-compensated over the range from 1 to 40°C. Excellent calibration stability has also been observed.

ACKNOWLEDGMENTS

This work was partially supported by the U.S. Department of Interior, Bureau of Mines. The authors would like to thank Drs. J. Emery Chilton and George Schnakenberg of the Bureau of Mines, whose many helpful suggestions and comments contributed significantly to the technology developments described here.

REFERENCES

1. Gruber, A.H., A.G. Goldstein, and A.B. LaConti. 1979. A new family of miniaturized self-contained CO dosimeters and direct reading detectors. Paper presented at U.S. Environmental Protection Agency Symposium on Personal Air Pollution Monitors, Chapel Hill, NC, January 11-13.

2. Kosek, J.A., A.B. LaConti, and A.G. Goldstein. 1979. Development of fuel cell gas detection instruments for use in a mine atmosphere. Final report, U.S. Bureau of Mines Contract HO 357078, March.

3. LaConti, A.B., M.E. Nolan, J.A. Kosek, and J.M. Sedlak. 1980. Recent developments in electrochemical SPE sensor cells for measuring CO and oxides of nitrogen. pages 551-573 in ACS Symposium Series No. 149, paper no. CHAS 40, Second Chemical Congress of the North American Continent, Las Vegas, NE, August.

4. Kosek, J.A., and A.H. Gruber. 1981. Development of improved detection instruments for toxic gas contaminants in mining atmospheres. Interim report, U.S. Bureau of Mines Contract HO 395132, February.

5. Kosek, J.A., and A.B. LaConti. 1982. Development of improved detection instruments for toxic gas contaminants in mining atmospheres. Final report, U.S. Bureau of Mines Contract HO 395132, January.

LABORATORY STUDIES OF A PASSIVE ELECTROCHEMICAL INSTRUMENT FOR MEASURING CARBON MONOXIDE

Vincent A. Forlenza

Energetics Science
Division of Becton Dickinson and Company

ABSTRACT

Diffusion or passive electrochemical sensors offer manufacturers and end users many advantages, such as lower cost and less maintenance. Despite these advantages, many professional hygienists have been skeptical of the accuracy of these sensors when they are exposed to variable bulk air movements. This study quantifies the effect of convection on the ECOLYZER 210 passive carbon monoxide monitor. The instrument was operated at constant concentration, while the face velocity of the sample impinging on the sensing system was varied from approximately 5 ft/min to 2,426 ft/min. Tests were run at 25 ppm and 197 ppm. The errors in concentration reading registered by the instrument were less than 6.5 percent. The ECOLYZER 210 convection barrier attenuates most of the unwanted effects of convection on the sensor, eliminating any strong dependency on face velocity.

INTRODUCTION

Health and safety professionals require small, lightweight, portable, and reliable monitors for many chemical and physical agents. Devices that rely on sample pumps in many cases are too bulky to be effectively and comfortably used as personal monitors. Recent developments in passive monitoring devices have enabled manufacturers to market small instruments and badges that are ideal for personal monitoring. Easily worn on a collar or a belt, these devices minimize the distraction and discomfort of wearing a monitor. They often offer the user the additional benefits of lower cost, and less maintenance, because they have fewer parts. When the monitor is a passive type instrument, it generally requires less power than the sample-draw type, so that the need for large battery packs is eliminated.

In the early 1970's, electrochemical sample-draw devices for measuring ambient carbon monoxide, such as the ECOLYZER 2000 series from Energetics Science, provided the health and safety professional with a portable and

highly accurate survey tool, but one that was too large for personal monitoring. The ECOLYZER 210 is designed as a personal monitor. The ECOLYZER 210 has a digital display for survey work and alarm functions for use as a safety tool. It weighs only thirteen ounces, and can be worn on a belt. This paper presents laboratory test data on this passive monitor.

The Theory of Passive CO Monitoring Devices

The ideal passive carbon monoxide monitor is not affected by changes in temperature, pressure, humidity, the presence of other chemical species, or convection, but only by changes in ambient concentration of carbon monoxide. The effect of convection on active monitors is eliminated by the use of a constant-volume pump. Passive devices use other means to eliminate the effect of bulk air movement. William J. Lautenberger and fellow researchers (1) list four means of eliminating the effect of convection on a passive monitor. They are:

1. The use of wire screens followed by a stagnant air space.

2. The use of thin attenuating sheets.

3. The use of a tube-like cavity, such as the Palmes tube or a series of cavities that have a length-to-diameter ratio greater than three.

4. The use of a permeation membrane directly in front of the collection medium.

The ECOLYZER 210 employs three of these four means of attenuating convection, the thin attenuating sheet, the tube-like cavity, and a permeation membrane.

The ECOLYZER 210 Sensing System

The ECOLYZER 210 carbon monoxide sensing system consists of three parts: the electrochemical sensor, an interference filter, and a convection barrier, or attenuating sheet. Figure 1 is a diagram of the system. The sensor is an Energetics Science patented three-electrode electrochemical cell. The cell functions according to the following mechanism. Carbon monoxide diffuses through a semipermeable membrane into the cell. The cell contains a sulfuric acid electrolyte. Inside the cell carbon monoxide molecules are oxidized to CO_2 according to the following equation:

$$CO + H_2O \rightarrow CO_2 + 2H^+ + 2E^- \qquad (1)$$

This reaction generates an electrical current that is proportional to the ambient concentration of carbon monoxide. The current flows between a working and counter electrode. A third electrode is used as a reference electrode to maintain the cell at a constant bias. The current is then amplified and used to drive a digital display, showing the concentration in parts per million.

A selective absorbent is placed between the ambient air and the cell

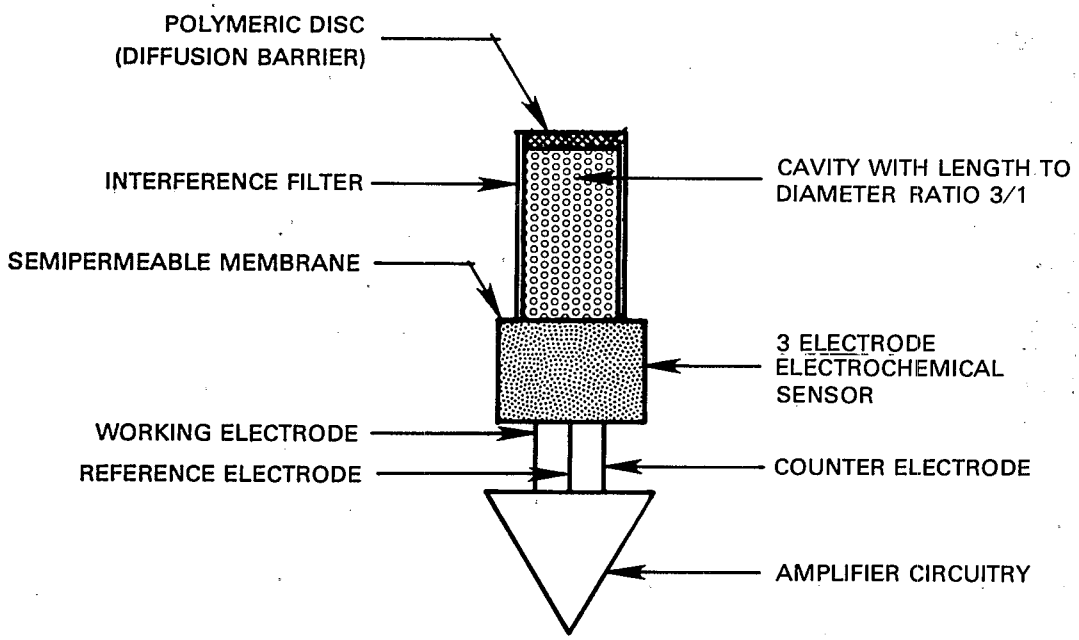

Figure 1. ECOLYZER 210 CO sensing system.

to remove any interfering gases that might give spurious readings. In sample-draw instruments, the sample is pumped through the interference filter and over the semipermeable membrane, where the CO diffuses into the cell. In a passive instrument, the sample must diffuse through the selective filter, so sizing of the filter and its media is critical. In applications where selectivity is not critical, the interference filter can be eliminated.

In order to eliminate the effects of bulk air movement, a polymeric disc is used in conjunction with the interference filter to eliminate most convection through the filter. In instances where the interference filter is not employed, the disc is used with a tube that has a length-to-diameter ratio greater than 3:1. The polymeric disc was chosen so that pore size and thickness allowed maximum diffusion of carbon monoxide, while attenuating most of the convection. If the effects of convection can be eliminated, then Fick's Law of Diffusion applies:

$$J = \frac{-D \Delta C}{\Delta X} \qquad (2)$$

where J = mass flux of migrating carbon monoxide
D = diffusion coefficient of the carbon monoxide
$\frac{\Delta C}{\Delta X}$ = concentration gradient that exists in space

In order to verify this, a constant gas concentration was passed over the sensing system at various velocities. Data from tests run at 197 ppm

CO and 25 ppm CO in air are presented in Figures 2 and 3. Table 1 gives the error due to changing the face velocity for the test at 197 ppm. The data from both tests show only a very slight dependence on face velocity over an extremely wide range. Below 20.6 ft/min, the errors are slightly negative. At these low air velocities, the sensor is being starved. The concentration gradient is changing as the sensor oxidizes CO to CO_2; however, the errors are small, only 3.1 percent at 5.1 ft/min for the 197 ppm test. It is safe to assume that these velocities are outside the normal use conditions for the instrument. On the other hand, the positive error due to face velocity is only 6.3 percent at 27.5 mi/hr (2,425 ft/min) in the 197 ppm test. Data from the 30 ppm test show a similar trend, indicating that the convection barrier is effective over a range of concentrations.

TABLE 1. INSTRUMENT ERROR DUE TO THE EFFECT OF FACE VELOCITY

Face velocity (ft/min)	Percent error*
5.1	-3.1
10.3	-2.1
20.6	0
51.6	1.6
103.2	2.6
154.9	3.6
206.5	3.6
258.0	4.2
310.0	4.2
361.0	4.7
413.0	4.7
464.5	4.7
516.0	5.2
731.0	5.2
970.0	5.7
1218.0	5.7
1311.0	5.7
2426.0	6.3

*Percent error =[(Instrument - actual)X 100]/actual.

To highlight the effectiveness of the barrier, a test was run with and without the convection barrier in place. Figure 4 illustrates the strong flow dependency of the system once the barrier has been removed. This is as expected, and is supported by results from many sample-draw systems.

Instrument Response Time

The porosity of the diffusion barrier and the diffusion path length will certainly affect response time. There are actually three resistances in series through which the gas must diffuse: the polymeric disc, the interference filter, and the semipermeable membrane of the cell. Figure 5

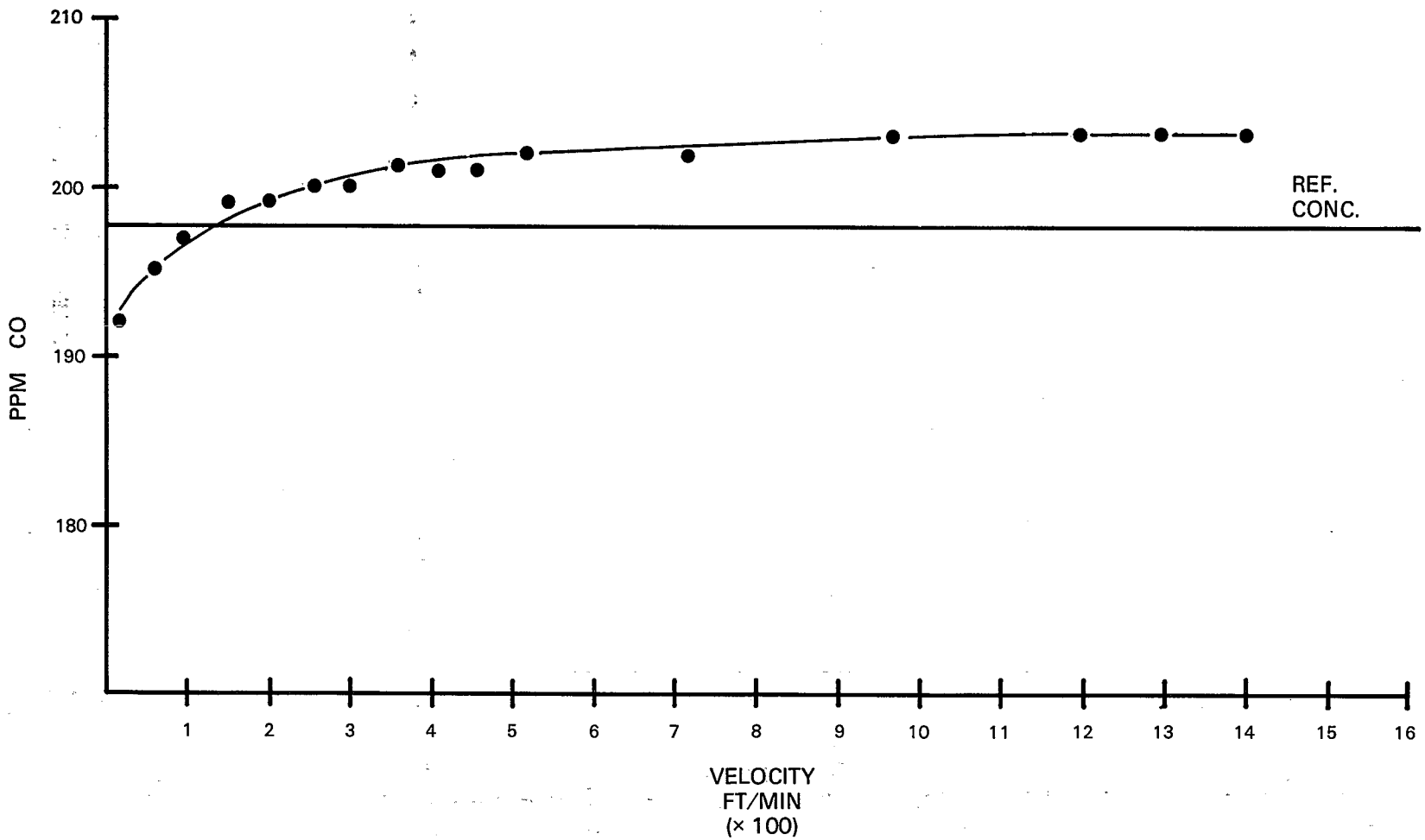

Figure 2. Instrument reading vs. face velocity at constant gas concentration.

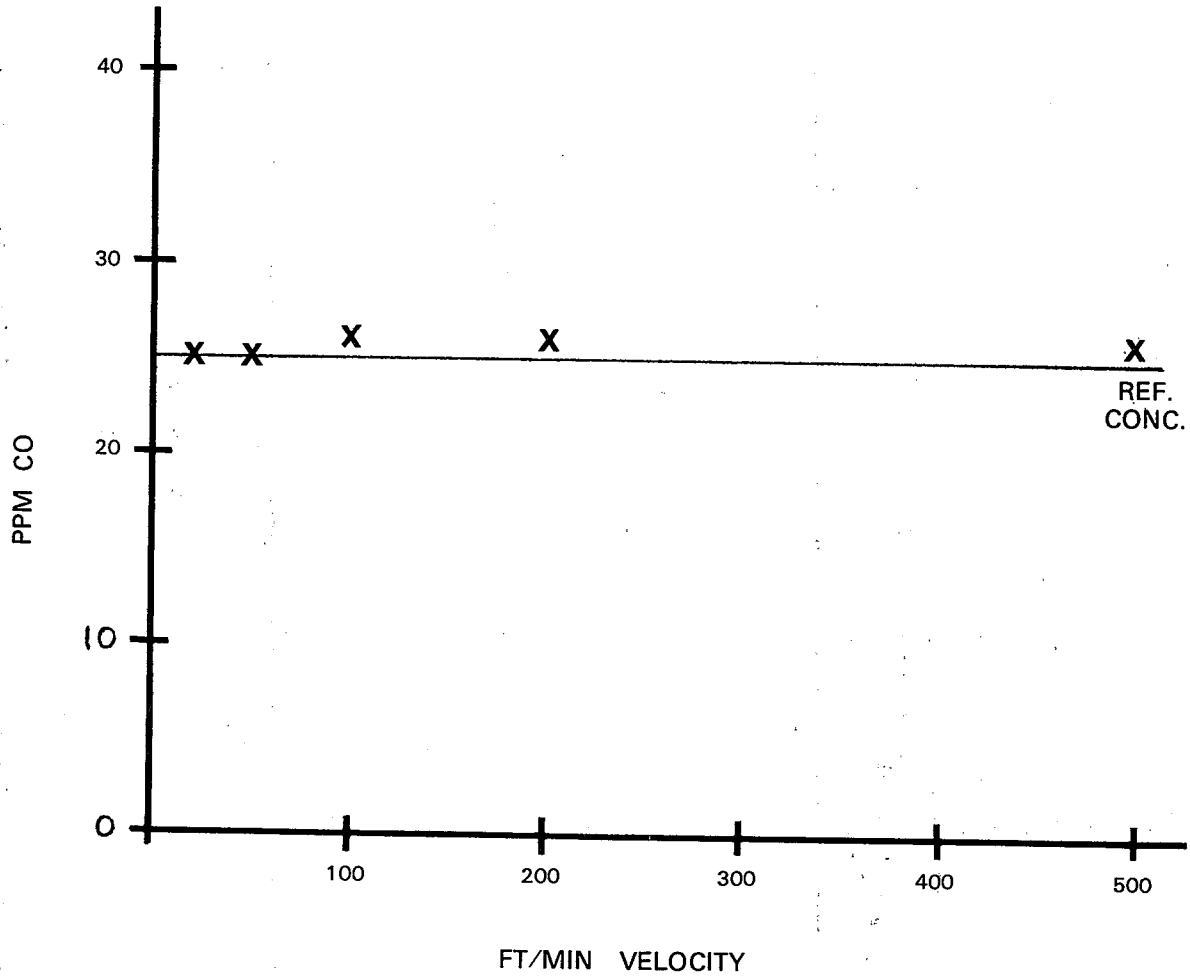

Figure 3. Ambient readings from the ECOLYZER 210 vs. face velocity at constant CO concentration.

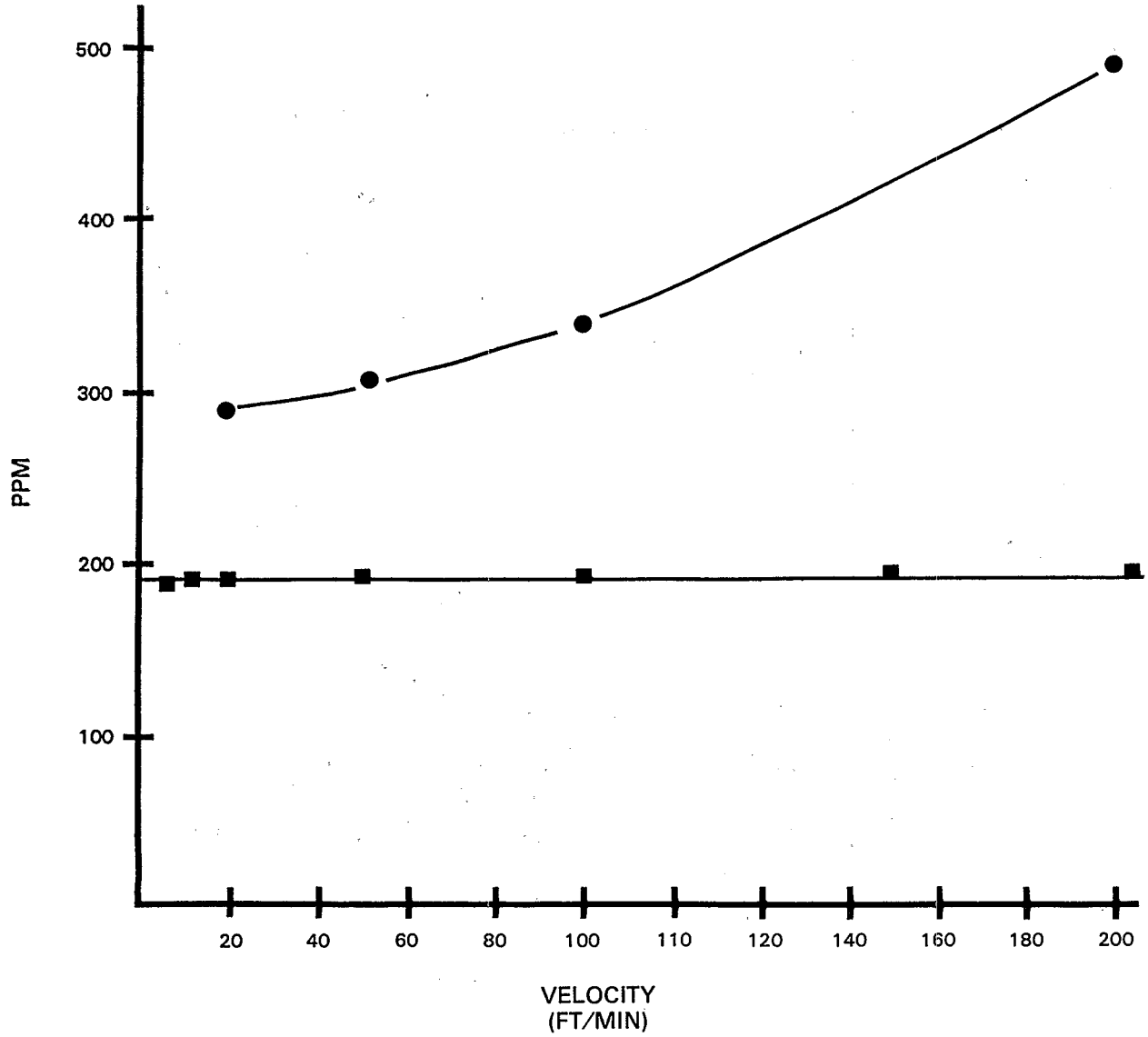

Figure 4. ECOLYZER 210 reading at constant CO concentration with and without convection barrier.

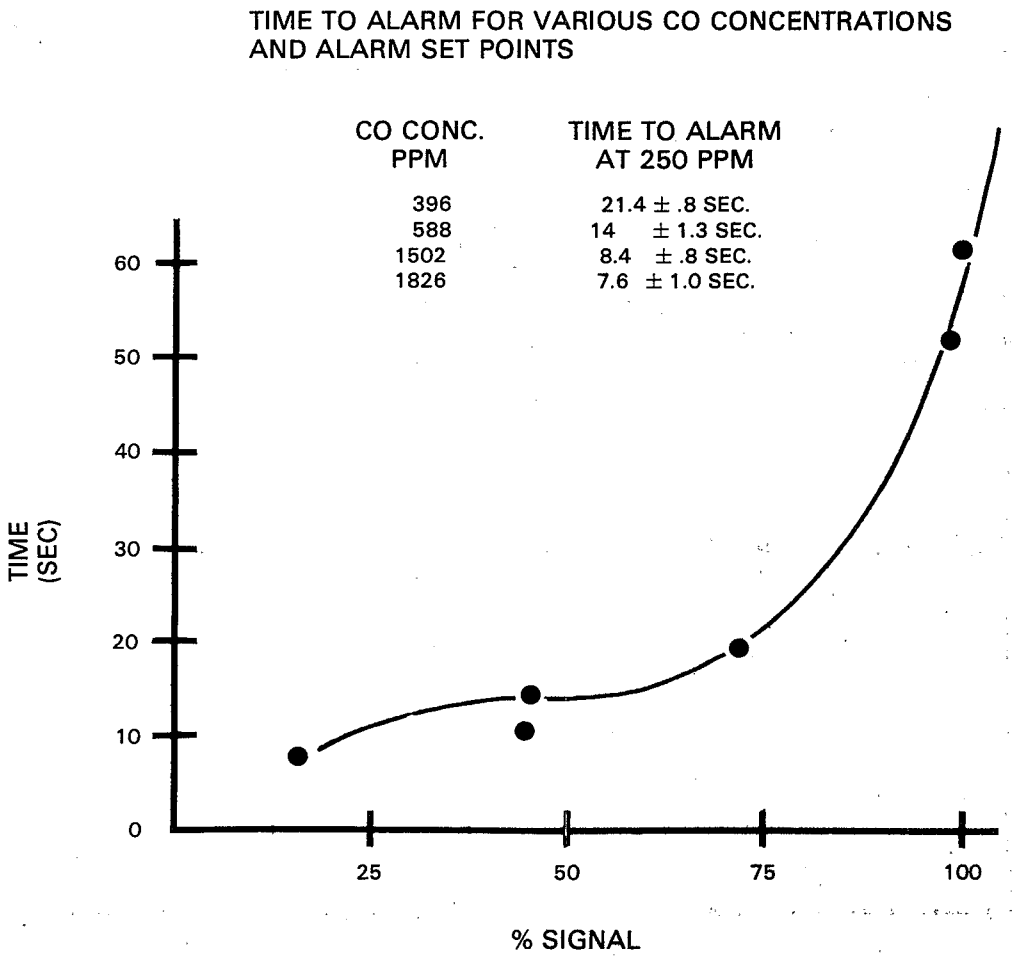

Figure 5. Percent signal vs. time for ECOLYZER 210-averaged data from five instruments.

shows that 90 percent of signal is achieved in less than 60 seconds. Typical alarm data are also shown to illustrate that instrument response is quite rapid.

Linearity

The instrument reading should be proportional to the partial pressure of the gas to be measured in the ambient air. Figure 6 shows that this is indeed the case over the range of the instrument, which is 0-1999 ppm of carbon monoxide for the ECOLYZER 210.

Specificity

The ECOLYZER 210 was exposed to a series of gases commonly found in the workplace. Table 2 shows the interference equivalent defined as the concentration necessary to register as 1 ppm on the instrument. For example, 270 ppm NO_2 will register as 1 ppm on the instrument. No response differs from no interference in this case. No response indicates that up to the concentration tested, the instrument did not respond to the gas tested. It is possible that, above that concentration, the instrument may respond to the gas. Ethane illustrates this phenomenon. No interference indicates that the instrument will not respond to any concentration. The data in Table 2 are with the interference filter in place. Inspection of the data shows that the ECOLYZER 210 exhibits excellent specificity towards carbon monoxide.

TABLE 2. INTERFERENCE EQUIVALENTS FOR CO DIFFUSION SENSOR

Gas tested	Concentration tested	Interference equivalent (ppm)
CH_4 (methane)	99%	No interference
CO_2 (carbon dioxide)	99.8%	No interference
NH_3 (ammonia)	29.4 ppm	135
NO (nitric oxide)	48.2 ppm	No response
NO_2 (nitrogen dioxide)	387 ppm	270
SO_2 (sulfur dioxide)	21.2 ppm	145
H_2S (hydrogen sulfide)	27.2 ppm	130
C_2H_2 (acetylene)	100 ppm	170
C_2H_4 (ethylene)	19.4 ppm	135
C_2H_6 (ethane)	50 ppm	No response
	500 ppm	1200
C_3H_8 (propane)	105 ppm	425
CH_3OH (methanol)	500 ppm	No response
C_2H_5OH (ethanol)	500 ppm	140
2-Propanol	500 ppm	750

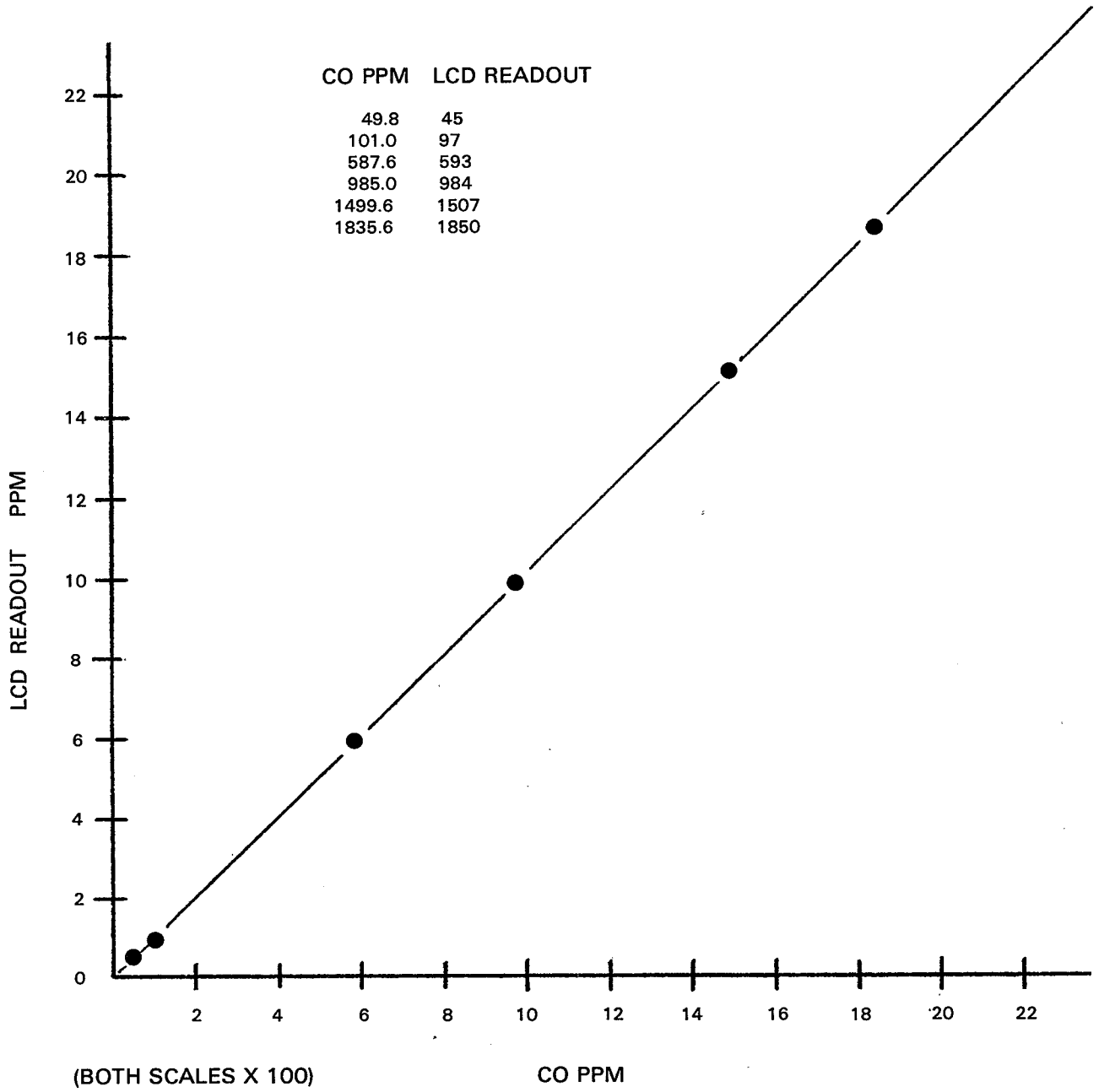

Figure 6. CO vs. LCD readout (ppm).

CONCLUSIONS

1. The ECOLYZER 210 convection barrier sensing system is a highly effective attenuating system, which all but eliminates the effect of face velocity on the instrument.

2. Below a velocity of 20 linear ft/min, the sensor becomes starved. However, the errors are not significant, even for velocities as low as 5 linear ft/min.

3. The instrument shows excellent linearity, response time, and specificity.

REFERENCES

1. Lautenberger, W.J., E.V. Kring, and J.A. Morello. 1981. Theory of passive monitors. Ann. Am. Conf. Gov. Ind. Hyg. 1:91-99.

RESULTS OF TESTING DIFFUSION-TYPE NITROGEN DIOXIDE PERSONAL MONITORS AT LOW CONCENTRATION

James B. Flanagan

Rockwell International Environmental Monitoring and Services Center
Chapel Hill, NC

and

Joseph Ryan

U.S. Environmental Protection Agency
Research Triangle Park, NC

INTRODUCTION

Facilities of the U.S. Environmental Protection Agency's (EPA) Clinical Environmental Laboratories (CEL) were used to test a commercially available diffusion-type personal NO_2 monitor based on a design by E.D. Palmes (1), under conditions simulating sub-industrial exposure levels and while being worn by human subjects. Like many other personal monitors commercially available, the Palmes tube design is optimized for the higher levels of industrial exposure. The monitors were tested with low ambient pollutant concentrations under a variety of conditions to establish their accuracy, precision, collection efficiency, and the effects of orientation and human wearers.

The CEL provides chambers large enough for human subjects to exercise and move around normally while being exposed to accurately controlled levels of pollutant gases with controlled conditions of temperature and humidity. Delivery of controlled amounts of the inorganic criteria air pollutants has been engineered into the system, so that levels approximating the amounts seen in the ambient environment can be delivered with high precision and accuracy. In addition to air pollutant delivery, temperature and relative humidity can be varied and controlled.

The Palmes tube system tested is manufactured by MDA Corporation (2). The monitor consists of a tube approximately 4 inches long, open at one end, and with a wire mesh coated with triethanolamine absorbent at the other. Mass transfer is accomplished by passive diffusion of NO_2 in air. Assuming no convective mixing in the tube, diffusion provides a constant sampling rate almost independent of temperature and pressure. After

exposure of several hours, the NO_2 is analyzed by standard chemical, colorimetric techniques.

The colorimetric-microprocessor supplied by MDA in the Palmes tube kit has simple lighted switches controlling its timing and analysis functions. A yellow filter over a small incandescent bulb provides the "monochromated" light source for the analyzer. Percent transmittance and calculated ppm-hr dosage is read out via LED display. The internal microprocessor controls the timer (for timing the color reaction), provides percent transmittance, and calculates the ppm-hr result using internal calibration curves. Accumulated dosages in the range from 1 to 50 ppm-hr can be measured. The readout device has a resolution of 0.1 ppm-hr; for a typical 8-hour exposure, this would yield a maximum resolution of 0.012 ppm in mean concentration.

EXPERIMENTAL

Before use in the controlling mode with the Palmes tubes, CEL analyzers were calibrated no more than three days before the exposure. Follow-up calibrations within two weeks of the initial calibration were also routinely used to check for drift. Follow-up calibrations made after the exposures showed no cases of excessive calibration drift.

Nitrogen dioxide standard was a dilute NO tank that was NBS-traceable. Bendix model 8101B analyzers were calibrated using this gas directly for NO. Titration with ozone was used to calculate conversion efficiency for the NO/NO_x instruments. Exposures in the chamber used the analyzers as a transfer standard.

Additional exposures were made utilizing the CEL gas calibration system. The source of calibration gas was a tank of 109 ppm NO_2 in N_2 (Airco Industrial Gases), which was traceable to NBS. Partially humidified zero air was mixed using Tylan mass flow controllers with controlling voltage set manually with potentiometers. Data acquisition was under automatic control of the CEL gas computer system. The concentrations of NO_2 thus obtained were monitored by two recently calibrated Bendix $NO-NO_x$ monitors. A 3-liter flask was used as the exposure chamber when calibrations were done. Flow rates through the 3-liter flask were typically between 2 to 5 liters per minute. A positive gas flow from the exhaust tube was checked before and after each session to assure proper operation with no leakage. Calibration gas ran through the flask at least 15 minutes prior to insertion of tubes.

For all concentration measurements, the recently calibrated analyzers were taken as the standard. Through careful quality control, quarterly audits, and reference to NBS permeation tubes at each calibration, these analyzers are thought to be accurate within ±5 percent.

RESULTS

Manual checks of the microprocessor's calculations of dosage were carried out using samples spiked with standard sodium nitrite solution. The results of this calibration are shown in Table 1. The expected ppm-hr doses are calculated for the spikes using the formula in literature provided by the manufacturer (2):

$$Q = 2.3 \text{ X (ppm-hr)} \quad (1)$$

In the present case, Q (quantity of NO_2) is known, and (ppm-hr) is to be derived. The conversion factor is obtained from the assumed stoichiometry of the color reaction (3) and from diffusion theory, assuming a diffusion coefficient of 0.154 and the geometric constants of the device. Units for Q in the above equation are nanoequivalents nitrite in a 2-cm^3 volume.

TABLE 1. RESULTS OF $NaNO_2$ CALIBRATION

Q	%T	Abs.	Colorimeter	Eqn.(1)
blank	98.9	0.005	----	----
4 neq.	80.5	0.094	2.3 ppm-hr	1.74 ppm-hr
8	64.7	0.189	4.7	3.48
12	52.5	0.280	7.0	5.22
20	33.8	0.471	11.9	8.70
40	12.9	0.889	22.4	17.4

Linear regression of the data shown in Table 1 and Figure 1 revealed a slope different from unity (m=1.28, b=0.28). When the manufacturer was contacted, it was found that the microprocessor algorithm included an undocumented "efficiency factor" of 0.72 in the calculation of ppm-hr from a given percent T. Equation (1) then becomes

$$Q = 2.3 \text{ X } (0.72) \text{ X (ppm-hr)} \quad (2)$$

Use of this factor corrects the slope of the regression line to within about 8 percent of theoretical, so that the algorithm used by the microprocessor-colorimeter appears to be valid. The need for the efficiency factor in the wet impinger techniques utilizing reagents similar to those used in the Palmes tubes is thought to arise from a combination of stoichiometric factors in the color reaction and the uptake efficiency of the absorbent during sampling. It is a simple matter to convert the final ppm-hr reading from the colorimeter to a different assumed efficiency factor:

$$\text{(new ppm-hr)} = \text{(old ppm-hr) X } 0.72 \text{ / (new factor)} \quad (3)$$

Table 2 summarizes the testing carried out in the chamber and calibration systems. Table 2 includes only exposures made in a stationary

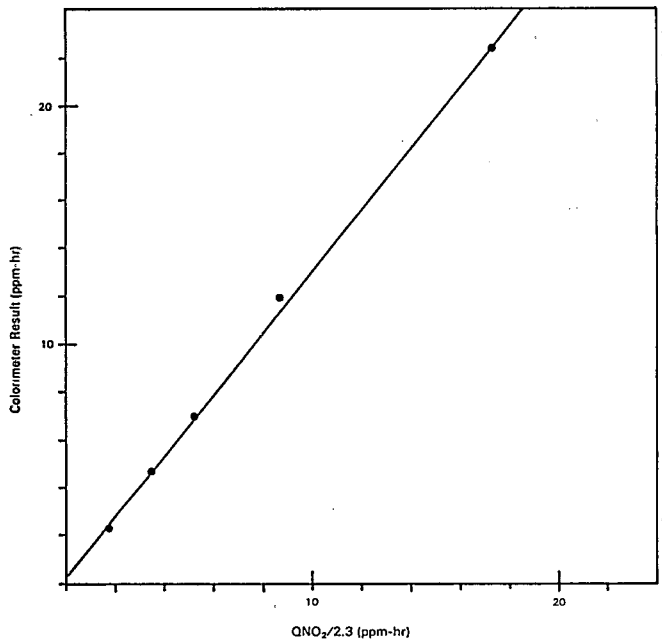

Figure 1. Calibration of Palmes tubes analysis system with standard $NaNO_2$.

position, either in the CEL or in the calibration flask. Tabular results of subject wear are given later.

The first set of data taken (18 sample tubes), as shown in Table 2, illustrates the difficulty of obtaining measurements at extremely low levels of net exposure: the ratio of the analyzed dosage to the dosage supplied by the CEL system is in error by a large percentage, though the scatter as reflected in the relative standard deviation is fairly good. The next two entries in Table 2, (four sample tubes) are blanks exposed to atmospheres free of NO_2 for different lengths of time. This shows that the high values at low dosage were not due to zero offset. The next set of twelve replicate samples was exposed to approximately 2 ppm-hr dosage at 0.5 ppm concentration. The precision of estimate was excellent, but the measured/actual ratio was still high. The next group of samplers (18 tubes) was exposed to high levels of NO_2 approximating 10 ppm. Due to a design limitation of the CEL, control of concentrations at these levels is very poor, so that an accurate estimate for concentration and true net dose is not available. The reproducibility of the ensemble of tubes thus exposed is excellent, however. The next groups of exposures in Table 2 were done in the calibration system rather than in the CEL. The purpose was to obtain results over a wider variety of conditions of concentration and duration of exposure than is possible in the CEL. There was no significant influence of concentration on accuracy (as expresed by the measured/actual ratio), although there was an apparent positive correlation when the measured/actual ratio was fit to a linear function of net dose.

Figure 2 illustrates results of virtually all of the individual

TABLE 2. PALMES TUBES NO_2 EXPOSURE RESULTS
STATIONARY EXPOSURE

Exposure time	Exposure conc	Calculated dosage	Palmes dosage (ppm-hr) Mean	S.D.	N	R.S.D.	Meas./actual
(T = 85° F, RH = 60 % in CEL)							
1.5 hr	0.5 ppm	0.75 ppm-hr	1.65	0.18	6	10%	2.2
0.75	1.0	0.75	1.72	0.25	6	14%	2.3
1.5	1.0	1.5	2.52	0.13	6	5%	1.68
5.0	0*	0*	0.2	--	2	--	--
20	0†	0†	0.1	--	2	--	--
(T = 72°, RH = 40% in CEL)							
4.08	0.5	2.04	3.0	0.15	12	5%	1.47
(T = 70° F, RH = 50% in CEL)							
0.5	‡	‡	4.42	0.37	6	8%	--
1.07	‡	‡	11.25	0.31	6	3%	--
1.35	‡	‡	11.7	0.56	6	5%	--
(T = 72°, RH = 40% (appx.), Calibration system)							
2.65	1.7	4.5	5.4	0.28	2	5%	1.2
4.03	0.88	3.55	4.1	0.21	3	5%	1.15
0.60	3.00	1.8	2.0	0.21	3	10%	1.11
8.45	0.87	7.35	9.3	2.72	3	29%	1.27
24.27	0.116	2.82	2.9	0.28	5	10%	1.03
15.68	0.407	6.38	8.6	1.08	3	13%	1.35
(horizontally in flask)							
2.33	0.946	2.21	2.6	0.18	6	7%	1.17
(vertically in flask)							
2.33	0.946	2.21	2.8	0.12	6	4%	1.26

*Ozone + NH_4NO_3 in chamber.
†Sealed tubes kept approximately 24 hours before analysis.
‡Beyond capability of CEL system to control/analyze - manually set to appx 5-10 ppm. Included to illustrate R.S.D. of identically exposed tubes only.

Ratio Palmes' Result/CEL vs. Dose

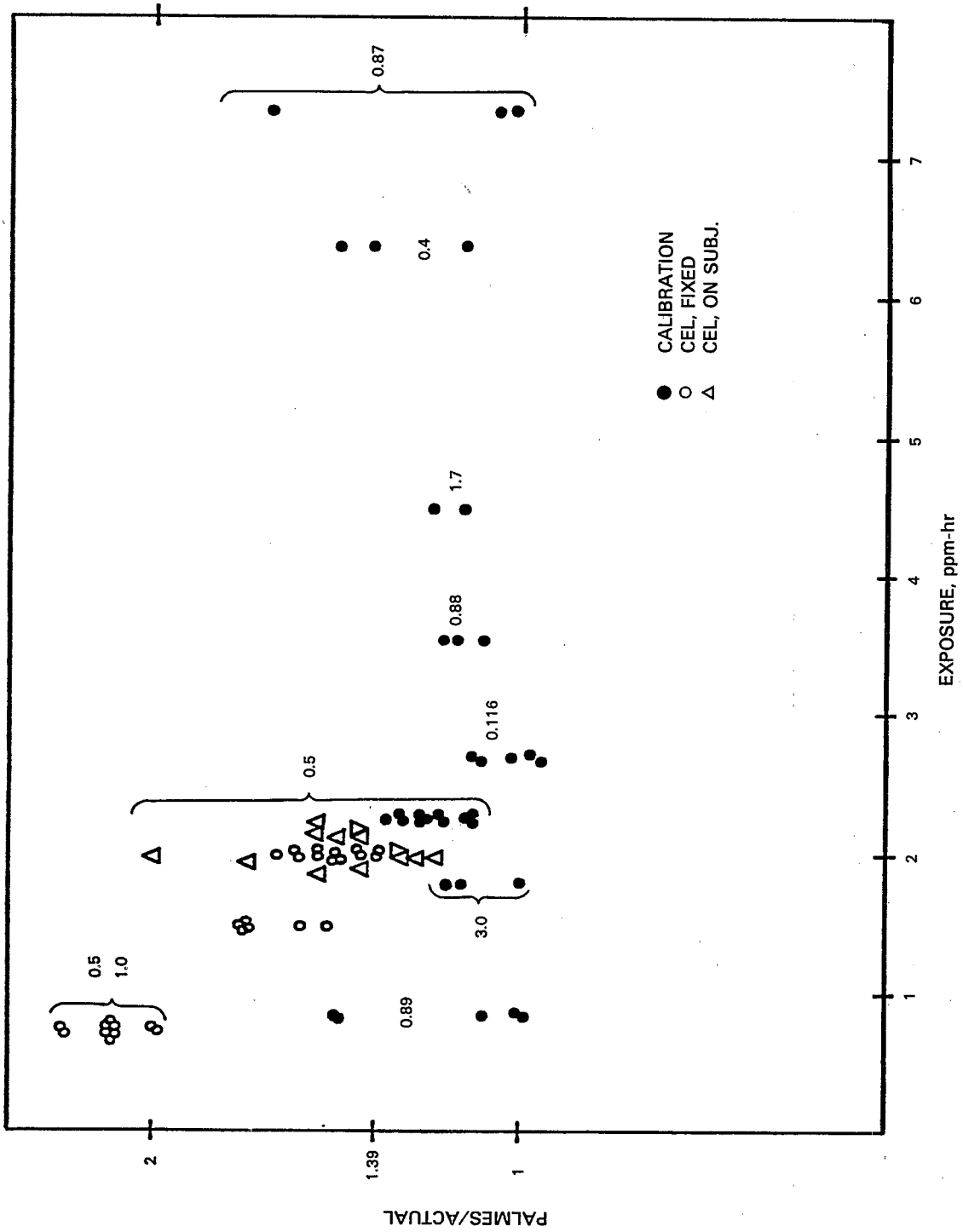

Figure 2. Ratio of Palmes result/CEL versus dose.

exposures made during this testing. Data are plotted as the ratio of measured/actual ratio versus net exposure. The actual concentrations used are indicated by each group of points. It can be seen that the scatter between samples exposed simultaneously is significant, and that relative accuracy becomes poorer as net exposure decreases. At lower concentrations, blank errors become more significant, with clearly discernible effects on accuracy at the left side of the graph (low net dosage).

An orientation effect test was carried out in the flask to check if the positioning of tubes in the flask contributed any bias in the analysis (final entries in Table 2). The means of six tubes in each group were found to be within 7 percent (0.2 ppm-hr). Student's t-test analysis gave a borderline significant difference. Horizontal position of the tubes was used in all other testing in the calibration system. Examination of Figure 2 also reveals a tendency for the analysis results to be higher than the actual exposure levels.

Investigation of the literature related to the method of nitrogen dioxide analysis used by the Palmes tubes has revealed considerable uncertainty in the efficiency of uptake of the pollutant by various absorbing media that have been used in the standard methods of analysis. The standard method proposed by EPA (4) uses a factor of 0.82 in its arsenite bubbler. Other workers have proposed values for the efficiency factor between 0.62 and 1.00 (5). Palmes himself recommended an efficiency factor of 1.00 (1). Our present work seems to indicate an efficiency between 0.72 and 1.00, although the scatter in the data prevents assignment of a more specific value. If a factor of unity, rather than 0.72, were assumed for the data of Figure 2, the expectation value for the ratio of Palmes/actual dosage would be raised to 1.39. There is also evidence in the literature for a concentration dependence of the efficiency factor (5, 6, 7), although our data do not show clear evidence of this in the range of concentrations employed.

Figure 3 illustrates the same data set as Figure 2, but with actual observations rather than ratios on the vertical axis. The two darker lines are the expectation lines for efficiency factors of 1.00 and 0.72. The lighter line is the actual regression line through the points shown.

Because of their size and sensitivity range, the Palmes tubes were ideally suited to in-chamber testing on subjects of the biomedical protocols. Exposures were made during two scheduled sessions, with monitors both on subjects and in a stationary location in the chamber. One exposure was to 0.5 ppm NO_2 gas, while the second was to ozone with NH_4NO_3 aerosol as a control exposure. Table 3 illustrates the results of these tests. Each tube was on a separate subject.

In order to gain a larger statistical basis in the chamber, a further experiment was done. A total of 24 tubes were exposed. Twelve of these were on a single subject, and twelve were stationary. The following exposures were made:

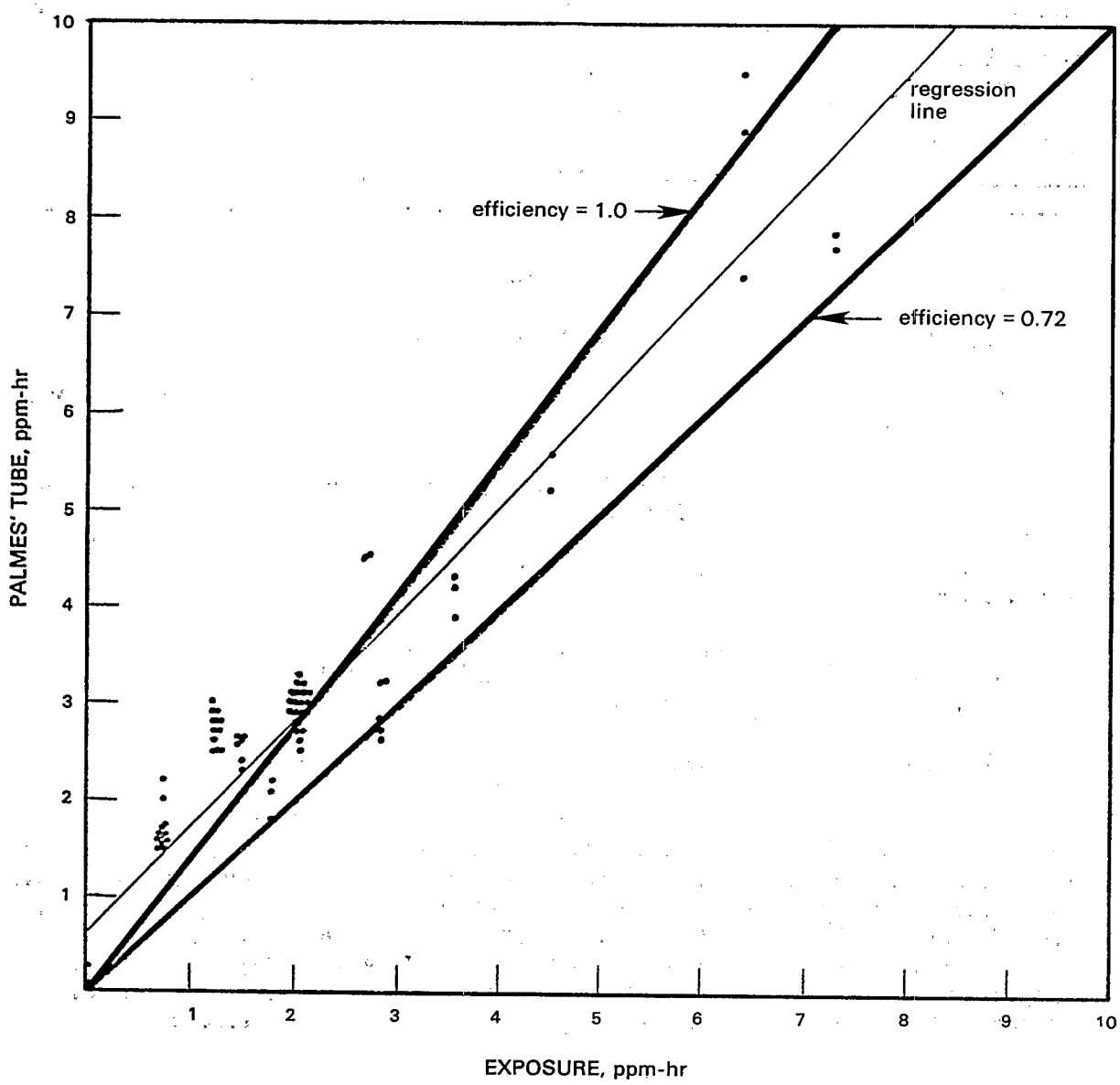

Figure 3. Palmes results versus dosage.

TABLE 3. ON-SUBJECT EXPOSURES IN CHAMBER

(T = 85° F, RH = 60%)

Exposure time	Exposure conc	Calculated dosage	Palmes dosage (ppm-hr) Mean	S.D.	N	R.S.D.	Meas./actual
(on subjects)							
4 hr	0.5	2.0	3.5	0.55	3	16%	1.75
(stationary)							
5 hr 20 min	0.5	2.7	4.5	0	2	--	1.66

(a) 6 samplers worn on upper body, around first button of shirt.

(b) 6 samplers worn on lower body, clipped to belt.

(c) 6 samplers held in vertical position in the chamber, clipped to an equipment rack.

(d) 6 samplers in horizontal position, in a wicker chair to allow free flow of gas past the tubes.

Subject activity during all exposures consisted of the following approximate proportions:

30 minutes - treadmill, 3.5 mph
30 minutes (approximate) - miscellaneous activity
3 hours - sitting in chair

4 hours - total exposure

As can be seen from Table 4, no important differences were seen between any groups except the lower body group, which is slightly low. Since much of the exposure was done in a sitting position, it is possible that occlusion of the openings by contact with the subject's clothing caused the difference observed. Statistical tests of the four group results indicate that the mean from the six tubes clipped to the lower body is significantly different ($p<0.05$) than the means of the other three groups. No other statistically significant differences were found.

SUMMARY

It was found that dosages as low as 2.0 ppm-hr could be reliably measured with the commercially available Palmes tube kit, although for best precision, higher levels of exposure are desirable. The design of the sampler is presently optimized for "industrial hygiene" levels, and could be modified to improve sensitivity in the lower limits of exposure.

TABLE 4. EXPOSURE OF PALMES TUBES IN CEL CHAMBER

(T = 70° F, RH = 40%)

Exposure time	Exposure conc.	Calculated dosage	Palmes dosage (ppm-hr) Mean	S.D.	N	R.S.D.	Meas./actual
On subject, upper body							
4	0.5	2.0	3.04	0.144	6	4.7%	1.52
On subject, lower body*							
4	0.5	2.0	2.75	0.217	6	7.9%	1.38
Stationary, vertical							
4	0.5	2.0	2.98	0.133	6	4.5%	1.49
Stationary, horizontal							
4	0.5	2.0	3.06	0.186	6	6.1%	1.53

*Statistically significant difference of mean from means of other three groups ($p<0.05$).

Specific modifications to achieve this goal might include:

1. Shorter diffusion length to increase capture of pollutant gas because of steeper diffusion gradient in tube. Use of a membrane or multi-cavity diffuser could be considered if the diffusion permeability is greater than the present design.

2. Larger absorption cross-section to increase the amount of material for analysis. In combination with a shorter diffuser, a badge type configuration might be achieved.

ACKNOWLEDGMENTS

The work presented here was sponsored by the U.S. Environmental Protection Agency. The kit used for testing was loaned by the U.S. Bureau of Mines. George Schnakenberg and Emory Chilton of the U.S. Bureau of Mines and Roberta McMahon of MDA Corporation provided helpful discussions.

REFERENCES

1. Palmes, E.D. 1976. Personal sampler for nitrogen dixoide. Am. Ind. Hyg. Assoc. J. 37:570.

2. McMahon, R. 1980. New technology for personal sampling of NO_2 and NO_x in the workplace. American Chemical Society Exposition Symposium, 1980. MDA-M-FS-4, MDA Corporation, Glenview, IL.

3. Saltzman, B.E. 1954. Colorimetric determination of nitrogen dioxide in the atmosphere. Anal. Chem. 26:1949-1955.

4. U.S. Environmental Protection Agency. 1976. Guidelines for development of a quality assurance program: Vol. XVI - Method for the determination of nitrogen dioxide in the atmosphere (sodium arsenite procedure). EPA-650/4-74-005-p.

5. Crecilius, H.J., and W. Forwerg. 1970. Investigations of the "Saltzman Factor." Staub-Reinhalt. Luft. 30:23-25.

6. Blacker, J.H. 1973. Triethanolamine for collecting nitrogen dioxide in the TLV range. Am. Ind. Hyg. Assoc. J. 34:390-395.

7. Huygens, Ir.C. 1970. Reaction of nitrogen dioxide with griess type reagents. Anal. Chem. 42:407-409.

* U.S. GOVERNMENT PRINTING OFFICE: 1983 - 659-095/1942